U.S. Department
of Commerce

Volume 102
Number 1
January 2004

Fishery Bulletin

U.S. Department of Commerce
Donald L. Evans
Secretary

National Oceanic and Atmospheric Administration
Vice Admiral
Conrad C. Lautenbacher Jr., USN (ret.)
Under Secretary for Oceans and Atmosphere

National Marine Fisheries Service
William T. Hogarth
Assistant Administrator for Fisheries

The *Fishery Bulletin* (ISSN 0090-0656) is published quarterly by the Scientific Publications Office, National Marine Fisheries Service, NOAA, 7600 Sand Point Way NE, BIN C15700, Seattle, WA 98115-0070. Periodicals postage is paid at Seattle, WA, and at additional mailing offices. POSTMASTER: Send address changes for subscriptions to Fishery Bulletin, Superintendent of Documents, Attn.: Chief, Mail List Branch, Mail Stop SSOM, Washington, DC 20402-9373.

Although the contents of this publication have not been copyrighted and may be reprinted entirely, reference to source is appreciated.

The Secretary of Commerce has determined that the publication of this periodical is necessary according to law for the transaction of public business of this Department. Use of funds for printing of this periodical has been approved by the Director of the Office of Management and Budget.

For sale by the Superintendent of Documents, U.S. Government Printing Office, Washington, DC 20402. Subscription price per year: $55.00 domestic and $68.75 foreign. Cost per single issue: $28.00 domestic and $35.00 foreign. **See back for order form.**

Fishery Bulletin

Scientific Editor
Dr. Norman Bartoo

Associate Editor
Sarah Shoffler

National Marine Fisheries Service, NOAA
8604 La Jolla Shores Drive
La Jolla, California 92037

Managing Editor
Sharyn Matriotti

National Marine Fisheries Service
Scientific Publications Office
7600 Sand Point Way NE, BIN C15700
Seattle, Washington 98115-0070

Editorial Committee

Dr. Harlyn O. Halvorson	University of Massachusetts, Boston
Dr. Ronald W. Hardy	University of Idaho, Hagerman
Dr. Richard D. Methot	National Marine Fisheries Service
Dr. Theodore W. Pietsch	University of Washington, Seattle
Dr. Joseph E. Powers	National Marine Fisheries Service
Dr. Harald Rosenthal	Universität Kiel, Germany
Dr. Fredric M. Serchuk	National Marine Fisheries Service
Dr. George Watters	National Marine Fisheries Service

***Fishery Bulletin* web site: www.fishbull.noaa.gov**

The *Fishery Bulletin* carries original research reports and technical notes on investigations in fishery science, engineering, and economics. It began as the Bulletin of the United States Fish Commission in 1881; it became the Bulletin of the Bureau of Fisheries in 1904 and the *Fishery Bulletin* of the Fish and Wildlife Service in 1941. Separates were issued as documents through volume 46; the last document was No. 1103. Beginning with volume 47 in 1931 and continuing through volume 62 in 1963, each separate appeared as a numbered bulletin. A new system began in 1963 with volume 63 in which papers are bound together in a single issue of the bulletin. Beginning with volume 70, number 1, January 1972, the *Fishery Bulletin* became a periodical, issued quarterly. In this form, it is available by subscription from the Superintendent of Documents, U.S. Government Printing Office, Washington, DC 20402. It is also available free in limited numbers to libraries, research institutions, State and Federal agencies, and in exchange for other scientific publications.

U.S. Department of Commerce
Seattle, Washington

Volume 102
Number 1
January 2004

Fishery Bulletin

Contents

Articles

1–13 **Alonzo, Suzanne H., and Marc Mangel**
The effects of size-selective fisheries on the stock dynamics of and sperm limitation in sex-changing fish

14–24 **Baba, Katsuhisa, Toshifumi Kawajiri, Yasuhiro Kuwahara, and Shigeru Nakao**
An environmentally based growth model that uses finite difference calculus with maximum likelihood method: its application to the brackish water bivalve *Corbicula japonica* in Lake Abashiri, Japan

25–46 **Brodeur, Rick D., Joseph P. Fisher, David J. Teel, Robert L. Emmett, Edmundo Casillas, and Todd W. Miller**
Juvenile salmonid distribution, growth, condition, origin, and environmental and species associations in the Northern California Current

47–62 **García-Rodríguez, Francisco J., and David Aurioles-Gamboa**
Spatial and temporal variation in the diet of the California sea lion (*Zalophus californianus*) in the Gulf of California, Mexico

63–77 **Jung, Sukgeun, and Edward D. Houde**
Recruitment and spawning-stock biomass distribution of bay anchovy (*Anchoa mitchilli*) in Chesapeake Bay

78–93 **Kellison, Todd G., and David B. Eggleston**
Coupling ecology and economy: modeling optimal release scenarios for summer flounder (*Paralichthys dentatus*) stock enhancement

94–107 **Kritzer, Jacob P.**
Sex-specific growth and mortality, spawning season, and female maturation of the stripey bass (*Lutjanus carponotatus*) on the Great Barrrier Reef

The conclusions and opinions expressed in *Fishery Bulletin* are solely those of the authors and do not represent the official position of the National Marine Fisheries Service (NOAA) or any other agency or institution.

The National Marine Fisheries Service (NMFS) does not approve, recommend, or endorse any proprietary product or proprietary material mentioned in this publication. No reference shall be made to NMFS, or to this publication furnished by NMFS, in any advertising or sales promotion which would indicate or imply that NMFS approves, recommends, or endorses any proprietary product or proprietary material mentioned herein, or which has as its purpose an intent to cause directly or indirectly the advertised product to be used or purchased because of this NMFS publication.

108–117 **Orr, Anthony J., Adria S. Banks, Steve Mellman, Harriet R. Huber, Robert L. DeLong, and Robin F. Brown**
Examination of the foraging habits of Pacific harbor seal (*Phoca vitulina richardsi*) to describe their use of the Umpqua River, Oregon, and their predation on salmonids
Companion paper with Purcell et al., see "Notes" below.

118–126 **Park, Wongyu, R. Ian Perry, and Sung Yun Hong**
Larval development of the sidestriped shrimp (*Pandalopsis dispar* Rathbun) (Crustacea, Decapoda, Pandalidae) reared in the laboratory

127–141 **Pearson, Donald E., and Franklin R. Shaw**
Sources of age determination errors for sablefish (*Anoplopoma fimbria*)

142–155 **Powell, Allyn B., Robin T. Cheshire, Elisabeth H. Laban, James Colvocoresses, Patrick O'Donnell, and Marie Davidian**
Growth, mortality, and hatchdate distributions of larval and juvenile spotted seatrout (*Cynoscion nebulosus*) in Florida Bay, Everglades National Park

156–167 **Santana, Francisco M., and Rosangela Lessa**
Age determination and growth of the night shark (*Carcharhinus signatus*) off the northeastern Brazilian coast

168–178 **Smith, Keith R., David A. Somerton, Mei-Sun Yang, and Daniel G. Nichol**
Distribution and biology of prowfish (*Zaprora silenus*) in the northeast Pacific

179–195 **Ward, Peter, Ransom A. Myers, and Wade Blanchard**
Fish lost at sea: the effect of soak time on pelagic longline catches

196–206 **Watanabe, Chikako, and Akihiko Yatsu**
Effects of density-dependence and sea surface temperature on interannual variation in length-at-age of chub mackerel (*Scomber japonicus*) in the Kuroshio-Oyashio area during 1970–1997

Notes

207–212 **Llanos-Rivera, Alejandra, and Leonardo R. Castro**
Latitudinal and seasonal egg-size variation of the anchoveta (*Engraulis ringens*) off the Chilean coast

213–220 **Purcell, Maureen, Greg Mackey, Eric LaHood, Harriet Huber, and Linda Park**
Molecular methods for the genetic identification of salmonid prey from Pacific harbor seal (*Phoca vitulina richardsi*) scat
Companion paper with Orr et al., see "Articles" above.

221–229 **Weng, Kevin C., and Barbara A. Block**
Diel vertical migration of the bigeye thresher shark (*Alopias superciliosus*), a species possessing orbital retia mirabilia

231 *Subscription form*

The effects of size-selective fisheries on the stock dynamics of and sperm limitation in sex-changing fish

Suzanne H. Alonzo

Institute of Marine Sciences and the Center for Stock Assessment Research (CSTAR)
University of California Santa Cruz
1156 High Street
Santa Cruz, California 95064
E-mail address: shalonzo@ucsc.edu

Marc Mangel

Department of Applied Mathematics and Statistics
Jack Baskin School of Engineering and the Center for Stock Assessment Research (CSTAR)
University of California Santa Cruz
1156 High Street
Santa Cruz, California 95064

Abstract—Fisheries models have traditionally focused on patterns of growth, fecundity, and survival of fish. However, reproductive rates are the outcome of a variety of interconnected factors such as life-history strategies, mating patterns, population sex ratio, social interactions, and individual fecundity and fertility. Behaviorally appropriate models are necessary to understand stock dynamics and predict the success of management strategies. Protogynous sex-changing fish present a challenge for management because size-selective fisheries can drastically reduce reproductive rates. We present a general framework using an individual-based simulation model to determine the effect of life-history pattern, sperm production, mating system, and management strategy on stock dynamics. We apply this general approach to the specific question of how size-selective fisheries that remove mainly males will impact the stock dynamics of a protogynous population with fixed sex change compared to an otherwise identical dioecious population. In this dioecious population, we kept all aspects of the stock constant except for the pattern of sex determination (i.e. whether the species changes sex or is dioecious). Protogynous stocks with fixed sex change are predicted to be very sensitive to the size-selective fishing pattern. If all male size classes are fished, protogynous populations are predicted to crash even at relatively low fishing mortality. When some male size classes escape fishing, we predict that the mean population size of sex-changing stocks will decrease proportionally less than the mean population size of dioecious species experiencing the same fishing mortality. For protogynous species, spawning-per-recruit measures that ignore fertilization rates are not good indicators of the impact of fishing on the population. Decreased mating aggregation size is predicted to lead to an increased effect of sperm limitation at constant fishing mortality and effort. Marine protected areas have the potential to mitigate some effects of fishing on sperm limitation in sex-changing populations.

Manuscript approved for publication 23 July 2003 by Scientific Editor.

Manuscript received 20 October 2003 at NMFS Scientific Publications Office.

Fish. Bull 102:1–13 (2004).

Fisheries models are generally used to predict the impact of fishing on stock dynamics and yield (Quinn and Deriso, 1999; Haddon, 2001). Classic models have focused mainly on growth, fecundity, and survival of species, without considering the impact of mating patterns on reproduction, survival, and recruitment. It is now recognized that life-history strategies and mating behavior will affect stock dynamics. Even so, general quantitative predictions regarding the effect of specific life-history patterns on fished populations are limited and further theory is needed (Levin and Grimes, 2002). It is likely that management strategies taking into account a species' reproductive behavior will greatly improve our ability to manage stocks (e.g. Beets and Friedlander, 1999). We would also like to know when the mating behavior and reproductive strategies of a stock will be worth investigating and when traditional management techniques will be sufficient. For example, in a management context, how do sex-changing stocks differ from separate-sex species? Here, we take an initial step toward generating a theory of the combined effect of life history and mating patterns on stock dynamics by focusing on the potential for and effect of sperm limitation in a protogynous (female to male) sex-changing stock. We focus on protogyny for this article because numerous protogynous species are commercially important, namely red porgy (*Pagrus pagrus*), gag grouper (*Mycteroperca microlepis*), and California sheephead (*Semicossyphus pulcher*).

Sex-changing fish present a unique challenge for management because size-selective fisheries have the potential to drastically reduce reproductive rates and population size at levels of fishing that would not pose a problem for dioecious (separate-sex) species (Huntsman and Schaaf, 1994; Armsworth, 2001; Fu et al., 2001). On the other hand, protogynous stocks may be less sensitive to the removal of large individuals if females are not fished and fertilization rates remain high. Many commercially important species are known to change sex (Bannerot et al., 1987; Shapiro, 1987; Coleman et al., 1996; Brule et al., 1999; Adams et al., 2000; Armsworth, 2001; Fu et al., 2001). Previous models have shown that sex-changing fish may be vulnerable to fishing (Bannerot et al., 1987; Huntsman and Schaaf, 1994; Armsworth, 2001; Fu et al., 2001).

Complications arise because the effect of fishing on a sex-changing species is mediated by many aspects of their reproductive biology, such as sex ratio, size-dependent fecundity, spawning aggregation size, and reproductive skew. Furthermore, patterns of sex change have cascading effects on the sex ratio, social interactions, population

fecundity, and male sperm production—all of which can affect stock dynamics. Thus, we cannot treat sex change as an isolated aspect of a species. Instead, we must consider sex change within the context of the mating system and the life history of the species to make general predictions. Behaviorally appropriate models are required to generate constructive qualitative and quantitative theory. Past theory has indicated that sex-changing populations exhibit stock dynamics that often differ from those of dioecious populations (Bannerot et al., 1987; Huntsman and Schaaf, 1994; Armsworth, 2001; Fu et al., 2001). Furthermore, protogynous stocks are predicted to be sensitive to fishing pattern and may exhibit nonlinear dynamics that could lead to population crashes (Armsworth, 2001). However, it is not known which aspects of the mating behavior and life history pattern of sex-changing stocks drive these differences. Here we focus on comparing a protogynous stock with an otherwise identical dioecious population to determine the effect of mating aggregation size, fertilization rates, and life history pattern on stock dynamics.

Size-selective (or age-selective) fisheries can impact a species through a decrease in spawning stock biomass, in general and through the removal of highly fecund larger and older individuals, in particular (Sadovy, 2001). However, in protogynous species, fisheries that preferentially remove large males can also change the population sex ratio; however, the exact effect of fishing pressure on stock dynamics in a protogynous species is complex. At one extreme, the complete removal of males from the population would cause a stock to crash, potentially making sex-changing species more vulnerable than dioecious species in the face of high fishing pressures. At the other extreme, sex-changing species may be less affected by size-selective fisheries if female fecundity limits recruitment and males are not removed in such numbers as to reduce mating or fertilization rates. Currently, there is no theory that predicts the potential for sperm limitation in protogynous stocks as a function of gamete production, fertilization rates, and mating pattern.

It has been suggested that marine reserves may be a viable management option for species where highly fecund older individuals are critical to reproduction (Levin and Grimes, 2002). However, no theory exists that can predict the impact of marine reserves on stock dynamics in sex-changing species. We consider the impact of a no-take marine reserve on the stock dynamics. We compare the effect of setting aside 0–30% of the spawning population in a reserve. We assume that larval production is exported from within the reserve to the rest of the population and determine whether the reserve can mediate some of the effects of fishing outside the reserve because this represents the optimal scenario for marine reserves. We also compare mean catch rates in the presence and absence of a reserve as a function of fishing mortality.

Spawning-per-recruit (SPR) measures are often used to estimate the impact of fishing on a stock (Parkes, 2000; Jennings et al., 2001). Ideally, a spawning-per-recruit measure would keep track of per-recruit production of larvae or eggs (Jennings et al., 2001). However, spawning stock biomass per recruit (SSBR) is commonly used to estimate the reproductive output per recruit at different intensities of fishing. One assumes that the biomass of mature fish is linearly related to reproductive output, which may be the case when egg production limits biomass and fecundity increases linearly with biomass. In protogynous stocks, overfishing of males alone may decrease fertilization rates and hence reproductive output without affecting either female biomass or egg production. Thus, in protogynous stocks or sex-selective fisheries, classic measures of spawning per recruit may misrepresent the impact of fishing on the stock's reproduction and hence population stability (Punt et al., 1993). We examine a variety of per-recruit measures and determine their ability to predict changes due to exploitation in mean population size.

In this study, we describe a general approach using sex- and size-dependent individual-based simulation models that predict reproduction, size distribution, and sex ratio in fished populations as a function of mating system and sex-change pattern. We examine the case where sex change occurs at a specific size threshold. We recognize that plastic and socially mediated sex-change patterns have been observed, and our results will apply only to species with fixed sex change. We explore the impact of mating aggregation size, sperm production, and asymptotic fertilization rates on the predicted stock dynamics in the presence of exploitation. We make predictions regarding the effects of fishing on population size, reproduction, sex ratio, size distribution, and fertilization rates. We also compare our results to previous work and discuss future directions.

Methods

We used an individual-based simulation to predict the size distribution, individual and population fecundity, population sex ratio, fertilization rate, and population size as a function of fishing mortality (Fig. 1). Individuals vary in age, size, sex, and mating site. Population size varies as a function of baseline survival, fishing mortality, reproduction, and larval recruitment. Reproduction depends on the pattern of sex change, mating system, sex ratio, mating site, and fecundity (or fertility) of individual males and females. For each annual time period, we determined individual survival, the size and age of these individuals in the next time period, and the total production of surviving offspring by those individuals. Initial analyses showed that a stationary size, sex, and age distribution is found within approximately 50 time periods and is independent of the initial population conditions. Thus, we simulated 100 time periods prior to examining the impact of fishing on stock dynamics to ensure that the population had already reached the stationary size and sex distribution for that scenario and set of parameters. We then examined the model for 100 reproductive seasons in the presence of fishing with a constant mean fishing mortality. Because a number of elements of the model were stochastic, we examined 20 simulations for each scenario and set of parameter values. Initial analyses indicated that 20 simulations were more than sufficient to lead to low variability in the key measures of interest. We assumed that reproduction occurs at the level of the mating

group at different reproductive sites. Individual survival, maturation, sex change, and mating site were determined stochastically as described below.

Fishing and adult survival

We assumed that adult survival is density independent but depends on fishing selectivity, fishing mortality, and baseline adult mortality in the absence of fishing. For simplicity, we assumed that age and size do not affect nonfishing adult mortality μ_A. We assumed that the fishery is size selective; we let L represent fish size, F represent annual fishing mortality, L_f represent the size at which there is 50% chance an individual of that size will be taken, and r represent the steepness of the selectivity pattern. Then fishing selectivity per size class $s(L)$ is given by

$$s(L) = \frac{1}{1+\exp\left(-r(L-L_f)\right)} \tag{1}$$

and adult annual survival becomes

$$\sigma(L) = \exp\left(-\mu_A - Fs(L)\right). \tag{2}$$

We assumed that fishing does not differentially affect the sexes independent of size. We recognize, however, that for some species this may not be the case. We also assumed that fishing occurs each year prior to reproduction and can represent either pulse or continuous fishing with an annual mortality F. We let $N_a(t)$ represent the number of individuals in age class a at time t so that population size $N(t) = \Sigma_a N_a(t)$.

Population dynamics

We assumed that the number of larvae that enter the population is determined by the production of fertilized eggs $P(t)$ and the probability that those larvae will survive to recruit. $P(t)$ is determined by the adult fecundity and fertilization rates described below. For computational tractability, we also assumed that a population ceiling $N_{\max}$ exists (Mangel and Tier, 1993, 1994). However, we chose $N_{\max}$ large enough that the stable population size was below the ceiling. Larval survival has both density-independent and density-dependent components (e.g. Cowen et al., 2000; Sale, 2002). We used a Beverton-Holt recruitment function to determine larval survival to the next age class (Quinn and Deriso, 1999; Jennings et al., 2001). Larvae represented the zero-age class $N_0(t)$ and thus the number of larvae surviving to recruit in any year t is given by

$$\begin{aligned} N_0(t) &= \left(\alpha P(t)\right)/\left(1+\beta P(t)\right) && \text{if } \left(\alpha P(t)\right)/\left(1+\beta P(t)\right) + \sum_{a=1} N_a(t) \le N_{\max} \\ N_0(t) &= \max\left(0, N_{\max} - \sum_{a=1} N_a(t)\right) && \text{if } \left(\alpha P(t)\right)/\left(1+\beta P(t)\right) + \sum_{a=1} N_a(t) > N_{\max}, \end{aligned} \tag{3}$$

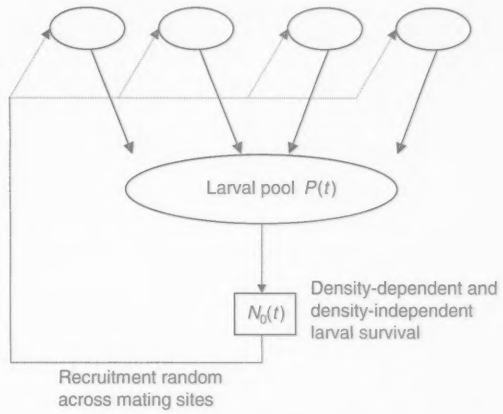
MATING SITES
Adult survival determined by baseline mortality and fishing pattern
Reproduction determined by group fecundity and fertility
No migration between mating sites
Larval pool P(t)
N0(t)
Density-dependent and density-independent larval survival
Recruitment random across mating sites

Figure 1

Structure and population dynamics of the individual-based model. We assumed that all mating sites contribute to a single larval pool.

where α gives density-independent survival; and β determines the strength of the density-dependence in the larval phase. In this function, we used the number of fertilized eggs produced, $P(t)$, rather than spawning stock size. We selected parameter values for larval survival that allowed the mean population size to be stationary near the ceiling in the absence of fishing. We assumed a single larval pool and that larvae recruit to mating sites at random (Fig. 1). The population was open between mating sites and we were simulating the entire stock. Thus, there was no emigration to or immigration from outside populations.

Growth dynamics

We assumed that all larvae enter the population at the same size, L_0. We assumed that growth is deterministic and independent of sex or reproductive status. We used a discrete time version of the von Bertalanffy growth equation (Beverton, 1987, 1992) to determine growth between age classes of surviving adults in which $L_{\inf}$ represents the asymptotic size and k is the growth rate. Then an individual of length $L(t)$ at time t will grow in the next time period to size $L(t+1)$ as follows:

$$L(t+1) = L_{\inf}\left(1+\exp(-k)\right) + L(t)\exp(-k). \tag{4}$$

Mating system

We assumed that reproduction occurs at the level of the mating group, and we examined the effect of varying mating group size and the number of mating sites. We assumed

that juveniles and adults exhibit site fidelity but that larvae settle randomly among mating sites. We also assumed that the population carrying capacity is split equally among the mating sites and that the total capacity of all mating sites exceeds the maximum population size in the absence of fishing as determined by adult mortality and the recruitment function. Therefore, mating sites do not limit recruitment but may affect reproductive rates. We examined three cases: 1) the entire population mates at one site (one mating site with up to 1000 individuals); 2) a few large mating groups exist (10 sites with a maximum of 100 individuals per site); and 3) many small mating aggregations exist (20 mating sites with a maximum of 50 individuals per site). For simplicity, we assumed that within a mating site, individuals mate in proportion to their fertility and fecundity. Therefore, large males and females have higher expected reproductive success. However, we assumed that all males that are large enough to change sex have a chance of reproducing proportional to their fertility. This is equivalent to assuming that females exhibit a mate choice threshold (Janetos, 1980) that has evolved with the size-at-sex change and that females have an equal probability of mating with males above this size threshold. However, a large male mating advantage clearly still exists. We also assumed that fishing mortality remains constant as mating aggregation size varies. Thus, we assumed that fishing effort per site does not increase as the number of mating sites decreases. An alternative would be to assume that total fishing mortality increases as the number of mating aggregations decreases.

Maturity

The probability that an individual matures $p_m(L)$ is determined by size. Once an individual matures, she remains female until sex change (see below). We let L_m represent the length at which 50% of the individuals will have matured.

$$p_m(L) = \frac{1}{1+\exp\left(-q(L-L_m)\right)}, \tag{5}$$

where q determines the steepness of the probability function.

Sex change

The probability of sex change, $p_c(L)$, is a logistic function of absolute size L

$$p_c(L) = \frac{1}{1+\exp\left(-\rho(L-L_c)\right)}, \tag{6}$$

where L_c represents the size at which 50% of the individuals will change sex from female to male and ρ is a constant.

Reproduction

We assumed that female fecundity $E(L)$ depends on individual size according to the allometric relationship

$$E(L)=aL^b, \tag{7}$$

where a and b are constants.

Once an individual has changed sex (as determined by the sex change rule described above) sperm production (in millions) $S(L)$ is given by

$$S(L)=cL^d, \tag{8}$$

where c and d are constants.

Size-dependent fecundity has been measured in many fish species (e.g. Gunderson, 1997). A general allometric relationship between sperm production and size has not been established. Therefore, we assumed that male gamete production increases with size at the same rate as that for females (b=d). We also assumed that males produce many more sperm at any body length than females produce eggs. Clearly, other possible patterns exist. We examined the case where males produce from 10^2 to 10^6 sperm for every egg produced by a female. In the pelagic spawning wrasse (*Thalassoma bifasciatum*), large males release approximately 1000 times more sperm than females release eggs (Schultz and Warner, 1991; Warner et al., 1995).

We used recently published data on sperm production and fertilization rates in the bluehead wrasse (*Thalassoma bifasciatum*) to generate a biologically appropriate fertilization function for our model (Warner et al., 1995; Petersen et al., 2001). It is critical to consider a biologically appropriate form for the function to express fertilization rates when considering the potential for sperm limitation. The probability an egg will be fertilized is an increasing function of the number of sperm available for that mating (Fig. 2). The number of eggs released per mating also affects the fertilization rate (Fig. 2). For simplicity, we calculated the average expected fertilization rate per mating site based on the total production of sperm and eggs at the site. We let S represent the number of sperm released (in millions) and E the number of eggs released at each mating site. We assumed that the proportion of eggs fertilized per mating site p_F is given by

$$p_F = \frac{S}{1+(\kappa E+\chi)S}, \tag{9}$$

where κ and χ are constants fitted to the data.

The number of eggs fertilized per group is $p_F E$ and the total production of fertilized eggs, $P(t)$, is the sum of the number of eggs fertilized in all mating groups.

Measures of spawning stock biomass per recruit

To measure the impact of fishing on stock dynamics, we computed the total spawning stock biomass per recruit starting from the beginning of fishing for the next 50 years. We used the generally recognized pattern that fish wet weight tends to be approximately proportional to the cube of fish length (Gunderson, 1997) to convert fish length, L, into relative biomass, $B(L)$~L^3. Then we calculated total female and male spawning stock biomass

per recruit (SSBR). We also kept track of the total fecundity (egg production per recruit), fertility (sperm production per recruit), and eggs fertilized per recruit.

Marine reserves

We examined the effect of no-take marine reserves on the predicted stock dynamics by comparing the stock dynamics in the presence and absence of reserves. Without a reserve, individuals at all mating sites are subject to fishing. In the presence of a no-take marine reserve, we "protect" a percentage of the mating sites (and thus the population) from fishing. We examined cases in which 0%, 10%, 20%, and 30% of mating sites were protected from fishing. We assumed that the population is completely open among mating sites. Thus, eggs produced from all mating sites enter one larval pool and recruitment occurs randomly between mating sites. Clearly other possibilities exist and could be considered in future analyses, but this case represents a reasonable baseline situation to consider because many marine fish have pelagic larval phases. We also recognize that these analyses ignore the effect of interactions between species within the reserve on stock dynamics. We examined two situations. In the first case, reduced fishing effort occurs when mean fishing mortality is decreased in the presence of reserves because fishing mortality (F) at the unprotected sites remains the same as before the reserve. In the second case, the redistribution of fishing effort occurs when mean fishing mortality across all sites remains the same because fishing mortality increases at the unprotected sites.

Comparison of sex-changing stocks and dioecious stocks

Ideally, we would like to distinguish the effects of sex change in isolation from the confounding effects of mating pattern, sex ratio, survival, growth, and population fecundity on stock dynamics. To differentiate whether sex change in isolation or other aspects of the mating system determine the predicted stock dynamics, we also examined a version of the model described above for a population where sex is fixed at birth. In this dioecious population, we keep all aspects of the stock constant except for the pattern of sex determination (whether the species changes sex or is dioecious). One would generally expect a dioecious population with no differences between the sexes in mortality to exhibit a 50:50 sex ratio (Fisher, 1930; Trivers, 1972; Charnov, 1982). However, we wanted to control for all differences between the dioecious and protogynous stocks other than the sex-determination pattern. Therefore, we considered the same sex ratio at maturity (0.67=the proportion of adults that are female) as found in the sex-changing population in the absence of fishing. Assuming no sex-specific differences in survival to maturity, this is the same as assuming a 0.67 sex ratio at birth. In this model, individuals remain one sex (determined randomly at birth) throughout their lifetime. Fishing is size but not sex selective. We assumed that males mature at the same size as females.

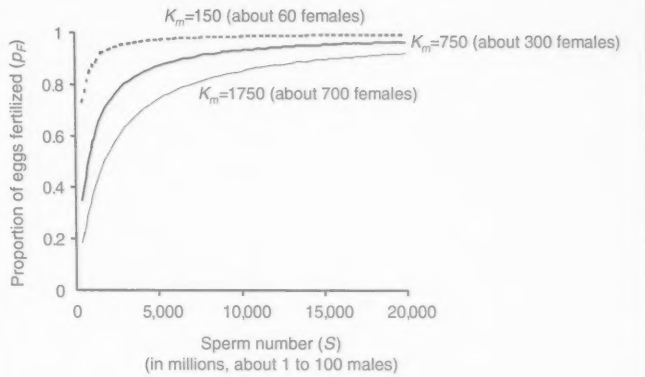

Figure 2

Fertilization rate as a function of the number of eggs and sperm per mating site. The saturation parameter $K_m=\kappa E+\chi$ is taken from Equation 9.

Parameter values

We used previous research on California sheephead (Labridae, *Semicossyphus pulcher*), a commercially important sex-changing fish, to provide evolutionarily and ecologically reasonable parameters for the model. Although the growth, survival, and reproduction of this species have been studied, less is known about the factors that induce sex change and mating behavior. In this species, sex change occurs at approximately 30 cm although the exact pattern varies among populations (Warner, 1975; Cowen, 1990). It is not known whether sex change is fixed or socially mediated. Because nothing is known about fertilization rates in the California sheephead, we generated κ and χ (Eq. 9) by fitting a line through the estimated values of K_m for small and large bluehead wrasse females as a function of their mean egg production (see Table 1 and Fig. 2; Warner et al., 1995; Petersen et al., 2001). For parameter values and sensitivity analyses see Table 1.

Results

We present the average across 20 simulations of the mean population measures of the last 50 years for each simulation. The variation around the mean in all measures considered was very low (hundredths of a percent of the mean or less). For the spawning per recruit (SPR) measures we give the mean value across the first 50 years of fishing to ensure that the entire cohort had died before the end of the simulation. When the ratio of sperm to eggs is 10^4 to 10^6, a single male can fertilize all of the eggs in the population. When the ratio of sperm to eggs is 10^2, sperm limitation occurs even in the absence of fishing. Therefore, we present results for the case where the ratio of sperm to eggs is 10^3

Table 1

The following parameters were used in the model.

Parameter	Baseline values	Definition and source
Growth		
k	0.05	growth rate (based on Cowen, 1990)
L_{inf}	90 cm	asymptotic size (based on Cowen, 1990)
L_0	8 cm	larval size at recruitment
Population		
N_{max}	1000	maximum population size
μ_A	0.35	adult mortality (based on Cowen, 1990)
α	0.0001	density-independent larval mortality
β	$\alpha/(1-\exp(-\mu_A))N_{max}(3.33 \times 10^{-7})$	larval recruitment function parameter (see text)
Fishing		
r	1 (0.1)	steepness of selectivity curve
L_f	30 (25, 35)	length at which 50% chance a fish will be removed
F	0–3	fishing mortality
Reproduction		
a	7.04	constant in the fecundity relationship (Warner, 1975)
b	2.95	exponent in the fecundity relationship (Warner, 1975)
c	$10^{-3}a$ ($10^{-2}a$, $10^{-4}a$)	constant in the sperm production function (measured in millions of sperm)
d	b	exponent in the fertility relationship (Warner, 1975)
κ	0.000003	slope of fertilization function parameter
χ	0.09	intercept of fertilization function parameter (based on Peterson et al., 2001) see text for details
Maturity		
L_m	20 cm	length at which 50% of fish mature (Warner, 1975; Cowen, 1990)
q	1	shape parameter in the maturity function
Sex change		
L_c	30 cm	length at which 50% of fish change sex (Warner, 1975; Cowen, 1990)
ρ	1	shape parameter in the sex change function

and fertilization rates are 100% in the absence of fishing, but the population must have multiple males for high fertilization rates. For all the results presented in our study we assumed a fixed sex-change pattern, mating among males and females at each site proportional to gamete production, and larval export among mating sites. We also assumed, unless otherwise noted, a sharp size-selective fishing pattern (r=1) and that the probability of sex change and removal of sex-changing fish by the fishery are centered at the same mean size or L_f=L_c. Clearly, the results presented in our study may not apply to cases where these assumptions are not met.

General patterns predicted by the model

First, we examined the general effect of fishing mortality on the sex-changing stock for the case when one mating site exists. When $L_f = L_c$, eggs produced per recruit decrease only slightly with fishing mortality (e.g. a 3% drop as fishing mortality increased from 0 to 3, Fig. 3A). However, the mean number of eggs fertilized (both total and per recruit) decreases sharply as fishing mortality increases (e.g. a 30% drop as fishing mortality increased from 0 to 3, Fig. 3A). The number of recruits per year decreases as well. As fishing mortality increases, male spawning stock biomass per recruit decreases dramatically, whereas changes in female spawning stock biomass would be practically undetectable (90% drop for male SSBR, compared with a 3% drop for female SSBR as F increases from 0 to 3, Fig. 3B). Because of the drop in male SSBR, total spawning stock biomass (males and females) per recruit also decreases as fishing mortality increases. Sperm production per recruit is predicted to decrease with increasing fishing mortality (Fig. 3C).

Sensitivity of stock dynamics to fishing pattern

In general, mean population size decreases as fishing pressure increases (Fig. 4A). The adult sex ratio (measured as

the percentage of mature individuals that are female) also increases as fishing mortality increases (Fig. 4B) and the mean size of adults in the population decreases. These patterns depend on fishing being size selective, which causes a disproportional take of males. If the size-selectivity of the fishery targeted smaller size classes (L_f<L_c), a decline in annual biomass removed by the fishery is predicted with increasing F and the stock is predicted to crash at a relatively low fishing mortality (Fig. 4C). If the fishery is less selective (r=0.1, L_f=L_c), the population is also predicted to crash for most fishing mortalities. Thus, allowing some proportion of mature males to consistently escape fishing is critical even at low fishing mortality. As fishing mortality increases, the predicted biomass removed by the fishery increases with diminishing returns (Fig. 4C). When L_f=L_c, the biomass removed by the fishery does not continue to increase with F because all males above the size at sex change are being removed by the fishery. In this case, the males in the population are essentially breeding only once before they are taken by the fishery. For the range of fishing mortality considered, we did not observe a decline in biomass taken with increasing F unless L_f<L_c or r=0.1. If more size classes are allowed to escape fishing (L_f>L_c), the general patterns remain the same, but for the same fishing mortality (F), the effect of fishing on the population is less (Fig. 4). Female biomass does not decrease much with fishing mortality when L_f=L_c even though some females are removed by the fishery because the probability of a female changing sex is the probability of it being fished. Therefore, female loss due to the fishery affects male biomass rather than female biomass in the population.

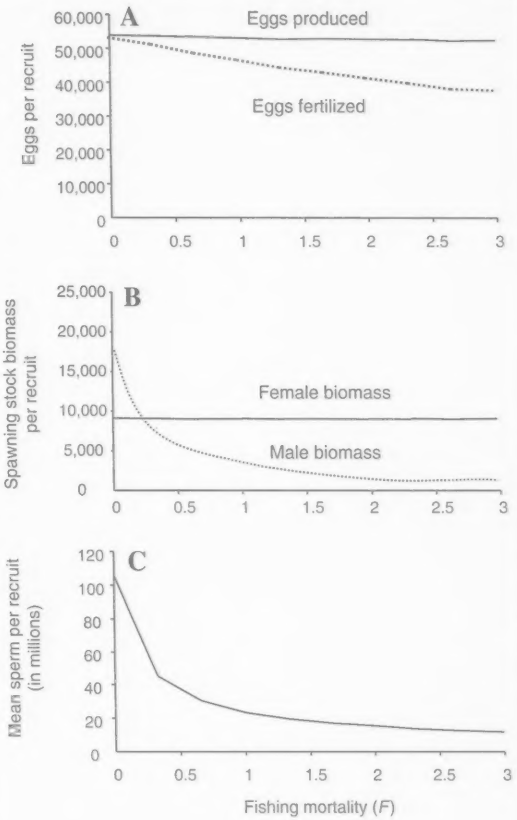

Figure 3

Spawning-per-recruit measures. Results are presented for the sex-changing stock with one mating site when $L_f = L_c$ and r=1. Means across 20 simulations are given. For details see the general text.

Sperm limitation and production

The removal of large males from the population is predicted to cause sperm limitation and decreased fertilization rates (Fig. 3, A and C), leading to a decrease in mean population size (Fig. 4A). The degree to which the fertilization rate and thus the population size decreases depends to a great extent on the pattern of sperm production and fertilization. We assumed that only a few males are needed to fertilize the eggs of many females (Fig. 2). We also assumed that per-capita reproduction and recruitment are high even at a low population size (Barrowman and Myers, 2000). Thus, protogynous populations with lower sperm production or fertilization rates would experience greater effects from fishing than predicted in the present study. Similarly, populations with lower production or survival would experience larger decreases in population size even with the same level of sperm limitation and fishing. In general, however, the removal of males alone from a protogynous population with a fixed sex change is predicted to cause decreased fertilization rates and lower mean population size even when the fertilization rate function is asymptotic and individual male sperm production is high.

Mating aggregation size

As mating aggregation size decreased and fishing mortality and effort remained constant, the effect of fishing on the population increased. As described above, we assumed that fishing effort would not be concentrated on the few large mating aggregations and thus increase total fishing mortality. The sex ratio, mean size, mean fecundity, and mean fertility all remained the same across different mating aggregation sizes with constant fishing mortality. However, the mean fertilization rate and number of fertilized eggs per recruit decreased with mating group size (Fig. 5) even though male biomass and SSBR remained the same. Both predicted mean population size and biomass taken decreased as fishing mortality increased (Fig. 5). This pattern was generated by sperm limitation in small mating groups. Smaller groups have higher probabilities that sperm production within the group will not be sufficient to fertilize the eggs produced within the mating group. Small mating aggregations may not only be sperm limited but also be male limited and fail to reproduce completely; populations with small group sizes (50 individuals or less) were predicted to become extinct in

5–25% of the simulations as fishing mortality (F) increased from 0 to 1. The impact of mating group size on stock dynamics is thus predicted to be nonlinear. A threshold mating aggregation size appeared to exist below which sperm limitation and reproductive failure become common.

Spawning-per-recruit measures

For size-selective fishing, the spawning stock biomass per recruit of females is not predicted to decrease significantly with increased fishing mortality as long as some male size classes escape fishing ($L_f \geq L_c$). However, male biomass per recruit and sperm production per recruit are both predicted to decrease. Although egg production is not predicted to decrease with increasing size-selective fishing pressure, the number of fertilized eggs is predicted to decrease. When all male size classes are fished ($L_f \geq L_c$), the stock is predicted to crash and therefore clearly female biomass and egg production are predicted to decrease with fishing mortality. In general, the predicted decrease in mean population size and reproduction is driven for the most part by decreased sperm production and consequently a reduction in the number of eggs fertilized per recruit. The relationships between fishing pressure and the classic spawning-per-recruit measures do not indicate the true effect that fishing is predicted to have on the protogynous population (Fig. 6). When $L_f \geq L_c$, female spawning stock biomass per recruit and eggs produced per recruit showed almost no effect of fishing on the population, even as mean population size decreased. Because of the size-selective fishing pattern, total and male biomass per recruit decreased with fishing mortality and decreasing mean population size. However, male and total biomass per recruit did not reflect the increased effect of fishing on populations with smaller mating aggregations. The production of fertilized eggs per recruit decreased with increased fishing pressure and decreased more sharply for smaller mating aggregations. Only the number of fertilized eggs per recruit could assess the predicted effect of fishing on the protogynous population. Thus, classic SPR measures were predicted to fail in the presence of sperm limitation to assess the impact of fishing on a protogynous stock.

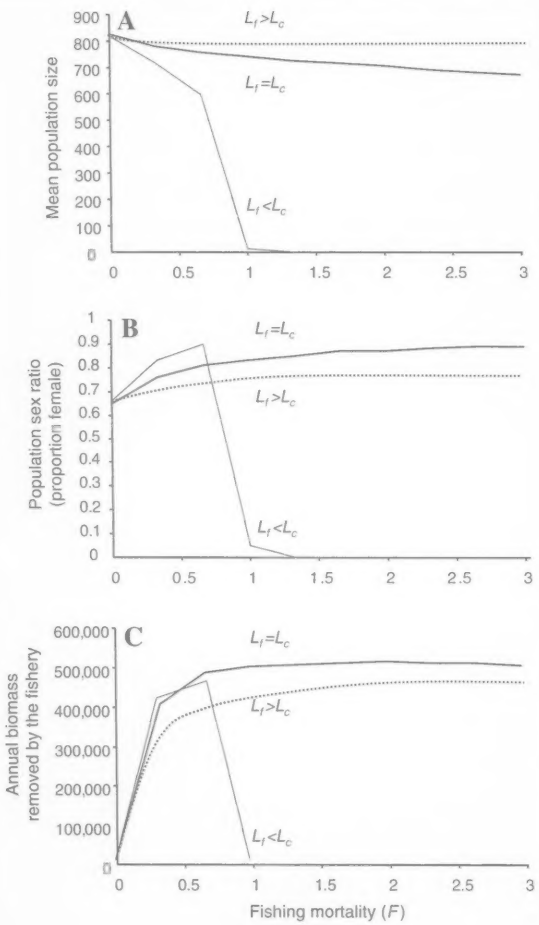

Figure 4

The effect of size-selective fishing on stock dynamics. We present results for the sex-changing stock with one mating site when r=1. Means across 20 simulations are given. For details see the general text.

Marine reserves and fishery management

In the situation considered in this study, the pattern of fishing is more important to stock dynamics than the presence of marine reserves. We assumed a size-selectivity that allowed on average 50% of individuals of sex-changing size to escape the fishing gear. Thus, although the sex ratio does increase (become more female) by 20–40%, all males are not lost from the population (when $L_f \geq L_c$ and r=1). If fishing selectivity occurs at a smaller size, then the effects on the population are predicted to be much greater and the protogynous stock would suddenly become more affected than the dioecious population. For example, at L_f=25 cm the protogynous stock is predicted to crash whenever $F \geq 1$. This occurs not because of a reduction in the production of eggs but rather because of a failure to fertilize the eggs produced by surviving females. When males of all size classes are fished, populations can become male limited and fertilization rates drop drastically. A decrease in the production of fertilized eggs can lead to a decrease in female biomass, but it is the removal of males rather than females that causes this decline.

When fishing effort is not redistributed after the formation of a reserve, the impact of fishing on the mean population size and SPR measures is predicted to decrease (e.g. Fig. 7A). However, if fishing effort is redistributed among unprotected areas, the benefit of the reserves to the protogynous stock decreases (Fig. 8A). Protecting some sites allows large males to

escape fishing and thus increases the production of fertilized eggs at the population level. However, yield decreased proportionally to the percentage of sites protected by the reserve unless fishing effort is redistributed among the remaining sites. We assumed that fish do not move between sites after the larval stage, and thus larger and older individuals do not leave the reserve and become exposed to fishing. Although this assumption is clearly appropriate for some species, it is important to realize that the dynamics and predictions would differ for more closed populations or migratory species. For the fishing pattern and biological scenario examined in this study, marine reserves are not predicted to increase biomass available to the fishery (Figs. 7B and 8B).

Dynamics of dioecious versus protogynous stocks

In the dioecious stock with a single randomly mating aggregation, both male and female biomass per recruit and fecundity or fertility per recruit are predicted to decrease as fishing mortality increases (Fig. 6). Because both egg production and sperm production decrease with increased fishing pressure in the dioecious stock, the number of eggs fertilized per recruit did not differ much from the other SPR measures. Thus, SSBR and eggs per recruit also indicated the impact of fishing on the stock in dioecious stocks with large mating aggregations. The percent drop in population size and fertilized egg production is predicted to be much greater in dioecious species and occurred more quickly than in the sex-changing stock because of a reduction in overall population fecundity even in the absence of decreased fertilization rates. However, dioecious stocks are predicted to exhibit larger mean population size for the same fishing mortality and to support a larger fishery because of the additional egg production of large fecund females. At very small mating aggregations, sperm limitation is predicted even in the dioecious stock and fertilized eggs per recruit become a better indicator of stock dynamics in the presence of fishing. Dioecious stocks are also predicted to benefit from marine no-take reserves through the protection of large fecund females (Fig. 7).

Discussion

In this study we developed a general framework that examines the consequences to

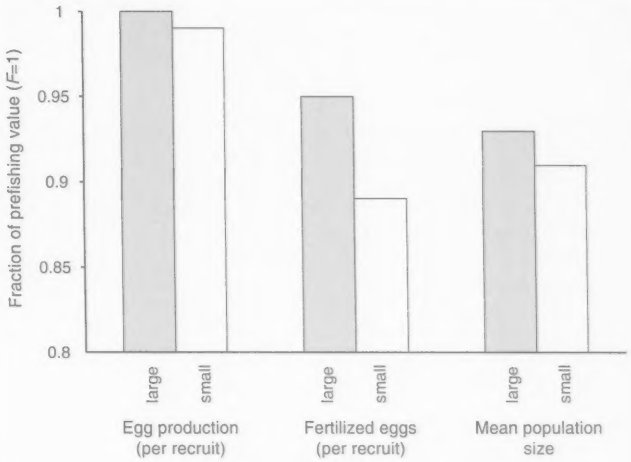

Figure 5

Mating aggregation size affects the response to fishing. Large (one large mating aggregation) and small (10 smaller mating aggregations) situations are compared. Percent change in the presence of fishing (from F=0 to F=1) in egg production per recruit, mean fertilized egg production per recruit, and mean population size are given. Total population fecundity and mean body size are lower for the smaller mating aggregations.

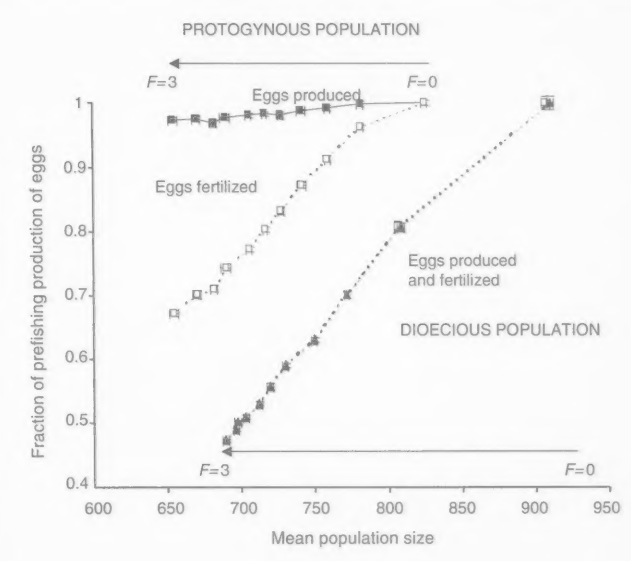

Figure 6

Spawning-per-recruit (SPR) measures in a protogynous (squares) and dioecious (triangles) stock: Mean egg production per recruit (filled) and mean fertilized eggs per recruit (open) are shown for a randomly mating population with one large mating group. Error bars indicate the standard error of the mean. For the dioecious population, the two SPR measures overlap.

fisheries management of a behaviorally and evolutionary reasonable life-history and sex-change pattern. We based our assumptions and parameter values on patterns observed in natural populations that have presumably evolved given the life history tradeoffs and expected reproductive success associated with these behaviors. However, we made various assumptions that affect the predicted patterns such as a fixed sex-change pattern, male mating success proportional to sperm production, and a very resilient recruitment function. Despite these assumptions, a number of general patterns emerge.

Life-history pattern is important but not sufficient to predict stock dynamics

In general, we predicted that a protogynous stock with fixed sex change will respond to the same fishing pressure differently than an otherwise identical dioecious stock. Understanding the life history of the population is clearly important to our understanding of stock dynamics. However, it is not possible to classify protogynous stocks simply as more or less sensitive to fishing. The differences between dioecious and sex-changing fish are relatively complex, and it is not the case that one life history is expected to be more or less vulnerable to fishing. Although the sex change and fishing pattern are important, they must be seen in the context of the mating system, reproductive behavior, and population dynamics of the species. If no male size classes escape fishing, then the sex-changing population will be much more sensitive to fishing and may crash even at low fishing mortality. When some male size classes escape fishing, an identical dioecious stock is predicted to experience a greater decrease in mean population size than the protogynous population. However, the protogynous species is predicted to be much more sensitive to mating aggregation size and sperm limitation. Protogynous stocks are predicted to benefit from marine protected areas at high levels of fishing mortality where sperm limitation is common at fished mating sites. In contrast, the dioecious stock is predicted to derive a greater benefit of marine reserves even at low fishing mortality because of the protection of large fecund females (Fig. 7). Although the sex-changing population is predicted to be less sensitive to fishing mortality overall, it is clearly very important to understand the exact details of the sex-change pattern and the size-selectivity of fishing in relation to sex change. It will also be important to understand the mating system and patterns of fertilization success and sperm production in males when managing a protogynous stock. Given the sensitivity of the sex-changing stock to the size-selective pattern of fishing, we recommend the precautionary approach of keeping fishing mortality sufficiently low so that some males of all size classes always escape fishing (Fig. 4C). Clearly, protogynous stocks cannot be managed as if they were dioecious.

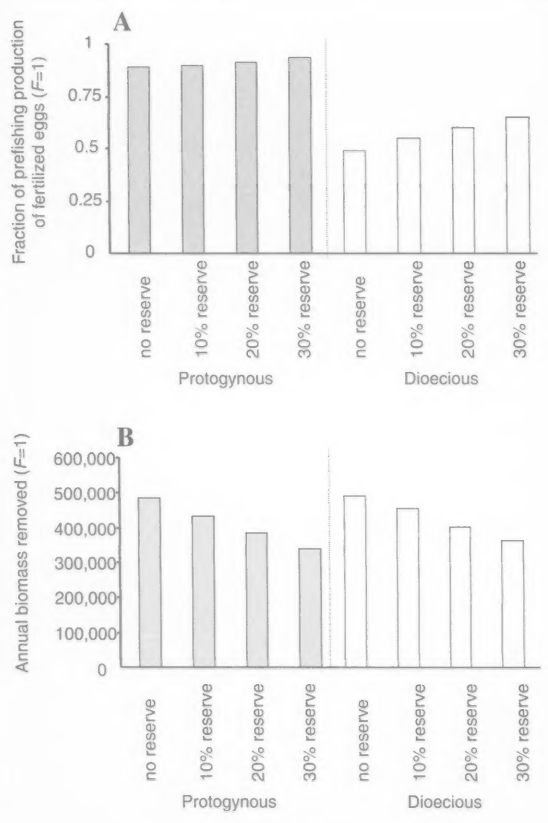

Figure 7

The effect of marine reserves on protogynous and dioecious populations when fishing effort is decreased (case 1). (**A**) Percent change in the presence of fishing (F=1) in the production of fertilized eggs compared to in the absence of fishing. (**B**) Annual biomass removed by the fisheries varies with marine reserve and sex-change pattern. Numbers shown are for 10 mating sites when F=1.

Sperm limitation and mating aggregation size affect stock dynamics

The removal of large males from the population can cause sperm limitation, decreased fertilization rates, and decreased population size even in a resilient species with high sperm production. Sperm limitation will increase as mating group size decreases. In the present model, even small males produced relatively large amounts of sperm. If males are removed, populations with lower sperm production are predicted to be more sensitive to the removal of large fertile males. Our assumption of fertilization rates determined by total egg and sperm production per mating site will, if anything, have underestimated the potential for sperm limitation. Other mating systems and reproductive behaviors could lead to greater sperm limitation than predicted in our study. For example, species that have not evolved under sperm competition should be more affected by the removal of large males than

species with sperm competition because of decreased allocation to sperm production. Pair spawning among individuals could also lead to decreased fertilization rates. Reproductive behaviors often found in sex-changing species, such as territoriality, female choice, resource-defense polygyny, and mate monopolization, all lead to skewed reproductive success for males and could further decrease fertilization rates. Sperm limitation is predicted to occur, and an understanding of such factors as fertilization rate, sperm production, mating skew, and mating group size will increase our ability to understand and predict stock dynamics.

Traditional spawning-per-recruit measures can fail in the presence of sperm limitation

Although problems exist with traditional spawning-per-recruit measures in general (Parkes, 2000), they are especially problematic for sex-changing stocks. In the dioecious stock, the relationship between female and total spawning stock biomass per recruit exhibits a roughly linear relationship with population size. In the sex-changing stock, female fecundity does not reflect the changes in mean population size. Although total or male spawning stock biomass per recruit did decrease with decreased population size, the fit between these measures will depend greatly on the size-dependent sperm production of males, mating aggregation size, and other factors determining the potential for sperm limitation. Male or total spawning stock biomass per recruit alone cannot predict sperm limitation and thus will fail to predict the potential population crashes that may result. We conclude that any measure of spawning per recruit in a sex-changing species that does not consider sperm limitation and reduced fertilization rates has the potential to underestimate the impact of fishing on the population. The number of eggs produced or female spawning stock biomass can remain relatively unchanged in the face of high fishing mortality even as the population is predicted to decline. However, the failure of classic spawning-per-recruit measures in the presence of declines due to sperm limitation or decreased fertilization rate will not be limited to protogynous stocks. Although sperm production patterns and fertilization rates are not known for many commercially important species, this information can be collected to develop a general sense of how sperm production depends on individual size. We also have a general sense of the factors that are expected to affect fertilization rates (Birkhead and Møller, 1998) and these can be easily studied in any species where spawning grounds are accessible to researchers. It is clear that new management measures must be developed for sex-changing species that consider the potential for sperm limitation because biomass alone may miss the potential for rapid population crashes. One purpose of theory is to tell us what we need to know more about and to stimulate further research. Our results clearly indicate that we need to know more about sperm production and fertilization rates when managing protogynous stocks.

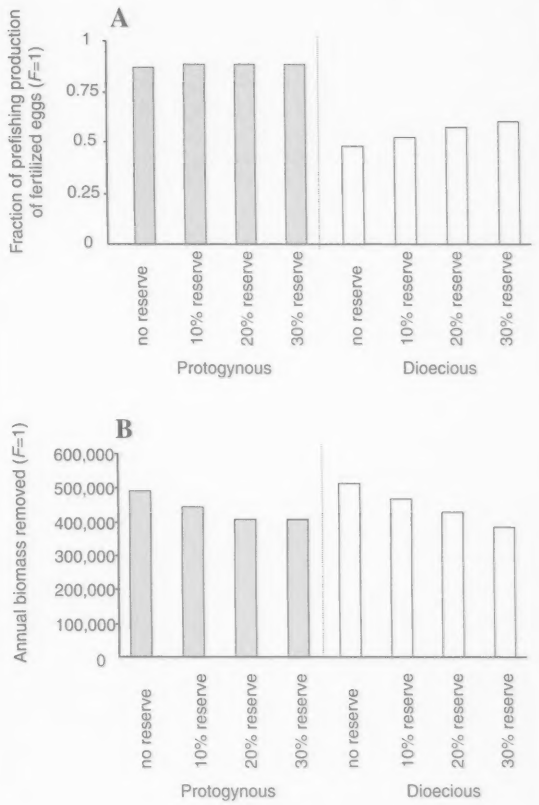

Figure 8

The effect of marine reserves on protogynous and dioecious populations when fishing effort is redistributed (case 2). (**A**) Percent change in the presence of fishing (F=1) in the production of fertilized eggs compared to percent change in the absence of fishing. (**B**) Annual biomass removed by the fisheries varies with marine reserve and sex-change pattern. Numbers shown are for 10 mating sites when F=1.

Marine reserves and size-selective fishing can be used to manage protogynous stocks

Marine reserves clearly have the potential to decrease the impact of fishing on populations. Large highly fecund or fertile individuals may be protected from size-selective fisheries. However, the benefits of a marine reserve will be significantly decreased if fishing effort is simply redistributed to unprotected sites (Figs. 7 and 8; Guenette and Pitcher, 1999; Apostolaki et al., 2002). It is usually recognized that the larval export and import dynamics will be crucial to whether reserves increase mean population size. We predict that the degree to which stocks respond to no-take reserves will also depend on their life-history pattern, mating system, and size-dependent fecundity and fertility. The protection of large and fecund (or fertile)

fish will certainly increase reproduction and decrease the impact of fishing on the population. However, the benefit of marine reserves will be much greater in populations where larger or older individuals play a key role in reproduction. Given the predicted extreme sensitivity of the protogynous population to the pattern of size-selective fishing, marine protected areas could represent a precautionary management strategy to ensure that some males are not subject to fishing mortality.

A comprehensive approach to stock dynamics

Managing fishing on stocks of sex-changing fish will require considering the sex-change pattern. However, one must also consider the sex change pattern within the context of the mating system. Although the pattern of sex determination does affect the stock dynamics, simple statements regarding whether dioecious or sex-changing populations are more sensitive to fishing are not possible. The differences among dioecious and sex-changing stocks are complex, and the management of these stocks will depend as much on their mating system, the type of fishing strategies used to capture them, and mating aggregation size as on the sex determination pattern. Classic SPR measures cannot measure sperm limitation and reduced fertilization rates, and thus will not always measure or predict the impact of fishing mortality on the population. Rather than relying on measures of spawning stock biomass per recruit alone, management groups should also monitor protogynous sex-changing stocks for a reduction in fertilization rates

Acknowledgments

We thank Phil Levin, Alec McCall, Steve Ralston, and Bob Warner for their comments on an earlier version of this manuscript. This research was supported by National Science Foundation grant IBN-0110506 to Suzanne Alonzo and the Center for Stock Assessment Research (CSTAR).

Literature cited

Adams, S., B. D. Mapstone, G. R. Russ, and C. R. Davies.
2000. Geographic variation in the sex ratio, sex specific size, and age structure of *Plectropomus leopardus* (Serranidae) between reefs open and closed to fishing on the Great Barrier Reef. Can. J. Fish. Aquat. Sci. 57:1448–1458.

Apostolaki, P., E. J. Milner-Gulland, M. K. McAllister, and G. P. Kirkwood.
2002. Modelling the effects of establishing a marine reserve for mobile fish species. Can. J. Fish. Aquat. Sci. 59: 405–415.

Armsworth, P. R.
2001. Effects of fishing on a protogynous hermaphrodite. Can. J. Fish. Aquat. Sci. 58:568–578.

Bannerot, S., W. F. Fox, and J. E. Powers.
1987. Reproductive strategies and the management of snappers and groupers in the gulf of Mexico and Caribbean. *In* Tropical snappers and groupers: biology and fisheries management (J. J. Polovina and S. Ralston, eds.), p. 561–603. Westview Press, Boulder, CO.

Barrowman, N. J., and R. A. Myers.
2000. Still more spawner-recruitment curves: The hockey stick and its generalizations. Can. J. Fish. Aquat. Sci. 57: 665–676.

Beets, J., and A. Friedlander.
1999. Evaluation of a conservation strategy: a spawning aggregation closure for red hind, *Epinephelus guttatus*, in the U.S. Virgin Islands. Environ. Biol. Fishes 55:91–98.

Beverton, R. J. H.
1987. Longevity in fish: some ecological and evolutionary considerations. *In* Evolution of longevity in animals. (A. D. Woodhead and K. H. Thompson, eds.) p. 161–185. Plenum, New York, NY.
1992. Patterns of reproductive strategy parameters in some marine teleost fishes. J. Fish Biol. 41 (suppl. B):137–160.

Birkhead, T. R., and A. P. Møller.
1998. Sperm competition and sexual selection, 826 p. Academic Press, San Diego, CA.

Brule, T., C. Deniel, T. Colas-Marrufo, and M. Sanchez-Crespo.
1999. Red grouper reproduction in the southern Gulf of Mexico. Trans. Am. Fish. Soc. 128:385–402.

Charnov, E. L.
1982. The theory of sex allocation, 355 p. Princeton Univ. Press, Princeton, NJ.

Coleman, F. C., C. C. Koenig, and L. A. Collins.
1996. Reproductive styles of shallow-water groupers (Pisces: Serranidae) in the eastern Gulf of Mexico and the consequences of fishing spawning aggregations. Environ. Biol. Fishes 47:129–141.

Cowen, R. K.
1990. Sex change and life history patterns of the labrid, *Semicossyphus pulcher*, across an environmental gradient. Copeia 1990:787–795.

Cowen, R. K., K. M. M. Lwiza, S. Sponaugle, C. B. Paris, and D. B. Olson.
2000. Connectivity of marine populations: Open or closed? Science 287:857–859.

Fisher, R. A.
1930. The genetical theory of natural selection, 272 p. Clarendon Press, Oxford.

Fu, C., T. J. Quinn, II, and T. C. Shirley.
2001. The role of sex change, growth and mortality in *Pandalus* population dynamics and management. ICES J. Mar. Sci. 58:607–621.

Guenette, S., and T. J. Pitcher.
1999. An age-structured model showing the benefits of marine reserves in controlling overexploitation. Fish. Res. 39:295–303.

Gunderson, D. R.
1997. Trade-off between reproductive effort and adult survival in oviparous and viviparous fishes. Can. J. Fish. Aquat. Sci. 54:990–998.

Haddon, M.
2001. Modelling and quantitative methods in fisheries, 406 p. Chapman and Hall, Boca Raton, FL.

Huntsman, G. R., and W. E. Schaaf.
1994. Simulation of the impact of fishing on reproduction of a protogynous grouper, the graysby. No. Am. J. Fish. Manag. 14:41–52.

Janetos, A. C.
1980. Strategies of female mate choice: a theoretical analysis. Behav. Ecol. Sociobiol. 7:107–112.

Jennings, S., M. J. Kaiser, and J. D. Reynolds.
2001. Marine fisheries ecology, 417 p. Blackwell Science, Oxford.

Levin, P. F., and C. B. Grimes.
2002. Reef fish ecology and grouper conservation and management. *In* Coral reef fishes: dynamics and diversity in a complex ecosystem (P. F. Sale, ed.) p. 377–390. Academic Press, Amsterdam.

Mangel, M., and C. Tier.
1993. A simple direct method for finding persistence times of populations and application to conservation problems. Proc. Nat. Acad. Sci. USA 90:1083–1086.
1994. Four facts every conservation biologist should know about persistence. Ecology 75:607–614.

Parkes, G.
2000. Understanding SPR and its use in U.S. fishery management, 62 p. Center for marine conservation, Washington D.C.

Petersen, C. W., R. R. Warner, D. Y. Shapiro, and A. Marconato.
2001. Components of fertilization success in the bluehead wrasse, *Thalassoma bifasciatum*. Behav. Ecol. 12: 237–245.

Punt, A. E., P. A. Garratt, and A. Govender.
1993. On an approach for applying per-recruit measures to a protogynous hermaphrodite, with an illustration for the slinger *Chrysoblephus puniceus* (Pisces: Sparidae). S. Afr. J. Sci. 13:109–119.

Quinn, T. J., and R. B. Deriso.
1999. Quantitative fish dynamics, 542 p. Oxford Univ. Press, New York, NY,

Sadovy, Y.
2001. The threat of fishing to highly fecund fishes. J. Fish Biol. 59:90–108.

Sale, P. F.
2002. The science we need to develop more effective management. *In* Coral reef fishes: dynamics and diversity in a complex ecosystem (P. F. Sale, ed.) p. 361–376. Academic Press, Amsterdam.

Schultz, E. T., and R. R. Warner.
1991. Phenotypic plasticity in life-history traits of female *Thalassoma bifasciatum* (Pisces: Labridae): 2. Correlation of fecundity and growth rate in comparative studies. Environ. Biol. Fishes 30:333–344.

Shapiro, D. Y.
1987. Reproduction in groupers. *In* Tropical snappers and groupers: biology and fisheries management (J. J. Polvina and S. Ralston, eds.) p. 295–328. Westview Press, Boulder, CO.

Trivers, R. L.
1972. Parental investment and sexual selection. *In* Sexual selection and the descent of man (B. Campbell, ed.), p. 136–179. Aldine-Atherton, Chicago.

Warner, R. R.
1975. The reproductive biology of the protogynous hermaphrodite *Pimelometopon pulchrum* (Pisces: Labridae). Fish. Bull. 73:262–283.

Warner, R. R., D. Y. Shapiro, A. Marcanato, and C. W. Petersen.
1995. Sexual conflict: Males with highest mating success convey the lowest fertilization benefits to females. Proc. R. Soc. Lond. B. Biol. Sci. 262:135–139.

Abstract—We present a growth analysis model that combines large amounts of environmental data with limited amounts of biological data and apply it to *Corbicula japonica*. The model uses the maximum-likelihood method with the Akaike information criterion, which provides an objective criterion for model selection. An adequate distribution for describing a single cohort is selected from available probability density functions, which are expressed by location and scale parameters. Daily relative increase rates of the location parameter are expressed by a multivariate logistic function with environmental factors for each day and categorical variables indicating animal ages as independent variables. Daily relative increase rates of the scale parameter are expressed by an equation describing the relationship with the daily relative increase rate of the location parameter. *Corbicula japonica* grows to a modal shell length of 0.7 mm during the first year in Lake Abashiri. Compared with the attainable maximum size of about 30 mm, the growth of juveniles is extremely slow because their growth is less susceptible to environmental factors until the second winter. The extremely slow growth in Lake Abashiri could be a geographical genetic variation within *C. japonica*.

An environmentally based growth model that uses finite difference calculus with maximum likelihood method: its application to the brackish water bivalve *Corbicula japonica* in Lake Abashiri, Japan

Katsuhisa Baba
Hokkaido Hakodate Fisheries Experiment Station
1-2-66, Yunokawa, Hakodate
Hokkaido 042-0932, Japan
E-mail address: babak@fishexp.pref.hokkaido.jp

Toshifumi Kawajiri
Nishiabashiri Fisheries Cooperative Association
1-7-1, Oomagari, Abashiri
Hokkaido 093-0045, Japan

Yasuhiro Kuwahara
Hokkaido Abashiri Fisheries Experiment Station
31, Masuura, Abashiri
Hokkaido 099-3119, Japan.

Shigeru Nakao
Graduate School of Fisheries Sciences
Hokaido University
3-1-1, Minato, Hakodate
Hokkaido 041-8611, Japan

Manuscript approved for publication 14 August 2003 by Scientific Editor.
Manuscript received 20 October 2003 at NMFS Scientific Publications Office.
Fish. Bull. 102:14–24 (2004).

Extreme fluctuations, both short-term and seasonal, in food availability (e.g. phytoplankton density) make it difficult to determine relationships between the growth of filter-feeding bivalves and environmental factors (Bayne, 1993). However, it is becoming easier to acquire large amounts of environmental data through the use of data loggers, submersible fluorometers, or remote-sensing satellites, which enable environmental monitoring at daily or subdaily intervals. The development of these devices could solve difficulties in data collection. However, analytical methods that combine large amounts of environmental data with limited amounts of biological data (e.g. shell length) are not yet well developed. We present an environmentally based growth model that combines such unbalanced data sets. This model is useful in elucidating relationships between environmental factors and growth of filter feeders from field data.

Complex box models, such as ecophysiological models, can derive the relationships between environmental factors and the growth of filter-feeding bivalves (Campbell and Newell, 1998; Grant and Bacher, 1998; Scholten and Smaal, 1998). These models are useful for estimating impacts of cultivated species on an ecosystem or the carrying capacity of a species (or both) (Dame, 1993; Héral, 1993; Grant et al., 1993). They are suitable for animals that have been widely studied, such as *Mytilus edulis*, because they are derived by integrating a huge amount of ecophysiological knowledge acquired mainly from laboratory experiments. However, extrapolation of such knowledge to natural conditions is still controversial (Jørgensen, 1996; Bayne, 1998). Our model treats complicated eco-

physiological processes as a black box; we constructed the model directly from fluctuations in environmental factors and growth rates. Our approach is reasonable for animals for which ecophysiological knowledge is limited, especially when the main purpose of investigation is to derive the relationships between environment and growth.

We applied the model to a single cohort of *Corbicula japonica* juveniles spawned in August 1997. We did not consider any bias caused by adjacent cohorts because *C. japonica* failed to spawn in 1995, 1996, and 1998 in Lake Abashiri owing to low water temperatures during the spawning season (Baba et al., 1999). Such investigations provide important basic information, such as the shape of the distribution of a single cohort, and the relationship between growth rate and expansion rate of size variation in a single cohort.

Corbicula spp. are harvested commercially in Japan. The annual catch ranged from 19,000 to 27,000 metric tons in 1996 to 2000 (Ministry of Agriculture, Forestry and Fisheries[1]), of which *C. japonica* was the main species. *Corbicula japonica* is distributed in brackish lakes and tidal flats of rivers from the south of Japan to the south of Sakhalin (Kafanov, 1991), is a dominant macrozoobenthos in these lakes, and has important roles in bioturbation and energy flow (Nakamura et al., 1988; Yamamuro and Koike, 1993). Juvenile *C. japonica* growth is fast in southern habitats. Their spats collected in Lake Shinji, which lies in the southern part of its range, grow to a mean shell length of around 6.7 mm in natural conditions by the first winter (Yamane et al.[2]). In northern habitats, growth is also believed to be fast; Utoh (1981) reported that mean shell length at the first annual mark was around 5.7 mm in Lake Abashiri. In Utoh's study differences between the shell lengths at the first annual marks and the shell lengths of individuals aged to be one year were also reported. The purposes of the present study are to elucidate juvenile growth and its relationship to environmental factors in Lake Abashiri.

Materials and methods

Overview of the model

Our model expresses relative growth rate for *C. japonica* by a sigmoid function with environmental factors and animal ages as independent variables. Modeling processes in general follow five steps: 1) Shell lengths of a single cohort are summarized by an adequate probability density function, which is expressed by a location parameter and a scale parameter; 2) Daily relative increase rate of the location parameter (dRIRL) is approximated by a sigmoid function with environmental factors and animal ages as independent variables; 3) Daily relative increase rate of the scale parameter is approximated by a simple function with the dRIRL as an independent variable; 4) The model is optimized by a maximum likelihood method; and 5) The best model is selected by Akaike information criterion (AIC). The AIC is an information-theoretic criterion extended from Fisher's likelihood theory and is useful for simultaneous comparison of models (Akaike, 1973; Burnham and Anderson, 1998).

Study site and sampling method

To collect juveniles of *C. japonica* spawned in August 1997, sediments were sampled with a 0.05-m^2 Smith–McIntyre grab once or twice a month from September 1997 to July 1999 at a depth of 3.5–4.0 m in Lake Abashiri (Fig. 1). The habitat of *C. japonica* is restricted to areas shallower than 6-m depth because the deeper area, the lower stratum of the lake, is covered by anoxic polyhaline water. We assumed that the selectivity of the sampling gear on *C. japonica* juveniles was negligible because the gear grabs the juveniles with the sediment. Because the magnitude of spawning in 1997 was relatively small (Baba et al., 1999), we selected a sampling site where we found abundant settled juveniles in our preliminary investigations. Samples could not be obtained during winter because of ice cover. Sediments were washed with tap water on 2- mm and 0.125-mm mesh sieves from September 1997 to October 1998, and on 4.75-mm and 0.125-mm mesh sieves from April to July 1999. To separate the juveniles from the retained sediments, we treated the sediments with zinc chloride solution as described by Sellmer (1956). Then we sorted the juveniles under a binocular microscope. Identification of the cohort spawned in 1997 was quite easy because *C. japonica* failed to spawn in 1995, 1996, and 1998 owing to low water temperatures during the spawning season (Baba et al., 1999). We considered all the individuals that passed through the larger-mesh sieves and that were retained on the smaller-mesh sieve as the 1997 cohort. Shell lengths were measured under a profile projector (V-12, Nikon Ltd., Chiyoda, Tokyo) at 50× magnification with a digital caliper (Digimatic caliper, Mitsutoyo Ltd., Kawasaki, Kanagawa), which has a 0.02-mm precision.

Environmental factors

Values for water temperature (°C), water fluorescence (fluorescence equivalent to uranin density, μg/L), salinity (psu, practical salinity unit), and turbidity (equivalent to kaolin density, ppm) were obtained for 0.1-m intervals from unpublished data at the Abashiri Local Office of the Hokkaido Development Bureau.[3] The variables were measured by a submersible fluorometer (Memory Chlorotec, ACL-1180-OK, Alec Electronics Ltd., Kobe, Hyogo) at four sites in Lake Abashiri at intervals of about one week (Fig. 1). The average values of each variable between the depths of 1 m and 6 m were used for later analyses. Values between the measured dates were interpolated linearly

[1] Ministry of Agriculture, Forestry and Fisheries. 1996–2002. Statistics on fisheries and water culture production. Association of Agriculture and Forestry, 1-2-1 Kasumigaseki, Chiyoda, Tokyo 100-0013, Japan.

[2] Yamane, K., M. Nakamura, T. Kiyokawa, H. Fukui, and E. Shigemoto. 1999. Experiment on the artificial spat collection. Bull. Shimane Pref. Fish. Exp. Stn., p. 232–234. Unpubl. rep. Shimane Prefectural Fisheries Experimental Station, 25-1 Setogashima, Hamada, Shimane 697-0051, Japan. [In Japanese.]

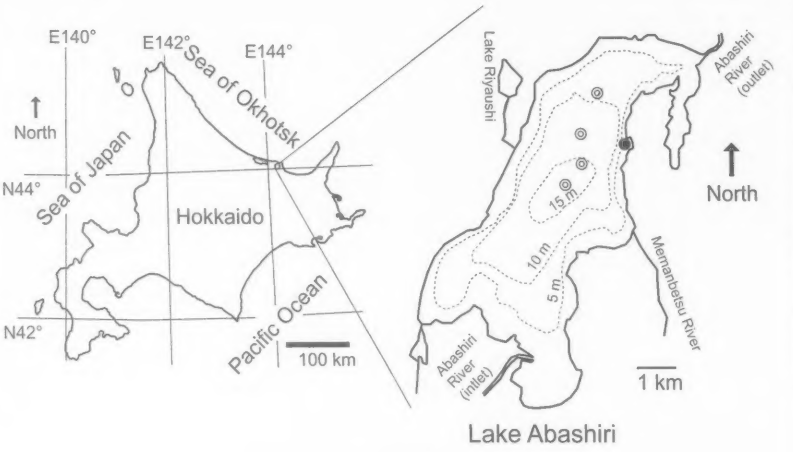

Figure 1

Location of sampling site for *Corbicula japonica* juveniles in Lake Abashiri, Japan (●). Environmental factors—water temperature, water fluorescence, salinity, and turbidity—were measured at four sites, designated by ◎.

for subsequent analysis with the environmentally based growth model. The water fluorescence reflects the density of phytoplankton.

Model structure

Modeling the distribution of a single sample Normal distribution is usually used to describe a single cohort in fishes and aquatic invertebrates (e.g. Pauly, 1987; Founier and Sibert, 1990; Yamakawa and Matsumiya, 1997). However, an adequate function to describe a single cohort of each animal should be selected to avoid biases caused by any inadequacies of the function. Probability density functions of many distributions are applicable for that purpose, and the appropriate can be selected among easily calculable functions to ensure convergence of the model. Characteristics of many distributions are well described by Evans et al. (1993). We used two distributions: normal distribution and largest extreme value distribution. The normal distribution is symmetric. The largest extreme value distribution is asymmetric with a longer tail toward the larger side. These are expressed by a location parameter and a scale parameter.

To use all the information inherent in data, parameters of the distribution functions are estimated from raw data (e.g. lengths), not from summarized data such as length frequency. This estimation method is described by Sakamoto et al. (1983). The most adequate distribution is selected by AIC. Log-likelihood functions of the distributions take the following forms:

Normal distribution

$$\log_e L_{normal}(a,b) = \sum_{i=1}^{n} \log_e \left\{ \frac{1}{\sqrt{2\pi b^2}} \exp\left[-(l_i - a)^2 / 2b^2\right] \right\}, \quad (1)$$

Largest extreme value distribution

$$\log_e L_{largest}(a,b) = \sum_{i=1}^{n} \log_e \left\{ (1/b) \exp\left[-(l_i - a)/b\right] \times \exp\left\{-\exp\left[-(l_i - a)/b\right]\right\} \right\}, \quad (2)$$

where n = number of data;
l_i = length of ith individual;
a = location parameter; and
b = scale parameter.

The location parameter is a mean in the normal distribution. The location parameter is a mode in the largest extreme distributions. The scale parameter is a standard deviation in the normal distribution.

The AIC is calculated by

$$\text{AIC} = -2 \log_e (\textit{maximum likelihood}) + 2m, \quad (3)$$

where m = number of parameters to be estimated.

The model with the minimum AIC is the best model. A difference of more than 1 or 2 is regarded as significant in terms of AIC (Sakamoto et al., 1983).

Modeling the change in the location Values of the location and scale parameters usually increase with the growth of an animal. The relative increase rate in a certain time step is defined as

[3] Abashiri Local Office of the Hokkaido Development Bureau, 2-6-1 Shinmachi, Abashiri, Hokkaido 093-0046, Japan.

$$r_i = (P_i - P_{i-1}) / P_{i=1}, \tag{4}$$

where r_i = relative increase rate of a parameter in the ith time step; and
P_i = parameter value after the ith time step.

Relationships between the parameter value and the relative increase rate of the parameter can be expressed by

$$\begin{aligned} P_1 &= P_0(1+r_1) \\ P_2 &= P_1(1+r_2) = P_0(1+r_1)(1+r_2) \\ P_3 &= P_2(1+r_3) = P_0(1+r_1)(1+r_2)(1+r_3) \\ &\vdots \\ P_n &= P_0\prod_{i=1}^{n}(1+r_i), \end{aligned} \tag{5}$$

where P_0 = parameter value at the first sampling;
P_i = parameter value after the ith time step; and
r_i = relative increase rate of the parameter in the ith time step.

We used one day as the time step in this study. In our environmentally based growth model, we assumed that the daily relative increase rate of location parameter (dRIRL) depends on the age of the animal and on environmental factors for each day. Sigmoid functions that take values between 0 and a certain maximum are empirically appropriate for expressing the relationships between the dRIRL and independent variables, especially for measures such as shell length that do not show negative growth. Therefore, using categorical variables indicating animal ages and environmental factors for each day as independent variables, we express the dRIRL by the multivariate logistic function

$$s_i = s_{\max} / \left\{1+\exp\left[-\left(\sum_{j=1}^{n_A}\alpha_j A_j + \sum_{k=1}^{n_E}\beta_k E_{ki}\right)\right]\right\}, \tag{6}$$

where s_i = dRIRL on the ith day from the first sampling;
$s_{\max}$ = potential maximum dRIRL of the animal;
α_j, β_k = coefficients of each independent variable;
A_j = categorical variable (a dummy variable indicating animal ages) that takes the value 1 or 0;
E_{ki} = the kth environmental factor on the ith day from the first sampling;
n_A = number of age categories; and
n_E = number of environmental factors.

The categorical variable takes the value of 1 when the animal is the category, otherwise it takes 0. The multivariate logistic function with $s_{\max} = 1$ is used for logistic regressions (Sokal and Rohlf, 1995). A method of giving a value to the categorical variable is described by Zar (1999).

Modeling the change in scale The daily relative increase rate of scale parameter (dRIRS) and dRIRL must be correlated because the dRIRS is larger when the dRIRL is larger. Therefore, we estimated the dRIRS from an equation expressing the relationship to the dRIRL. We tested two functions,

$$t_i = \begin{cases} \gamma_1 + \gamma_2 s_i & (\gamma_1 + \gamma_2 s_i > 0) \\ 0 & (\gamma_1 + \gamma_2 s_i \le 0) \end{cases} \tag{7}$$

and

$$t_i = \begin{cases} (s_i - \gamma_1)^{\gamma_2} & (s_i - \gamma_1 > 0) \\ 0 & (s_i - \gamma_1 \le 0) \end{cases}, \tag{8}$$

where t_i = dRIRS on the ith day from the first sampling;
γ_1, γ_2 = coefficients of the equations; and
s_i = dRIRL on the ith day from the first sampling.

Model estimation

Likelihood function The location and scale parameters at the first sampling (a_0 and b_0), the coefficients of Equation 6 ($s_{\max}$, α_j and β_k), and the coefficients of Equations 7 and 8 (γ_1 and γ_2) are estimated as values that maximize total log-likelihood. The total log-likelihood is evaluated by the adequate probability density function selected in the first step. The log-likelihood functions take the following forms:

Normal distribution

$$\begin{aligned} &\log_e L_{normal}(a_0, b_0, s_{\max}, \alpha_j, \beta_k, \gamma_1, \gamma_2) \\ &= \sum_{q=1}^{N}\sum_{i=1}^{n_q}\log_e\left\{\frac{1}{\sqrt{2\pi\hat{b}_q^2}}\exp\left[-(l_{qi}-\hat{a}_q)/2\hat{b}_q^2\right]\right\}; \end{aligned} \tag{9}$$

Largest extreme value distribution

$$\begin{aligned} &\log_e L_{largest}(a_0, b_0, s_{\max}, \alpha_j, \beta_k, \gamma_1, \gamma_2) \\ &= \sum_{q=1}^{N}\sum_{i=1}^{n_q}\log_e\left\{(1/\hat{b}_q)\exp\left[-(l_{qi}-\hat{a}_q)/\hat{b}_q\right]\right. \\ &\left.\times\exp\left\{-\exp\left[-(l_{qi}-\hat{a}_q)/\hat{b}_q\right]\right\}\right\}, \end{aligned} \tag{10}$$

where a_0, b_0 = values of the location and scale parameters, respectively, at the first sampling;
$s_{\max}, \alpha_j, \beta_k$ = coefficients of Equation 6;
γ_1, γ_2 = coefficients of Equations 7 and 8;
N = number of samplings;
n_q = number of data at the qth sampling;
$\hat{a}_q$ = location parameter at the qth sampling estimated by Equation 5 (r_i=s_i);
$\hat{b}_q$ = scale parameter at the qth sampling estimated by Equation 5 (r_i=t_i); and
l_{qi} = length of the ith individual at the qth sampling.

AIC is used to select significant environmental factors, the age categorization, and the equation to express the

relationship between dRIRL and dRIRS, i.e. Equation 7 or 8.

Confidence intervals To evaluate uncertainties of coefficient values and model selection, we estimated the 95% confidence intervals of all coefficients—i.e. a_0, b_0, s_{max}, α_j, β_k, γ_1, and γ_2—based on profile likelihood. For example, the 95% confidence interval of a_0—$a_{0,95}$—was estimated as an interval that suffices in the following equation:

$$2\Big\{\max\log_e L(\hat{a}_0,\hat{b}_0,\hat{s}_{\max},\hat{\alpha}_j,\hat{\beta}_k,\hat{\gamma}_1,\hat{\gamma}_2) - \max\log_e L(\hat{a}_0,\hat{b}_0,\hat{s}_{\max},\hat{\alpha}_j,\hat{\beta}_k,\hat{\gamma}_1,\hat{\gamma}_2 \mid a_0=\alpha_{0.96})\Big\} \le \chi_1^2(0.05), \quad (11)$$

where $x_1^2(0.05)$ = value of a chi-squared distribution at an upper probability of 0.05 with one degree of freedom, i.e. 3.84.

The characteristics of the interval are explained by Burnham and Anderson (1998).

We used Microsoft Excel (Microsoft Corp., Redmond, WA) as the analysis platform, and Solver (Microsoft Corp., Redmond, WA) as the nonlinear optimization tool.

Model selection

We used three procedures for model selection to achieve the best model. First, we constructed an *a priori* set of base models based on biological variables; then we selected the best base model. Fixation of the base model drastically decreases possible candidate models to be tested. To test all possible combinations of independent variables and model forms is quite impractical. Second, we excluded insignificant factors from the best base model. Third, we checked the significance of environmental factors that were not included in the base models. If one was significant, we included it in the best base model. All of these procedures were performed by AIC. The construction of the *a priori* set of candidate models is partially subjective, but it is an important part of the model construction (Burnham and Anderson, 1998).

Seasonal growth in bivalves is influenced by water temperature and food supply (Bayne and Newell, 1983). The growth rate of *Corbicula fluminea* changes with age (McMahon, 1983). Therefore, we constructed base models combining water temperature, water fluorescence, and categorical variables indicating age for the independent variables of Equation 6. We tested two types of categorization of age. The first segregates ages based on real age, i.e. two categories: 0+ or 1+. The second segregates ages in relation to winter, i.e. three categories: before the first winter, from the first to the second winter, and after the second winter. For the real-age categorization, age was segregated based on 1 September, because the spawning season was in August 1997. For the winter-base age categorization, we segregated ages based on 1 January. No biases should have occurred because of the segregation date of the winter base categorization and because the growth of *C. japonica* is negligible during winter. Four base models were constructed combining the two types of age categorization and two types of equations expressing the relationship between the dRIRL and the dRIRS, i.e. Equations 7 or 8. We selected the best base model by AIC.

To check the significance of each environmental factor and age categorization, we removed the independent variables one by one from the best base model and re-optimized the model. When the model was significantly improved by the removal in terms of AIC, the effect of the variable was insignificant on the model; therefore we excluded it.

To check the significance of salinity and turbidity, which were not included in the base models, we included them one at a time into the best base model and re-optimized the model. When the model was improved by the inclusion, the effect of the variable was significant on the model; therefore we included it.

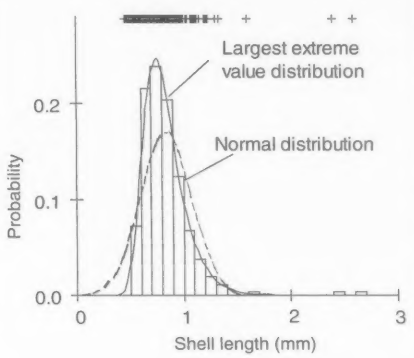

Figure 2

Two distributions fitted by the maximum-likelihood method to the shell lengths of *Corbicula japonica* juveniles spawned in 1997 and sampled on 22 April 1999. Raw data are shown by +. The shell length composition is shown by the histogram.

Results

Modeling the distribution of a single sample

The largest extreme value distribution was the best in terms of AIC except for data sampled on 13 May 1998 (results are not shown). The exception is due probably to the small sample size (n=38) on that date. The largest extreme value distribution was therefore used to evaluate likelihood in later analyses: we selected Equation 10 from Equations 9 and 10. The result of fitting the two distributions to the shell lengths sampled on 22 April 1999 is shown in Figure 2 as a representative example. The largest extreme value distribution is apparently better than the normal distribution for describing the single cohort of *C. japonica* spawned in 1997.

Table 1

Values of location and scale parameters at the first sampling, coefficients, log-likelihood, and AIC of models constructed based on the largest extreme value distribution. The best AIC among four base models (models 1–4) is enclosed by a single line. The best AIC of all models is enclosed by a double line. dRIRL = daily relative increase rate of location parameter, dRIRS = daily relative increase rate of scale parameter, Temp. = water temperature, WF = water fluorescence, Sal. = salinity, Turb. = turbidity, C1 = before the first winter, C2 = from the first to the second winter, C3 = after the second winter.

Model no.	Parameters at 1st sampling		Max. dRIRL	Age categorization			Environmental factors				Expressing relationship between dRIRS and dRIRL			Log-L	AIC
	a_0	b_0	s_{max}	A_1 α_1	A_2 α_2	A_3 α_3	Temp. β_1	WF β_2	Sal. β_3	Turb. β_4	γ_1	γ_2	Eq. no		
				0+	1+										
1	0.299	0.040	0.012	−62.6	−23.7		0.16	2.61			0.0000	1.686	7	850.4	−1682.9
2	0.297	0.040	0.011	−56.1	−22.1		0.20	2.44			0.0001	0.887	8	852.3	−1686.5
				C1	C2	C3									
3	0.299	0.042	0.011	−16.8	−16.7	−9.1	0.61	0.41			−0.0076	2.902	7	950.4	−1880.9
4	0.299	0.042	0.011	−17.5	−17.6	−9.6	0.65	0.42			0.0034	0.760	8	952.2	−1884.4
4.1	0.299	0.042	0.011	−18.3[1]		−10.0	0.68	0.44			0.0034	0.760	8	952.2	−1886.3
4.2	0.297	0.038	0.005	127.9	−26.8[1]		0.34	4.15			0.0000	0.895	8	735.0	−1451.9
4.3	0.295	0.037	0.008	−47.3	−16.3	−8.8		1.47			0.0033	0.766	8	848.9	−1679.9
4.4	0.299	0.041	0.013	-4.9	-8.9	-4.9	0.40				0.0020	0.806	8	909.6	-1801.1
4.5	0.299	0.042	0.011	−16.7[1]		−9.1	0.62	0.42	−0.25		0.0033	0.762	8	952.4	−1884.8
4.6	0.299	0.042	0.011	−18.5[1]		−10.2	0.68	0.44		0.007	0.0034	0.760	8	952.2	−1884.4

[1] One common coefficient was used for the two categorical variables.

Model selection and application

Model 4 was the best in terms of AIC among four base models (Table 1, models 1–4); ages were categorized in relation to winter; and the relationship between dRIRL and dRIRS was expressed by Equation 8.

Four models were made by removing each independent variable from model 4 (Table 1, models 4.1 to 4.4). The effect of one age categorization—segregation of ages between the first and second winters—was insignificant on the model, because the model was significantly improved by its removal in terms of AIC. The effects of the other independent variables were significant on the model, because the model was significantly worse by their removal in terms of AIC. The effects of salinity and turbidity were insignificant on the model, because adding each variable made the model significantly worse in terms of AIC (Table 1, models 4.5 and 4.6). Consequently, model 4.1 was the best model to describe the relationships among environmental factors, ages, and growth of *C. japonica* juveniles spawned in 1997.

The coefficient value for age categorization of before the second winter (−18.3) is much smaller than that of after the second winter (−10.0) (Table 1). This difference suggests that the growth response of *C. japonica* juveniles is much less susceptible to environmental factors before the second winter than after.

Peaks of the dRIRL corresponded with peaks of water fluorescence, when the water temperature was warmer than about 10°C, especially before the second winter (Fig. 3, B and C). Therefore, food supply is the most influential factor when the water temperature is above about 10°C. The slow growth or no growth during winter is due to the low water temperatures. The dRIRL reached a plateau after 30 May 1999. This was due to two factors: water fluorescence was relatively intense after 30 May 1999 (Fig. 3B); and the growth response of *C. japonica* to the environmental factors was more susceptible after the second winter than before.

The confidence limits of all the coefficients seem to be reasonably estimated by the profile likelihood method (Table 2). These results also guarantee the convergence of the model because the model was frequently optimized to seek each confidence limit with different starting values. We repeated the optimization at least 20 times to seek each confidence limit. On other models, we also confirmed the convergences as well.

The largest extreme value distributions estimated by model 4.1 fitted the shell lengths of *C. japonica* juveniles very well (Fig. 4).

Discussion

Model formulation and application

Largest extreme value distribution is apparently better than normal distribution to describe the single cohort of *C. japonica* that spawned in 1997. This distribution has a mode and a longer tail toward the larger side. If the shell

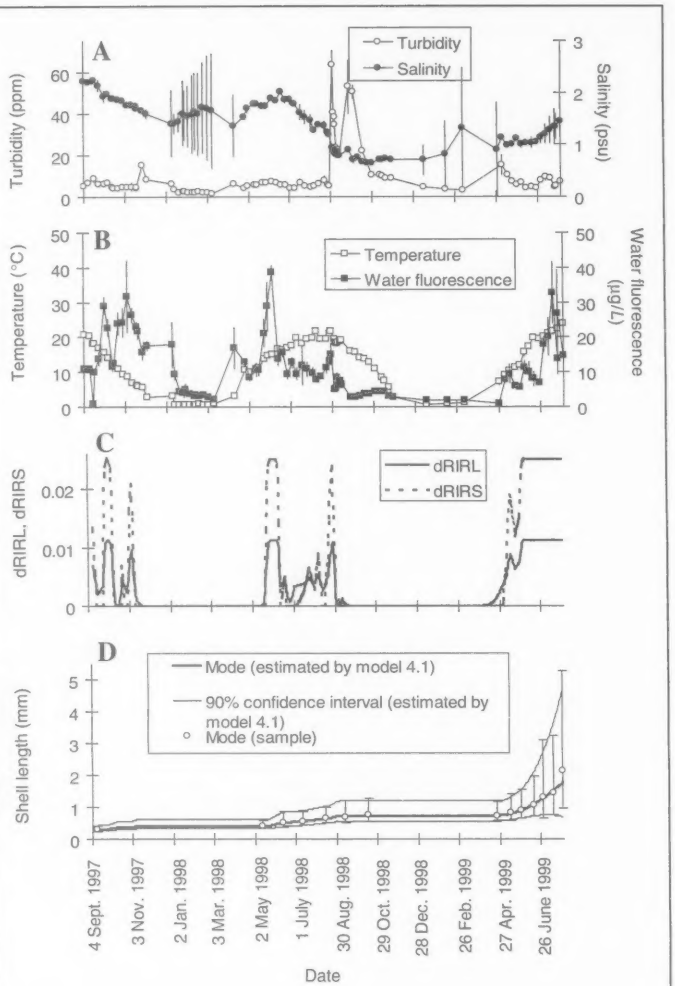

Figure 3

Environmental fluctuations and prediction of the growth of *Corbicula japonica* juveniles spawned in 1997 in Lake Abashiri by the best model (Model 4.1 in Table1). (**A**) Insignificant environmental factors (factors excluded in the model selection), turbidity (equivalent to kaolin density, ppm) and salinity (psu, practical salinity unit). (**B**) Significant environmental factors (factors included in the model selection), temperature (°C) and water fluorescence (equivalent to uranin density, µg/L). (**C**) Daily relative increase rate of location parameter (dRIRL) and daily relative increase rate of scale parameter (dRIRS) estimated by the model. (**D**) Growth of *Corbicula japonica*; vertical bars represent 90% confidence intervals for the shell lengths of the samples.

length distribution becomes asymmetric during growth, skewness of the distribution would increase according to growth. However, there is no correlation between the skewness and the means of the shell lengths. Therefore, we thought that the shell length distribution of the cohort was already asymmetric just after settlement. Such a distribution might be influenced by fluctuations in larval settlement during the spawning season; and larval settlement would be influenced by fluctuations in larval supply from the water column. During the spawning season of 1997, the average planktonic larval density gradually increased from 26 ind/m^3 on 25 July to a maximum of 603 ind/m^3 on

Table 2

95% confidence limits of location and scale parameters at the first sampling and coefficients of the best model constructed based on the largest extreme value distribution (models 4.1 in Table 1) estimated by profile likelihood method. dRIRL = daily relative increase rate of location parameter, dRIRS = daily relative increase rate of scale parameter, Temp. = water temperature, WF = water fluorescence, Sal. = salinity, Turb. = turbidity.

	Parameters at 1st sampling		Max. dRIRL	Age categorization			Environmental factors				Expressing relationship between dRIRS and dRIRL	
				A_1	A_2	A_3	Temp.	WF	Sal.	Turb.		
	a_0	b_0	s_{max}	α_1	α_2	α_3	β_1	β_2	β_3	β_4	γ_1	γ_2
Lower 95 %	0.294	0.039	0.010	–26.6[1]		–14.6	0.41	0.27			0.0027	0.734
Upper 95 %	0.304	0.045	0.013	–11.5[1]		–6.4	1.00	0.64			0.0039	0.793

[1] One common coefficient for the two categorical variables.

13 August. Then it sharply decreased to 3 ind/m^3 on 19 August (Baba et al., 1999). Such a pattern of larval-density fluctuation might have caused the asymmetric distribution of shell lengths of the settled juveniles. Another possible factor that influenced the shapes of the shell length distributions and the relationship between dRIRL and dRIRS is size-dependent mortality, e.g. predations and fisheries. Size-dependent mortality has been reported in several marine bivalves (e.g. Nakaoka, 1996). Potential predators of *C. japonica* are fishes, such as Japanese dace (*Tribolodon hakonensis*) (also known as big-scaled Pacific redfin, FAO), Pacific redfin (*Tribolodon brandtii*), common carp (*Cyprinus carpio*), and the So-iny mullet (*Liza haematocheila*) (Kawasaki[4]). In our study, the size-dependent mortality was negligible because the range of the shell lengths observed in this study was very narrow.

The shape of the distribution to describe a single cohort should be determined from the data. In contrast, single cohorts are usually separated from multicohort data by assuming a normal distribution of lengths in a single cohort (e.g. Fournier and Sibert, 1990). Therefore, it is possible that multicohort analysis done without selection of an adequate distribution to describe a single cohort causes substantial bias in estimations of various stock features of animal populations, such as age composition, growth, mortality, and recruitment. In our preliminary analyses, we also tested smallest extreme value distribution, inverse Gaussian distribution, and lognormal distribution. The inverse Gaussian distribution was the best for two samples; the lognormal distribution, was the best for two samples; the largest extreme value distribution was the best for ten samples. Therefore, it is reasonable to select the largest extreme value distribution. We selected a single distribution for our analyses, otherwise a discontinuous point would have appeared in the growth curve.

Relatively large confidence intervals were obtained in the coefficients of the linear component of Equation 6, i.e. α_j, and β_k (Table 2). The relatively large confidence intervals may indicate that the number of estimated coefficients is somewhat larger than the number of samplings. Therefore, to estimate these coefficients more precisely, we may need to investigate more cohorts spawned in other years in future investigations.

Growth of *C. japonica*

We identified extremely slow growth in *C. japonica* juveniles, which grew to a modal shell length of 0.7 mm during the first year in Lake Abashiri, which lies at 43.7°N. Spats of *C. japonica* collected from 1992 to 1997 in Lake Shinji, which lies at 35.5°N, grew to a mean shell length of 6.7 mm in natural conditions by the first winter (Yamane et al.[2]). Using environmental factors measured in Lake Shinji from 1990 to 1998 at monthly intervals (Seike[5]), we simulated the growth of *C. japonica* with model 4.1. *Corbicula japonica* grew to a mean shell length of 1.4 mm (standard error, 0.37) by the first winter in the simulations. Therefore, the large difference in juvenile growth between the two habitats cannot be explained by environmental differences because the results of the simulation were apparently an underestimate. We think that the extremely slow growth of the juveniles (prolonged phase of meiobenthic development) in Lake Abashiri is probably a geographical variation, which is genetically determined, within *C. japonica*. However, there remains a possibility that the juvenile growth differences depend on other environmental factors not measured in this study. Therefore, the geographical

[4] Kawasaki, K. 1997. Lagoon structure and fish production in Ogawara-ko Lagoon. *In* Final reports on fisheries in Ogawara-ko Lagoon (Tohoku Construction Corporation ed.), p. 4–33. Unpubl. rep. Construction Office for Takasegawa General Development of Tohoku Regional Construction Bureau, 3 Ishido, Hachinohe, Aomori 039-1165, Japan.

[5] Seike, Y. 1990–98. Gobiusu: monthly report of water quality in Lake Shinji and Lake Nakaumi. Unpubl. rep. Faculty of Science and Engineering, Shimane University, 1060 Nishikawatsu, Matsue, Shimane 690-0823, Japan.

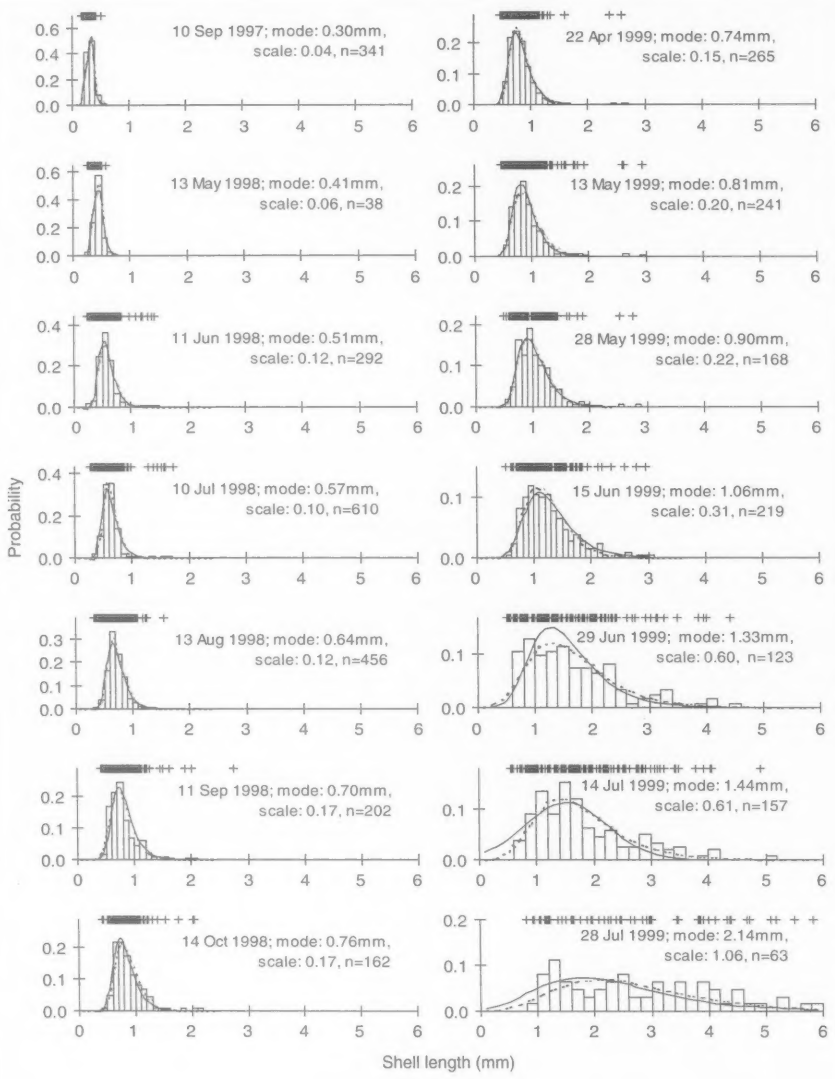
10 Sep 1997; mode: 0.30mm, scale: 0.04, n=341
22 Apr 1999; mode: 0.74mm, scale: 0.15, n=265
13 May 1998; mode: 0.41mm, scale: 0.06, n=38
13 May 1999; mode: 0.81mm, scale: 0.20, n=241
11 Jun 1998; mode: 0.51mm, scale: 0.12, n=292
28 May 1999; mode: 0.90mm, scale: 0.22, n=168
10 Jul 1998; mode: 0.57mm, scale: 0.10, n=610
15 Jun 1999; mode: 1.06mm, scale: 0.31, n=219
13 Aug 1998; mode: 0.64mm, scale: 0.12, n=456
29 Jun 1999; mode: 1.33mm, scale: 0.60, n=123
11 Sep 1998; mode: 0.70mm, scale: 0.17, n=202
14 Jul 1999; mode: 1.44mm, scale: 0.61, n=157
14 Oct 1998; mode: 0.76mm, scale: 0.17, n=162
28 Jul 1999; mode: 2.14mm, scale: 1.06, n=63
Probability
Shell length (mm)

Figure 4

Shell-length compositions of a single cohort of *Corbicula japonica* spawned in 1997. The raw data (shell lengths) are shown by +. The largest extreme value distribution estimated by the best model (model 4.1 in Table 1) is shown by a solid line. The largest extreme value distribution independently fitted by the maximum likelihood method is shown by a dashed line. The sampling date and values of location parameter (mode) and scale parameter independently fitted by the maximum likelihood method are shown in each panel.

variation should be validated by reciprocal transplantations or laboratory experiments (or both) in future investigations. Prolonged phases of meiobenthic development have been reported in some marine bivalves (Nakaoka, 1992; Harvey and Gage, 1995). However, a prolonged phase of meiobenthic development as a geographical variation is rarely reported.

In many species of bivalve, populations from higher latitudes have a slower initial growth rate; but longevity and ultimate size in these populations are frequently greater than at lower latitudes (Newell, 1964; Seed, 1980). The extremely slow growth of *C. japonica* juveniles in Lake Abashiri may be an extreme example of this phenomenon. In Lake Abashiri, *C. japonica* failed to spawn in ten out of 21 years for which

data were available because of low water temperatures during the summer spawning season (Baba et al., 1999). This means that a long life span is essential to sustain populations of *C. japonica* in northern habitats. We think that a long life span is the ultimate factor for the extremely slow growth rate of *C. japonica* juveniles in Lake Abashiri.

The growth response of *C. japonica* juveniles is much less susceptible to environmental factors before the second winter than after and is the proximate factor for an extremely slow growth rate. *Nuculoma tenuis*, a detritus feeder, develops its palp proboscides, its feeding apparatus, during the prolonged phase of meiobenthic development (Harvey and Gage, 1995). The change of growth susceptibility to environmental factors in young ages may suggest that some functional morphological changes occur in *C. japonica*, also a filter feeder. In our preliminary analyses, we could not find a better model when we used different values of s_{max} in Equation 6 between ages instead of categorical variables indicating ages. Therefore, we conclude that the difference in growth rates between ages is not due to a difference in potential maximum growth rate, at least in the range of the shell length observed in our study. When our model is applied to a wider range of the shell lengths or other species, it is best to examine the age dependence of s_{max}.

Acknowledgments

We express our thanks to T. Kato, Vice-Head of the River Improvement Section in the Abashiri Local Office of the Hokkaido Development Bureau, for providing environmental data on Lake Abashiri. We also thank the reviewers of Fishery Bulletin for providing helpful suggestions on our manuscript.

Literature cited

Akaike, H.
1973. Information theory and an extension of the maximum likelihood principle. *In* Second international symposium on information theory (B. N. Petrov and F. Csaki, eds.), p. 267–281. Akademiai Kiado, Budapest.

Baba, K., T. Kawajiri, and Y. Kuwahara.
1999. Effects of water temperature and salinity on spawning of the brackish water bivalve *Corbicula japonica* in Lake Abashiri, Hokkaido, Japan. Mar. Ecol. Prog. Ser. 180: 213–221.

Bayne, B. L.
1993. Feeding physiology of bivalves: time dependence and compensation for changes in food availability. *In* Bivalve filter feeders and marine ecosystem processes (R. F. Dame ed.), p. 1–24. Springer Verlag, New York, NY.
1998. The physiology of suspension feeding by bivalve molluscs: an introduction to the Plymouth "TROPHEE" workshop. J. Exp. Mar. Biol. Ecol. 219:1–19.

Bayne, B. L., and R. C. Newell.
1983. Physiological energetics of marine molluscs. *In* The Mollusca, 4(1) (A. S. M. Saleuddin and K. M. Wilbur eds.), p. 407–515. Academic Press, New York, NY.

Burnham, K. P., and D. R. Anderson.
1998. Model selection and inference, 349 p. Springer, New York, NY.

Campbell, D. E., and C. R. Newell.
1998. MUSMOD, a production model for bottom culture of the blue mussel, *Mytilus edulis* L. J. Exp. Mar. Biol. Ecol. 219:171–203.

Dame, R. F.
1993. The role of bivalve filter feeder material fluxes in estuarine ecosystems. *In* Bivalve filter feeders in estuarine and coastal ecosystem processes: NATO ASI Series (R. F. Dame ed.), p. 245–269. Springer-Verlag, Berlin, Heidelberg.

Evans, M., N. Hastings, and B. Peacock.
1993. Statistical distribution, 170 p. John Wiley & Sons, New York, NY.

Fournier, D. A., and J. R. Sibert.
1990. MULTIFAN a likelihood-based method for estimating growth parameters and age composition from multiple length frequency data sets illustrated using data for southern bluefin tuna (*Thunnus maccoyii*). Can. J. Fish. Aquat. Sci. 47:301–317.

Grant, J., and C. Bacher.
1998. Comparative models of mussel bioenergetics and their validation at field culture sites. J. Exp. Mar. Biol. Ecol. 219:21–44.

Grant, J., M. Dowd, K. Thompson, C. Emerson, and A. Hatcher.
1993. Perspectives on field studies and related biological models of bivalve growth and carrying capacity. *In* Bivalve filter feeders in estuarine and coastal ecosystem processes: NATO ASI Series (R. F. Dame ed.), p. 371–420. Springer-Verlag, Berlin, Heidelberg.

Harvey, R., and J. D. Gage.
1995. Reproduction and recruitment of *Nuculoma Tenuis* (Bivalvia: Nuculoida) from Loch Etive, Scotland. J. Moll. Stud. 61:409–419.

Héral, M.
1993. Why carrying capacity models are useful tools for management of bivalve molluscs culture. *In* Bivalve filter feeders in estuarine and coastal ecosystem processes: NATO ASI Series (R. F. Dame ed.), p. 455–477. Springer-Verlag, Berlin, Heidelberg.

Jørgensen, C. B.
1996. Bivalve filter feeding revisited. Mar. Ecol. Prog. Ser. 142:287–302.

Kafanov, A. I.
1991. Bivalves on continental shelf and continental slope of Northern Pacific, p. 81–82. Science Acad. USSR, Vladivostok.

MacMahon, R. F.
1983. Ecology of an invasive pest bivalve, *Corbicula*. *In* The Mollusca, 6(12) (W. D. Russell-Hunter, ed.), p. 505–561. Academic Press, Orlando, FL.

Nakamura, M., M. Yamamuro, M. Ishikawa, and H. Nishimura.
1988. Role of the bivalve *Corbicula japonica* in the nitrogen cycle in a mesohaline lagoon. Mar. Biol. 99: 369–374.

Nakaoka, M.
1992. Age determination and growth analysis based on external shell rings of the protobranch bivalve *Yoldia notabilis* Yokoyama in Otsuchi Bay, Northeastern Japan. Benthos Res. 43:53–66.
1996. Size-dependent survivorship of the bivalve *Yoldia notabilis* (Yokoyama, 1920): the effect of crab predation. J. Shellfish Res. 15:355–362.

Newell, G. E.
1964. Physiological aspects of the ecology of intertidal molluscs. *In* Physiology of Mollusca (K. M. Wilbur and C. M. Yonge eds.), p. 59–81. Academic Press, London.

Pauly, D.
1987. A review of the ELEFAN system for analysis of length

frequency data in fish and aquatic invertebrates. *In* Length-based methods in fisheries research (D. Pauly and G. R. Morgan eds.), p. 7–34. ICLARM conference proceedings 13, 688 International Center for Living Aquatic Resource Management, Manila, Philippines and Kuwait Institute for Scientific Research, Safet, Kuwait.

Sakamoto, Y., M. Ishiguro, and G. Kitagawa.
1983. Statistics based on information amount (Jouhouryou Toukei Gaku), 236 p. Kyoritu Shuppan, Tokyo. [In Japanese.]

Scholten, H., and A. C. Smaal.
1998. Responses of *Mytilus edulis* L. to varying food concentrations: testing EMMY, an ecophysiological model. J. Exp. Mar. Biol. Ecol. 219:217–39.

Seed, R.
1980. Shell growth and form in the Bivalvia. *In* Skeletal growth of aquatic organisms (D. G. Rhoads ed.), p. 23–67. Plenum Press, New York, NY.

Sellmer, G. P.
1956. A method for the separation of small bivalve molluscs from sediments. Ecology 37:206.

Sokal, R. R. and F. J. Rohlf.
1995. Biometry, 3rd ed., 887 p. W. H. Freeman and Company, New York, NY.

Utoh, H.
1981. Growth of the brackish water bivalve, *Corbicula japonica* Prime, in Lake Abashiri. Sci. Rep. Hokkaido Fish. Exp. Stn. 23:65–81. [In Japanese.]

Yamakawa, T,. and Y. Matsumiya.
1997. Simultaneous analysis of multiple length frequency data sets when the growth rates fluctuate between years. Fish. Sci. 63:708–714.

Yamamuro, M., and I. Koike.
1993. Nitrogen metabolism of the filter-feeding bivalve *Corbicula japonica* and its significance in primary production of a brackish lake in Japan. Limnol. Oceanogr. 38: 997–1007.

Zar, J. H.
1999. Biostatistical analysis, 663 p. Prentice Hall, Upper Saddle River, NJ.

Juvenile salmonid distribution, growth, condition, origin, and environmental and species associations in the Northern California Current*

Rick D. Brodeur
Northwest Fisheries Science Center
National Marine Fisheries Service, NOAA
2030 S. Marine Science Drive
Newport, Oregon 97365
E-mail address: Rick.Brodeur@noaa.gov

Joseph P. Fisher
College of Ocean and Atmospheric Sciences
Oregon State University
Corvallis, Oregon 97331

David J. Teel
Northwest Fisheries Science Center
National Marine Fisheries Service, NOAA
Seattle, Washington 98112

Robert L. Emmett
Northwest Fisheries Science Center
National Marine Fisheries Service, NOAA
2030 S. Marine Science Drive
Newport, Oregon 97365

Edmundo Casillas
Northwest Fisheries Science Center
National Marine Fisheries Service, NOAA
Seattle, Washington 98112

Todd W. Miller
Cooperative Institute for Marine Resources Studies
Oregon State University
Newport, Oregon 97365

Abstract—Information is summarized on juvenile salmonid distribution, size, condition, growth, stock origin, and species and environmental associations from June and August 2000 GLOBEC cruises with particular emphasis on differences related to the regions north and south of Cape Blanco off Southern Oregon. Juvenile salmon were more abundant during the August cruise as compared to the June cruise and were mainly distributed northward from Cape Blanco. There were distinct differences in distribution patterns between salmon species: chinook salmon were found close inshore in cooler water all along the coast and coho salmon were rarely found south of Cape Blanco. Distance offshore and temperature were the dominant explanatory variables related to coho and chinook salmon distribution. The nekton assemblages differed significantly between cruises. The June cruise was dominated by juvenile rockfishes, rex sole, and sablefish, which were almost completely absent in August. The forage fish community during June comprised Pacific herring and whitebait smelt north of Cape Blanco and surf smelt south of Cape Blanco. The fish community in August was dominated by Pacific sardines and highly migratory pelagic species. Estimated growth rates of juvenile coho salmon were higher in the GLOBEC study area than in areas farther north. An unusually high percentage of coho salmon in the study area were precocious males. Significant differences in growth and condition of juvenile coho salmon indicated different oceanographic environments north and south of Cape Blanco. The condition index was higher in juvenile coho salmon to the north but no significant differences were found for yearling chinook salmon. Genetic mixed stock analysis indicated that during June, most of the chinook salmon in our sample originated from rivers along the central coast of Oregon. In August, chinook salmon sampled south of Cape Blanco were largely from southern Oregon and northern California; whereas most chinook salmon north of Cape Blanco were from the Central Valley in California.

Manuscript approved for publication 30 June 2003 by Scientific Editor.
Manuscript received 20 October 2003 at NMFS Scientific Publications Office.
Fish. Bull 102:25–46 (2004).

The need to understand the direct and indirect linkages between oceanographic conditions and salmon survival in the marine environment has increased with the listing of many West Coast salmon stocks as threatened or endangered. Recent studies have shown that long-term changes in climate affect oceanic structure and produce abrupt differences in salmon marine survival and returns (Francis and Hare, 1994; Mantua et al., 1997). A major regime shift in the subarctic and California Current ecosystems during the late 1970s may have been a factor in reducing ocean survival of salmon in the Pacific Northwest and in increasing marine survival in Alaska (Hare et al., 1999). Fluctuations in mortality of salmon in the freshwater and marine environments have been shown to be almost equally significant sources of annual salmonid recruitment variability (Bradford, 1995). Unlike in the freshwater environment, the physical and biological mechanisms and factors in the marine environment that cause mortality of salmon are largely unknown. Predation, inter- and intraspecific competition, food availability, smolt quality and health, and physical ocean conditions likely influence survival of salmon in the marine environment. Thus, increasing our understanding of nearshore ocean environments, their linkages to oceanographic conditions, and the role they play in salmonid survival, could provide management options for increasing adult returns. Characterization of the space-time variability of the environmental conditions that smolts encounter when they enter the nearshore ocean, and the eventual survival of these smolts will allow us to identify which biotic and abiotic ocean conditions are correlated with various ocean survival levels.

Many anadromous salmonid populations along the west coast of the United States have declined over the last few decades (Nehlsen et al., 1991), and most stocks show a regional north-south pattern in degree of extinction risk (Kope and Wainwright, 1998). This pattern suggests that both marine habitat conditions and mesoscale climate patterns affect salmonid population status (e.g. Lawson, 1993). A dramatic example is the population trend of coho salmon (*Oncorhynchus kisutch*) along the Oregon coast. Populations along the coast north of Cape Blanco (43°N) have exhib-

* Contribution number 364 of the U.S. GLOBEC program, NEP Office, Oregon State University, Corvallis, OR.

ited a strong decline in size and survival in the mid-1990s; whereas populations south of Cape Blanco have not shown this trend (Lewis[1]). This finding suggests that these two populations have experienced different ocean conditions.

The quality of the marine habitat (in terms of habitat complexity, prey density, and temperature) undoubtedly influences fish growth and condition. Growth and indices of condition can be used as measures of habitat quality for juvenile salmon and to identify essential links between oceanographic conditions and survival of salmon populations during the critical juvenile life history phase. Measures such as growth (growth rate, size variation, and allometric relationships) (Lorenzen, 1996; McGurk, 1996) and accumulation of energetic reserves used in growth and sustenance during the low-productivity winter periods have been used previously to characterize habitat quality and to describe how it ultimately affects the individual and the population (Perry et al., 1996; Paul and Willette, 1997). Environmental factors are known to affect growth, reproduction, survival, and ultimately population recruitment (Hinch et al., 1995; Marschall and Crowder, 1995; Friedland and Haas, 1996). As such, fish condition, growth rate, and size in the pre-adult stages are parameters that can be used to identify the influence of natural and anthropogenic ocean conditions on marine survival.

Much of our current knowledge of the dominant nekton of the pelagic ecosystem off the coasts of Oregon and Washington is derived from a series of 17 cruises conducted by Oregon State University (OSU) from 1979 to 1985. These collections, consisting of >900 quantitative purse seine sets in the northern California Current, were made to examine geographic distributions and temporal trends of the dominant nekton and how these relate to physical and biotic conditions at the time of capture. The primary purpose of these cruises was to collect data for assessment of the abundance, distribution, growth, migration, and ecology of juvenile salmon in coastal waters. Data on the distribution, migration and growth of juvenile salmon from these cruises have been summarized in Fisher and Pearcy (1988; 1995), Pearcy and Fisher (1988, 1990), and Pearcy (1992). Analysis of the nonsalmonid data includes studies on their abundance and distribution (Brodeur and Pearcy, 1986; Emmett and Brodeur, 2000), feeding habits (Brodeur et al., 1987) and interannual variability in relation to oceanographic conditions (Brodeur and Pearcy, 1992). In addition, the distribution of juvenile salmon (mainly coho and chinook salmon [*O. tshawytscha*]) has been studied more recently as a component of a multiyear Columbia River Plume study (Emmett and Brodeur, 2000; Teel et al., 2003; Brodeur et al., 2003). However, all these cruises extended only as far south as Cape Blanco, with the exception of one cruise (July 1984), which extended as far south as Eureka, California, but included only a few collections south of Cape Blanco (Pearcy and Fisher, 1990). Thus, the region south of Cape Blanco is almost completely unknown in terms of juvenile salmon distribution, pelagic nekton, and biological oceanography in general, despite being an area of very strong upwelling and high productivity. Also, the fine-scale distribution of juvenile salmon in relation to environmental variables has not been studied in any detail.

The California Current is not homogeneous but rather can be divided into distinct subunits or regions, each with its own physical and biological characteristics (U.S. GLOBEC, 1994). A break between the northernmost two regions occurs at Cape Blanco, where the equatorward upwelling jet veers sharply off the shelf and into the California Current (Barth et al., 2000). The upwelling zone north of the cape is narrow, extending out about 30 km, whereas south of Cape Blanco, it can extend up to 100 km offshore. This area also appears to represent a faunal break for some zooplankton communities (McGowan et al., 1999; Peterson and Keister, 2002) and is a break point for alternative salmon migration strategies (Weitkamp et al., 1995; Weitkamp and Neely, 2002).

During the summer of 2000, we conducted broad-scale sampling and fine-scale process studies from central Oregon to northern California to examine the distribution of juvenile salmon and associated species in relation to environmental conditions. This was one component of a multidisciplinary U.S. Global Ocean Ecosystem Dynamics (GLOBEC) Northeast Pacific study examining the northern California Current ranging in scope from the physics up to the top trophic levels (Batchelder et al., 2002). We were interested in examining the distribution of juvenile salmon north and south of Cape Blanco, the origin of these fish, and any regional differences in growth and condition of salmon across the range of sampling. Evidence exists that the physical conditions and the associated biota are different within this geographical scale. Thus, analyses of the relationship between oceanographic conditions and the response of resident biota can provide insights into the linkages associated with physical and biological processes that shape the biological community, and in particular, those associated with salmon recruitment.

Methods

Field surveys

Surveys were conducted over two time periods—early summer (29 May–18 June, 2000) and late summer (28 July–15 August, 2000). Each survey consisted of a mesoscale grid along designated GLOBEC transects that had been monitored for several years and by fine-scale process sampling at stations of interest based on features observed in the physical environment (fronts or eddies) or by acoustic sampling conducted by two accompanying oceanographic vessels (RV *Wecoma* and RV *New Horizon*). Further details on the physical and biological conditions occurring at the time of our sampling have been reported by Batchelder et al. (2002).

For the mesoscale survey, stations were established at 1, 5, 10, 15, 20, 25 and 30 nautical miles from shore on each of five transects. Inclement weather, particularly

[1] Lewis, M. A. 2002. Stock assessment of anadromous salmonids 2001. Monitoring program report OPSW-ODFW-2002-04, 57 p. Oregon Dept. Fish Wildlife, Portland, OR 97207.

during the first cruise, prevented us from sampling all the stations along each transect. At each station, a Nordic 264 rope trawl built by Nor'Eastern Trawl Systems, Inc. (Bainbridge Island, WA) was towed in surface waters by a chartered fishing vessel (FV *Sea Eagle*) at a speed of 6 km/h. This rope trawl has a maximum mouth opening of approximately 30 m × 18 m. Mesh sizes ranged from 162.6 cm in the throat of the trawl near the jib lines to 8.9 cm in the codend. To maintain catches of small fish and squid, a 6.1-m long, 0.8-cm mesh knotless liner was sewn into the codend. All tows were 30 minutes in duration. All fish and squid caught were counted and measured at sea. After fork length (FL) was measured to the nearest mm, all juvenile salmon were immediately frozen for later determinations of growth, condition, food habits, genetic analysis, and assessment of pathological condition.

The physical and biological environment was monitored and sampled at each station immediately prior to setting the trawl. A CTD (conductivity, temperature, and depth) cast was made with a Sea-Bird SBE 19 Seacat profiler to 100 m at deep stations or within 10 m of the bottom at shallow stations. Chlorophyll and nutrient samples were collected from 3 m depth with a Niskin water sampler. A neuston tow with a 1-m^2 mouth containing 333-μm mesh net was towed for 5 minutes out of the wake of the vessel at each station. General Oceanics flow meters were placed inside the net to measure the amount of water sampled. Additional details on the analysis of these neuston trawls are available in Reese et al.[2]

Condition and growth analysis

Each salmonid was remeasured (FL to the nearest mm) and weighed (to the nearest 0.1 g) in the laboratory. A portion of hepatic and muscle tissue was excised, placed in individual capsules, frozen in liquid nitrogen, and stored at –80°C until analyzed. The bioenergetic health of juvenile salmon was evaluated by assessing changes in water content (as a surrogate measure of fat accumulation) of liver and muscle to estimate dry tissue weight. The water content was determined by drying tissue samples to a constant weight at 105°C. The accumulation of energy reserves during the growth season (energy reserves of salmon in August in relation to salmon collected in June) that would enhance survival of juveniles during the winter when food availability is lower was also measured. The condition of juvenile salmon was assessed by examining weight residuals (by using either the wet weight or dry weight) derived from the allometric relationship between length and weight of individual juvenile salmon after logarithmic transformation (Jakob et al., 1996) of salmon captured in June and August. Wet-weight residuals are representative of the traditional condition index of animals and are a reflection of somatic tissue growth. Dry-weight residuals are responsive to accumulation of fat stores and are a reflection of the bioenergetic health of the individual animal (Sutton et al., 2000; Post and Parkinson, 2001).

To contrast growth characteristics during 2000 in different latitudinal ranges of the California Current, we compared ocean growth rates of juvenile coho salmon south and north of Cape Blanco in the GLOBEC study area, and in the area from Newport, Oregon, north to northern Washington. The physical and biological characteristics of these three regions of the coastal ocean differ greatly (U.S. GLOBEC, 1994), and these differences may impact the distribution and abundance of prey of juvenile salmonids and therefore may also affect salmonid growth. Data north of Newport, Oregon, were collected during a separate study of the Columbia River plume and the adjacent coastal ocean (hereafter called the "plume study") using the same trawl and a similar sampling strategy as in the GLOBEC study (see Emmett and Brodeur [2000] and Teel et al. [2003] for details).

Scales were examined from 45 juvenile coho salmon caught during the June and August 2000 GLOBEC cruises and 252 juvenile coho salmon caught during the 2000 plume cruises. The scales were mounted on gummed cards from which acetate impressions were made. Using a video camera attached to a compound microscope and Optimas® imaging software (vers. 5.1, Optimas Inc., Seattle, WA) we measured the distance (scale radius) along the anterior-posterior axis of each scale from the focus (F) to the ocean entry mark (OE) and to the scale margin (Fig. 1). The fork-length of each fish at the time of ocean entry (FL_{OE}) was estimated from the scale radius (SR_{OE}) at ocean entry using the Fraser and Lee back-calculation method (Ricker, 1992):

$$FL_{OE} = \frac{(FL - 36.07)}{SR} \times SR_{OE} + 36.07,$$

where FL = length at capture;
SR = scale radius at capture; and
36.07 = the intercept from a regression of SR on FL for juvenile coho salmon caught in the ocean (Fig. 2A).

In an analogous fashion, fish weight at time of ocean entry (Wt_{OE}) was back-calculated from the estimated fish fork length at ocean entry (FL_{OE}):

$$\ln(Wt_{OE}) = \frac{(\ln(Wt) + 12.633)}{\ln(FL)} \times \ln(FL_{OE}) - 12.633,$$

where Wt = weight at capture; and
–12.633 = the intercept from a linear regression of $\ln(Wt)$ on $\ln(FL)$ for juvenile coho salmon caught in the ocean (Fig. 2B).

The growth rate in FL,

$$(FL - FL_{OE}) / \Delta d,$$

[2] Reese, D. C., T. W. Miller, and R. D. Brodeur. 2003. Community structure of neustonic zooplankton in the northern California Current in relation to oceanographic conditions, 22 p. Unpubl. manuscript. Northwest Fisheries Science Center, NMFS, 2030 S. Marine Science Drive, Newport, OR 97365.

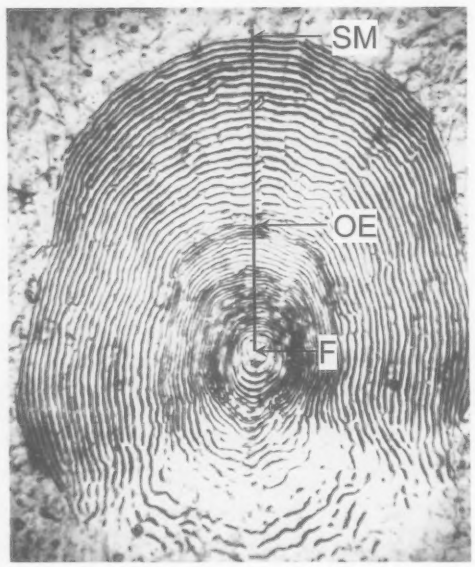

Figure 1

Scale from a 352-mm FL male juvenile coho salmon (*Oncorhynchus kisutch*) caught during the August 2000 GLOBEC cruise showing the axis of measurement (black line), the focus (F), the mark of ocean entry (OE), and the scale margin (SM).

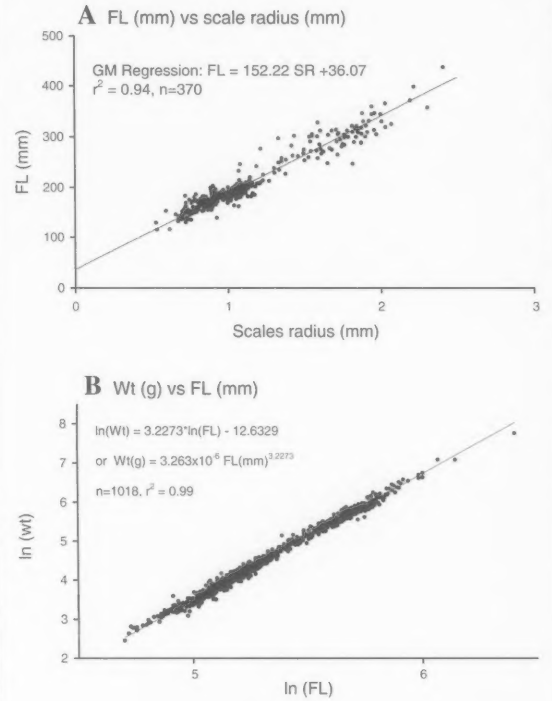
A FL (mm) vs scale radius (mm)
GM Regression: FL = 152.22 SR +36.07
r^2 = 0.94, n=370
FL (mm)
Scales radius (mm)
B Wt (g) vs FL (mm)
ln(Wt) = 3.2273*ln(FL) - 12.6329
or Wt(g) = 3.263x10^{-6} FL(mm)$^{3.2273}$
n=1018, r^2 = 0.99
ln (wt)
ln (FL)

Figure 2

(**A**) Regression of fork length (FL) on scale radius and, (**B**) regression of ln(*Wt*) on ln(*FL*) for juvenile coho salmon (*Oncorhynchus kisutch*) caught during the May 1998–September 2000 Columbia River plume study.

and the instantaneous growth rate in weight:

$$G = \left(\ln(Wt) - \ln(Wt_{OE})\right) / \Delta d,$$

where Δd = estimated days between ocean entry and capture, were estimated for each salmon.

The meaning of the instantaneous growth rate G can be stated as follows: if salmon growth is exponential between ocean entry and capture, then

$$\frac{Wt}{Wt_{OE}} = e^{G \times \Delta d},$$

and at any *instant* the fish's weight increases at the *rate* of G of its body weight per day. G can be multiplied by 100 to give the instantaneous growth rate in terms of percentage of body weight per day.

Although the dates of ocean entry of individual fish were unknown, seaward migration of coho salmon smolts in California, Oregon, and Washington rivers occurs mainly between mid-April and mid-June, and there is no consistent latitudinal trend in timing of the migration (Weitkamp et al., 1995). Peak downstream migration of coho salmon smolts was between mid-May and very early June in the Columbia River estuary, 1978–83 (Dawley et al., 1985), and in the lower Trinity River, California, 1997–2000 (USFWS[3]). In 2000, peak downstream migration of mainly nonhatchery coho salmon smolts at 13 monitoring sites in coastal Oregon rivers north of Cape Blanco occurred from April 2 to May 20; median peak migration occurred 26 April (Solazzi et al.[4]) From the information available on timing of seaward migration of coho salmon smolts, we used an ocean entry date of 15 May when calculating Δd and estimating ocean growth rates of unmarked coho salmon from scales.

In addition to estimating growth rates of juvenile coho salmon from scales, we also estimated instantaneous growth rates in weight between hatchery release and capture in the ocean of 28 coded-wire–tagged (CWT) juvenile coho salmon:

[3] USFWS (U.S. Fish and Wildlife Service). 2001. Juvenile salmonid monitoring on the mainstem Klamath River at Big Bar and mainstem Trinity River at Willow Creek, 1997–2000, 106 p. Annual report of the Klamath River Fisheries Assessment Program. Arcata Fish and Wildlife Office, Arcata, CA 95521.

[4] Solazzi, M. F., S. L. Johnson, B. Miller, and T. Dalton. 2002. Salmonid life-cycle monitoring project 2001. Monitoring program report OPSW-ODFW-2002-2, 25 p. Oregon Dept. Fish and Wildlife, Portland, OR 97207.

$$G = \left(\ln(Wt) - \ln(Wt_R)\right) / \Delta d,$$

where Wt = weight of the CWT fish at capture;
Wt_R = the average weight of fish in the CWT group at time of release; and
Δd = days between hatchery release and capture in the ocean.

Estimated growth rates of these CWT fish, of known release date and known average release weight were used to validate the growth rates estimated from scale analysis

Our analysis of the growth of chinook salmon based on scale characteristics is not far enough advanced to report in this article. We plan to present these data in a later article.

Contribution of hatchery coho salmon to catches

The total numbers, percentages of marked fish (any external fin clips or internal tags) and grand average weights of hatchery coho salmon smolts released in 2000 are summarized for different release regions in Appendix Table 1. These data were used to compare the estimated average weights of fish at time of ocean entry (from scale analysis) with the average weights of hatchery fish at time of release, and also to estimate the proportions of hatchery coho salmon in our catches. We calculated the expected percentage ($E\%$) of marked fish in each catch if 100% of the fish were hatchery fish:

$$E\% = \sum R_i \times A_i,$$

where R_i = the proportional contribution of region i to the catch (this paper for the GLOBEC catches, and from Teel et al., 2003 for the plume study catches); and
A_i = the percentage of hatchery fish that were marked in region i (from Appendix Table 1).

The percentage of hatchery fish in each catch sample ($H\%$) was then estimated as

$$H\% = \frac{O\%}{E\%} \times 100,$$

where $O\%$ = observed percentage of marked fish.

Genetic analysis

The freshwater origins of juvenile chinook and coho salmon and steelhead (*O. mykiss*) were studied by using standard methods of genetic mixed stock analysis (Milner et al., 1985; Pella and Milner, 1987). According to the methods described by Aebersold et al. (1987), samples of eye, liver, heart, and skeletal muscle were extracted from frozen whole juvenile salmon and analyzed with horizontal starch-gel protein electrophoresis. Data from previous studies characterizing genetic (allozyme) differences among spawning populations in California and the Pacific Northwest were then used as baseline data to estimate the stock compositions of our ocean caught mixed-stock samples. Baselines consisted of 32 gene loci and 116 populations for chinook salmon (Teel et al.[5]), 58 loci and 49 populations for coho salmon (Teel et al., 2003), and 55 loci and 57 populations for steelhead (Busby et al., 1996). Estimates of stock compositions were made by using the maximum likelihood procedures described by Pella and Milner (1987) and the Statistical Package for Analyzing Mixtures (Debevec et al., 2000). Estimates of individual baseline populations were then summed to estimate contributions of regional stock groups. Precision of the stock composition estimates was estimated by bootstrapping the estimates 100 times with resampling of the baseline and mixture genetic data as described in Pella and Milner (1987).

Habitat and assemblage analysis

The raw numbers of fish and squid caught from each trawl were converted to densities based on the volume filtered per trawl to standardize for differences in effort between tows. Density contours of juvenile salmon and other nekton were produced using specialized graphics programs. We then tested whether the habitat associations of the dominant salmonids were significantly different from the total habitat sampled by following the methods outlined in Perry and Smith (1994). This procedure involved comparing the cumulative distributions of salmon catch with observed environmental conditions (temperature, salinity, chlorophyll-*a* at one meter, water depth, and neuston displacement volume). We performed 5000 randomizations of the data and used the Cramér-von Mises test statistic recommended by Syrjala (1996) as being robust to the effects of inordinately large catches.

To explore the relationship between juvenile salmon and other fish species and environmental variables, we used several types of multivariate analyses (McCune and Grace, 2002). Original data from each of the two cruises formed complimentary species and environmental matrices. The June and August cruises were analyzed individually to look at spatial patterns of species composition in relation to environmental gradients (Gauch, 1982). To avoid spurious effects of rare species, we excluded species from the data matrix that had a frequency of occurrence of less than 10% of the possible occurrences for each cruise (McCune and Grace, 2002). To minimize the effect of very large catches, the data were log transformed. Stations with no species present were eliminated from the data set to allow for analysis of sample units in species space. Data transformations and their effects on the summary statistics were examined prior to analysis. Analyses of data were performed by using PC-ORD version 4.28 (McCune and Mefford, 1999).

Agglomerative hierarchical cluster analysis (AHCA) using the Bray-Curtis dissimilarity measure and Wards

[5] Teel, D. J., P. A. Crane, C. M. Guthrie, III, A. R. Marshall, D. M. Van Doornik, W. D. Templin, N. V. Varnavskaya, and L. W. Seeb. 1999. Comprehensive allozyme database discriminates chinook salmon from around the Pacific Rim. (NPAFC document 440), 25 p. Alaska Department of Fish and Game, Division of Commercial Fisheries, 333 Raspberry Road, Ancorage, AK 99518.

linkage function was applied to arrange the nekton species assemblages and stations into cluster groups. The cutoff level to form optimal groups within the species and station dendrograms was based on several criteria: 1) biological meaning; 2) significance tests of groups using a multi-response permutation procedure (MRPP); and 3) comparison of cutoff level MRPP results with those groups obtained from one cutoff level below and above the level of interest. A nonparametric procedure, MRPP compares the *a priori* groupings from AHCA and tests the hypothesis of no difference between the groups. For cluster analysis of stations, indicator species analysis (ISA) was used to determine nekton species strongly associated with individual groups. ISA assigns indicator values to each species according to relative abundance and frequency, then tests the significance (Monte-Carlo permutation test) of the highest species-specific indicator value assigned to a particular group.

Nonmetric multidimensional scaling (NMS; Kruskal, 1964) was used to ordinate sample units in species space and to compare station cluster groups to environmental gradients. NMS was chosen for this analysis because it is robust to data that are non-normal and that have high numbers of zeros. Initial runs of NMS from both cruise datasets resulted in three-dimensional solutions. Subsequent reapplication of NMS using a three-dimensional solution (Sorensen distance, 400 maximum iterations, and 40 runs with real data) was applied for the final ordinations. To examine the environmental or station factors associated with each NMS axis that may have affected the distribution of the dominant taxa, we correlated the NMS station and species scores to a suite of environmental variables including water depth, distance offshore, latitude, surface temperature, surface salinity, chlorophyll-*a* concentration, and neuston zooplankton settled volumes. Pearson and Kendall correlations with each ordination axis were used to measure strength and direction of individual species and environmental parameters.

Results

Distribution of juvenile salmon and other species

We collected a total of 18,852 nekton individuals: two cephalopod, one agnathan, two elasmobranch, and 57 fish taxa from 163 surface trawls (see Table 1 for scientific names of all species). With the exception of market squid in June and blue shark in August, most of the nonteleost nekton occurred in only a few collections. Substantially fewer fish were caught in the June cruise than in the August cruise, but the diversity was much higher in the June cruise. The catch in June was dominated by forage fishes such as Pacific herring, surf and whitebait smelt, and juvenile rockfishes, sablefish, and flatfishes. Salmonids, mainly juvenile chinook and coho salmon and steelhead, comprised a relatively minor proportion of the catches (only 114 juvenile salmonids; 1.9 % of the total).

The August cruise was dominated by several large catches of Pacific sardine (Table 1). Jack mackerel was the most common nonsalmonid caught. Many of the juvenile fish taxa caught during the June cruise were absent during the August cruise; those that did occur (sablefish, rex sole) were much lower in abundance. Mesopelagic fishes of the family Bathylagidae and Myctophidae were collected only during the August cruise, mainly because of the inclusion of more offshore stations and occasional collections during nondaylight hours. As in the earlier cruise, salmonids comprised a relatively minor percentage of the catch (3.1%) but were more common and abundant during this survey.

Juvenile chinook salmon were broadly distributed latitudinally during both cruises, but their distribution was mainly restricted to nearshore stations within the 100-m isobath (Fig. 3). Coho salmon juveniles were more common north of Cape Blanco during both cruises and were found generally farther offshore than chinook salmon juveniles (Fig. 3). In contrast, steelhead juveniles were found mainly south of Cape Blanco, especially in June, but their zonal distribution overlapped that of coho salmon juveniles.

Size and condition of juvenile salmon

Fork length of yearling chinook salmon averaged 227 ±42 mm FL in June and 230 ±30 mm FL in August and averaged 135 ±12 mm FL for subyearling chinook salmon in August, whereas juvenile coho salmon averaged 162 ±32 mm FL in June and 286 ±46 mm FL in August (Table 2). No significant differences in fork length of juvenile chinook or coho salmon north or south of Cape Blanco were evident.

Juvenile coho salmon weighed significantly more on a wet-weight basis for a given fork length in the region north of Cape Blanco compared to juveniles captured south of Cape Blanco (Fig. 4). This pattern was also similar and significant when evaluated on a dry-weight basis (bioenergetic growth). Although the stock composition in the two regions could account for some of these differences, the growth responses likely reflect habitat-specific features in the region north of Cape Blanco that benefit coho salmon. No difference in condition of yearling chinook salmon captured north or south of Cape Blanco, on either a wet- or dry-weight basis, was evident (Fig. 4). Information regarding size and condition of subyearling chinook salmon are not presented because few subyearling chinook salmon were caught in June and all but one subyearling chinook salmon in August were caught in the region south of Cape Blanco, OR. Insufficient subyearling chinook salmon were available for an analysis comparable to that done for yearling chinook and coho salmon.

Proportions of wild and hatchery coho salmon

Most of the juvenile coho salmon caught during the plume study north of Newport, Oregon, originated in hatcheries (Table 3). In June and September 2000 we estimated that wild fish comprised only 10% and 25%, respectively, of the catch. Wild fish, however, comprised a proportionally much higher percentage of the catch of coho salmon in the GLOBEC study area in June north of Cape Blanco (67%), and in August south of Cape Blanco (61%), than in the plume study area farther to the north. Most jacks and

Table 1

Phylogenetic listing of nekton catch in numerical composition, frequency of occurrence (F.O.) and size range caught for each cruise. (j) indicates juvenile stage; (a) adult. ML = mantle length, TL = total length, FL = fork length, SL = standard length (in mm).

			June (84 stations)			August (79 stations)		
Class and Family	Common name	Scientific name	Number	F.O.	Size range	Number	F.O.	Size range
Cephalopoda								
Onychoteuthidae	Pacific clubhook squid	*Onychoteuthis borealijaponicus*	19	6	21–80 ML	302	6	21–227 ML
Loliginidae	Market squid	*Loligo opalescens*	301	14	33–122 ML	1	1	35 ML
Agnatha								
Petromyzontidae	Pacific lamprey	*Lampetra tridentata*				1	1	625 TL
Chondrichthyes								
Alopiidae	Thresher shark	*Alopias vulpinus*	1	1	36–576 TL			
Carcharhinidae	Blue shark	*Prionace glauca*				18	10	1300–1660 TL
Osteichthyes								
Xenocongridae	Eel leptocephalus	*Thalassenchelys coheni*	3	1	214–243 TL	2	2	260–305 TL
Clupeidae	Pacific herring	*Clupea pallasi*	1022	9	127–195 FL			
	Pacific sardine	*Sardinops sagax*	7	2	237–260 FL	10,327	15	178–290 FL
Engraulididae	Northern anchovy	*Engraulis mordax*				49	12	148–165 FL
Salmonidae	Chinook salmon (j,a)	*Oncorhynchus tshawytscha*	56	18	121–780 FL	252	26	109–910 FL
	Coho salmon (j,a)	*Oncorhynchus kisutch*	35	15	122–580 FL	111	25	210–736 FL
	Cutthroat trout (j,a)	*Oncorhynchus clarki*	1	1	186 FL	3	3	258–341 FL
	Steelhead trout (j,a)	*Oncorhynchus mykiss*	22	8	176–284 FL	36	13	261–430 FL
Osmeridae	Smelt (j)	Osmeridae	14	4	37–52 SL	74	5	31–50 SL
	Surf smelt	*Hypomesus pretiosus*	846	8	128–184 FL	351	7	140–187 FL
	Whitebait smelt	*Allosmerus elongatus*	946	6	60–114 FL	79	3	76–132 FL
Bathylagidae	Popeye blacksmelt	*Bathylagus ochotensis*				1	1	76 SL
Paralepidae	Slender barracudina	*Lestidium ringens*				3	1	72–76 SL
Myctophidae	Northern lampfish	*Stenobrachius leucopsarus*				96	4	14–70 SL
	Bigfin lanterfish	*Symbolophorus californiensis*				61	4	89–102 SL
	Blue laternfish	*Tarletonbeania crenularis*				10	3	33–87 SL
Gadidae	Gadid (j)	Gadidae	10	3	42–58 SL	13	3	53–57 SL
	Pacific cod (j)	*Gadus macrocephalus*	23	1	38–60 SL			
	Pacific tomcod (j)	*Microgadus proximus*	6	4	35–55 SL	8	2	49–80 SL
Scomberesocidae	Pacific saury	*Cololabis saira*	26	1	182–229 FL	66	6	131–194 FL
Atherinidae	Jacksmelt	*Atherinopsis californiensis*				1	1	302 FL
Trachipteridae	King–of–the–salmon (j)	*Trachipterus altivelis*	2	2	71–270 SL	12	2	40–83 SL
Gasterosteidae	Threespine stickleback	*Gasterosteus aculeatus*	1	1	60 SL			
Scorpaenidae	Pacific ocean perch (j)	*Sebastes alutus*	1	1	33 SL			
	Darkblotched rockfish (j)	*Sebastes crameri*	154	14	29–54 SL	1	1	53 SL
	Yellowtail rockfish (j)	*Sebastes flavidus*	1350	24	20–63 SL	1	1	18 SL
	Shortbelly rockfish (j)	*Sebastes jordani*	1	1	37 SL			
	Black rockfish (j,a)	*Sebastes melanops*	1	1	30 SL	1	1	335 FL
	Bocaccio (j)	*Sebastes paucispinis*	20	5	21–36 SL			
	Canary rockfish (j)	*Sebastes pinniger*	27	5	22–39 SL			
	Bank rockfish (j)	*Sebastes rufus*	8	1	16–28 SL			
	Stripetail rockfish (j)	*Sebastes saxicola*	13	3	32–37 SL			
Hexagrammidae	Lingcod (j)	*Ophiodon elongatus*	20	9	76–81 FL			
Anoplopomatidae	Sablefish (j)	*Anoplopoma fimbria*	182	14	55–136 FL	4	2	173–241 FL

continued

Table 1 (continued)

Class and Family	Common name	Scientific name	June (84 stations) Number	F.O.	Size range	August (79 stations) Number	F.O.	Size range
Cottidae	Irish lord (j)	*Hemilepidotus* spp.	2	1	38–40 FL			
	Cabezon (j)	*Scorpeanichthys marmoratus*	12	7	33–38 SL			
	Pacific staghorn sculpin	*Leptocottus armatus*	1	1	180 TL			
Agonidae	Sturgeon poacher (j)	*Podothecus acipenserinus*				1	1	80 TL
Cyclopteridae	Pacific spiny lumpsucker	*Eumicrotremus orbis*				1	1	253 TL
Carangidae	Jack mackerel	*Trachurus symmetricus*	111	3	364–583 FL	839	20	227–589 FL
Bramidae	Pacific pomfret	*Brama japonica*				5	2	387–434 FL
Anarhichadidae	Wolf-eel (j)	*Anarrhichthys ocellatus*	15	13	215–555 TL	8	7	442–582 TL
Ammodytidae	Pacific sandlance	*Ammodytes hexapterus*	4	4	45–82 SL			
Zaprodidae	Prowfish (j)	*Zaprora silenus*	1	1	68 SL			
Scombridae	Chub mackerel	*Scomber japonicus*				74	6	266–421 FL
Centrolophidae	Medusafish	*Icichthys lockingtoni*	3	3	37–50 SL	8	6	87–129 FL
Bothidae	Sanddabs (j)	*Citharichthys* spp.	23	13	35–43 SL	3	2	269–288 TL
	Pacific sanddab (j)	*Citharichthys sordidus*	32	4	32–44 SL			
	Speckled sanddab (j)	*Citharichthys stigmaeus*	60	10	30–43 SL			
Pleuronectidae	Dover sole (j)	*Microstomus pacificus*	2	2	40–50 SL	3	1	27–34 SL
	Sand sole (j)	*Psettichthys melanostictus*	3	3	22–39 SL			
	Slender sole (j)	*Eopsetta exilis*				1	1	66 SL
	Starry flounder	*Platichthys stellatus*				2	1	349–399 TL
	Curlfin sole (j)	*Pleuronichthys decurrens*	5	3	25–31 SL			
	English sole	*Parophrys vetulus*	1	1	303 TL			
	Rex sole (j)	*Errex zachirus*	581	12	34–79 SL	48	11	44–70 SL
Molidae	Ocean sunfish	*Mola mola*				1	1	620 TL
Total			5974			12,878		

about one half of the nonjacks caught north of Cape Blanco in August were hatchery fish.

Two factors, however, may have lead to inaccuracies in estimation of hatchery-wild ratios of coho salmon in the GLOBEC study area. First, because of low sample sizes, the data were pooled from both June and August catches for the genetic stock analysis; therefore we do not know the proportional contributions of the different release areas to the catches in either month alone. Second, all the fish released from Klamath River and Trinity River hatcheries had been clipped on the maxillary. We were unaware that the maxillary clip was being used, did not look for it, and consequently may have classified fish with this mark as unmarked. Therefore, the proportion of hatchery fish in the catch of coho salmon during GLOBEC may have been higher than is shown in Table 3.

Age and growth of juvenile coho salmon

Forty-three percent (24 of 56) of the juvenile coho salmon caught during the August GLOBEC cruise were precocious males ("jacks") according to the testes-weight to body-weight criteria of Pearcy and Fisher (1988). This is a much higher percentage of jacks than found among juvenile fish caught in September 2000 in the plume study off Oregon and Washington, where only 4.5% of fish (6 of 132) were precocious males or females according to the same criteria. Because the jacks were considerably larger than the nonjacks, average growth rates of the two groups were reported separately.

Estimated average growth rates in FL between ocean entry and capture were higher for fish caught in the August 2000 GLOBEC cruises (1.56–2.22 mm/d) than for fish caught in any other cruises (Table 3). The fish caught in August 2000 were also larger when they entered the ocean (average170–178 mm FL) than fish caught in other cruises (average154–160 mm FL). Average growth rate of jacks from north of Cape Blanco (2.22 mm/d), was significantly higher (t-test, $P<0.05$) than growth rates of nonjacks (1.56–1.67 mm/d). Growth rates of nonjacks north and south of Cape Blanco were not significantly different (t-test, $P<0.05$). The combination of large size at ocean entry

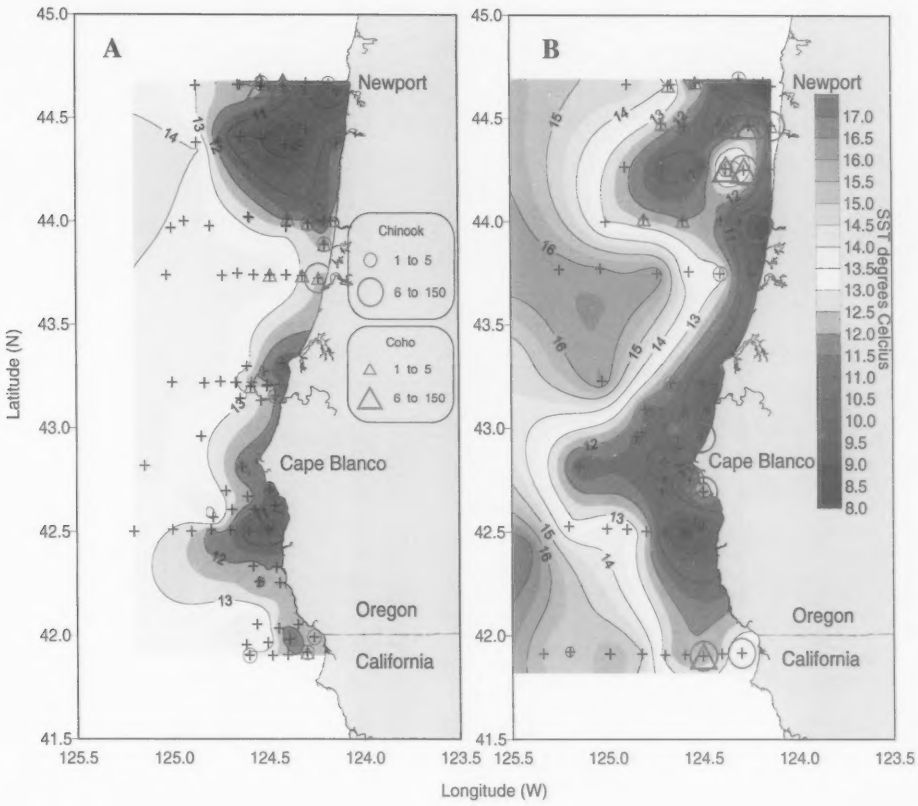

Figure 3

Catch distribution for juvenile coho (*Oncorhynchus kisutch*) and chinook salmon (*O. tshawytscha*) for the (**A**) June and (**B**) August cruise overlaid on surface temperature contours. Plus signs are stations sampled where no salmon were caught.

and favorable conditions for growth in the ocean probably contributed to the very high percentage of jack coho salmon in August 2000 in the GLOBEC study area.

Estimated average growth rates between ocean entry and capture of juvenile coho salmon were higher in the GLOBEC area than in the plume study area (t-tests, $P<0.05$). For fish caught in June, average growth rate was 1.06 mm/d and 0.63 mm/d in the GLOBEC and plume study areas, respectively. For fish caught in August or September, average growth rate was 1.57–2.22 mm/d in the GLOBEC study area and 1.17 mm/d plume in the study area (Table 3). The higher growth rates of coho salmon caught in the GLOBEC study area suggests that in 2000 conditions for growth were better there than those in the plume study area farther north off Oregon and Washington. Average instantaneous growth rates in weight were also higher (t-tests, $P<0.05$) for the fish caught in the June and August 2000 GLOBEC cruises (2.0 and 2.1–2.8% body wt/d, respectively) than for the fish caught in the June and September 2000 plume study cruises (1.2 and 1.7 % body wt/d, respectively; Table 4A).

In addition, the average condition index (CI) of juvenile coho salmon in June was significantly higher (t-test, $P=0.03$) in the GLOBEC study area (1.12, $n=32$, SD=0.087) than in the plume study area (1.07, $n=245$, SD=0.117). Similarly, the average CI of nonjack juvenile coho salmon was higher (t-test, $P=0.002$) in August in the GLOBEC study area (1.24, $n=32$, SD=0.096) than in September in the plume study area (1.18, $n=132$, SD=0.100). Both the high instantaneous growth rates in weight and the high CI of juvenile coho salmon caught in the GLOBEC study area suggest that conditions for growth of coho salmon in this area were very good in 2000. Growth rates estimated from the few CWT fish caught during these cruises (Table 4B) were similar to, and help validate, the growth rates estimated from scales (Table 4A).

Average weights at time of ocean entry back-calculated from scales for coho salmon caught in June in the GLOBEC area and in all months in the plume study area (Table 4A) were slightly higher than the average weights of hatchery coho salmon at time of release (Appendix Table 1). For example, in the plume study area, average back calculated weights at ocean entry ranged from 37.5 g to 42.4 g (Table 4A)—slightly higher than the expected average weights at release of about 32–33 g based on the stock composi-

Table 2

Summary of mean, standard deviation, and range of FL measured in the field, weight measured in the laboratory, and condition index (CI) of subyearling (age 0.0) and yearling (age 1.0) chinook salmon and yearling (age 1.0) coho salmon caught during the June and August cruises north (N) and south (S) of Cape Blanco (latitude 42.837°). Precocious coho salmon are indicated with a "J".

	Field FL (mm)				Laboratory weight (g)			C.I. ($wt \times 10^5 / FL^3$)	
	n	Mean	SD	Range	Mean	SD	Range	Mean	SD
Chinook (age 0.0)									
June (N)	1	121	—	—	18	—	—	1.04	—
August (N)	1	172	—	—	70	—	—	1.37	—
August (S)	125	134	12	109–175	28	9	12–70	1.10	0.08
Chinook (age 1.0)									
June (N)	27	229	42	144–280	178	91	33–306	1.32	0.10
June (S)	1	174	—	—	67	—	—	1.28	—
August (N)	54	229	26	187–318	164	72	80–468	1.32	0.09
August (S)	35	231	35	190–349	176	94	80–535	1.32	0.07
Coho (age 1.0)									
June (N)	30	161	33	122–276	56	51	19–292	1.13	0.08
June (S)	2	172	0	172–172	49	1	48–49	0.95	0.01
August (N-J)	24	365	31	310–415	690	209	375–1198	1.38	0.12
August (N)	24	285	51	210–385	326	188	97–766	1.26	0.10
August (S)	8	293	33	239–334	308	103	157–433	1.19	0.05

Table 3

Catch, percentage of the catch that was marked, estimated percentage of hatchery origin, size of scale sample, FL at ocean entry (OE) back calculated from scales, FL at capture, and estimated growth rate in FL while in the ocean for juvenile coho salmon caught during the 2000 GLOBEC and Columbia River plume studies. All length data are from the scale sample only. An ocean entry date of 15 May was used when calculating growth rate in FL.

Cruise	Catch (*n*)	Marked	Estimated % hatchery origin	Scale sample (*n*)	Back-calculated FL at OE (mm) mean (SD)	FL at capture (mm) mean (SD)	Growth rate (mm/d) mean (SD)
GLOBEC							
June 2000	32	32%	33%	11	155 (29.0)	177 (42.3)	1.06 (1.01)
Aug 2000							
North of C. Blanco							
Jacks	24	71%	74%	19	170 (22.8)	370 (28.1)	2.22 (0.35)
Nonjacks	24	46%	48%	9	178 (21.6)	309 (46.1)	1.67 (0.51)
South of C. Blanco							
Nonjacks	8	38%	39%	6	178 (13.0)	303 (29.3)	1.56 (0.22)
Plume study							
May 2000	165	68%	76–80%[1]	79	157 (16.5)	166 (17.7)	0.97 (1.15)
Jun 2000	245	76%	90%	97	160 (14.5)	185 (23.4)	0.63 (0.53)
Sep 2000	132	65%	75%	76	154 (19.0)	305 (24.9)	1.17 (0.23)

[1] No genetic stock analysis was available. The higher estimate assumes the same stock composition as in June, the lower estimate assumes that all hatchery fish were from the Columbia River.

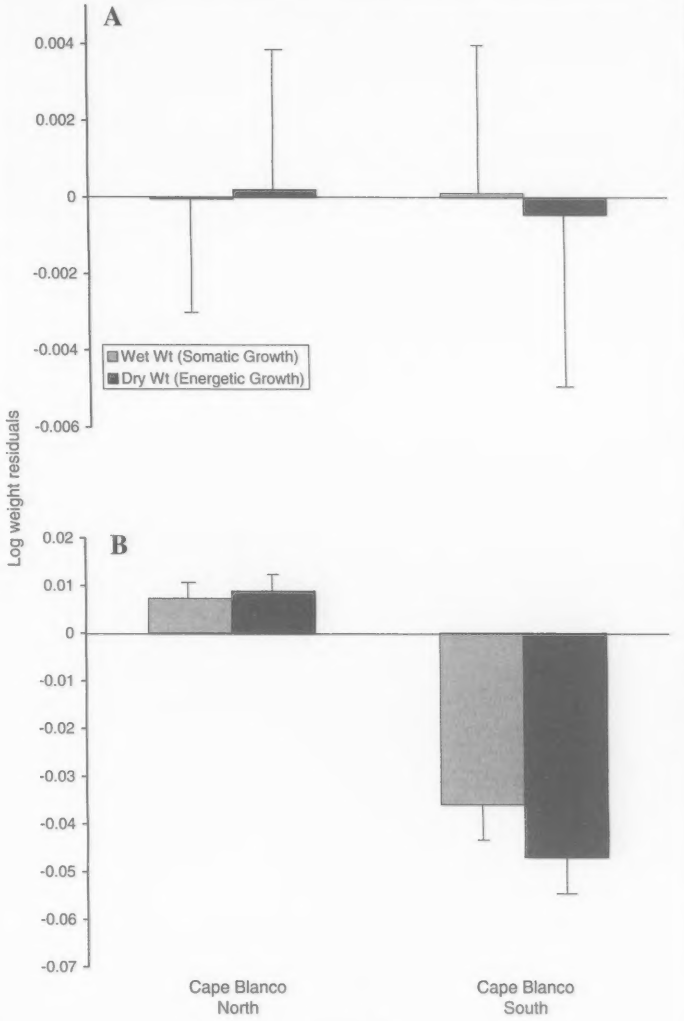

Figure 4

Wet and dry weight residuals (+1 standard error) for (**A**) yearling chinook (*Oncorhynchus tshawytscha*) and (**B**) juvenile coho salmon (*O. kisutch*) collected North and South of Cape Blanco. Weight residuals are derived from the linear relationship between fork length and wet or dry weight (log-transformed data) of juvenile salmon captured in June and August.

tion of these catches (Teel et al., 2003) and the release weights (Appendix Table 1). Similarly, the back-calculated weight at ocean entry in June in the GLOBEC area (45.5 g) was slightly higher than the expected average weight at hatchery release (about 41 g) based on the stock composition (Table 5) and the average release weights. These fairly small differences between back-calculated size at ocean entry and average size at release could be due to growth during downstream migration, selectively higher mortality of small smolts, or a bias in the back-calculation procedure.

However, the average back-calculated weights at time of ocean entry of fish caught in August in the GLOBEC study area (60–69 g) were over two standard deviations above the average weights of hatchery fish released from the Oregon coast or northern California—the main contributors to this catch (Appendix Table 1). These were obviously atypical coho salmon, and the very high proportion of jacks (preco-

Table 4

(**A**) Weights at ocean entry (OE) back-calculated from scales, weights at capture, and estimated instantaneous rates of growth while in the ocean (G) for juvenile coho salmon caught during the 2000 GLOBEC and Columbia River plume studies. An ocean entry date of 15 May was used when calculating growth rate. (**B**) Similar data for CWT fish. Growth rates of the CWT coho salmon were estimated for the periods between hatchery release and capture in the ocean.

		Back-calc. Wt. at OE (g)	Weight at capture (g)	G
A Cruise	n	mean (SD)	mean (SD)	mean (SD)
GLOBEC				
June 2000	11	45.5 (26.8)	78.0 (76.4)	0.020 (0.015)
Aug 2000				
North of C. Blanco				
Jacks	19	68.9 (27.2)	719.7 (200.0)	0.028 (0.005)
Nonjacks	9	59.5 (26.3)	419.2 (177.2)	0.023 (0.006)
South of C. Blanco				
Nonjacks	6	60.3 (12.8)	336.2 (96.2)	0.021 (0.002)
Plume study				
May 2000	79	39.4 (10.8)	47.9 (14.6)	0.020 (0.024)
Jun 2000	97	42.4 (12.5)	71.9 (33.3)	0.012 (0.009)
Sep 2000	75	37.5 (13.7)	347.2 (158.3)	0.017 (0.003)
		Wt. at release (g)	Wt. at capture (g)	G
B Cruise	n	mean (SD)	mean (SD)	mean (SD)
GLOBEC				
Jun 2000	4	44.4 (1.3)	86.6 (30.9)	0.018 (0.005)
Aug 2000	3	35.6 (9.8)	395.7 (215.0)	0.024 (0.003)
Plume study				
Jun 2000	11	28.3 (4.5)	66.1 (32.3)	0.012 (0.005)
Sep 2000	10	33.4 (10.9)	392.4 (283.3)	0.018 (0.002)

cious, sexually developed males) among the fish was probably a consequence of their very large size at ocean entry and their high rates of growth in the ocean.

Freshwater origins of juvenile salmonids

Allozyme data were collected from samples of 247 chinook salmon, 88 coho salmon, and 58 steelhead. Genetic mixed stock analyses indicated that chinook salmon in June were predominately (54%, SD=0.18) from rivers and hatcheries along the mid Oregon coast, an area immediately north of Cape Blanco (Table 5, Fig. 5). In August, chinook salmon were largely from rivers that enter the sea south of Cape Blanco. Fish from the Sacramento and San Joaquin rivers in northern California were estimated to comprise 90% (SD=0.07) of the chinook salmon sampled in August north of Cape Blanco. The largest concentration of chinook salmon we sampled was south of Cape Blanco in August, and these fish were mostly from rivers in southern Oregon (53%, SD=0.10) and the Sacramento and San Joaquin rivers (20%, SD=0.05). Chinook salmon from the Columbia River Basin were also present, but were estimated to comprise only 18% (SD=0.15) of the June sample and 8% (SD=0.05) of the August sample north of Cape Blanco. Recoveries of hatchery chinook salmon bearing coded-wire tags (CWT) provided direct evidence of stock origins for ten fish, all taken in trawls north of Cape Blanco (Table 5). These data reveal that hatchery fish released from the Umpqua River on the central Oregon coast (n=6), Columbia River Basin (n=3) and Sacramento River (n=1) contributed to our sample of chinook salmon. The proportion of CWT fish from the Umpqua River in our August catch north of Cape Blanco (8%) indicated that the contribution of mid Oregon coastal fish was underestimated in the genetic analysis likely because of the small size of the mixture sample.

Genetic estimates of coho salmon indicated that most fish originated from coastal Oregon rivers north of Cape Blanco (47%, SD=0.10) and from the Columbia River (13%, SD=0.08) (Table 5). However, a substantial proportion (40%, SD=0.09) of coho salmon were from coastal rivers south of Cape Blanco, a region that includes spawning populations in the Rogue and Klamath rivers. Eight coho salmon in our sample contained CWTs and showed that fish from

Table 5

Estimated percentage stock compositions, samples sizes, and recoveries of coded wire tags (CWTs) for chinook and coho salmon and steelhead sampled in trawl surveys along the Oregon and California coasts in 2000. Some of the major baseline stocks are given for coastal stock groups. None of the steelhead sampled contained coded wire tags.

	June (n=35) Entire Study Area			August (n=157) South of Cape Blanco			August (n=55) North of Cape Blanco		
Chinook salmon stock group	Est.	SD	CWT	Est.	SD	CWT	Est.	SD	CWT
Columbia and Snake Rivers	18	0.15	2	3	0.03		8	0.05	1
North Oregon coast (Nehalem, Trask, Alsea, and Siuslaw Rivers)	0	0.00		0	0.00		0	0.00	
Mid Oregon coast (Umpqua, Coquille, Sixes, and Elk Rivers)	54	0.18	3	3	0.03		1	0.02	3
South Oregon coast (Rogue, Chetco, and Winchuck Rivers)	26	0.16		53	0.10		0	0.00	
Klamath and Trinity Rivers	0	0.00		14	0.07		0	0.00	
North California Coast (Mad, Eel, and Mattole Rivers)	2	0.05		7	0.07		1	0.04	
Sacramento and San Joaquin Rivers	0	0.00		20	0.05		90	0.07	1

	June and August (n=88) Entire study area		
Coho salmon stock group	Est.	SD	CWT
Columbia River	13	0.08	2
North and Mid Oregon coast (Nehalem, Siletz, Alsea, Umpqua, and Coos Rivers)	47	0.10	5
Rogue and Klamath Rivers	40	0.09	1
North California Coast (Mad, Russian, Little, and Scott Rivers)	0	0.00	

	June and August (n=58) Entire study area	
Steelhead trout stock group	Est.	SD
Columbia and Snake Rivers	0	0.00
North and Mid Oregon coast (Nehalem, Siletz, Alsea, Umpqua, Coos, and Coquille Rivers)	1	0.03
South Oregon coast (Elk, Rogue, Chetco, and Winchuck Rivers)	53	0.08
Smith, Klamath, and Trinity Rivers	0	0.00
North California Coast (Mad, Eel, and Ten Mile Rivers)	10	0.05
Sacramento and San Joaquin Rivers	14	0.05
Central and South California Coast (San Lorenzo River and Scott, Pauma, and Gaviota Creeks	3	0.02
Unknown	19	—

hatcheries in the Umpqua River (n=5), Rogue River (n=1), and Columbia River (n=2) were in our study area.

Genetic analysis of steelhead samples showed that a large proportion were from the Rogue River and nearby coastal streams (53%, SD=0.08). Steelhead from the Sacramento and San Joaquin rivers (14%, SD=0.05) and northern California coastal rivers (10%, SD=0.05) were also present. Estimates for steelhead originating from rivers north of Cape Blanco and from south of the San Francisco Bay were near zero. Approximately 19% of the steelhead mixture was not allocated to any source population, suggesting that our baseline data for the species is incomplete. No steelhead in our collections contained CWTs.

Species associations of juvenile salmonids and other species

From cluster analysis of species based on station assemblages (Fig. 6), MRPP of both sample periods showed strong within-group agreement (P<0.0001) at the first level (two groups); all subsequent groups had sequentially higher levels of within-group agreement. As a result, the cutoff level was determined by balancing a lower percent information remaining (<30%) in the model while retaining biologically meaningful groups. For June this cutoff resided at the second level (three groups) and for August, at the third level (four groups). For the June cruise, all salmonids includ-

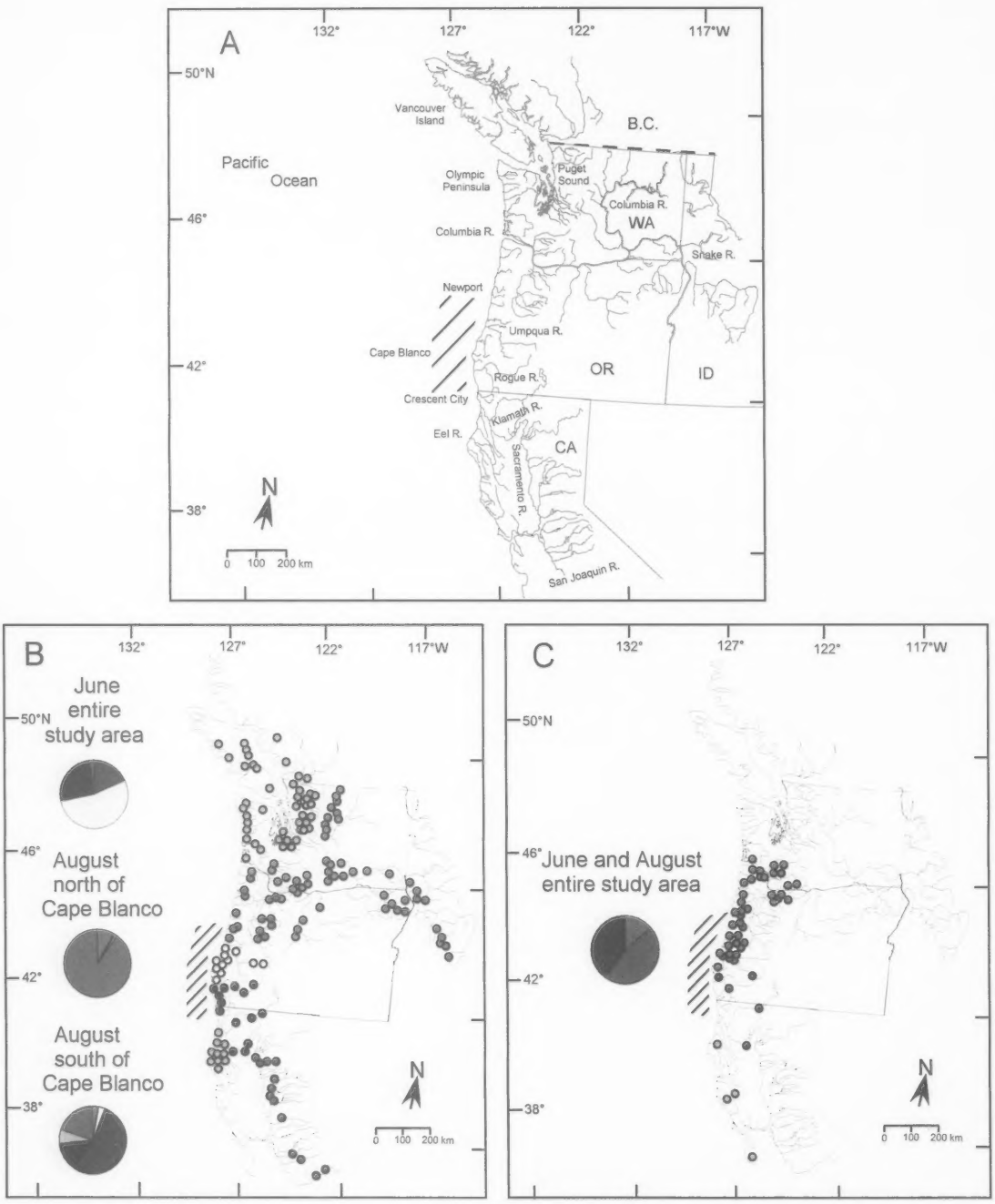

Figure 5

(**A**) Map of study area and location of GLOBEC sampling (hatching). (**B**) Stock compositions of chinook salmon (*Oncorhynchus tshawytscha*). Stock groups are North of Columbia River (grey), Columbia River Basin (green), north Oregon coast (pink), mid Oregon coast (yellow), south Oregon coast (dark blue), Klamath River Basin (black), north California coast (light blue), and Central Valley (red). (**C**) Stock compositions of coho salmon (*O. kisutch*). Stock groups are Columbia River (green), mid and north Oregon coast (dark pink), Rogue and Klamath rivers (blue), and north California coast (orange).

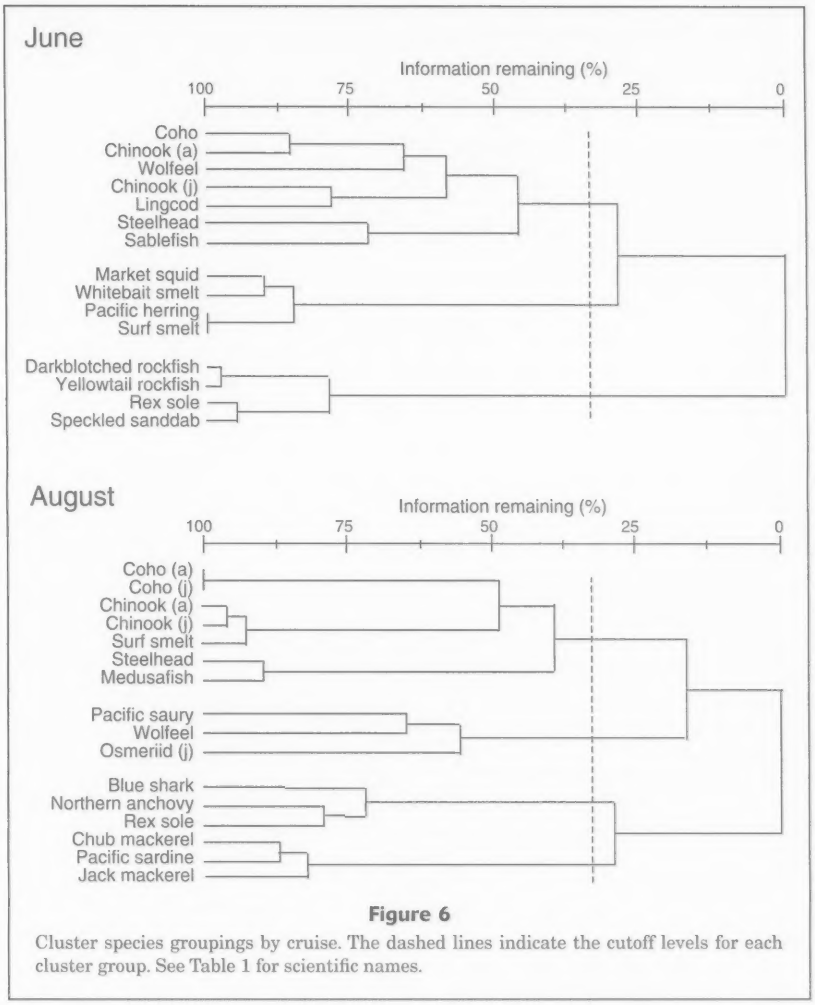

Figure 6

Cluster species groupings by cruise. The dashed lines indicate the cutoff levels for each cluster group. See Table 1 for scientific names.

ing steelhead were classified within the same grouping that included several pelagic juvenile taxa, including wolf-eel, lingcod, and sablefish (Fig. 6). Two other clusters that were not associated with juvenile salmon included a southern inshore group consisting of market squid, Pacific herring, and two species of smelt and an offshore northern group consisting primarily of juvenile rockfish and rex sole. For the August cruise, all salmonid juveniles and adults again clustered together in one large group with surf smelt and medusafish (Fig. 6). The remaining three groups were much smaller and consisted primarily of offshore pelagic species.

Cluster analysis of stations based on species assemblages, and subsequent examination of the cutoff level using MRPP, resulted in three groupings from both sample periods (Fig. 7). MRPP revealed strong within-group agreement for all levels ($P<0.0001$); however, delineation at three groups was based on maintaining lower percent information remaining (<30%) and still having a meaningful level of resolution. There was some measure of geographic separation among the three groups (Fig. 7). In June, group A was predominantly inshore and mostly in the southern half of the sampling area, group B was found mainly in the middle shelf region and was more northern, and group C was found predominantly offshore. In August, group A consisted of only three stations, all south of Cape Blanco, whereas groups B and C both spanned the entire shelf and offshore region and had no particular north-south affinity (Fig. 7). ISA of the groups from both sampling periods showed that only groups A and C had indicator species (Tables 6 and 7), whereas the intermediate groups had none.

Ordination analyses and environmental correlates

NMS ordination of the June sampling period (Fig. 8A) revealed most of the variance in the data: axes 1 and

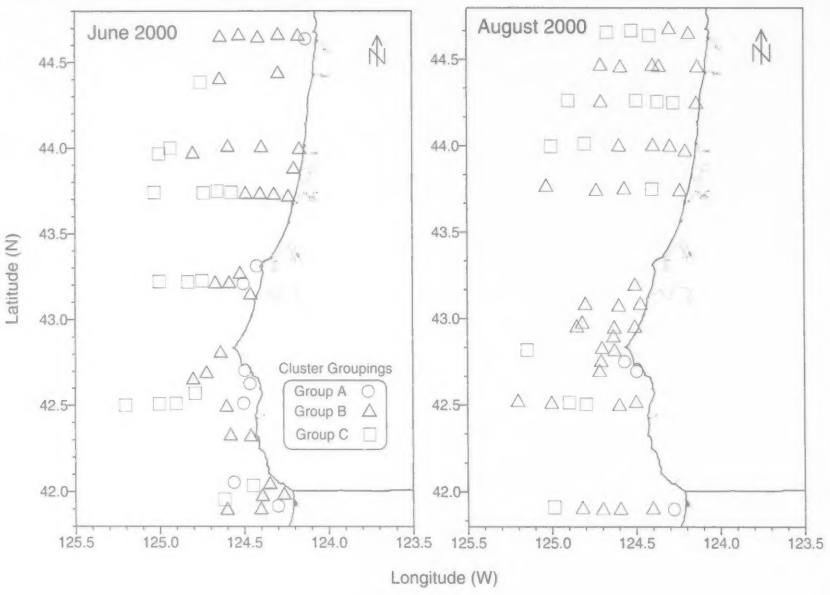

Figure 7

Map showing locations of cluster station groupings by cruise.

Table 6

Indicator species analysis showing indicator values for dominant pelagic nekton captured in pelagic trawls during June 2000 and mean, standard deviations (SD), and *P*-values for each cluster grouping. Cluster Group B did not have any species that were determined to be indicators of that group.

Group	Species	Observed indicator value (IV)	Indicator value IV from randomized groups		
			Mean	SD	*P*-value
A	chinook (age 0.0)	61.0	15.7	6.54	<0.001
A	lingcod	26.1	12.6	5.67	0.024
A	Pacific herring	71.7	12.8	5.88	<0.001
A	surf smelt	86.5	11.8	5.59	<0.001
A	whitebait smelt	31.5	10.4	5.55	0.007
A	market squid	50.8	15.0	6.20	<0.001
C	darkblotched rockfish	66.8	15.8	6.31	<0.001
C	rex sole	46.0	15.0	6.24	0.002
C	sablefish	31.1	16.2	6.32	0.035
C	speckled sanddab	52.5	13.4	5.94	0.001
C	yellowtail rockfish	98.8	19.0	6.30	<0.001

3 represented 31% and 23%, respectively (stress=16.3). Temperature, depth and salinity best explained the ordination of stations, representing a cross shelf gradient from nearshore high levels of salinity to increasing temperature and depth offshore. Ordination of August stations (Fig. 8B) represented 42% of the variance in the data, and 23% of the variance was loaded on axis 2 and 19% on axis 3 (stress=19.4). As with June, salinity increased toward the coast and temperature and depth increased off the shelf. The groups derived from the cluster analysis tended to group together in multivariate space, with the exception of group B in the June cruise (triangles in Fig. 8A).

Table 7

Indicator Species Analysis showing indicator values for dominant pelagic nekton captured in pelagic trawls during August 2000 and mean, standard deviations (SD), and *P*-values for each cluster grouping. Cluster Group B did not have any species that were determined to be indicators of that group.

Group	Species	Observed indicator value (IV)	Indicator value IV from randomized groups		
			Mean	SD	*P*-value
A	chinook (age 1.0)	76.5	21.3	11.18	0.004
A	chinook (age 0.0)	80.4	22.1	11.62	0.003
A	surf smelt	97.9	12.4	8.21	<0.001
C	chub mackerel	33.3	12.8	8.88	0.021
C	jack mackerel	73.7	23.0	11.86	0.006

Table 8

Results of statistical tests for habitat associations between juvenile salmon and environmental or station variables from each cruise in 2000. Fish marked by zeros indicate subyearlings and those marked with one indicate yearlings. Shown are the *P*-levels for 5000 randomizations of the cumulative frequency of the habitat variable and the proportion of the standardized salmon catch associated with each habitat observation. Results are based on the Cramér von-Mises test statistic determined from binned data for depth and neuston biomass. Significance values <0.05 are shown in boldface.

Cruise	Taxon and age	Surface temp.	Surface salinity	1-m chlorophyll	Bottom depth	Neuston biomass
Jun	chinook (age 1.0)	0.30	0.60	0.13	0.18	0.13
	coho (age 1.0)	0.33	0.48	0.21	0.17	0.31
Aug	chinook (age 0.0)	0.36	0.25	0.13	0.35	0.42
	chinook (age 1.0)	**0.04**	**<0.01**	**<0.01**	**0.02**	0.29
	coho (age 1.0)	0.68	**0.04**	0.07	**0.02**	0.45

There were few instances where the habitat associations of juvenile salmon were significantly different from the distribution of environmental variables sampled (Table 8). None of the variables were significant for yearling chinook and coho salmon in the June sampling (no subyearling salmon were caught during that cruise). In August, all the variables except neuston biomass were significant for yearling chinook salmon. These fish were collected at cooler temperatures, higher salinities, higher chlorophyll-*a* concentrations, and at shallower depths than have been typically recorded (Fig. 9). Coho salmon juveniles were found in higher salinities and shallower depths than at the sampled habitat (Fig. 9). These results correlated with the capture of juvenile chinook salmon and to a lesser with extent coho salmon at nearshore stations in the upwelling zone.

Discussion

Understanding the mechanisms underlying the dynamics of multispecies communities is one of the biggest challenges in ecology. Most communities contain many interacting species, each of which is likely to be affected by multiple biotic and abiotic factors. In order to effectively characterize a system, we need to differentiate variability resulting from both temporal and spatial factors. Our observations took place during two time periods of about 20 days each and thus were not synoptic "snapshots" of the system. Indeed, during our June sampling, conditions changed markedly from the beginning to the end of the cruise because of the arrival of an anomalous major southwest storm (Batchelder et al., 2002), which likely completely altered the hydrography and biology of the system. Thus, short-term temporal variability may obscure patterns observed over the spatial scale of our sampling.

The pelagic nekton community sampled during these cruises was not that different from what had previously been shown for purse seine and trawling collections off the coast of Oregon and Washington (Brodeur and Pearcy, 1986; Emmett and Brodeur, 2000; Brodeur et al., 2003). The early summer nekton community was dominated by coastal forage fishes such as smelts and Pacific herring, but also comprised juveniles of many rockfish, sculpin, and flatfish species. These winter-spring spawning species eventually settle out to demersal habitats sometime in summer (Shenker, 1988; Doyle, 1992), which may in part explain the paucity of these taxa in the August cruise. In contrast, the August nekton community consisted of large,

highly migratory species such as Pacific sardines, jack mackerel, and chub mackerel. Pacific sardine, which was almost completely absent from the system in the 1980s, has undergone a substantial resurgence and is now one of the most abundant species off the coast in summer (Brodeur et al., 2000; Emmett and Brodeur, 2000; McFarlane and Beamish, 2001). It should be noted, however, that some of the differences between cruises could be accounted for by the inclusion of substantially more offshore stations during the second cruise. Our results from the community analyses suggest that juvenile salmon tend to co-occur with each other and with a variety of other pelagic nekton, including adult salmon, and that this spatial overlap varies temporally. Brodeur et al. (2003), in analyzing community structure based on previous pelagic sampling data off Oregon and Washington, arrived at similar results. In both studies, the geographic boundaries of the pelagic assemblages often overlap and are not as distinct as demersal assemblages. However, the pelagic environment is much more spatially and temporally heterogeneous than the demersal environment, and many of the species examined in our study are highly mobile and are likely to respond quickly to changing conditions. Research is presently underway to examine the trophic interactions among salmonids and with other sympatric nekton species in order to determine what ecological relationships (e.g. predation, competition), if any, are occurring in this system.

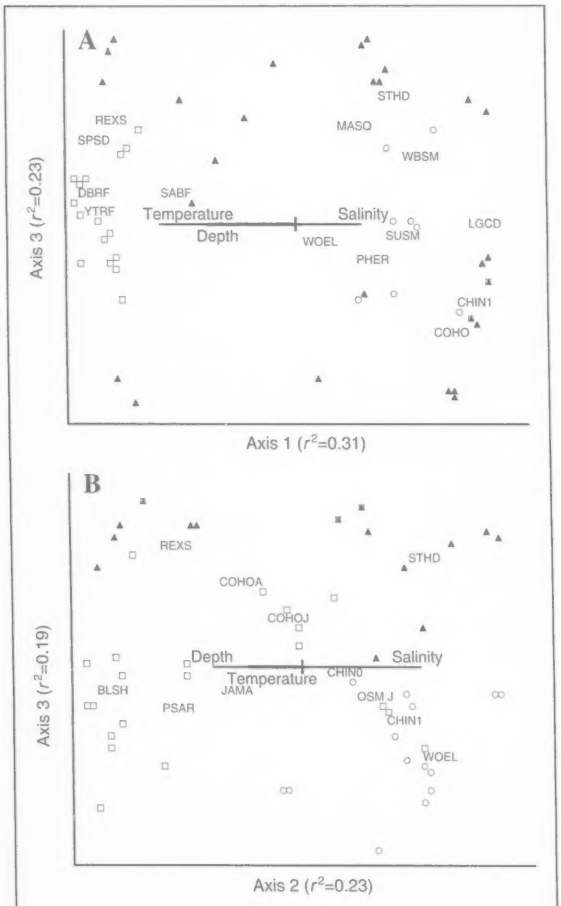

Figure 8

Nonmetric multidimensional scaling (NMS) ordination plot of stations and nekton species with environmental parameters from June (**A**) and August (**B**) 2000 GLOBEC cruises. Station symbols denote: onshore (○), mid-shelf (▲), and slope (□) groupings; Species abbreviations denote the following taxa: CHIN 0 (chinook, age 0), CHIN 1 (chinook, age ≥1.1), STHD (steelhead trout), SUSM (surf smelt), PSAU (Pacific saury), WOEL (wolf-eel juvenile), OSM J (osmerid juvenile), REXS (rex sole, larval), MEDF (medusafish), PSAR (Pacific sardine), JAMA (jack mackerel), CHMA (chub mackerel), NANC (northern anchovy), BLSH (blue shark).

From the results of our sampling, we concluded that juvenile salmonids, with the possible exception of steelhead, occupy the cool, high salinity, inshore upwelling regions off the southern Oregon coast. However, particularly for the June cruise, many of the coho and chinook salmon juveniles collected may have recently entered the ocean with little time to disperse offshore, so that the capture location may not reflect true habitat preferences. Moreover, the vertical dimensions of our trawl also precluded us from sampling the nearshore, subtidal regions where some subyearling chinook may reside shortly after entering the ocean.

Salmon and steelhead differed considerably in stock composition. The pattern for coho salmon was similar to that of chinook salmon in that fish from sources both north and south of Cape Blanco contributed to our catches. However, steelhead from rivers north of Cape Blanco were absent, presumably having migrated offshore and north shortly after entering the sea, as shown by Pearcy et al. (1990). Although our stock composition estimates for steelhead should be viewed with caution because of an incomplete genetic baseline and a relatively small number of samples, our findings support Pearcy et al.'s suggestion that steelhead from rivers south of Cape Blanco have a unique marine distribution and reside throughout the summer in the upwelling zone off northern California and southern Oregon.

Our study revealed seasonal shifts in the abundance and stock composition of juvenile salmonids. Although salmonids comprised small portions of the vertebrate catches of both the June and August cruises, juvenile chinook salmon, coho salmon, and steelhead were much more abundant later in the summer, likely indicating that fish moving into our study area are from shoreline or riverine habitats. The greater abundance of chinook salmon in late summer can be explained in part by the northern migration of fish that originated in rivers south of our study area. Chinook salmon from the Sacramento and San Joaquin rivers in California's Central Valley comprised substantial proportions in the August catches both south (20%) and north (90%) of Cape Blanco. In contrast, the few chinook salmon caught in June were mostly (54%) from streams that enter the sea immediately north of Cape Blanco such as the Umpqua, Coquille, Sixes, and Elk rivers. Chinook salmon

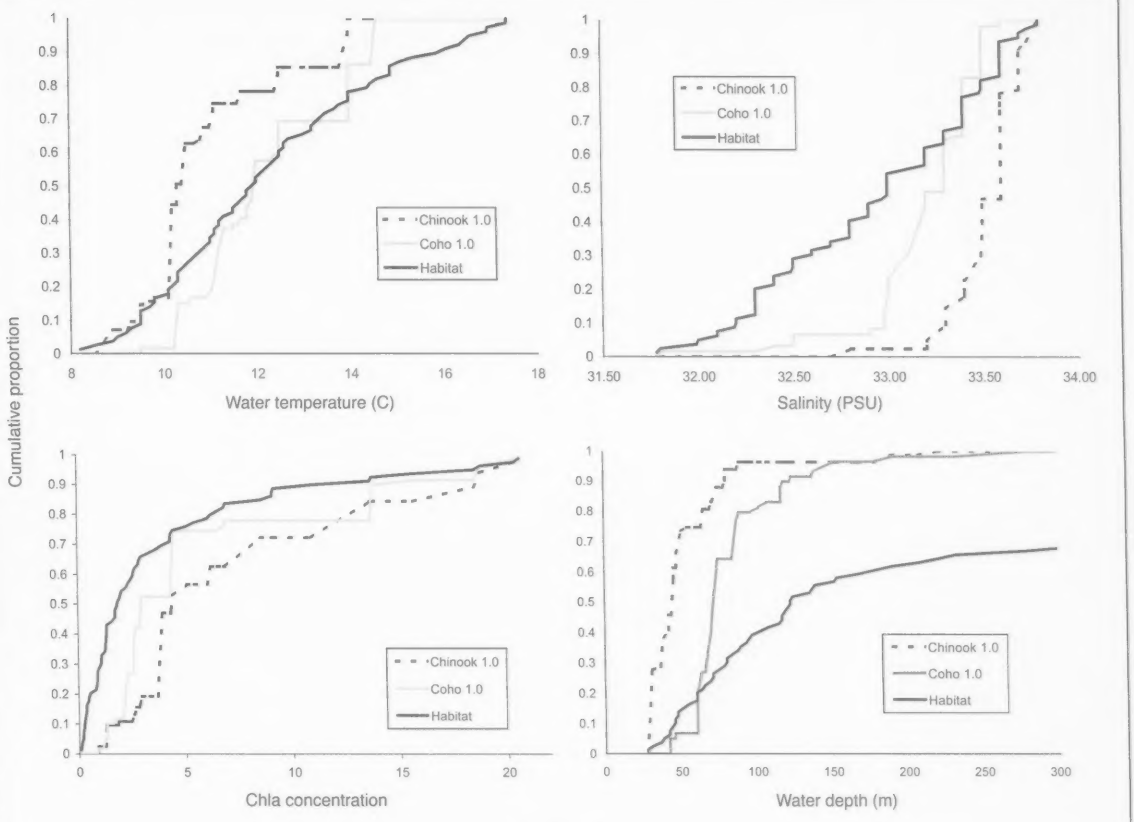

Figure 9

Cumulative distribution curves for salmon and environmental or station variables. Only the August variables that showed at least one significant difference are included. See Table 8 for results of the statistical tests.

from these rivers are known to primarily migrate north of our study area along the coast (Nicholas and Hankin, 1988). By August, fish from these stocks were nearly absent from our samples. Oregon rivers south of Cape Blanco, an area that includes the Rogue, Chetco, and Winchuck rivers, produce chinook salmon with a more southerly pattern of ocean migration (Nicholas and Hankin, 1988; Myers et al., 1998). Chinook salmon from these rivers were found throughout the summer and contributed 53% to our largest catches of chinook salmon along transects south of Cape Blanco in August.

Results from our 2000 GLOBEC cruises identified Cape Blanco as an important breakpoint in salmonid life-history variation. Stock distributions of both juvenile salmon and steelhead indicated that different migration patterns of fish originating from southern and northern rivers are evident during their early marine phase. Our August survey also revealed sharp contrasts in life-history type and freshwater origin between the juvenile chinook salmon population in the marine area north of Cape Blanco and that to the south. Chinook salmon captured north of Cape Blanco were nearly all yearlings and largely from the Sacramento River drainage. Subyearlings predominated in our catches south of Cape Blanco and included a much larger proportion of fish from coastal streams in southern Oregon and northern California.

Comparisons of our results with similar studies conducted further north show differences in salmonid migrations on a somewhat broader geographic scale. In several years of sampling during the summers of 1981 through 1985 off the central Oregon to northern Washington coast, most juvenile chinook salmon bearing CWTs were from Columbia River hatcheries (Pearcy and Fisher, 1990; Fisher and Pearcy, 1995). Only one tagged chinook salmon from a river south of Cape Blanco (Klamath River) was captured. Pearcy and Fisher also found that juvenile coho salmon were largely from the Columbia River and that smaller contributions were from coastal rivers north of Cape Blanco. Their findings have been corroborated by more recent surveys in the same region (Emmett and Brodeur, 2000) using genetic

data (Teel et al., 2003). Samples from subsequent cruises will be used to examine the persistence of such fine- and broad-scale geographic structure in the juvenile migrations of salmonid stocks.

A major source of error in our estimates of growth rates of juvenile coho salmon back-calculated from scales was uncertainty of when individual fish entered the ocean. We used a single date of ocean entry for all fish (15 May), but individual fish, of course, entered the ocean at different times over the course of a month or more. Consequently, coefficients of variation were relatively large (84–119% and 75–120% of mean growth rate in FL and weight, respectively) for fish caught in May and June, when errors in estimated growth periods likely were large in relation to the actual growth periods. Conversely, coefficients of variation were relatively small (14–30% and 10–26% of growth rate in FL and weight, respectively) for fish caught in August or September, when errors in estimated growth periods likely were small in relation to the actual growth periods. (Note the decrease in standard deviation of mean growth rates with month of capture in Tables 3 and 4A). Growth rates of CWT coho salmon between hatchery release and capture in the ocean (Table 4B) were very similar to the growth rates of unmarked salmon estimated from scales for the same months and areas. In addition, the growth rates of the former group (CWT coho salmon) helped to validate the growth rates of the latter group (Table 4A).

Significant differences in growth and condition of juvenile coho salmon indicate that different oceanographic environments exist north and south of Cape Blanco. The length of the fish indicated that substantial growth occurred in juvenile coho salmon during the study period. Assessment of other growth features (condition) revealed that juvenile coho salmon grew better north of Cape Blanco. Because we included measurement of condition in both the June and August period in the evaluation, changes in stock composition, described earlier, may be partly responsible for this observation. Although genetic stock composition was different between months, month of sampling was not a significant factor, suggesting that stock composition is not likely a significant factor affecting the difference in condition (a performance metric) of juvenile salmon north and south of Cape Blanco.

Several lines of evidence further support the hypothesis that areas north of Cape Blanco benefit juvenile yearling chinook and coho salmon. There were greater numbers of juvenile yearling chinook and coho salmon to the north of Cape Blanco. Although our overall sampling effort was greater north of Cape Blanco, in the mesoscale portion of our survey designed to assess general distribution patterns, more yearling chinook and coho salmon were captured north of Cape Blanco. Secondly, when we evaluated the growth rate of juvenile coho salmon in the GLOBEC region compared to juveniles captured off northern Oregon and Washington, juveniles from the GLOBEC region grew much better. The similar tracking of resource (distribution and abundance) and performance (measured in terms of either somatic and energetic growth or growth rate) metrics for juvenile yearling chinook salmon and coho salmon north of Cape Blanco suggests that habitat quality in this region was better. The results of this study help define the biogeographical zones for salmon growth and establish regional-based management strategies for depleted salmon stocks.

Acknowledgments

We thank the captain and crew of the FV *Sea Eagle* for their expert help in conducting the trawling operations under sometimes adverse weather conditions. We are grateful to Jackie Popp-Noskov, Paul Bentley, Marcia House, and Becky Baldwin for assistance in field sampling. Donald Van Doornik and David Kuligowski collected the genetic data. We thank Anne Marshall for the use of unpublished chinook salmon allele frequency data. Stephen Smith and Alex De Robertis helped with the statistical analysis. Earlier versions of this manuscript were improved by the helpful comments of two anonymous journal reviewers. Research was conducted as part of the U.S. GLOBEC program and was jointly funded by the National Science Foundation (Grant no. OCE-0002855) and the National Oceanic and Atmospheric Administration (NOAA). We also acknowledge the Bonneville Power Administration for funding the plume study.

Literature cited

Aebersold, P. B., G. A. Winans, D. J. Teel, G. B. Milner, and F. M. Utter.
1987. Manual for starch gel electrophoresis: a method for the detection of genetic variation. NOAA Tech. Rep. NMFS 61, 19 p.

Batchelder, H. P., J. A.Barth, M. P. Kosro, P. T. Strub, R. D. Brodeur, W. T. Peterson, C. T. Tynan, M. D. Ohman, L. W. Botsford, T. M. Powell, F. B. Schwing, D. G. Ainley, D. L. Mackas, B. M. Hickey, and S. R. Ramp.
2002. The GLOBEC Northeast Pacific California Current System program. Oceanogr. 15:36–47.

Barth, J. A., S. D. Pierce, and R. L. Smith.
2000. A separating coastal upwelling jet at Cape Blanco, Oregon and its connection to the California Current System. Deep-Sea Res. 47(part II):783–810.

Bradford, M. J.
1995. Comparative review of Pacific salmon survival rates. Can. J. Fish. Aquat. Sci. 52:1327–1338.

Brodeur, R. D., P. J. Bentley, R. L. Emmett, T. Miller, and W. T. Peterson.
2000. Sardines in the ecosystem of the Pacific Northwest. Proc. sardine 2000 symposium. Pacific States Marine Fish. Comm., p. 90–102. [Available from Pacific States Marine Fisheries Commission, Portland, OR.]

Brodeur, R. D., J .P. Fisher, Y. Ueno, K. Nagasawa, and W. G. Pearcy.
2003. An east-west comparison of the Transition Zone coastal pelagic nekton of the North Pacific Ocean. J. Oceanog. 59(4):415–434.

Brodeur, R. D., H. V. Lorz, and W. G. Pearcy.
1987. Food habits and dietary variability of pelagic nekton off Oregon and Washington, 1979–1984. NOAA Tech. Rep. NMFS 57, 32 p.

Brodeur, R. D., and W. G. Pearcy.
1986. Distribution and relative abundance of pelagic non-

salmonid nekton off Oregon and Washington, 1979–1984. NOAA Tech. Rep. NMFS 46, 85 p.

1992. Effects of environmental variability on trophic interactions and food web structure in a pelagic upwelling ecosystem. Mar. Ecol. Prog. Ser. 84:101–119.

Busby, P. J., T. C. Wainwright, G. J. Bryant, L. Lierheimer, R. S. Waples, F. W. Waknitz, and I. V. Lagomarsino.

1996. Status review of west coast steelhead from Washington, Idaho, Oregon, and California. NOAA Tech. Memo. NMFS-NWFSC-27, 261 p.

Dawley, E. M., R. D. Ledgerwood, and A. Jensen.

1985. Beach and purse seine sampling of juvenile salmonids in the Columbia River estuary and ocean plume, 1977–1983. Vol. 1, Procedures, sampling effort, and catch data. NOAA Tech. Memo. NMFS F/NWC-74, 260 p.

Debevec, E. M., R. B. Gates, M. Masuda, J. Pella, J. Reynolds, and L. W. Seeb.

2000. SPAM (Version 3.2): Statistics program for analyzing mixtures. J. Hered. 91:509–511.

Doyle, M. J.

1992. Neustonic ichthyoplankton in the northern region of the California Current ecosystem. Calif. Coop. Oceanic Fish. Invest. Rep. 33:141–161.

Emmett, R. L., and R. D. Brodeur.

2000. The relationship between recent changes in the pelagic nekton community off Oregon and Washington and physical oceanographic conditions. Bull. North Pac. Anadr. Fish. Comm. 2:11–20.

Fisher, J. P., and W. G. Pearcy.

1988. Growth of juvenile coho salmon (*Oncorhynchus kisutch*) off Oregon and Washington, USA in years of differing coastal upwelling. Can. J. Fish. Aquat. Sci. 45: 1036–1044.

1995. Distribution, migration, and growth of juvenile chinook salmon, *Oncohychus tshawytscha*, off Oregon and Washington. Fish. Bull. 93:274–289.

Francis, R. C., and S. R. Hare.

1994. Decadal-scale regime shifts in large marine ecosystems of the Northeast Pacific: a case for historical science. Fish. Oceanogr. 3:279–291.

Friedland, K. D., and R. E. Haas.

1996. Marine post-smolt growth and age at maturity of Atlantic salmon. J. Fish Biol. 48:1–15.

Gauch, H. G., Jr.

1982. Multivariate analysis in community ecology. Cambridge Univ. Press, N.Y. 298 p.

Hare, S. R., N. J. Mantua, and R. C. Francis.

1999. Inverse production regimes: Alaska and West Coast salmon. Fisheries 24:6–14.

Hinch, S. G., M. C. Healey, R. E. Diewert, K. A.Thomson, R. Hourston, M. A. Henderson, and F. Juanes.

1995. Potential effects of climate change on marine growth and survival of Fraser River sockeye salmon. Can. J. Fish. Aquat. Sci. 52:2651–2659.

Jakob, E. M., S. D. Marshall, and G. W. Uetz.

1996. Estimating fitness: a comparison of body condition indices. Oikos 77: 61–67.

Kope, R., and T. Wainwright.

1998. Trends in the status of Pacific salmon populations in Washington, Oregon, California, and Idaho. North Pac. Anadr. Fish. Comm. Bull. 1:1–12.

Kruskal, J. B.

1964. Nonmetric multidimensional scaling: a numerical method. Psychometricka 29:115–129.

Lawson, P. W.

1993. Cycles in ocean productivity, trends in habitat quality, and the restoration of salmon runs in Oregon. Fisheries 18:6–10.

Lorenzen, K.

1996. The relationship between body weight and natural mortality in juvenile and adult fish: A comparison of natural ecosystems and aquaculture. J. Fish Biol. 49: 627–647.

Mantua, N. J., S. R. Hare, Y. Zhang, J. M. Wallace, and R. C. Francis.

1997. A Pacific interdecadal oscillation with impacts on salmon production. Bull. Am. Meteorol. Soc. 78: 1069–1079.

Marschall, E. A., and L. B. Crowder.

1995. Density-dependent survival as a function of size in juvenile salmonids in streams. Can. J. Fish. Aquat. Sci. 52:136–140.

McCune, B., and J. B. Grace.

2002. Analysis of ecological communities, 300 p. MjM Software Design, Gleneden Beach, OR.

McCune, B., and M. J. Mefford.

1999. PC-ORD, multivariate analysis of ecological data, users guide, 237 p. MjM Software Design, Gleneden Beach, OR.

McFarlane, G. A., and R. J. Beamish.

2001. The re-occurrence of sardines off British Columbia characterises the dynamic nature of regimes. Prog. Oceanogr. 49:151–165.

McGowan, J. A., D. B. Chelton, and A. Conversi.

1999. Plankton patterns, climate, and change in the California Current. *In* Large marine ecosystems of the Pacific Rim: assessment, sustainability, and management (K. Sherman and Q. Tang, eds.), p. 63–105. Blackwell Science, Malden, MA.

McGurk, M. D.

1996. Allometry of marine mortality of Pacifc salmon. Fish. Bull. 94:77–88.

Milner, G. B., D. J. Teel, F. M. Utter, and G. A. Winans.

1985. A genetic method of stock identification in mixed populations of Pacific salmon, *Oncorhynchus* spp. Mar. Fish. Rev. 47:1–8.

Myers, J. M., R. G. Kope, G. J. Bryant, D. J. Teel, L. J. Lierheimer, T. C. Wainwright, W. S. Grant, F. W. Waknitz, K. Neely, S. T. Lindley, and R. S. Waples.

1998. Status review of chinook salmon in Washington, Idaho, Oregon, and California. NOAA Tech. Memo. NMFS-NWFCS-35, 443 p.

Nehlsen, W., J. E. Williams, and J. A. Lichatowich.

1991. Pacific salmon at the crossroads: stocks at risk from California, Oregon, Idaho, and Washington. Fisheries 16: 4–21.

Nicholas, J. W., and D. G. Hankin.

1988. Chinook salmon populations in Oregon coastal river basins: Description of life histories and assessment of recent trends in run strengths. Oregon Department of Fish and Wildlife, Fish Division Information Report 88-1, 359 p.

Paul, A. J., and T. M. Willette.

1997. Geographical variation in somatic energy content of migrating pink salmon fry from PWS: a tool to measure nutritional status. *In* Proceedings of the international symposium on the role of forage fishes in marine ecosystems. Alaska Sea Grant College Program, Report 97-01, p. 707–720. Univ. Alaska, Fairbanks, AK.

Pearcy, W. G.

1992. Ocean ecology of North Pacific salmonids, 179 p. Univ. Washington Press, Seattle, WA.

Pearcy, W. G., R. D. Brodeur, and J. P. Fisher.

1990. Distribution and biology of juvenile cutthroat trout

(*Oncorhynchus clarki clarki*) and steelhead (*O. mykiss*) in coastal waters off Oregon and Washington. Fish. Bull. 88: 697–711.

Pearcy, W. G., and J. P. Fisher.
1988. Migrations of coho salmon, *Oncorhynchus kisutch*, during their first summer in the ocean. Fish. Bull. 86: 173–195.
1990. Distribution and abundance of juvenile salmonids off Oregon and Washington, 1981–1985. NOAA Tech. Rep. NMFS 93:1–83.

Pella, J., and G. B. Milner.
1987. Use of genetic marks in stock composition analyses. *In* Population genetics and fishery management, (N. Ryman and F. Utter, eds.), p. 247–276. Washington Sea Grant, Univ. Washington Press, Seattle, WA.

Perry, R. I., B. Hargreaves, B. J. Waddell, and D. L. Mackas.
1996. Spatial variations in feeding and condition of juvenile pink and chum salmon off Vancouver Island, British Columbia. Fish. Oceanogr. 5:73–88.

Perry, R. I., and S. J. Smith.
1994. Identifying habitat associations of marine fishes using survey data: an application to the Northwest Atlantic. Can. J. Fish. Aquat. Sci. 51:589–602.

Peterson, W. T., and J. E. Keister.
2002. The effect of a large cape on distribution patterns of coastal and oceanic copepods off Oregon and northern California during the 1998-1999 El Niño-La Niña. Prog. Oceanogr. 53:389–411.

Post, J. R., and E. A. Parkinson.
2001. Energy allocation strategy in young fish: allometry and survival. Ecology 82:1040–1051.

Ricker, W. E.
1992. Back-calculation of fish lengths based on proportionality between scale and length increments. Can. J. Fish. Aquat. Sci. 49:1018–1026.

Shenker, J. M.
1988. Oceanographic associations of neustonic larval and juvenile fishes and Dungeness crab megalopae off Oregon. Fish. Bull. 86:299–317.

Sutton, S. G., T. P. Bult, and R. L. Haedrich.
2000. Relationship among fat weight, body weight, water weight, and condition factors in wild Atlantic salmon parr. Trans. Am. Fish. Soc. 129:527–538.

Syrjala, S. E.
1996. A statistical test for a difference between the spatial distributions of two populations. Ecology 77:75-80.

Teel, D. J., D. M. Van Doornik, D. R. Kuligowski, and W. S. Grant.
2003. Genetic analysis of juvenile coho salmon (*Oncorhynchus kisutch*) off Oregon and Washington reveals few Columbia River wild fish. Fish. Bull. 101:640–652.

U.S. GLOBEC.
1994. A science plan for the California Current. U.S. GLOBEC Rep. 11, 134 p. Univ. California, Berkeley, CA.

Weitkamp, L., and K. Neely.
2002. Coho salmon (*Oncorhynchus kisutch*) ocean migration patterns: insight from marine coded-wire tag recoveries. Can. J. Fish. Aquat. Sci. 59:1100–1115.

Weitkamp, L. A., T. C. Wainright, G. J. Bryant, G. B. Milner, D. J. Teel, T. G. Kope, and R. S. Waples.
1995. Status review of coho salmon from Washington, Oregon, and California. NOAA Tech. Memo. NMFS-NWFSC-24, 258 p.

Appendix Table 1

Summary of releases of coho salmon smolts in 2000 by region. This summary of releases of all hatchery coho salmon smolts by region was calculated from data in the Pacific States Marine Fisheries Commission Regional Mark Information System (http://www.rmis.org/ [accessed 5 April 2003]) and in USFWS 2001 (see Footnote 2 in the general text).

	No. of release groups	Total fish released	Release weight (g)	
			Marked	mean (SD)
All British Columbia	250	13,612,715	71.4%	19.6 (5.7)
Washington: St. Juan de Fuca, Puget Sound, Skagit River, Nooksack River, etc.	83	15,316,299	86.4%	29.1 (19.7)
Washington:				
North of Columbia River to Cape Flattery	63	7,630,257	76.7%	31.6 (5.3)
Columbia River	140	29,879,137	89.0%	32.0 (6.4)
Oregon Coast north of Cape Blanco	14	809,962	95.6%	41.6 (7.4)
Southern Oregon and Northern California: Rogue, Klamath, and Trinity Rivers	5	745,060	99.8%[1]	42.1 (4.4)

[1] 100% of the fish released from Klamath and Trinity Rivers were clipped on the maxillary.

Spatial and temporal variation in the diet of the California sea lion (*Zalophus californianus*) in the Gulf of California, Mexico

Francisco J. García-Rodríguez
David Aurioles-Gamboa
Centro Interdisciplinario de Ciencias Marinas-Instituto Politécnico Nacional
Departamento de Biología Marina y Pesquerías
Apdo. Postal 592
La Paz, Baja California Sur, México
E-mail address (for F. J. García-Rodríguez): fjgrodri@cibnor.mx

Abstract—Between June 1995 and May 1996 seven rookeries in the Gulf of California were visited four times in order to collect scat samples for studying spatial and seasonal variability California sea lion prey. The rookeries studied were San Pedro Mártir, San Esteban, El Rasito, Los Machos, Los Cantiles, Isla Granito, and Isla Lobos. The 1273 scat samples collected yielded 4995 otoliths (95.3%) and 247 (4.7%) cephalopod beaks. Fish were found in 97.4% of scat samples collected, cephalopods in 11.2%, and crustaceans in 12.7%. We identified 92 prey taxa to the species level, 11 to genus level, and 10 to family level, of which the most important were Pacific cutlassfish (*Trichiurus lepturus*), Pacific sardine (*Sardinops caeruleus*), plainfin midshipman (*Porichthys* spp.), myctophid no. 1, northern anchovy (*Engraulis mordax*), Pacific mackerel (*Scomber japonicus*), anchoveta (*Cetengraulis mysticetus*), and jack mackerel (*Trachurus symmetricus*). Significant differences were found among rookeries in the occurrence of all main prey ($P \leq 0.04$), except for myctophid no. 1 ($P > 0.05$). Temporally, significant differences were found in the occurrence of Pacific cutlassfish, Pacific sardine, plainfin midshipman, northern anchovy, and Pacific mackerel ($P < 0.05$), but not in jack mackerel ($\chi^2 = 2.94$, df=3, $P = 0.40$), myctophid no. 1 ($\chi^2 = 1.67$, df= 3, $P = 0.64$), or lanternfishes ($\chi^2 = 2.08$, df=3, $P = 0.56$). Differences were observed in the diet and in trophic diversity among seasons and rookeries. More evident was the variation in diet in relation to availability of Pacific sardine.

Manuscript approved for publication 9 October 2003 by Scientific Editor.
Manuscript received 20 October 2003 at NMFS Scientific Publications Office.
Fish. Bull. 102:47–62 (2004).

The population of the California sea lion (*Zalophus californianus*), in the Gulf of California numbers approximately 23,000 individuals, 82% of which inhabit the northern region of the gulf above latitude 28° (Aurioles-Gamboa and Zavala-González, 1994). In this region are found the most important reproductive areas and the highest pup production of the Gulf. Aurioles-Gamboa and Zavala-González (1994) suggested that the high concentration of animals in this region is related to high abundance of pelagic fish such as Pacific sardine (*Sardinops caeruleus*) (also known as South American pilchard, FAO), Pacific mackerel (*Scomber japonicus*), Pacific thread herring (*Opisthonema libertate*), and anchoveta (*Cetengraulis mysticetus*) (Cisneros-Mata et al., 1987[1]; Cisneros-Mata et al., 1991[2]; Cisneros-Mata et al., 1997[3]).

Despite the importance of the northern gulf region, feeding studies of the California sea lion at Gulf of California rookeries have been few and have been conducted at different time periods. Researchers have studied sea lion diet in Los Islotes (Aurioles-Gamboa et al., 1984; García-Rodríguez, 1995), Los Cantiles (Isla Angel de la Guarda), Isla Granito (Sánchez-Arias, 1992; Bautista-Vega, 2000), and Isla Racito (Orta-Dávila, 1988). These studies have shown that sea lions consume a variety of prey and that differences exist between the diet of sea lions found at different rookeries within the Gulf of California. At Los Islotes, the most important prey were cusk eel (*Aulopus bajacali*), bigeye bass (*Pronotogrammus eos*), threadfin bass (*Pronotogrammus multifasciatus*), and splitail bass (*Hemanthias* sp.) (Aurioles-Gamboa et al., 1984; García-Rodríguez, 1995). At Los Cantiles and Isla Granito important prey were lanternfish (*Diaphus* sp.), northern anchovy (*Engraulis mordax*), Pacific cutlassfish (*Trichiurus nitens*), shoulderspot (*Caelorinchus scaphopsis*), and Pacific whiting (*Merluccius productus*) (Sanchez-Arias, 1992; Bautista-Vega, 2000), whereas at Isla Racito, important prey were Pacific sardine (*Sardinops caeruleus*), Pacific mackerel (*Scomber japonicus*), grunt (*Haemulopsis* spp.), rockfish (*Sebastes*

[1] Cisneros-Mata, M. A., J. P. Santos-Molina, J. A. De Anda M., A. Sánchez-Palafox, and J. J. Estrada. 1987. Pesquería de sardina en el noroeste de México (1985/86). Informe Técnico, 79 p. Centro Regional de Investigaciones Pesqueras de Guaymas. INP. SEPESCA. Calle 20 No. 605 Sur Col. La Cantera. Guaymas, Son. CP. 85400.

[2] Cisneros-Mata, M. A., M. O. Nevarez-Martínez, G. Montemayor-López, J. P. Santos-Molina, and R. Morales-Azpeitia. 1991. Pesquería de sardina en el Golfo de California de 1988/89–1989/90. Informe Técnico, 80 p. Centro Regional de Investigaciones Pesqueras de Guaymas. INP. SEPESCA. Calle 20 No. 605 Sur Col. La Cantera. Guaymas, Son. CP. 85400.

[3] Cisneros-Mata, M. A., M. O. Nevárez-Martínez, M. A. Martínez-Zavala, M. L. Anguiano-Carranza, J. P. Santos-Molina, A. R. Godínez-Cota, and G. Montemayor-López. 1997. Diagnosis de la pesquería de pelágicos menores del Golfo de California de 1991/92 a 1995/96. Informe Técnico, 59 p. Centro Regional de Investigaciones Pesqueras de Guaymas. INP. SEMARNAP. Calle 20 No. 605 Sur Col. La Cantera. Guaymas, Son. CP. 85400.

spp.), and Pacific whiting (*Merluccius* spp.) (Orta-Dávila, 1988).

Some California sea lion prey are important fisheries resources in Mexico. The Pacific sardine, for example, is the target of a fishery begun in 1967 and which, along with the northern anchovy, contributed to most of the volume of the catch (200,870 t during the 1995–96 season) obtained in the Gulf (Cisneros-Mata et al.[3]). The central and northern regions of the Gulf of California harbor the greatest abundance of sea lions and schooling fishes, such as the sardine and anchovy. Because of this, knowledge of sea lion feeding habits and their temporal and spatial variability is relevant to understanding the potential interaction between sea lions and fisheries in the area (Orta-Dávila, 1988; Sánchez-Arias, 1992; Bautista-Vega, 2000).

In this article, we present the results of concurrent diet studies conducted at various rookeries and haulout areas of sea lions in the northern rookeries of the Gulf of California to examine the prey consumed, and spatial and temporal variability in their diet.

Materials and methods

Scat samples of California sea lions were collected at Isla San Pedro Mártir (SPM, 28°24′00″N, 112°25′3″W), Isla San Esteban (EST, 28°42′00″N, 112°36′00″W), Isla Rasito (RAS, 28°49′30″N, 112°59′30″W), Isla Granito (GRA, 29°34′30″N, 113°32′15″W), Isla Lobos (LOB, 30°02′30″N, 114°, 28′30″W), and at two colonies of Isla Angel de la Guarda known as Los Machos (MAC, 29°20′00″N, 113°30′00″W), and Los Cantiles (CAN, 29°32′00″N, 113°29′00″W, Fig. 1). The total number of California sea lions in these seven rookeries was approximately 15,000 animals (that were hauled out) of which about 12.2% inhabit San Pedro Mártir, 34.7% San Esteban, 2.8% El Rasito, 10.0% Los Machos, 8.7% Los Cantiles, 11.0% Isla Granito, and 20.6% Isla Lobos (Aurioles-Gamboa and Zavala-González, 1994). All the animals were spread out along the shoreline of each island, except at Isla Angel de la Guarda, where they were clustered within two areas: Los Cantiles, on the eastern shoreline and Los Machos on the western shoreline.

Scat samples were obtained at reproductive and nonreproductive haulout areas between June 1995 and May 1996. At El Rasito, sampling was done only at one reproductive area; fresh and dried samples were collected (Fig. 2). If for any reason a scat was not collected (because it was found in pieces or in poor condition), it was destroyed and the site was cleared to avoid collection during subsequent trips. All fresh and dried samples collected were pooled to represent each sampling period. We assumed that the diet information corresponded to a time period close to the collection trip, but some dried scats could have been deposited shortly after the last collection.

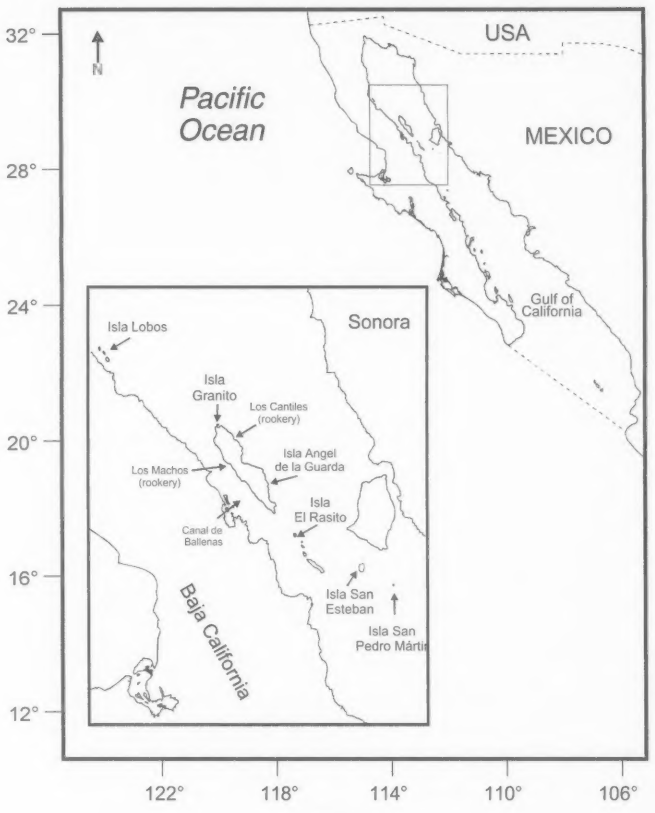

Figure 1

Map of Baja California showing location of California sea lion rookeries that were studied in the Gulf of California.

Scats were stored in plastic bottles and then dried shortly thereafter to prevent decomposition of fish otoliths and other hard parts (which were used in subsequent prey identification) until the scats could be processed at a later date. The samples were processed by soaking in a weak biodegradable detergent solution for 1 to 7 days before being sifted through nested sieves of 2.00-, 1.18-, and 0.5-mm mesh size. Fish bones and scales, eye lenses of fish and squid, otoliths, cephalopod beaks, and crustacean fragments were extracted from the samples. Cephalopod beaks were stored in 70% ethanol, and the other items were dried and stored in vials. Sagittal otoliths and cephalopod beaks were used to identify teleost fish and cephalopods, respectively. Identifications were made by using photographs and diagrams from Clarke (1962), Fitch (1966), Fitch and Brownell (1968), and Wolff (1984), as well as voucher specimen material from the 1) Center Interdisciplinario de Marinas Ciencias (CICIMAR), 2) Instituto Tecnólogico y de Estudios Superiores de Monterrey, Guaymas, 3) Los Angeles County Museum of Natural History, California, and 4) Centro de Investigación Científica y de Educación Superior de Ensenada (CICESE), Baja California, Mexico. Prey species identifed to family level were coded by using

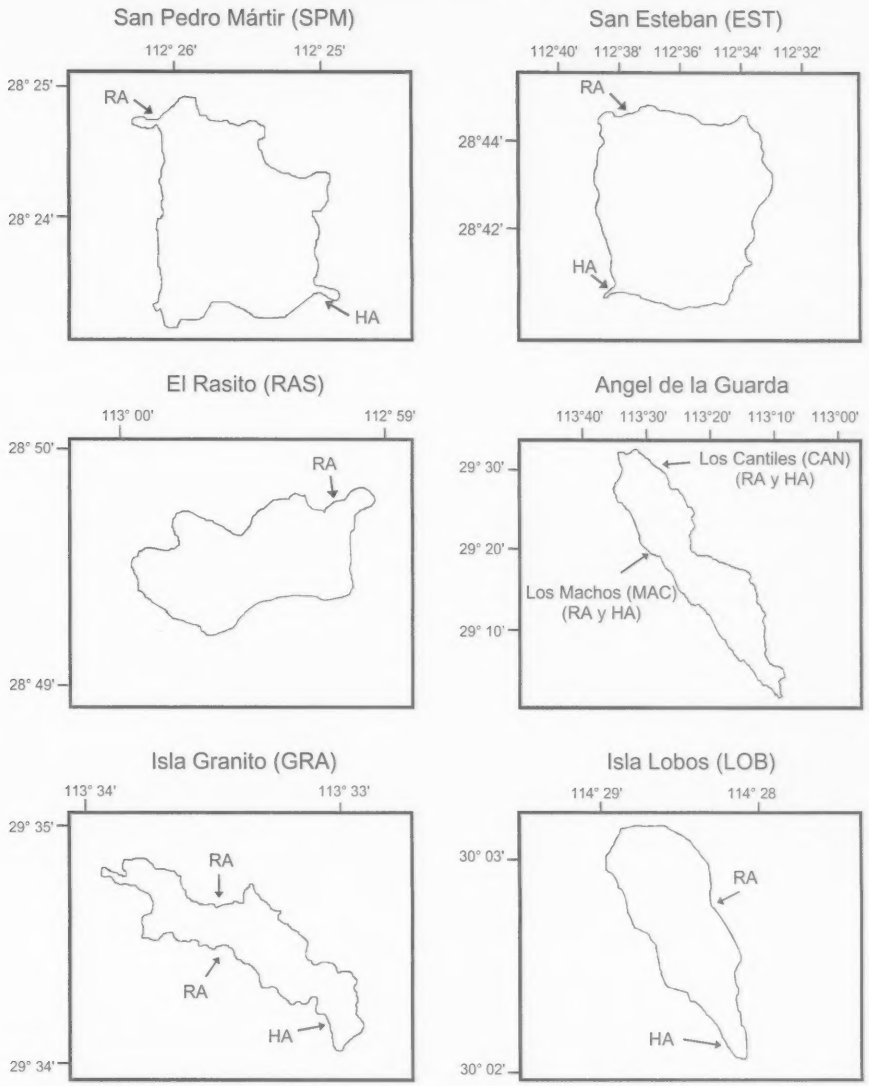

Figure 2

Location of sites where samples of California sea lion scats were collected at each island. RA = reproductive area; HA = haulout area.

the family name plus a sequential number. Otoliths from prey species that were not identified to species, genus, or family level were coded with "fish species" plus a number.

Three indices were used to describe the diet of sea lions. Percent number (PN) represents the percentage of the number of individuals for each prey taxon over the total number of individuals found in all scat samples. Percent of occurrence (PO) represents the percentage of scats having a given prey taxon and indicates the percentage of the population that is consuming a particular prey species. The third index, index of importance (IIMP) incorporates PN and PO and is defined as

$$\mathrm{IIMP}_i = \frac{1}{U}\sum_{j=1}^{U}\frac{X_{ij}}{X_j}, \qquad (1)$$

where x_i = number of individuals of taxon i in scat j;
X_j = total number of individuals from all taxa found in scat j; and
U = total number of samples with prey.

The IIMP, developed for scat analysis (García-Rodríguez, 1999), was used to determine the importance of prey species, their spatial and temporal variation in the diet,

diversity of prey estimates, and measures of similarity among rookeries. Crustaceans were not incorporated into the IIMP index because it was not possible to quantify the number of individuals in the samples.

We used the IIMP Index because it is less sensitive to changes in the number of prey in an individual scat compared to PN. For example, if a scat contains a single prey taxon, the IIMP does not change regardless of the number of individuals of that taxon, in that scat. However, as one increases the number of individuals of a given prey taxon in the scat, the PN will also increase for that prey. The IIMP allows each scat to contribute an equal amount of information, whereas PN can be dominated by a few scats with a large number of a single prey-taxon otoliths. In this manner the IIMP is similar to the split-sample frequency of ocurrence (SSFO) index, developed by Olesiuk (1993), where each scat is treated as a sampling unit and does not assume, as does PN, that the distribution of prey hard parts between scats is uniform. However, with the SSFO index, each prey taxon in a given scat is given an equal weight for that scat. If only one species occurs in a sample, its occurrence is scored as 1, if two species occur, each occurrence is scored as 0.5, and so forth (Olesiuk, 1993). The IIMP index incorporates more information than the SSFO index, regardless of the number of individuals of each taxon in the scat.[4]

Percent number (PN) was used only to show differences between broad prey groups (fishes and cephalopods) and PO was used to review the temporal and spatial changes from each main prey (those with average IIMP of at least 10% at any rookery). For all estimations, a single otolith (right or left) or single cephalopod beak (upper or lower) represented one individual prey. We tested the hypothesis that the occurrence of the main prey was independent of the rookery and of the date collection using contingency tables and an estimator of chi-square (χ^2) (Cortés, 1997).

Total length of the otoliths (mm) and the linear equation obtained by Alvarado-Castillo[5] were used to estimate the length of the Pacific sardine (total length mm=7.41+(47.24×otolith length mm); r=0.85, n=2740). Insufficient data did not allow estimating the size of specimens from May. All estimated lengths were transformed using log10, followed by an ANOVA among sampling periods. The size of Pacific sardine consumed by California sea lion was compared to those caught in the commercial fishery. We chose to estimate the size of Pacific sardines because of the broad information available concerning age and growth and other aspects about the fishery and because we found many sardine otoliths in good condition.

Spatial and temporal correlation in composition of diet was compared by using the Spearman rank correlation coefficient (R_S) (Fritz, 1974). Pairs of IIMP values were used for each prey taxon in a pair of sampling events (rookeries or sampling dates) to examine the correlation among them. This analysis was limited to prey that had an IIMP value of 10% or more. Cluster analysis of average IIMP data for the seven rookeries was used to assess the similarity of the diet among rookeries. The dendrogram for the cluster analysis was based on relative Euclidean distances and unweighted pair-grouping methods (UPGMA) strategy (Ludwig and Reynolds, 1988). We included only prey that, for at least one occasion, had IIMP values ≥10%.

Trophic diversity was evaluated by using diversity curves (Hurtubia, 1973) developed from IIMP index data. For each date and colony, the cumulative diversity was calculated for increasing numbers of sequentially numbered (but we assumed randomly deposited and collected) scat samples. The diversity curves also allowed us to evaluate sample size (Hurtubia, 1973; Hoffman, 1978; Magurran, 1988, Cortés, 1997) by identifying the point at which the curve flattens. The diversity was estimated by using the Shannon index:

$$H' = -\sum_{i=1}^{S} p_i \ln p_i, \quad (2)$$

where H' = trophic diversity;
S = total number of prey taxa; and
P_i = $IIMP_i$, and represents the relative abundance of taxon i obtained from each scat and pooled from scat 1 up to the total number of scats collected.

The values of trophic diversity were then plotted against the number of pooled scats.

Results

Identification of prey

The 1273 scat samples collected during June 1995 through May 1996 (Table 1) yielded fish remains in 97.4% of the samples, cephalopod remains in 11.2%, and crustacean remains in 12.7%. Fish and cephalopods represented 95.3% and 4.7%, respectively, of the 5242 individual prey (excluding crustaceans). The occurrence and number of these prey groups changed temporally and spatially (Fig. 3). We identified 92 prey taxa to the species level, 11 to the genus level, and 10 to family level from 851 scats (Table 2). Remaining scats had damaged prey structures in a condition that prevented us from identifying species to the genus or family level.

We found nine main prey with IIMP average values ≥10% (Table 3): the Pacific cutlassfish (*Trichiurus lepturus*), the Pacific sardine (*Sardinops caeruleus*), the plainfin midshipman (*Porichthys* spp.), myctophid no. 1, the northern anchovy (*Engraulis mordax*), Pacific mackerel (*Scomber japonicus*), the anchoveta (*Cetengraulis mysticetus*), jack mackerel (*Trachurus symmetricus*), and the lanternfish (unid. myctophid).

[4] García-Rodríguez, F. J., and J. De la Cruz-Agüero. In prep. An index to measure the specie prey importance of California sea lion (*Zalophus californianus*) based on scat samples.

[5] Alvarado-Castillo, R. Unpubl. data. Departamento de Biología y Pesquerías, Centro Interdisciplinario de Ciencias Marinas. Avenida IPN S/N Col. Palo Playa de Santa Rita, La Paz, Baja California Sur, México 23070.

Table 1

Number of scats collected at each rookery for each sampling period.

	June 1995	September 1995	January 1996	May 1996	Total
San Pedro Mártir (SPM)	22	33	88	29	172
San Esteban (EST)	50	66	91	67	274
El Rasito (RAS)	11	56	58	25	150
Los Cantiles (CAN)	20	58	47	35	160
Isla Granito (GRA)	24	20	41	19	104
Los Machos (MAC)	39	32	36	0	107
Isla Lobos (LOB)	72	139	72	23	306
Total	238	404	433	198	1273

Spatial and temporal variability of the main prey

The importance (IIMP) of the Pacific cutlassfish was greater in Los Cantiles (28.4%), Isla Lobos (20.8%), and Isla Granito (48.5%) than at other sites (Fig. 4). The Pacific sardine was the dominant prey at Los Machos and to the south. There was a significant correlation across the seasons between Los Machos and El Rasito (r=0.998, P=0.04), but not between Los Machos and Isla Granito (r=0.602, P=0.59). The IIMP of sardine was also correlated between El Rasito and San Esteban (r=0.95, P=0.04). The plainfin midshipman did not show a clear pattern, but its presence in the diet increased northeastward from Isla Angel de la Guarda. Lanternfishes, especially myctophid no. 1, were the dominant prey at San Pedro Mártir, San Esteban, and El Rasito. The presence of Pacific mackerel was positively correlated with the presence of the Pacific sardine. The anchoveta was only found at Isla Lobos, and jack mackerel at El Rasito, San Pedro Mártir, and Isla Granito.

The changes in the PO of the main prey coincided with the variations of the IIMP. The occurrence of Pacific cutlassfish, Pacific sardine, plainfin midshipman, northern anchovy, Pacific mackerel, and jack mackerel was significantly different (P<0.04) among rookeries. Myctophid no. 1 showed no significant difference in ocurrence (χ^2=11.04, df=6, P=0.09); but when all lanternfishes were pooled, their occurrence among rookeries was significantly different (χ^2=11.13, df=6, P=0.04). We found significant temporal differences in the occurrence of Pacific cutlassfish, Pacific sardine, plainfin midshipman, northern anchovy, and Pacific mackerel (P<0.05), but no significant differences were found among seasons in the occurrence of jack mackerel (χ^2=2.94, df=3, P=0.40), myctophid no. 1 (χ^2=1.67, df=3, P=0.6428), or lanternfish (χ^2=2.08, df=3, P=0.5562).

Size of Pacific sardine consumed by sea lions

The estimated size of the Pacific sardine found in scat was between 101.8 mm and 179.7 mm (mean length of 150.4 mm ±13.7 mm). Significant differences were found among sampling periods (F=4.79, df=2, P=0.01), specifically between June and January (Newman-Keuls test; P=0.04) and between September and January (Newman-Keuls test; P=0.01). The average size was 147.4 mm (±16.1 mm) in June, 151.7 mm (±13.0 mm) in September, and 136.5 mm (±13.7 mm) in January (Fig. 5). A similar pattern was found in Los Cantiles, Los Machos, and Isla Granito.

Spatial and temporal correlation in diet

We identified 25 prey taxa that had an IIMP index value of ≥10% (Table 3) for a given collection. The Spearman rank correlation coefficient of IIMP between any pair of rookeries during June, September, January, and May was not significant (P>0.08). There was no positive correlation among any pair of sampling periods for any rookery (P>0.14), except between January and May at San Pedro Mártir (R_S=0.64, P<0.05) and El Rasito (R_S=0.66, P<0.05) and between January and June as well as between January and May at Isla Lobos (R_S=0.56, P=0.05; and R_S=0.59, P=0.05, respectively).

The similarity in diet was related to the distance between rookeries. A clustering for the seven rookeries was obtained from these 25 prey taxa (Fig 6). We arbitrarily used a "cut-off" distance of 0.3 and 0.4 on the dendrogram as reference points for identifying clusters. The group obtained by using the first distance (0.3) showed four feeding areas: one located in the south (area I: San Pedro Mártir, San Esteban, and El Rasito), another in Canal de Ballenas (area II: Los Machos) and two in the north (area III: Los Cantiles and Isla Lobos; and area IV: Isla Granito). When the second distance (0.4) was used, the seven rookeries grouped into two clusters: 1) the southern region and Canal de Ballenas, and 2) the region north of Angel de la Guarda.

Spatial and temporal variability in trophic diversity

Temporal variability in trophic diversity was evident between the rookeries (Fig. 7). In general, two patterns could be differentiated: one in which the diversity varied little throughout the year and the other in which diversity was high in January and low in September. The rookeries San Pedro Mártir and Isla Lobos showed the first pattern and Los Machos and Isla Granito (and to a lesser extent, San Esteban and El Rasito) showed the second pattern. In September, when diversity was low, the dominant prey at

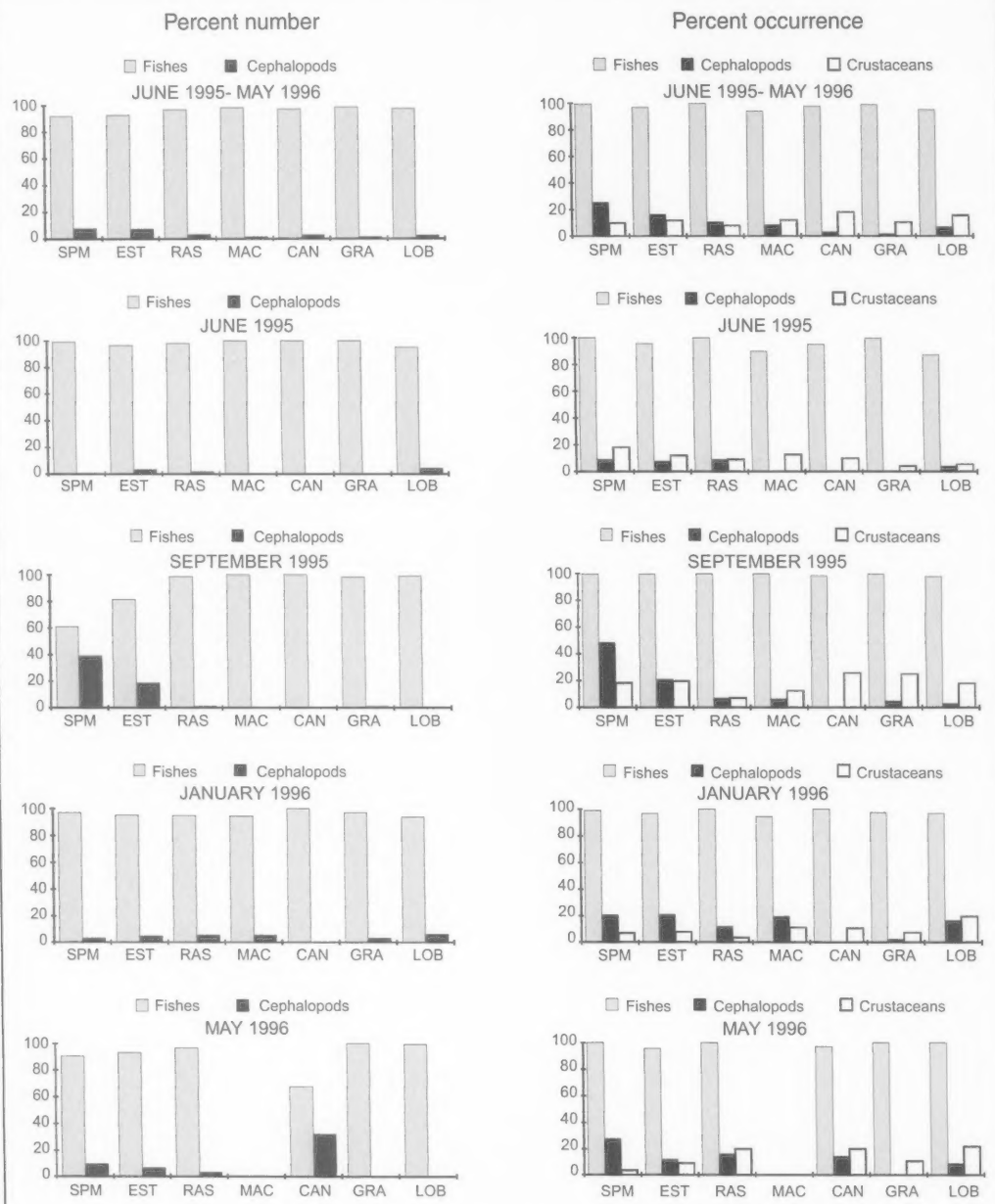

Figure 3

Percent number (PN) and percent occurrence (PO) index values for fishes, cephalopods, and crustaceans found in samples of California sea lion scats collected at seven rookeries in the Gulf of California, Mexico, for all sampling periods combined and for each sampling period.

San Esteban, El Rasito, and Los Machos was Pacific sardine, whereas at Isla Granito, it was Pacific cutlassfish (Fig. 4). The curves obtained for Los Cantiles showed a clear pattern of diversity only in September, although the trend in the January curve would suggest a higher diversity in January than in September.

Table 2

Prey of California sea lion identified from scat samples collected at Isla San Pedro Martir, Isla San Esteban, Isla El Rasito, Los Cantiles, Isla Granito, Los Machos and Isla Lobos from June 1995 through May 1996. *n* ind. = number of individuals in the sample; PN = percent number; n occurr = number of occurrences; PO = percentage of occurrence; IIMP = index of importance.

Scientific name	Common name	*n* Ind.	PN	*n* Occurr.	PO	IIMP
Trichiurus lepturus	Pacific cutlassfish	306	5.837	128	15.041	16.392
Sardinops caeruleus	Pacific sardine	358	6.829	88	10.341	10.020
Porichthys spp.	midshipman	456	8.699	95	11.163	9.297
Myctophid no. 1	lanternfish	714	13.621	119	13.984	7.901
Engraulis mordax	northern anchovy	430	8.203	43	5.053	5.199
Scomber japonicus	Pacific mackerel	103	1.965	42	4.935	3.403
Cetengraulis mysticetus	anchoveta	410	7.821	15	1.763	2.404
Loliolopsis diomedeae	squid	77	1.469	35	4.113	2.399
Trachurus symmetricus	jack mackerel	111	2.118	41	4.818	2.273
Merluccius spp.	Pacific whiting	55	1.049	25	2.938	2.206
Pontinus spp.	scorpionfish	61	1.164	26	3.055	1.842
Enoploteuthid no. 1	squid	95	1.812	23	2.703	1.754
Caelorinchus scaphopsis	shoulderspot	65	1.240	25	2.938	1.728
Octopus sp. no. 1	octopus	24	0.458	17	1.998	1.614
Sebastes macdonaldi	Mexican rockfish	42	0.801	18	2.115	1.496
Citharichthys sp no. 1	sanddab	120	2.289	23	2.703	1.220
Fish species no. 1	—	49	0.935	25	2.938	1.153
Haemulopsis leuciscus	white grunt	176	3.357	21	2.468	1.093
Peprilus snyderi	salema butterfish	163	3.110	33	3.878	1.025
Prionotus spp.	searobin	12	0.229	9	1.058	0.855
Prionotus stephanophrys	lumptail searobin	53	1.011	14	1.645	0.814
Argentina sialis	Pacific argentine	19	0.362	13	1.528	0.754
Fish species no. 2	—	55	1.049	27	3.173	0.737
Hemanthias peruanus	splittail bass	60	1.145	22	2.585	0.602
Fish species no. 3	—	9	0.172	6	0.705	0.592
Micropogonias ectenes	slender croaker	13	0.248	9	1.058	0.547
Lepophidium spp.	cusk-eel	9	0.172	3	0.353	0.532
Fish species no. 4	—	10	0.191	3	0.353	0.511
Sebastes exsul	buccanner rockfish	15	0.286	10	1.175	0.505
Cranchiid no. 2	Squid	20	0.382	12	1.410	0.501
Haemulon flaviguttatum	yellowspotted grunt	11	0.210	3	0.353	0.468
Selar crumenophthalmus	bigeye scad	24	0.458	12	1.410	0.431
Fish species no. 5	—	33	0.630	19	2.233	0.384
Paralabrax sp. no. 1	sea bass	9	0.172	5	0.588	0.373
Synodus sp. no. 3	lizardfish	10	0.191	3	0.353	0.341
Lepophidium prorates	prowspine cusk-eel	5	0.095	4	0.470	0.335
Fish species no. 6	—	9	0.172	5	0.588	0.324
Synodus sp. no. 1	lizardfish	25	0.477	10	1.175	0.324
Octopus sp, no. 2	octopus	8	0.153	7	0.823	0.308
Gonatus berryi	squid	5	0.095	5	0.588	0.274
Mugil cephalus	striped mullet	1	0.019	1	0.118	0.265
Paranthias colonus	Pacific creole-fish	1	0.019	1	0.118	0.265
Balistes polylepis	finescale triggerfish	13	0.248	4	0.470	0.245
Physiculus nematopus	charcoal mora	30	0.572	12	1.410	0.244
Hemanthias spp.	sea bass	9	0.172	6	0.705	0.234
Fish species no. 7	—	10	0.191	8	0.940	0.233
Uroconger varidens	conger eel	8	0.153	5	0.588	0.189
Larimus spp.	drum	8	0.153	6	0.705	0.174
Apogon retrosella	barspot cardinalfish	5	0.095	4	0.470	0.173
Dosidicus gigas	squid	8	0.153	5	0.588	0.171

continued

Table 2 (continued)

Scientific name	Common name	*n* Ind.	PN	*n* Occurr.	PO	IIMP
Merluccius productus	Pacific whiting	1	0.019	1	0.118	0.167
Fish species no. 8	—	2	0.038	2	0.235	0.159
Synodus sp. no. 2	lizardfish	12	0.229	5	0.588	0.132
Scorpaena sonorae	Sonora scorpionfish	2	0.038	1	0.118	0.130
Eucinostomus spp.	mojarra	13	0.248	5	0.588	0.129
Fish species no. 9	—	3	0.057	3	0.353	0.127
Cynoscion reticulatus	striped weakfish	23	0.439	7	0.823	0.124
Fish species no. 10	—	10	0.191	1	0.118	0.122
Caulolatilus affinis	bighead tilefish	4	0.076	3	0.353	0.114
Paralabrax auroguttatus	goldspotted sand bass	18	0.343	4	0.470	0.110
Fish species no. 11	—	3	0.057	2	0.235	0.102
Cranchiid no. 5	squid	1	0.019	1	0.118	0.097
Bodianus diplotaenia	mexican hogfish	1	0.019	1	0.118	0.087
Prionotus sp. no. 1	searonbin	2	0.038	2	0.235	0.087
Strongylura exilis	california needlefish	1	0.019	1	0.118	0.083
Synodus spp.	lizardfish	6	0114	5	0.588	0.146
Fish species no. 12	—	3	0.057	3	0.353	0.074
Fish species no. 13	—	2	0.038	1	0.118	0.065
Fish species no. 14	—	3	0.057	1	0.118	0.060
Fish species no. 15	—	2	0.038	1	0.118	0.058
Fish species no. 16		2	0.038	2	0.235	0.056
Porichthys sp. 1	midshipman	1	0.019	1	0.118	0.052
Fish species no. 17	—	5	0.095	3	0.353	0.049
Calamus brachysomus	Pacific porgy	5	0.095	2	0.235	0.043
Fish species no. 18	—	1	0.019	1	0.118	0.042
Fish species no. 19	—	5	0.095	2	0.235	0.041
Ophididae no. 1	—	1	0.019	1	0.118	0.040
Fish species no. 20	—	5	0.095	3	0.353	0.039
Sebastes sinesis	blackmouth rockfish	2	0.038	1	0.118	0.039
Symphurus spp.	tonguefish	3	0.057	1	0.118	0.038
Fish species no. 21	—	2	0.038	1	0.118	0.036
Pronotogrammus multifasciatus	threadfin bass	8	0.153	2	0.235	0.029
Fish species no. 22	—	2	0.038	2	0.235	0.027
Fish species no. 23	—	2	0.038	1	0.118	0.021
Orthopristis reddingi	Bronze-striped grunt	16	0.305	1	0.118	0.020
Fish species no. 24	—	2	0.038	1	0.118	0.020
Fish species no. 25	—	1	0.019	1	0.118	0.016
Cranchiidae no. 4	squid	2	0.038	2	0.235	0.014
Fish species no. 26	—	2	0.038	2	0.235	0.014
Histioteuthis heteropsis	squid	1	0.019	1	0.118	0.014
Scorpaenidae no. 1	—	1	0.019	1	0.118	0.011
Fish species no. 27	—	3	0.057	2	0.235	0.011
Fish species no. 28	—	1	0.019	1	0.118	0.010
Fish species no. 29	—	1	0.019	1	0.118	0.008
Cranchiidae no. 3	squid	1	0.019	1	0.118	0.006
Bollmannia spp.	goby	1	0.019	1	0.118	0.006
Fish species no. 30	—	1	0.019	1	0.118	0.005
Cranchiidae no. 1	squid	1	0.019	1	0.118	0.004
Paralabrax maculatofasciatus	spotted sand bass	1	0.019	1	0.118	0.003
Ophidion scrippsae	basketweave cusk-eel	1	0.019	1	0.118	0.003
Physiculus spp.	cod, codling, mora	2	0.038	1	0.118	0.003
Ophididae no. 2	—	4	0.076	1	0.118	0.002
Unid. Carangidae	jacks	8	0.153	3	0.353	0.141

continued

Table 2 (continued)

Scientific name	Common name	*n* Ind.	PN	*n* Occurr.	PO	IIMP
Unid. Engraulidae	anchovies	1	0.019	1	0.118	0.248
Unid. Haemulidae	grunts	13	0.248	11	1.293	0.509
Unid. Labridae	wrasses	1	0.019	1	0.118	0.005
Unid. Mycthophidae	lanternifishes	216	4.121	71	8.343	4.895
Unid. Ophididae	cusk-eel	2	0.038	1	0.118	0.098
Unid. Scianidae	drums	13	0.248	9	1.058	0.643
Unid. Scorpaenidae	scorpionfishes	30	0.572	18	2.115	1.078
Unid. Serranidae	sea bass	13	0.248	6	0.705	0.176
Unid. Triglidae	searobins	1	0.019	1	0.118	0.002
	Unid. fishes	39	0.744	16	1.880	1.819
	Unid. cephalopods	4	0.076	4	0.470	0.373
	Unid. fishes (very eroded)	381	7.268	231	27.145	
	Remains of cephalopods			14	1.645	
	Remains of crustaceans			162	19.036	

Discussion

Stomach acids attack otoliths, affecting their size and number and consequently the estimate of prey occurrence and importance. Erosion of otoliths during digestion has been analyzed in studies of pinnipeds in captivity. Bowen (2000) reviewed nine studies that estimated the proportion of otoliths recovered in scat samples to obtain a prey-number correction factor (NCF). He found that NCF is greater than 1.0 because many prey species are not recovered in the scat samples. Additionally, the erosion level can be significantly different among prey species (Bowen, 2000) because of differences in the shape and microstructure of otoliths. Therefore, estimates of biomass based on scat analysis should be carefully interpreted because the consumption of some prey species can be under- or overestimated. Correction factors are needed to compensate for differential erosion for the prey species of each pinniped.

In this study the most important prey of California sea lions were pelagic fish with small, thin, and fragile otoliths (Nolf, 1993). The lanternfish also have small otoliths—perhaps smaller than those of any other prey taxa found in the scats. Their true importance in California sea lion feeding may be underestimated because of erosion caused by stomach acids (Da Silva and Neilson, 1985; Murie and Lavigne, 1985; Jobling and Breiby, 1986; Jobling, 1987; Tollit et al., 1997). Similarly, the presence of cephalopods may have been underestimated because their jaws are composed of chitin, which is harder to digest, and frequently are regurgitated (Pitcher, 1980; Hawes, 1983). However, the high resistence to digestion of cephalopod beaks allows recovery of them in good shape. Thus they are a good choice to use in such diet analyses (Lowry and Carretta, 1999).

A numerical index of prey species importance may over- or underestimate the dominance of prey species in the diet because it does not consider the weight of the prey. For IIMP, a numerical index that assumes a similar weight for all prey species, the true importance of the individual large prey in the diet can be underestimated and the importance of individual small prey can be overestimated. This problem is also present when the PO, PN, and the SSFO index are used because these are all based only upon the number and occurrence of otoliths and cephalopods beaks. As when using PN, and the SSFO, the IIMP does not work for species that cannot be enumerated, such as crustaceans.

Given the tendencies of the trophic diversity curves, the sample size was suitable in almost all cases. However, at San Pedro Mártir a few more samples would have been useful to fully depict the diet. At Los Cantiles, except during September 1995, the samplings should have been more intense because the flattened portion of the diversity curves are not clear. The information, therefore, that comes from those samples could be biased. However, the number of scats that we analyzed contained a high percentage of the consumed species, especially the main prey.

The results of this study indicate that the California sea lion consumed mainly fish and some crustaceans and cephalopods. According to the PN index, fish were more important than cephalopods in the diet of sea lions. In addition, fish were more frequent (PO) than crustacean and cephalopods.

Crustaceans were represented in a similar manner in scats from all rookeries. Cephalopods, however, were more important at San Pedro Mártir and San Esteban, probably because they are more common towards the southern gulf. Species of the suborder Oegopsida, which includes oceanic species (Roper and Young, 1975), were most commonly found in scats from these rookeries. Orta-Dávila (1988) and Sánchez-Arias (1992) have also noted the low consumption of cephalopods at the northern rookeries. Fish were the most diverse and commonly eaten prey. In contrast to cephalopods, fish were slightly less important in the southern region.

The availability and abundance of the various prey resources influenced the diet of the sea lions in the Gulf

Table 3

Prey of California sea lions having IIMP index values ≥10% in at least one sampling period for seven rookeries in the Gulf of California, Mexico. Blank indicate that species were not recorded in diet; "—" means unavailable data.

	Prey species	June 1995	September 1995	January 1996	May 1996	Average
San Pedro	*Engraulis mordax*	29.7		2.1	0.5	8.1
Martir	myctophid no. 1	29.0	10.5	9.0	20.5	17.3
	Porichthys spp.	11.2	2.0	6.8	15.5	8.9
	Prionotus stephanophrys	0.6	3.3	3.3	10.9	4.5
	enopleoteuthid no.1		27.3	0.8		7.0
	Sebastes macdonaldi		10.4			2.6
	Haeumulopsis leuciscus			16.7	6.0	5.7
San Esteban	*Trichiurus lepturus*	24.9	3.4		3.0	7.8
	Sardinops caeruleus	10.0	34.1		4.2	12.1
	unid. Myctophidae	13.79	3.4	4.3	10.9	8.1
	myctophid no. 1	2.8	11.8	8.9	18.8	10.6
	enopleoteuthid no. 1		16.9			4.2
	Sebastes macdonaldi		2.1	9.7	1.4	3.3
	fish species no. 1			1.7	11.0	3.2
El Rasito	*Porichthys* spp.	26.2	4.0	2.3		8.1
	unid. Myctophidae	16.4	1.5	8.1	16.4	10.6
	Scomber japonicus	13.8	3.2	3.7	2.5	5.8
	Pontinus spp.	11.5	5.1	4.1	10.9	7.9
	Octopus sp. no.1	11.5		2.9	7.7	5.5
	myctophid no. 1	6.6	5.1	21.4	6.8	10.0
	Sardinops caeruleus	1.6	40.1	0.9	7.3	12.5
	Trachurus symmetricus		22.0	5.0	23.4	12.6
	Caelorinchus scaphopsis		3.6	13.5	10.5	6.9
Los Machos	*Sardinops caeruleus*	21.0	64.1	16.8	—	34.0
	Scomber japonicus	19.0		10.9	—	10.0
	Merluccius spp.	15.4		8.2	—	7.9
	Trichiurus lepturus	11.7	5.4		—	5.7
	Sebastes macdonaldi	1.8		11.3	—	4.4
Los Cantiles	*Porichthys* spp.	66.7	15.5			20.6
	Trichiurus lepturus	22.2	38.2		53.1	28.4
	Engraulis mordax	3.7	0.4	14.3		4.6
	myctophid no. 1		17.6	4.8		5.6
	Sardinops caeruleus		6.8	19.0		6.5
	fish species no. 3		0.9	14.3		3.8
	unid. fishes		0.9	19.0		5.0
	unid. Scianidae			14.3		3.6
	Lepophidium spp.			14.		3.5
	Loliolopsis diomedeae				21.1	5.3
Isla Granito	*Engraulis mordax*	49.3	7.8			14.3
	Trichiurus lepturus	22.0	70.1	2.0	100.0	48.5
	unid. myctophidae	1.7	1.1	12.6		3.9
	Sardinops caeruleus	0.9		18.7		4.9
	Porichthys spp.	0.5	18.2	4.6		5.8
	Citharichthys sp. no. 1			21.7		5.4
Isla Lobos	*Cetengraulis mysticetus*	32.7	0.1	6.8	27.8	16.9
	Trichiurus lepturus	25.2	27.7	15.8	14.3	20.8
	Porichthys spp.	9.0	10.3	23.2	35.5	19.5
	Loliolopsis diomedeae	4.9	2.2	11.6	3.5	5.6
	Peprilus snyderi		23.5	5.2		7.2

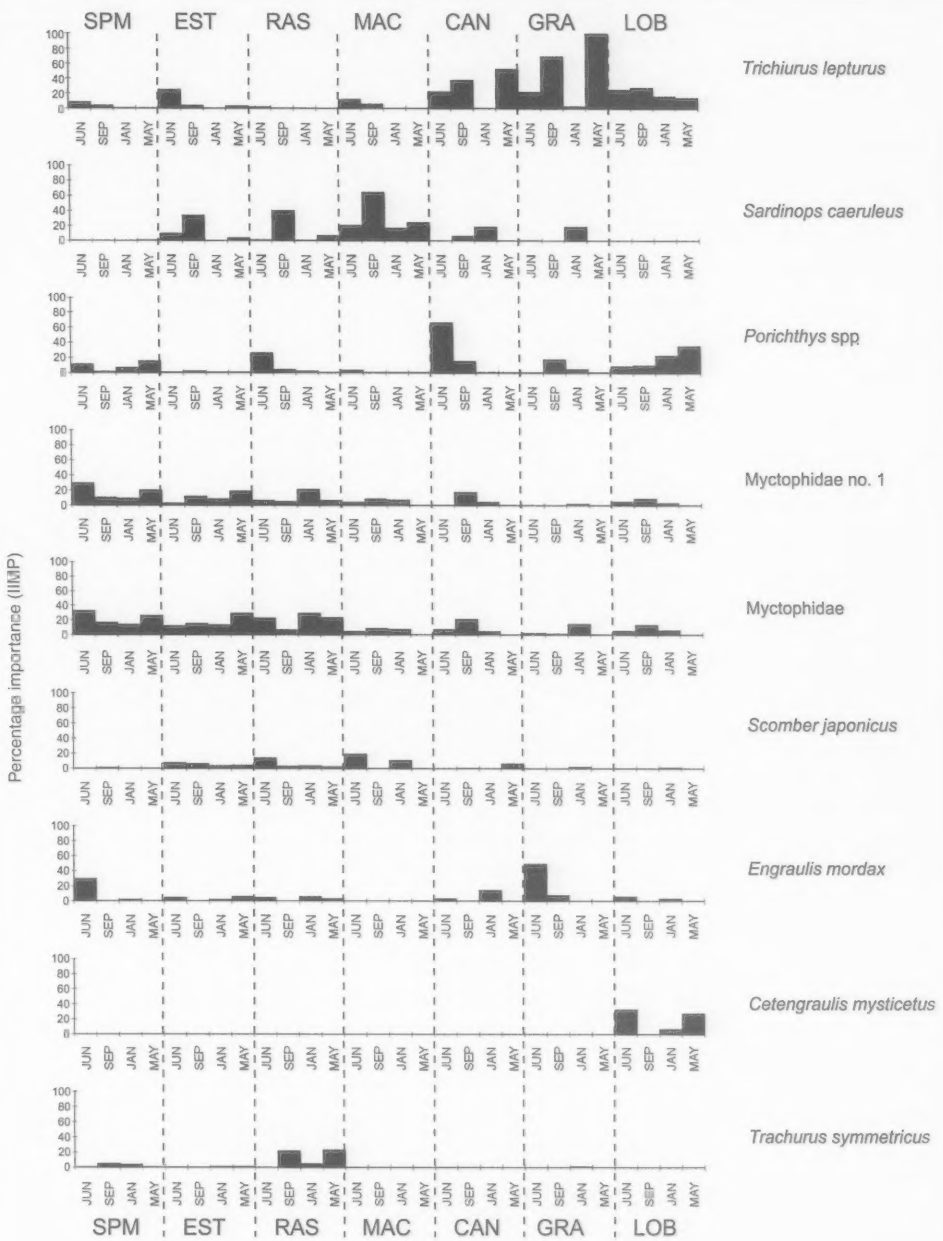

Figure 4

Index of importance (IIMP) for nine prey species identified from samples of California sea lions scats collected at seven rookeries in the Gulf of California, Mexico, during June and September 1995, and January and May 1996.

of California. The distribution pattern of Pacific sardine closely agrees with its importance in the sea lions diet. The Pacific sardine occurred in high concentrations around Angel de la Guarda and Isla Tiburon during the summer and along the coast of southern Sonora during the winter, where spawning occurs (Cisneros-Mata et al.[3]). Sardines

were consumed in the Canal de Ballenas region during the summer (September), when they are very abundant. Larger size Pacific sardines were consumed by sea lions most frequently during the summer when adult sardines occur more frequently in the Canal de Ballenas. As adult sardine left Canal de Ballenas (Cisneros-Mata et al., 1997), the proportion of young individuals in the diet of sea lions increased. The fish eaten by sea lions were apparently smaller than those captured by the commercial fisheries. The average estimated size of the sardines consumed was 150.4 mm, whereas the average size of commercially caught fish during the 1995–96 season was 162.4 mm (Cisneros-Mata et al.[3]). This 7% difference in size may have been caused by an underestimation of otolith size because of digestive erosion (Jobling and Breiby, 1986). If this is so, then the size of Pacific sardines consumed by sea lions is similar to the size of those captured by the fishery.

Isla Lobos was the only rookery where Pacific sardine was not consumed. This finding differs from those of Cisneros-Mata et al.[3] which show the Pacific sardines present as far north as Isla Lobos. However, their study period was during the 1991–92 El Niño episode, whereas our study occurred during normal oceanographic conditios in 1995–96.

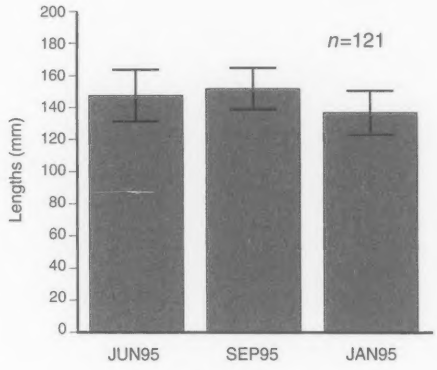

Figure 5

Size of Pacific sardine (*Sardinops caeruleus*) estimated from otoliths found in California sea lions scats collected in Isla San Esteban, El Rasito, Granito, Los Cantiles, and Los Machos. One standard deviation is indicated from each mean.

Less is known about the spatial and temporal availability of other important prey. As with commercial captures (Arvizu-Martinez, 1987), Pacific mackerel occurred together with Pacific sardine. Similar variations in occurrence for both species have been noticed from stomach content analyses of the giant squid (*Dosidicus gigas*) (Ehrhardt, 1991). Lanternfishes were abundant north of Isla Angel de la Guarda (Robison, 1972); however they were not important in the diet of the California sea lion in this region. Their greater importance in the diet at southern rookeries was probably due to the absence of more preferred prey such as Pacific sardine, Pacific cutlassfish, or anchoveta. The consumption of northern anchovy tended to be less important towards Canal de Ballenas, where Pacific sardine reached its maximum importance. The low spatial overlap of these two species has also been noted in other studies. The anchoveta was present only at Isla Lobos. This is an estuarine-lagoon species, typical of coastal lagoons of northern Sinaloa and Sonora (Castro-Aguirre et al., 1995). The presence of this prey in Isla Lobos is possibly due to the sandy coast (Walker, 1960), which is similar to that of the Sinaloa-Sonora coast.

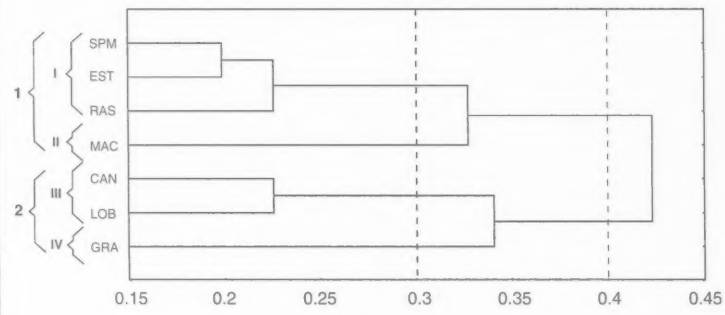

Figure 6

Dendrogram of cluster analysis of seven rookeries determined with Euclidean distance (computed from the IIMP of the 25 prey that had on at least one occasion a value ≥10%) and the UPGMA (unweighted pair-grouping methods) strategy. The vertical lines represent the points of references to delimit the groups.

The diet of California sea lions differed among rookeries, probably due to differences in feeding sites and prey availability. Antonelis et al. (1990) studied the foraging characteristics of the northern fur seal (*Callorhinus ursinus*) and the California sea lion at San Miguel Island and found differences between foraging areas among species. The northern fur seal was found most frequently foraging in oceanic water within 72.4 km from the island, whereas Califorinia sea lions forgaged more often in the shallower neritic zone, within 54.2 km from the island. Different foraging distances in California sea lions from San Miguel Island were found by Melin and DeLong (1999). During the nonbreeding season a higher percentage of foraging locations occurred at distances less than 100 km, whereas during the breeding season most of the foraging locations occurred at distances greater than 100 km. These differences are probably due to the increased California sea lion population in San Miguel; this increase in population forces sea lions to exploit new areas as a density-dependent response to population

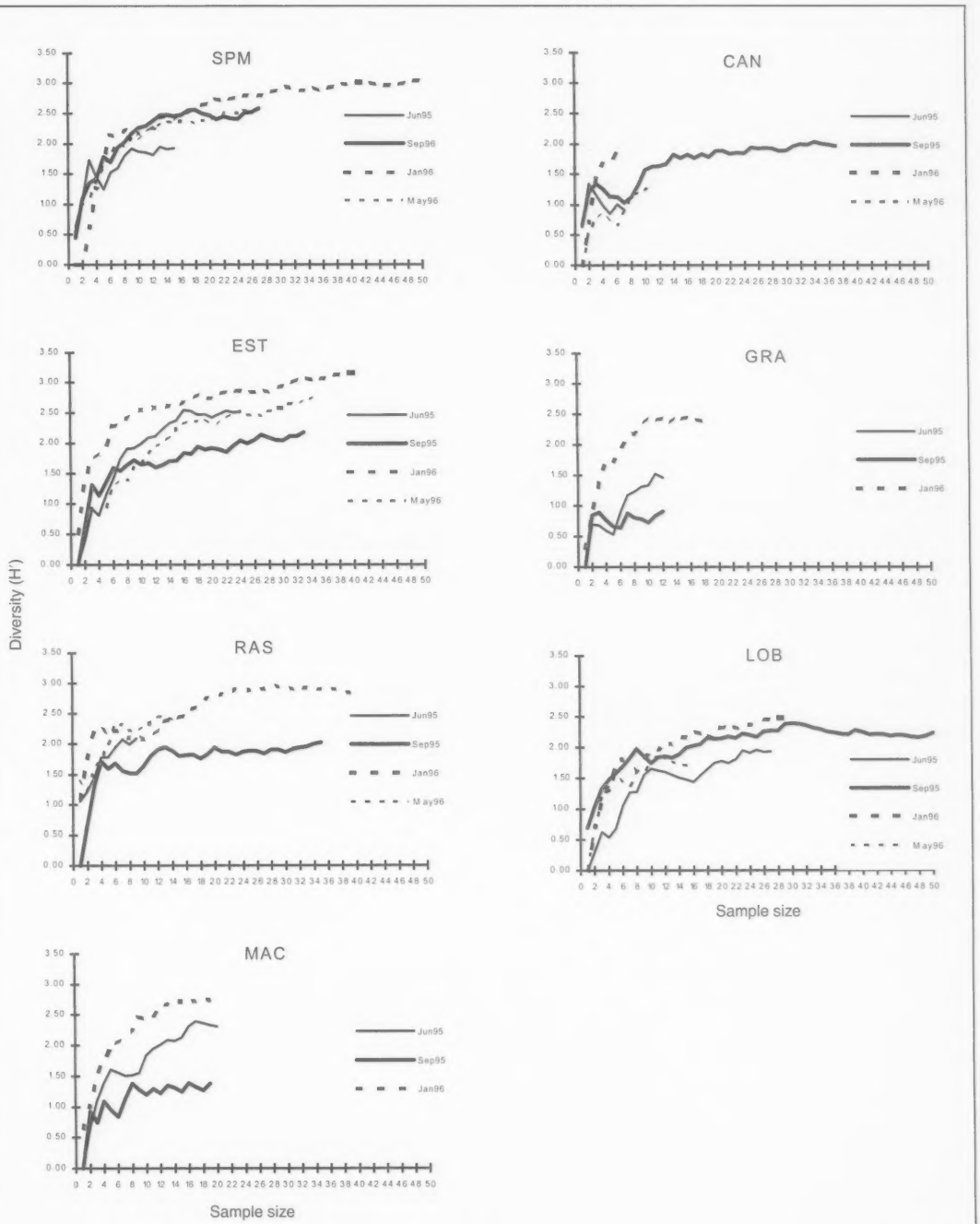

Figure 7

Trophic diversity curves for California sea lions determined from scat samples collected at seven rookeries in the Gulf of California, Mexico. SPM = San Pedro Mártir; EST = San Esteban; RAS = Isla Rasito; MAC = Los Machos; CAN = Los Cantiles; GRA = Isla Granito; LOB = Isla Lobos.

growth. Although, these differences could also be due to variability in the distribution of prey (Melin and DeLong, 1999), as suggested by Antonelis and Fiscus (1980), foraging areas might change with season and annual variations in prey availability and abundance.

Foraging areas in the Gulf of California could lie closer to rookeries than those recorded for San Miguel Island sea lions because the diet was different among rookeries in spite of the shorter distance between them (54.2 km). At Los Islotes, Baja California Sur, adult females fed within 20 km of the colony (Durán-Lizárraga, 1998). Kooyman and Trillmich (1986a, 1986b) reported similar data in sea lion colonies of the Galapagos Islands. In the northern region of the Gulf of California, feeding range could be shorter than that at Los Islotes because of the higher concentration of food at high nutrient concentrations (phosphate, nitrate, nitrite, and silicate) in Canal de Ballenas that is associated with strong tidal mixing (Alvarez-Borrego, 1983).

Four foraging zones were discerned from dietary differences in sea lions from the seven rookeries studied. Zone I, which included San Pedro Mártir, San Esteban, and El Rasito, was characterized by the consumption of lanternfish; zone II, which included Los Machos was characterized by the consumption of Pacific sardine and Pacific mackerel; zone III, which included Isla Granito, by the consumption of Pacific cutlassfish and the northern anchovy; and zone IV, Los Cantiles and Isla Lobos, was characterized by the consumption of the plainfin midshipman and the Pacific cutlassfish. These four zones may indicate differences in habits used by sea lions or may indicate different oceanographic conditions exploited by sea lions. The eastern coast of the Gulf of California displays high photosynthetic pigment concentrations, associated with upwelling induced by winds from the northwest in the winter. These conditions may make Canal de Ballenas one of the most important for the distribution of Pacific sardine during the summer.

Trophic diversity varied spatially and temporally. San Pedro Mártir and Isla lobos sea lions seem to depend on a more stable feeding areas compared to sea lions at rookeries on Isla Granito and Los Machos, where changes in diversity of consumed species indicated that sea lions feed on fewer species during certain times of the year. Similar results in relation to the changes in diversity were also noticed in the rookeries of the Channel Islands and Farallon Islands, California (Bailey and Ainley, 1982; Antonelis et al., 1984; Lowry et al., 1990; Lowry et al., 1991). Perhaps the tendency to have the highest values of diversity and little seasonal variation at San Pedro Mártir is the result of this rookery being located in a zone of transition between two biogeographical areas. This geographical position confers greater environmental heterogeneity and greater ecological diversity (Walker, 1960).

California sea lions in the upper region of the Gulf of California obtain the main portion of their diet from a relatively small number of species. The decrease in abundance of any of these food resources can seriously affect the population, particularly at Isla Granito and Los Machos because sea lions from these rookeries depend on a few species.

Acknowledgments

We wish to thank Secretaria de Marina, Armada de Mexico, for its great support during the field activities, and the Consejo Nacional de Ciencia y Tecnologia (CONACYT) for funding this study under grant number 26430-N. The Secretaria de Medio Ambiente, Recursos Naturales y Pesca (SEMARNAP) provided permits for field work (DOO.-700-(2)01104 and DOO.-700(2).-1917). We would like to thank Robert Lavenberg and Jeff Siegel for allowing us the use of otoliths from the collection at the Natural Museum History of Los Angeles County and also Lawrence Barnes for his logistical support during the stay of first author at Los Angeles; we also thank Manuel Nava for allowing us the use of otoliths from the collection in Tecnologico de Monterrey, Campus Guaymas. We are also grateful to Unai Markaida for his assistance in prey identification based on the examination of cephalopods beaks. We thank Mark Lowry for commenting on an earlier draft of the paper, Norman Silverberg for reviewing the manuscript in English, and two anonymous reviewers for their valuable suggestions and criticism. The first author would like to thank Centro Interdisciplinario de Ciencias Marinas-IPN for a scholarship (PIFI, Programa Institucional para la Formación de Investigadores) assigned for postgraduate studies.

Literature cited

Alvarez-Borrego, S.
1983. Gulf of California. *In* Estuaries and enclosed seas (B. H. Ketchum, ed.), p 427–449. Elsevier Scientific Publishing Co., Amsterdam.

Antonelis, G. A, and C. H. Fiscus.
1980. The pinnipeds of the California Current. Calif. Coop. Oceanic Fish. Invest. Rep. 21:68–78.

Antonelis, G. A., C. H. Fiscus, and R. L. DeLong.
1984. Spring and summer prey of California sea lions, *Zalophus californianus*, at San Miguel Island, California 1978–79. Fish. Bull. 82:67–75.

Antonelis, G. A., B. S. Stewart, and W. F. Perryman.
1990. Foraging characteristics of females northern fur seals (*Callorhinus ursinus*) and California sea lion (*Zalophus californianus*). Can J. Zool. 68:150–158.

Arvizu-Martínez, J.
1987. Fisheries activities in the Gulf of California, México. Calif. Coop. Oceanic Fish. Invest. Rep. 28:32–36.

Aurioles-Gamboa, D., C. Fox, F. Sinsel, and G. Tanos.
1984. Prey of sea lions (*Zalophus californianus*) in the bay of La Paz, Baja California Sur, México. J. Mammal. 65(3): 519–21.

Aurioles-Gamboa, D., and A. Zavala-González.
1994. Algunos factores ecológicos que determinan la distribución y abundancia del lobo marino de California, *Zalophus californianus*, en el Golfo de California. Ciencias Marinas 20(4):535–553.

Bailey, K. M., and D. G. Ainley.
1982. The dynamics of California sea lion predation on Pacific hake. Fish. Res. 1:163–176.

Bautista-Vega, A. A.
2000. Vartiación estacional en la dieta del lobo marino común, *Zalophus californianus*, en las Islas Ángel de la Guarda y Granito, Golfo de California, México. Tesis de Licenciatura,

113 p. Universidad Nacional Autónoma de México. México, D.F.

Bowen, W. D.
2000. Reconstruction of pinniped diets: accounting for complete digestion of otoliths and cephalopod beaks. Can. J. Fish. Aquat. Sci. 57:898–905.

Castro-Aguirre, J. L., E. F. Balart, and J. Arvizu-Martínez.
1995. Contribución al conocimiento del origen y distribución de la ictiofauna del Golfo de California, México. Hidrobiológica 5(1-2):57–78.

Clarke, M. R.
1962. The identification of cephalopod "beaks" and the relationship between beak size and total body weight. Bull. British Museum (Natural History) Zoology 8(10):419–480.

Cortés, E.
1997. A critical review of methods of studying fish feeding based on analysis of stomach contents: application to elasmobranch fishes. Can. J. Fish. Aquat. Sci. 54:726–738.

Da Silva, J., and J. D. Neilson.
1985. Limitations of using otoliths recovered in scats to estimate prey consumptions in seals. Can. J. Fish. Aquat. Sci. 42:1439–1442.

Durán-Lizárraga, M. E.
1998. Caracterización de los patrones de buceos de alimentación de lobo marino *Zalophus californianus* y su relación con variables ambientales en la Bahía de La Paz, B.C.S. Tesis de Maestria, 82 p. CICIMAR, La Paz, B.C.S., México.

Ehrhardt, N. M.
1991. Potential impact of a seasonal migratory jumbo squid (*Dosidicus gigas*) stock on a Gulf of California sardine (*Sardinops sagax caerulea*) population. Bull. Mar. Sci. 49(1–2):325–332.

Fitch, J. E.
1966. Additional fish remains, mostly otoliths, from a Pleistocene deposit at Playa del Rey, California. Los Angeles County Mus., Cont. in Sci. (119):1–16.

Fitch, J. E., and R. L. Brownell.
1968. Fish otoliths in Cetacean stomachs and their importance in interpreting feeding habits. J. Fish. Res. Board Canada. 25(12):2561–2574.

Fritz, E. S.
1974. Total diet comparison in fishes by Spearman rank correlation coefficients. Copeia (1974):210–214.

García-Rodríguez, F. J.
1995. Ecología alimentaria del lobo marino de California, *Zalophus californianus californianus* en Los Islotes, B.C.S., México. Tesis de Licenciatura, 106 p. Universidad Autónoma de Baja California Sur. La Paz, B.C.S., México.
1999. Cambios espaciales y estacionales en la estructura trófica del lobo marino de California, *Zalophus caliornianus*, en la región de la grande islas, Golfo de California. Tesis de Maestría, 73 p. CICIMAR. La Paz, B.C.S, México.

Hawes, D.
1983. An evaluation of California sea lion scat samples as indicators of prey importance. Master's thesis, 50 p. San Francisco State Univ., San Francisco, CA.

Hoffman, M.
1978. The use of Pielou's method to determine sample size in food studies. *In* Fish food habits studies: proceedings of the second Pacific Northwest technical workshop (S. J. Lipovsky and C. A. Simenstad, eds.), p 56–61. Washington Sea Grant Publication, Seattle, WA.

Hurtubia, J.
1973. Trophic diversity measurement in sympatric predatory species. Ecology 54(4):885–890.

Jobling, M.
1987. Marine mammal faeces samples as indicators of prey importance—a source of error in bioenergetics studies. Sarsia 72:255–260.

Jobling, M., and A. Breiby.
1986. The use and abuse of fish otoliths in studies of feeding habits of marine piscivores. Sarsia 71:265–274.

Kooyman, G. L., and F. Trillmich.
1986a. Diving behavior of Galapagos fur seals. *In* Fur seals: maternal strategies on land and at sea (R. L. Gentry and G. L. Kooyman, eds), p. 186–195. Princeton Univ. Press, New Jersey, NJ.
1986b. Diving behavior of Galapagos sea lions. *In* Fur seals—maternal strategies on land and at sea (R. L. Gentry and G. L. Kooyman, eds.), p. 209–220. Princeton Univ. Press, Princeton, NJ.

Lowry, M. S., and J. V. Carretta.
1999. Market squid (*Loligo opalescens*) in the diet of California sea lions (*Zalophus californianus*) in southern California (1981–1995). Calif. Coop. Oceanic Fish. Invest. Rep. 40:196–207.

Lowry, M. S., C. W. Oliver, C. Macky, and J. B. Wexler.
1990. Food habits of California sea lions *Zalophus californianus* at San Clemente Island, California, 1981–86. Fish. Bull. 88:509–521.

Lowry, M. S., B. S. Stewart, C. B. Heath, P. K. Yochem, and J. M. Francis.
1991. Seasonal and annual variability in the diet of California sea lions *Zalophus californianus* at San Nicolas Island, California, 1981–86. Fish. Bull. 89:331–336.

Ludwig, J. A., and J. F. Reynolds.
1988. Statistical ecology: a primer on methods and computing, 338 p. John Wiley and Sons, New York, NY.

Magurran, A. E.
1988. Ecological diversity and its measurement, 178 p. Princeton Univ. Press, Princeton, NJ.

Melin, S. R., and R. L. DeLong.
1999. At-sea distribution and diving behavior of California sea lion females from San Miguel Island, California. *In* Proceeding of the fifth California islands symposium (D. R. Browne, K. L. Mitchell, and H. W. Chaney, eds.), p. 407–402. Santa Barbara Museum of Natural History, Santa Barbara, CA.

Murie, D. J., and D. M. Lavigne.
1985. A technique to recovery of otoliths from stomach contents of piscivorous pinnipeds. J. Wildl. Manag. 49: 910–912.

Nolf, D.
1993. A survey of perciform otoliths and their interest for phylogenetic analysis, with an iconographic synopsis of the Percoidei. Bull. Mar. Sci. 52(1):220–239.

Olesiuk, P. F.
1993. Annual prey consumption by harbor seals (*Phoca vitulina*) in the Strait of Georgia, British Columbia. Fish. Bull. 91:491–515.

Orta-Dávila, F.
1988. Hábitos alimentarios y censos globales del lobo marino (*Zalophus californianus*) en el Islote El Racito, Bahía de las Ánimas, Baja California. México durante octubre 1986–1987. Tesis de Licenciatura, 59 p. Universidad Autónoma de Baja California. Ensenada, B.C.

Pitcher, K. W.
1980. Stomach contents and feces as indicators of harbour seal, *Phoca vitulina*, foods in the Gulf of Alaska. Fish. Bull. 78:797–798.

Robison, B. H.
1972. Distribution of the midwater fishes of the Gulf of California. Copeia (1972):449–61.
Roper, C. F. E., and R. E. Young.
1975. Vertical distribution of pelagic cephalopods. Smithsonian Contribution to Zoology 209(51):31.
Sánchez-Arias, M.
1992. Contribución al conocimiento de los hábitos alimentarios del lobo marino de California *Zalophus californianus* en las Islas Ángel de la Guarda y Granito, Golfo de California, México. Tesis de Licenciatura, 63 p. Universidad Nacional Autónoma de México. México, D.F.
Tollit, D. J., M. J. Steward, P. M. Thompson, G. J. Pierce, M. B. Santos, and S. Hughes.
1997. Species and size differences in the digestion of otoliths and beaks: implications for estimates of pinniped diet composition. Can. J. Fish. Aquat. Sci. 54:105–119.
Walker, B. W.
1960. The distribution and affinities of the marine fish fauna of the Gulf of California. System. Zool. 9(3):123–133.
Wolff, G. A.
1984. Identification and estimation of size from the beaks of 18 species of cephalopods from the Pacific Ocean. NOAA Tech. Rep. NMFS 17, 49 p.

Recruitment and spawning-stock biomass distribution of bay anchovy (*Anchoa mitchilli*) in Chesapeake Bay*

Sukgeun Jung
Edward D. Houde
University of Maryland Center for Environmental Science
Chesapeake Biological Laboratory
1 Williams St., P.O. Box 38
Solomons, Maryland 20688
E-mail address (for S. Jung): jung@cbl.umces.edu

Abstract—Recruitment of bay anchovy (*Anchoa mitchilli*) in Chesapeake is related to variability in hydrological conditions and to abundance and spatial distribution of spawning stock biomass (SSB). Midwater-trawl surveys conducted for six years, over the entire 320-km length of the bay, provided information on anchovy SSB, annual spatial patterns of recruitment, and their relationships to variability in the estuarine environment. SSB of anchovy varied sixfold in 1995–2000; it alone explained little variability in young-of-the-year (YOY) recruitment level in October, which varied ninefold. Recruitments were low in 1995 and 1996 (47 and 31×10^9) but higher in 1997–2000 (100 to 265×10^9). During the recruitment process the YOY population migrated upbay before a subsequent fall-winter downbay migration. The extent of the downbay migration by maturing recruits was greatest in years of high freshwater input to the bay. Mean dissolved oxygen (DO) was more important than freshwater input in controlling distribution of SSB and shifts in SSB location between April–May (prespawning) and June–August (spawning) periods. Recruitments of bay anchovy were higher when mean DO was lowest in the downbay region during the spawning season. It is hypothesized that anchovy recruitment level is inversely related to mean DO concentration because low DO is associated with high plankton productivity in Chesapeake Bay. Additionally, low DO conditions may confine most bay anchovy spawners to the downbay region, where production of larvae and juveniles is enhanced. A modified Ricker stock-recruitment model indicated density-compensatory recruitment with respect to SSB and demonstrated the importance of spring-summer DO levels and spatial distribution of SSB as controllers of bay anchovy recruitment.

Manuscript approved for publication 30 September 2003 by Scientific Editor.
Manuscript received 20 October 2003 at NMFS Scientific Publications Office.
Fish. Bull. 102:63–77 (2004).

Recruitment for marine fishes is variable and is regulated or controlled by a combination of density-dependent and density-independent processes. It has been hypothesized that density-independent processes dominate from the egg to larval stages whereas density-dependent control by predation may be more important in the juvenile stage (Sissenwine, 1984; Houde, 1987). Density-dependent processes may be stock dependent, regulated by adult abundances, or dependent on abundances of the early-life stages (Ricker, 1975). In estuarine systems, where hydrological conditions (e.g. dissolved oxygen, temperature, and circulation) vary widely, the roles of density-independent physical factors on fish recruitments may be dominant, making it difficult, but still important, to partition density-dependent and density-independent processes, particularly for short-lived small pelagic fishes such as anchovies and sardines.

Bay anchovy (*Anchoa mitchilli*) (Engraulidae) is a coastal species distributed broadly in the western Atlantic from Maine to Mexico. This small fish is the most abundant and ubiquitous fish in Chesapeake Bay, the largest estuary on the east coast of North America (Houde and Zastrow, 1991; Able and Fahay, 1998). It is not fished, yet there is evidence that recruitment is variable (Newberger and Houde, 1995). It feeds on zooplankton—primarily copepods and other small crustacea—and is a major prey of piscivores, including several economically important fishes (Baird and Ulanowicz, 1989; Luo and Brandt, 1993; Hartman and Brandt, 1995). Male and female bay anchovy in Chesapeake Bay mature at 40–45 mm fork length (44–50 mm total length) at about 10 months of age, and peak spawning occurs in July (Zastrow et al., 1991). Most eggs are produced by age-1 individuals (Luo and Musick, 1991; Zastrow et al., 1991). Bay anchovy may survive to age 3+ and reach approximately 100 mm length and 5 g wet weight (Newberger and Houde, 1995; Wang and Houde, 1995).

Newberger and Houde (1995) noted large differences in annual survey abundances of bay anchovy that apparently resulted from variability in annual recruitments. In Chesapeake Bay, abundance, growth, and mortality rates of bay anchovy eggs and larvae vary temporally and spatially (Dorsey et al., 1996; MacGregor and Houde, 1996; Rilling and Houde, 1999a, 1999b). Individual-based models were developed to test the hypothesis that recruitment of bay anchovy is determined by variable growth and mortality during early-life stages that are regulated by density-dependent processes (Wang et al., 1997; Cowan et al., 1999; Rose et al., 1999). In previous research, there was little knowledge of levels of spawning stock biomass or density-independent environmental factors that may control recruitment through their effects on spatial and temporal variability in growth and mortality of prerecruit anchovy.

* Contribution 3696 of the University of Maryland Center for Environmental Science, Chesapeake Biological Laboratory, Solomons, MD 20688.

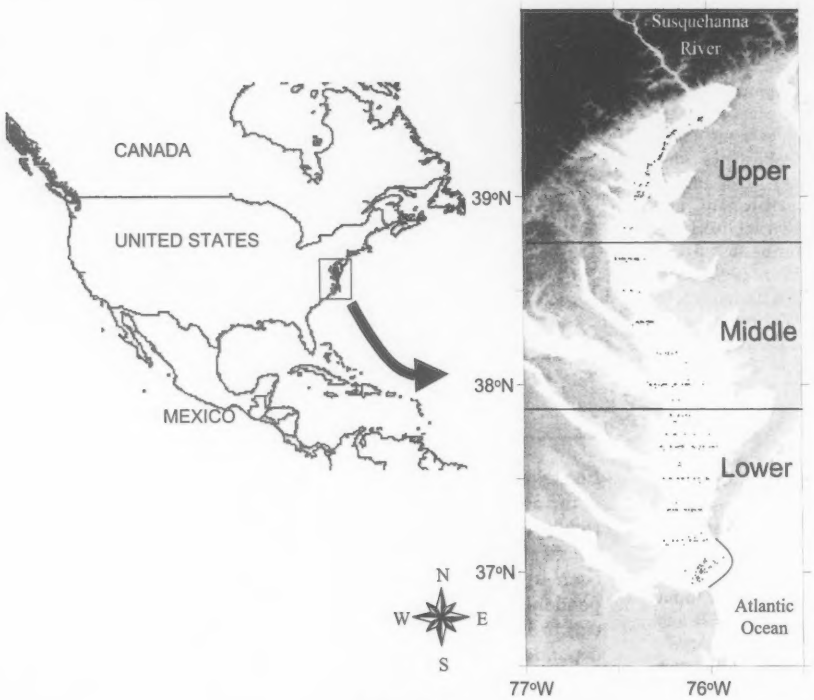

Figure 1

Chesapeake Bay and stations sampled by the midwater trawl in the 1995–2000 surveys. Horizontal lines indicate boundaries of three designated regions.

We evaluated environmental factors, spatial distribution of spawning stock biomass (SSB), and possible ontogenetic migrations of prerecruits (Dovel, 1971; Loos and Perry, 1991; Wang and Houde, 1995; Kimura et al., 2000) with respect to bay anchovy recruitment variability. Our objectives were 1) to estimate annual and regional variability in bay anchovy recruitment, 2) to evaluate effects of hydrological conditions (mainly, freshwater input, and dissolved oxygen concentration) on stage-specific distribution, ontogenetic migration, and recruitment, and 3) to identify mechanisms and describe patterns or trends in the bay anchovy recruitment process. Data were obtained in a six-year, multidisciplinary research program conducted throughout Chesapeake Bay.

Materials and methods

Study area

Chesapeake Bay is a coastal plain estuary of partially mixed fresh water and sea water. Its 320-km mainstem varies in width from about 6 to 50 km (Fig. 1). The Bay is shallow; less than 10% of its area is >18 m deep and approximately 50% is <6 m deep. More than 80% of the freshwater entering the bay is from tributaries on its northern and western sides (Chesapeake Bay Program[1]). Salinity grades from near-full seawater at the mouth of the bay to freshwater near its head. Water temperatures reach 28–30°C in mid summer, and fall to 1–4°C in late winter (Murdy et al., 1997). Despite shallow depth, the bay usually has a strongly developed pycnocline, and has seasonally strong vertical gradients in temperature, salinity, and dissolved oxygen.

Surveys

Trawl surveys were conducted three times annually over the entire bay (April–May, June–August, and October), 1995–2000 (Table 1, Fig. 1). Midwater-trawl (MWT) fish collections[2] were made on transects in three regions: the lower bay (37°05′N–37°55′N), middle bay (37°55′N–38°45′N), and upper bay (38°45′N–39°25′N). As defined, the lower bay contains 51% of water volume, the middle bay 32%, and the upper bay 17% (Fig. 1). The number of midwater trawl sta-

[1] Chesapeake Bay Program. 2000. Chesapeake Bay: Introduction to an ecosystem. U.S. Environmental Protection Agency, publ. EPA 903-R-00-001, 30 p. EPA, 410 Severn Ave, Suite 109, Annapolis, MD 21403.

[2] Trophic interactions in estuarine systems, midwater trawl survey. University of Maryland Center for Environmental Science, Chesapeake Biological Laboratory. http://www.chesapeake.org/ ties/mwt [accessed 15 October 2003].

Table 1

Cruise dates, mean temperatures (°C), salinities (psu), and dissolved oxygen (mg/L), integrated from surface to bottom, and pooled standard errors for individual cruises, years, seasons, and regions of Chesapeake Bay, 1995–2000. CV = coefficient of variation for annual means.

	Temperature	SE	Salinity	SE	Oxygen	SE
Cruise date (departure)						
28 Apr 95	13.88	0.11	15.01	0.42	8.53	0.13
23 Jul 95	28.13	0.12	15.48	0.44	6.50	0.14
28 Oct 95	17.26	0.12	17.39	0.45	7.59	0.14
28 Apr 96	13.87	0.10	10.84	0.36	10.21	0.11
17 Jul 96	24.66	0.11	11.80	0.41	7.43	0.13
22 Oct 96	16.10	0.10	11.26	0.36	8.55	0.11
20 Apr 97	10.93	0.13	11.41	0.50	10.01	0.16
11 Jul 97	25.28	0.13	13.59	0.51	7.10	0.16
29 Oct 97	14.64	0.13	18.19	0.51	8.01	0.16
11 Apr 98	12.26	0.12	8.90	0.44	9.95	0.14
04 Aug 98	26.15	0.12	12.89	0.46	7.01	0.15
19 Oct 98	18.60	0.13	16.64	0.49	8.64	0.15
19 Apr 99	11.97	0.13	13.51	0.49	10.04	0.16
26 Jun 99	23.52	0.15	16.02	0.56	5.75	0.18
23 Oct 99	16.30	0.14	17.38	0.53	8.87	0.17
29 Apr 00	12.95	0.17	12.51	0.64	8.98	0.20
25 Jul 00	24.26	0.14	14.06	0.53	5.17	0.17
17 Oct 00	17.89	0.15	16.73	0.56	7.63	0.18
Year						
1995	19.76	0.07	15.96	0.25	7.54	0.08
1996	18.21	0.06	11.30	0.22	8.73	0.07
1997	16.95	0.08	14.40	0.29	8.37	0.09
1998	19.00	0.07	12.81	0.27	8.53	0.08
1999	17.26	0.08	15.64	0.30	8.22	0.10
2000	18.36	0.09	14.43	0.33	7.26	0.11
CV	5.8%		12.5%		7.2%	
Season						
April–May	12.64	0.05	12.03	0.20	9.62	0.06
June–August	25.33	0.05	13.97	0.20	6.49	0.06
October	16.80	0.05	16.27	0.20	8.22	0.06
Region of bay						
Lower	18.40	0.04	21.19	0.16	8.15	0.05
Middle	18.33	0.05	14.06	0.19	8.33	0.06
Upper	18.04	0.06	7.02	0.23	7.85	0.07

tions per survey ranged from 24 to 52 (six-year total=597). Additional baywide surveys (August 1997 and September 1998) and partial surveys (June 1997, July 1998, and July 1999) also provided data (total stations =146).

An 18-m^2 mouth-opening midwater trawl (MWT), with 3-mm codend mesh was deployed from the stern of the 37-m research vessel *Cape Henlopen*. All trawling was conducted at night. Standardized tows of 20-min duration were conducted and the trawl was deployed at graded depth intervals from surface to bottom (2 minutes at each depth interval) in order to provide a sample of fish from the entire water column. Fish catches (or subsamples) were counted, measured (to the nearest 1.0 mm), and weighed on deck immediately after a tow.

Abundance and biomass of bay anchovy recruits and spawners

We separated bay anchovy catches into YOY and spawners based on total length (TL). The minimum length of bay anchovy retained by the MWT was 21 mm TL, which we also defined as the minimum TL for recruited YOY bay

anchovy. Modal lengths of young-of-the-year (YOY) bay anchovy cohorts were determined from length-frequency distributions in MWT catches and a modal analysis (Bhattacharya, 1967; King, 1995). Based on the modal analysis of summer and fall survey data, the maximum TL of YOY bay anchovy and, therefore, the minimum TL of spawners, were estimated (Table 2).

Length-dependent gear selectivity for bay anchovy was adjusted by comparing catches of the MWT and a 2-m^2 Tucker trawl with catches from 707-μm meshes at the same stations during a September 1998 baywide survey. The length-specific MWT:Tucker-trawl catch ratios (N_{MWT}/N_{TT}=catch per unit of effort MWT ÷ catch per volume of water Tucker trawl) for anchovies 21–70 mm TL indicated that both gears fished with a consistent selectivity for bay anchovy of 30–48 mm TL, and with a slight decrease in N_{TT} for 48–70 mm TL. However, the values of N_{MWT}/N_{TT} were lower by factors of 1~7 for 21–30 mm TL fish, indicating that small anchovies were collected less efficiently by the MWT. We concluded that length classes of anchovies >30 mm TL were equally vulnerable to the MWT and those >48 mm TL were less vulnerable to the Tucker trawl. Accordingly, we adjusted MWT catches of ≤30 mm TL anchovy by multiplying them by a weighting factor estimated from the regression of values of N_{MWT}/N_{TT} for 21–30 mm TL bay anchovy.

$$(\textit{Weighting factor}) = -0.59\ TL + 19.08, \qquad (r^2=0.96)$$

where TL = total length.

The weighting factor equals 1.0 for anchovy >30 mm TL because MWT selectivity is constant for anchovy >30 mm TL. To estimate water sampled in a 20-min MWT tow,

$$D_N = N_{MWT}/V_{MWT} = (1/s) \times N_{TT}/V_{TT}$$

and

$$V_{MWT} = s \times (N_{MWT}/N_{TT}) \times V_{TT},$$

where D_N = the concentration of 31–48 mm TL bay anchovy at a station (i.e. number/m^3);
N_{MWT} = the number of 31–48 mm TL bay anchovy collected per 20-min MWT tow at a station; V_{MWT} = the effective water volume sampled by a 20-min MWT tow (m^3);
N_{TT} = the number of 31–48 mm TL bay anchovy collected by the 2-m^2 Tucker trawl at the same station;
s = vulnerability to the Tucker trawl (s=1 if all bay anchovies in water volume, V_{TT}, are collected); and V_{TT} is the volume filtered by the Tucker trawl (m^3) estimated from a flowmeter in its mouth.

The mean of N_{MWT}/N_{TT} for 30–48 mm TL bay anchovy during the September 1998 survey indicated that V_{MWT} = 4961 m^3, if 30–48 mm TL bay anchovy did not significantly avoid the mouth of the 2-m^2 Tucker trawl (i.e. s=1). Assuming s=1 (i.e. V_{MWT}=4961 m^3), we estimated "relative" baywide abundance and biomass of YOY and spawners for the 18 surveys from 1995 to 2000.

Table 2

Estimated maximum total lengths of young-of-the-year bay anchovy (mm) from Chesapeake Bay, based on analysis of length-frequency distributions.

Year	Date	Length (mm)
1995	23 Jul	52
	28 Oct	69
1996	17 Jul	57
	22 Oct	68
1997	11 Jul	30
	2 Aug	56
	29 Oct	66
1998	4 Aug	50
	7 Sep	62
	19 Oct	69
1999	26 Jun	30
	23 Oct	65
2000	25 Jul	52
	17 Oct	67

To coarsely estimate a typical value of s, "absolute" baywide spawner biomasses in June–August were estimated for 1995–2000 according to an egg production method (Parker, 1985; Rilling and Houde, 1999a). Bay anchovy eggs had been collected in a 1-m^2 Tucker trawl during the same surveys and provided estimates of egg abundance. The coverage of stations and sampling design for the Tucker trawl was comparable to that of the MWT, but the Tucker trawl was deployed during both day and night. We presumed that all eggs collected between 00:00 and 20:00 h had been spawned near a midnight peak (00:00 h) (Zastrow et al., 1991) and decreased in abundance at a mean instantaneous mortality (reported for bay anchovy eggs in Chesapeake Bay as M = 0.066/h; Dorsey et al., 1996). Based on the estimated number of eggs spawned at 00:00 h for each station, the regional mean weight of individual spawners (defined by the minimum TL in Table 2) in MWT catches, and the reported fecundity-weight relationship for females (Zastrow et al., 1991), we were able to coarsely estimate "absolute" baywide spawner biomass. We assumed that the spawning fraction of adult females per day was essentially 1.0 (i.e. all adult females participated in spawning, Zastrow et al., 1991) and the fecundity-weight relationship was constant over years.

Comparison of the baywide estimates of spawner biomass in June–August based on the egg production method ("absolute" biomass) with estimates based on the MWT catch-per-unit-of-effort ("relative" biomass) indicated that, on average, for 1995 to 2000, s is equal to 0.20. Therefore, the mean effective water volume fished by a 20-min MWT tow was 4961 × 0.20 = 989 m^3.

Because N_{MWT} of bay anchovy was highly variable, even at stations on the same sampling transect, and a mixed model (SAS version 6.12, SAS Inst. Inc., Cary, NC) including spatial covariance (variogram) did not significantly improve precision in annual, seasonal, and regional means or differences of N_{MWT}, a stratified sampling design (Steel and Torrie, 1980), i.e. stratum = region, was adopted. Based on the mean effective water volume ($= s \times V_{MWT}$), we estimated regional "absolute" abundance and biomass (number and wet weight) and related standard errors of the linear combination by regional subvolumes (Samuels, 1989) of bay anchovy ≥21 mm TL for all MWT surveys from 1995 to 2000 by multiplying regional mean MWT catch by $V_r/989$, where V_r represents the water volume (m^3) in each bay region (Cronin, 1971):

$$N_{total} = (N_l \times V_l + N_m \times V_m + N_u \times V_u)/(s \times V_{MWT}) \times V_{total}$$

$$SE_N = Sc_N \sqrt{V_l^2 / n_l + V_m^2 / n_m + V_u^2 / n_u},$$

where N_{total} = baywide absolute abundance;
N_l, N_m, N_u = mean values of N_{MWT} for the lower (l), middle (m), and upper (u) bay;
V_l, V_m, V_u = bay subvolumes for the lower (l), middle (m), and upper (u) bay (from Cronin, 1971), $V_l = 26.7 \times 10^9$ m^3, $V_m = 16.8 \times 10^9$ m^3, $V_u = 8.7 \times 10^9$ m^3, $V_{total} = V_l + V_m + V_u = 52.1 \times 10^9$ m^3;
SE_N = standard error of N_{total};
n_l, n_m, n_u = number of midwater trawl stations for the lower (l), middle (m), and upper (u) bay;
Sc_N = pooled standard deviation of N_{MWT} = square root of mean squares within groups in analysis of variance table = $\sqrt{(SS_l + SS_m + SS_u)/(n_{total} - 3)}$, where SS_l, SS_m, SS_u = sum of squares of N_{MWT} for the lower (l), middle (m), and upper (u) bay, and $n_{total} = n_l + n_m + n_u$.

Environmental factors

Depth profiles of temperature, salinity, and dissolved oxygen (DO) concentration were determined from conductivity-temperature-depth (CTD) casts at sampling stations. DO data were adjusted by calibrating against Winkler titration data from water samples collected in Niskin bottles deployed with the CTD cast. However, DO data from the CTD could not be adjusted for the 1999 summer and all calendar year 2000 cruises because Winkler titrations were not conducted. To estimate regional means for the water column, we averaged temperature, salinity, and DO values by integrating the observed values with respect to depth, after dividing the water column into "above pycnocline" and "subpycnocline" layers.

Ontogenetic migration

We analyzed length-frequency distributions along the south-north axis of the bay (i.e. by latitude) to delineate possible ontogenetic migrations of YOY and adult bay anchovy. To parameterize the distribution of YOY and adult abundance and biomass, we estimated the biomass-weighted mean latitudes of occurrence for each length class (3-mm interval).

$$\bar{L}_{B,l} = \sum_k B_{k,l} L_k / \sum_k B_{k,l},$$

where $\bar{L}_{B,l}$ = biomass-weighted mean latitude of a length class, l;
L_k = latitude of the station, k; and
B = biomass (g, wet weight) per 20-min tow.

We devised a metric to parameterize the location of bay anchovy SSB. We assumed that the baseline boundary for SSB distribution during the spring was at the mouth of the bay (37°00′N). Then, the upbay difference between biomass-weighted mean latitude of SSB (in decimal units) in Jun–August and the baseline for SSB during the spring (ΔL) was calculated:

$$\Delta L = \left(\begin{array}{c} \text{biomass-weighted mean latitude of} \\ \text{SSB in June – August} \end{array} \right) - 37.00.$$

Recruitment model

As an exploratory step, a correlation analysis was undertaken to examine the relationships between bay anchovy SSB, migration patterns, and recruitment levels with respect to regional and depth-layer-specific mean temperature, mean salinity, mean DO, their gradients, and monthly mean freshwater flow from the Susquehanna River. Cross-correlations revealed that SSB migration pattern (ΔL), regional mean DO concentrations, and October YOY recruitment level were closely correlated. Regional mean DO concentration provided the best fit to YOY recruitment level in October when baywide SSB also was included as an explanatory variable in multiple regressions. However, because there is uncertainty in the uncalibrated DO measurements in 1999 and 2000, we did not use regional mean DO in our recruitment model. Instead, we developed a modified Ricker-type stock-recruitment model (Ricker, 1975) that included ΔL as an explanatory variable:

$$R_y = a\, S \exp(-\beta_1 S - \beta_2 \Delta L) + \varepsilon_y \quad \text{(modified Ricker model)}$$

where R_y = recruitment level = October YOY abundance in each year (1995–2000);
y; a, β_1 and β_2 = regression coefficients;
S = estimated baywide SSB (male+female) in metric tons for April–May; and
ε_y = the error term.

In this model, if ΔL is held constant, R_y is maximum at $S = 1/\beta_1$. Although no abiotic factor was included explicitly in the model, ΔL is strongly correlated with regional mean DO and serves as a proxy for it. For the modified Ricker model, collinearity, and jackknife influence diagnostic tools were

Table 3

Seasonal mean freshwater flow entering Chesapeake Bay from the Susquehanna River (m^3/s). Data source: http://va.water.usgs.gov/chesbay/RIMP/adaps.html.

Period	1995	1996	1997	1998	1999	2000
Jan–Mar	1289	2495	1474	2563	1325	1379
Apr–Jun	728	1702	920	1625	791	1627
Jul–Sep	238	768	239	334	294	393
Oct–Dec	923	2230	746	194	642	504
Annual mean	795	1799	845	1179	763	976

applied to evaluate reliability of the regression model (Belsley et al., 1980; SAS, 1989).

Results

Environmental factors

Stream flows from the Susquehanna River (Table 3) varied annually and seasonally. Freshwater stream flows were higher in 1996 and 1998 than in other years. Baywide mean values of water temperature, salinity, and DO concentration, averaged from surface to bottom, varied annually, seasonally, and regionally (Table 1). Annually, mean temperature was highest in 1995 and lowest in 1997. Mean salinity was highest in 1995 and lowest in 1996. Mean DO concentration was highest in 1996 and lowest in 2000. Regionally, salinity was more variable than temperature and DO concentration. Seasonally, temperature and DO concentration were more variable than salinity. Temperature was highest in the June–August period, the spawning season of bay anchovy. Seasonally, salinity increased progressively from April–May to October. Mean DO concentration was consistently lowest in June–August.

Trends in abundance and recruitment

Estimates of bay anchovy abundance reported in our study are for the entire mainstem of Chesapeake Bay. The estimated recruitment levels (baywide abundance of YOY bay anchovy >30 mm TL in October) varied ninefold and were low in 1995 and 1996 (47.5 ±16.6 and 30.6 $\pm 8.6 \times 10^9$ individuals) but much higher in 1997–2000 (99.6 ±12.4 to 264.8 $\pm 32.6 \times 10^9$). Baywide estimates of bay anchovy biomass for individuals >30 mm TL increased from April to October in each year (Table 4). October baywide biomass varied sevenfold from 27.1 $\pm 5.5 \times 10^3$ to 192.9 $\pm 20.4 \times 10^3$ tons and was highest in 1998 and lowest in 1996.

Estimated spawning stock biomass (SSB) in April–May was lowest in 1995 (3.3 $\pm 1.1 \times 10^3$ tons), and highest in 1997 (20.1 $\pm 5.3 \times 10^3$ tons), indicating sixfold variability. SSB in June–August was lowest in 1996 (2.4 $\pm 0.2 \times 10^3$ tons), and highest in 1997 (21.1 $\pm 2.3 \times 10^3$ tons). The SSBs in April–May and June–August did not show any obvious relationship to YOY abundance (recruitment) in October.

Ontogenetic migration

The length-specific mean locations (latitudes of occurrence) of bay anchovy revealed an apparent ontogenetic migration. Small juveniles of bay anchovy tended to move upbay and were located primarily upbay until they were approximately 45 mm TL, after which they began to move downbay (Fig. 2). In April–May, age-1 bay anchovy <60 mm TL, consisting of individuals recruited from the previous year, varied annually in their mean latitude of occurrence, whereas large (≥age 1, ≥60 mm TL) bay anchovy had relatively stable locations near the boundary between the lower and middle bay regions, centered at latitude 37°40′N (Fig. 2A). Compared to April–May, age-1+ bay anchovy in June–August were more variable in their annual mean locations, but both YOY and adult bay anchovy tended to occur upbay of latitude 38°00′N, except in year 2000 (Fig. 2B). In 1997 and 1999, when annual mean temperatures were lowest (Table 1), YOY bay anchovy were too small to be sampled by the MWT in June–August and are not represented in Figure 2B. In October, mean latitudes of occurrence (Fig. 2C) indicated a consistent distribution pattern and an apparent ontogenetic migration by YOY anchovy. The most probable explanation for the observed latitudinal distributions was that small YOY bay anchovy tended to move upbay initially, but then downbay at about 45 mm TL. Distribution of age-1+ individuals in October was variable.

The SSB of bay anchovy (excludes YOY) from 1995 to 2000 was centered near 38°00′N in April–August except in June–August of 1995 and 1996, when the SSB was centered farther upbay (Fig. 3A). In 2000, the migration pattern differed from other years. Spawning bay anchovy in 2000 were located farther downbay in July than in April (Fig. 3A). The April–May location of prespawning SSB was mostly explained by the mean flow of the Susquehanna River from June of the previous year to February of the current year (r^2=0.94, P=0.0012; Fig. 3B). But, in June–August, the mean location of spawning fish was more strongly and significantly related to the subpycnocline-layer mean

Table 4

Baywide abundance and biomass estimates for bay anchovy >30 mm TL (young-of-the-year + adult). SE = standard error.

		Abundance ($\times 10^9$)		Biomass ($\times 10^3$ metric tons)	
Year	Period	Estimate	SE	Estimate	SE
1995	April–May	2.1	0.7	3.3	1.1
	June–August	57.8	28.1	32.6	17.5
	October	47.5	16.6	51.9	21.0
1996	April–May	4.9	1.1	8.9	2.0
	June–August	5.3	1.6	3.7	1.3
	October	30.6	8.6	27.1	5.5
1997	April–May	11.8	3.3	20.1	5.3
	June–August	9.4	2.3	21.1	5.0
	October	99.6	12.4	85.6	10.8
1998	April–May	3.5	0.7	6.1	1.3
	June–August	14.4	4.5	17.0	7.9
	October	264.8	32.6	192.9	20.4
1999	April–May	6.9	1.4	10.6	2.2
	June–August	5.5	1.2	10.6	2.4
	October	124.5	28.3	115.3	25.0
2000	April–May	6.2	4.1	13.0	6.6
	June–August	144.6	51.2	56.0	17.0
	October	169.1	43.7	152.9	40.0

DO during that same period in the middle bay (r^2=0.75, P=0.02; Fig. 3C).

Correlations

Correlation analyses suggested that regional mean DO concentrations are the most important environmental correlate associated with spatial distribution of SSB and recruitment processes of bay anchovy. The mean locations (latitudes of occurrence), abundances, and biomasses for YOY and adult bay anchovy were analyzed with respect to environmental variables (Table 5). Recruitment levels (YOY abundance) in October were consistently inversely correlated with DO concentrations in the lower and middle bay in June–August (r=–0.13 to –0.89). Biomass-weighted mean latitude of SSB (age 1+) in April–May was consistently and positively correlated with regional salinities in April–May (r=0.30 to 0.88). On the other hand, in June–August, surface-layer mean salinity in the lower Bay and subpycnocline-layer mean DO in the lower and middle bay were significantly and positively correlated with mean latitude of SSB or ΔL (r=0.82 to 0.91). Baywide SSB in April–May and June–August tended to be negatively correlated with water temperature in April–May (r=–0.45 to –0.90).

Recruitment model

Although SSB alone did not correlate significantly with recruitment level, mean DO in June–August was significantly related to the mean latitude of SSB in June–August (or ΔL) and bay anchovy recruitment level in October (Figs. 3C and 4). ΔL was selected as the explanatory variable, rather than DO, because DO data were uncalibrated in 1999 and 2000. The correlation observed between ΔL and DO (Fig 3C) suggested that ΔL can serve as a proxy for DO in the stock-recruitment model. Including ΔL and SSB for April–May in a modified Ricker model provided a good fit to bay anchovy recruitment levels observed from 1995 to 2000 (Fig. 5). The model is

$$R_y = 365\, S \exp(-0.19\, S\, 1.35\, \Delta L) \quad \text{(modified Ricker model)}.$$

In the model, if ΔL is held constant, predicted recruitment level of bay anchovy is maximum when baywide SSB in April–May is approximately 5.3×10^3 tons. Collinearity and influence diagnostic statistics did not indicate collinearity between the two independent variables (S and ΔL), or that an observation in any year had a dominating influence on parameter estimates.

Discussion

Complex environmental processes and biological interactions control bay anchovy recruitment in Chesapeake Bay. Dissolved oxygen (DO), freshwater flow, salinity, and temperature acting on prerecruits and adults are important factors affecting bay anchovy distribution and levels of recruitment. Spawning stock size also is related to recruit-

ment level. Our results have demonstrated that there is a strong spatial component in the recruitment dynamics of bay anchovy. Although fish recruitment processes historically have been difficult to understand, our six-year, spatially extensive research has provided new insights into processes that control bay anchovy recruitment.

Ontogenetic migration pattern

It is apparent that ontogenetic migration plays a role in the spatial and temporal patterns in abundance, biomass, and production of bay anchovy. There are several lines of evidence. Rilling and Houde (1999a), in a baywide analysis, reported that mean density of eggs and larvae in June and July 1993 was very high in the lower Chesapeake Bay compared to more upbay sites. Dovel (1971) and Loos and Perry (1991) reported possible upbay or upriver migration of bay anchovy larvae and juveniles in the mainstem and tributaries of the Bay. Recent otolith microchemical analyses have strongly supported the hypothesis that an upbay ontogenetic migration by small YOY anchovy (≥25 mm, late larvae and small juveniles) occurs (Kimura et al., 2000). In the middle Hudson River estuary (Schultz et al., 2000) and Chesapeake Bay (North and Houde, in press), selective tidal-stream transport was suggested as a mechanism for up-estuary movements of bay anchovy larvae. Our conceptual model of the bay anchovy life cycle includes migration patterns in the bay based on available knowledge and evidence (Fig. 6).

It is uncertain what benefits YOY bay anchovy derives from upbay migration in summer and whether the migration is passive or active before a subsequent reverse migration in the fall. To explain upbay movements of estuarine fishes, Dovel (1971) proposed that there is a "critical zone" of low salinity and high prey production in the upper bay, which is important as a nursery for bay anchovy and other fish species. In late spring and early summer, age-1 and age-1+ bay anchovy mature and move upbay while spawning, although the year 2000, when mean freshwater streamflow during the previous fall-winter was lowest, was an exception. Recruited YOY bay anchovy apparently overwinter primarily, but not entirely, downbay until spring.

There remains a possibility of significant immigration to the bay by adult bay anchovy in some years from the coastal ocean or tidal tributaries of the bay. Without such immigration, baywide adult abundance would decrease continuously during the April–October period through natural mortality. However, in two years of our six-year study, 1995 and 1998, estimated adult abundance increased substantially from April to July, and in 1999 adult abundance increased from June to October, implying significant immigration to the bay in those years (Jung, 2002).

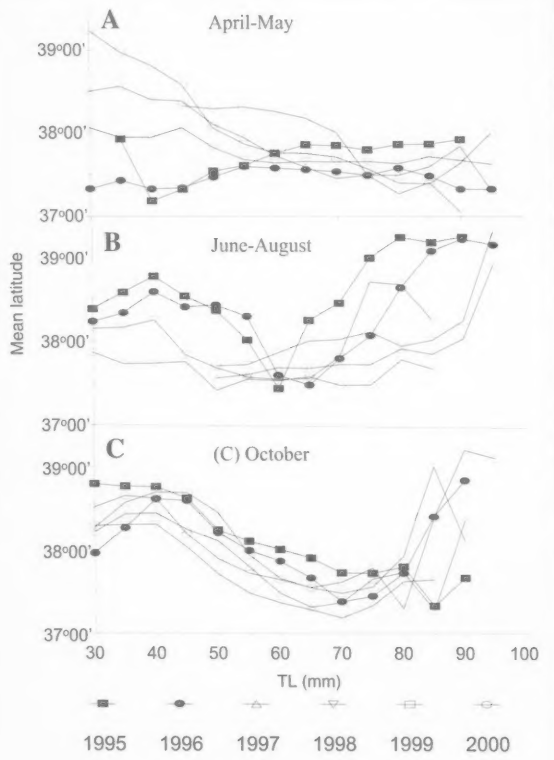

Figure 2

Abundance-weighted mean latitude of occurrence of bay anchovy (*Anchoa mitchilli*) in Chesapeake Bay, 1995–2000.

Recruitment control and regulation

The modified Ricker recruitment model that included SSB and ΔL as explanatory variables provided a good fit to bay anchovy recruitments. Although the model fitted well, there were only six years of data, and the underlying mechanisms explaining relationships between the distribution and level of SSB, hydrological conditions, and density-dependent regulatory processes in recruitment of bay anchovy are not yet clear. Nevertheless, correlations and the recruitment model clearly indicated a density-dependent effect of SSB level and also implicated environmental factors (at the mesoscale) that are related to mean DO concentration, latitudinal distribution of SSB (ΔL), and the recruitment level of bay anchovy (Fig. 4).

The modified Ricker model for bay anchovy (Fig. 5) indicates a density-compensatory stock-recruitment relationship (Ricker, 1975), although we do not know at what life stages density-dependent processes are most important. Without accounting for the controlling effect of ΔL and mean DO on a regional scale, the density-dependence might have gone undetected (Fig. 4). Recent individual-based models suggest that density-dependent processes during early-life stages could stabilize bay anchovy recruitments (Wang et al., 1997; Cowan et al., 1999; Rose et al., 1999). At the small scales of several meters modeled by Wang et al. (1997) and Cowan et al. (1999), larval-stage feeding

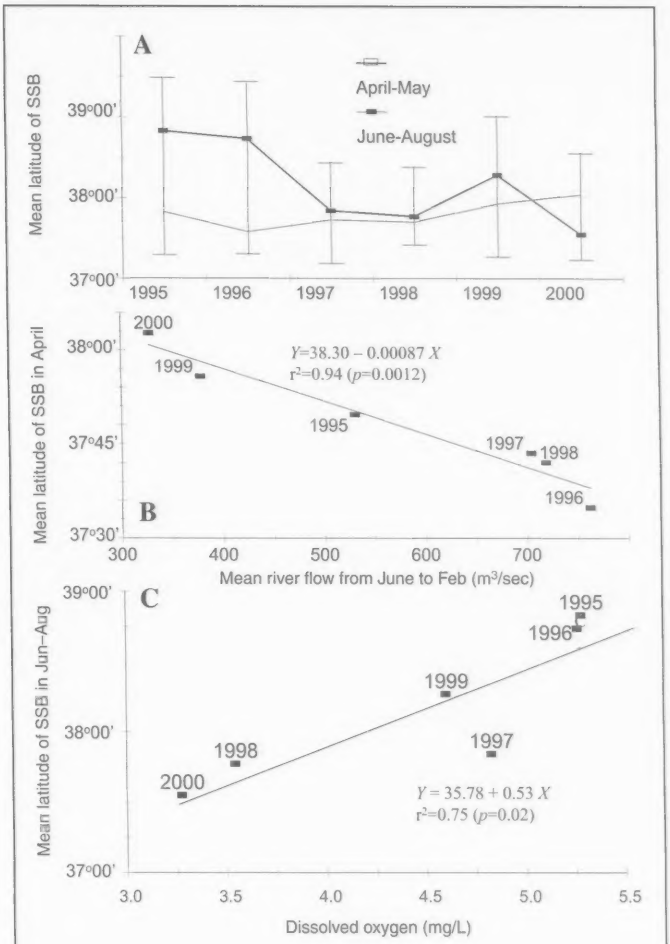

Figure 3

Mean location (latitude) of adult bay anchovy (*Anchoa mitchilli*) spawning stock biomass (SSB) in Chesapeake Bay. (**A**) Mean latitude and standard deviation in April–May and in June–August. The upper vertical bar represents mean + standard deviation for June–August, and the lower vertical bar represents mean–standard deviation for April–May. (**B**) Mean latitude in April–May and mean Susquehanna River flow from June of the previous year to February of the current year. (**C**) Mean latitude in June–August and mean dissolved oxygen in the subpycnocline layer of the middle bay in June–August.

processes were important and high adult SSB could produce abundant first-feeding larvae with subsequent density-dependent food competition. In Tampa Bay, Florida, Peebles et al. (1996) hypothesized that bay anchovy's size-specific fecundity is directly related to prey availability for adults. Modeled results of Rose et al. (1999) suggested that density-dependent growth of bay anchovy larvae and juveniles in Chesapeake Bay would lead to density-dependent survival of these stages. Hunter and Kimbrell (1980) and Alheit (1987) proposed that cannibalism by adults on eggs and larvae provides a degree of density-dependent regulation in anchovies of the genus *Engraulis*. Analyses of feeding by adult bay anchovy did not indicate that pelagic fish eggs were a significant part of bay anchovy diet (Vazquez-Rojas, 1989; Klebasko, 1991), although no specific study of cannibalism has been undertaken.

We propose three hypotheses that may explain the relationships among regional DO concentration, the latitudinal shift in SSB distribution during the spawning season (ΔL), and recruitment levels of bay anchovy in October. The

hypotheses are the following: 1) averaged DO concentration is inversely related to levels of plankton productivity in a region and high plankton productivity favors high recruitments of planktivorous bay anchovy; 2) low dissolved oxygen concentrations can restrict spatial distribution of bay anchovy SSB to the lower bay insuring high egg and

Table 5

Cross-correlation coefficients for bay anchovy distribution and abundance with respect to region- and layer-specific means of temperature, salinity, and dissolved oxygen from 1995 to 2000. Mean latitude is biomass-weighted mean latitude of occurrence of bay anchovy. Abundance and biomass are baywide total estimates. ΔL = (mean latitude in June–August) –37.00. Abbreviations are as follows: SAL = salinity, TEM = water temperature, OXY = dissolved oxygen; the fourth and fifth digits: 04 = April–May, 07 = June–August; the sixth character: L = lower bay, M = middle bay, U = upper bay; The last character: S = layer above the pycnocline, B = layer below the pycnocline. * = significant at $\alpha = 0.05$.

	Young-of-the-year		Adult			
	Mean latitude	Abundance	Mean latitude		Biomass	
	October	October	April–May	June–August (or ΔL)	April–May	June–August
SAL04LS	0.29	–0.43	0.74	0.26	–0.17	–0.52
SAL04MS	0.45	–0.63	0.30	0.71	–0.41	–0.22
SAL04US	0.27	–0.60	0.42	0.53	–0.18	–0.02
SAL04LB	–0.24	0.01	0.88*	–0.16	–0.14	–0.31
SAL04MB	0.08	–0.17	0.59	0.33	–0.39	–0.05
SAL04UB	0.29	–0.61	0.45	0.46	–0.03	0.05
SAL07LS	0.83*	–0.75		0.91*		–0.46
SAL07MS	–0.12	0.06		0.14		0.31
SAL07US	0.06	–0.03		–0.04		–0.33
SAL07LB	0.70	–0.75		0.64		–0.11
SAL07MB	–0.41	0.60		–0.31		0.19
SAL07UB	0.15	–0.20		0.01		–0.42
TEM04LS	0.16	–0.25	–0.03	0.65	–0.90*	–0.48
TEM04MS	0.50	–0.46	0.14	0.65	–0.71	–0.85*
TEM04US	0.53	–0.32	–0.36	0.52	–0.56	–0.85*
TEM04LB	0.29	–0.49	0.19	0.71	–0.72	–0.45
TEM04MB	0.22	–0.42	0.39	0.47	–0.55	–0.62
TEM04UB	0.40	–0.26	–0.39	0.48	–0.60	–0.77
TEM07LS	–0.49	–0.04		0.11		0.45
TEM07MS	–0.16	–0.21		0.47		0.14
TEM07US	–0.29	–0.08		0.39		0.38
TEM07LB	–0.68	0.24		–0.11		0.38
TEM07MB	–0.24	–0.10		0.37		–0.04
TEM07UB	–0.45	0.16		0.21		0.46
OXY04LS	0.63	–0.22	–0.80	0.39	–0.10	–0.30
OXY04MS	–0.27	0.56	0.23	–0.81	0.55	–0.04
OXY04US	–0.43	0.41	–0.30	–0.30	0.30	0.88*
OXY04LB	0.93**	–0.68	–0.59	0.63	0.04	–0.38
OXY04MB	0.47	–0.35	–0.31	–0.09	0.70	–0.12
OXY04UB	–0.57	0.65	–0.32	–0.46	0.21	0.78
OXY07LS	0.18	–0.30		0.29		0.32
OXY07MS	0.01	–0.13		0.29		0.56
OXY07US	0.23	–0.32		0.50		0.10
OXY07LB	0.67	–0.48		0.82*		–0.28
OXY07MB	0.72	–0.89*		0.87*		–0.04
OXY07UB	0.01	0.16		0.21		0.37

larval production there; and 3) density-depensatory predator satiation occurs when concentrations of bay anchovy larvae and juveniles at the mesoscale (10–100 km) are high in relation to satiation potential of predators, which favors larval production and high anchovy recruitments.

First, averaged DO level in the bay or its regions may be an indicator of ecosystem metabolism and secondary production. DO level in the subeuphotic layer is an indicator of respiration and secondary production by planktonic and benthic communities (Kemp and Boynton, 1980; Kemp et al., 1992). Recruitment levels of bay anchovy increased substantially in 1997 and in subsequent years. We speculate that enhanced detrital production potentially increased zooplankton prey abundances in the subsequent year and that associated elevated levels of respiration by detrital microorganisms and zooplankton contributed to low mean DO. Increased zooplankton prey abundances, in turn, may have promoted production of larval and juvenile bay anchovy in 1997 and 1998. Thus, increased prey availability, associated with low mean DO concentration, could have enhanced recruitment (Fig. 4).

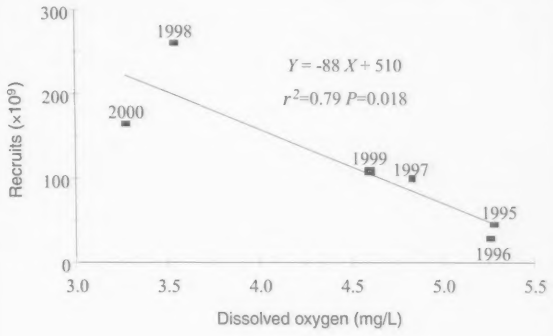

Figure 4

Relationship between mean dissolved oxygen below the pycnocline in the middle Chesapeake Bay during the June–August period and recruitment level of bay anchovy in October. r^2 = coefficient of determination.

The second hypothesis proposes that spatial restriction of SSB by low DO is a factor controlling bay anchovy recruitment. Based on our results, hypoxic conditions in the bay appear to define the distribution and potential for upbay migration of bay anchovy SSB (Fig. 3C). In years when the baywide subpycnocline mean DO level was low, spawning bay anchovy tended to be most concentrated in the lower bay (Table 5, Fig. 3, A and C), possibly because hypoxia in deeper waters of the mid-bay region discouraged upbay migration. The region selected by adult anchovy as the predominant spawning area and its variability played

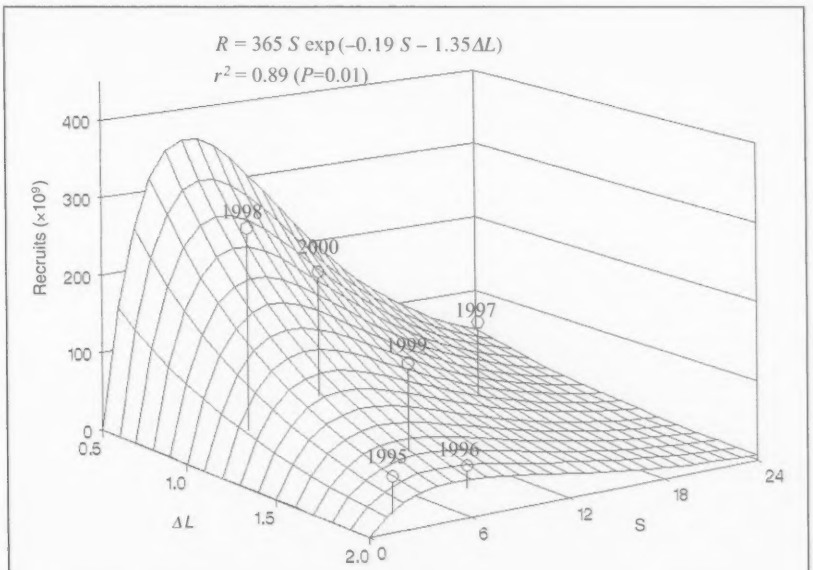

Figure 5

Stock-recruitment model (modified Ricker model). R = baywide number of recruits in October ($\times 10^9$). ΔL = location of bay anchovy (*Anchoa mitchilli*) spawning stock biomass in June–August in relation to the baseline latitude at the mouth of the bay, 37°00′N. S = baywide spawning stock biomass (SSB $\times 10^3$ metric tons for April–May). Balloon symbols are observed data from 1995 to 2000.

a strong role in controlling YOY recruitment levels. The four highest recruitment years in our series had the lowest mean subpycnocline DO levels and had distribution patterns of SSB that differed little between the prespawning April–May and spawning June–August periods (Fig. 4). Although we do not fully understand how DO, and possibly hypoxic conditions, affect migratory behavior and distribution patterns of bay anchovy, hypoxia in Chesapeake Bay has been demonstrated in other research to affect spatial and temporal patterns of fish abundance, including bay anchovy (Breitburg, 1992; Keister et al., 2000).

Our third hypothesis proposes that predation is an important regulator of fish recruitment in early-life stages (Sissenwine, 1984; Bailey and Houde, 1989). We hypothesize that abundant and spatially concentrated larval or juvenile anchovy, as observed in the lower bay, could promote early-life survival by satiating predators, even if some predators migrate to areas where larval and juvenile anchovy are abundant. At mesoscale distances of 10–100 km, distribution of predators (e.g. YOY and age-1 weakfish [*Cynoscion regalis*]) may be important. If the maximum number of prey that can be eaten by predators is reasonably constant, the effect of predation can be density-dependent (Hilborn and Walters, 1992), i.e. predation mortality rate decreases as prey density increases.

In support of the third hypothesis, a correspondence analysis on fish species assemblages by year, season, region, and life stage (Jung and Houde, 2003) indicated that distributions and abundances of YOY weakfish, a major predator of bay anchovy in Chesapeake Bay (Hartman and Brandt, 1995), and YOY bay anchovy were closely associated spatially, seasonally, and annually in our six-year study. The major spawning area of bay anchovy is spatially restricted. If predator migration to the area is limited, then as the supply of larvae and juveniles increases, it may saturate predator demand, the condition necessary for depensation to be important.

It may seem contradictory to propose that density-compensation with respect to SSB (the negative sign of β_1) and density-depensation with respect to ΔL (the second or third hypothesis) can act simultaneously during larval and juvenile stages. Under this circumstance, the number of surviving postlarval anchovies is hypothesized to decrease because of food limitation when larval abundance is high, reducing subsequent predation-related mortality rate on postlarvae and small juveniles. Low abundance of anchovy early-life stages will lead to the opposite effect (Fig. 7). The proposed opposing responses of the early-larval and late-larval–juvenile stages are explained by differences in the spatial scales of distribution and densities of life stages of bay anchovy (Fig. 7). The spatial scale of processes that affect distributions of late-stage larvae and juveniles is large compared to that for early-stage larvae because of the increased dispersal and swimming ability of juveniles. Comparing early-larval and late-larval–juvenile stages of bay anchovy, we propose that effects of prey concentration (the first hypothesis) and SSB level (density-compensation) act primarily on the dynamics of early-larval stages, whereas predation mortality and the inhibitory effects of low DO (density-depensation; the second and third hypotheses) are more important regulators and controllers, respectively, during late-larval and juvenile stages.

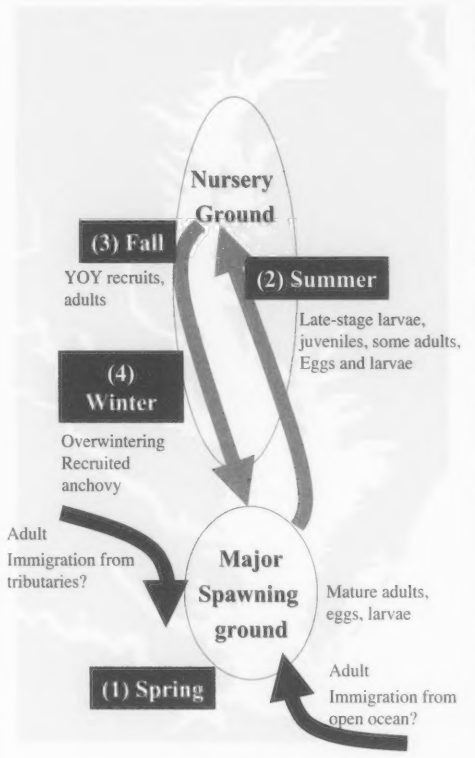

Figure 6

Conceptual model representing bay anchovy (*Anchoa mitchilli*) life cycle and ontogenetic migration within Chesapeake Bay, and possible immigration of adults from tributaries and coastal ocean.

The three hypotheses that relate DO, SSB distribution, and recruitment of bay anchovy are not mutually exclusive. If low mean DO level is an indicator of enhanced prey production and availability to larvae and juveniles, increased prey productivity in the lower bay could enhance bay anchovy recruitment potential by supplying enough zooplankton prey to spawning adults, larvae, and juveniles. At the same time, low mean DO in the mid-Bay could confine most spawning bay anchovy to the lower bay, thus increasing spawning and larval production there, and possibly enhancing survival of juveniles by predator satiation. Ultimately, other hypotheses may provide better explanations of the relationships between regional mean DO, latitudinal shifts in distribution of spawners, abundances of spawners, and recruitment of bay anchovy. For example, abundant gelatinous organisms, such as the scyphomedusa (*Chrysaora quinquecirra*) and the lobate ctenophore (*Mnemiopsis leidyi*), can be important predators on early-stage anchovy and competitors with juveniles and adults (Purcell et al.,

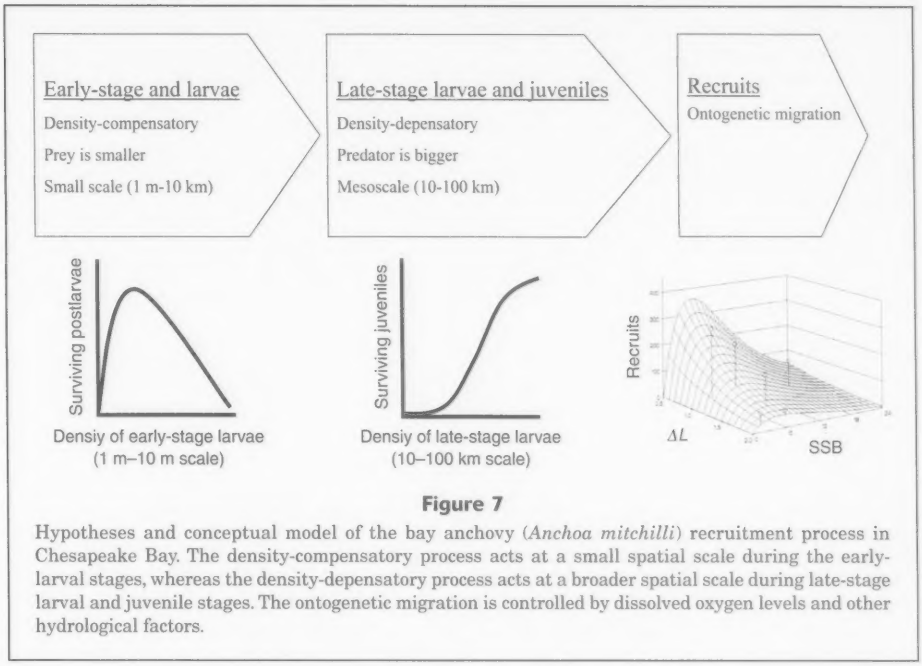

Figure 7

Hypotheses and conceptual model of the bay anchovy (*Anchoa mitchilli*) recruitment process in Chesapeake Bay. The density-compensatory process acts at a small spatial scale during the early-larval stages, whereas the density-depensatory process acts at a broader spatial scale during late-stage larval and juvenile stages. The ontogenetic migration is controlled by dissolved oxygen levels and other hydrological factors.

1994), but their potential role with respect to bay anchovy recruitment could not be defined in our study. For the present, it is clear that most spawning occurs in the lower and mid Chesapeake Bay, from which larval and juvenile anchovies disperse upbay. We hypothesize that food availability is the major factor controlling production of bay anchovy early-larval stages whereas predation becomes more important during late-larval and juvenile stages. Our results and hypotheses implicate density-related processes, operating at different spatial scales, as regulators of recruitment of bay anchovy in Chesapeake Bay.

Acknowledgments

We thank S. Leach, E. North, J. Hagy, C. Rilling, J. Cleveland, A. Madden, D. O'Brien, B. Pearson, D. Craige, T. Auth, and the able crew of RV *Cape Henlopen* for assistance in field surveys. T. Miller and E. Russek-Cohen provided comments and assistance on statistical analyses. This research was supported by a U.S. National Science Foundation, Land Margin Ecosystem Research (LMER) program grant, "Trophic interactions in estuarine systems (TIES)" (grant DEB94-12113). Additional support was provided by NSF Grant OCE-9521512 and by National Oceanic and Atmospheric Administration grant NOAA, NA17OP2656.

Literature cited

Able, K. W., and M. P. Fahay.
1998. The first year in the life of estuarine fishes in the Middle Atlantic Bight, 342 p. Rutgers Univ. Press, New Brunswick, NJ.

Alheit, J.
1987. Egg cannibalism versus egg predation: their significance in anchovies. S. Afr. J. Mar. Sci. 5:467–470.

Bailey, K. M., and E. D. Houde.
1989. Predation on eggs and larvae of marine fishes and the recruitment problem. Adv. Mar. Bio. 25:1–83.

Baird, D., and R. E. Ulanowicz.
1989. The seasonal dynamics of the Chesapeake Bay ecosystem. Ecol. Monogr. 59:329–364.

Belsley, D. A., E. Kuh, and R. E. Welsch.
1980. Regression diagnostics: identifying influential data and sources of collinearity, 292 p. John Wiley and Sons, Inc., New York, NY.

Bhattacharya, C. G.
1967. A simple method of resolution of a distribution into Gaussian components. Biometrics 23:115–135.

Breitburg, D. L.
1992. Episodic hypoxia in Chesapeake Bay: Interacting effects of recruitment, behavior, and physical disturbance. Ecol. Monogr. 62:525–546.

Cowan, J. H., K. A. Rose, E. D. Houde, S. B. Wang, and J. Young.
1999. Modeling effects of increased larval mortality on bay anchovy population dynamics in the mesohaline Chesapeake Bay: evidence for compensatory reserve. Mar. Ecol. Prog. Ser. 185:133–146.

Cronin, W. B.
1971. Volumetric, areal, and tidal statistics of the Chesapeake bay estuary and its tributaries, 15 p. Chesapeake Bay Institute, Johns Hopkins Univ., Baltimore, MD.

Dorsey, S. E., E. D. Houde, and J. C. Gamble.
1996. Cohort abundances and daily variability in mortality of eggs and yolk-sac larvae of bay anchovy, *Anchoa mitchilli*, in Chesapeake Bay. Fish. Bull. 94:257–267.

Dovel, W. L.
1971. Fish eggs and larvae of the upper Chesapeake Bay. Chesapeake Biological Laboratory, special report 4, 71 p. Natural Resource Institute, Univ. Maryland, College Park, MD.

Harding, L. W., M. E. Mallonee, and E. S. Perry.
2002. Toward a predictive understanding of primary productivity in a temperate, partially stratified estuary. Estuar. Coast. Shelf Sci. 55:437–463.

Hartman, K. J., and S. B. Brandt.
1995. Predatory demand and impact of striped bass, bluefish, and weakfish in the Chesapeake Bay: applications of bioenergetics models. Can. J. Fish. Aquat. Sci. 52: 1667–1687.

Hilborn, R., and C. J. Walters.
1992. Stock and recruitment. *In* Quantitative fisheries stock assessments: choice, dynamics, and uncertainty (R. Hilborn and C. J. Walters, eds.), p. 241–296. Chapman & Hall, New York, NY.

Houde, E. D.
1987. Fish early life dynamics and recruitment variability. Am. Fish. Soc. Symp. 2:17–29.

Houde, E. D., and C. E. Zastrow.
1991. Bay anchovy. *In* Habitat requirements for Chesapeake Bay living resources, 2nd ed. (S. L. Funderburk, J. A. Mihursky, S. J. Jordan, and D. Riley, eds.), p. 8.1 to 8.14. Living Resources Subcommittee, Chesapeake Bay Program, Annapolis, MD.

Hunter, J. R., and C. A. Kimbrell.
1980. Egg cannibalism in the northern anchovy, *Engraulis mordax*. Fish. Bull. 78:811–816.

Jung, S.
2002. Fish community structure and the spatial and temporal variability in recruitment and biomass production in Chesapeake Bay. Ph.D. diss., 349 p. Univ. Maryland, College Park, MD.

Jung, S., and E. D. Houde.
2003. Spatial and temporal variability of pelagic fish community structure and distribution in Chesapeake Bay, U.S.A. Estuar. Coast. Shelf Sci. 58:335–351.

Keister, J. E., E. D. Houde, and D. L. Breitburg.
2000. Effects of bottom-layer hypoxia on abundances and depth distribution of organisms in Patuxent River, Chesapeake Bay. Mar. Ecol. Prog. Ser. 205:43–59.

Kemp, W. M., and W. R. Boynton.
1980. Influence of biological and physical processes on dissolved oxygen dynamics in an estuarine system: implications for measurement of community metabolism. Estuar. Coast. Mar. Sci. 11:407–431.

Kemp, W. M., P. A. Sampou, J. Garber, J. Tuttle, and W. R. Boynton.
1992. Seasonal depletion of oxygen from bottom waters of Chesapeake Bay: roles of benthic and planktonic respiration and physical exchange processes. Mar. Ecol. Prog. Ser. 85:137–152.

Kimura, R., D. H. Secor, E. D. Houde, and P. M. Piccoli.
2000. Up-estuary dispersal of young-of-the-year bay anchovy *Anchoa mitchilli* in the Chesapeake Bay: inferences from microprobe analysis of strontium in otoliths. Mar. Ecol. Prog. Ser. 208:217–227.

King, M.
1995. Fisheries biology, assessment and management, 341 p. Fishing News Books, Oxford.

Klebasko, M. J.
1991. Feeding ecology and daily ration of bay anchovy, *Anchoa mitchilli* in the mid-Chesapeake Bay. M.S. thesis, 103 p. Univ. Maryland, College Park, MD.

Loos, J. J., and E. S. Perry.
1991. Larval migration and mortality rates of bay anchovy in the Patuxent River. *In* Larval fish recruitment and research in the Americas: proceedings of the 13th annual fish conference, 21–26 May 1989, Merida, Mexico (R. D. Hoyt, ed.), p. 65–76. NOAA Technical Report NMFS 95.

Luo, J., and S. B. Brandt.
1993. Bay anchovy *Anchoa mitchilli* production and consumption in mid-Chesapeake Bay based on a bioenergetics model and acoustic measurement of fish abundance. Mar. Ecol. Prog. Ser. 98:223–236.

Luo, J., and J. Musick.
1991. Reproductive biology of the bay anchovy in Chesapeake Bay. Trans. Am. Fish. Soc. 120:701–710.

MacGregor, J. M., and E. D. Houde.
1996. Onshore-offshore pattern and variability in distribution and abundance of bay anchovy *Anchoa mitchilli* eggs and larvae in Chesapeake Bay. Mar. Ecol. Prog. Ser. 138: 15–25.

Murdy, E. O., R. S. Birdsong, and J. A. Musick.
1997. Fishes of Chesapeake Bay, 324 p. Smithsonian Institution Press, Washington, D.C. and London.

Newberger, T. A., and E. D. Houde.
1995. Population biology of bay anchovy *Anchoa mitchilli* in the mid Chesapeake bay. Mar. Ecol. Prog. Ser. 116:25–37.

North, E. W., and E. D. Houde.
In press. Transport and dispersal of bay anchovy (*Anchoa mitchilli*) eggs and larvae in Chesapeake Bay. Estuar. Coast. Shelf Sci..

Parker, K.
1985. Biomass model for the egg production method. *In* An egg production method for estimating spawning biomass of pelagic fish: application to the northern anchovy, *Engraulis mordax* (R. Lasker, ed.), p. 5–7. NOAA Tech. Rep. NMFS 36.

Peebles, E. B., J. R. Hall, and S. G. Tolley.
1996. Egg production by the bay anchovy *Anchoa mitchilli* in relation to adult and larval prey fields. Mar. Ecol. Prog. Ser. 131:61–73.

Purcell, J. E., D. A. Nemazie, S. E. Dorsey, E. D. Houde, and J. C. Gamble.
1994. Predation mortality of bay anchovy *Anchoa mitchilli* eggs and larvae due to scyphomedusae and ctenophores in Chesapeake Bay. Mar. Ecol. Prog. Ser. 114 :47–58.

Ricker, W. E.
1975. Computation and interpretation of biological statistics of fish population. Bull. Fish. Res. Board Can. 191: 1–382.

Rilling, G. C., and E. D. Houde.
1999a. Regional and temporal variability in distribution and abundance of bay anchovy (*Anchoa mitchilli*) eggs, larvae, and adult biomass in the Chesapeake Bay. Estuaries 22: 1096–1109.
1999b. Regional and temporal variability in growth and mortality of bay anchovy, *Anchoa mitchilli*, larvae in Chesapeake Bay. Fish. Bull. 97:555–569.

Rose, K. A., J. H. Cowan, M. E. Clark, E. D. Houde, and S. B. Wang.
1999. An individual-based model of bay anchovy population dynamics in the mesohaline region of Chesapeake Bay. Mar. Ecol. Prog. Ser. 185:113–132.

SAS Institute Inc.
1989. SAS/STAT user's guide, version 6, 4th ed., 1686 p. SAS Institute Inc., Cary, NC.

Samuels, M. L.
1989. Statistics for the life sciences, p. 409–42. Prentice-Hall, Inc., Upper Saddle River, NJ.
Schultz, E. T., R. K. Cowen, K. M. M. Lwiza, and A. M. Gospodarek.
2000. Explaining advection: Do larval bay anchovy (*Anchoa mitchilli*) show selective tidal-stream transport? ICES J. Mar. Sci. 57:360–371.
Sissenwine, M. P.
1984. Why do fish populations vary? *In* Exploitation of marine communities (R. M. May, ed.), p. 59–94. Springer-Verlad, Berlin.
Smith, E. M., and W. M. Kemp.
2001. Size structure and the production/respiration balance in a coastal plankton community. Limnol. Oceanogr. 46: 473–485.
Steel, R. G. D., and J. H. Torrie.
1980. Principles and procedures of statistics. A biometrical approach. 2nd ed., 633 p. McGraw-Hill Inc. New York, NY.
Vazquez-Rojas, A. V.
1989. Energetics, trophic relationships and chemical composition of bay anchovy, *Anchoa mitchilli* in the Chesapeake Bay. M.S. thesis, 166 p. Univ. Maryland, College Park, MD.
Wang, S. B., J. H. Cowan, K. A. Rose, and E. D. Houde.
1997. Individual-based modelling of recruitment variability and biomass production of bay anchovy in mid-Chesapeake Bay. J. Fish Biol. 51 (suppl. A):121–134.
Wang, S. B., and E. D. Houde.
1995. Distribution, relative abundance, biomass and production of bay anchovy *Anchoa mitchilli* in the Chesapeake Bay. Mar. Ecol. Prog. Ser. 121:27–38.
Zastrow, C. E., E. D. Houde, and L. G. Morin.
1991. Spawning, fecundity, hatch-date frequency and young-of-the-year growth of bay anchovy *Anchoa mitchilli* in mid-Chesapeake Bay. Mar. Ecol. Prog. Ser. 73:161–171.

Coupling ecology and economy: modeling optimal release scenarios for summer flounder (*Paralichthys dentatus*) stock enhancement

G. Todd Kellison

David B. Eggleston

Department of Marine, Earth, and Atmospheric Sciences,
North Carolina State University
Raleigh, North Carolina 27695-8208
Present address (for G. T. Kellison, contact author): National Park Service/Biscayne National Park
9700 SW 328th St, Homestead, Florida 33033

E-mail address (for G. T. Kellison): todd_kellison@nps.gov

Abstract—Increasing interest in the use of stock enhancement as a management tool necessitates a better understanding of the relative costs and benefits of alternative release strategies. We present a relatively simple model coupling ecology and economic costs to make inferences about optimal release scenarios for summer flounder (*Paralichthys dentatus*), a subject of stock enhancement interest in North Carolina. The model, parameterized from mark-recapture experiments, predicts optimal release scenarios from both survival and economic standpoints for varyious dates-of-release, sizes-at-release, and numbers of fish released. Although most stock enhancement efforts involve the release of relatively small fish, the model suggests that optimal results (maximum survival and minimum costs) will be obtained when relatively large fish (75–80 mm total length) are released early in the nursery season (April). We investigated the sensitivity of model predictions to violations of the assumption of density-independent mortality by including density-mortality relationships based on weak and strong type-2 and type-3 predator functional responses (resulting in depensatory mortality at elevated densities). Depending on postrelease density, density-mortality relationships included in the model considerably affect predicted postrelease survival and economic costs associated with enhancement efforts, but do not alter the release scenario (i.e. combination of release variables) that produces optimal results. Predicted (from model output) declines in flounder over time most closely match declines observed in replicate field sites when mortality in the model is density-independent or governed by a weak type-3 functional response. The model provides an example of a relatively easy-to-develop predictive tool with which to make inferences about the ecological and economic potential of stock enhancement of summer flounder and provides a template for model creation for additional species that are subjects of stock enhancement interest, but for which limited empirical data exist.

Manuscript approved for publication 17 July 2003 by Scientific Editor.

Manuscript received 20 October 2003 at NMFS Scientific Publications Office.

Fish. Bull. 102:78–93 (2004).

Commercially important marine fish and invertebrate populations are declining worldwide in response to overexploitation and habitat degradation (Rosenberg et al., 1993; FAO 1998). This reduction in harvestable fishery resources has stimulated increasing interest in the use of hatchery-reared (HR) animals to enhance wild stocks (Munro and Bell, 1997; Travis et al., 1998; Cowx, 1999; Kent and Drawbridge, 1999). Unfortunately, many stock enhancement programs proceed before ecological concerns are adequately addressed (Blankenship and Leber, 1996), and without the identification of goals or the evaluation of the success of enhancement efforts (Cowx, 1999). If fishery managers can satisfactorily determine that enhancement efforts will have no ecologically significant negative ramifications, then managers should establish specific, quantifiable goals and objectives of enhancement efforts as part of a responsible approach to stock enhancement (Blankenship and Leber, 1996; Heppell and Crowder, 1998). Once such goals have been established, managers should identify stocking approaches that will lead to the most cost-efficient realization of enhancement goals—a process that can be accomplished with the aid of coupled ecological and economic models. Although numerous (advanced) models (conceptual and species-specific) exist to predict the biological and ecological impact of alternative enhancement scenarios (e.g. Botsford and Hobbs, 1984; Salvanes et al., 1992; Barbeau and Caswell, 1999; Sutton et al., 2000), there are few models (of which we are aware) that have attempted to link the biological and ecological results of stocking efforts (e.g. addition of biomass to a stocked population) with the economic costs associated with various release scenarios (e.g. Botsford and Hobbs, 1984; Hobbs et al., 1990; Hernandez-Llamas, 1997; Kent and Drawbridge, 1999). Such a link is critical to the responsible use of funding to rebuild or manage fisheries, and for the comparison of predicted costs of enhancement versus alternative management techniques.

In North Carolina, there has been recent interest in stock enhancement with summer flounder (*Paralichthys dentatus*) (Waters, 1996; Rickards, 1998; Waters and Mosher, 1999; Burke et al., 2000; Copeland et al.[1]) because of a combination of heavy commercial and recreational exploitation, established techniques for mass hatchery-rearing (Burke et al., 1999), and considerable knowledge of summer flounder life history (Powell and Schwartz, 1977; Burke et al., 1991; Burke, 1995). Nevertheless, there have been no large-scale release experiments (and subsequent collection of data) by which to make empirical inferences about stock enhancement potential for this species. We present a compartmental model, parameterized from mark-recapture field experiments,

[1] Copeland, B. J., J. M. Miller, and E. B. Waters. 1998. The potential for flounder and red drum stock enhancement in North Carolina. Summary of workshop, 30–31 March, 1998, 22 p. [Available from North Carolina State Univ, Raleigh, NC 27695.]

Table 1

Range of numbers of summer flounder (*Paralichthys dentatus*) released (and resulting postrelease densities), sizes-at-release, and dates of release simulated in the model.

Number released	Postrelease density	Size-at-release	Dates of release
100–400,000	0.001–4.0	30–80 mm	1 April–15 July

that incorporates size of fish released, date-of-release, and number of fish released to calculate 1) predicted numbers of survivors and 2) economic costs associated with varying release scenarios under density-independent mortality. We investigated the sensitivity of model predictions to violations of the assumption of density-independent mortality because there is abundant evidence that mortality rates, or processes underlying mortality rates (e.g. growth), are affected by density-dependent relationships in the wild (see, for recent examples, Buckel et al., 1999; Bystroem and Garcia-Berthou, 1999; Jenkins et al., 1999; Kimmerer et al., 2000). We did so by repeating model simulations under varying density-mortality relationships (depensatory in nature at elevated densities), using experimental evidence from our own field studies and published observations for similar species to parameterize density-mortality relationships. Additionally, we used a scenario in which the density-mortality relationship changed over time to make inferences about the effect of more complex density-mortality relationships on postrelease mortality of juvenile summer flounder. Finally, we generated predicted temporal patterns of field densities under varying density-mortality relationships and compared them with observed (in the field) patterns to determine whether model output under the considered density-mortality relationships matched actual patterns in the field. The model provides an example of a relatively easy-to-develop predictive tool with which to make inferences about the ecological and economic potential of stock enhancement with summer flounder and provides a template for model creation for additional species that are subjects of stock enhancement interest, but for which limited empirical data exist.

Materials and methods

Background

In North Carolina, wild summer flounder recruit to shallow-water estuarine nursery habitats from February to May, after which small juvenile (20–35 mm total length [TL]) densities range from ~0.1 to 1.0 fish/m^2 (Burke et al., 1991; Kellison and Taylor[2]). Juveniles subsequently make an ontogenetic habitat shift to deeper waters (Powell and Schwartz, 1977), apparently after reaching a total length of ~80 mm (Kellison and Taylor[2]). By mid-July, densities of juvenile summer flounder in the shallow water nursery habitats are near zero (Kellison and Taylor[2]).

Model pathway

Our compartmental model simulated the daily mortality and growth of different-size hatchery-reared (HR) fish released in the field over a 105-day period (1 April to 15 July, based on observed field abundances) in a hypothetical release habitat of 10 hectares. The model predicted the percentage of released fish surviving and economic cost-per-survivor under 2730 release scenarios for a specified number of fish released (see below). To begin the model, a value of number of fish released (NFR) ranging from 100 to 400,000 (Table 1) was chosen (Fig. 1), resulting in postrelease densities (assuming even postrelease distribution) of 0.001–4.0 fish/m^2. These values included a range of densities of juvenile summer flounder observed in wild nursery habitats (~0–1 fish/m^2; mean ~0.05 fish/m^2; Kellison and Taylor[2]), but also included unusually high densities (>1 fish/m^2) in order to examine how such release strategies would affect model output (we did not examine densities >4 fish/m^2 because of a lack of data on fish response to resource limitation likely to occur as densities increased past values for which we had empirical growth data). Each group of NFR was initially assigned a "size-(TL) at-release" of 30 mm (the smallest size-at-release simulated in the model), after which a size-dependent economic cost associated with the release of the 30-mm-TL fish was calculated (see below). The release group was then assigned a minimum Julian "day of release" of 92 (corresponding to 1 April, the earliest release date simulated in the model). A range of Julian days of release was included in the model because field-estimated growth rates were dependent on Julian day (Kellison, 2000), and growth rates are potentially important to the determination of mortality rates (Rice et al. 1993). With this model, we then calculated daily mortality and growth (described below) in the hypothetical release habitat over the number of days at large (DAL), where

$$DAL = 197 \text{ (the Julian day corresponding to 15 July)} - 92 \text{ (Julian release day)},$$

and output a number of survivors and a calculated cost-per-survivor (CPS), where

$$CPS = \textit{cost associated with release} \div \textit{predicted number of survivors},$$

[2] Kellison, G. T., and J. C. Taylor. 2000. Unpubl. data. Department of Marine, Earth, and Atmospheric Sciences, North Carolina State University, Raleigh, NC 27695-8208.

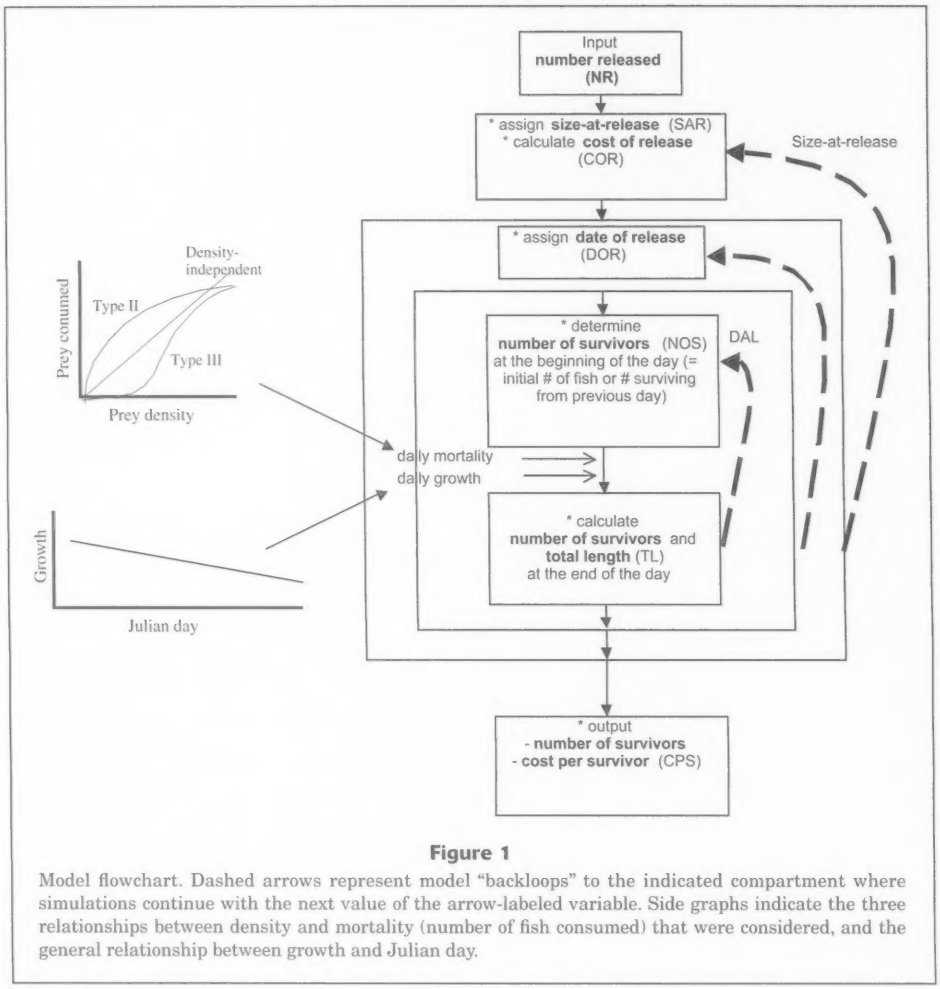

Figure 1

Model flowchart. Dashed arrows represent model "backloops" to the indicated compartment where simulations continue with the next value of the arrow-labeled variable. Side graphs indicate the three relationships between density and mortality (number of fish consumed) that were considered, and the general relationship between growth and Julian day.

for the initial release scenario of fish size = 30 mm TL, Julian day = 92, and an NFR input determined by the modeler). The model then looped back to the "date-of-release" step and simulated the release of the 30-mm-TL fish for Julian release days 93–197, outputting a predicted number of survivors and cost-per-survivor for each release date. The model then repeated all previous steps under sequentially larger size-at-release scenarios, looping back to the "size-at-release" step and simulating the release of fish ranging in size from 32–80 mm TL fish in steps of 2 mm TL. The model output was a predicted number of survivors and economic cost-per-survivor for each release day (92–197) for each size-at-release (Fig. 1). Thus, for each input NFR, there were 26 size-at-release possibilities × 105 Julian days of release possibilities, which resulted in 2730 simulations, each of which resulted in a predicted number of survivors and cost-per-survivor for that particular release scenario. For each input NFR, the results from the 2730 simulations were plotted on two response surfaces, with an x-axis of size-at-release, a y-axis of date-of-release, and a z-axis of either 1) predicted number of survivors (NOS), or 2) cost-per-survivor (CPS), to identify release scenarios resulting in the maximum predicted number of survivors and minimum cost-per-survivor, respectively. The scenarios resulting in the maximum predicted number of survivors and minimum cost-per-survivor were not necessarily identical.

Calculation of mortality, growth, survival, and economic costs associated with release

During each day at large (DAL), released fish were subjected to a density-independent daily mortality rate of 0.02153, derived from postrelease mark-recapture data of HR summer flounder (Kellison et al., 2003b). In deriving this value, mean postrelease densities were used to estimate a total number of survivors from experimental releases. Daily survival was then calculated with the equation

$$NFR \times S_D^{DAL} = NOS,$$

where NFR = number released;
S_D = daily survival;
DAL = days at large (from release date until Julian day 197); and
NOS = estimated number of survivors.

Daily mortality (M_D) was then calculated from the equation

$$M_D = 1 - S_D.$$

At the end of each simulated day, all fish that were alive increased in growth according to the equation

$$G_D = -0.0061 \times \text{Julian day} + 1.2487,$$

which was derived from mark-recapture data (Kellison, 2000), and in which G_D is daily growth in millimeters. Fish reaching 80 mm TL during the model (i.e. by 15 July) were considered to make an ontogenetic habitat shift to deeper waters. These fish were then subjected to one half year of natural mortality to simulate mortality-related losses from deeper-water habitats (M=0.28; Froese and Pauley, 2001). Remaining fish, now having survived ~one year of natural mortality, were considered to be survivors (available to the commercial fishery), which is a conservative assumption because 1-yr-old summer flounder are only partially recruited to the commercial fishery. All fish not reaching a total length of 80 mm were assumed to perish.

To determine size-dependent economic costs of fish production, we used the following regression equation derived for Japanese flounder (*Paralichthys olivaceus*) by Sproul and Tominaga (1992) because equivalent economic data for summer flounder were unavailable:

$$C_{PF} = 14.24 + 1.234 \times TL,$$

where C_{PF} = the cost per fish in Japanese yen (¥); and
TL = the total length of the HR fish.

Costs were then converted into US$ by using an exchange rate of 106.7¥ per 1 US$ (universal currency converter). We feel use of this cost-of-fish-production equation is appropriate because the Japanese flounder is closely related and similar in life history traits to the summer flounder (Tanaka et al., 1989; Burke et al., 1991), resulting in similar optimal rearing practices for hatchery-reared Japanese and summer flounder (Burke et al., 1999), and thus likely similar rearing costs. Additionally, the scale of Japanese flounder hatchery production is similar to, or greater than, other government subsidized hatchery production programs (e.g. red drum in Texas, cod in Norway [Svåsand, 1998]).

Density-mortality relationships

We tested the sensitivity of the model results (optimal predicted number of survivors and cost-per-survivor estimates under varying NFRs) to violations of the assumption of density-independent mortality by incorporating varying types and strengths of density-dependent mortality (depensatory in nature at elevated densities; see below) into the model. As a basis for these sensitivity analyses, we assumed that predation was the driving mechanism underlying the postrelease mortality of HR summer flounder under the densities examined (Kellison et al., 2000; Kellison et al., 2003b). Thus, we made daily mortality rates correspond to either a type-2 or type-3 predator functional response (Holling, 1959; see Lindholm et al., 2001 for example), in which proportional mortality due to predation decreases with increasing density (type-2 response) or increases initially with increasing density, reaches a zenith, and then decreases with increasing density (type-3 response) (Fig. 2). Both type-2 and type-3 responses result in decreasing (depensatory) mortality at elevated prey densities due to predator satiation. We did not include scenarios in which mortality increased at elevated densities (as would be expected when densities reached those likely to result in resource limitation) because we did not include in the model elevated release densities likely to result in resource limitation. We parameterized the daily mortality curves so that each response (type 2 or 3) incorporated the daily mortality rate of 0.02153. These mortality curves contain mortality values that are within ranges reported in the literature for other species of juvenile marine fishes (Bax, 1983; Houde, 1987; Nash, 1998; Rose et al., 1999). To make further inferences about the importance of density-dependent mortality to model results, we included a 1) weak and 2) strong form of each functional response (types 2 and 3) (Fig. 2), as well as scenarios in which the response shifted temporally from 3) type 2 to 3, and 4) type 3 to 2 at the midpoint of the nursery season (Julian day 145). We included both the weak and strong forms of the type-2 and type-3 functional responses to determine the extent to which variation in the strength of the functional response would affect model predictions. The strength of the functional response could vary because of annual variation in the presence or abundance of prey or because predators could affect the density-mortality relationship (see, for example, Hansen et al., 1998).

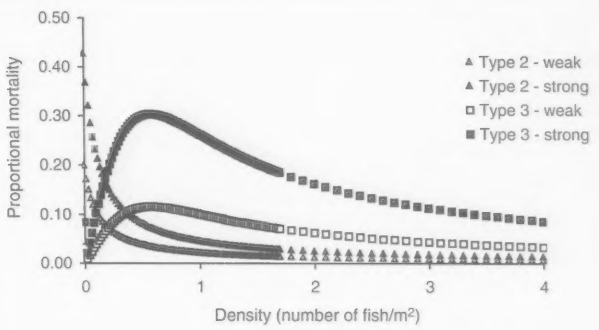

Figure 2

Proportional mortality curves for juvenile summer flounder corresponding to weak and strong type-2 and type-3 mortality responses.

For example, a strong positive (compensatory) density-mortality relationship driven by predators might become weaker in years when predator abundance was lower than average. We included the temporally shifting functional response scenarios to determine the extent to which temporal variation in the form of the functional response would affect model predictions. Temporal variation in the form of the functional response might occur because of temporal changes in the predator community, or because of changing predator-prey size dynamics (e.g. Stoner, 1980; Black and Hairston, 1988). For example, as the nursery season for summer flounder progresses, proportionately greater numbers of juveniles grow to sizes at which they are capable of preying on smaller juveniles (Kellison, personal obs.). If cannibalistic summer flounder exhibit a different predatory functional response from that of the predator guild community predominating earlier in the season, then the density-mortality relationship may change seasonally.

We replicated all model simulations over each of the six density-mortality relationships (weak and strong types 2 and 3, and shifting patterns [type 2 to 3 and type 3 to 2]) to determine optimal release scenarios (maximum number of survivors, minimum cost-per-survivor) under each relationship. We then compared results to those obtained under density-independent mortality to make inferences about the importance of density-mortality relationships to model results.

Correspondence between predicted and observed temporal abundance patterns

Different density-mortality relationships may result in distinct temporal patterns of abundance (e.g. rapid versus more gradual declines in abundance) depending on initial densities. We generated predicted patterns of temporal field abundance of juvenile summer flounder under density-independent mortality and four additional density-mortality relationships (governed by weak and strong type 2 and 3 functional responses) and under varying initial densities (0.1, 0.3, and 0.5 fish/m^2) to examine whether the different density-mortality relationships would result in distinct temporal patterns of abundance. We used 1998–99 field data and logarithmic or polynomial regression models to generate curves that best fitted (based on r^2 values) observed (from natural nursery sites) temporal declines in abundance under varying initial densities. We compared the best-fit curves to those predicted by the model under density-independent and four additional density-mortality relationships. These comparisons allowed us to make qualitative inferences about which density-mortality relationship(s) resulted in the best match between predicted and observed temporal patterns of abundance.

Model assumptions

The assumptions of the model are the following:

1 Daily mortality is independent of size. Although there is strong evidence that mortality of fishes in the wild is size-dependent (Lorenzen, 2000), particularly in regard to the importance of size to susceptibility to predation (see, for example, Elis and Gibson, 1995; Furuta, 1999; Manderson et al., 1999), we found no evidence (from recaptures of released hatchery-reared fish) of size-selective daily mortality for juvenile summer flounder ranging in size from ~30–80 mm TL in shallow-water nursery areas (Kellison et al., 2003a). Implications for violations of this assumption are addressed in the "Discussion" section.

2 Daily growth is independent of fish density. We based this assumption on field experiments that indicated no growth limitation at densities roughly equal to the maximum densities explored in the model (Kellison et al., 2003b). Similar findings (i.e. no food-limitation or density-dependent growth) have been reported for similar-size plaice in shallow-water nursery habitats (van der Veer and Witte, 1993).

3 Economic cost per fish (C_{PF}) is independent of the number of fish acquired for release (i.e. within the range of numbers of fish released in model simulations, there is no decrease in cost per fish as the number of fish acquired from the production hatchery for release increases). This assumption is likely to be valid over changes in numbers of fish released common to stock enhancement programs (Sproul and Tominaga, 1992) but may not be valid as numbers released change over orders of magnitude because of economy of scale (Adams and Pomeroy 1991; Garcia et al., 1999).

4 There is no emigration from the release habitat until fish exhibit an ontogenetic shift in habitat at 80 mm TL. Although pre-ontogenetic habitat shift emigration may not truly be zero, we feel that it is also unlikely that pre-ontogenetic habitat-shift emigration accounts for more than a minimal amount of loss of released fish from the habitat of release, as supported by several points. First, rates of pre-ontogenetic shift emigration in wild juveniles are apparently low (Kellison and Taylor[2]), suggesting that large-scale spatial migrations may not be part of the behavioral repertoire of early juvenile summer flounder. Second, irregular temporally replicated sampling outside of experimental release sites resulted in zero captures of emigrating hatchery-reared fish (Kellison et al., 2003b). Third, emigration rates of closely related HR Japanese flounder (*Paralichthys olivaceus*) are reported to be very low (Tominaga and Watanabe, 1998). In combination, these points suggest that our zero emigration assumption is appropriate.

5 Fish that do not grow to 80 mm TL during the model period (i.e. by 15 July) do not survive. Although this assumption cannot be examined with our field data, data do show that juvenile summer flounder are absent from shallow-water nursery habitats by mid to late July (Kellison et al.[3]). Thus, all fish have either perished or made ontogenetic habitat shifts to deeper habitats by this time. Our field observations suggest that the deeper habitats to which larger flounder

[3] Kellison, G. T., J. C. Taylor, and J. S. Burke. 2000. Unpubl. data. Department of Marine, Earth, and Atmospheric Sciences, North Carolina State Univ., Raleigh, NC 27695-8208.

make ontogenetic habitat shifts are inhabited by relatively high densities of potential predators (e.g. blue crabs, age 1+ flounders, red drum [*Sciaenops ocellatus*], searobin [*Prionotus* sp.], and lizardfish [*Synodus* sp.]), which may be considerably less abundant in shallow-water habitats. These relatively large and abundant predators would presumably expose small migrating fish to high rates of predation (see, for example, Elis and Gibson, 1995; Furuta, 1999; Manderson et al., 1999). This assumption is supported by research with the congener Japanese flounder (*Paralichthys olivaceus*). Although a range of sizes of hatchery-reared Japanese flounder may survive within relatively shallow nursery habitats, fishes less than 90 mm TL moving into relatively deep waters are poorly represented in subsequent age classes, most likely due to predation-induced mortality (Yamashita et al., 1994; Furuta, 1999).

6 There is no relationship between length of rearing period (time spent in the hatchery environment) and probability of postrelease mortality related to behavioral deficits (Olla et al., 1998). Hatchery-specific selection pressures may result in HR fish that are behaviorally selected to survive in the hatchery and not in the wild (see Olla et al., 1998; Kellison et al., 2000; for discussion). We assume that behavioral deficits are not exacerbated with time spent in the hatchery (i.e. behavioral deficits are equal for all sizes-at-release).

Results

The most important factor affecting the number of survivors (and therefore percent survival) was size-at-release because the greatest numbers and percentages of survivors were always produced by releasing the largest fish possible (80 mm TL in the model). Number of survivors decreased with decreasing size-at-release and with increasing Julian day of release (Fig. 3A). The cost-per-survivor (CPS) was also most affected by size-at-release, such that CPS decreased with increasing size-at-release (Fig. 3B). CPS generally increased with increasing Julian day of release (Fig. 3B), although this effect was less important than the effect of size-at-release. Because mortality was originally assumed to be density-independent, the optimal cost-per-survivor did not vary with the number of fish released (Fig. 4), and the relationship between number of fish released and number of survivors was linear (Fig. 4), such that the maximum number of survivors were generated from the greatest number of fish released (NFR=400,000).

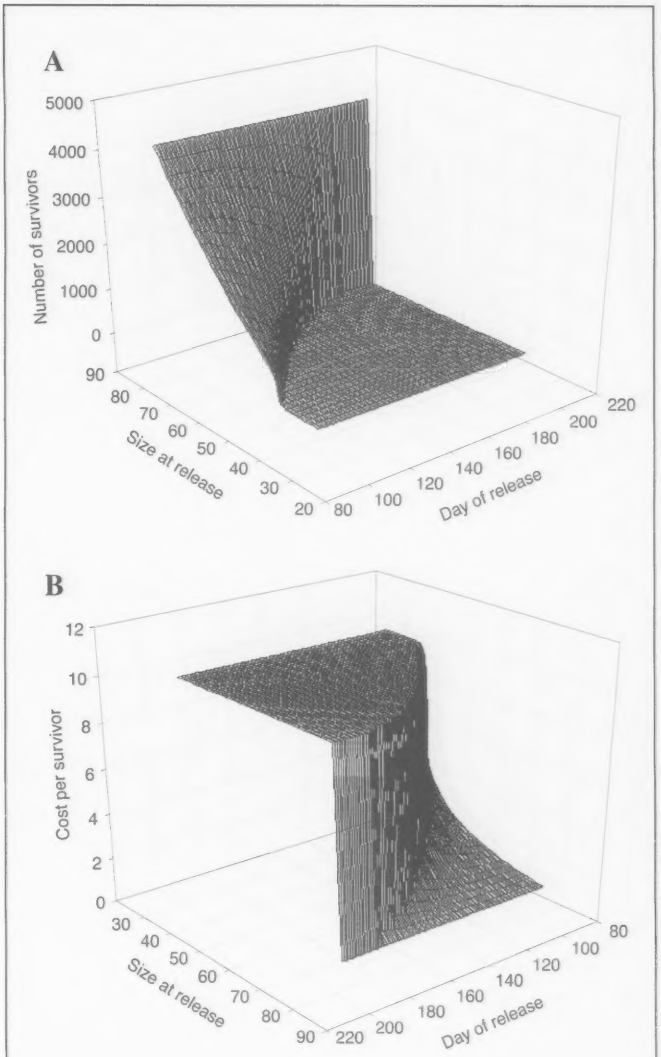

Figure 3

Response surfaces of (**A**) number of fish survivors (summer flounder) and (**B**) cost-per-survivor (CPS) as a function of date of release and size at release at number released (NR) = 5000 (postrelease density=0.05) under density-independent mortality. CPS values greater than $10 were set equal to $10 for ease of presentation.

Sensitivity of model predictions to violations of density-independent mortality assumption

Model results varied considerably under the various density-mortality relationships (Fig. 5, A and B), indicating the importance of knowledge of the relationship between numbers of fish released (density) and mortality in the wild to predicting optimal release scenarios. Variation in model output was dependent on the type and strength of

the density-mortality relationship. For example, at postrelease densities of 0.5 fish/m^2 (NFR=50,000), survival of released flounder under density-independent mortality was ~28% higher than that predicted under strong type-3 mortality, but only ~2% higher than that predicted under weak type-2 mortality (Fig. 5A). At postrelease densities of 0.001 fish/m^2 (NFR=100), survival of released flounder under density-independent mortality was ~41% higher than that predicted under strong type-2 mortality, but ~2% less than that predicted under strong type-3 mortality (Fig. 5A). In contrast, when postrelease densities were relatively high, there was less of an impact of density-mortality relationship on postrelease survival and costs associated with stock enhancement. For example, at postrelease densities of three fish/m^2 (NFR=300,000), survival of released flounder differed by less than 4% between density-independent, weak or strong type-2, and weak type-3 mortality, although survival under strong type-3 mortality was ~9% less than that predicted under density-independent mortality and ~11% less than that predicted under strong type-2 mortality (Fig. 5A). Thus, the model results were most sensitive to violations of the assumption of density-independent mortality at low densities of fish released in the field.

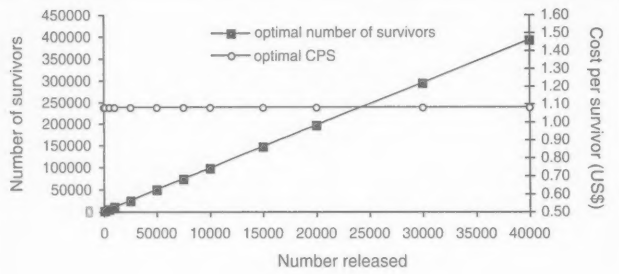

Figure 4

Optimal number of fish survivors and cost-per-survivor as a function of varying numbers of summer flounder released under density-independent mortality.

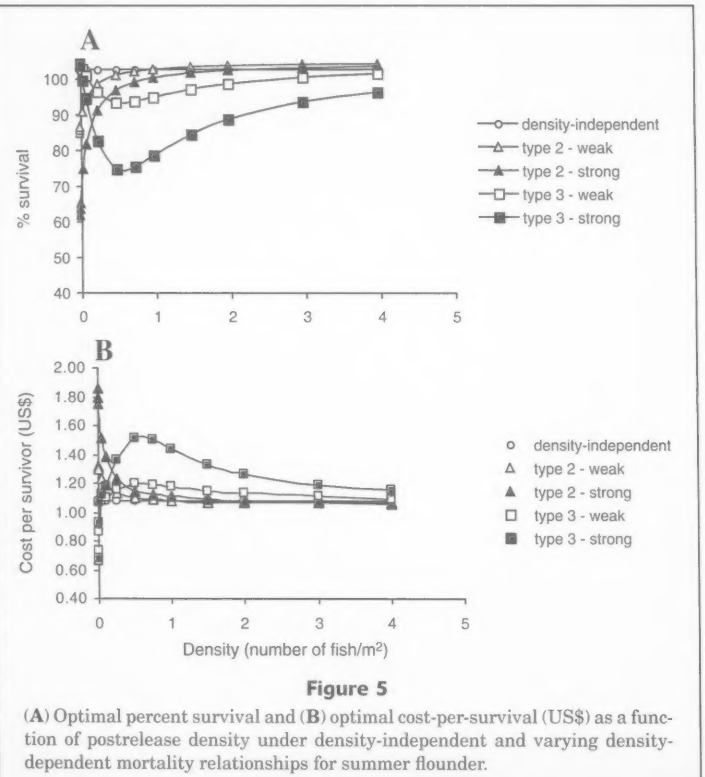

Figure 5

(**A**) Optimal percent survival and (**B**) optimal cost-per-survival (US$) as a function of postrelease density under density-independent and varying density-dependent mortality relationships for summer flounder.

Type-2 mortality As with density-independent mortality, the most important factor affecting number of survivors and cost per survivor under type-2 mortality was size-at-release (Fig. 6, A and B). In all simulations, the greatest number of survivors was produced by releasing the largest fish possible. Number of survivors decreased with increasing Julian day of release (Fig. 6A). There was a considerable interaction between size-at-release and number of fish released, such that low postrelease densities were subjected to relatively high proportional mortality. Thus, when fish were released in low numbers and at small sizes, the fish were subjected to relatively high proportional mortality rates for long periods of time (while they grew towards the 80-mm-TL ontogenetic shift size) and consequently produced few or no survivors (Fig. 6A). Optimal release scenarios under strong type-2 mortality produced substantially lower (>40% in some cases) percent survival (and therefore substantially higher cost-per-survivor) estimates at low to moderate numbers released (NFR=100–50,000; postrelease density=0.001–0.5 fish/m^2) than under density-independent mortality (Fig. 5, A and B). Differences in percent survival estimates (and thus cost-per-survivor estimates) between density-independent survival and weak or strong type-2 mortality declined to less than 5% when the numbers released increased to 25,000 (postrelease density=0.25 fish/m^2) under weak type-2 mortality and 75,000 (postrelease density=0.75 fish/m^2) under strong type-2 mortality (Fig. 5A). Thus, model predictions under density-independent mortality differed most from predictions under mortality governed by

a type-2 predator functional response when postrelease densities were relatively low.

Type-3 mortality As in all other simulations, the most important factor affecting number of survivors under type-3 mortality was size-at-release, such that the greatest numbers of survivors were always produced by releasing the largest fish possible (Fig. 7A). Number of survivors decreased with increasing Julian day of release (Fig. 7A). Percent survival was considerably lower (>25% in some cases) under type-3 mortality than under density-independent mortality at moderate to high numbers released (NFR=10,000–400,000) (Fig. 5A).

In nearly all simulations, the lowest CPS values were produced by releasing the largest fish possible (Fig. 7B). The exceptions to the "large size = optimal CPS" rule occurred when postrelease densities were small (corresponding to numbers released of 100, 500, and 1000) and the mortality curve was type 3 (weak or strong). In these instances, mortality was sufficiently low at low release densities (Fig. 7B) so that the difference in overall survival between small- and large-released fish was small enough to be overridden by the increased cost of the larger fish, and the minimum CPS was obtained when small (42–44 mm TL) fish were released (e.g. Fig. 7B).

At low numbers released (NFR=100–1000), optimal cost-per-survivor was considerably lower (>45% in some cases) under type-3 mortality than under density-independent mortality (Fig. 5A). As NFR increased, CPS under type-3 mortality became greater (~40% in some cases) than that achieved under density-independent mortality (Fig. 5B).

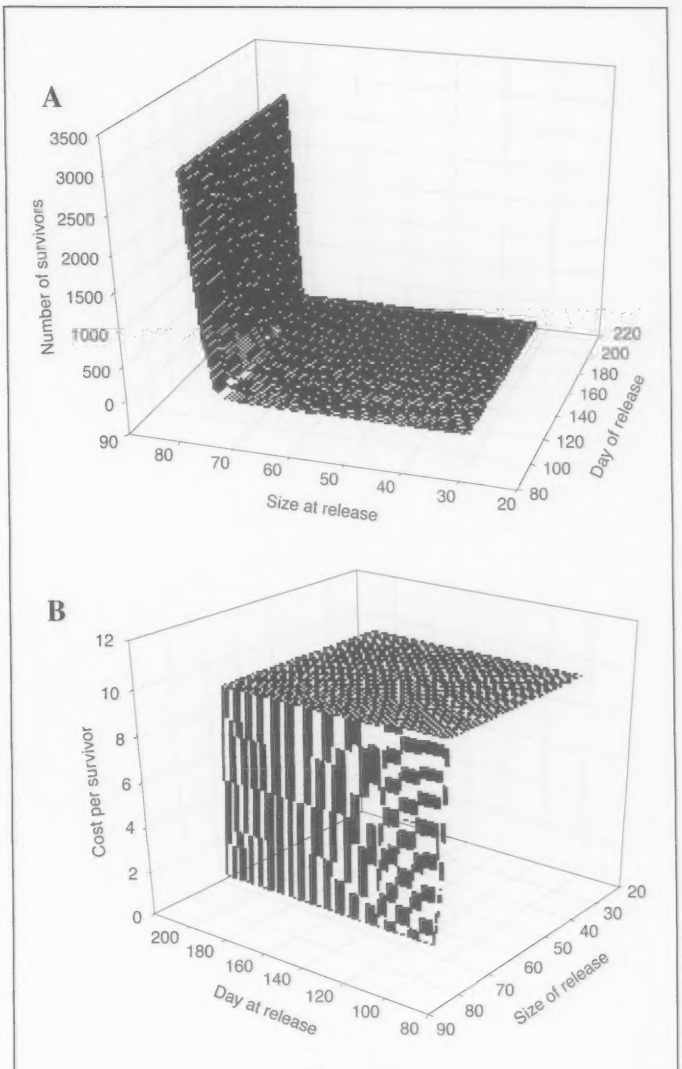

Figure 6

Response surfaces of (**A**) number of fish (summer flounder) survivors and (**B**) cost-per-survivor (CPS) as a function of date of release and size at release at number released (NR) = 5000 (postrelease density=0.05) under a strong type-2 functional response. CPS values greater than $10 were set equal to $10 for ease of presentation.

Temporal shift in functional response from type 2 to type 3, and from type 3 to type 2 The optimal numbers of survivors under varying numbers released were identical, and optimal CPS values nearly identical, when the form of the functional response changed from a type 2 to a type 3, and from a type 3 to a type 2, midway through the juvenile nursery season (Fig. 8, A and B). The differences at low postrelease densities between optimal CPS values under shifting type 2 to type 3 and type 3 to type 2 scenarios (Fig. 8A) occurred because initial mortality under the type-3 functional response was sufficiently low that the difference in overall survival between small- and large-released fish was small enough to be overridden by the increased cost of the larger fish (Fig. 8A). The minimum CPS was obtained when small (42–44 mm TL) fish were released (in all other cases, optimal results were obtained when size-at-release was maximized) (Fig. 8A). The major difference between the two shifting scenarios is that the release dates producing optimal results for a given number of fish released varied depending on the direction of the shifting functional response. For example, when the functional response shifted from a type 2 to a type 3, a release of 100,000 HR organisms achieved optimal results when release occurred early in the season (Julian day ≤145) (Fig. 9A). When the functional response shifted from a type 3 to a type 2, a release of 100,000 HR summer flounder achieved optimal results only when releases occurred later in the season (Julian day >145) (Fig. 9B). When the

functional response shifted from a type 3 to a type 2, releasing 100,000 HR organisms prior to Julian day 146 resulted in markedly decreased survival (and therefore increased CPS) compared to results obtained from releases after day 146 (e.g. releasing on Julian day 92 resulted in a decrease in number of survivors and an increase in CPS of 22.8% and 29.7%, respectively) (Fig. 9B). Thus, date-of-release had a significant effect on the results (and therefore in determining optimal release strategies) when the relationship between density and mortality changed temporally, suggesting that the presence of a temporal shift in the functional response of the predator guild would have considerable effects on the number of survivors and CPS for stock enhancement efforts with juvenile summer flounder.

Correspondence between predicted and observed temporal abundance patterns

Under the assumption of a type-2 functional response, predicted declines in juvenile summer flounder density over time were rapid when initial density was relatively low (i.e. 0.1 fish/m^2) (Fig. 10, A and B). These predictions contrast with those observed in the field, in which declines at relatively low initial densities were gradual (compare Fig. 10A and 10B to Fig. 10F). Under the assumption of a type-3 functional response, predicted declines were rapid when initial density was relatively high (i.e. 0.5 fish/m^2) (Fig. 10, C and D). These results generally contrast with those observed in the field, in which declines at relatively high densities were much less rapid than those predicted under a strong type-3 functional response, and somewhat less rapid than those predicted under a weak type-3 functional response (Figs. 10F and 11). Under density-independent mortality, there was little difference in predicted declines in juvenile summer flounder density over time between the three initial density levels (0.1, 0.3, and 0.5 fish/m^2); in each case there was a gradual decrease in density over time (Fig. 10E). These results were similar to those observed in the field, although declines at relatively high densities in the field were somewhat more rapid than those predicted under density-independent mortality (compare Figs. 10E and 10F). Thus, a density-mortality relationship lying between that generated under density-independence and that generated under the weak type-3 functional response in the model would most closely predict the temporal declines observed in the field.

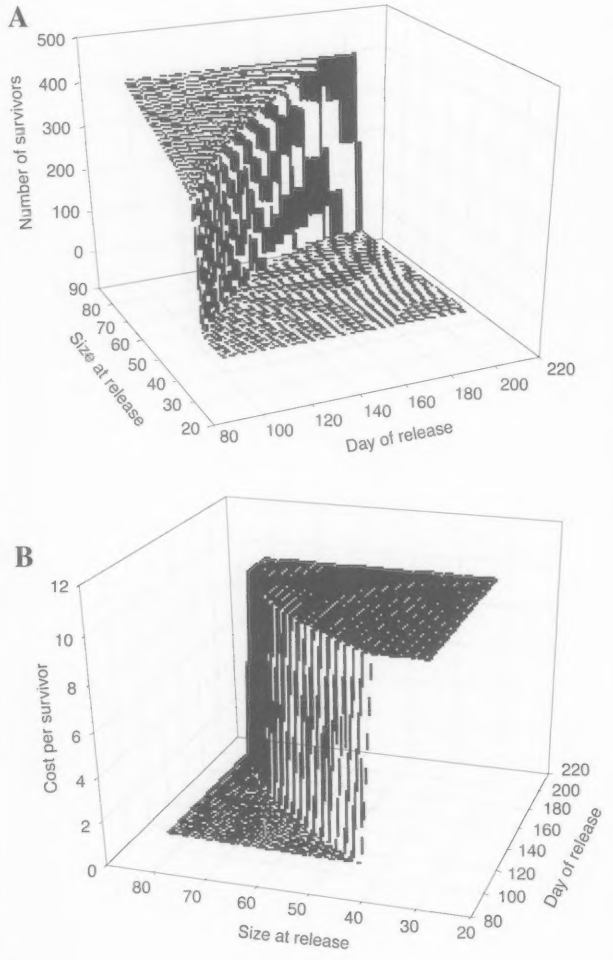

Figure 7

Response surfaces of (**A**) number of fish (summer flounder) survivors and (**B**) cost-per-survivor (CPS) as a function of date of release and size at release at number released (NR) = 500 (postrelease density=0.005) under a strong type-3 functional response. CPS values greater than $10 were set equal to $10 for ease of presentation.

Discussion

Implications for stock enhancement of summer flounder

Regardless of the relationship between density and mortality, size-at-release was the most important variable in the model affecting survival and costs associated with stock enhancement of summer flounder. The model predicts that under all release scenarios, 1) survival will be maximized and 2) costs associated with stock enhancement (i.e. cost per survivor) will be minimized when HR fish are released at the largest size possible. From a survival standpoint, these results are not

surprising. Larger fish spend fewer days than smaller fish in the wild nursery habitats before making an ontogenetic habitat shift to deeper waters and thus are susceptible to daily natural mortality for fewer numbers of days than are smaller fish. Thus, total mortality of smaller fish is greater than that of larger fish. Additionally, although we chose to make mortality independent of size in the model, abundant literature suggests that natural mortality (especially due to predation) may decrease with increasing size by mechanisms such as enhanced resistance to starvation, decreased vulnerability to predators, and better tolerance of environmental extremes (Sogard, 1997; Hurst and Conover, 1998; Lorenzen, 2000). Thus, the difference in predicted survival between 1) relatively large and relatively small fish and 2) fish released early versus late in the season in our model would be even greater if larger summer flounder suffered lower natural mortality than smaller fish. Furthermore, the daily mortality estimate used in the density-independent simulations and to parameterize the different types of density-mortality relationships may have been an underestimate of daily mortality (Kellison, 2000). If a greater estimate of daily mortality had been used, the difference in predicted survival between relatively large and relatively small fish in our model would have been further exacerbated because smaller fish spend longer amounts of time in the model growing to the 80-mm-TL ontogenetic shift size. These conclusions are supported by empirical research demonstrating that relatively large released HR fish suffer lower mortality than relatively small HR fish released in the field (e.g. Yamashita et al., 1994; Leber, 1995; Willis et al., 1995; Tominaga and Watanabe, 1998; Svåsand et al., 2000).

Although the survival predictions of the model (total mortality decreases with increasing size-at-release) are not surprising, the economic (cost-per-survivor) predictions were unexpected. The paradigm for stock enhancement strategy is that the rearing of relatively large fish for release is cost prohibitive, so that mass releases of relatively small, inexpensive-to-rear fish are a better strategy than the release of larger, expensive-to-rear fish (Kellison, personal obs.). Thus, relatively small juveniles are released in virtually all current stock enhancement programs (e.g. Russell and Rimmer, 1997; Masuda and Tsukamoto, 1998; McEachron et al., 1998; Svåsand, 1998; Serafy et al., 1999). Nevertheless, large-scale hatcheries and grow-out facilities are using ever-increasing technology to minimize the costs associated with the production of relatively large fishes (Sproul and Tominaga, 1992). Thus, for species for which 1) hatcheries are capable of producing relatively large fish at relatively low costs (as is likely for summer flounder), and 2) postrelease survival rates increase with release size, release scenarios utilizing the largest fish possible may maximize the potential (i.e. produce maximum survival at minimum costs) of stock enhancement efforts. In these cases, the "small fish maximize stock enhancement potential" paradigm might be replaced with a "large fish maximize potential" paradigm. As a caveat, this "large fish" strategy may be limited by spatial limitations of hatcheries in producing large numbers of relatively large fish. Because reared fish generally must be kept below critical densities in hatchery environments because of water quality and fish interaction issues (e.g. cannibalism), larger fish necessarily require more space than smaller fish for rearing. If the demand for space to rear large quantities of large fish can be realized, then the model simulations indicate that stock enhancement strategies in which size-at-release is maximized will produce the maximum number of survivors.

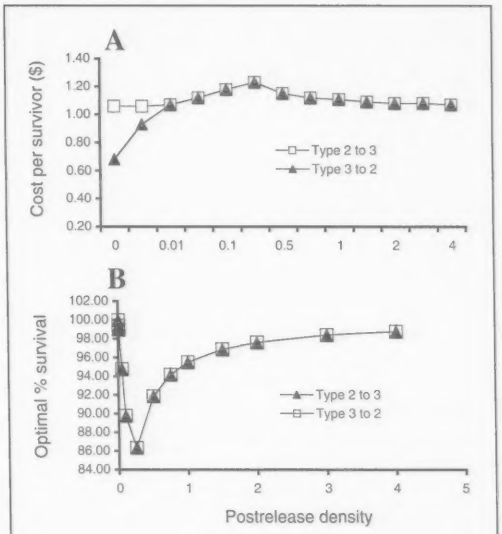

Figure 8

Optimal (**A**) economic cost-per-survivor and (**B**) percent survival of released hatchery-reared summer flounder under temporally shifting functional responses of type 2 to type 3 and type 3 to type 2.

Although not as important as size-at-release, Julian day of release had a significant effect on survival and cost-per-survivor in the model, such that enhancement efforts were always more successful (more survivors, lower costs) when fish were released at the earliest Julian day possible. These results occurred because growth in the model decreased with increasing Julian Day. Although the mechanisms underlying this decrease in growth with increasing Julian day are unknown, they may be related to decreased prey availability or metabolic efficiency as temperatures increase with increasing Julian day (Malloy and Targett, 1994a, 1994b; Fujii and Noguchi, 1996; Howson, 2000). Thus, for a given size-at-release, fish released earlier in the season experienced greater growth rates than fish of the same size-at-release released later in the season and therefore reached the 80-mm-TL ontogenetic shift size faster (over a period of fewer days) than fish released later in the season. Thus, fish released earlier in the season were susceptible to natural mortality for fewer days than fish released later in the season and therefore suffered lower total mortality. These results emphasize the importance of knowledge of possible time-dependent growth in the field prior to stock enhancement efforts.

Is density important? Effects of varying density-mortality relationships

Our results suggest that the relationship between density and mortality has the potential to significantly affect optimal release scenarios associated with stock enhancement efforts. Because the original simulations were performed under density-independent mortality, the number of survivors originally increased linearly with the number released, resulting in a density-independent cost-per-survivor. Thus, when mortality is independent of density (over a given range of densities) for a target species for stock enhancement, managers will maximize the number of survivors produced by releasing the greatest number of fish possible within that range for a given size class. When mortality varied with density of released fish, the number of survivors and cost-per-survivor depended on the density-mortality relationship. In some cases, optimal results (maximum survival and minimum cost) differed depending on whether the response variable was number of survivors or cost-per-survivor. Under the assumption of a strong type-3 functional response and under relatively low postrelease densities, survival was optimized (maximized) by releasing the largest fish (80 mm TL) possible; however, cost-per-survivor was optimized (minimized) by releasing smaller fish (42–44 mm TL). This result occurred because mortality at low postrelease densities was sufficiently low that the difference in total mortality attributed to the longer "susceptibility" period of the smaller fish was insufficient to override the economic advantage of releasing smaller fish. Simulations under shifting functional responses (type 2 to type 3 and type 3 to type 2) produced optimal results similar to those obtained when nonshifting type-2 or type-3 functional responses were employed because densities were generally reduced to such low numbers by the time the shift occurred that the changing density-mortality relationship was inconsequential. Importantly, when functional responses shifted temporally, the predicted number of survivors and economic cost per survivor was at times very dependent on date of release, suggesting that identifying or ruling out shifting functional responses in the wild may be critical to accurate prediction of response variables (survivors and economic costs) associated with stock enhancement. Although we are not aware of reports in the literature of shifting functional responses in the wild, we are also not aware of studies that have tested for such a phenomenon, possibly because of the logistical difficulties inherent in identifying a shifting functional response.

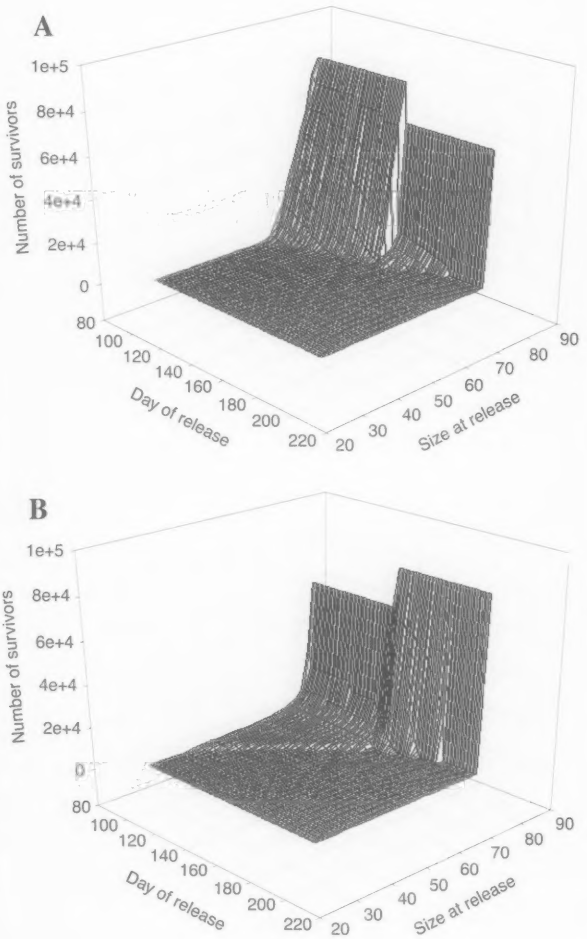

Figure 9

(**A**) Response surface of optimal number of summer flounder survivors as a function of date of release and size at release at number released (NR) = 100,000 (postrelease density=1.0 fish/m^2) under the assumption of a temporally shifting functional responses from type 2 to type 3. (**B**) Response surfaces of optimal number of survivors as a function of date of release and size at release at number released (NR) = 100,000 (postrelease density=1.0 fish/m^2) under the assumption of a temporally shifting functional responses from type 3 to type 2.

Correspondence between predicted and observed temporal abundance patterns

Predictions of field abundance patterns of juvenile flounder density over time were noticeably different under density-independent mortality and density-dependent mortality governed by type-2 and type-3 functional responses. For example, our simulations predict that fish density should decrease rapidly under relatively low initial densities if the functional response is type 2, decrease rapidly at relatively high initial densities if the functional response is type 3, and

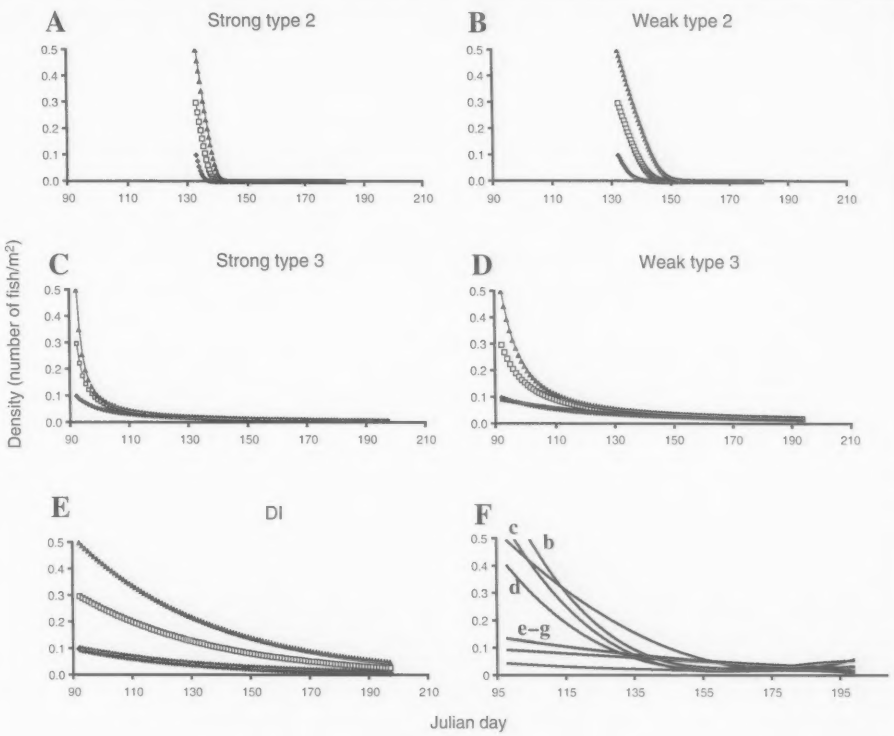

Figure 10

Predicted temporal trends in summer flounder abundance under initial densities of 0.5, 0.3, and 0.1 fish/m^2 under the assumption of a functional response that is a (**A**) strong type 2, (**B**) weak type 2, (**C**) strong type 3, (**D**) weak type 3, and under the assumption of (**E**) density-independent (DI) mortality. The curves in (**F**) are best fitted (highest r^2 value) to data collected in Duke Beach 1999 (curve a, r^2=0.82), Haystacks Marsh 1999 (curve b, r^2=0.73), Prytherch Marsh 1999 (curve c, r^2=0.82), Towne Beach 1999 (curve d, r^2=0.91), Radio Beach 1999 (curve e, r^2 = 0.27), Duke Beach 1998 (curve f, r^2=0.31), and Prytherch 1998 (curve g, r^2=0.16) (see Fig. 11 for data).

gradually decrease regardless of initial density if mortality is density independent. From examinations of temporal abundance patterns from several nursery sites (see Kellison et al., 2003b, for site descriptions), it is evident that observed declines at relatively low initial densities are similar to predicted declines under both density-independent mortality and a weak type-3 functional response; whereas observed declines at relatively high initial densities are somewhat less gradual than predicted under density-independent mortality, but somewhat more gradual than predicted under the weak type-3 functional response. These results suggest that model predictions made under the assumption of a weak type-3 response may give reasonably accurate but conservative predictions of juvenile summer flounder mortality and economic costs associated with stock enhancement for comparison with alternative management methods. As a caveat, although we found no evidence of size-dependent daily mortality over the range of fish sizes examined in this study, it is very likely that such a relationship exists to some extent (Sogard, 1997; Lorenzen, 2000). Incorporating size-dependent mortality into the model would decrease the slopes of the predicted temporal abundance curves but should not change the conclusion that the observed data lie somewhere between values predicted under density-independent mortality and those governed by a weak type-3 functional response, respectively. Additionally, because the portions of the curves used to delineate between temporal abundances expected under density-independent versus varying density-mortality relationships are from early in the growth season (later parts of the curve converge on very low densities) and because nearly all fish in these portions of the curves are at sizes well below that at which ontogenetic emigration occurs, the exclusion of emigration from these simulations should not affect the general conclusions reached. These issues could be clarified with further field trials to investigate the dependence of daily mortality rates on fish size.

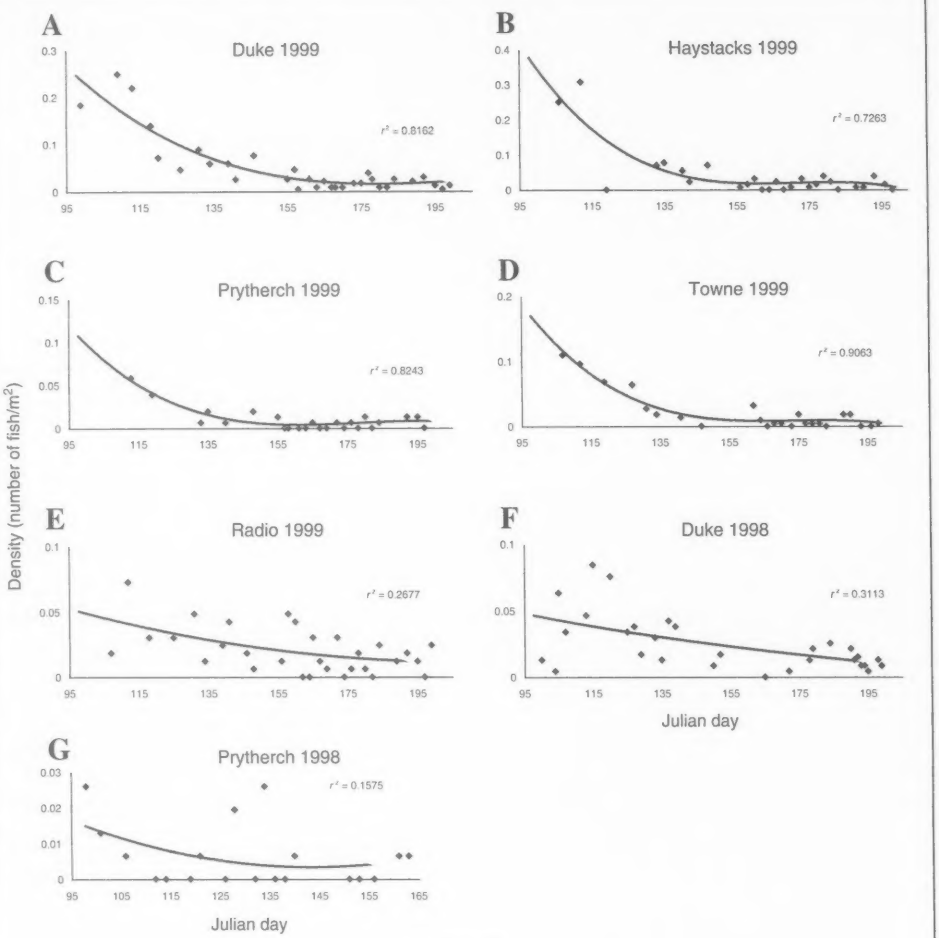

Figure 11

Temporal density patterns from (**A**) Duke Beach, 1999; (**B**) Haystacks Marsh, 1999; (**C**) Prytherch Marsh, 1999; (**D**) Towne Beach, 1999; (**E**) Radio Beach, 1999; (**F**) Duke Beach, 1998; and (**G**) Prytherch Marsh 1998. Densities are corrected for gear bias (see Kellison, 2000).

Model utility and implications

Although model results varied considerably under the various density-mortality relationships, the overall predictions that survival would be maximized and economic costs minimized when relatively large fish were released early in the season were unaffected by the density-mortality relationship. These results suggest that managers may use this model to make inferences about optimal release scenarios even if density-mortality relationships are unknown. Additionally, these results have important implications for the cost efficiency of stock enhancement programs. Managers can use the model to determine the release scenarios under which they can 1) maximize the number of survivors, given a financial limit (e.g. given a budget of x dollars, what release scenario or scenarios will produce the greatest number of survivors?), and 2) minimize costs, given a goal of number-of-survivors-produced (e.g. given a goal of producing x survivors, what release scenario or scenarios will be most cost efficient?).

In conclusion, the compartmental model used in this study provides an example of a relatively easy-to-develop predictive tool with which to make inferences about the ecological and economic potential of stock enhancement, in relation to alternative management approaches, to rebuild depleted fisheries.

Acknowledgments

We thank Brian Burke (NCSU) for tutelage in the use of Visual Basic. Mike Denson (South Carolina Department of Natural Resources) and Pete Schuhmann (UNC-Wilmington) greatly contributed to the editing of an earlier version of this manuscript. Mark Wuenschel, Michael Martin, Brian Degan, Lisa Etherington, and Mikael Currimjoe provided valuable laboratory and field assistance necessary for parameter estimation. This project was partially funded by the University of North Carolina at Wilmington/North Carolina State University Cooperative Ph.D. Program, and a grant from the National Science Foundation (OCE 97-34472) to D. Eggleston.

Literature cited

Adams, C. M., and R. S. Pomeroy.
1991. Scale economies in hard clam aquaculture. J. Shellfish Res. 10:307–308.

Barbeau, M. A., and H. Caswell.
1999. A matrix model for short-term dynamics of seeded populations of sea scallops. Ecol. Appl. 9:266–287.

Bax, N. J.
1983. Early marine mortality of marked juvenile chum salmon (*Oncorhynchus keta*) released into Hood Canal, Puget Sound, Washington, in 1980. Can. J. Fish. Aquat. Sci. 40:426–435.

Black, R. W. II, and N. G. Hairston Jr.
1988. Predator driven changes in community structure. Oecologia 77:468–479.

Blankenship, H. L., and K. M. Leber.
1996. A responsible approach to marine stock enhancement. *In* Developing and sustaining world fisheries resources: the state of science and management (D. A. Hancock, D. C. Smith, A. Grant, and J. P. Beumer, eds.), p. 485–491. CSIRO, Collingwood, Australia.

Botsford, L. W., and R. C. Hobbs.
1984. Optimal fishery policy with artificial enhancement through stocking: California's white sturgeon as an example. Ecol. Model. 23:293–312.

Buckel, J. A., D. O. Conover, N. D. Steinberg, and K. A. McKown.
1999. Impact of age-0 bluefish (*Pomatomus saltatrix*) predation on age-0 fishes in the Hudson River estuary: evidence for density-dependent loss of juvenile striped bass (*Morone saxatilis*). Can. J. Fish. Aquat. Sci. 56:275–287.

Burke, J. S.
1995. Role of feeding and prey distribution on summer and southern flounder in selection of estuarine nursery habitats. J. Fish Biol. 47:355–366

Burke, J. S., J. M. Miller, and D. E. Hoss.
1991. Immigration and settlement pattern of *Paralichthys dentatus* and *P. lethostigma* in an estuarine nursery ground, North Carolina, U.S.A. Neth. J. Sea Res. 27:393–405.

Burke, J. S., J. P. Monaghan, and S. Yokoyama.
2000. Efforts to understand stock structure of summer flounder (*Paralichthys dentatus*) in North Carolina, USA. J. Sea Res. 44:111–122.

Burke, J. S., T. Seikai, Y. Tanaka, and M. Tanaka.
1999. Experimental intensive culture of summer flounder, *Paralichthys dentatus*. Aquaculture 176: 135–144.

Bystroem, P., and E. Garcia-Berthou.
1999. Density dependent growth and size specific competitive interactions in young fish. Oikos 86: 217–232.

Cowx, I. G.
1999. An appraisal of stocking strategies in the light of developing country constraints. Fish. Manag. Ecol. 6: 21–34.

Elis, T., and R. N. Gibson.
1995. Size-selective predation of 0-group flatfishes in a Scottish coastal nursery ground. Mar. Ecol. Prog. Ser. 127:27–37.

FAO (Food and Agriculture Organization of the United Nations).
1998. Summary: The state of world fisheries and aquaculture. http://www.fao.org/WAICENT/FAOINFO/FISHERY/FISHERY.HTM. [Accessed: June 1998.]

Froese, R., and D. Pauly, eds.
2001. FishBase. World wide web electronic publication. http://www.fishbase.org. [Accessed: January 2001.]

Fujii, T., and M. Noguchi.
1996. Feeding and growth of Japanese flounder (*Paralichthys olivaceus*) in the nursery ground. *In* Proceedings of an international workshop: survival strategies in early life stages of marine resources, p. 141–154. A. A. Balkema Publishers, Brookfield, VT.

Furuta, S.
1999. Seasonal changes in abundance, length distribution, feeding condition and predation vulnerability of juvenile Japanese flounder, *Paralichthys olivaceus*, and prey mysid density in the Tottori coastal area. Nippon Suisan Gakkaishi 65:167–174.

Garcia, L. MaB., R. F. Agbayani, M. N. Duray, G. V. Hilomen-Garcia, A. C. Emata, and C. L. Marte.
1999. Economic assessment of commercial hatchery production of milkfish (*Chanos chanos* Forsskål) fry. J. Applied Ichthyol. 15:70–74.

Hansen, M. J., M. A. Bozek, J. R. Newby, S. P. Newman, and M. D. Staggs.
1998. Factors affecting recruitment of walleyes in Escanaba Lake, Wisconsin, 1958–1996. North Am. J. Fish. Manag. 18:764–774.

Heppell, S. S., and L. B. Crowder.
1998. Prognostic evaluation of enhancement programs using population models and life history analysis. Bull. Mar. Sci. 62:495–507.

Hernandez-Llamas, A.
1997. Management strategies of stocking density and length of culture period for the Catarina scallop *Argopecten circularis* (Sowerby): A bioeconomic approach. Aquacult. Res. 28:223–229.

Hobbs, R. C., L. W. Botsford, and R. G. Kope.
1990. Bioeconomic evaluation of the culture/stocking concept for California halibut. The California halibut, *Paralichthys californicus*, resource and fisheries, 1990, p. 417–450. Cal. Dep. Fish Game Fish. Bull., vol. 174.

Holling, C. S.
1959. Some characteristics of simple types of predation and parasitism. Canadian Entomologist 91: 385–398.

Houde, E. D.
1987. Fish early life history dynamics and recruitment variability. Am. Fish. Soc. Symp. 2:17–29.

Howson, U. A.
2000. Nursery habitat quality for juvenile paralichthyid flounders: Experimental analysis of the effects of physicochemical parameters. Ph.D. diss., 129 p. Univ. Delaware, Newark, DE. 129 p.

Hurst, T. P., and D. O. Conover.
1998. Winter mortality of young-of-the-year Hudson River bass (*Morone saxatilis*): Size-dependent patterns and effects on recruitment. Can. J. Fish Aquat. Sci. 55: 1122–1130.

Jenkins, T. M. Jr., S. Diehl, K. W. Kratz, and S. D. Cooper.
1999. Effects of population density on individual growth of brown trout in streams. Ecol. 80:941–956.

Kellison, G. T.
2000. Evaluation of stock enhancement potential for summer flounder (*Paralichthys dentatus*): an integrated laboratory, field and modeling study. Ph.D. diss., 196 p. NC State Univ., Raleigh, NC.

Kellison, G. T., D. B. Eggleston, and J. S. Burke.
2000. Comparative behaviour and survival of hatchery-reared versus wild summer flounder (*Paralichthys dentatus*). Can. J. Fish. Aquat. Sci. 57:1870–1877.

Kellison, G. T., D. B. Eggleston, J. C. Taylor, and J. S. Burke.
2003a. An assessment of biases associated with caging, tethering, and habitat-specific trawl sampling of summer flounder (*Paralichthys dentatus*). Estuaries 26:64–71.

Kellison G. T., D. B. Eggleston, J. C. Taylor, J. S. Burke, and J. A. Osborne.
2003b. Pilot evaluation of summer flounder stock enhancement potential using experimental ecology. Mar. Ecol. Prog. Ser. 250:263–278.

Kent, D. B., and M. A. Drawbridge.
1999. Developing a marine ranching programme: A multidisciplinary approach. Marine ranching: Global perspectives with emphasis on the Japanese experience. FAO fisheries circular 943:66–78. FAO, Rome.

Kimmerer, W. J., J. H. Cowman Jr., L. W. Miller, and K. A. Rose.
2000. Analysis of an estuarine striped bass (*Morone saxatilis*) population: influence of density-dependent mortality between metamorphosis and recruitment. Can. J. Fish. Aquat. Sci. 57:478–486.

Leber, K. M.
1995. Significance of fish size-at-release on enhancement of striped mullet fisheries in Hawaii. J. World. Aquacult. Soc. 26:143–153.

Lindholm, J. B., P. J. Auster, M. Ruth, and L Kaufman.
2001. Modeling the effects of fishing and implications for the design of marine protected areas: juvenile fish responses to variation in seafloor habitat. Conserv. Biol. 15:424–437.

Lorenzen, K.
2000. Allometry of natural mortality as a basis for assessing optimal release size in fish stocking programmes. Can. J. Fish. Aquat. Sci. 57:2374–2381.

Malloy, K. D., and T. E. Targett.
1994a. The use of RNA:DNA ratios to predict growth limitation of juvenile summer flounder (*Paralichthys dentatus*) from Delaware and North Carolina estuaries. Mar. Biol. 118:367–375.
1994b. Effects of ration limitation and low temperature on growth, biochemical condition, and survival of juvenile summer flounder from two Atlantic Coast nurseries. Trans. Am. Fish. Soc. 123:182–193.

Manderson, J. P., B. A. Phelan, A. J. Bejda, L. L. Stehlik, and A. W. Stoner.
1999. Predation by striped searobin (*Prionotus evolans*, Triglidae) on young-of-the-year winter flounder (*Pseudopleuronectes americanus*, Walbaum): examining prey size selection and prey choice using field observations and laboratory experiments. J. Exp. Mar. Biol. Ecol. 242:211–231.

Masuda, R., and K. Tsukamoto.
1998. Stock enhancement in Japan: review and perspective. Bull. Mar. Sci. 62:337–358.

McEachron, L. W., R. L. Colura, B.W. Bumguardner, and R. Ward.
1998. Survival of stocked red drum in Texas. Bull. Mar. Sci. 62:359–368.

Munro, J. L., and J. D. Bell.
1997. Enhancement of marine fisheries resources. Rev. Fish. Sci. 5:185–222.

Nash, R. D. M.
1998. Exploring the population dynamics of Irish Sea plaice, *Pleuronectes platessa* L., through the use of Paulik diagrams. J. Sea Res. 40:1–18.

Olla, B. L., M. W. Davis, and C. H. Ryer.
1998. Understanding how the hatchery environment represses or promotes the development of behavioural survival skills. Bull. Mar. Sci. 62:531–550.

Powell, A. B., and F. J. Schwartz.
1977. Distribution of paralichthid flounders (Bothidae: Paralichthys) in North Carolina estuaries. Chesapeake Sci. 18: 334–339.

Rice, J. A., T. J. Miller, K. A. Rose, L. B. Crowder, E. A. Marschall, A. S. Trebitz, and D. L. DeAngelis.
1993. Growth rate variation and larval survival: Inferences from an individual-based size-dependent predation model. Can. J. Fish. Aquat. Sci. 50:133–142.

Rickards, W. L.
1998. Sustainable flounder culture and fisheries: a regional approach involving Rhode Island, New Hampshire, Virginia, North Carolina, and South Carolina. *In* Nutrition and technical development of Aquaculture, Nov. 1998, p. 17–20. Sea Grant, Durham, NH.

Rose, K. A., J. H. Cowan Jr, M. E. Clark, E. D. Houde, and S-B Wang.
1999. An individual-based model of bay anchovy population dynamics in the mesohaline region of Chesapeake Bay. Mar. Ecol. Prog. Ser. 185:113–132.

Rosenberg, A. A., M. J. Fogarty, M. P. Sissenwine, J. R. Beddington, and J. G. Shepard.
1993. Achieving sustainable use of renewable resources. Science 262:828–829.

Russell, D. J., and M. A. Rimmer.
1997. Assessment of stock enhancement of barramundi *Lates calcarifer* (Bloch) in a coastal river system in far northern Queensland, Australia. Developing and sustaining world fisheries resources. *In* Developing and sustaining world fisheries resources: the state of science and management, p. 498–503. CSIRO, Collingwood (Australia).

Salvanes, A. G. V., D. L. Aksnes, and J. Giske.
1992. Ecosystem model for evaluating potential cod production in a west Norwegian fjord. Mar. Ecol. Prog. Ser. 90: 9–22.

Serafy, J. E., J. S. Ault, T. R. Capo, and D. R. Schultz.
1999. Red drum, *Sciaenops ocellatus* L., stock enhancement in Biscayne Bay, FL, USA: assessment of releasing unmarked early juveniles. Aquacult. Res. 30:737–750.

Sogard, S. M.
1997. Size-selective mortality in the juvenile stage of teleost fishes: a review. Bull. Mar. Sci. 60: 1129–1157.

Sproul, J. T., and O. Tominaga.
1992. An economic review of the Japanese flounder stock enhancement project in Ishikari Bay, Hokkaido. Bull. Mar. Sci. 50:75–88.

Stoner, A.W.
1980. Feeding ecology of *Lagodon rhomboides* (Pisces: Sparidae): variation and functional responses. Fish. Bull. 78: 337–352.

Sutton, T. M., K. A. Rose, and J. J. Ney.
2000. A model analysis of strategies for enhancing stocking success of landlocked striped bass populations. N. Am. J. Fish. Manag. 20:841–859.

Svåsand, T.
1998. Cod enhancement studies in Norway—background and results with emphasis on releases in the period 1983–1990. Bull. Mar. Sci. 62:313–324.
Svåsand, T. S., T. Kristiansen, T. Pedersen, A. G. V Salvanes, R. Engelsen, G. Naevdal, and M. Nodtvedt.
2000. The enhancement of cod stocks. Fish Fisheries 1: 173–205.
Tanaka, M., T. Goto, M. Tomiyama, and H. Sudo.
1989. Immigration, settlement and mortality of flounder *Paralichthys olivaceus* larvae and juveniles in a nursery ground, Shijiki Bay, Japan. Neth. J. Sea Res. 24:57–67.
Tominaga, O., and Y. Watanabe.
1998. Geographical dispersal and optimum release size of hatchery-reared Japanese flounder *Paralichthys olivaceus* released in Ishikari Bay, Hokkaido, Japan. J. Sea Res. 40: 73–81.
Travis, J., F. C. Coleman, C. B. Grimes, D. Conover, T. M. Bert, and M. Tringali.
1998. Critically assessing stock enhancement: an introduction to the Mote Symposium. Bull. Mar. Sci. 62: 305–311.
van der Veer, H. W., and J. I. Witte.
1993. The "maximum growth/optimal food condition" hypothesis: A test for 0-group plaice *Pleuronectes platessa* in the Dutch Wadden Sea. Mar. Ecol. Prog. Ser. 101: 81–90.
Waters, E. B.
1996. Sustainable flounder culture and fisheries. NC Sea Grant Publication UNC-SG-96-14, 12 p. Sea Grant, Raleigh, NC.
Waters, E. B., and K. Mosher, eds.
1999. Flounder aquaculture and stock enhancement in North Carolina: issues, opportunities and recommendations. NC Sea Grant Publication, UNC-SG-99-02, 24 p. Sea Grant, Raleigh, NC.
Willis, S. A., W. W. Falls, C. W. Dennis, D. E. Roberts, and P. G. Whitechurch.
1995. Assessment of season of release and size-at-release on recapture rates of hatchery-reared red drum. Uses and effects of cultured fishes in aquatic ecosystems. Am. Fish. Soc. Symp. 15:354–365.
Yamashita, Y., S. Nagahora, H. Yamada, and D. Kitigawa.
1994. Effects of release size on survival and growth of Japanese flounder *Paralichthys olivaceus* in coastal waters off Iwate Prefecture, northeastern Japan. Mar. Ecol. Prog. Ser. 105:269–276.

Sex-specific growth and mortality, spawning season, and female maturation of the stripey bass (*Lutjanus carponotatus*) on the Great Barrier Reef

Jacob P. Kritzer

School of Marine Biology & Aquaculture
and CRC Reef Research Centre–Effects of Line Fishing Project
James Cook University
Townsville, Queensland 4811, Australia
Present address: Department of Biological Sciences
University of Windsor
401 Sunset Avenue
Windsor, Ontario N9B 3P4, Canada
E-mail address: kritzer@uwindsor.ca

Abstract—Sex-specific demography and reproductive biology of stripey bass (*Lutjanus carponotatus*) (also known as Spanish flag snapper, FAO) were examined at the Palm and Lizard island groups, Great Barrier Reef (GBR). Total mortality rates were similar between the sexes. Males had larger L_∞ at both island groups and Lizard Island group fish had larger overall L_∞. Female:male sex ratios were 1.3 and 1.1 at the Palm and Lizard island groups, respectively. The former is statistically different from 1, but is unlikely significantly different in a biological sense. Females matured on average at 2 years of age and 190 mm fork length at both locations. Female gonadal lipid body indices peaked from August through October, preceding peak gonadosomatic indices in October, November, and December that were twice as great as in any other month. However, ovarian staging revealed 50% or more ovaries were ripe from September through February, suggesting a more protracted spawning season and highlighting the different interpretations that can arise between gonad weight and gonad staging methods. Gonadosomatic index increases slightly with body size and larger fish have a longer average spawning season, which suggests that larger fish produce greater relative reproductive output. Lizard Island group females had ovaries nearly twice as large as Palm Island group females at a given body size. However, it is unclear whether this reflects spatial differences akin to those observed in growth or effects of sampling Lizard Island group fish closer to their date of spawning. These results support an existing 250 mm minimum size limit for *L. carponotatus* on the GBR, as well as the timing of a proposed October through December spawning closure for the fishery. The results also caution against assessing reef-fish stocks without reference to sex-, size-, and location-specific biological traits.

Manuscript approved for publication 22 July 2003 by Scientific Editor.

Manuscript received 22 July 2003 at NMFS Scientific Publications Office.

Fish Bull. 102:94–107 (2004).

Lutjanid snappers are among the most prominent species comprising the catch of hook-and-line fisheries on tropical reefs worldwide (Dalzell, 1996). A notable exception is the line fishery on Australia's Great Barrier Reef (GBR). There, the finfish catch, and therefore the majority of fisheries research, is dominated by coral trouts of the genus *Plectropomus* (Mapstone et al.[1]). However, the GBR finfish harvest is diverse and the catch of many secondary species has risen steadily since the early 1990s (Mapstone et al.[1]). Furthermore, over the past decade, the GBR fishery has changed with the advent of the lucrative Asian live reef-fish market. At present, only a handful of the many species harvested on the GBR are exported to the live reef-fish market. However, continued expansion of the trade coupled with the depletion of fish stocks in other source nations (Bentley[2]) has the potential to introduce demand for a wider range of species. Even in the absence of changes in the species composition of live reef-fish exports, increased demand for secondary species due to changes in either domestic preferences or availability of primary species has the potential to elevate harvest of currently nontarget species (Kritzer, 2003).

Effective multispecies management of the GBR fishery will ultimately require understanding the biology of more than simply the primary target species. For example, spawning closures of the fishery have been proposed for nine-day periods around the new moon in October, November, and December on the rationale that this will protect spawning activity of a wide range of harvested species (Queensland Fisheries Management Authority[3]). Yet, spawning season information for species beyond the common coral trout (*P. leopardus*) (Ferreira, 1995; Samoilys, 1997) is nearly nonexistent. The GBR fishery is in a fortunate position with respect to management of many species for which exploitation is still at relatively low levels because baseline biological characteristics can be estimated before stock structure is drastically altered by fishing. These data can then be used in both formulating management strategies and monitoring effects of fishing.

[1] Mapstone, B. D., J. P. MacKinlay, and C. R. Davies. 1996. A description of the commercial reef line fishery log book data held by the Queensland Fisheries Management Authority. Report to the Queensland Fisheries Management Authority, 480 p. Primary Industries Building, GPO Box 46, Brisbane, Queensland 4001, Australia.

[2] Bentley, N. 1999. Fishing for solutions: can the live trade in wild groupers and wrasses from Southeast Asia be managed? TRAFFIC Southeast Asia report, 143 p. Unit 9-3A, 3rd Floor, Jalan SS23/11, Taman SEA, 47400 Petaling Jaya, Selangor, Malaysia.

[3] Queensland Fisheries Management Authority. 1999. Queensland coral reef fin fish fishery. Draft management plan and regulatory impact statement, 80 p. Primary Industries Building, GPO Box 46, Brisbane, Queensland 4001, Australia.

One of the most prominent secondary species in the GBR fishery is the stripey bass (*Lutjanus carponotatus*) (Spanish flag snapper, FAO). In relation to other large predators on the GBR, *L. carponotatus* is highly abundant on inshore reefs, common on mid-continental shelf reefs, and absent from outer-shelf reefs (Newman and Williams, 1996; Newman et al., 1997; Mapstone et al.[4]). Although this affinity for inshore reefs has the potential to make the species more susceptible to recreational fishing, the limited available data do not suggest that it is heavily exploited by the recreational fleet (Higgs, 1993) in relation to the commercial fleet (Mapstone et al.[1]). *Lutjanus carponotatus* has a broad-based diet, consuming a wide variety of smaller reef fishes and invertebrates (Connell, 1998). Its role as a predator coupled with its abundance, particularly on inshore reefs, suggests that the species might have an important ecological function on the GBR in addition to its role as a fishery resource.

Davies (1995) and Newman et al. (2000) have collected basic demographic data for *L. carponotatus* on the northern and central GBR, respectively. They both reported a pronounced asymptote in the growth trajectory and that most growth occurred over the first three to five years and little subsequent growth over a lifespan that can reach 15 to 20 years. Newman et al. (2000) also reported a heavily male-biased sample and larger body sizes among males. Unlike age and growth data, no information on reproduction of *L. carponotatus* has been available despite that fact that existing (minimum size limits) and proposed (spawning closures) fisheries regulations are based largely on reproductive traits (Queensland Fisheries Management Authority[3]).

Specific aims of this study were 1) to estimate sex ratios and sex-specific schedules of growth and mortality; 2) to estimate age- and size-specific schedules of female maturation; 3) to identify the spawning season; and 4) to determine whether reproductive output is proportional to body size by examining the ovary weight-body weight relationship and the average spawning duration of large and small fish. All traits were estimated at the Palm Island group on the central GBR. Additionally, sex-specific growth and female maturity schedules were also examined at the Lizard Island group on the northern GBR to develop spatial comparisons.

Materials and methods

Field methods

Size, age, and reproductive data were obtained for 465 *L. carponotatus* collected by spear fishing on fringing reef slopes during monthly fishery independent sampling at Pelorus, Orpheus, and Fantome Islands in the Palm Island group on the central GBR (Fig. 1) from April 1997 through March 1998. No sampling took place in January 1998 because of severe flooding in the area. To develop spatial comparisons, samples of 118 and 18 fish were obtained in October 1997 and April 1999, respectively, by spear fishing at the Lizard Island group approximately 400 km north of the Palm Island group (Fig. 1). Fish were collected from depths of 2 to 15 m by teams of two to four scuba divers. *Lutjanus carponotatus* most commonly inhabits depths less than 15 m (Newman and Williams, 1996); therefore sampling efforts encountered the majority of the population. Fish were targeted as encountered, without preference based on size, in order to collect as representative a sample as possible. Fish <150 mm fork length (FL) were rare in the samples because they were infrequently observed on reef slopes (Kritzer, 2002). Therefore, supplemental spear fishing on reef flats targeting smaller fish was conducted at the Palm Island group (n=24) in April and December 1999 and at the Lizard Island group (n=25) in May 1999 to obtain growth data for size classes against which the primary sampling was biased.

Total weight (TW, g) and FL (mm) of each specimen were recorded. Ovaries and testes of small lutjanids on the GBR are characterized by a lipid body running along the length of each lobe, akin to that found in tropical acanthurids (Fishelson et al., 1985). Gonads and these associated lipid bodies were removed and preserved in FAAC (formaldehyde 4%, acetic acid 5%, calcium chloride 1.3%). Sagittal otoliths were removed, cleaned, and stored for later analyses.

Gonad processing and ovarian staging

The lipid body was removed from each ovary or testis after fixation and the weight of the gonad (GW) and lipid body (LW) were measured to the nearest 0.01 g. A gonadosomatic index (GSI) and lipidsomatic index (LSI; after Lobel, 1989) were calculated for each sample as the percentage of TW represented by GW and LW, respectively. Features of whole fixed ovaries including color, speckling, and surface texture were noted as potential criteria for macroscopic staging after comparison with samples processed histologically. Sex of the April 1999 Lizard Island group samples was determined macroscopically only, and was therefore used in sex-specific growth analyses but not in analysis of maturity. Fish <150 mm FL had undeveloped gonads and sex of these specimens was not determined or assigned a reproductive stage.

A subsample of 131 ovaries spanning the range of gonad sizes and external appearances were prepared for histological examination. Samoilys and Roelofs (2000) found that medial gonad sections were adequate for determination of reproductive status. Therefore, a medial section was removed from one gonad lobe, dehydrated, and embedded in paraffin. Embedded ovarian tissues were sectioned at 5 μm and stained with hematoxylin and eosin. Ovaries were staged on the basis of the most advanced oocyte stage present (West, 1990). Additional features used in histological staging included the presence of brown bodies and atretic

[4] Mapstone, B. D., A. M. Ayling, and J. H. Choat. 1998. Habitat, cross shelf and regional patterns in the distributions and abundances of some coral reef organisms on the northern Great Barrier Reef. Great Barrier Reef Marine Park Authority research publication 48, 71 p. GPO Box 1379, Townsville, Queensland 4810, Australia.

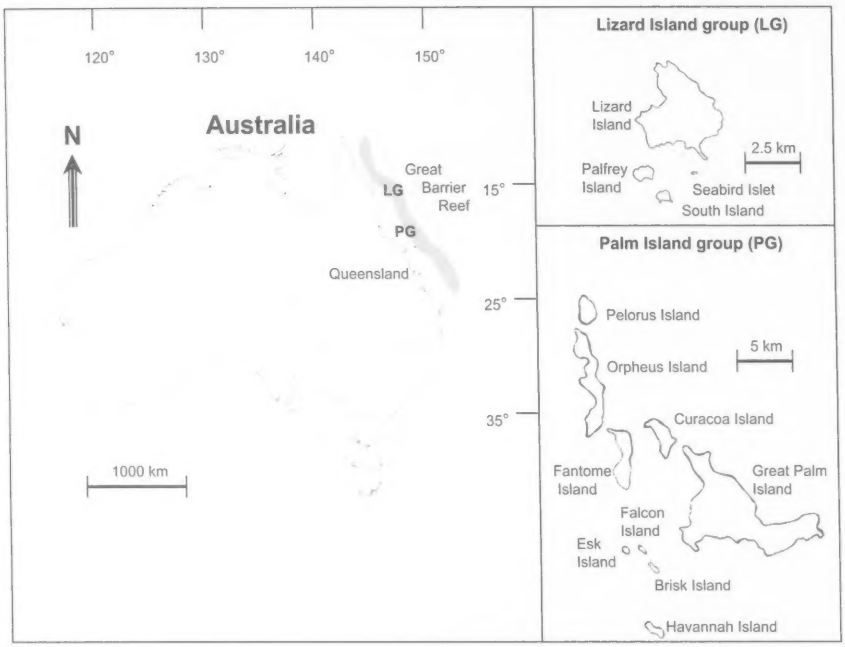

Figure 1

Location of the Palm Island group (PG) and Lizard Island (LG) group within the Great Barrier Reef off the coast of Queensland, Australia.

oocytes and, in the case of inactive ovaries, the relative thickness of the gonad wall and the compactness of the ovarian lamellae (Samoilys and Roelofs, 2000). For those samples processed histologically, macroscopic features were compared within and between reproductive stages to determine whether any macroscopic characteristics could be used to accurately stage ovaries

Age determination

Ages of fish were determined in order to estimate age-based schedules of growth, mortality, and maturation. Otoliths lacking broad, opaque macro-increments were processed to enumerate finer presumed daily micro-increments. These otoliths were ground by hand first from the anterior end and then the posterior end through a progressively finer series of P1200 sandpaper, 12-µm lapping film, and 9-µm lapping film until a thin section through the nucleus remained. Micro-increments were enumerated on two independent occasions. If the two counts for one specimen did not deviate by more than 5% of their mean, the mean was used as the age estimate. Otherwise, a third reading was performed and the mean of this and the more similar of the first two readings was used as the age estimate, again provided that the counts differed by no more than 5% of their mean.

Macro-increments in the otoliths of *L. carponotatus* have been validated as annuli by tetracycline labeling (Cappo et al., 2000). A pilot analysis indicated that age estimates did not differ between readings of whole left and right otoliths (paired t-test: df=59; t=0.60; P=0.55); therefore one otolith was randomly selected from each sample for age determination. All otoliths were initially read whole. A second pilot analysis compared whole and sectioned age estimates for a subsample of *L. carponotatus* otoliths. This comparison suggested that whole readings began to drastically underestimate age beyond approximately sectioned age 12 (see Kritzer, 2002). To capitalize on both the greater efficiency of whole readings and the greater accuracy of sectioned readings, whole readings were used for all fish except for those for which any whole reading exceeded 10 or for which there was not agreement in at least two out of three independent whole readings. If at least two out of three independent readings of either whole or sectioned otoliths (as appropriate) agreed, then that value was used as the age estimate. Ferreira and Russ (1994) have described the whole- and sectioned-otolith preparation and reading methods used in the present study.

Sex-specific demography

Early growth of *L. carponotatus* was estimated by linear regression of FL on age for those samples processed to read subannual micro-increments. Separate regressions were performed for the Palm and Lizard island groups and these were compared by analysis of covariance (ANCOVA). Because of the undeveloped nature of the gonads of the smallest fish, early growth was estimated without refer-

ence to sex. Sex ratios at each island group were compared with an expected ratio of 1:1 by χ^2 goodness-of-fit tests by using all specimens (i.e. immature and mature) whose sex could be determined.

Lifetime growth parameters were estimated for males and females from each island group by fitting the von Bertalanffy growth function (VBGF),

$$L_t = L_\infty\left(1-\exp\left(-K(t-t_0)\right)\right),$$

where L_t = FL at age t;
L_∞ = the mean asymptotic FL;
K = the Brody growth coefficient; and
t_0 = the age at which fish have theoretical FL of 0.

Growth functions were fitted by nonlinear least-squares regression of FL on age by using samples for which sex was determined. Because VBGF parameter estimates can be sensitive to the range of ages and sizes used (see Ferreira and Russ, 1994, for an empirical example), a common t_0 equivalent to the x-intercept of the early growth estimates was used in all models (see "Results" section). Although the sex-specific sample sizes at the Lizard Island group were smaller (n=65 for females; n=62 for males), VBGF parameter estimates achieved high precision at sample sizes between 50 and 100 (Kritzer et al., 2001); therefore the Lizard Island group data were included in the analysis. Growth parameters were compared by plotting 95% confidence regions of the parameters K and L_∞ (Kimura, 1980) for each sex from each location and assessing the degree of overlap.

Sex-specific total mortality rates, Z, were estimated by using the age-based catch curve of Ricker (1975) as the slope of a linear regression of natural log-transformed frequency on age class. Everhart and Youngs (1981) proposed that catch curve analysis should exclude age classes with n<5 and Murphy (1997) proposed that age structures used in catch curves should be truncated at the first age class with n<5. Alternatively, Kritzer et al. (2001) proposed that a sample should contain an average of at least ten fish per age class irrespective of age class-specific sample sizes. Therefore catch curves were fitted by two different methods for each sex at the Palm Island group. The first catch curve began at the modal age class and stopped before the first age class with $n<5$. The second catch curve likewise began at the modal age class but included all age classes that were thereafter represented in the data set. Sex-specific sample sizes for the Lizard Island group were too small by any of these criteria and this location was excluded. Mortality estimates for Palm Island group fish were compared between the fitting methods within each sex as well as between sexes by ANCOVA.

Reproductive biology

Maturation schedules of female fish were estimated for each island group by fitting a logistic model,

$$P_i = 1/\left(1+\exp(a-ri)\right),$$

where P_i = the proportion of mature fish in age or 20-mm size class i;
a adjusts the position of the curve along the abscissa; and
r determines its steepness.

Age- and size-specific maturity functions were used to estimate the mean age, t_{50}, and size, L_{50}, at which 50% of females are mature at each island group.

Monthly mean LSI and GSI values of mature Palm Island group fish were plotted separately for males and females to determine seasonal patterns of energy storage and the peak spawning period of *L. carponotatus*. The proportion of specimens at each mature female reproductive stage in each month was also plotted to examine ovarian development patterns throughout the year and the degree of spawning activity occurring outside of peak months.

To examine whether relative reproductive output increases with body size, GW and GSI for stage-IV ovaries collected during peak spawning months were regressed against TW. Residual plots were used to assess deviation from a linear relationship and to identify three outliers, which were removed from the regression analysis. Regression slopes were compared between the two island groups by ANCOVA. Also, mean GSI values and the proportion of Palm Island group females with stage-IV ovaries during spawning months were compared between females ≤230 mm FL and those >230 mm FL to examine whether the duration of spawning varies between size classes (*nota bene*: 230 mm FL is approximately the mean size of mature Palm Island group females and splits each month's sample approximately in half).

Results

Ovarian staging

Five female reproductive stages were identified through histological analysis (Table 1) and were based largely on the scheme of Samoilys and Roelofs (2000). Ovarian stages I (immature) and II (resting mature) have similar oocyte stages. These can be distinguished by the presence of brown bodies or atretic oocytes, which are typically products of prior spawning (e.g. Ha and Kinzie, 1996; Adams et al., 2000) and are usually absent from stage-I ovaries. However, these structures will not necessarily persist in ovaries that have spawned, and in fact were rare among the samples; therefore identification of immature females was based primarily on structural organization of the ovary. Stage-I ovaries typically have a thin ovarian wall and more compacted oocytes, whereas ovaries that have previously spawned tend to have a thicker ovarian wall and a more disorganized arrangement of oocytes (Table 1). Also, there were distinct size differences between stage-I ovaries and other stages. The mean GW of stage-I ovaries was approximately one-third that of stage-II ovaries, and mean GSI was approximately one-half of that at stage II (Table 1), and the distribution of body sizes of fish at stage I had much lower minimum, maximum, and modal size

Table 1

Description of histological and macroscopic features (after fixation in a formaldehyde, acetic acid, calcium chloride solution) of ovarian developmental stages of *Lutjanus carponotatus*. Stage definitions and descriptions are largely a modification of the scheme proposed by Samoilys and Roelofs (2000). Mean ovary weight (GW) and gonosomatic index (GSI) for the larger Palm Island group sample are provided.

	Stage	Histological features	Macroscopic features
Inactive	I Immature	Relatively thin ovarian wall; lamellae well packed; only darkly purple staining previtellogenic oocyte stages (oogonia and perinucleolar stages) present.	Always even white color over entire surface; smooth surface texture; lobes quite small (typically <2 cm long) and thin (mean GW=0.33 g; mean GSI=0.24%).
	II Resting	Relatively thick ovarian wall; spaces between lamellae common; only previtellogenic oocyte stages and possibly brown bodies and few atretic vitellogenic oocytes present.	Even white to cream or tan color over gonad surface; surface may be smooth or somewhat convoluted; small white stage II ovaries are difficult to distinguish from stage I without histology (mean GW=1.01 g; mean GSI=0.43%).
Active	III Ripening	Most advanced oocytes are at yolk globule or migratory nucleus stage; atretic oocytes or brown bodies possibly present.	Color sometimes white but more often cream to tan; surface is commonly convoluted; difficult to distinguish from stage II without histology (mean GW=1.18 g; mean GSI=0.53%).
	IVa Ripe	Most advanced oocytes at yolk vesicle stage; atretic oocytes or brown bodies possibly present.	Color tan to brown or mustard with opaque speckles that become larger and more dense as late stage oocytes become more numerous; convoluted surface sometimes with prominent vascularization (mean GW=4.04 g; mean GSI=1.39%).
	IVb Running ripe	Similar to stage IVa but large, irregularly shaped, clear to lightly coloured hydrated oocytes are present.	External appearance identical to stage IVa and can only be differentiated histologically (no samples found at Palm Island group).

classes compared with the distribution of body sizes of fish at stage II (Fig. 2).

Stage-III (ripening) ovaries contain oocytes at the yolk vesicle vesicle stage, which some authors classify as vitellogenic (e.g. Samoilys and Roelofs, 2000) and others classify as previtellogenic (e.g. West 1990). Like stage-II ovaries, stage-III ovaries can, but do not necessarily, contain brown bodies or atretic oocytes as evidence of probable prior spawning. Although the fish might not have spawned previously, stage III is considered to be a mature stage in the present study because the appearance of yolk vesicles is associated with the initial development of the yolk globule and represents advanced development of the oocyte beyond perinucleolar stages (West, 1990). Therefore, the fish is preparing for spawning and will soon be part of the mature population if it is not already. Mean age and size of stage-II (4.4. years and 219 mm FL), stage-III (5.0 years and 222 mm FL), and stage-IV (6.5 years and 261 mm FL) females were much more similar to one another than they were to stage-I females (1.9 years and 119 mm FL). Moreover, size-frequency distributions of fish at stages II, III, and IV showed considerable overlap and similarity with one another and were all quite distinct from the size-frequency distribution for stage-I females (Fig. 2). This suggests a division between immature fish and those that are spawning or are nearly ready to do so. The pronounced difference in GW and GSI between stage-I and stage-III ovaries and similarity in these metrics between stage-II and stage-III fish (Table 1) further support this division.

Most immature ovaries and all ripe ovaries could be identified macroscopically. Because certain macroscopic features were common to multiple ovarian stages, additional histological features was required to separate the largest immature from the smallest resting ovaries and all ripening from resting ovaries among the samples remaining after the initial comparison between histological and macroscopic features. Only one ovary with fully hydrated oocytes, collected at the Lizard Island group, was found among the samples prepared for histological analysis; therefore stages IVa and IVb were treated as a single stage. Stage IV sufficiently represents final development toward spawning on the broad seasonal time scale adopted in this study but encompasses a wide range of ovarian characteristics and would need to be divided into more detailed stages for finer temporal scale studies of lunar or diel spawning patterns. No samples exhibited features of truly "spent" ovaries.

Sex-specific demography

Differences were not apparent in early growth of *L. carponotatus* between the island groups (ANCOVA: df=1, 46; F=1.07; P=0.301); therefore the data were pooled to

estimate an early growth rate of 0.76 mm/d, assuming daily periodicity of micro-increments (Fig. 3). This rate of growth represents quite rapid growth, given that fish are adding 100 mm of length in around 4 months, increasing from approximately 20 to 120 mm FL (Fig. 3). The x-intercept of the early growth curve (=–17.98 d) was divided by 365 d/yr to estimate a common t_0 (=–0.049 yr) for all VBGF models.

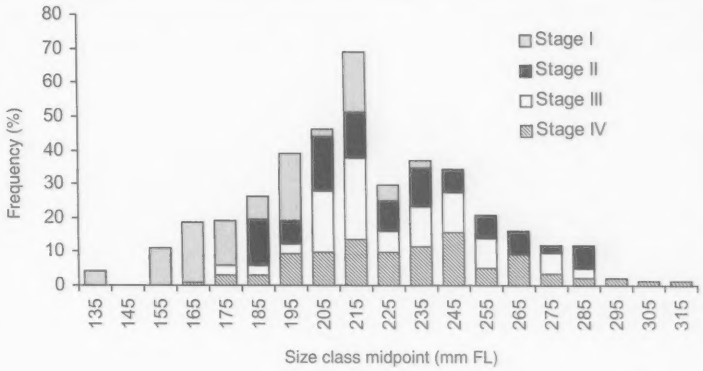

Figure 2

Size-frequency distributions of female Palm Island group *Lutjanus carponotatus* at each of the four stages of ovarian development. Stage descriptions are provided in Table 1.

Although size at age for both sexes at both island groups was characterized by substantial individual variability, different growth trajectories were evident for males and females (Fig. 4, A and B). Estimates (Table 2) and 95% joint confidence regions (Fig. 4C) for the VBGF parameters indicated that the primary differences in these trajectories at each island group lay in L_∞ (which indicated that males grow larger than females). In contrast, the common range of K values spanned by the sexes within each island group indicated similar curvature (Table 2, Fig. 4C). However, use of a common t_0 restricts the range of possible fitted K values (Kritzer et al., 2001). In addition to the differences between the sexes, the data revealed a general pattern of larger body sizes at the Lizard Island group (Table 2, Fig. 4).

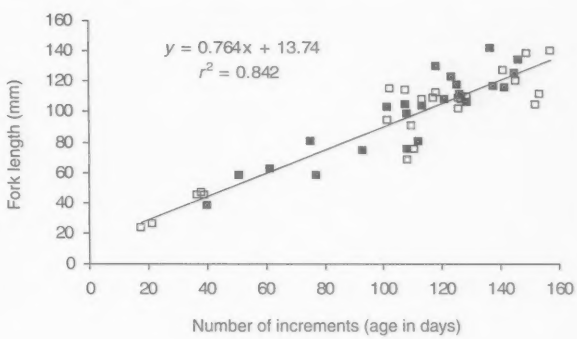

Figure 3

Fork length at microincrement count for *Lutjanus carponotatus* lacking the first annulus at the Palm (□; n=24) and Lizard (■; n=25) island groups. Periodicity of increments is presumed to be daily. Data from each island group are distinguished, but a pooled linear growth curve is presented as separate growth curves did not differ (ANCOVA: df=1, 46; F=1.07; P=0.301).

Mortality estimates at the Palm Island group were slightly higher when all age classes beyond 1 year were included compared with exclusion of age classes with $n < 5$ (Fig. 5). These higher mortality estimates contrast with Murphy's (1997) finding that truncation of the age structure results in higher least-squares estimates of Z. The differences between mortality rates estimated with and without age classes with $n < 5$ were minor for both males (ANCOVA: df=1, 20; F=0.009; P=0.92) and females (ANCOVA: df=1, 23; F=1.35; P=0.26). Therefore, for comparisons between the sexes, the estimates that included all age classes greater than 1 yr were used. In contrast to the sex-specific growth differences, Z estimates of 0.26/yr and 0.29/yr (Fig. 5) corresponding to annual survivorship of 77% and 75% for females and males, respectively, at the Palm Island group were similar between the sexes (ANCOVA: df=1, 27; F=0.505; P=0.483). Murphy's (1997) results also suggested that least-squares mortality estimates are likely to be around 30% less than the true mortality rate when n = 200 and the true Z = 0.2/yr. Correcting these mortality estimates based upon this potential bias results in Z estimates up to 0.37/yr and 0.41/yr for females and males, respectively, with corresponding annual survivorship of 69% and 66%. However, the catch curve estimates (Fig. 5) corresponded well with estimates based upon Hoenig's (1983) empirically derived relationship between Z and maximum age, t_{max} (females: t_{max}=18 yr, Z=0.23/yr; males: t_{max}=16 yr; Z=0.26/yr).

The observed female-to-male sex ratios of 1.3 and 1.1 were close to unity at the Palm and Lizard Island groups, respectively (Table 2). However, χ^2 tests suggest this ratio is statistically different from 1 at the Palm Island group (df= 1; χ^2=7.74; P=0.005) but not at the Lizard Island group (df=1; χ^2=0.031; P=0.86).

Age and size at maturity

Although there was some indication that Palm Island group females mature at slightly younger ages and smaller sizes

than Lizard Island group females, maturation schedules were generally similar (Fig. 6). At both island groups, age 2 was the age at both earliest maturity and 50% maturity, and 93–100% of females had matured by age 4 (Fig. 6A, Table 3). Thus, maturation was rapid, beginning early in life and ending within a 2-year period with nearly all members of a cohort mature. Length-specific maturation schedules also exhibited similarity between the island groups with mature fish first appearing in the 160–179 mm FL size class, estimated 50% maturation in the 180–199 mm FL size class, and 93–100% maturity at the 220–239 mm FL size class (Fig. 6B, Table 3).

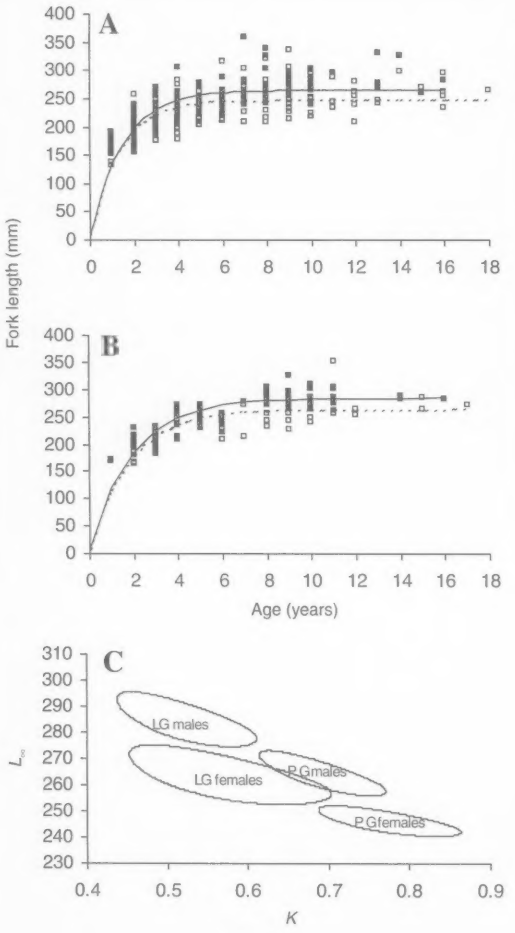

Figure 4

Fork length at age and estimated von Bertalanffy growth curves for male (■, solid lines) and female (□, broken lines) *Lutjanus carponotatus* at the Palm (**A**) and Lizard (**B**) island groups and estimated 95% joint confidence regions of the parameters K and L_∞ (**C**). Parameter estimates are presented in Table 2.

Spawning season

Mature female LSI values were highest in August through October with a maximum in September (Fig. 7A). The peak in GSI lagged that of LSI by two months with the highest values occurring from October through December and with a maximum in November (Fig. 7A). The absence of a January sample unfortunately leaves some ambiguity as to whether GSI, and therefore presumably spawning activity, would still be high at this time or if it would have begun to decline. Male GSI values also exhibited a November maximum (Fig. 7B). Male LSI values, however, did not show any clear trend of increase and decline throughout the year and peaks in April, May, and August that did not correlate with future GSI values as clearly as seen in the female data (Fig. 7). Unlike LSI values for females, monthly mean male LSI values were always greater than the corresponding GSI values.

The seasonal pattern of *L. carponotatus* spawning activity suggested by monthly trends in the proportions of mature ovarian stages can be interpreted as different from that suggested by GSI values. The lowest GSI values in the October–December peak period were close to twice as great as the next highest values in September and February (Fig. 7A). However, the percentage of stage-IV ovaries in the September sample was greater than 50%, which is well over half the percentage of the October sample; whereas the February sample comprised approximately the same percentage of stage-IV ovaries as October (Fig. 8). Also, more than 50% of the March sample was stage-IV ovaries (Fig. 8), whereas its GSI value was close to that of the months with relatively few ripe ovaries (Fig. 7A). Furthermore, September and March had the highest proportions of ripening (stage-III) females and thus far fewer resting mature (stage-II) females than the April to August period of limited spawning activity (Fig. 8). Therefore, regardless of whether September, February, and March are defined as nonspawning months or months of limited spawning activity based upon GSI, analysis of ovarian stage frequencies suggests these to be periods of greater spawning activity than might be predicted with GSI. Clearly, the presence of advanced oocytes is a much better indication of imminent spawning than any measure of gonad size; therefore the reproductive stage-frequency data undoubtedly provide the more accurate picture of *L. carponotatus* spawning patterns.

Of 59 ovaries staged from the October 1997 Lizard Island group sample, eight were at stage I, two were at stage II, and 49 (96% of mature females in the sample) were at stage IV. This finding suggests that the island groups share at least October as a common period of active spawning.

Reproductive differences between locations and among size classes

The variation in GW among females of like body sizes during peak spawning months increased to some degree with increasing TW, but there was a generally homogeneous spread of data around the predicted regression

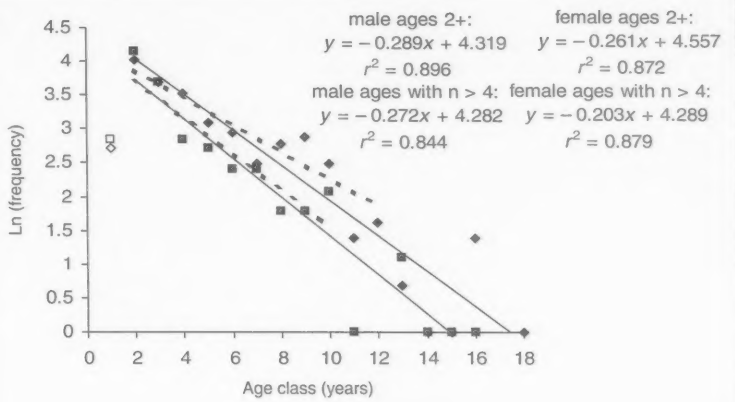

Figure 5

Age-based catch curves for female (■, higher elevation lines) and male (♦, lower elevation lines) *Lutjanus carponotatus* at the Palm Island group fitted to all age classes >1 (solid lines) and age classes >1 with n >4 (dashed lines). Open symbols represent age class 1, which was not used in the analysis.

Table 2

Sex-specific von Bertalanffy growth parameters for *Lutjanus carponotatus* at the Palm and Lizard Island groups, Great Barrier Reef. n is sample size; $\bar{L}_F$ is the mean fork length (mm); K is the Brody growth coefficient (per yr); L_∞ is the mean asymptotic fork length (mm); a common t_0 of –0.049 yr was used in all growth models. Standard errors are provided below parameter estimates.

	n	$\bar{L}_F$	K	L_∞	r^2
Palm Island group					
females	263	224.2	0.77	246.3	0.515
		(2.11)	(0.032)	(2.25)	
males	202	224.7	0.69	264.3	0.629
		(2.78)	(0.028)	(3.26)	
sex ratio	1.3:1				
Lizard Island group					
females	65	239.9	0.56	263.5	0.618
		(4.76)	(0.043)	(4.24)	
males	62	256.4	0.51	284.8	0.714
		(4.77)	(0.032)	(4.03)	
sex ratio	1.1:1				

lines across body sizes (Fig. 9A). This suggests that on average GW at stage IV during peak spawning months is a linear function of TW. Lizard Island group fish generally had larger ovaries at a given size than did Palm Island group fish (Fig. 9A), a difference supported by ANCOVA (df=1, 125; F=34.7; P<0.001). In fact, regression slopes of 0.25 and 0.52 suggest relative ovary weights at the Lizard Island group were approximately twice as large as those at the Palm Island group. There were no differences in the GW-TW relationship among October, November, and December at the Palm Island group, and therefore the differences in this relationship between the island groups was consistent whether only the Palm Island group October data were used or whether the October through December data were used.

Although GW is a linear function of TW, the nonzero regression constants (Fig. 9A) mean that GW is not a constant proportion of TW. Consequently, GSI increases with increasing TW (Fig. 9B). The relationship between TW and GSI is not strong, with regression slopes close to zero and low r^2 values at both island groups (Fig. 9B). Despite this, the relationship is statistically strong at both the Palm (ANOVA: df=1,82; F=12.70; P=0.006) and Lizard (ANOVA: df= 1,42; F=22.95; P<0.0001) Island groups. Also, there is

some suggestion that, like the GW-TW relationship, the GSI-TW relationship varies between the island groups, although to a much lesser extent (ANCOVA: df=1,125; F=7.44; P=0.007).

There is some indication that larger fish spawn over a longer period at the Palm Island group. During the September–February spawning season, mean GSI values were always higher for mature Palm Island group females >230 mm FL compared with mature females ≤230 mm FL at the same location (Fig. 10). This pattern is likely due in part to the higher relative gonad weights of larger fish (Fig. 9B) but also seems to be driven by greater proportions of stage-IV ovaries among larger mature females in September, October, and February compared with fish ≤230 mm FL (Fig. 10). During these months, 13%, 13% and 25% more large fish were at stage IV, respectively, than were small fish.

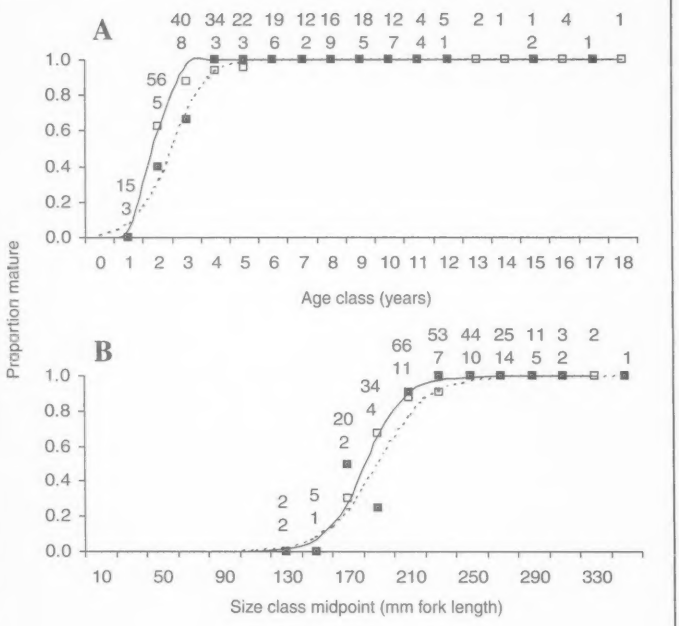

Figure 6

Proportion of mature female *Lutjanus carponotatus* and estimated age-specific (**A**) and size-specific (**B**) logistic maturation schedules at the Palm (■, solid lines) and Lizard (□, broken lines) island groups. Sample sizes for the Palm (top value) and Lizard (lower value) Island groups are presented above the data for each age or size class. Parameters of the maturity functions are provided in Table 3.

Discussion

Demography and reproduction of *L. carponotatus*

Growth of *L. carponotatus* is rapid for the first two years of life, slows over the next two years, and nearly ceases by age 4. The slowing and cessation of growth coincide with the ages at 50% and 100% maturity, respectively, and support the argument of Day and Taylor (1997) that maturation represents a pivotal physiological transformation and consequently a fundamental shift in the growth trajectory. Further supporting the idea that reproductive development occurs at the expense of somatic growth is the apparently longer average spawning season among larger fish that have ceased most somatic growth. The limited growth over much of the lifes-

Table 3

Parameters of age- and size-specific logistic maturation schedules and estimated ages and fork lengths at 50% maturity of female *Lutjanus carponotatus* at the Palm and Lizard Island groups, Great Barrier Reef. a adjusts the position of the logistic function along the abscissa; r determines the steepness of the logistic function; t_{50} is the age at 50% maturity; L_{50} is the fork length at 50% maturity. Standard errors are provided below parameter estimates.

	a	r	r^2	t_{50} or L_{50}
Age-specific				
Palm Island group	6.40	3.42	0.985	1.9 years
	(1.42)	(0.12)		
Lizard Island group	4.16	1.73	0.990	2.4 years
	(0.48)	(0.19)		
Size-specific				
Palm Island group	14.72	0.081	0.994	182 mm
	(1.49)	(0.008)		
Lizard Island group	11.61	0.061	0.908	189 mm
	(3.84)	(0.020)		

pan of *L. carponotatus* can explain the apparently constant mortality rate over many age classes (evidenced by high catch curve r^2 values) given that mortality is often largely a function of body size (Roff, 1992).

The development and regression of visceral fat stores preceding increases in ovary weight is a pattern that has been observed in other reef fishes, including tropical surgeonfishes (Acanthuridae: Fishelson et al., 1985) and groupers (Serranidae: Ferreira, 1995) and temperate rockfishes (Scorpaenidae: Guillemot et al., 1985). These patterns suggest that the stored lipid is fuelling the energetic costs of spawning. The lack of a similar pattern for males supports the idea that energetic costs associated with production of sperm are low in relation to eggs (Wootton, 1985) thus enabling male *L. carponotatus* to attain larger sizes, as also reported by Newman et al. (2000). Alternatively, males might spawn more frequently throughout the year than females and the lack of seasonal patterns in lipid storage among males might reflect a more regular energetic demand that precludes energy storage. In any case, these sex-specific growth patterns, coupled with similar mortality rates between the sexes and sex ratios that are at unity or that are at most only slightly female-biased (see below), suggest that females are limiting reproduction of this species. Therefore stock dynamics should be modeled in terms of female biology (Hilborn and Walters, 1992).

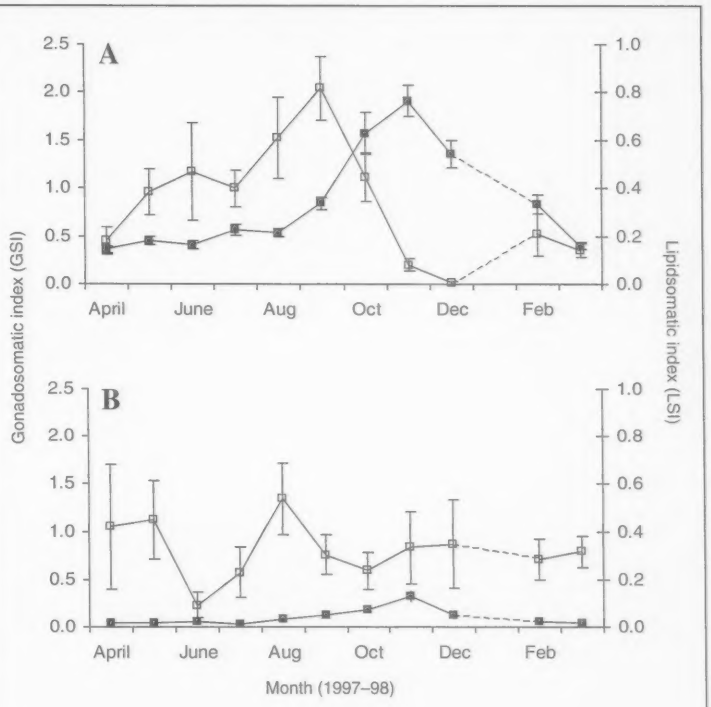

Figure 7

Monthly mean gonadosomatic index (GSI ±SE; ■) and lipidsomatic index (LSI ±SE; □) values for mature female (**A**) and all male (**B**) *Lutjanus carponotatus* at the Palm Island group.

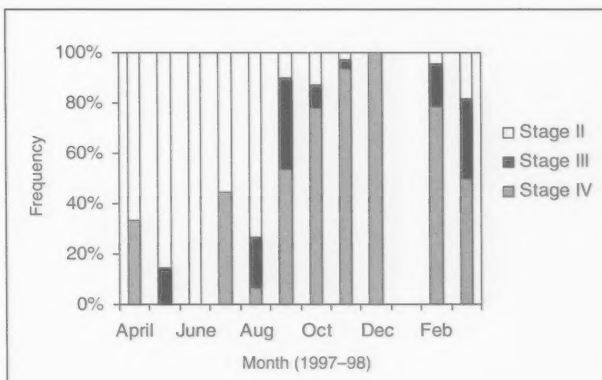

Figure 8

Monthly frequencies of ovarian stages of mature *Lutjanus carponotatus* at the Palm Island group. Stage descriptions are provided in Table 1.

The apparently female-biased sex ratio at the Palm Island group starkly contrasts with the heavily male-biased sex ratio reported for mid-shelf reefs of the central GBR by Newman et al. (2000). However, neither a male- nor female-biased sex ratio would be expected from a nonhermaphrodite that is not known to possess a complex mating system such as defense of females or territories. It is possible that the spawning sex ratio (i.e. excluding juveniles) is closer to unity if males mature earlier than females, but this ratio is not possible to assess because male maturation has not yet been examined for this species. The difference between the sex ratio reported in this study and that by Newman et al. (2000) might be due to variation in mating systems across a cross-shelf density gradient (Newman and Williams, 1996). Alternatively, the sampling by traps and line fishing conducted by Newman et al. (2000) could be more heavily biased toward males than the sampling by spear fishing used in the present study because of larger size, wider gape, or more aggressive behavior toward bait among males (Cappo and Brown, 1996). Furthermore, it is likely that a female-biased sex ratio as observed at the

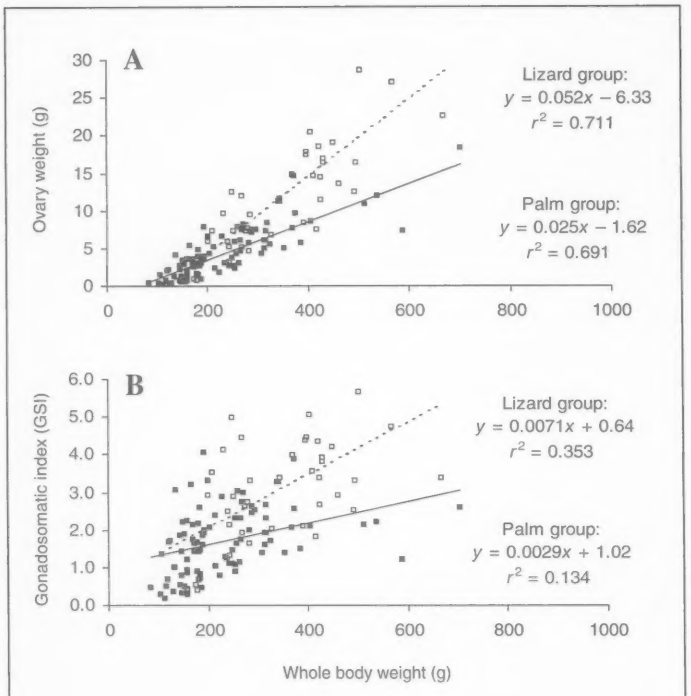

Figure 9

Fixed ovary weight (**A**) and gonadosomatic index (**B**) at fresh whole body weight for mature female *Lutjanus carponotatus* at ovarian stage IV (see Table 1) collected during peak spawning months (Oct–Dec) at the Palm (■, solid lines) and Lizard (□, dashed lines) island groups.

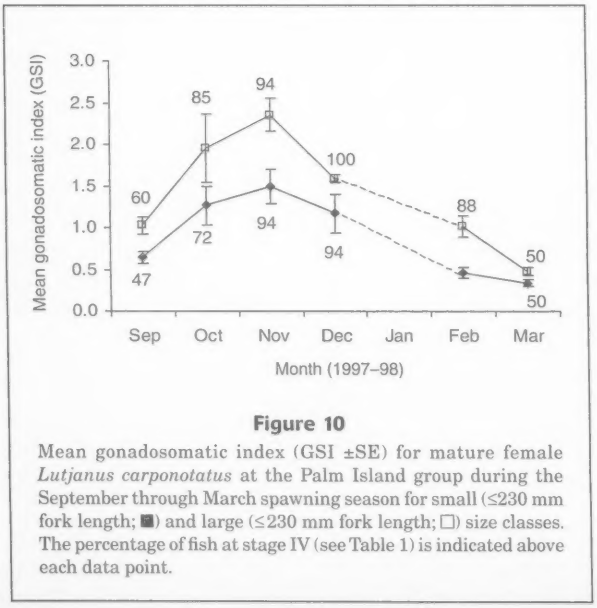

Figure 10

Mean gonadosomatic index (GSI ±SE) for mature female *Lutjanus carponotatus* at the Palm Island group during the September through March spawning season for small (≤230 mm fork length; ■) and large (≤230 mm fork length; □) size classes. The percentage of fish at stage IV (see Table 1) is indicated above each data point.

Palm Island group is not a prevalent feature of *L. carponotatus* populations. Rather, the strong statistical suggestion of a sex ratio quite different from unity might be due to the fact that sex ratios often show temporal variability (e.g. Stergiou et al., 1996) coupled with the propensity to achieve statistically significant differences when using large sample sizes (Johnson, 1999).

Maturation schedules and sex-specific growth differences were consistent between the island groups, but overall growth patterns differed, with Lizard Island group fish reaching larger asymptotic body sizes. Given the vast distance between the island groups, these differences might be due to inherent genetic differences between the populations. Or, effects of temperature (the Palm Island group sits at a higher latitude), turbidity, freshwater run-off (the Palm Island group sits closer to a river mouth and has more developed mangrove systems), or other environmental factors could be driving the differences. Of course, these possibilities are not mutually exclusive.

The larger ovaries observed among Lizard Island females might be due to further spatial differences or might be an effect of timing of sampling. The temporal resolution of sampling aimed to identify the extent of the spawning season but was too coarse to account for intramonth differences in ovarian development. Large changes in ovary size might occur within stage IV, and the final progression to immediate prespawning stages can be rapid (e.g. Davis and West, 1993). The Lizard Island group sample was collected from 17 to 23 October 1998, whereas the corresponding Palm Island group sample was collected from 11 to 12 October 1998. The October 1998 new moon was on the 20th, and *P. leopardus*, the only GBR species for which lunar spawning patterns have been reported, spawns primarily around the new moon (Samoilys, 1997). If *L. carponotatus* spawning is also centered around the new moon, the spatial differences in ovary weight at body weight might be due to more advanced development toward full hydration within the Lizard Island group sample. In fact, the higher proportion of stage-IV ovaries within the October Lizard Island group sample (96%) compared with the October Palm Island group sample (78%), coupled with the higher relative ovary weights at the Lizard Island group in October, can be taken as preliminary evidence that *L. carponotatus* spawns at the new moon.

Comparison with other reef fishes

The growth differences between male and female *L. carponotatus* contrast with a general trend of larger body sizes among female lutjanids observed in Atlan-

tic, Caribbean, and Hawaiian species (Grimes, 1987). However, the pattern observed in the present study seems common in the Indo-Pacific where males frequently (Davis and West, 1992; McPherson and Squire, 1992; Newman et al., 1996, 2000), but not universally (Hilomen, 1997), are the larger sex. As noted above, these differences are consistent with predictions based on energetic costs of producing sperm and eggs.

Lutjanus carponotatus spawning patterns identified by using both GSI and ovarian stage frequencies show pronounced seasonal differences: there are at least five months of very limited or no spawning activity from April through August. This finding supports Grimes's (1987) observation that continental lutjanid populations tend to have more restricted spawning seasons than populations associated with oceanic islands, which spawn more or less continuously throughout the year. Although seasonal patterns exist, the prominence of ripe gonads over seven months from September through March suggests an extended spawning season and supports the general observation that tropical reef fishes spawn over longer periods within the year than do cooler water species (Lowe-McConnell, 1979). However, a study with finer temporal resolution is needed to verify that spawning actually occurs in months with a high proportion of stage-IV ovaries.

Female *L. carponotatus* mature on average at approximately 75% of their mean asymptotic size, 54% of their maximum observed size, and 11% of their maximum longevity. The relative size at maturity contrasts with Grimes's (1987) observations that shallow-water continental lutjanid populations like those of *L. carponotatus* on the GBR typically mature at smaller relative sizes (≈42% maximum size) compared to deep-water populations associated with oceanic islands (≈50% maximum size). Two sympatric shallow-water species, *L. russelli* (Sheaves, 1995) and *L. fulviflamma* (Hilomen, 1997), likewise contrast with the general familial trend and mature at approximately 50% and 75% of their maximum size, respectively. Hence, a general pattern of relative size at maturity might exist among shallow-water lutjanids in the GBR region that is different from those regions covered by Grimes's (1987) review. Lutjanids on the GBR are generally lightly fished (Mapstone et al.[1]); therefore the geographic difference in sizes at maturity might be due to fishing pressure selecting for smaller sizes at maturity in other regions.

The relative age at maturity of *L. carponotatus* cannot be as readily placed in a broader familial context given that ages at maturity were not widely estimated for lutjanids at the time of Grimes's (1987) review. However, an array of published studies suggests that many tropical and subtropical demersal fishes share the absolute, but not relative, ages of *L. carponotatus* at 50% and 100% maturity at 2 and 4 years, respectively. These include other small gonochores on the GBR (Sheaves, 1995; Hart and Russ, 1996; Hilomen, 1997), as well as a range of gonochores in other regions (Grimes and Huntsman, 1980; Davis and West, 1993; Ross et al., 1995) and hermaphrodites on the GBR and elsewhere (Ferreira, 1993, 1995; Bullock and Murphy, 1994). The ubiquity of this maturity schedule, despite a wide array of maximum body sizes (160–1200 mm) and longevities (6–56 years) among these species, perhaps suggests a common physiological threshold toward which many species gravitate in order to maximize lifetime reproductive success. More comprehensive analysis of life history trade-offs (e.g. Roff, 1992) is needed to test this hypothesis.

Fisheries management

Harvest of *L. carponotatus* is currently restricted to fish greater than 250 mm total length (approximately 233 mm FL) with the aim of allowing 50% of fish to spawn at least once, and this regulation is proposed to remain after revision by the GBR fishery management plan (Queensland Fisheries Management Authority[3]). The estimated size at 50% maturity of 190 mm FL suggests that the regulation is meeting its objective. However, the objective itself might not adequately protect the reproductive potential of *L. carponotatus* and similar species if individuals require multiple spawning years to ensure sufficient replenishment of the stock. The extensive longevities of many reef fishes have been hypothesized to be a mechanism for coping with low and irregular recruitment rates through a process dubbed the "storage effect" (Warner and Chesson, 1985). The rationale behind the storage effect hypothesis is that fish must reproduce during many breeding seasons in order to endure poor recruitment years and realize high reproductive success during the unpredictable and intermittent good recruitment years. If this process is important for population dynamics of *L. carponotatus* and other species, management will need to protect an intact natural population structure in some areas within the fishery. Protecting older age classes cannot be achieved by using maximum size limits for species like *L. carponotatus* that have a pronounced asymptote in the growth trajectory because body sizes are similar over a broad range of age classes and size is therefore poorly correlated with age. Protecting natural age structure could be accomplished through a system of strategically designed marine protected areas that allow some populations to experience natural survival free of fishing mortality.

Proposed closures of the GBR line fishery during nine-day periods around the new moon in October, November, and December are aimed at protecting spawning activity and particularly spawning aggregations of *P. leopardus* and other harvested species (Queensland Fisheries Management Authority[3]). *Lutjanus carponotatus* shares a peak spawning period during these months with *P. leopardus* (Ferreira, 1995; Samoilys 1997) and several other sympatric exploited species (McPherson et al., 1992; Sheaves, 1995; Hilomen, 1997; Brown et al.[5]). In addition, the larger ovaries of the Lizard Island group fish, which were collected closer to the new moon, may indicate that, like *P. leopardus* (Samoilys, 1997), *L. carponotatus* spawns at

[5] Brown, I. W., P. J. Doherty, B. Ferreira, C. Keenan, G. McPherson, G. Russ, M. Samoilys, and W. Sumpton. 1994. Growth, reproduction and recruitment of Great Barrier Reef food fish stocks. Final report to the Fisheries Research and Development Corporation, FRDC Project 90/18, Queensland Department of Primary Industries, 154 p. Southern Fisheries Centre, GPO Box 76, Deception Bay, Queensland 4508, Australia.

the new moon. Therefore, the timing of the proposed spawning closures seems appropriate. However, it is not known whether *L. carponotatus* aggregate to spawn; therefore the goal of protecting spawning aggregations might not be relevant for this species. In fact, the prevalence and ecological importance of spawning aggregations for any species on the GBR is largely unknown; therefore the efficacy of the proposed closures is difficult to predict.

Beyond the implications for management regulations, these data have implications for modeling *L. carponotatus* stock dynamics. In particular, the results suggest that reproductive output by a unit of *L. carponotatus* biomass cannot be predicted on the basis of that biomass alone. Relative ovary weight increases slightly with increasing body size and there is evidence that larger fish spawn more frequently. The greatest difference in the proportion of ripe ovaries between size classes occurred in February 1998 after severe flooding in January. It is possible that the lower proportion of ripe ovaries among small fish in February was due to stresses caused by changes in salinity or increased run-off and is not a regular trait. However, increased resilience to environmental stresses that allows more frequent spawning would also increase the relative reproductive success of large fish. Therefore, a population comprising fewer larger fish is likely to show greater annual egg production than a population with equivalent biomass that comprises more numerous but smaller fish. Additionally, the sex-specific patterns reported in this study further suggest gross biomass might be an inadequate index of replenishment potential and that female biomass needs to be considered. Therefore, stock structure, in terms of sex ratio and the frequency of size classes, and not simply overall biomass needs to be considered when predicting reproductive potential.

Acknowledgments

I thank the numerous assistants who participated in fieldwork, as well as Sam Adams and Sue Reilly for assistance with histological examinations. The manuscript was greatly improved by comments from Howard Choat, Carl Walters, Tony Fowler, Campbell Davies, Sam Adams, Bruce Mapstone, an anonymous thesis examiner, and two anonymous reviewers. This work was conducted while the author was supported by an international postgraduate research scholarship from the Commonwealth of Australia and a postgraduate stipend from the CRC Reef Research Centre. Final preparation of the manuscript took place while the author was supported by a postdoctoral fellowship funded jointly by the University of Windsor and the Canadian National Science and Engineering Research Council (collaborative research opportunity grant no. 227965-00) to Peter Sale and others).

Literature cited

Adams, S., B. D. Mapstone, G. R. Russ, and C. R. Davies.
2000. Geographic variation in the sex ratio, sex specific size, and age structure of *Plectropomus leopardus* (Serranidae) between reefs open and closed to fishing on the Great Barrier Reef. Can. J. Fish. Aquatic Sci. 57: 1448–1458.

Bullock, L. H., and M. D. Murphy.
1994. Aspects of the life history of the yellowmouth grouper, *Mycteroperca interstitialis*, in the eastern Gulf of Mexico. Bull. Mar. Sci. 55:30–45.

Cappo, M., and I. W. Brown.
1996. Evaluation of sampling methods for reef fish of commercial and recreational interest. CRC Reef Research Centre Technical Report 6, 72 p.

Cappo, M., P. Eden, S. J. Newman, and S. Robertson.
2000. A new approach to validation of periodicity and timing of opaque zone formation in the otoliths of eleven species of *Lutjanus* from the central Great Barrier Reef. Fish. Bull. 98:474–488.

Connell, S. D.
1998. Patterns of piscivory by resident predatory reef fish at One Tree Reef, Great Barrier Reef. Mar. Freshw. Res. 49:25–30.

Dalzell, P.
1996. Catch rates, selectivity and yields of reef fishing. *In* Reef fisheries (N. V. C. Polunin and C. M. Roberts, eds.), p. 161–192. Chapman and Hall, London.

Davies, C. R.
1995. Patterns of movement of three species of coral reef fish on the Great Barrier Reef. Ph.D. diss, 212 p. James Cook University, Queensland, Australia.

Davis, T. L. O., and G. J. West.
1992. Growth and mortality of *Lutjanus vittus* (Quoy and Gaimard) from the North West Shelf of Australia. Fish. Bull. 90:395–404.
1993. Maturation, reproductive seasonality, fecundity, and spawning frequency in *Lutjanus vittus* (Quoy and Gaimard) from the North West Shelf of Australia. Fish. Bull. 91: 224–236.

Day, T., and P. D. Taylor.
1997. Von Bertalanffy's growth equation should not be used to model age and size at maturity. Am. Nat. 149: 381–393.

Everhart, W. H., and W. D. Youngs.
1981. Principles of fishery science, 349 p. Cornell Univ. Press, Ithaca, NY.

Ferreira, B. P.
1993. Reproduction of the inshore coral trout *Plectropomus maculatus* (Perciformes: Serranidae) from the central Great Barrier Reef, Australia. J. Fish Biol. 42:831–844.
1995. Reproduction of the common coral trout *Plectropomus leopardus* (Serranidae: Epinephelinae) from the central and northern Great Barrier Reef, Australia. Bull. Mar. Sci. 56: 653–669.

Ferreira, B. P., and G. R. Russ
1994. Age validation and estimation of growth rate of the coral trout, *Plectropomus leopardus*, (Lacepede 1802) from Lizard Island, northern Great Barrier Reef. Fish. Bull. 92:46–57.

Fishelson, L., W. L. Montgomery, and A. A. Myrberg.
1985. A new fat body associated with the gonad of surgeonfishes (Acanthuridae: Teleostei). Mar. Biol. 86:109–112.

Grimes, C. B.
1987. Reproductive biology of the Lutjanidae: a review. *In* Tropical snappers and groupers: biology and fisheries management (J. Polovina and S. Ralston., eds.), p. 239–294. Westview Press, London.

Grimes, C. B., and G. R. Huntsman.
1980. Reproductive biology of the vermilion snapper,

Rhomboplites aurorubens, from North Carolina and South Carolina. Fish. Bull. 78:137–146.

Guillemot, P. J., R. J. Larson, and W. H. Lenarz.
1985. Seasonal cycles of fat and gonad volume in five species of northern California rockfish (Scorpaenidae: *Sebastes*). Fish. Bull. 83:299–311.

Ha, P. Y., and R. A. Kinzie.
1996. Reproductive biology of *Awaous guamensis*, an amphidromous Hawaiian goby. Environ. Biol. Fish. 45:383–396.

Hart, A. M. and G. R. Russ.
1996. Response of herbivorous fishes to crown-of-thorns *Acanthaster planci* outbreaks. III. Age, growth, mortality and maturity indices of *Acanthurus nigrofuscus*. Mar. Ecol. Prog. Ser. 136:25–35.

Higgs, J. B.
1993. A descriptive analysis of records of the recreational reef-line fishery on the Great Barrier Reef. M.Sc. thesis, 128 p. James Cook Univ., Queensland, Australia.

Hilborn, R., and C. J. Walters.
1992. Quantitative fisheries stock assessment: choice, dynamics and uncertainty, 570 p. Kluwer Academic, Boston, MA.

Hilomen, V. V.
1997. Inter- and intra-habitat movement patterns and population dynamics of small reef fishes of commercial and recreational significance. Ph.D. diss., 277 p. James Cook Univ., Queensland, Australia.

Hoenig, J. M.
1983. Empirical use of longevity data to estimate mortality rates. Fish. Bull. 82:898–902.

Johnson, D. H.
1999. The insignificance of statistical significance testing. J. Wildlife Manag. 63:763–772.

Kimura, D. K.
1980. Likelihood methods for the von Bertalanffy growth curve. Fish. Bull. 77:765–776.

Kritzer, J. P.
2002. Variation in the population biology of stripey bass *Lutjanus carponotatus* within and between two island groups on the Great Barrier Reef. Mar. Ecol. Prog. Ser. 243:191–207.
2003. Biology and management of small snappers on the Great Barrier Reef. *In* Bridging the gap: a workshop linking student research with fisheries stakeholders (A. J. Williams, D. J. Welch, G. Muldoon, R. Marriott, J. P. Kritzer, and S. Adams eds.), p. 62–80. CRC Reef Research Centre, Townsville, Queensland, Australia.

Kritzer, J. P., C. R. Davies, and B. D. Mapstone
2001. Characterizing fish populations: effects of sample size and population structure on the precision of demographic parameter estimates. Can. J. Fish. Aquat. Sci. 58: 1557–1568.

Lobel, P. S.
1989. Ocean current variability and the spawning season of Hawaiian reef fishes. Env. Biol. Fish. 24:161–171.

Lowe-McConnell, R. H.
1979. Ecological aspects of seasonality in fishes of tropical waters. Symp. Zool. Soc. Lond. 44:219–241.

McPherson, G. R., and L. Squire
1992. Age and growth of three dominant *Lutjanus* species of the Great Barrier Reef inter-reef fishery. Asian Fish. Sci. 5:25–36.

McPherson, G.R., L. Squire, and J. O'Brien
1992. Reproduction of three dominant *Lutjanus* species of the Great Barrier Reef inter-reef fishery. Asian Fish. Sci. 5:15–24.

Murphy, M. D.
1997. Bias in Chapman-Robson and least-squares estimators of mortality rates for steady state populations. Fish. Bull. 95:863–868.

Newman, S. J., and D. M. Williams
1996. Variation in reef associated assemblages of the Lutjanidae and Lethrinidae at different distances offshore in the central Great Barrier Reef. Environ. Biol. Fish. 46: 123–138.

Newman, S. J., D. M. Williams, and G. R. Russ
1996. Age validation, growth and mortality rates of the tropical snappers (Pisces: Lutjanidae) *Lutjanus adetii* (Castelnau, 1873) and *L. quinquelineatus* (Bloch, 1790) from the central Great Barrier Reef, Australia. Mar. Freshw. Res. 47:575–584.
1997. Patterns of zonation of assemblages of the Lutjanidae, Lethrinidae and Serranidae (Epinephilinae) within and among mid-shelf and outer-shelf reefs in the central Great Barrier Reef. Mar. Freshw. Res. 48:119–128.

Newman, S. J., M. Cappo, and D. M. Williams
2000. Age, growth and mortality of the stripey, *Lutjanus carponotatus* (Richardson) and the brown-stripe snapper, *L. vitta* (Quoy and Gaimard) from the central Great Barrier Reef, Australia. Fish. Res. 48:263–275.

Ricker, W. E.
1975. Computation and interpretation of biological statistics of fish populations, 382 p. Bull. Fish. Res. Board Can. 191.

Roff, D.A.
1992. The evolution of life histories, 535 p. Chapman and Hall, New York, NY.

Ross, J. L., T. M. Stevens, and D. S. Vaughan
1995. Age, growth, mortality, and reproductive biology of red drums in North Carolina waters. Trans. Am. Fish. Soc. 124:37–54.

Samoilys, M. A.
1997. Periodicity of spawning aggregations of coral trout *Plectropomus leopardus* (Pisces: Serranidae) on the northern Great Barrier Reef. Mar. Ecol. Prog. Ser. 160: 149–159.

Samoilys, M. A., and A. Roelofs.
2000. Defining the reproductive biology of a large serranid, *Plectropomus leopardus*. CRC Reef Research Centre Technical Report 31, 36 p.

Sheaves, M.
1995. Large lutjanid and serranid fishes in tropical estuaries: are they adults or juveniles? Mar. Ecol. Prog. Ser. 129: 31–40.

Stergiou, K. I., P. Economidis, and A. Sinis.
1996. Sex ratio, spawning season and size at maturity of red bandfish in the western Aegean Sea. J. Fish. Biol. 49: 561–572.

Warner, R. R., and P. L. Chesson.
1985. Coexistence mediated by recruitment fluctuations: a field guide to the storage effect. Am. Nat. 125:769–787.

West, G.
1990. Methods of assessing ovarian development in fishes: a review. Aust. J. Mar. Freshw. Res. 41:199–222.

Wootton, R. J.
1985. Energetics of reproduction. *In* Fish energetics: new perspectives (P. Tytler and P. Calow, eds.), p. 231–254. Croom Helm, London.

Examination of the foraging habits of Pacific harbor seal (*Phoca vitulina richardsi*) to describe their use of the Umpqua River, Oregon, and their predation on salmonids

Anthony J. Orr
Adria S. Banks
Steve Mellman
Harriet R. Huber
Robert L. DeLong
National Marine Mammal Laboratory
Alaska Fisheries Science Center, NMFS, NOAA
7600 Sand Point Way NE
Seattle, Washington 98115
E-mail address (for A. J. Orr, contact author): tony.orr@noaa.gov

Robin F. Brown
Oregon Department of Fish and Wildlife
2040 S. E. Marine Science Drive
Newport, Oregon 97365

Abstract—The increase in harbor seal (*Phoca vitulina richardsi*) abundance, concurrent with the decrease in salmonid (*Oncorhynchus* spp.) and other fish stocks, raises concerns about the potential negative impact of seals on fish populations. Although harbor seals are found in rivers and estuaries, their presence is not necessarily indicative of exclusive or predominant feeding in these systems. We examined the diet of harbor seals in the Umpqua River, Oregon, during 1997 and 1998 to indirectly assess whether or not they were feeding in the river. Fish otoliths and other skeletal structures were recovered from 651 scats and used to identify seal prey. The use of all diagnostic prey structures, rather than just otoliths, increased our estimates of the number of taxa, the minimum number of individuals and percent frequency of occurrence (%FO) of prey consumed. The %FO indicated that the most common prey were pleuronectids, Pacific hake (*Merluccius productus*), Pacific staghorn sculpin (*Leptocottus armatus*), osmerids, and shiner surfperch (*Cymatogaster aggregata*). The majority (76%) of prey were fish that inhabit marine waters exclusively and fish found in marine and estuarine areas (e.g. anadromous spp.) which would indicate that seals forage predominantly at sea and use the estuary for resting and opportunistic feeding. Salmonid remains were encountered in 39 samples (6%); two samples contained identifiable otoliths, which were determined to be from chinook salmon (*O. tshawytscha*). Because of the complex salmonid composition in the Umpqua River, we used molecular genetic techniques on salmonid bones retrieved from scat to discern species that were rare from those that were abundant. Of the 37 scats with salmonid bones but no otoliths, bones were identified genetically as chinook or coho (*O. kisutch*) salmon, or steelhead trout (*O. mykiss*) in 90% of the samples.

Manuscript approved for publication 9 October 2003 by Scientific Editor.
Manuscript received 20 October 2003 at NMFS Scientific Publications Office.
Fish. Bull. 102:108–117 (2004).

The Pacific harbor seal (*Phoca vitulina richardsi*) is found along the west coast of North America from the Aleutian Islands, Alaska, to the San Roque Islands, Baja California (King, 1983; Reeves et al., 1992). Before the passage of the Marine Mammal Protection Act (MMPA) of 1972, harbor seals in Oregon were kept at relatively low numbers (fewer than 500 animals in 1968) because of bounties offered by the state and harassment from commercial and sport fishermen (Pearson and Verts, 1970). Since passage of protective legislation, harbor seals in Oregon have increased an average of 6% to 7% annually between 1978 and 1998, although, in recent years, numbers appear to be leveling at about 8000 individuals (Brown and Kohlmann, 1998).

The rapid increase in harbor seal numbers has revived fishery-managers' interest in seal diet because of the potential for increased consumption of commercial fish species. In addition, there has been a heightened concern about greater harbor seal abundance in rivers and estuaries during migrations of depressed salmonid populations because of the potential negative impact on the recovery of these fishes (NMFS, 1997). Because of the tenuous status of many salmonid (*Oncorhynchus* spp.) species along the west coast, the National Marine Fisheries Service (NMFS) recommended that the United States Congress modify the MMPA to allow lethal removal of seals from river mouths where they may prey on depressed salmonid populations (NMFS, 1997). Predation of salmonids by harbor seals in Oregon has been documented (Brown, 1980; Harvey, 1987; Brown et al., 1995; Riemer and Brown, 1997; Beach et al.[1]). The proportion of salmonids in the diet of harbor seals varied from 1% to 30% depending on area, season, and sampling method (NMFS, 1997).

Pinniped prey consumption can be determined from direct observations in some systems, if prey is consumed at

[1] Beach, R., A. Geiger, S. Jefferies, S. Treacy, and B. Troutman. 1985. Marine mammals and their interactions with fisheries of the Columbia River and adjacent waters, 1980–1982. NWAFC (Northwest Alaska Fisheries Science Center) processed rep. NWAFC 85-04, 316 p. NWAFC, National Marine Fisheries Service, Seattle, WA, 98115.

the surface (Bigg et al., 1990); however, consumption is typically determined by examining scat (fecal) samples. In the past, species-specific sagittal otoliths found in scats were used exclusively to determine the identification of prey taxa. However, because otoliths can be partially or completely digested, or are not present in scats (because the head of the prey was not consumed), they are not always an adequate representation of diet. Recently, investigators have begun to use additional structures (e.g. cranial elements, vertebrae) recovered from scats to identify prey (e.g. Olesiuk et al., 1990; Cottrell et al., 1996; Riemer and Brown, 1997; Browne et al., 2002; Lance et al.[2]). These structures usually are more common than otoliths and frequently can be identified to species; however, bones of some species can be identified to family only (e.g. salmonids). Consequently, the National Marine Mammal Laboratory (NMML) collaborated with the Conservation Biology Molecular Genetics Laboratory (CBMGL; Northwest Fisheries Science Center, Seattle, WA) to develop molecular genetic identification of salmonid species (Purcell et al., 2004). Because of the complex salmonid species composition in the Umpqua River, genetic identification was vital to distinguish species that were rare from those that were abundant.

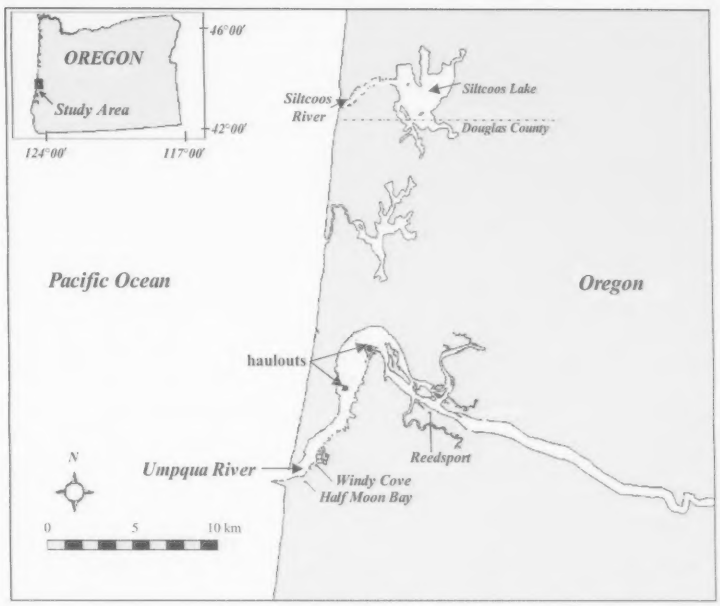

Figure 1

Map of the lower section of the Umpqua River, Oregon, where scat samples were collected at two haulout sites during 1997 and 1998.

The original impetus of this study was to assess the impact of harbor seal predation on the recovery of the Umpqua River sea-run cutthroat trout (*O. clarkii*) that were listed as endangered under the Endangered Species Act (ESA) during 1996 (Johnson et al., 1999). Umpqua River cutthroat trout were removed from the ESA in 2000 because they were identified to be part of the larger Oregon Coast evolutionary significant unit (U.S. Fish and Wildlife Service, 2000). The present study was continued despite the "delisting" of cutthroat trout because the Umpqua is inhabited year-round by harbor seals that haul out several kilometers upriver and is, thus, ideal for determining whether the presence of a pinniped species within a system is indicative of substantial feeding on fish species of concern within that environment. In addition, the Umpqua River contains several other salmonid species whose status is precarious (NMFS, 1997). Therefore, the development of genetic identification techniques was considered valuable for this system, as well as for future foraging studies in which species-specific identification may be desirable but impossible by way of conventional identification methods.

The objectives of this study were 1) to determine by an examination of diet if harbor seals that haul out in the Umpqua River feed primarily in the river or elsewhere, and 2) to apply genetic techniques to identify salmonid prey species.

Materials and methods

Study area

The Umpqua River, located in southern Oregon (Fig. 1), is a natal river for sea-run cutthroat trout, as well as chinook (*O. tshawytscha*), coho (*O. kisutch*) salmon, and steelhead trout (*O. mykiss*). The Umpqua estuary is also inhabited year-round by approximately 600–1000 harbor seals and has been designated as an area where pinnipeds and salmonids significantly co-occur (NMFS, 1997). Scat samples for this study were collected from two haulouts located within 4.8 km of the river's mouth and within 1.6 km of each other (Fig. 1).

Scat collection and analysis

Samples were collected during two seasons: "spring" (March through June) and "fall" (August to December). "Spring" corresponded to the migration of anadromous cutthroat trout adults and some juveniles to the ocean and "fall" coincided approximately with the freshwater return of spawning anadromous adults. The migratory and spawn-

[2] Lance, M., A. Orr, S. Riemer, M. Weise, and J. Laake. 2001. Pinniped food habits and prey identification techniques protocol. AFSC Proc. Rep. 2001-04, 36 p. AFSC, NMFS, NOAA, 7600 Sand Point Way NE, Seattle, WA 98115.

Table 1

Collection dates of harbor seal scats and numbers of scats with identifiable prey remains, without identifiable remains, and without remains from the Umpqua River, Oregon, during 1997 and 1998. Fall and spring periods correspond to timing of cutthroat trout runs on the Umpqua River.

Collection dates	With identifiable remains	Without identifiable remains	Without remains	Total
Fall, 1997				
16–23 Sep	26	1	2	29
27 Sep–6 Oct	5	0	3	8
12–24 Oct	31	0	7	38
31 Oct–10 Nov	21	0	6	27
12–25 Nov	36	0	10	46
Total	119	1	28	148
Spring 1998				
24–25 Mar	27	5	2	34
13–15 Apr	59	5	7	71
26–27 Apr	45	4	4	53
13–14 May	41	0	4	45
27–28 May	12	0	1	13
11–12 Jun	35	2	1	38
Total	219	16	19	254
Fall 1998				
5–6 Aug	142	1	1	144
19–20 Aug	111	1	3	115
6–9 Sep	28	3	3	34
19–21 Sep	13	0	0	13
7–8 Oct	19	0	1	20
Total	313	5	8	326

ing periods of chinook and coho salmon, and steelhead trout also occur during these times.

During fall 1997, all harbor seal scats present at the haulouts were collected every other day during the daytime low tide, weather permitting (Table 1). In 1998, biweekly attempts were made to pick a minimum of 50 scats during low tides at the haulout sites (Table 1). Scats were collected, placed in individual plastic bags, and frozen for later processing. At the laboratory samples were thawed and rinsed in nested sieves (1.0 mm, 0.71 mm, and 0.5 mm in 1997; 1.4 mm, 1.0 mm, and 0.5 mm in 1998). Fish structures were dried and stored in glass vials and cephalopod remains were stored in vials with 70% isopropyl or ethyl alcohol.

Prey were identified to the lowest possible taxon by using sagittal otoliths, skeletal, and cartilaginous remains from fish and beaks and statoliths from cephalopods. Other invertebrate remains were discarded from analysis because of the uncertainty of identifying them as primary or secondary prey. Unknown prey were categorized as "unidentified" and "unidentifiable" (Browne et al., 2002). Items that were categorized as "unidentifiable" were excluded from analyses because they could not be distinguished from prey already identified in the sample. Otoliths, beaks, and diagnostic bones were identified by using an extensive reference collection at the NMML and voucher samples verified by Pacific Identifications (Victoria, British Columbia).

After identification, otoliths were separated by side (left, right, or unknown) and enumerated to determine minimum number of specific prey. Unique diagnostic structures (e.g. quadrates, angulars, basioccipitals, vomers) were used for identification and enumeration of fish. Non-unique skeletal structures such as gillrakers and teeth were used to identify but not enumerate taxa (i.e. their presence indicated only a single individual) unless the structures were from different size classes. Vertebrae were treated like other non-unique structures; however, for salmon, if the number of vertebrae reflected more than one individual, then they were used for enumeration. Cephalopod beaks were separated by side (upper, lower, or unknown) and enumerated to determine number of prey.

To discern where harbor seals were feeding, identified prey were categorized as those exclusively found in rivers or estuaries (e.g. gobiids, cyprinids), those found exclusively in marine waters (e.g. gadids, myxinids), and those that could potentially be found in either environment (e.g. anadromous species, osmerids, petromyzontids) by using Eschmeyer et al. (1983). A seal was considered to feed in the river-estuary system if all the prey taxa identified in the scat were definitely or could potentially be found in the system. For example, a sample containing remains of peamouth chub (*Mylocheilus caurinus*), threespine stickleback (*Gasterosteus aculeatus*), river lamprey (*Lampetra ayresii*), and chinook salmon would be classified as a riverine-

estuarine species because these prey items could feasibly be consumed in the river. It was assumed that the seal was feeding in the marine environment if a sample contained exclusively marine prey, such as Pacific hagfish (*Eptatretus stoutti*), Pacific hake (*Merluccius productus*), and rockfish (*Sebastes* spp.). If a scat comprised prey taxa that potentially could be found in a riverine-estuarine system or marine waters (e.g. salmonids, osmerids), as well as those found exclusively in marine waters, then it was assumed that the feeding environment was marine or mixed.

Salmonid skeletal remains were sent to the CBMGL for species identification. Remains to be analyzed genetically were selected by number or size (or both) to represent different species or individuals present in each scat. For example, if a scat had 95 approximately equal-size vertebrae (a salmonid has approximately 65 vertebrae; Butler, 1990), then at least two vertebrae (potentially representing at least two individuals) were sent for genetic identification. Also, if a sample had a very large gillraker and three small vertebrae, then the gillraker and one vertebra were sent for genetic identification. The size of diagnostic structures was also used to categorize salmon remains as juvenile or adult, when possible. The CBMGL identified salmonid species by direct sequencing of mitochondrial DNA or analysis of restriction fragment length polymorphism (Purcell et al., 2004).

The abundance of prey taxa in harbor seal diet for each period was described by using the minimum number of individuals (MNI) and percent frequency of occurrence (%FO). We compared the effect of including bone on the number of prey consumed by estimating MNI using the greater number of right or left otoliths and then again using all diagnostic skeletal remains. Cephalopod MNI was estimated from the greater number of upper or lower beaks. The %FO of prey taxon i was defined as

$$\%FO_i = \frac{\sum_{k=1}^{s} O_{ik}}{s} \times 100,$$

where O_{ik} = absence (0) or presence (1) of taxon i in scat k; and

s = the total number of scats that contained identifiable prey remains.

The presence of taxon i in scat k was determined by using otoliths and then again using all structures. To account for variability in diet, point estimates of %FO for a prey taxon were determined during each sampling period and then averaged for each season.

Results

Scats

Over 725 scats were collected during all periods. The number of scats collected with identifiable remains was 119 (99%; n=148) in fall 1997, 219 (93%; n=254) in spring 1998, and 313 (98%; n=326) in fall 1998 (Table 1). Of the 651 samples with identifiable prey remains, 605 (93%) contained fish bones, 347 (53%) had fish otoliths, 231 (36%) contained remains from cartilaginous fish, and 41 (6%) had cephalopod beaks. A majority (65% fall 1997, 65% spring 1998, 63% fall 1998) of scats with identifiable remains had one to three prey taxa present and less than 4% contained more than ten taxa. Approximately 40 prey taxa, representing at least 25 families, were identified throughout the study (Tables 2 and 3).

For nearly all prey taxa, MNI was greater when all skeletal remains were identified than when otoliths were used exclusively (Table 2). For several species, such as Pacific hake, Pacific herring (*Clupea pallasii*), and Pacific sardine (*Sardinops sagax*), MNI at least tripled when all structures were used for enumeration (Table 2). For most salmonids, cartilaginous fishes, three-spine stickleback, Irish lords (*Hemilepidotus* spp.), and Pacific mackerel (*Scomber japonicus*), no otoliths were recovered; therefore other skeletal elements had to be used for identification (Table 2). For a few prey, such as cyprinids, gobiids, and butter sole (*Isopsetta isolepis*), only otoliths were recovered (Table 2).

Foraging habits

The %FO for most prey taxa was greater when all structures were used than when just otoliths were used (Table 3). The %FO indicated that the prey most frequently consumed were pleuronectids, Pacific hake, Pacific staghorn sculpin (*Leptocottus armatus*), osmerids, and shiner surfperch (*Cymatogaster aggregata*). Prey frequently found in scats included those that were exclusively marine (e.g. Pacific hake, rex sole (*Glyptocephalus zachirus*), English sole (*Parophrys vetulus*), and myxinids), and those that occur in both marine and estuarine waters (e.g. Pacific staghorn sculpin, and shiner surfperch [Table 3]). Only 24% of scats were composed entirely of prey taxa that could be found in riverine-estuarine systems (Fig. 2). Consequently, a majority of the scats contained prey species that were exclusively marine ($\bar{x}$=25.3%) or were a mixture of marine and potentially marine species ($\bar{x}$=50.8%; Fig. 2).

Salmonids

Salmonid remains were found in only 6% (39/651) of the samples. Five chinook smolts were identified from otoliths in two samples collected during fall 1997; in the remaining 37 samples, salmonid bones were unidentifiable to species with conventional techniques. With the cooperation of CBMGL, we examined 116 salmonid bones using molecular genetic techniques. Species identification was successful for 67% (78/116) of the bones and teeth from 90% (35/39) of the scat samples that contained salmonid structures. In the four samples that remained unidentified, three contained only a single salmonid bone that failed to produce any DNA. Most of the other bones where DNA could not be extracted were small or fragmented and highly digested. Seventeen of the samples contained chinook salmon bones (including the two samples with chinook salmon otoliths); 11 contained coho salmon bones, four contained steelhead trout bones, and three contained bones from two salmonid

Table 2

Minimum number of individuals (MNI) of fish prey derived from sagittal otoliths and all structures retrieved from harbor seal scats collected at the Umpqua River during 1997 and 1998. *s* represents the number of scats with identifiable remains. na indicates taxon did not have sagittal otoliths to be used for identification.

		Fall 1997 (*s*=119)		Spring 1998 (*s*=219)		Fall 1998 (*s*=313)	
Family	Species	MNI otoliths	MNI all structures	MNI otoliths	MNI all structures	MNI otoliths	MNI all structures
Ammodytidae	Pacific sand lance	205	208	317	321	3	7
Bothidae	Pacific sanddab	12	13	9	9	1	2
Clupeidae	American shad	1	2	4	11	1	15
	Pacific herring	6	22	3	10	121	345
	Pacific sardine	0	0	50	235	39	185
Cottidae	Pacific staghorn sculpin	44	65	25	48	30	85
	unidentified cottid	0	0	0	0	0	8
Cyprinidae	peamouth chub	1	1	4	4	4	4
Embiotocidae	shiner surfperch	104	109	209	274	23	104
Engraulididae	northern anchovy	1	3	0	0	1	2
Gadidae	Pacific hake	1	35	10	44	58	199
	Pacific tomcod	9	21	19	52	8	26
Gasterosteidae	threespine stickleback	0	1	0	0	0	0
Gobiidae	unidentified gobiid	2	2	1	1	0	0
Hexagrammidae	lingcod	0	1	0	0	1	1
Myxinidae	Pacific hagfish	0	20	0	13	0	61
Ophidiidae	spotted cusk-eel	0	0	4	4	2	2
Osmeridae	unidentified osmerid	42	54	14	41	105	132
Petromyzontidae	Pacific lamprey	na	5	na	89	na	41
	river lamprey	na	2	na	1	na	0
Pholididae	saddleback gunnel	3	7	1	3	0	1
Pleuronectidae	English sole	38	41	37	39	75	84
	Dover sole	1	4	5	6	27	51
	slender sole	1	1	18	24	28	42
	butter sole	1	1	15	15	2	2
	rex sole	19	44	44	53	96	125
	petrale sole	0	0	0	0	1	1
	starry flounder	10	17	8	12	6	31
Rajidae	unidentified rajid	na	1	na	7	na	4
Scombridae	Pacific mackerel	0	2	0	3	0	2
Scorpaenidae	*Sebastes* spp.	0	15	6	19	2	3
Trichodontidae	Pacific sandfish	0	0	0	1	2	3
Zoarcidae	unidentified zoarcid	0	0	0	0	2	2
Salmonidae	coho salmon						
	unknown	0	4	0	0	0	0
	juvenile	0	1	0	4	0	2
	adult	0	0	0	1	0	3
	Steelhead or rainbow trout						
	unknown	0	0	0	2	0	2
	juvenile	0	0	0	0	0	1
	chinook salmon						
	unknown	5	6	0	0	0	3
	juvenile	0	5	0	2	0	5
	adult	0	1	0	0	0	0
	unidentified salmonid						
	unknown	0	2	0	1	0	2
	juvenile	0	1	0	0	0	1

Table 3

Mean percent frequency of occurrence (%FO) of common prey recovered from harbor seal scat samples collected at haulout sites in the Umpqua River, Oregon, during 1997 and 1998. SD indicates standard deviation.

		Fall 1997	Spring 1997	Fall 1998
Family	Species	Mean (±SD)	Mean (±SD)	Mean (±SD)
Ammodytidae	Pacific sand lance	12.5 ±8.3	12.6 ±8.3	9.1 ±8.9
Bothidae	Pacific sanddab	11.4 ±7.5	4.1 ±2.5	3.0 ±3.2
Clupeidae	American shad	4.3 ±0.6	13.0 ±2.3	5.3 ±3.1
	Pacific herring	16.9 ±13.7	7.3 ±6.9	35.9 ±21.8
	Pacific sardine	0	16.1 ±12.2	17.9 ±9.1
Cottidae	Pacific staghorn sculpin	23.9 ±8.5	21.0 ±19.0	11.8 ±4.5
	unidentified cottid	16.5 ±20.4	3.2 ±0.7	0.8 ±0.1
Cyprinidae	peamouth chub	3.8	2.3 ±0.6	2.8
Embiotocidae	shiner surfperch	18.2 ±8.2	23.6 ±19.4	7.0 ±2.9
Engraulididae	northern anchovy	5.5 ±3.2	0	2.1 ±2.0
Gadidae	Pacific hake	27.9 ±9.7	17.0 ±5.7	41.6 ±25.5
	Pacific tomcod	15.4 ±7.8	16.1 ±7.0	12.3 ±8.3
Gasterosteidae	threespine stickleback	2.8	0	0
Gobiidae	unidentified gobiid	7.7	1.7	0
Hexagrammidae	lingcod	3.8	0	0.7
Loliginidae	market squid	12.8 ±10.2	3.5 ±1.3	0
Myxinidae	Pacific hagfish	17.5 ±7.9	6.7 ±3.5	16.5 ±9.4
Octopodidae	*Octopus rubescens*	3.8 ±1.4	8.3 ±2.6	8.4 ±7.0
Ophidiidae	spotted cusk-eel	0	0	0.9
Osmeridae	unidentified osmerid	20.8 ±11.3	14.6 ±8.2	19.5 ±10.0
Petromyzontidae	Pacific lamprey	7.7 ±8.2	20.5 ±10.1	8.2 ±2.9
	river lamprey	5.6	3.7	0
Pholididae	saddleback gunnel	14.7 ±16.9	2.6 ±0.3	5.3
Pleuronectidae	English sole	21.9 ±1.7	8.7 ±5.2	17.5 ±12.0
	Dover sole	7.4 ±5.9	4.6 ±0.7	13.5 ±13.6
	slender sole	0	11.0 ±7.2	14.9 ±14.9
	butter sole	3.8	7.2 ±3.7	1.4
	rex sole	27.4 ±12.1	14.2 ±9.6	19.9 ±20.5
	petrale sole	0	0	0.7
	starry flounder	15.8 ±7.4	3.7 ±1.0	5.8 ±1.2
Rajidae	unidentified rajid	2.8	5.0 ±1.6	2.8
Scombridae	Pacific mackerel	3.8 ±1.4	4.6 ±4.0	0.8 ±0.1
Scorpaenidae	*Sebastes* spp.	15.7 ±8.3	9.1 ±2.6	2.1
Trichodontidae	Pacific sandfish	0	1.7	2.1
unidentifed bothid/ pleuronectid	unidentified flatfish	38.5 ±15.9	20.2 ±10.3	14.8 ±2.5
Zoarcidae	unidentified zoarcid	0	0	1.4
Salmonidae	coho salmon			
	unknown	5.8 ±3.6	0	0
	juvenile	4.8	3.3 ±2.3	0.7
	adult	0	2.4	6.2 ±6.2
	steelhead/rainbow trout			
	unknown	0	2.7 ±1.4	0.7
	juvenile	0	0	0.9
	adult	0	0	0.9
	chinook salmon			
	unknown	7.6 ±3.5	0	0.8 ±0.1
	juvenile	4.0 ±1.1	3.4	3.6 ±3.0
	adult	4.8	0	0
	unidentified salmonid(s)			
	unknown	4.3 ±0.6	2.4	0.8 ±0.1
	juvenile	4.8	0	7.7

species (two with coho and chinook salmon and one with coho salmon and steelhead trout, Table 2). No cutthroat trout were identified with conventional or molecular genetic techniques.

Using otoliths and other diagnostic skeletal structures, we enumerated at least 54 individual salmonids in 39 scats (Table 2). All individuals identified as adults (n=5) were coho salmon, except one chinook salmon from spring 1997. Individual juveniles identified as steelhead trout (n=1), coho salmon (n=7), chinook salmon (n=12), or unidentified salmonids (n=2) were present during all periods. Because of the difficulty of determining age from size-variable structures such as gillrakers and teeth, most individuals (n=27) were designated as "unknown age."

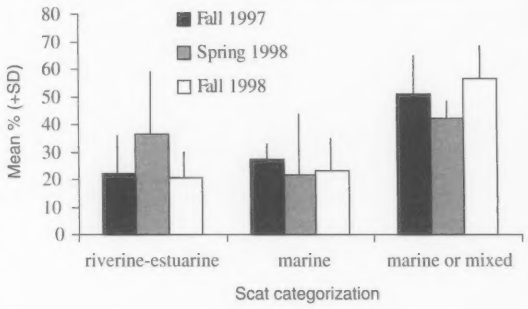

Figure 2

Mean percentage plus standard deviation (SD) of scats that were classified as "riverine-estuarine" (i.e. samples composed of prey taxa that are exclusively or potentially (e.g. anadromous species, osmerids) found in rivers or estuaries), "marine" (i.e. samples composed exclusively of prey that inhabit marine waters), and "marine or mixed" (i.e. samples composed of prey taxa exclusively found in marine waters or those that might inhabit marine waters at some stage in their life).

Discussion

Investigating diet is essential to assessing the role of harbor seals in marine and freshwater ecosystems in order to quantify their interactions with fisheries and determine their impact on the recovery of endangered species. All methods used to investigate diet of seals and other pinnipeds have some limitations (Murie and Lavigne, 1985, 1986; Harvey, 1989). With scats, it is assumed that the relative frequency of prey identified from undigested remains reflects the frequency of prey eaten (Tollit et al., 1997). However, several investigators have determined that this assumption may be seriously biased in several ways (Hawes, 1983; da Silva and Neilson, 1985; Jobling, 1987; Dellinger and Trillmich, 1988; Harvey, 1989; Pierce and Boyle, 1991; Cottrell et al., 1996; Tollit et al., 1997; Bowen, 2000; Orr and Harvey, 2001). No diet study can estimate detrimental or lethal impacts to prey resulting from harassment by pinnipeds. In addition, once a prey is captured, a seal might consume only the soft tissue (especially of larger prey), which would not leave identifiable evidence in scats. Additionally, because skeletal remains from different prey species pass through the alimentary canal and erode at different rates they may not reflect the true number or proportions of prey consumed (Hawes, 1983; Harvey, 1989; Pierce and Boyle, 1991; Cottrell et al., 1996; Tollit et al., 1997). Therefore, predation estimates determined from scat samples should be regarded as a measure of minimum impact. Although there are complications inherent in the use of scats to describe the diet of seals, scat analysis remains useful because many scats can be collected quickly, with minimum effort and without harm to the animals (Harvey, 1989).

Scats

Recently, skeletal remains other than otoliths and beaks have begun to be used to identify and enumerate prey of pinnipeds (e.g. Olesiuk et al., 1990; Cottrell et al., 1996; Riemer and Brown, 1997; Browne et al., 2002). There are constraints, however, for using all skeletal elements to identify prey species, including the need for a reference collection and the extensive training of personnel to identify digested prey structures (Cottrell et al., 1996). Moreover, there is usually a bias in the recovery and recognition of prey structures from different taxa (Cottrell et al., 1996; Laake et al., 2002). This bias may be a significant problem in estimating relative abundance of prey or biomass consumption by harbor seals and is the reason these indices were not considered in this study.

Despite these complications, the use of all available structures increased our estimates of prey diversity, MNI, and %FO for most prey taxa. Examination of all diagnostic structures also allowed us to consider a greater sample size because 93% of scats with identifiable remains contained bones, whereas only 53% of scats contained otoliths. Species not represented by otoliths, such as salmonids (during 1998) and cartilaginous fishes, were detected because all structures were used. In addition, the MNI of important prey such as Pacific hake, Pacific herring, and Pacific sardine would have been greatly underestimated had otoliths been used exclusively because the MNI derived by using all structures was at least threefold greater. Although there are complexities associated with estimating MNI from all structures, this method avoids the use of numerical correction factors determined from recovery rates of otoliths fed to captive seals during laboratory experiments (Browne et al., 2002). Results from captive experiments are highly variable between repeated trials for the same individual and among different individuals (Harvey, 1989; Bowen et al., 2000; Orr and Harvey, 2001).

Foraging habits

Harbor seals in the lower Umpqua River consumed prey from over 35 taxa; however, only a few prey taxa were dominant in their diet, as reflected by %FO. Overall, the five most abundant families of prey were Clupeidae, Cot-

tidae, Embiotocidae, Gadidae, and Pleuronectidae. These are similar to those reported in other studies of harbor seal diet in Oregon (Riemer and Brown, 1997; Browne et al., 2002; Riemer et al.[3, 4]).

It was evident by the presence of prey like Pacific hake, Pacific sardine, hagfish, and various flatfishes that seals fed offshore in pelagic and demersal areas. Harbor seals also consumed prey (e.g. Pacific staghorn sculpin) commonly found inshore or in estuarine waters. The NMFS recommendations to remove pinnipeds from systems where endangered prey also occur, rely on the assumption that pinnipeds are primarily feeding (on ESA-listed species) in that system. Our study indicated that this was not the case. Although the seals at the Umpqua hauled out several kilometers up river, they foraged primarily at sea.

Because of the life histories of many of the prey taxa, our foraging habitat categories must be considered estimations of where the prey might have been consumed. For example, we estimated that 24% of scats contained prey attributable to the riverine-estuarine environment. However, this may actually be an overestimation because some of these species potentially inhabit the marine environment at some time in their life and may have been consumed there. Additionally, scats categorized as marine or mixed may reflect that the seal fed solely in the marine environment (because all the taxa can potentially be found in marine waters) or fed at sea and within the river. Nevertheless, these categories are useful for a broad apportioning of foraging habitat. Even though we were able to determine that approximately 76% of the scats contained marine and potentially marine prey taxa, we were unable to assess whether this reflected a seal population with homogeneous or heterogeneous foraging patterns. In other words, because the scats could not be attributed to a particular individual, we had no way of discerning: 1) whether the entire seal population foraged roughly three-fourths of the time at sea and one-fourth of the time in the river, or 2) whether 76% of the seals fed at sea whereas 24% foraged closer to shore and in the river. This distinction may be important if only a subgroup of seals is feeding in the river and preying on fish that are seasonally abundant in the estuary, such as salmonids. Studies that incorporate radio- or satellite-telemetry or genetic identification of individual prey items in scats may reveal these distinctions in the future.

Because the seals haul out almost 5 km upriver and have been observed as far as 32 km upriver, it is clear that seals use the river environment. However, the prevalence of marine fish remains in the scat samples indicates that the seals that haul out at the Umpqua River do not feed exclusively in the river. The predominance of marine prey may reflect a foraging strategy in which the effort required to find marine sources of food is offset by the energy gained by exploiting large aggregations of marine schooling fish (e.g. Pacific hake and Pacific sardine). In this scenario, the seals in the Umpqua estuarine-riverine system may depend on marine resources while taking advantage of protected estuarine waters that provide a sheltered place to rest and occasionally feed.

Salmonids

We used two methods to estimate the number of salmonids eaten by harbor seals: prey remains and genetic analyses of scat samples. Analysis of skeletal remains was of limited value because the majority of salmonid structures recovered from scat samples were bones, which could be identified only to family. This study represents a novel application of genetic techniques to identify salmonid species from bones found in scats. These techniques allowed us to determine species for a majority of the salmonid samples that would have otherwise remained unidentified because they did not contain otoliths.

Salmonid bones or otoliths were found in 6% of the harbor seal scats collected during our study—a finding that is comparable to the 5% found by Laake et al. (2002) at the Columbia River. However, it is about one-half of what was found by Riemer and Brown (13%; 1997) at selected sites in Oregon. Brown et al. (1995) found salmonids in 12% of gastrointestinal tracts of harbors seals taken incidentally by commercial salmon gillnet fishing operations, and Roffe and Mate (1984) observed that salmonids made up 30% of the prey for harbor seals surface feeding in the Rogue River. Regardless of sampling method, in these studies, most of the salmonids could be identified only to family because few otoliths were recovered and genetic techniques to identify bones to species had not yet been developed.

Salmonids are present in the Umpqua River year-round although species and age composition change throughout the year. In this study, most salmonid prey of known age were juveniles; however, we could determine age of only one-half of the individuals. Juveniles are found in the Umpqua River system year-round and may be easier for seals to catch than adults. Alternatively, perhaps seals did not consume many adult skeletal elements because adult salmonids are large fish, which may be ripped apart rather than swallowed whole.

Our sampling seasons encompassed at least some portion of the migrations of all salmonids, all of which (except cutthroat trout) were prey of harbor seals. The fact that portions of all migrations were included in the sampling design was noteworthy because there were a large number of seals in the river throughout the year and yet we found no evidence through genetic or otolith identification that seals consumed cutthroat trout in the Umpqua River. The genetic identification tools developed and applied in our collaboration with CBMGL were useful in discerning

[3] Riemer, S. D., R. F. Brown, and M. I. Dhruv. 1999. Monitoring pinniped predation on salmonids in the Alsea and Rogue River estuaries: fall, 1997. *In* Pinniped predation on salmonids: preliminary reports on field investigations in Washington, Oregon, and California, p. 104–152. Compiled by National Marine Fisheries Service, Northwest Region. [Available from ODFW, 7118 NE Vandenberg Avenue, Corvallis, OR 97330.]

[4] Riemer, S. D., R. F. Brown, and M. I. Dhruv. 1999. Monitoring pinniped predation on salmonids in the Alsea and Rogue River estuaries: fall, 1998. *In* Pinniped predation on salmonids: preliminary reports on field investigations in Washington, Oregon, and California, p. 153–188. Compiled by National Marine Fisheries Service, Northwest Region. [Available from ODFW, 7118 NE Vandenberg Avenue, Corvallis, OR 97330.]

scarce from abundant salmonids. These techniques may be useful in identifying other pinniped prey that lack species-specific structures and would allow managers to better assess the impact of pinniped predation on threatened or endangered species.

Acknowledgments

This study was proposed and initiated in collaboration with Joe Scordino. Scat collection and harbor seal counts were conducted by Lawrence Lehman, Kirt Hughes, Merrill Gosho, Sharon Melin, and Robert DeLong. The U.S. Coast Guard Umpqua River Station provided boat storage and a location for keeping a chest freezer during the 1997 field season. We would like to thank the Oregon Institute of Marine Biology, Charleston, OR, where the samples collected during 1997 were processed. We greatly appreciate the collaboration with Conservation Biology Molecular Genetics Laboratory, which resulted in the identification of our salmon remains based on genetic methods. We would also like to thank Susan Reimer who kindly helped us with difficult identifications, as well as Lawrence Lehman and Jason Griffith for their verification of bone and otolith identifications. We thank Patience Browne, Patrick Gearin, John Jansen, Mark Dhruv, and three anonymous reviewers for providing helpful comments on earlier drafts of this manuscript.

Literature cited

Bigg, M. A., G. Ellis, P. Cottrell, and L. Milette.
1990. Predation by harbour seals and sea lions on adult salmon in Comox Harbour and Cowichan Bay, British Columbia. Can. Tech. Rep. Fish. Aquat. Sci. 1769, 31 p.

Bowen, W. D.
2000. Reconstruction of pinnipeds diets: accounting for complete digestion of otoliths and cephalopod beaks. Can. J. Fish. Aquat. Sci. 57:898–905.

Brown, R. F.
1980. Abundance, movements and feeding habits of the harbor seal, *Phoca vitulina*, at Netarts Bay, Oregon. M.S. thesis, 69 p. Oregon State Univ., Corvallis, OR.

Brown, R. F., S. D. Riemer, and S. Jefferies.
1995. Food of pinnipeds collected during the Columbia River Area Commercial Salmon Gillnet Observation Program, 1991–1994. ODFW (Oregon Dep. Fish Wildlife), Wildlife Diverstiy Program Tech. Rep. 95-6-01, 16 p.

Brown, R. F., and S. Kohlmann.
1998. Trends in abundance and current status of the Pacific harbor seal (*Phoca vitulina richardsi*) in Oregon: 1977–1998. ODFW, Wildlife Diverstiy Program Tech. Rep. 98-6-01, 16 p.

Browne, P., J. L. Laake, and R. L. DeLong.
2002. Improving pinniped diet analyses through identification of multiple skeletal structures in fecal samples. Fish. Bull. 100:423–433.

Butler, U. L.
1990. Distinguishing natural from cultural salmonid deposits in Pacific Northwest North America. Ph.D. diss., 218 p. Univ. of Washington, Seattle, WA.

Cottrell, P. E., A. W. Trites, and E. H. Miller.
1996. Assessing the use of hard parts in faeces to identify harbour seal prey: results of captive-feeding trials. Can. J. Zool. 74:875–880.

da Silva, J., and J. Neilson.
1985. Limitations of using otoliths recovered in scats to estimate prey consumption in seals. Can. J. Fish. Aquat. Sci. 42:1439–1442.

Dellinger, T., and F. Trillmich.
1988. Estimating diet composition from scat analysis in otariid seals (Otariidae): is it reliable? Can. J. Zool. 66: 1865–1870.

Eschmeyer, W. N., E. S. Herald, and H. Hammann.
1983. A field guide to Pacific Coast fishes of North America, 336 p. Houghton Mifflin Co., Boston, MA.

Harvey, J. T.
1987. Population dynamics, annual food consumption, movements and dive behaviors of harbor seals, *Phoca vitulina richardsi*, in Oregon. Ph.D. diss., 177 p. Oregon State Univ., Corvallis, OR.
1989. Assessment of errors associated with harbor seal (*Phoca vitulina)* faecal sampling. J. Zool., Lond. 219: 101–111.

Hawes, S.
1983. An evaluation of California sea lion scat samples as indicators of prey importance. M.S. thesis, 50 p. San Francisco State Univ. San Francisco, CA.

Jobling, M.
1987. Marine mammal faeces samples as indicators of prey importance—a source of error in bioenergetics studies. Sarsia 72:255–260.

Johnson, O., M. Ruckelshaus, W. Grant, F. Waknitz, A. Garrett, G. Bryant, K. Neely, and J. Hard.
1999. Status review of coastal cutthroat trout from Washington, Oregon, and California. NOAA Tech. Memo. NMFS-NWFSC-37, 292 p.

King, J.
1983. Seals of the world, 240 p. Comstock Publishing Assoc., Cornell Univ. Press, New York, NY.

Laake, J. L., P. Browne, R. L. DeLong, and H. R. Huber.
2002. Pinniped diet composition: a comparison of estimation models. Fish. Bull. 100:434–447.

Murie, D., and D. Lavigne.
1985. A technique for the recovery of otoliths from stomach contents of piscivorous pinnipeds. J. Wildl. Manag. 49: 910-912.
1986. Interpretation of otoliths in stomach content analyses of phocid seals: Quantifying fish consumption. Can. J. Zool. 64:1152–1157.

NMFS (National Marine Fisheries Service).
1997. Investigation of scientific information on the impacts of California sea lions and Pacific harbor seals on salmonids and on the coastal ecosystem of Washington, Oregon, and California. NOAA Tech. Memo. NMFS-NWFSC-28, 172 p.

Olesiuk, P. F., M. A. Bigg, G. M. Ellis, S. J. Crockford, and R. J. Wigen.
1990. An assessment of the feeding habits of harbour seals (*Phoca vitulina*) in the Strait of Georgia, British Columbia, based on scat analysis. Can. Tech. Rep. Fish. Aquat. Sci. 1730, 135 p.

Orr, A. J., and J. T. Harvey.
2001. Quantifying errors associated with using fecal samples to determine the diet of the California sea lion (*Zalophus californianus*). Can. J. Zool. 79:1080–1087.

Pearson, J., and B. Verts.
1970. Abundance and distribution of harbor seals and northern sea lions in Oregon. Murrelet 51:1–5.
Pierce, G. J., and P. R. Boyle.
1991. A review of methods for diet analysis in piscivorous marine mammals. Ocean. Mar. Biol. Ann. Rev. 29:409–486.
Purcell, M, G. Mackey, E. LaHood, H. Huber, and L. Park.
2004. Molecular methods for the genetic identification of salmonid prey from Pacific harbor seal (*Phoca vitulina richardsi*) scat. Fish. Bull. 102:213–220.
Reeves, R., B. Stewart, and S. Leatherwood.
1992. The Sierra Club handbook of seals and sirenians, 359 p. Sierra Club Books, San Francisco, CA.
Riemer, S. D., and R. F. Brown.
1997. Prey of pinnipeds at selected sites in Oregon identified by scat (fecal) analysis, 1983–1996. ODFW Wildlife Diversity Program Tech. Rep. 97-6-02, 34 p.
Roffe, T., and B. Mate.
1984. Abundances and feeding habits of pinnipeds in the Rogue River, Oregon. J. Wildl. Manag. 48:1262–1274.
Tollit, D. J., M.J. Steward, P. M. Thompson, G. J. Pierce, M. B. Santos, and S. Hughes.
1997. Species and size differences in the digestion of otoliths and beaks: implications for estimates of pinniped diet composition. Can. J. Fish. Aquat. Sci. 54:105–119.
U. S. Fish and Wildlife Service.
2000. Endangered and threatened wildlife and plants; final rule to remove the Umpqua River cutthroat trout from the list of endangered wildlife. Federal Register: 26 April 2000, 65(81:24420–24422.

Larval development of the sidestriped shrimp (*Pandalopsis dispar* Rathbun) (Crustacea, Decapoda, Pandalidae) reared in the laboratory

Wongyu Park
School of Fisheries and Ocean Sciences
University of Alaska Fairbanks
Juneau, Alaska, 99801-8677
E-mail address: w.park@uaf.edu

R. Ian Perry
Pacific Biological Station,
Fisheries and Oceans
Nanaimo, British Columbia, V9R 5K6, Canada

Sung Yun Hong
Department of Marine Biology
Pukyong National University
Pusan, 608-737, Korea

Abstract—Larval development of the sidestriped shrimp (*Pandalopsis dispar*) is described from larvae reared in the laboratory. The species has five zoeal stages and one postlarval stage. Complete larval morphological characteristics of the species are described and compared with those of related species of the genus. The number of setae on the margin of the telson in the first and second stages is variable: 11+12, 12+12, or 11+11. Of these, 11+12 pairs are most common. The present study confirms that what was termed the fifth stage in the original study done by Berkeley in 1930 was the sixth stage and that the fifth stage in the Berkeley's study is comparable to the sixth stage that is described in the present study. The sixth stage has a segmented inner flagellum of the antennule and fully developed pleopods with setae. The ability to distinguish larval stages of *P. dispar* from larval stages of other plankton can be important for studies of the effect of climate change on marine communities in the Northeast Pacific and for marine resource management strategies.

Manuscipt approved for publication 23 June 2003 by Scientific Editor.
Manuscript received 20 October 2003 at NMFS Scientific Publications Office.
Fish. Bull. 102:118–126 (2004).

Sixteen species of the genus *Pandalopsis* have been recognized in the Southwestern Atlantic and North Pacific Oceans (Komai, 1994; Jensen, 1998; Hanamura et al., 2000). Most members of the genus attain a large body size and are valuable as commercial fishery resources (Holthuis, 1980; Baba et al., 1986). In the North Pacific, *P. dispar, P. ampla, P. aleutica, P. longirostris, P. lucidirimicola, and P. spinosior* have been reported. Of these, *Pandalopsis dispar* is an important component of the commercial shrimp fisheries along with several species of the genus *Pandalus*. Commercial landings of shrimp during 1999 totaled approximately 19 million tons (PSMFC, 1999).

Knowledge of the life histories of these species, including the duration and growth of their larvae, is important for stock assessment and management. However, remarkably little is known about their early life histories because most species of the genus live at considerable depths. Of the 16 *Pandalopsis* species, the larvae of only three species have been described partly or completely from plankton samples or from larvae reared in the laboratory. The larvae of *Pandalopsis japonica* were described completely from specimens reared in the laboratory by Komai and Mizushima (1993). Kurata (1964) described the first stage of *P. coccinata* from plankton samples and from larvae hatched in the laboratory. Thatje and Bacardit (2000) assumed that larvae of *P. ampla* occurring in Argentine waters were similar to those of *P. dispar* and *Pandalopsis coccinata*. Berkeley (1930) described four larval stages of *P. dispar* based on samples collected in British Columbia coastal waters. The first stage was obtained from ovigerous females, whereas the larvae of the other stages were separated from plankton samples. In addition, the stage described as the fifth stage was not clearly defined.

In this study, we describe the complete series of larval stages of *P. dispar* using specimens reared in the laboratory.

Materials and methods

Ovigerous females of *Pandalopsis dispar* were collected on 25 March

1999 by using a small shrimp trawl fished at depths of about 40 m near Gabriola Island in the vicinity of the Pacific Biological Station, Nanaimo, British Columbia (latitude 49°13′, longitude 123°55′). Water temperature at the collection site was around 9°C, and salinity was 29.0‰. The females were each kept in a 20-L jar with seawater. The larvae hatched on 1 April 1999. Hundreds of larvae hatched from one female. Of these, one hundred newly hatched larvae were transferred into individual 250-mL jars. To obtain samples for drawing and descriptions, a total of 150 larvae from the female were reared in a 20-L jar. Newly hatched *Artemia* nauplii were used to feed the larvae. We used filtered natural seawater from 40 m depth without adjusting the water temperature or salinity. Water temperature during the rearing experiments ranged from 8.7°C to 12.2°C (mean 10.5°C). Salinity during the rearing experiments ranged from 26.0‰ to 31.0‰ (mean 28.9‰). The water in each jar was changed daily.

All drawings were made with a drawing tube attached to a microscope. Carapace length (CL) was measured with an ocular micrometer from the posterior edge of the orbital arch to the middorsal posterior edge of the carapace. The anatomical terms used in this paper are from Pike and Williamson (1969) and Haynes (1985).

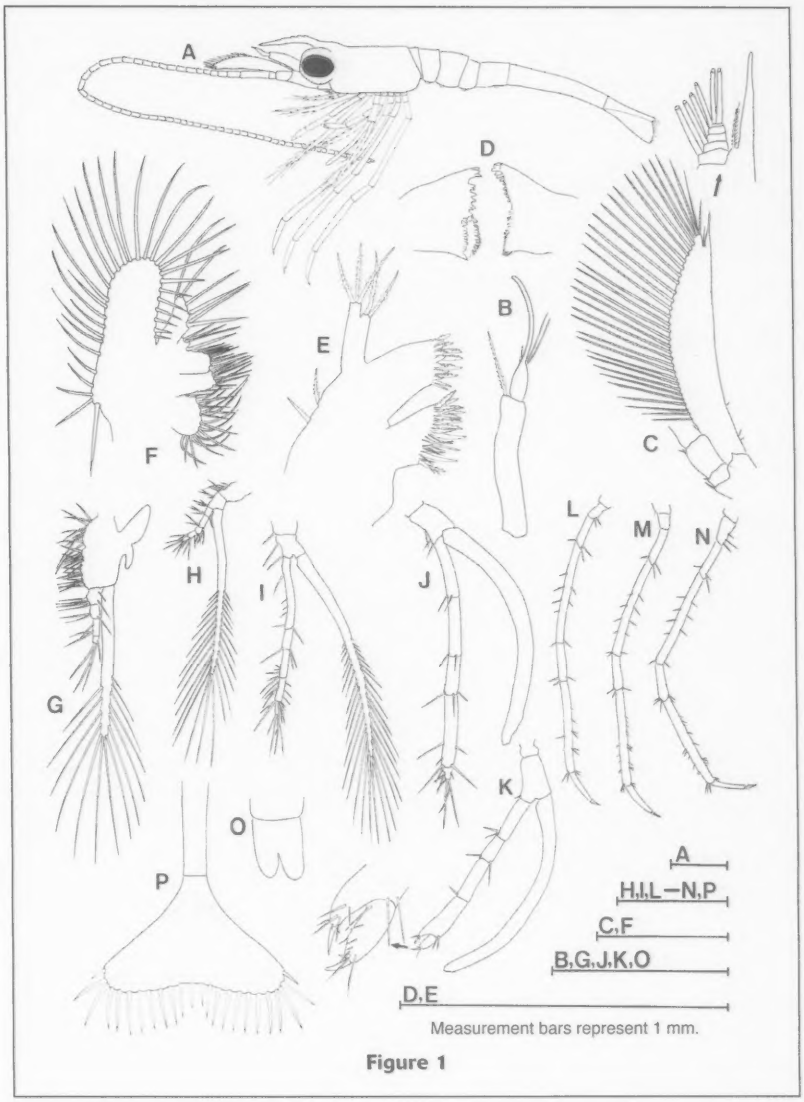

Figure 1

Results

In the complete larval development of *Pandalopsis dispar* there are five zoeal stages. In addition, there is one postlarval stage. The duration of each larval stage and the survival rate of *P. dispar* are shown in Table 1.

Larval description

First stage

Carapace (Fig. 1A) Carapace length (CL), 1.6 mm (SD: 0.06 mm, n=89); with concave lateral margin; rostrum long, well developed and directed forward and upward; weak

Table 1

Duration of each larval stage of *Pandalopsis dispar* at 8.7–12.2°C (mean 10.5°C) and 26.0–31.0‰ (mean 28.9‰). Stage 6 is a postlarval stage.

Stage	Mean duration (day)	Range (day)	Number of larvae observed
1	10.7	9–15	89
2	8.9	8–11	81
3	9.5	8–14	67
4	10	9–12	59
5	10.8	10–13	51
6	10.5	9–12	48

dorsal denticles and bare ventral tubercles on rostrum; rostrum about 0.7 times as long as carapace.

Eyes (Fig. 1A) Sessile.

Abdomen (Fig. 1A) 5 somites plus telson.

Antennule (Fig. 1, A and B) Peduncle unsegmented with a strong seta at distromesial margin; outer flagellum with 2+2 short aesthetascs.

Antenna (Fig. 1, A and C) Longer than the whole body length; flagellum segmented throughout its length; outer-distal corner terminated with an acute spine and a minute seta; inner-distal margin 5-segmented with 1, 1, 1, 1, 2 setae; inner margin fringed with 28–29 setae.

Mandible (Fig. 1D) Asymmetrical; without the same arrangement of denticles, however, almost the same size; incisor process not separated from molar process; armed with several teeth on molar part.

Maxillule (Fig. 1E) Coxal and basal endite with serially developed strong spines and multiple setae; endopod with 2+3 terminal setae

Maxilla (Fig. 1F) Palp with 2, 1, 1, 2 setae; coxal endite with 6 distal setae; basal endite with 8 distal setae; broad scaphognathite with narrow posterior lobes having long naked setae.

First maxilliped (Fig. 1G) Endites separated by shallow notch and with multiple setae; bilobed epipod; endopod 4-segmented with 6, 3, 3, 4 setae; exopod with 14 plumose natatory setae; terminal segment with 3 terminal spines and 1 subterminal spine.

Second maxilliped (Fig. 1H) Coxa with 7 setae; basis with 3 setae; no epipod; endopod 5 segmented with 5, 5, 2, 4, 4 setae; exopod with 27 plumose natatory setae.

Third maxilliped (Fig. 1I) Coxa with 1 seta; basis with 2 setae; endopod 5-segmented with various number of setae; exopod with 34–36 plumose natatory setae.

Pereiopods (Fig. 1, J–N) 1st pereiopod (Fig. 1J) not chelate; 3 long terminal spines on dactylus; dactylus short; propodus longer than carpus; exopod without natatory setae; endopod of 2nd pereiopod chelated (Fig. 1K); chela with numerous small spines; ischium and carpus of pereiopods 3–5 (Fig. 1, L–N) longer than 1st and 2nd ones; propodus armed with several minute spines.

Pleopods (Fig. 1O) Bilobed buds, not functional.

Telson (Fig. 1P) Triangular form; broadened at the end, posterolateral margin with 11+12 (12+12, 11+11) marginal spines; each spine with fine hairs.

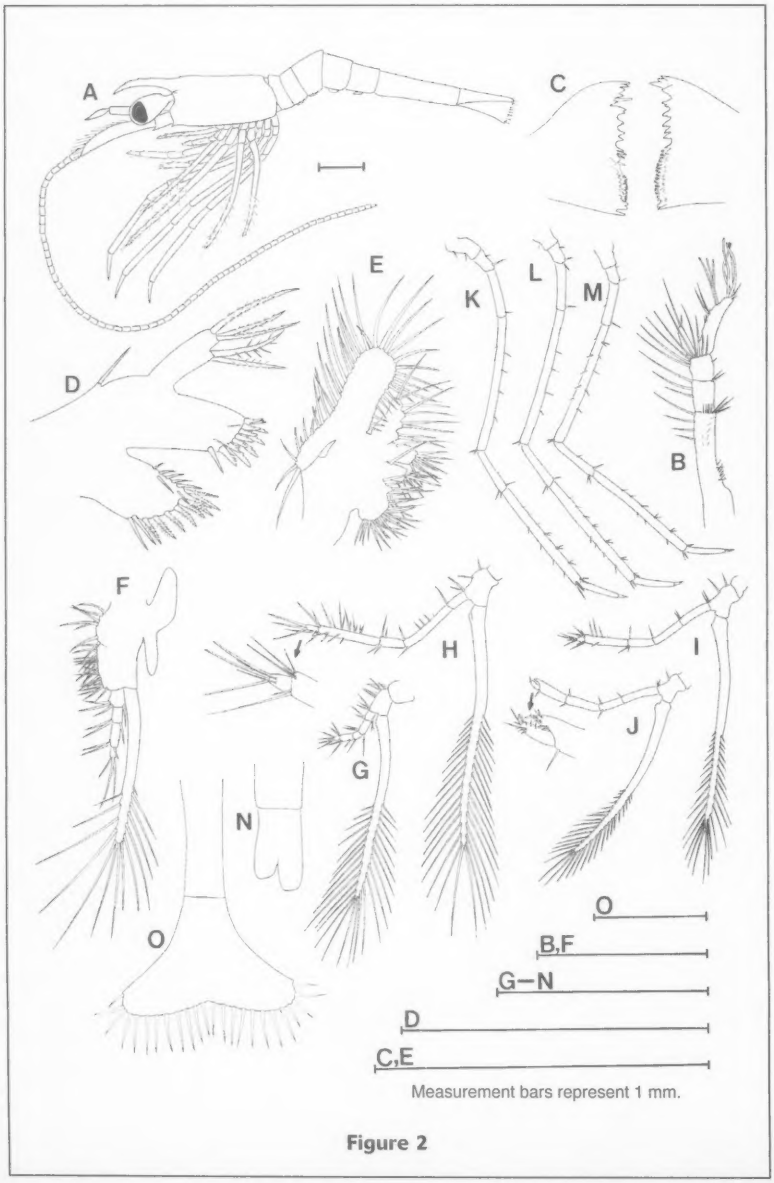

Figure 2

Second stage

Carapace (Fig. 2A) CL, 2.2 mm (SD: 0.11, n=81); rostrum not strongly curved upwards; 5–6 prominent dorsal denticles and 3–4 weak ventral spines; rostrum shorter than carapace; supraorbital spine present.

Eyes (Fig. 2A) Stalked; separated from carapace.

Antenna (Fig. 2A) General shape unchanged; longer than that of 1st stage.

Antennule (Fig. 2B) Peduncle 3-

segmented; inner flagellum with 2 distal setae; outer flagellum with 2, 3, 4, 2 aesthetascs on inner margin.

Mandible (Fig. 2C) General shape unchanged; bigger than that of 1st stage.

Maxillule (Fig. 2D) Coxal and basal endite with serially developed strong spines and multiple setae; endopodite with 2+3 spines; a strong subterminal seta.

Maxilla (Fig. 2E) Palp with 2, 2, 2, 3 setae; broad scaphognathite with narrow posterior lobe having a long naked seta; coxal endite with 6 distal setae; basal endite with 7 distal setae.

First maxilliped (Fig. 2F) Epipod bilobed; endopod with 3+1, 2+1, 2+1, 3 setae; exopod unsegmented with 14 plumose natatory setae.

Second maxilliped (Fig. 2G) One long and several intermediate sized spines in basal endite; endopod 5-segmented; exopod with 24 plumose natatory setae.

Third maxilliped (Fig. 2H) Endopod 5-segmented, armed with many spines; exopod of 36 plumose natatory setae.

Pereiopods (Fig. 2, I–M) Not chelate; 1st pereiopod of 4 spines in basal endite; 3 strong and two weak spines in dactylus of 1st pereiopod; general shape unchanged from 2nd pereiopod through 5th pereiopod.

Pleopods (Fig. 2N) Bilobed buds, not functional; no seta and hair on buds; no further development from the 1st stage.

Telson (Fig. 2O) Unchanged.

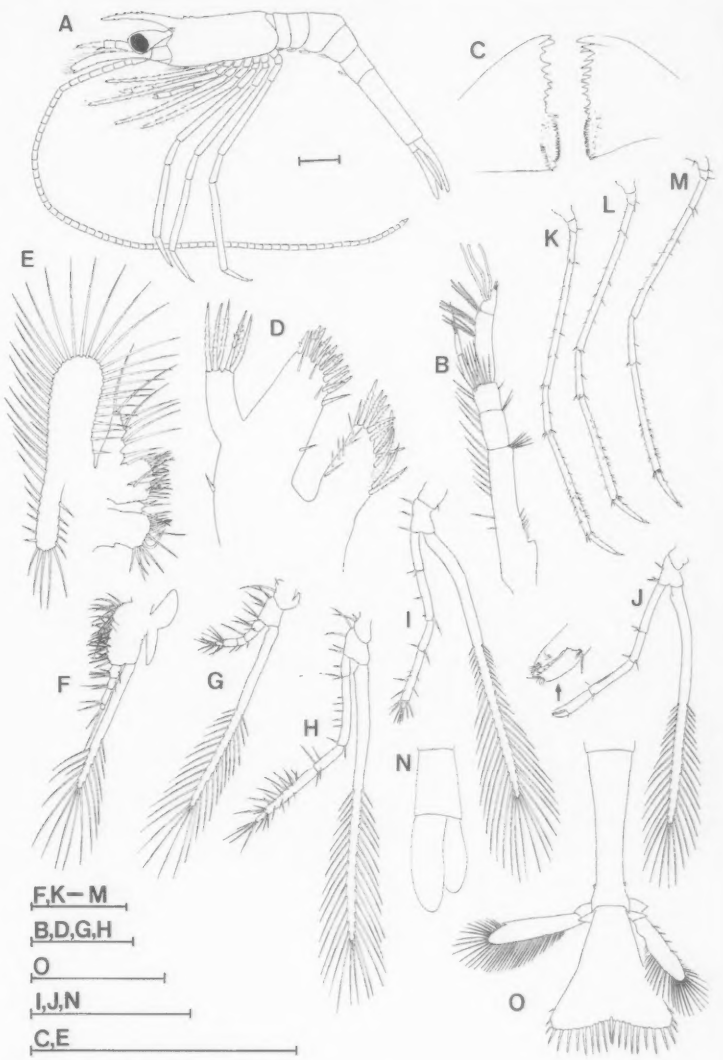

Figure 3

Third stage

Carapace (Fig. 3A) CL, 2.7 mm (SD: 0.12, n=67); longer rostrum than that of 2nd stage; almost 0.9 times as long as carapace; rostrum with 5-6 dorsal spines and 1-2 ventral spines.

Antennule (Fig. 3B) Inner flagellum 2-segmented with 0, 2 setae; outer flagellum 2-segmented with 3+3+3, 3+3 aesthetascs.

Antenna (Fig. 3A) General shape unchanged; longer than 2nd stage.

Mandible (Fig. 3C) Molar and incisor processes present; incisor process with 6-9 teeth; molar process with heavy teeth on biting edge.

Maxillule (Fig. 3D) Palp with 2+3 setae; a small subterminal spine; basal and coxal endite with numerous spines.

Maxilla (Fig. 3E) Protopodite unsegmented; palp with 1, 2, 2, 1+2 setae and with 4 lobes; broad scaphognathite with narrow posterior lobe bearing numerous setae.

First maxilliped (Fig. 3F) Epipod bilobed; endopod 4-segmented with 4, 2, 2, 2 setae; exopod with 15–16 plumose natatory setae;

Second maxilliped (Fig. 3G) Coxal endite with an epipod and a strong spine; endopod 5-segmented with 3, 2, 2, 4, 6 setae exopod with setae.

Third maxilliped (Fig. 3H) Coxal endite with one long and

one short spine; basal endite with 2 long and 2 intermediate sized spines; endopod 5-segmented with numerous setae; exopod with 25–26 plumose natatory setae.

Pereiopods (Fig. 3, I–M) General shape unchanged except addition of setae.

Pleopods (Fig. 3N) Buds biramous; much longer than that of 2nd stage.

Uropods (Fig. 3O) Biramous; endopod with a fused spine at distal quarter of outer margin and numerous setae on inner distal margin; exopod with 4 spines on outer margin and numerous setae on inner distal margin.

Telson (Fig. 3O). With 12 pairs of posterolateral spines plus a median spine.

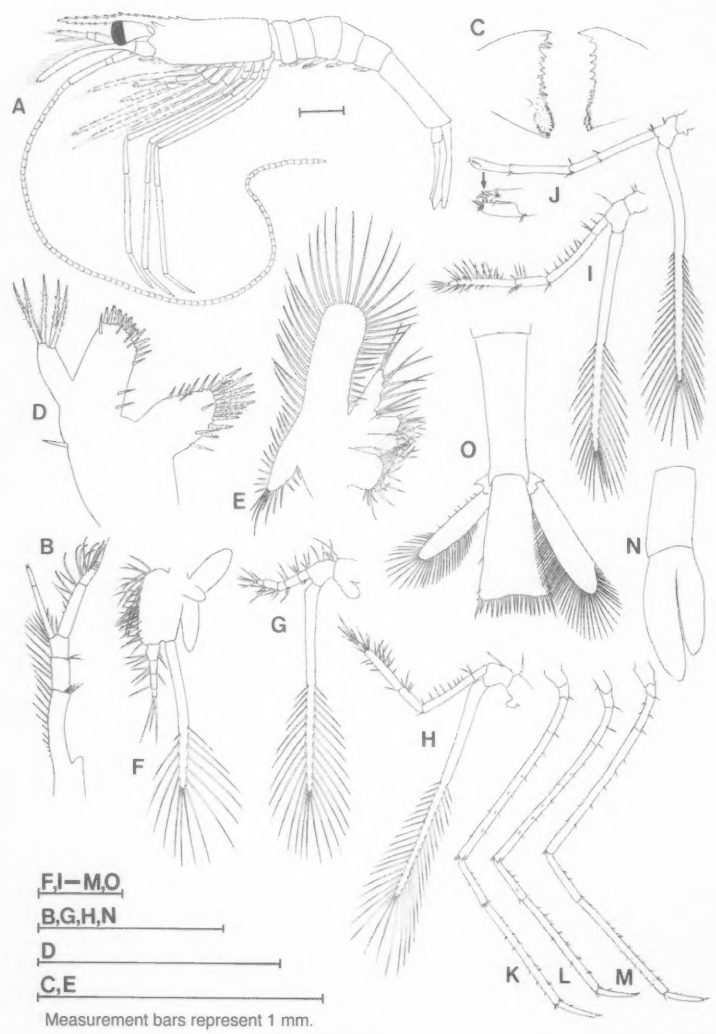

Figure 4

Fourth stage

Carapace (Fig. 4A) CL, 3.1 mm (SD: 0.13, n=59); Rostrum slightly longer than carapace and directed forward; rostrum with 15 dorsal spines and 6 ventral spines.

Antenna (Fig. 4A) General shape unchanged; longer than that of 3rd stage.

Antennule (Fig. 4B) Much longer inner flagellum than that of 3rd stage; inner flagellum about 0.9 times as long as outer flagellum, 2-segmented with 0, 2 setae; outer flagellum 6-segmented with 1, 2, 2, 3, 4 aesthetascs.

Mandible (Fig. 4C) Similar to third stage.

Maxillule (Fig 4D) General shape unchanged except addition of setae on endites.

Maxilla (Fig. 4E) Palp with 3, 2, 2, 3 setae; endites and scaphognathite added numerous setae.

First maxilliped (Fig. 4F) Expod with 15 plumose natatory setae.

Second maxilliped (Fig. 4G) Basal endite with an epipod and a long spine; exopod with 28–29 plumose natatory setae.

Third maxilliped (Fig. 4H) Expopod with 36–37 plumose natatory setae.

Pereiopods (Fig. 4, I–M) Number of spines increased.

Pleopods (Fig. 4N) Lobes much longer than those of third stage.

Uropods (Fig. 4O) Endopod and exopod with numerous setae on inner distal margin.

Telson (Fig. 4O) With 12 pairs of spines on posterolateral margin; a pair of lateral spines at distal third.

Fifth stage

Carapace (Fig. 5A) CL, 3.6 mm (SD: 0.15, n=51); Rostrum directed forward and upward, slightly longer than carapace; rostrum with 17–18 dorsal spines and 7–8 ventral spines.

Antennule (Fig. 5B) Inner flagellum 3-segmented and about 0.9 times as long as outer flagellum; outer flagellum with 2+2+3+3+3+2+3+5 aesthetascs and distal third 6-segmented.

Mandible (Fig. 5C) More advanced development than that of 6th; not much change in biting surface.

Maxillule (Fig. 5D) General shape unchanged except addition of setae on endites.

Maxilla (Fig. 5E) General shape unchanged.
First maxilliped (Fig. 5F) Exopod with 16 plumose natatory setae.
Second maxilliped (Fig. 5G) Exopod with 31–33 plumose natatory setae.
Third maxilliped (Fig. 5H) Exopod with 46–48 plumose natatory setae.
Pereiopods (Fig. 5, I–M) Ischium slightly expanded in first pereipod.
Pleopods (Fig. 5N) Much more developed than pleopods of 4th stage; exopod with 13, 1 setae; endopod with 6 setae and vestiges of appendix interna.
Uropod (Fig. 5O) Exopod with numerous minute spines on outer margin
Telson (Fig. 5O) Both lateral margins parallel; 19 terminal spines; 2 pairs of lateral spines.

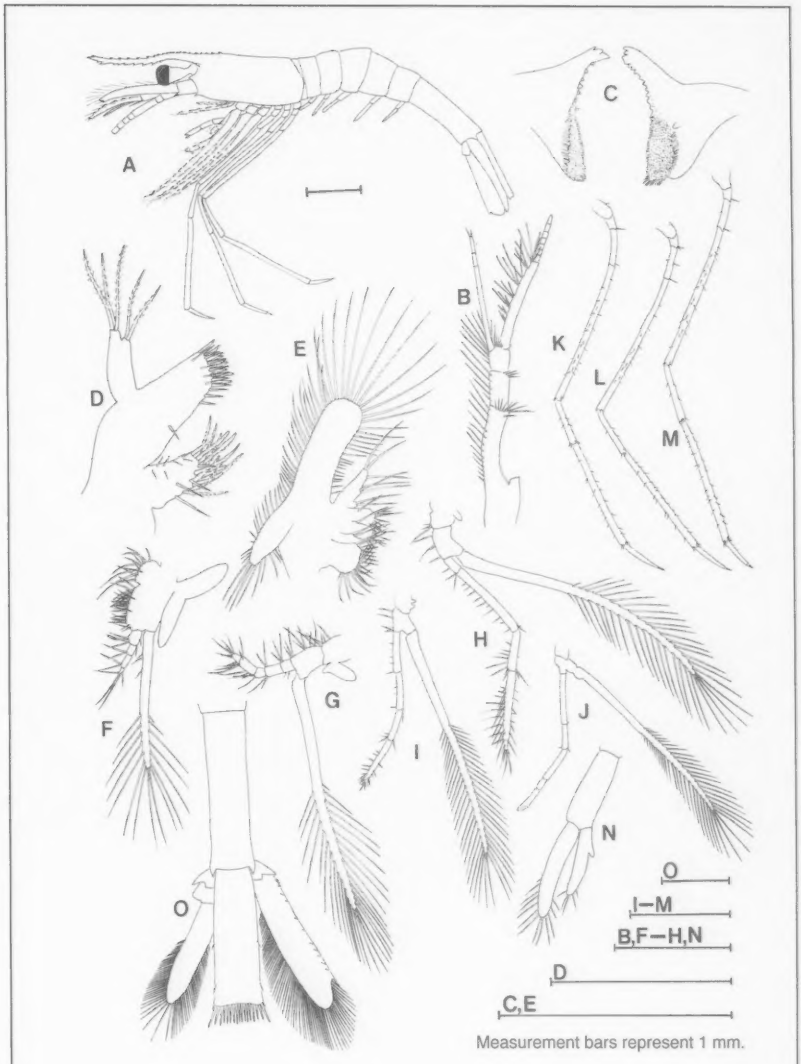

Figure 5

Sixth stage

Carapace (Fig. 6A) CL, 4.0 mm (SD: 0.21, n=48); adult-like.
Antennule (Fig. 6B) Inner flagellum as long as outer flagellum; inner flagellum with multisegments; outer flagellum with numerous segments.
Mandible (Fig. 6C) Incisor part separated from molar process and extended anteriorly.
Maxillule (Fig. 6D) 9 terminal spines on basal endite.
Maxilla (Fig. 6E) Palp with 2, 2, 2, 1+2 spines; broad scaphognathite with narrow posterior lobe bearing 3 long setae.
First maxilliped (Fig. 6F) Exopodite with 4+2, 2, 2 3 long and 1 short spines.
Second maxilliped (Fig. 6G) Basal endite with 2 long spines; vestigial dactylus.
Third maxilliped (Fig. 6H) Propodus armed with many spines; dactylus with 2 spines.
Pereiopods (Fig. 6, I–M) 1st pereipods with subchelated terminal segment; 1st pereiopod with slightly expanded ischium.
Pleopods (Fig. 6N) Endopod and exopod with numerous plumose natatory setae; endopod with epipod almost adult-like.
Uropods (Fig. 6O) Biramous; larger than those of fifth stage; adult-like.
Telson (Fig. 6O) Telson with 20 terminal spines and 4 pairs of lateral spines.

Discussion

The first stage larva of *Pandalopsis dispar* described by Berkeley (1930) is identical to the larva described in the present study. However, we found that she overlooked some important characteristics. She described the first stage larva as having 24 setae on the margin of the telson. We found, however, that the number of setae is variable, and that the larvae have 11+12, 12+12, or 11+11 marginal

setae. Of these, 11+12 pairs are more common than the others.

Berkeley (1930) described the fifth stage based on plankton materials. In the present study, what was described by Berkeley (1930) as the fifth stage larva turned out to be the sixth stage because the larvae of this stage have fully developed pleopods. Although the larvae of the fifth stage have somewhat natatory setose on their pleopods, they appear not to be completely functional. Compared to the larvae of *P. japonica*, *P. dispar* has one more stage than that of *P. japonica*. The pleopod development of *P. japonica* from the fourth stage to the fifth stage is very obvious, whereas that of *P. dispar* has another stage and the changes in its features between the fourth and sixth stages are easily seen.

The major characteristics of the six larval stages of *P. dispar* are summarized in Table 2. This table can be used for the identification of the larval stages of this species. Komai (1994) reviewed the morphological characters of the first larval stage of three *Pandalopsis* spp.: *P. dispar, P. coccinata,* and *P. japonica*. The larvae of *P. dispar* at this stage are quite different from those of the other two species. The larvae of *P. dispar* have a triangular telson, whereas those of *P. coccinata* and *P. japonica* have a semicircular telson.

The adults of the genus *Pandalopsis* differ from those of other pandalid shrimps by having a laminated expansion on the first pereiopod (Schmit, 1921; Butler, 1980). This character is also present in larvae of *P. coccinata* and *P. japonica,* whereas it is not present in larvae of *P. dispar*. From the third stage the ischium does indicate expansion, however, it is not distinctive. It is assumed that in *P. dispar,* the expansion should be distinctive after the larval stages.

In *P. coccinata* and *P. japonica* the ischium of the first pereiopod has a laminated expansion; however, in *P. dispar* it has no lamination. The structure of the ischium of the first pereiopod can be a diagnostic feature of *P. dispar* in addition to the shape of the telson.

Interspecific variation in the larval stages of pandalid shrimp is large, ranging from three to thirteen stages (Rothlisberg, 1980; Komai and Mizushima, 1993). Haynes (1980, 1985) assumed that *P. dispar* might have seven pelagic stages, or at least more than four. The present study has determined that *P. dispar* has five zoeal stages prior to the juvenile stage.

Pandalopsis dispar is one of the four principal target species of shrimp trawl fisheries in both offshore and inshore areas of the NE Pacific Ocean (PICES, 2001) but has undergone very large fluctuations in abundance, particularly in Alaska where it was reduced to extremely low levels during the late 1980s and through the 1990s. These fluctuations appear to have been associated first with climate fluctuations (Anderson, 2000), and second with intense harvesting (Oresanz et al., 1998). Anderson (2000) has suggested that pandalid shrimp population changes are one of the early in-

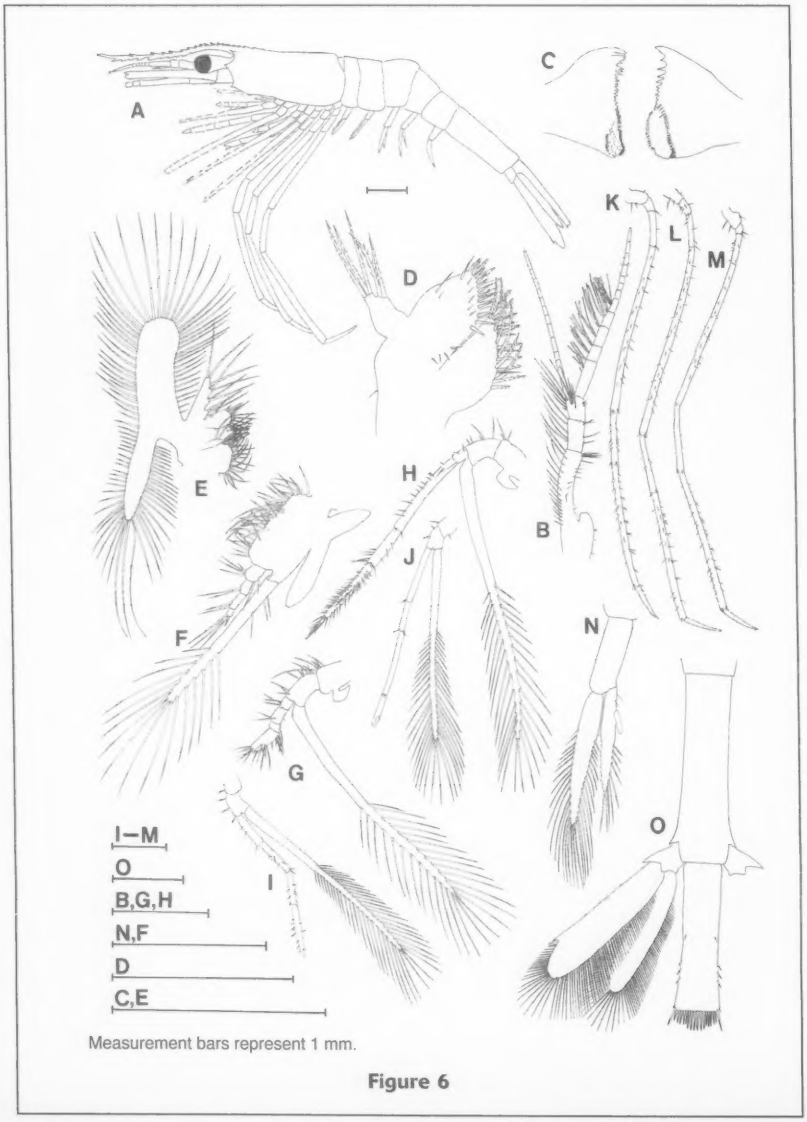

Figure 6

Table 2

Major characters of *Pandalopsis dispar* larvae.

Characters		Larval stage[1] 1	2	3	4	5	6 (postlarva)
Antenna flagellum	Inner	One strong spine	One peduncle with a few small spines	2 segments	2 segments	3 segments	Multisegmented over 14
	Outer	Not segmented	Slightly developed	2 segments	6 segments	7 segments	12 segments
Telson		12+11, 12+12, or 11+11		10 pairs of terminal spines, 2 pairs of uropods	One spine on each midlateral margin	2 spines on each lateral margin	4 spines on each lateral margin
Pleopod development		Wide as much as long	Longer than wide	Almost separated lobes	Longer lobes than those of stage 3	Lobes separated completely with natatory setae	Adult-like, with many natatory setae on both lobes

[1] Eyes of the first stage are sessile on carapace, whereas those of the second and later stages are stalked.

dicators of shifts in marine communities in this region. Orensanz et al. (1998) have suggested it is important to recognize that crustacean stocks can have multiscale spatial structures; species have possibly both widely distributed populations (such as in the oceanic offshore) and populations with discrete and localized distributions (as may occur in the nearshore inlets).

The ability to distinguish the larval stages of *Pandalopsis dispar* from routine plankton samples is therefore of use in studying both these problems of population fluctuations and population distributions. Early identification of trends in strong versus weak year classes can provide rapid indications of possible changes in large-scale climate conditions. Unambiguous identification of planktonic stages of *P. dispar* is also essential for studies of the spatial structure of its populations, for studies of transport pathways and potential mixing rates among populations, and ultimately for understanding the metapopulation structure of these populations. This latter point is critical for the development of improved management approaches, which may include identification of reproductive refugia (Orensanz et al., 1998).

Acknowledgments

We wish to thank Jim Boutillier and Steve Head for their support with this study. This study was supported by the Korea Research Foundation Grant (KRF-2002-013-H00005).

Literature cited

Anderson, P. J.
2000. Pandalid shrimp as indicators of ecosystem regime shift. J. Northw. Atl. Fish. Sci. 27:1–10.

Baba, K., K. Hayashi, and M. Toriyama.
1986. Decapod crustaceans from continental shelf and slope around Japan, 336 p. Japan Fisheries Resource Conservation Association, Tosho Printing Co. Ltd., Tokyo.

Berkeley, A.
1930. The post-embryonic development of the common pandalids of British Columbia. Cont. Can. Bio. Fish., New Series 6:79–163.

Butler, T. H.
1980. Shrimps of the Pacific coast of Canada. Can. Bull. Fish. Aquat. Sci. 202, 280 p.

Hanamura, Y., H. Khono, and H. Sakai.
2000. A new species of the deepwater pandalid shrimp of the genus *Pandalopsis* (Crustacea: Decapoda: Pandalidae) from the Kuril Islands, North Pacific. Crust. Res. 29:27–34.

Haynes, E.
1980. Larval morphology of *Pandalus tridens* and summary of the principal morphological characteristics of North Pacific pandalid shrimp larvae. Fish. Bull. 77:625–640.

Haynes, E.
1985. Morphological development, identification, and biology of larvae of Pandalidae, Hippolytidae and Crangonidae (Crustacea: Decapoda) of the northern North Pacific Ocean. Fish. Bull. 83:253–288.

Holthuis, L. B.
1980. Shrimps and prawns of the world, an annotated catalogue of species of interest to fisheries. FAO species Catalogue. FAO Fish. Syn. 125, FIR/S 125 Vol.1, 271 p.

Jensen, G. C.
1998. A new species of the genus *Pandalopsis* (Decapoda: Caridea: Pandalidae) from the Eastern Pacific, with notes on its natural history. Species Diversity 3:81–88.

Komai, T.
1994. Deep-sea shrimps of the genus *Pandalopsis* (Decapoda: Caridea: Pandalidae) from the Pacific Coast of eastern Hokkaido, Japan with the description of two new species. J. Crust. Biol. 14:538–559.

Komai, T., and T. Mizushima.
1993. Advanced larval development of *Pandalopsis japonica*

Balss, 1914 (Decapoda: Caridea: Pandalidae) reared in the Laboratory. Crustaceana 64:24–39.

Kurata, H.
1964. Larvae of deacapod Crustacea of Hokkaido. 3. Pandalidae. Bull. Hokkaido Reg. Fish. Res. Lab. 28:23–34.

Orensanz, J. M., J. Armstrong, D. Armstrong, and R. Hilborn.
1998. Crustacean resources are vulnerable to serial depletion—the multifaceted decline of crab and shrimp fisheries in the greater Gulf of Alaska. Rev. Fish Biol. Fisheries 8: 117–176.

Pike, R. B., and D. I. Williamson.
1964. The larvae of some species of Pandalidae (Decapoda). Crustaceana 6:265–284.

PICES.
2001. Commercially important crabs, shrimps and lobsters of the North Pacific Ocean. PICES Scientific Report 19, 79 p. North Pacific Marine Science Organization, Sidney, B.C., Canada

PSMFC (Pacific States Marine Fisheries Commission).
1999. 52nd annual report of the Pacific States Marine Fisheries Commission (A. J. Didier, ed.), 37 p. Pacific States Marine Fisheries Commission, Gladston, OR.

Rothlisberg, P. C.
1980. A complete larval description of *Pandalus jordani* Rathbun (Decapoda, Pandalidae) and its relation to other members of the genus *Pandalus*. Crustaceana 38:19–48.

Schmitt, W. L.
1921. The marine decapod Crustacea of California with special reference to the decapod Crustacea collected by the United States Bureau of Fisheries Steamer "Albatross" in connection with the biological survey of San Francisco bay during the years 1912–1913. Univ. California, Publ. Zool., vol. 23, 470 p.

Thatje, S., and R. Bacardit.
2000. Larval development of *Austropandalus grayi* (Cunningham, 1871) (Decapoda, Caridea, Pandalidae) from the southwestern Atlantic Ocean. Crustaceana 73:609–628.

Sources of age determination errors for sablefish (*Anoplopoma fimbria*)*

Donald E. Pearson
Santa Cruz Laboratory
National Marine Fisheries Service
110 Shaffer Road
Santa Cruz, California 95060
E-mail address: Don.Pearson@Noaa.Gov

Franklin R. Shaw
Alaska Fisheries Science Center
National Marine Fisheries Service
7600 Sand Point Way NE
Seattle, Washington 98118

Abstract—This study was undertaken to resolve problems in age determination of sablefish (*Anoplopoma fimbria*). Aging of this species has been hampered by poor agreement (averaging less than 45%) among age readers and by differences in assigned ages of as much as 15 years.

Otoliths from fish that had been injected with oxytetracycline (OTC) and that had been at liberty for known durations were used to determine why age determinations were so difficult and to help determine the correct aging procedure. All fish were sampled from Oregon southwards, which represents the southern part of their range. The otoliths were examined with the aid of image processing.

Some fish showed little or no growth on the otolith after eight months at liberty, whereas otoliths from other fish grew substantially. Some fish lay down two prominent hyaline zones within a single year, one in the summer and one in the winter. We classified the otoliths by morphological type and found that certain types are more likely to lay down multiple hyaline zones and other types are likely to lay down little or no zones. This finding suggests that some improvement could be achieved by detailed knowledge of the growth characteristics of the different types.

This study suggests that it may not be possible to obtain reliable ages from sablefish otoliths. At the very least, more studies will be required to understand the growth of sablefish otoliths.

Manuscript approved for publication 14 July 2003 by Scientific Editor.

Manuscript received 20 October 2003 at NMFS Scientific Publications Office.

Fish Bull. 102:127–141 (2004).

Sablefish (*Anoplopoma fimbria*) are a valuable groundfish resource off the west coast of North America. The fishery in California, Oregon, and Washington is tightly regulated according to periodic stock assessments. Between 1990 and 1998 landings averaged more than 8000 metric tons per year and an average exvessel (retail) value of 12.5 million dollars per year (PFMC, 1999).

Sablefish are distributed in the northeastern Pacific Ocean from Baja California to the Bering Sea and southeast to northern Japan (Miller and Lea, 1972). Males and females are sexually mature between 55 and 67 cm, although there is considerable variation (Fujiwara and Hankin 1988a; Hunter et al., 1989). Off Washington, Oregon, and California, sablefish spawn from October through April and spawning peaks in January and February. Sablefish are oviparous, releasing eggs that float near the surface (Hunter et al., 1989). After hatching, larvae and juveniles inhabit surface waters offshore for several years after which they migrate inshore and settle to the bottom.

Sablefish are found on the continental slope and are commercially fished at depths from 200 to 1400 meters (Leet et al., 1992). Adult sablefish feed on fish, cephalopods, and crustaceans (Laidig et al., 1998). They reach a maximum length of 102 cm (Miller and Lea, 1972) and are believed to be a very long-lived species (possibly 100 years or more).

Many physical features have been used to age this species, including scales, finrays, thin-sectioned otoliths, and broken and burned otoliths, but all methods have resulted in less than 45% agreement among readers (Lai, 1985; Fujiwara and Hankin 1988b; Kimura and Lyons, 1991; Heifetz et al., 1999). The broken and burned otolith method (Chilton and Beamish, 1982) is the principal method used in aging of the species in both the United States and Canada. Typically, age readers agree on ages less than 50% of the time, and for fish older than 7 years, agreement drops to less than 15% (Kimura and Lyons, 1991).

There have been repeated efforts at validating sablefish ages and developing aging criteria. Beamish et al. (1983) successfully used oxytetracycline (OTC) marking to validate ages and repeated his experiment in 1995 when additional marked fish were recovered (MacFarlane and Beamish, 1995). Lai (1985) validated the use of otoliths for aging sablefish. Fujiwara and Hankin (1988b) examined otolith growth characteristics to help refine aging criteria. Heifetz et al. (1999) validated the currently accepted aging practices and examined sources of error in the aging of sablefish. Kastelle et al. (1994) used radiometric methods to generally validate the aging criteria currently used. Even with all of these studies that have validated age

* Contribution 119 from the Santa Cruz Laboratory, National Marine Fisheries Service, Santa Cruz, CA 95060.

Figure 1

Map of California and southern Oregon showing the locations (black dots) of sablefish sampling and tagging in September and October of 1991.

determinations, independent age readings seldom are in agreement. This suggests that the methods used to validate the ages were insufficient to allow development of precise aging criteria. The lack of reliable age data has made stock assessments difficult and controversial (Crone et al., 1997), and in addition, accurate aging is needed to support ecological and habitat studies.

In September and October of 1991, a tagging and oxytetracycline (OTC) injection study was included as part of a fish trap survey of the abundance of sablefish in southern Oregon and California. The purpose of this study was to attempt, once more, to improve our ability to reliably age sablefish, thereby improving our ability to manage the species.

Methods

Capture, tagging, injection, and recovery

In September 1991, the fisheries research vessel *Alaska* was chartered by the National Marine Fisheries Service to conduct a trap survey from Coos Bay, Oregon, to Cortez Bank, California (Fig. 1). A total of nine sites were visited. At each site seven strings of ten traps were deployed in various depths between 250 and 1900 meters. The traps were retrieved after 24 hours, the catch was removed, and the traps reset for an additional 24 hours. All the sablefish were counted, otoliths were removed from the first 20 arbitrarily selected fish at each station, and the rest of the fish were tagged with blue spaghetti tags. Three of every four tagged fish were injected intraperitoneally with 30 mg of OTC per kilogram of fish (Beamish et al., 1983) and the fourth fish was used as a control. A complete description of the survey can be found in Parks and Shaw (1994).

A scientist visited the major commercial fishing ports in California and southern Oregon to make port samplers, commercial dealers, and fishermen aware of the importance of the study and to explain handling procedures in the study. A $50.00 reward was offered for the return of whole tagged fish.

When a tagged fish was returned, the port sampler measured it (fork length in mm), determined the sex, and removed the otoliths. The otoliths were cleaned and stored in painted glass vials (because the OTC mark was light labile) with a 50% ethanol solution.

Processing of the otoliths

Two pairs of otoliths were initially selected to develop the procedures to be used in the study. It was found that the OTC mark was very faint and upon heating (as required by conventional age determination methods), the mark disappeared. Accordingly, we developed a method to obtain images of the otoliths before and after heating, and to superimpose the two images of the same otolith; the first viewed under UV light and, the second, after heating, under white light.

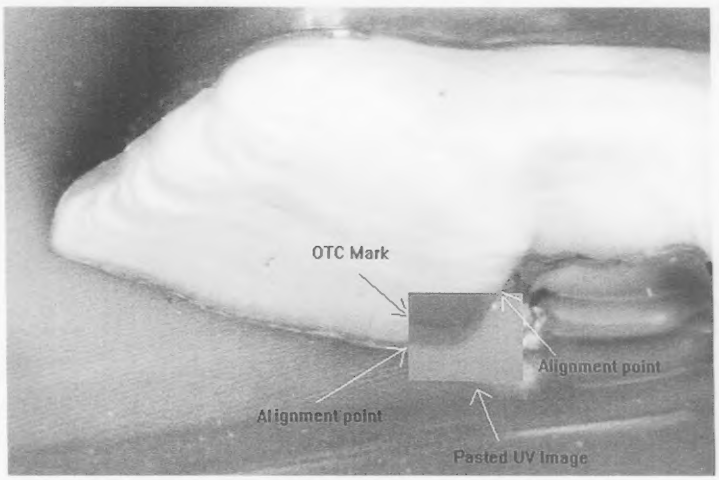

Figure 2

Composite image of a sablefish otolith. The otolith was first viewed under UV light and an image was captured. It was then baked and a second image was captured by using white light. Then a small rectangle from the UV image was electronically cut and pasted on the image of the baked otolith. The flourescent mark produced by the OTC appears as a dark line on the UV section. Points on the otolith used for correct positioning of the pasted section are shown.

The otoliths were embedded in epoxy casting resin. After the resin hardened, the blocks containing the otoliths were sliced in half across the dorsoventral axis with a diamond saw.

Images were captured in a two-stage process. The first stage used ultraviolet light to reveal the OTC mark, and the second stage used white light to reveal the growth marks used for age determination. In the first stage, the room was completely darkened and an image of the otolith, including the OTC mark, was captured by using a video camera capable of capturing images under low light conditions. We used an ultraviolet lamp which produced a strong beam of light at 365 angstroms. The otolith was viewed on a compound microscope using reflected light. The camera and image processing system were connected to a PC computer equipped with a frame grabber card. A version of NIH Image, a public domain image processing software (Scion Corporation, Frederick, MD), was used to process the images.

The embedded otolith was placed on the microscope and a drop of mineral oil was placed on the surface of the otolith. The limited amount of UV light available to the camera required the use of frame averaging. Usually 30 frames were sufficient to produce a sharp view of the otolith and the fluorescing mark. In some cases, the mark was too faint to allow an image to be captured. When there was sufficient fluorescence, two composite images were captured, one at 4× and one at 40×.

In the second stage, the same embedded otolith was placed in a small toaster oven at 270°C and heated for 20 to 25 minutes until it had turned dark brown. This baking process enhanced the growth rings for visual analysis and approximated what age readers see using the break and burn method; however, the latter process results in darker hyaline zones than those obtained with this method. After cooling, the otolith was viewed under white light. A second set of images was then captured. A section of each UV image was then electronically cut and pasted onto the image captured under visible light. With some experimentation it was found that the pasted sections could be aligned exactly over the visible light images, creating a final composite image as shown in Figure 2.

Initial examination of the otoliths

Initially, all OTC-marked otoliths were examined with knowledge of the year and season of release, but without any other information about the fish. Composite UV and white light images were obtained as previously described. The age reader determined the following: whether or not the OTC mark was visible; whether the OTC mark was in a hyaline or opaque zone; the number of annual hyaline zones visible beyond the OTC mark (and whether or not the edge was included in the count); edge type (hyaline, narrow opaque, wide opaque, or unidentifiable), and the shape of the otolith. In some cases the OTC mark could not be identified or the mark was too faint to be captured as a composite image; these specimens were excluded from subsequent analyses.

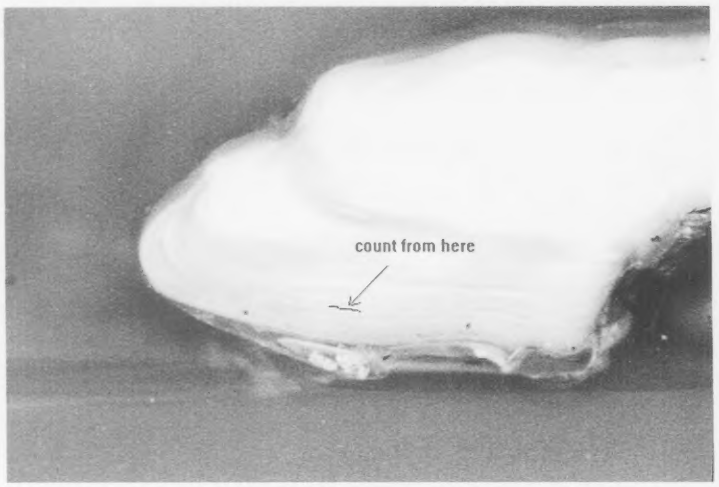

Figure 3

Example of an image of a baked sablefish otolith which has been annotated with a mark. The image is an example of one of the images provided to three researchers in order to obtain cross-reading comparisons.

Following standard age determination procedures (Chilton and Beamish, 1982), if a hyaline zone was not visible on the edge between January and March, then the edge was counted. If a mark was not visible on the edge between April and May and there was a wide opaque zone, then the edge was counted as a mark. If a mark was visible on the edge and the month was after May, the edge was not counted. This procedure is used to properly assign the fish to an annual cohort. Because the reader was not given the month of recapture, the ages were adjusted based on the count of hyaline zones, the month of recapture, and whether the edge had been counted. This adjustment provided a corrected reader count of annual marks. The corrected count was compared to the number of annual marks that would have been present if marks were laid down annually.

Previous experience suggested that there are different patterns of sablefish otolith growth. We attempted to classify and characterize these different types of growth patterns based on morphology of the otoliths as seen in cross section. After the otoliths had been examined, we developed a standard classification scheme of morphological classes and types which could be used to classify the most commonly observed morphological types. The otoliths were re-examined and reclassified to see if difficulties and discrepancies in aging were associated with morphological type. It was hoped that this process could be used to refine the aging criteria and improve precision.

Because sample size was small, we used a Fisher exact test (Agresti, 1990) to test for independence of morphological type versus tendency to over-estimate, correctly estimate, or under-estimate the number of annual marks. The columns in the test indicated whether the fish had been over-aged, correctly aged, or under-aged. The rows in the test were the four morphological types identified in this study.

Examination of the otoliths by the age readers

To determine how age readers would count the marks on the otoliths, we selected a subsample of 25 otoliths to be aged at four West Coast fisheries laboratories. The otolith selection was based on having good quality images and otoliths. The images of the baked otoliths (not the composite images) were annotated with a mark (Fig. 3). The mark was placed in a location which could be readily located on the actual otolith by the readers—on the zone just inside of the OTC mark. Readers were given the following: a set of printed images, an electronic file of the images for viewing on a computer screen, the embedded otolith, the month of capture, the size and sex of the fish from which the otolith came, and a set of instructions for examining the otoliths. Readers were not told where the mark on the image was placed in relation to where the OTC mark was in order to reduce bias from readers who may have known when the fish were injected and recaptured. Readers were asked to provide the following: the number of annual marks visible outside the mark on the image, whether the edge was counted, how confident they were of their readings, and any comments they might have.

Three readers participated in this analysis, two of whom had extensive, long-term experience in aging sablefish. The readings and age determination criteria (including edge count criteria) were compared to each other and to the time known to have passed between OTC marking and recapture.

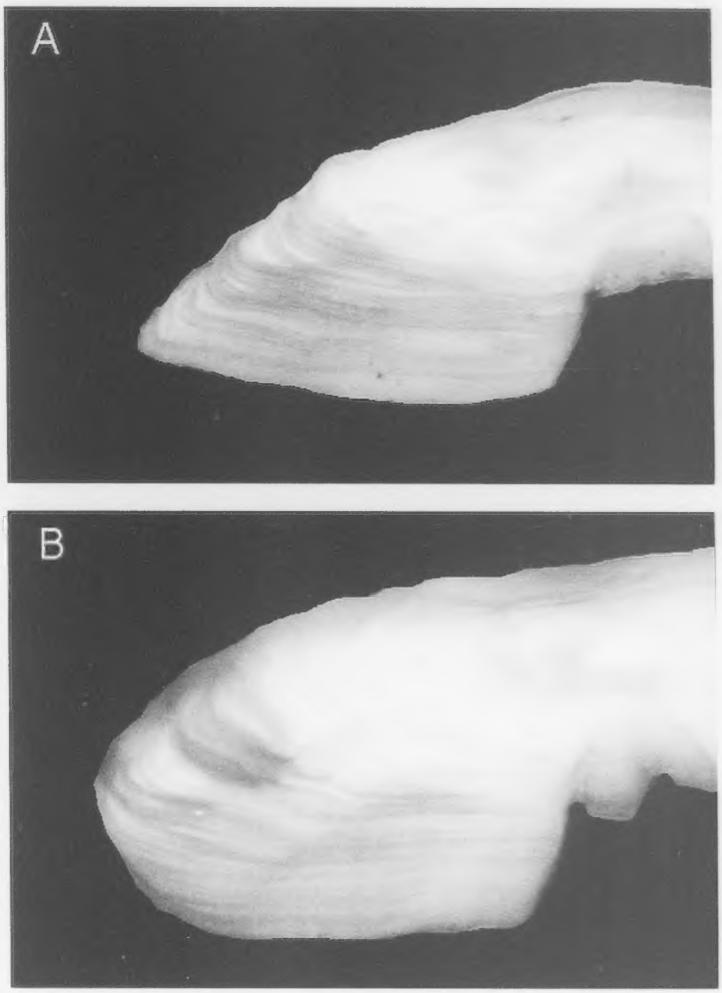

Figure 4

Images of four otolith morphological types. (**A**) Otolith is a wide type, (**B**) otolith is a wide, wedge subtype. (**C**) otolith is a thick type, and (**D**) otolith is a thick, wedge subtype.

To determine if age determination difficulties were related to sex, size, area of capture, depth of capture, or otolith morphological type; Fisher exact tests were performed. In each test, the variables were compared to whether the fish had been correctly aged, over aged, or under aged.

Results

Recoveries

A total of 2575 fish were tagged at the nine sites, and 368 tagged fish were recaptured. Of the recaptured fish, 284 had been injected with OTC. Of the 284 injected fish, usable otoliths were recovered from 191 fish; for the remaining fish, otoliths either were not recovered or were too badly damaged during removal to be used.

Otolith morphological types

After examination of all the otoliths, "wide" and "thick" morphological types were identified, and each type had a "wedge" subtype (Fig. 4). Each otolith in the study was then classified according to this scheme.

The wide type (Fig. 4A) is characterized by new growth that steadily increases cross sectional width along the dorsal and ventral surfaces. In the wedge subtype (Fig. 4B), initial growth increases the width, but the most

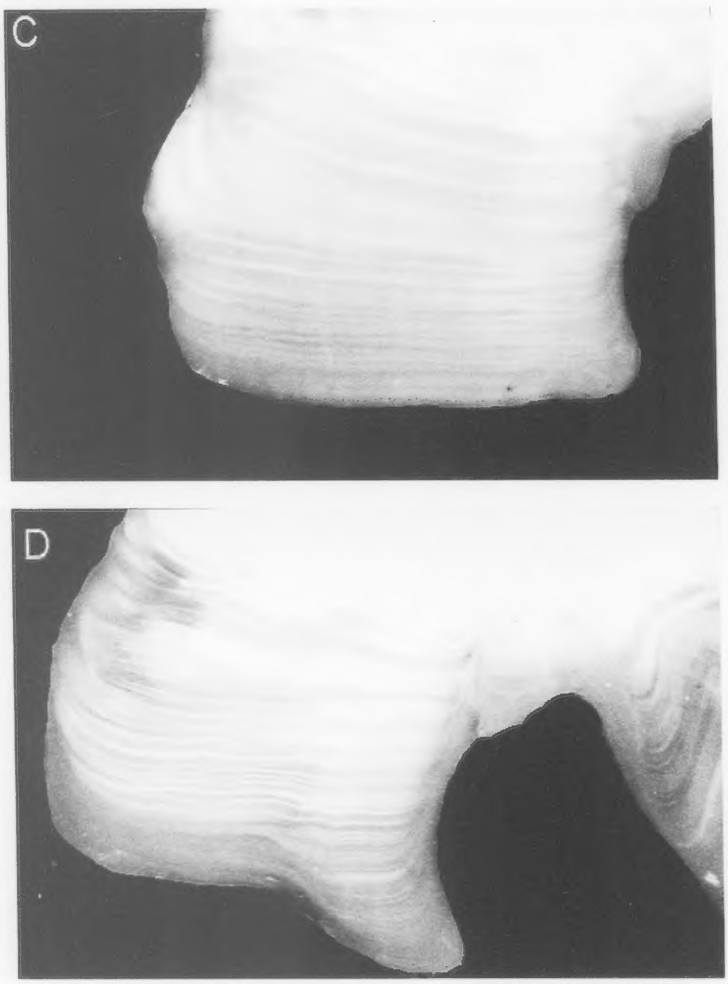

Figure 4 (continued)

recent growth is concentrated on the medial or lateral surface at the sulcus, decreasing towards the dorsal and ventral surfaces, resulting in a wedgelike appearance.

The thick type (Fig. 4C) is characterized by new growth that increases the thickness of the otolith without increasing the cross sectional width, causing the annulii to appear closely spaced on the lateral surfaces. In the wedge subtype (Fig. 4D), the most recent growth is concentrated at the sulcus and narrows towards the dorsal and ventral surfaces, forming a wedge shape.

It should be noted that these types and subtypes are not always clearly defined. It should also be noted that classification to the subtype is based on the most recent one or more hyaline zones. A wedge subtype is formed when a single hyaline zone widens near the sulcus and comes to a point at the outer edge.

Of the 191 otoliths examined, 63 (33.0%) were classified as "wide" types, 76 (39.7%) were classified as "wide, wedge subtypes," 32 (16.8%) were classified as "thick" types, 5 (2.6%) were classified as "thick, wedge subtypes,' and 15 (7.9%), could not be classified by this scheme.

Position of the OTC mark

There was no detectable OTC mark in 22 of 191 otoliths. The absence of marks appeared to be a random event, occurring in otoliths from several different recovery years and equally likely to be found among different sexes, otolith types, different depths, and locations.

Of the 169 otoliths with detectable marks, the OTC mark was found in a hyaline zone in 129 otoliths (76.3%), in an opaque zone in 36 otoliths (21.3%), and could not be reli-

Table 1

Frequency of otoliths with an OTC mark appearing on the edge versus those with the marks inside the edge. All fish were injected between September and October of 1991.

Year	Month	Mark on edge	Mark not on edge
1991	Oct	2	1
	Nov	1	3
	Dec	4	2
1992	Jan	2	4
	Feb	1	6
	Mar	7	4
	Apr	3	1
	May	7	26
	Jun	2	
	Jul	1	7
	Aug	1	4
	Sep	1	2
	Oct	5	
	Nov	3	
	Dec		

ably determined in four otoliths (2.4%) because the marks were between a hyaline and opaque zone. Of the 36 otoliths with the mark in an opaque zone, the mark occurred just after a hyaline zone in four otoliths. In 24 of the 36 otoliths with the mark in an opaque zone, the mark was on the edge where it can be difficult to determine whether it is opaque or hyaline. In no case did the reader indicate that the mark was in a hyaline zone at the edge and thus the edge appeared to be opaque in most cases.

The OTC mark occurred on the otolith edge in 30 of the otoliths recaptured prior to 1993 (up to 16 months after injection). Examination of the monthly distribution of otoliths with marks on the edge (Table 1) indicated that some fish exhibited little or no otolith growth for substantial lengths of time.

Otoliths from fish recaptured in 1992 with marks on the edge (i.e. showing little growth) were examined and classified by morphological type (Table 2). This examination indicated that the thick type is more likely to have little growth because 32% of the otoliths with marks on the edge were the thick type, yet they made up only 17% of the otoliths in the study. Conversely, only 18% of the otoliths with the mark on the edge were of the wide type; however, they made up 33% of the otoliths in the study. This trend was not statistically significant, however, because the *P*-value was 0.106.

Table 3

Number of visible hyaline zones occurring after an OTC mark on otoliths from fish recaptured in 1992. This is shown by three-month interval to show the progression of development of the hyaline zones. All fish were injected in September and October of 1991.

	No. of hyaline zones		
Interval	0	1	2
Jan–Mar	12	8	1
Apr–Jun	5	14	4
Jul–Sep	6	2	
Oct–Dec	3	1	

Number of visible hyaline zones

The number of prominent hyaline zones after the OTC mark for fish recaptured in 1992 at three-month intervals is shown in Table 3. This distribution shows the otoliths that had no detectable growth but also shows that a hyaline zone forms in many fish during the winter. It also shows that in some fish, a summer hyaline zone is formed; however, the sample size for October–December was small and this is a period when a summer hyaline zone would be expected to be fully visible.

The number of visible and prominent hyaline zones after the OTC mark for fish recaptured after 1992 (Table 4), compared with the number of zones which should have been counted, showed that if a reader had counted each of the prominent hyaline zones as an annulus, the count would have overestimated the age of the fish. An example of an otolith with a larger number of prominent hyaline zones than expected is shown in Figure 5. It should be noted that a reader would not necessarily have counted each of the

Table 2

Number of otoliths in 1992 with OTC marks on the edge by otolith morphological type. Also shown is the overall percentage of the morphological types in the present study. All fish were injected in September and October 1991.

	Otolith type							
	Wide		Wide, wedge		Thick		Thick, wedge	
	No.	Percent	No.	Percent	No.	Percent	No.	Percent
1992 otoliths	4	18	10	45	7	32	1	5
Otoliths in this study	63	33	76	40	32	17	5	3

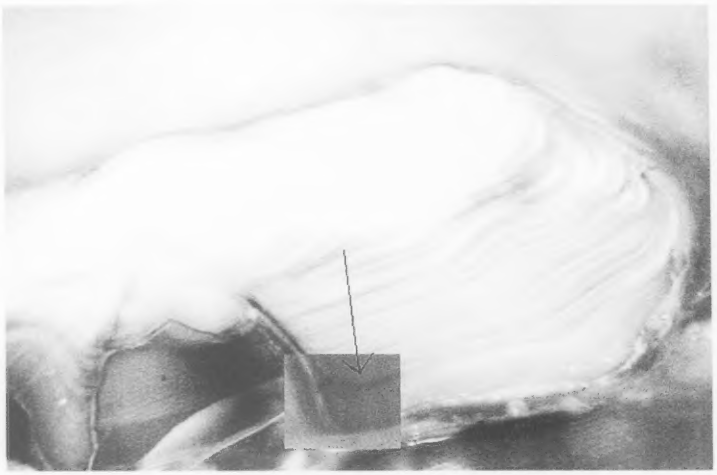

Figure 5

Image of a sablefish otolith having more prominent hyaline zones than should have been present. The fish was caught after eight months at liberty. A single hyaline zone should have formed; however, there is a zone on the edge and one midway between the dark OTC mark.

Table 4

Counts of the number of prominent hyaline zones versus the number of annual hyaline zones that should have been present after an OTC mark. These counts are for fish recaptured more than 15 months after initial capture. Agreement between counts and number of expected annual hyaline zones is shown in bold.

		No. of prominent hyaline zones										
Year	Expected number	0	1	2	3	4	5	6	7	8	9	10
1993	2	3	1	**7**	6	4	3					
1994	3	2		1	**5**	2	1	3	1			
1995	4	1				**2**		5	1	2	1	
1996	5					1	**1**		1	2		
1997	6				1			**1**	1		2	1

Table 5

Percent and number (in parentheses) of sablefish otoliths with more hyaline zones than were expected, with the expected number of hyaline zones (correct count), and with fewer hyaline zones than were expected for each otolith type.

Otolith type	More zones	Expected number of zones	Fewer zones
Thick	10.3% (3)	41.4% (12)	48.3% (14)
Thick, wedge	0 (0)	40.0% (2)	60.0% (3)
Wide	39.3% (22)	48.2% (27)	12.5% (7)
Wide, wedge	35.2% (25)	45.1% (32)	19.7% (14)

prominent hyaline zones as an annulus (they might have considered them to be checks). In many of these otoliths, there were less prominent zones that were not counted and which were interpreted as checks.

Thick type otoliths and thick, wedge subtype otoliths tend to have fewer visible hyaline zones than expected (Table 5). In contrast, wide type and the wide, wedge subtype otoliths are more likely to have more hyaline zones than expected. The Fisher exact test yielded a significant P-value of 0.001.

Blind comparisons of reader counts

A comparison of the counts of annual hyaline zones for each reader to the expected number of annual hyaline zones

Table 6

Comparison of number of annual hyaline zones counted by reader 1 versus the expected number of annual hyaline zones that should have been counted. Agreement with the expected counts are shown in bold.

	Reader 1 count						
Expected count	1	2	3	4	5	6	7
1	**2**	7	2	1			
2		**2**	4	1	1		
3		1			1		
4				**2**			
5			1				

Table 7

Comparison of number of annual hyaline zones counted by reader 2 versus the expected number of annual hyaline zones that should have been counted. Agreement with the expected counts are shown in bold.

	Reader 2 count						
Expected count	1	2	3	4	5	6	7
1		5	2	3	1	1	
2			3	2	2		1
3			**1**	1			
4						1	1
5					**1**		

Table 8

Comparison of number of annual hyaline zones counted by reader 3 versus the expected number of annual hyaline zones which should have been counted. Agreement with the expected counts are shown in bold.

	Reader 3 count						
Expected count	1	2	3	4	5	6	7
1	**10**	2					
2	2	**1**	3	1	1		
3	1	1					
4	2						
5	1						

after the OTC mark are shown in Tables 6, 7, and 8. In these tables, it is assumed that the readers should not have counted the zone in which the OTC mark occurred because that mark is presumed to have formed in the summer of 1991. Readers 1 and 2 tended to overestimate, whereas reader 3 (the least experienced age reader) had generally good agreement. Reader 1 agreed with the expected count 24% of the time, reader 2 agreed with the expected count 4% of the time, and reader 3 agreed with the expected count 44% of the time. The result for reader 3 is deceptive, however, because that reader did not follow accepted methods of when to count the edge.

Reader 1 and reader 2 agreed on whether to count the edge of the otolith in 24 of 25 otoliths (Table 9). Reader 3 agreed with reader 1 on whether to count the edge in 16 of 25 otoliths and 17 of 25 otoliths with reader 2. Had reader 3 followed accepted practice, agreement with the expected count would have been much less.

Efforts to determine what factors (depth of capture, location of capture, sex, size of the fish, and otolith morphological type) resulted in a miscount of the true number of annual marks were inconclusive. We first corrected the count for the fact that all readers counted the mark in which the OTC mark had occurred by subtracting one from their counts, and we then eliminated the readings from reader 3 because of his lack of experience and anomalous age determination criteria. Then we examined the relationship of how many otoliths had been over-aged, correctly aged, and under-aged to the above factors. Depth of capture was divided into two groups: less than 600 m and 600 or more m. Location was divided into two groups: north and south of latitude 39 north. Sizes were divided into two groups: <55 cm FL and ≥55 cm FL. And finally, we tested each of the four otolith morphological types.

We used Fisher exact tests to determine the probability that differences were due to chance alone. There were no detectable differences from the null hypothesis for depth, sex, or location of capture (Table 10); however, there was some evidence that fish length and otolith morphological type might be related to miscounting. Small fish showed a slightly greater tendency to be over counted (more rings than should have been present) than larger fish (P=0.150). Otolith morphological type showed some departure from randomness; thick types appeared to be more likely to be undercounted (fewer rings than should have been present) and wide types were more likely to be over counted (P=0.066).

Discussion

Position of mark

There was no visible mark on 22 of the 191 otoliths (11.5%). Beamish et al. (1983) reported that 14 of 129 OTC-injected fish (10.9%) had no detectable mark. They attributed this to improper handling of the fish after recapture. The similarity in the number of otoliths failing to show the OTC mark between their study and our study suggests that some portion of the population may not absorb sufficient OTC to produce a visible mark.

The finding that most of the OTC marks were in a hyaline zone is important. This indicates that many of the sablefish in our study laid down a prominent hyaline zone in the summer. Age readers who conventionally assume that an annual mark is laid down only in the winter

Table 9

Blind reading results of 25 sablefish otoliths by 3 readers. All fish had been captured and injected with OTC in September and October of 1991. The counts they provided are the number of annual marks outside of the OTC mark. "Expected count" indicates how many winter hyaline zones should have been present. The columns labeled "Edge" refer to whether or not the edge was included in the age reader's counts.

			Reader 1		Reader 2		Reader 3	
Fish ID no.	Recapture date	Expected count	Count	Edge	Count	Edge	Count	Edge
10375	4 May 92	1	2	Y	2	Y	1	N
10030	14 May 92	1	1	Y	2	Y	1	N
10267	17 May 92	1	2	Y	3	Y	1	N
10408	17 May 92	1	2	Y	2	Y	2	Y
10417	18 May 92	1	2	Y	3	Y	1	N
10630	25 May 92	1	4	Y	4	Y	1	N
12148	26 May 92	1	3	Y	4	Y	1	N
12176	26 May 92	1	2	Y	5	Y	1	N
12431	26 May 92	1	2	Y	2	Y	2	Y
10568	29 Jul 92	1	1	N	2	N	1	N
11121	1 Oct 92	1	2	N	6	N	1	N
11117	16 Oct 92	1	3	N	4	N	1	N
10400	12 Jan 93	2	3	Y	5	Y	3	Y
10370	14 Jan 93	2	4	Y	4	Y	3	Y
10870	15 Feb 93	2	2	Y	7	Y	5	Y
10246	15 Apr 93	2	3	N	3	Y	3	Y
11735	16 May 93	2	3	Y	3	Y	2	Y
11586	18 May 93	2	2	Y	4	Y	4	Y
11106	3 Aug 93	2	3	N	3	N	1	N
10617	2 Dec 93	2	5	N	5	N	1	N
10580	23 May 94	3	2	Y	4	Y	2	Y
10714	9 Dec 94	3	5	N	3	N	1	N
11516	3 Aug 95	4	4	N	7	N	1	N
11524	16 Dec 95	4	4	N	6	N	1	N
11761	25 Apr 96	5	3	Y	5	Y	3	N

Table 10

Comparison of the number of fish under counted, correctly counted, and over counted by two experienced age readers versus depth of capture, location (north or south of 39 degrees latitude), sex, fork length, and otolith morphological type. The *P*-value from the Fisher exact test is shown, indicating the level of significance.

	Under counted	Correctly counted	Over counted	*P*
Depth				
<600 meters	7	14	15	0.987
>600 meters	3	6	5	
Location				
South	4	8	10	0.606
North	3	12	7	
Sex				
Male	3	2	5	0.381
Female	7	18	15	
Length				
<55 cm	4	14	15	0.150
≥55 cm	6	6	5	
Otolith type				
Thick	4	2	2	0.066
Thick, wedge	1	1	0	
Wide	2	5	11	
Wide, wedge	3	12	7	

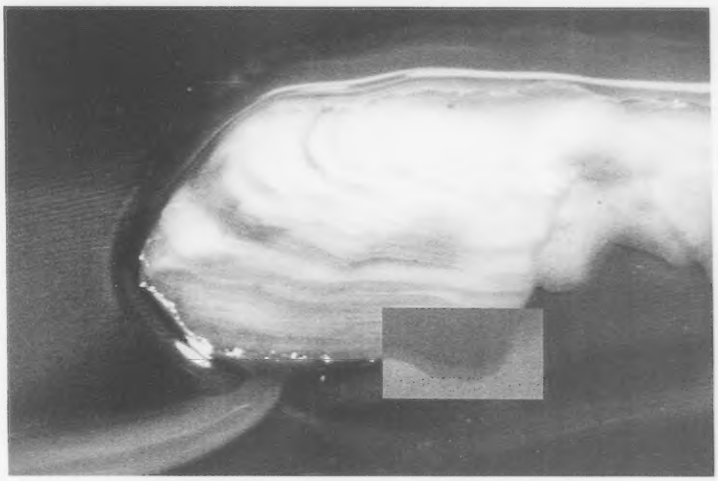

Figure 6

Image of a baked sablefish otolith with an electronically pasted section taken from an image captured under UV light. The dark OTC mark is clearly located within a hyaline zone, and the hyaline zone persists through the entire otolith. The fish was injected with OTC on 5 October 1991.

would probably mis-age these fish. Because the age readers who examined the otoliths without knowledge of the recapture information were not informed that the point they were counting from was just inside the summer mark, it was interesting to note that all three of them counted the hyaline zone in which the OTC mark had occurred as an annual hyaline zone in all cases. In other words, the summer hyaline zone did not appear to be a check to the readers. The readers indicated that the manner of preparation of the otoliths (embedded and baked) was not the manner in which they were accustomed to view otoliths and may have influenced their results. The fact that the hyaline zones were not as dark with the baking method as opposed to the burning method may have influenced the readers age estimates; however, some otolith burns can be quite light and experienced readers recognize the various levels of burning, particularly when cross reading otoliths from other age readers. Readers sometimes use multiple sections and are free to manipulate the otolith to improve viewing, which was not possible in the present study. Beamish et al. (1983) indicated that when readers knew how many marks to look for, they were able to identify false annual marks (checks). According to their study, a check is not persistent throughout the otolith. In Figure 6, the hyaline zone in which the OTC mark appeared clearly persists throughout the otolith. If the hyaline zone which contained the OTC mark began to be laid down in the winter, then there would be very little time for the formation of a wide opaque zone to form after injection in the fall. Because the age readers counted the hyaline zone in which the OTC mark occurred, they clearly assumed that it was not a check. If the age readers had known that the hyaline zone (in which the OTC mark occurred) had formed in the summer, then they presumably would not have counted it. It is therefore of interest to see the effect on agreement between reader counts minus the hyaline zone where the OTC mark occurred and the actual number of hyaline zones that should have been present. When we adjusted the reader counts by subtracting one year from their original counts and compared their adjusted counts to the expected number of annual marks (Table 11), agreement for readers 1 and 2 improved, whereas it decreased for reader 3 (the least experienced reader).

Also of importance is the fact that on some otoliths, even after eight months at liberty, no growth had occurred, as evidenced by the fact that the OTC mark was on the edge. For example, otoliths from two fish, recaptured after eight months at liberty showed marked differences in otolith growth (Fig. 7). On otolith A there was no detectable growth with the OTC mark on the edge, whereas on otolith B there was substantial growth. The OTC marks on both otoliths were very prominent. These otoliths came from similar fish; that is, otolith A came from a 597-mm female fish caught in 680 meters of water at 40°52′ latitude, and otolith B came from a 610-mm female fish caught in 480 meters of water at 41°54′ latitude. This provides strong evidence that otolith growth, and presumably fish growth, varies greatly among individual sablefish. Beamish et al. (1983) reported that the OTC mark was on or near the edge in 28 otoliths (18.1%) of 154 fish which had been at liberty for two to three years. In a similar time interval, we found that 34 of 126 (27.0%) had the OTC marks on or near the edge. Both the finding of a summer hyaline zone and the differences in growth of the otolith among individual fish

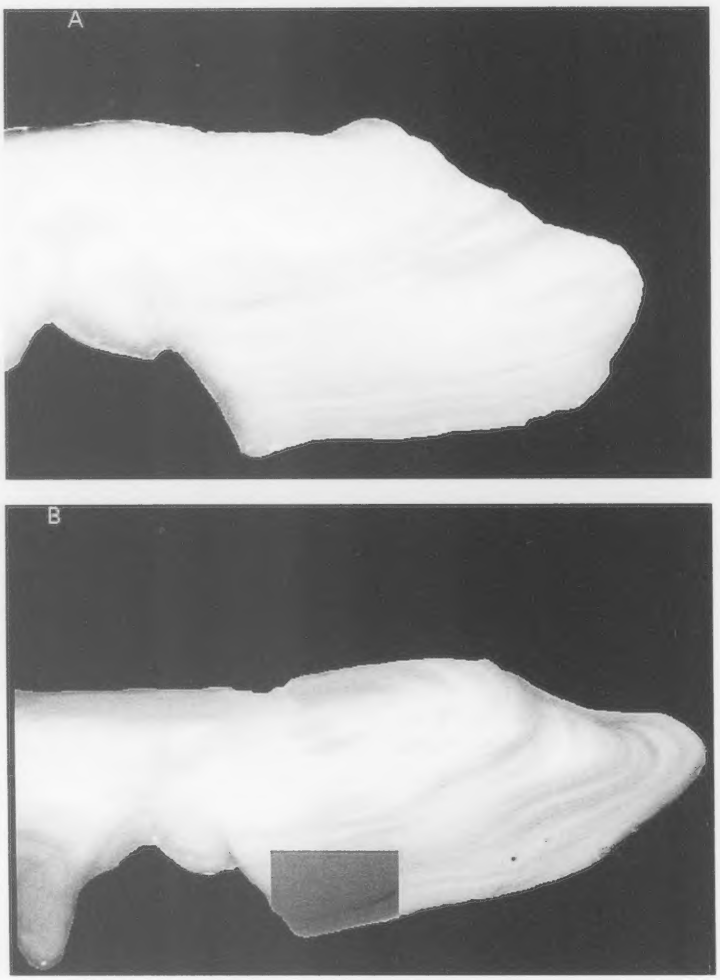

Figure 7

Images of otoliths from two sablefish showing differences in otolith growth rate. Both fish were injected with OTC in early October of 1991 and were recaptured in May of 1992. (**A**) Otolith was from a 597-mm female caught in 680 meters of water at 40°52′ latitude. (**B**) Otolith was from a 610-mm female fish caught in 480 meters of water at 41°52′ latitude. The OTC mark in A was on the edge, whereas the position of the OTC mark in B is shown on the insert.

are important factors in developing reliable and consistent age determination criteria.

The importance of using the same age determination criteria among readers cannot be overestimated. In the blind comparison, the readers were asked whether they had included the edge in their count of annual zones. With standard age determination methods, if no hyaline material is visible on the edge up to about May, then the edge is counted. This procedure is based on the assumption that a zone is in the process of forming but is not yet clearly visible. On the other hand, if hyaline material is observed on the edge after May, it is not counted because it is assumed to be either a check or the beginning of the next winter's hyaline zone. Reader 1 and reader 2 (the two most experienced age readers) agreed on whether to count the edge 96% of the time, indicating that they were using the same criteria. Reader 3, however, agreed with reader 1 only 64% of the time and with reader 2 only 68% of the time which suggests that reader 3 was using different edge-interpretation criteria.

Table 11

Percent agreement between number of hyaline zones counted by three age readers and the number which should have been present. Also shown is the effect of removing the count of a hyaline zone which formed in the summer and which should not have been counted as an annual mark.

Reader 1		Reader 2		Reader 3	
Original	Corrected	Original	Corrected	Original	Corrected
24%	44%	4%	36%	44%	20%

Effect of ages on stock assessments

Crone et al. (1997) noted that one of the problems with stock assessments of sablefish is that the size at 50% sexual maturity is between 55 and 67 cm (age 5–7) and that there is considerable variability in the these estimates. Further, they noted that there has been difficulty in determining age-specific selectivity because of problems with the ages used in previous assessments. Crone et al. (1997) further noted that there is a considerable discrepancy in ages among the age determination laboratories on the west coast. Finally, the model used to perform stock assessments has estimated that in order to obtain a good fit with the data, the actual level of aging error should be higher than has been reported. The lack of reliable age data has been used to criticize stock assessments.

Age and length at sexual maturity has been found to vary substantially by depth (Fujiwara and Hankin, 1988a). Fujiwara and Hankin found that both males and females had a length of 550 mm for the length at 50% sexual maturity in shallow water (<600 meters). In depths greater than 600 m, the size at 50% sexual maturity was 450 mm for males and 500 mm for females. To determine age, they used sectioned otoliths and methods that may not have been directly comparable to the methods used in other studies or the methods used in the present study; nonetheless, they found that both males and females matured at a younger age in deeper water. Saunders et al. (1997) also reported differences in length at maturity related to depth and location of capture. Methot[1] found that ontogenetic movement into deeper water for spawning was more closely related to age than size. If sexual maturity is more closely related to age than length as suggested by Methot, then unreliable ages may explain the variable maturity schedule for sablefish. In our study, fish were captured over a 900 nmi range at depths from 200 to more than 1000 m. If depth is related to growth of sablefish, then it is possible that the different morphometric types of otoliths observed in our study may also be a function of depth. If depth is responsible for the morphological types, it also suggests that reliability of ages may be a function of the depth at which the sablefish are found. Further, if depth influences growth, a fish which changes its depth over time, may exhibit different patterns of growth throughout its life which would further complicate the problem of determining reliable ages.

Potential sources of error in this study

This study used sablefish caught in the southern part of the sablefish range. Many species show latitudinal variation in growth (June and Reintjes, 1959; White and Chittenden, 1977; Leggett and Carscadden, 1978; Shepherd and Grimes, 1983; Pearson and Hightower, 1991). It is possible that the results of this study do not apply to the northern portion of their range.

Another potential source of error in our study is the effect of tagging on the growth of the sablefish. MacFarlane and Beamish (1990) found that tagged sablefish grew slower than untagged fish. If this is true, then the results of this study are much more difficult to interpret. MacFarlane and Beamish did not use OTC and as a result they based their ages on conventional aging methods. If they had injected the fish, it would have been interesting to note whether the ages for the fish in their study would have been interpreted differently. If fish do grow differently after tagging, many age, growth, and validation studies will need to be re-evaluated.

Conclusion

Obtaining accurate ages, with reasonable precision, for sablefish is very difficult. Previous aging studies of sablefish have obtained results similar to ours, even when the readers knew how many annual marks should have been present (Beamish et al. 1983; MacFarlane and Beamish, 1995). We found that some fish lay down two marks a year and others may not lay down any. We also found that certain morphological types of otoliths may be indicative of slow growing fish and others may be indicative of rapidly growing fish (assuming otolith growth relates to fish growth).

The fact that agreement among readers or with the correct age consistently ranges between 30% and 45% suggests that this imprecision may be inherent in sablefish aging. A substantial fraction of the population may not be able to be reliably aged: some otoliths do not appear to grow and others grow very rapidly, laying down prominent summer hyaline zones that even experienced age readers cannot differentiate from winter hyaline zones.

[1] Methot, R. D. 1995. Geographic patterns in growth and maturity of female sablefish off the U.S. west coast. Unpubl. manuscript, 39 p. NOAA, NMFS, Northwest Fisheries Science Center, Seattle, WA.

We believe the wide type and wide, wedge subtypes are often over-aged, and the thick type and thick, wedge subtypes are occasionally under-aged and further propose that readers be made aware that a hyaline zone typically forms in the winter, but that it is not uncommon for a second mark to form in the summer.

Another, less desirable approach, would be for age readers to record the morphological type of otolith as a routine part of aging. Users of the data could then incorporate this information into their studies by using a correction factor for fish likely to be under-aged and for fish likely to be over-aged. This factor could be in the form of an aging error matrix as suggested by Heifetz et al. (1999). This approach may not be practical until more data are available on the true effect on ages for the morphological types described in this study, including how many years would need to be added or subtracted for each type. Finally, a more complete description of the morphological types would be needed to assist the age readers.

Acknowledgments

We would like to express our gratitude to Delsa Anderl (Alaska Fisheries Science Center), Kristin Munk (Alaska Department of Fish and Game), Shayne MacLellan (Pacific Biological Station, Canadian Department of Fisheries and Oceans), and Bruce Pederson (Oregon Department of Fish and Wildlife) for participating in the otolith blind reading component of this paper. We would also like to thank Dan Kimura and Craig Kastelle of the Alaska Fisheries Science Center for their assistance in developing the design of this study. We would like to thank Michael Mohr (Southwest Fisheries Science Center, Santa Cruz, CA) for his valuable contribution to the statistical analyses used in this study. This study could not have been completed without the support of Gary Stauffer (Alaska Fisheries Science Center) who provided funding for the recovery of the sablefish. Additionally, this study would never have been completed without the assistance of numerous commercial market samplers, port biologists, commercial fishermen, and dealers who were responsible for collecting and processing the sablefish when they were caught. And finally, we would like to thank William Lenarz (Southwest Fisheries Science Center, retired) for his support of this study.

Literature cited

Agresti, A.
1990. Categorical data analysis, 558 p. Wiley, New York, NY.

Beamish, R. J., G. A. MacFarlane, and D. E. Chilton.
1983. Use of oxytetracycline and other methods to validate a method of age determination for sablefish. *In* Proceedings of the second international sablefish symposium, p. 95–116. Alaska Sea Grant Rep. 83-8, Univ. Alaska, Fairbanks, AK.

Chilton, D. E., and R. J. Beamish.
1982. Age determination methods for fishes studied by groundfish program at the Pacific Biological Station. Can Spec Publ. Fish. Aquat. Sci. 60:19–22.

Crone, P. R., R. D. Methot, R. J. Conser, R. R. Lauth, and M. E. Wilkins.
1997. Status of the sablefish resource off the U.S. Pacific Coast in 1997. Appendix G *in* Status of the Pacific Coast groundfish fishery through 1997 and recommended acceptable biological catches for 1998, 135 p. Pacific Fisheries Management Council 1998.

Fujiwara, S., and D. G. Hankin.
1988a. Sex ratio, spawning period, and size and age at maturity of sablefish Anoplopoma fimbria off northern California. Nippon Suisan Gakkaisha 54(8):1333–1338.
1988b. Aging discrepancy related to asymmetrical otolith growth for sablefish *Anoplopoma fimbria* in northern California. Nippon Suisan Gakkaishi 54(1):27–31.

Heifetz, J., D. Anderl, N. E. Maloney, and T. L. Rutecki.
1999. Age validation and analysis of aging error from marked and recaptured sablefish, *Anoplopoma fimbria*. Fish. Bull. 97:256–263.

Hunter, J. R., B. J. Macewicz, and C. A. Kimbrell.
1989. Fecundity and other aspects of the reproduction of sablefish, *Anoplopoma fimbria*, in central California waters. CalCOFI Rep. 30, 1989, p. 61–72.

June, F. C., and J. W. Reintjes.
1959. Age and size composition of the menhaden catch along the Atlantic coast of the United States, 1952–55: with a brief review of the commercial fishery. U.S. Fish and Wildl. Serv., Spec. Sci. Rep. Fish. 317, 65 p.

Kastelle, C. R, D. K. Kimura, A. E. Nevissi, and D. R. Gunderson.
1994. Using Pb-210/Ra-226 disequilibria for sablefish, *Anoplopoma fimbria*, age validation. Fish. Bull. 92:292–301.

Kimura, D. K., and J. J. Lyons.
1991. Between-reader bias and variability in the age determination process. Fish. Bull. 89:53–60.

Lai, H. L.
1985. Evaluation and validation of age determination for sablefish, pollock and yellowfin sole; optimum sampling design using age-length key; and implications of aging variability in pollock. Ph.D. diss., 426 p. Univ. Washington, Seattle, WA

Laidig, T. E., P. B. Adams, and W. M. Samiere.
1998. Feeding habits of sablefish, *Anoplopoma fimbria*, off the coast of Oregon and California. NOAA Tech. Rep NMFS 130:65–79.

Leet, W. S., C. M. Dewees, and C. W. Haugen.
1992. California's living marine resources and their utilization. Calif. Seagrant Publication UCSGEP-92-12, 257 p. Univ. California Davis, Davis, CA.

Leggett, W. C., and J. E. Carscadden.
1978. Latitudinal variation in reproductive characteristics of American shad (*Alosa sapidissima*): evidence for population specific life history strategies in fish. J. Fish. Res. Board Can. 35:1469–1478.

Macfarlane, G. A., and R. J. Beamish.
1990. Effect of an external tag on growth of sablefish (*Anoplopoma fimbria*), and consequences to mortality and age at maturity. Can. J. Fish. Aquat. Sci. 47:1551–1557.
1995. Validation of the otolith cross-section method of age determination for sablefish (*Anoplopoma fimbria*) using oxytetracycline. *In* Recent developments in fish otolith research (D. H. Secor, J. M. Dean, and S. E. Campana, eds.), p. 319–329. Univ. South Carolina Press, Columbia, SC.

Miller, D. J., and R. N. Lea.
1972. Guide to the coastal marine fishes of California. CDFG (Calif. Dep. Fish and Game) Fish Bull. 157, 249 p.

Parks, N. B., and F. R. Shaw.
1994. Relative abundance and size composition of sablefish

(*Anoplopoma fimbria*) in the coastal waters of California and southern Oregon, 1984–1991. NOAA Tech. Memo NMFS-AFSC-35, 38 p.

Pearson, D. E., and J. E. Hightower.
1991. Spatial and temporal variability in growth of widow rockfish (*Sebastes entomelas*). NOAA Tech. Mem. NOAA-TM-NMFS-SWFSC-167, 43 p.

PFMC (Pacific Fishery Management Council).
1999. Status of the Pacific Coast groundfish fishery through 1999 and recommended acceptable biological catches for 2000, 232 p. Pacific Fishery Management Council, Portland, Oregon.

Saunders, M. W., B. M. Leaman, G. A. McFarlane.
1997. Influence of ontogeny and fishing mortality on the interpretation of sablefish, *Anoplopoma fimbria*, life history. NOAA Tech Rep. NMFS 130:81–92.

Shepherd, G., and C. B. Grimes.
1983. Geographic and historic variations in growth of weakfish, *Cynoscion regalis*, in the middle Atlantic bight. Fish. Bull. 81:4:803–813.

White, M. L., and M. E. Chittenden.
1977. Age determination, reproduction, and population dynamics of the Atlantic croaker, *Micropogonius undulatus*. Fish. Bull. 75:109–123.

Growth, mortality, and hatchdate distributions of larval and juvenile spotted seatrout (*Cynoscion nebulosus*) in Florida Bay, Everglades National Park

Allyn B. Powell
Robin T. Cheshire
Elisabeth H. Laban
National Ocean Service
National Oceanic and Atmospheric Administration
Center for Coastal Fisheries and Habitat Research
101 Pivers Island Road
Beaufort, North Carolina 28516
E-mail address (for A. B. Powell): allyn.powell@noaa.gov

James Colvocoresses
Patrick O'Donnell
Florida Fish and Wildlife Commission
Florida Marine Research Institute
2796 Overseas Highway, Suite 119
Marathon, Florida 33050

Marie Davidian
Room 209, Patterson Hall
2501 Founder's Drive
North Carolina State University
Raleigh, North Carolina 27695

Abstract—Life history aspects of larval and, mainly, juvenile spotted seatrout (*Cynoscion nebulosus*) were studied in Florida Bay, Everglades National Park, Florida. Collections were made in 1994–97, although the majority of juveniles were collected in 1995. The main objective was to obtain life history data to eventually develop a spatially explicit model and provide baseline data to understand how Everglades restoration plans (i.e. increased freshwater flows) could influence spotted seatrout vital rates. Growth of larvae and juveniles (<80 mm SL) was best described by the equation $\log_e$ *standard length* = −1.31 + 1.2162 ($\log_e$ *age*). Growth in length of juveniles (12–80 mm SL) was best described by the equation *standard length* = −7.50 + 0.8417 (*age*). Growth in wet weight of juveniles (15–69 mm SL) was best described by the equation $\log_e$ *wet-weight* = −4.44 + 0.0748 (*age*). There were no significant differences in juvenile growth in length of spotted seatrout in 1995 between three geographical subdivisions of Florida Bay: central, western, and waters adjacent to the Gulf of Mexico. We found a significant difference in wet-weight for one of six cohorts categorized by month of hatchdate in 1995, and a significant difference in length for another cohort. Juveniles (i.e. survivors) used to calculate weekly hatchdate distributions during 1995 had estimated spawning times that were cyclical and protracted, and there was no correlation between spawning and moon phase. Temperature influenced otolith increment widths during certain growth periods in 1995. There was no evidence of a relationship between otolith growth rate and temperature for the first 21 increments. For increments 22–60, otolith growth rates decreased with increasing age and the extent of the decrease depended strongly in a quadratic fashion on the temperature to which the fish was exposed. For temperatures at the lower and higher range, increment growth rates were highest. We suggest that this quadratic relationship might be influenced by an environmental factor other than temperature. There was insufficient information to obtain reliable inferences on the relationship of increment growth rate to salinity.

Manuscript approved for publication 23 June 2003 by Scientific Editor.
Manuscript received 20 October 2003 at NMFS Scientific Publications Office.
Fish. Bull. 102:142–155 (2004).

The spotted seatrout (*Cynoscion nebulosus*) is an important recreational fish in Florida Bay and spends its entire life history within Florida Bay (Rutherford et al.,1989). The biology of adult spotted seatrout in Florida Bay is well known (Rutherford et al., 1982, 1989), as are the distribution and abundance of juveniles in the bay, including a description of the juvenile habitats and their diets (Hettler, 1989; Chester and Thayer, 1990; Thayer et al., 1999; Florida Department of Environmental Protection[1]). The temporal and spatial distribution and abundance of larval spotted seatrout in Florida Bay and adjacent waters, and the spatial and temporal spawning habits of these larvae also have been determined (Powell et al., 1989; Rutherford et al., 1989; Powell, 2003).

The early life history of spotted seatrout in other south Florida estuaries also has been well documented. Peebles and Tolley (1988) described the distribution, growth, and mortality of larval spotted seatrout in Naples and Fakahatchee Bays, and McMichael and Peters (1989) described the size distribution, growth, spawning, and diet of spotted seatrout in Tampa Bay.

Information on growth and mortality of larval and juvenile spotted seatrout in Florida Bay is lacking. Research on these topics would enhance our understanding of the entire life history of this valuable species, and in particular aid in eventually developing a spatially explicit model for spotted seatrout that is highly desired by the Program Management Committee for the South Florida Ecosystem Restoration Prediction and Modeling Program. In addition, these life history studies could help clarify juvenile growth and survival and provide needed information for the restoration

[1] Florida Department of Environmental Protection. 1996. Fisheries-independent-monitoring program, 1995 annual report, 58 p. Florida Department of Environmental Protection, Florida Marine Research Institute, 100 8th Avenue SE, St. Petersburg, FL 33701.

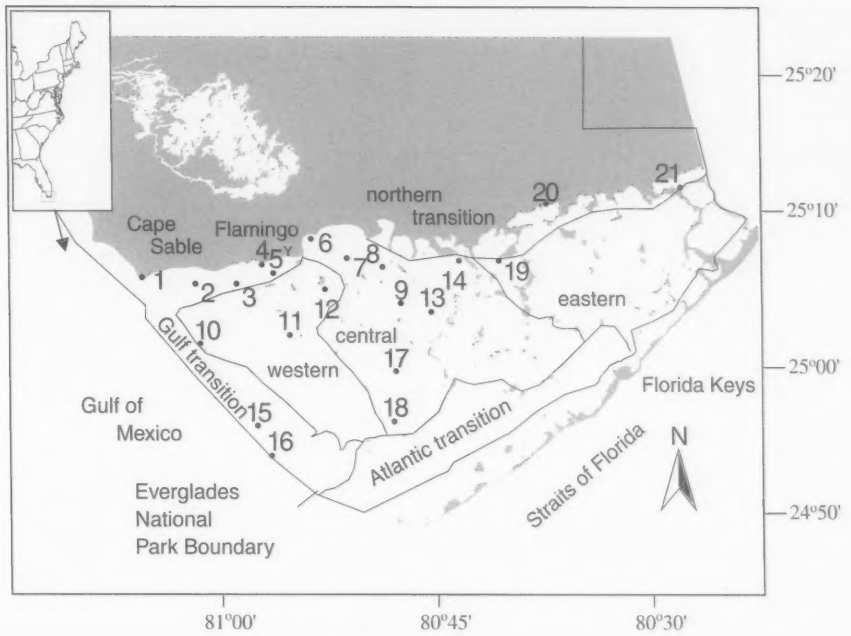

Figure 1

Location of sampling sites for spotted seatrout (*Cynoscion nebulosus*) in Florida Bay, Everglades National Park, Florida, including Florida Bay Subdivisions.

of the Everglades, including a return of historic freshwater flows into Florida Bay.

Two conceptual frameworks have been advanced to couple the role of growth and mortality in influencing cohort dynamics. Anderson (1988), in a review of hypotheses relating survival of prerecruits to recruitment, advocated a growth-mortality hypothesis as a rational framework for early life history studies that address recruitment variability. This concept predicts that survival of a cohort is directly related to growth rates during the early life stages. The growth-mortality framework, which includes several important integrated components and is based on bioenergetic principles of growth and ecological theory that predict growth rate, is directly related to survival. If it can be demonstrated that survival is a function of growth during the early life stage, then a valuable tool becomes available for examining mechanisms influencing recruitment of marine fishes.

Another framework suggests that the mortality rate does not operate alone in determining stage-specific survival, but it is the mortality:growth (M:G) ratio (mortality per unit of growth) that determines stage-specific survival (see citations in Houde, 1997). Houde (1997) advanced the idea of using the M:G ratio as an estimator of production and potential survivorship especially in early life stages when both mortality and growth are high and variable. This concept was partly based on the strong coupling of growth and mortality demonstrated by Ware (1975) who argued that when growth rate is poorer than average, larvae would be exposed to sources of mortality over a longer period and hence their mortality rate would increase. Growth and mortality values for successive cohorts would tend to form a cluster of points around a regression of mortality on growth based on average values for a particular species.

Our intent is not to test the growth-mortality hypothesis (*sensu* Hare and Cowen, 1997) as outlined by Anderson (1988), nor fully to develop the M:G ratio concept (Houde, 1997), but rather to use these concepts as a framework for our study. The major goal is to provide information on growth and survival of larval and, mainly, juvenile spotted seatrout that can ultimately be used to develop a spatially explicit model that can be linked to Everglades restoration activities. Therefore, the major objectives of this paper are 1) to determine overall growth rates of larval and juvenile spotted seatrout in Florida Bay; 2) to determine and compare juvenile growth rates geographically; 3) to estimate natural mortality rates of juveniles; 4) to estimate hatchdate distributions; 5) to compare cohort growth and mortality rates and G:M ratios for juveniles; and 6) to evaluate the effects of salinity and temperature on otolith growth—a surrogate for somatic growth.

Methods and materials

Field collections

Larval fish used for otolith microstructure analysis were collected from September 1994 through July 1997, mainly in the Gulf transition, western, and central subdivisions (Table 1, Fig. 1). These subdivisions designated by the

Table 1

Florida Bay sampling stations where otoliths from spotted seatrout were collected. Included are numbers (n) of larvae and juveniles used in the otolith microstructure analysis, and subdivisions as defined by the South Florida Ecosystem Restoration Prediction and Modeling Program, Program Management Committee.

Station number	Latitude (degrees and minutes)	Longitude (degrees and minutes)	Florida Bay subdivisions	Location	Juveniles (n)	Larvae (n)
1	25 06.81	81 05.27	Gulf transition	Cape Sable	—	4
2	25 06.37	81 01.42	Gulf transition	Middle Ground	1	10
3	25 06.40	80 58.58	Gulf transition	Conchie Channel	—	4
4	25 07.70	80 56.90	Gulf transition	Bradley Key	119	—
5	25 07.12	80 56.07	western	Murray Key	4	8
6	25 08.11	80 50.95	central	Snake Bight	3	—
7	25 09.45	80 53.42	central	Snake Bight	4	—
8	25 07.50	80 48.51	central	Rankin Lake	12	—
9	25 05.06	80 47.30	central	Roscoe Key	20	—
10	25 02.30	81 .1.12	Gulf transition	Sandy Key	49	—
11	25 02.90	80 55.00	western	Johnson Key Basin	125	—
12	25 06.00	80 52.50	western	Palm Key Basin	110	—
13	25 04.50	80 45.15	central	Whipray Basin	2	62
14	25 08.00	80 43.20	central	Crocodile Point	9	—
15	24 56.70	80 57.20	Gulf transition	Schooner Bank	2	—
16	24 54.70	80 56.31	Gulf Transition	Sprigger Bank	—	8
17	25 00.40	80 47.68	central	Sid Key Bank	6	—
18	24 57.03	80 47.52	central	Twin Key Basin	6	—
19	25 07.98	80 40.48	eastern	Madeira Point	1	—
20	25 11.85	80 37.15	northern	Little Madeira Bay	8	—
21	25 13.00	80 27.80	eastern	Shell Key	5	—

South Florida Ecosystem Restoration Prediction and Modeling Program, Program Management Committee, were based on modifications of the benthic mollusc community (Turney and Perkins, 1972). In 1994 and 1995, we used 60-cm bongo nets fitted with 0.333-mm mesh fished from the port side of a 5.4-m boat. Beginning in 1996, we used a paired 60-cm bow-mounted push net with 0.333-mm mesh nets similar to that described by Hettler and Chester (1990).

Juvenile spotted seatrout were obtained from monitoring programs established by the NOAA Center for Coastal Fisheries and Habitat Research (NOAA) and Florida Marine Research Institute (FMRI). NOAA collections were made from May 1995 through September 1997. Juveniles were collected with an otter trawl towed between two 5-m boats. The otter trawl measured 3.4 m (headrope) and was fitted with a 3.2-mm mesh tailbag with 6-mm mesh. FMRI collections were made in 1995 with a seine and a trawl. The 21.4-m center-bag drag seine was fitted with a 1.8 m × 1.8 m × 1.8 m bag of 3.2-mm mesh. The 6.1-m (headrope) otter trawl was fitted with a body of 38.1-mm stretch mesh and a 3.2-mm mesh tailbag. The majority of juveniles (86%) from NOAA and FMRI collections were collected in 1995.

Otolith microstructure analysis

Otolith processing Otolith removal and preparation generally followed the methods of Secor et al. (1991). All otoliths, except for the right sagitta, were mounted on a slide with mounting media and archived. The right sagittal otolith was embedded for transverse sectioning or polishing (or both). The left sagitta was embedded for transverse sectioning if the right was damaged. Sagittae were read with a light microscope at 1000× magnification under oil immersion. The first increment was determined as that following the core increment; which was defined as a well-defined dark increment surrounding the core (Powell et al., 2000). Two blind counts of increments were made by one reader and if the counts differed by more than 5, then the otolith was read again. If the counts were within the acceptable range, the two counts were averaged. Based on a previous validation study (Powell et al., 2000), 2.5 days were added to the increment counts to obtain the daily age. A total of 582 sagittal otoliths were aged. This total included 96 from larval collections from September 1994 through July 1997, 139 juveniles from NOAA collections from June 1995 through September 1997, and 347 from FMRI collections from June 1995 through December 1995.

Increment widths were measured on 347 otoliths from FMRI collections (1995) by using image analysis. The measuring path consisted of two segments: a ventral path from the core to the 21st increment and a ventral-medial path along the sulcus, from the 21st increment to the edge (Fig. 2). The 21st increment was selected as the transition point in these measuring paths by test reading 30 otolith sections representing the entire range of sample fish

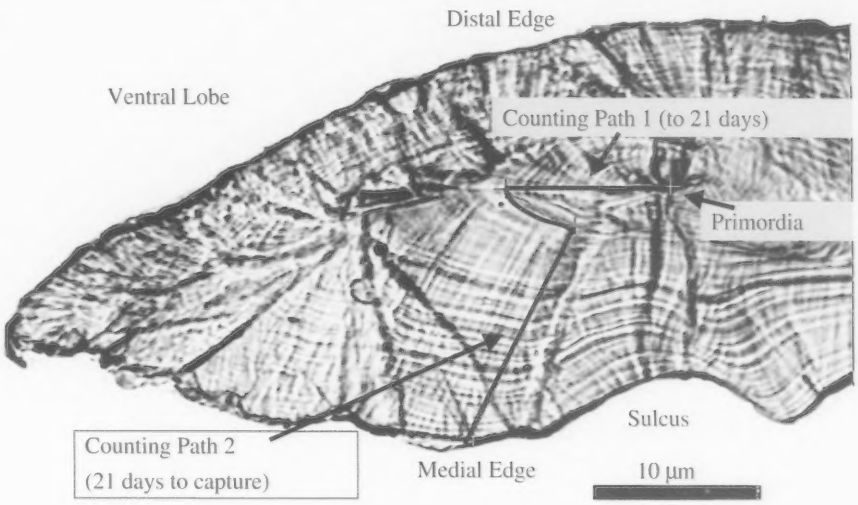

Figure 2

Transverse polished section of a spotted seatrout (*Cynoscion nebulosus*) (18 mm SL; age 48 days) otolith showing the counting paths.

lengths. In all samples, the 21st increment could easily be traced in both measuring paths and in all samples the first 21 increments could be measured within the same image. Increment widths were averaged over a 7-day period. Age estimates were also obtained and we eliminated any otolith used to measure increment widths if the difference in total increment count between the two methods (counts obtained directly from the microscope versus those attained by image analysis) was greater than 7 days or 10%. On this basis, 117 otoliths were removed from the increment width analysis.

We believed counts obtained directly from the microscope were more accurate than those obtained by summing the number of increments measured on the computer monitor with the image analysis system. Counting increments directly through the microscope lens allows the reader to optically section the otolith (by varying the focus), which helps in detecting daily increments. "Frozen" multiple images are a result of using the image analysis; hence optical sectioning is not possible.

Data analysis Data from all years and sources were used for 1) overall growth (i.e. larval and juvenile); 2) juvenile growth; and 3) estimates of juvenile mortality. Data from NOAA larval and juvenile collections were used to estimate a body-length–otolith-radius relationship. Data from 1995 FMRI and NOAA collections, which was the most complete data set, were used for growth comparisons between cohorts, and hatchdate distributions. Data from 1995 FMRI collections were used for 1) growth comparisons between geographical subdivisions; 2) estimating a wet-weight–age relationship to compute the ratio of wet-weight specific-growth to mortality (G:M ratios), which assesses the relative recruitment potential of individual cohorts (Houde, 1996; Rilling and Houde, 1999; Rooker et al., 1999); and 3) determining the influence of temperature on otolith increment width. We used the FMRI data set exclusively for the above analyzes because collections were spatially more localized and wet weights were available.

Natural mortality (M) estimates were derived by regressing $\log_e$ unadjusted numbers on age classes (5-day bins); the resulting slope provided an estimate of total mortality (Ricker, 1975). However, on the basis of the age-frequency distributions (Fig. 3), we considered juveniles ≥40 days old fully recruited to our gear and juveniles ≥90 days old appeared to avoid our gear. Hence, only juveniles between 40 and 90 days old were used to calculate mortality.

Hatchdate distributions were computed on a weekly basis and adjustments for mortality were made on individual juveniles by the equation

$$N_o = N_t / e^{-Zt},$$

where N_0 = estimated number at hatching;
N_t = number at time t (N_t=1 because N_0 was calculated for each individual fish);
Z = instantaneous daily mortality coefficient; and
t = age in days.

Spotted seatrout cohorts were divided into weekly units, but comparisons between cohort growth was done on a monthly basis because of inadequate numbers for weekly comparisons. A test of heterogeneity of slopes was imple-

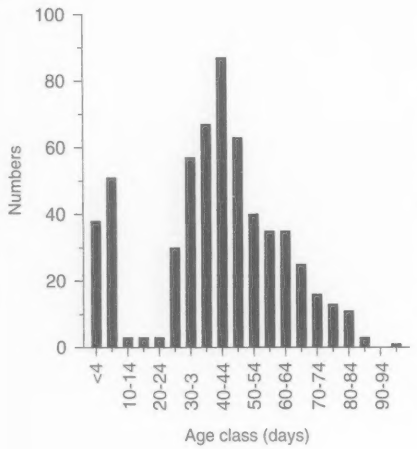

Figure 3

Frequency distribution of spotted seatrout (*Cynoscion nebulosus*) age classes used in determining minimum age at full recruitment to the sampling gear, and mortality.

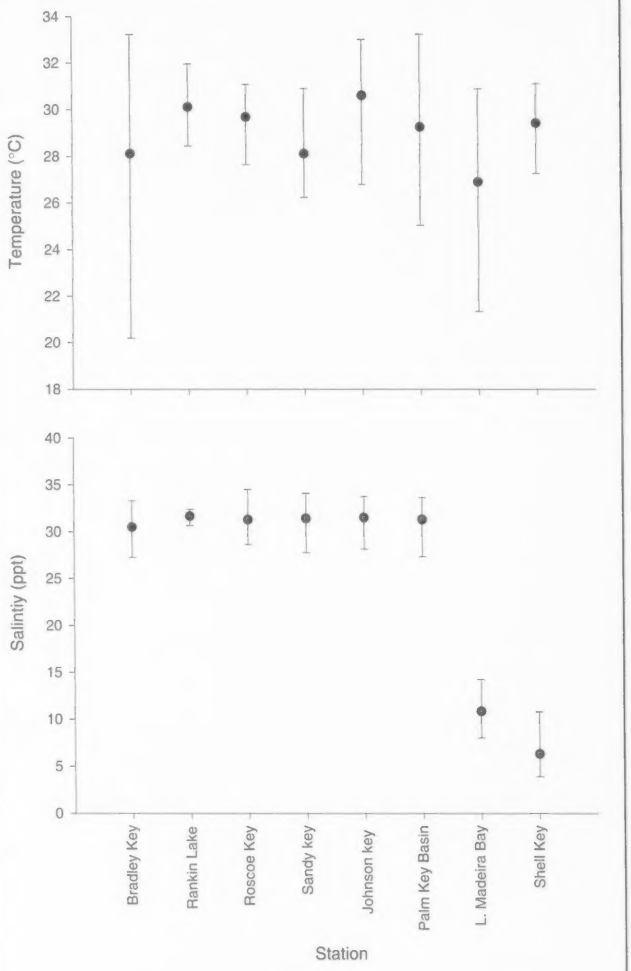

Figure 4

Mean and ranges of temperature and salinity data by station used in the otolith microstructure longitudinal analysis (relationship between increment width and temperature and salinity). For station locations relative to subdivisions, see Table 1 and Figure 1.

mented by using a generalized linear model (SAS/STAT software, version 6.12, SAS Institute, Cary, NC) to test if growth differed among cohorts. A general linear test (Neter et al., 1983) was used to compare growth between three geographical subdivisions (Gulf transition, western, and central). This test is a function of the error sum of squares of the reduced model minus the error sum of squares of the full model. Adequate numbers of juveniles were not available to compare growth in eastern and northern subdivisions (Table 1). Circular statistics (Batschelet, 1981) were used to determine if spawning, as determined from hatchdate distributions, was uniform over the lunar month. The phase of the moon for 1995 was identified by the fraction illuminated (U. S. Naval Observatory Applications Department, 1997). A 3-point moving average was used to test if spawning was cyclical.

Cohorts (1995) were categorized according to the following hatchdates: cohort A, 29 March–2 May ("April"); cohort B, 3 May–6 June ("May"); cohort C, 7 June–4 July ("June"); cohort D, 5 July–1 August ("July"); cohort E, 2 August–5 September ("August"); cohort F, 6 September–3 October ("September").

Comparisons of the relative recruitment potential of individual cohorts (G:M ratios) between all cohorts were unresolved. Although cohort mortality estimates could be generated, they were appropriate (by analyzing r^2 and P-values from regression analysis) for only three cohorts (cohorts B, D, and F).

A random coefficient model was used to investigate the relationship between growth rate of otoliths with age and temperature from juveniles collected in 1995. Most fish were exposed to salinities in a narrow range between 28 and 34 ppt; only 9 fish were exposed to salinities in the 5–13 ppt range (Fig. 4). Consequently, there was insufficient information to obtain reliable inferences on the relationship of growth rate to salinity or the relationship to salinity and temperature for growth information obtained by using either otolith measuring path. This was a disappointment because growth responses to salinity were considered an important objective in relation to proposed Everglades water management activities. Thus, investigation was restricted to the relationship of growth with temperature. A separate model was fitted for the first (1–21 increments)

and second (22–60 increments) measuring paths because otolith increment width changed at a constant (age-independent) rate for each path. We did not include fish with >60 increments because the relationship past this number was determined for only 10% of the fish and included obvious outliers. Letting Y_{ij} be the otolith width measurement for fish i at age α_{ij}, where j indexes time, the model for each path was

$$Y_{ij} = \alpha_{0i} + \alpha_{1i}\alpha_{ij} + e_{ij},$$

where α_{0i} and α_{1i} are the fish-specific intercept and slope describing the relationship between increment width and age for fish i, and e_{ij} is a normally distributed error term; thus, α_{1i} is the growth rate for fish i over the measuring path. Temperature exhibited only negligible change for any given fish over the measuring path; thus, temperature for fish i was summarized as t_i, the average temperature over the path for that fish. To determine an appropriate model for the relationship between intercept and growth rate and temperature, a preliminary analysis was performed in which ordinary least squares estimates of α_{0i} and α_{1i} were obtained separately for each fish i and plotted against temperature. For the first measuring path (1–21 increments), the appropriate model was

$$\alpha_{0i} = \beta_{00} + \beta_{0i}t_i + b_{0i},\ \alpha_{1i} = \beta_{10} + \beta_{11}t_i + \beta_{12}t_i^2 + b_{1i},$$

where b_{0i} and b_{1i} are normally distributed random effects, allowing growth rates for fish at the same temperature to vary across fish. For the second measuring path (22–60 increments), the appropriate model was,

$$\alpha_{0i} = \beta_{00} + \beta_{01}t_i + \beta_{02}t_i^2 + b_{0i},\ \alpha_{1i} = \beta_{10} + \beta_{11}t_i + \beta_{12}t_i^2 + b_{1i}.$$

By substitution, these considerations yielded models 1 and 2 for the first and second paths, respectively:

$$Y_{ij} = (\beta_{00} + \beta_{01}t_i) + (\beta_{10} + \beta_{11}t_i + \beta_{12}t_i^2)\, a_{ij} + b_{0i} + b_{1i}a_{ij} + e_{ij} \quad (1)$$

$$Y_{ij} = (\beta_{00} + \beta_{01}t_i + \beta_{02}t_i^2) + (\beta_{10} + \beta_{11}t_i + \beta_{12}t_i^2)\, a_{ij} + b_{0i} + b_{1i}a_{ij} + e_{ij} \quad (2)$$

thus representing otolith increment width in each case as having a straight line relationship with age, where the slope (age-independent growth rate) depends on average temperature according to a quadratic relationship. The random effects allow observations on the same fish to be correlated, whereas observations across fish are independent. Models 1 and 2 were implemented in SAS Proc Mixed (SAS/STAT software, version 6.12, SAS Institute, Cary, NC).

Daily temperature records were obtained from the United States Department of Interior's National Park Service, Florida Bay monitoring stations and averaged over a 7-day period. In 1995, temperature records were available only for Johnson Key Basin (JKB), Whipray Basin (WB), Little Blackwater Sound (LBS), and Little Madeira Bay (LMB), but spotted seatrout were also collected at other sites (Table 1). Daily temperatures were estimated for Sandy Key (SK) and Roscoe Keys (RK) from values recorded during sampling trips because both these stations are not in close proximity to National Park Service monitoring sites. Sandy Key values were regressed on JKB values (same dates). Sandy Key temperatures were collected from January 1994 through August 1996. The regression model for temperature was $SK = 0.76 + 0.9536\ JKB$ [r^2=0.89; n=25]. Roscoe Key values were regressed on WB values (same dates). Roscoe Key temperatures were collected from January 1994 through August 1996. The regression model for temperature was $RK = 5.60 + 0.7976\ WB$ [r^2=0.87; n=31). Temperature values were available at Murray Key (MK) in 1997. To attain values for our 1995 analysis we regressed MK on JKB (same dates). The temperature regression model was $MK = 0.77 + 0.9680$ JKB [r^2=0.99; n=342].

We reported measurements in standard length (SL). For preflexion and flexion larvae, standard length was measured from the tip of the snout to the tip of the notochord. For postflexion larvae and juveniles, standard length was measured from the tip of the snout to the base of the hypural plate.

Results

Overall growth of larvae and juveniles (<80 mm SL) was best described by the equation $\log_e$ *standard length* = $-1.31 + 1.2162$ ($\log_e$ *age*) [n=582; r^2=0.97]. Growth in body length of juveniles (12–80 mm SL) was best described by the linear equation *standard length* = $-7.50 + 0.8417$ (*age*) [n=486; r^2=0.84]; hence, juveniles between approximately age 20–100 days grew on average 0.84 mm/d. There were no significant differences in juvenile growth in body length among three geographical subdivisions [F^4_{327}=0.756; n=333] (Table 2), but there was a significant growth difference in length for one of six 1995 cohorts (Table 3, Fig. 5). Growth in wet weight of juveniles (15–69 mm SL) was best described by the equation $\log_e$ *wet weight* = $-4.44 + 0.0748$ (*age*) [n=347, r^2=0.84]. There was a significant growth difference in wet weight for one cohort (Table 4, Fig. 6).

Weekly 1995 hatchdate distributions, determined by using daily instantaneous mortality (0.0585, Fig. 7), indicated juveniles in collections (i.e. survivors) were from spawning that was cyclical and protracted (Fig. 8). The most intense successful spawning occurred during 21–27 June (9.2% of total). Using a 3-point moving average, we observed three similar cycles (Fig. 8). From data on survivors, ~25% of juveniles were spawned by late May, 50% by early July, and 75% by late August and from data on cohorts, three cohorts (cohorts C, D, and E; early June–late August) comprised 55% of the total estimated spawn of spotted seatrout. There was no correlation between spawning and moon phase (periodic regression r^2=0.019, P=0.754) (Fig. 8).

The relative recruitment potential (G:M ratio) of the 1995 year class estimated from the wet-weight specific growth coefficient (0.0748) and the instantaneous daily mortality rate (0.0585, Fig. 7) was 1.28. The G:M ratio for three cohorts (B, May; D, July; and F, September) was greater than the ratio for the total 1995 year class because mortal-

Table 2

Summary of growth data used to compare growth in length of spotted seatrout among three Florida Bay subdivisions. Growth was best described by the linear equation: *standard length* = $a + b$ (age in days).

Subdivision	Intercept	Slope	n	r^2	Size range (mm SL)
Gulf transition	–11.07	0.8914	139	0.86	16–69
Central	–12.23	0.9298	49	0.80	15–63
Western	–10.56	0.8834	145	0.85	17–69

Table 3

Summary of statistics for a test for heterogeneity of slopes for cohort somatic growth rates of spotted seatrout. Cohorts were categorized according to month of hatchdate (see text). The base parameter is cohort F and all parameter estimates are deviations from the base cohort. For growth equations, see Figure 5.

Parameter	Estimate	Standard error	t-value	P-value
Intercept	–7.97270	3.02829	–2.63	0.0088
Cohort A	–0.86811	4.31970	–0.20	0.8408
Cohort B	–11.85849	3.91387	–3.03	0.0026
Cohort C	1.65094	3.86470	0.43	0.6695
Cohort D	–6.70820	4.74936	–1.41	0.1586
Cohort E	1.02077	3.50931	0.29	0.7713
Slope	0.82088	0.05613	14.62	<0.001
Cohort A	0.04054	0.08604	0.47	0.6378
Cohort B	0.24578	0.07106	3.46	0.0006
Cohort C	–0.00113	0.07091	–0.02	0.9873
Cohort D	0.15741	0.08730	1.80	0.0721
Cohort E	0.04544	0.06821	0.67	0.5058

Table 4

Summary of statistics for a test for heterogeneity of slopes for cohort wet-weight growth rate of spotted seatrout. Cohorts were categorized according to month of hatch date (see text). The base parameter is cohort F and all parameter estimates are deviations from the base cohort. For growth equations, see Figure 6.

Parameter	Estimate	Standard error	t-value	P-value
Intercept	–4.27384	0.23763	–17.99	<0.0001
Cohort A	0.10201	0.37014	0.28	0.7830
Cohort B	–0.46348	0.34092	–1.36	0.1749
Cohort C	–0.27866	0.32116	–0.87	0.3862
Cohort D	–0.19540	0.38352	–0.51	0.6108
Cohort E	–0.38260	0.29853	–1.28	0.2009
Slope	0.06974	0.00439	15.88	<0.0001
Cohort A	0.00195	0.00729	0.27	0.7889
Cohort B	0.00679	0.00622	1.09	0.2754
Cohort C	0.00502	0.00575	0.87	0.3835
Cohort D	0.00759	0.00702	1.08	0.2808
Cohort E	0.01188	0.00564	2.11	0.0359

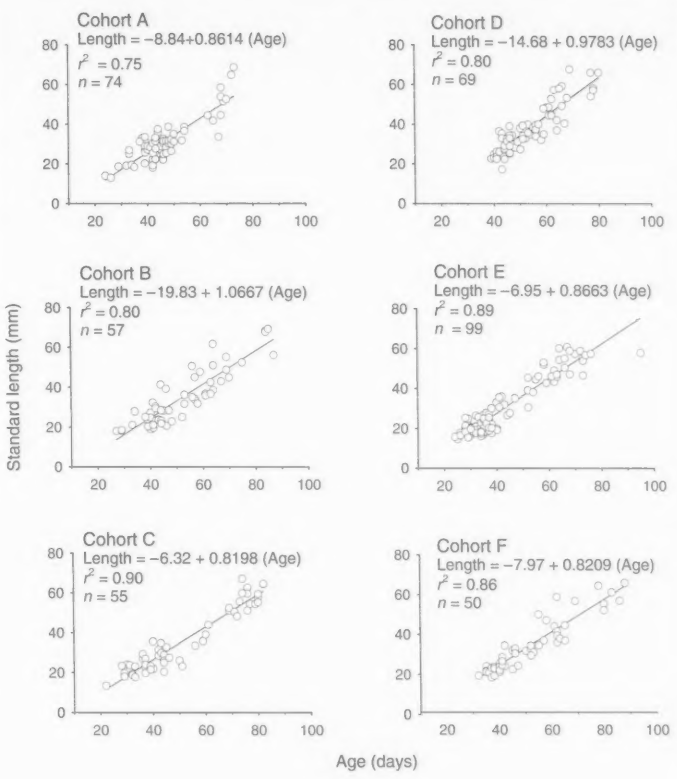

Figure 5

Comparison of growth in standard length among six spotted seatrout (*Cynoscion nebulosus*) cohorts collected in 1995. See text for cohort hatchdates.

Table 5

Daily growth (wet weight in grams) rates and daily mortality rates for three cohorts in Florida Bay in 1995. Cohorts were categorized according to month of hatchdate (see text). The G:M ratio derived from the growth and mortality rates is also presented. For growth equations and associated r^2 values, see Figure 6.

Cohort	Hatchdate month	Growth rate	Mortality rate	r^2	G:M ratio	Size range (mm SL)
B	May	0.0765	0.0445	0.54	1.72	28–62
D	July	0.0773	0.0565	0.82	1.37	37–68
F	September	0.0697	0.0354	0.67	1.97	37–66

ity rates appeared relatively low compared to the overall mortality rate (0.0585) for juveniles (Table 5). However, differences in mortality rates among these three cohorts were not significant (F^4_{21}=1.414). There were no significant differences in weight-specific coefficients among the three cohorts (B, D, and F) (Table 4), but a significant difference in length-specific coefficients among the three cohorts was found (Table 3). Cohort B (May) had a significantly higher growth rate than the other two cohorts.

There was a close relationship between otolith radius and body length (Fig. 9). A linear equation with the sagittal ventral radius, had a similar r^2 as a curvilinear equation with the sagittal dorsal radius. However, we were unable to measure increment widths along this plane and instead used a combination of a ventral path and a ventral medial path.

As an initial demonstration that otolith increment width increased with age along the 1–21 increment measuring path and decreased along the 22–60 increment path, simpli-

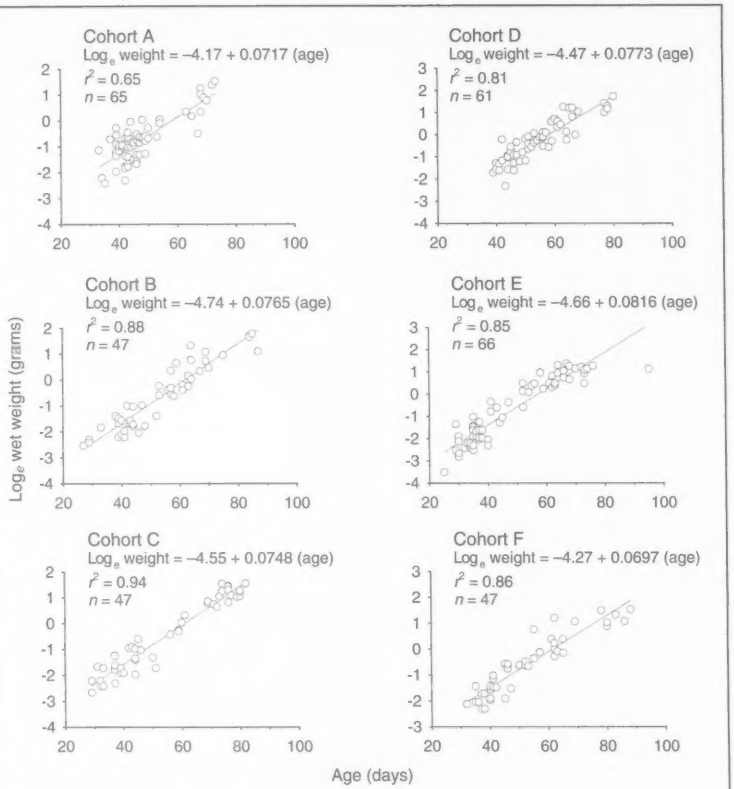

Figure 6

Comparison of growth in wet-weight (grams) among six spotted seatrout (*Cynoscion nebulosus*) cohorts collected in 1995. See text for cohort hatchdates.

fied versions of Equations 1 and 2 (see above) were fitted, in which all coefficients of temperature were set equal to zero, so that Equations 1 and 2 represent simple linear relationships with age. For the first path, the estimate of slope was 0.153 μm/d (P<0.0001); that for the second path was –0.065 μm/d (P<0.0001). Addition of quadratic terms to each model was not supported (P=0.81 and 0.12, respectively). For the first path, whether intercept or growth rate were associated with temperature was determined by testing whether the parameters β_{01}, β_{11}, and β_{12} were equal to zero. There was no evidence that any of these parameters were different from zero (P=0.45, 0.35, and 0.42, respectively); the latter two may indicate that the data do not support the contention that growth rate depends on temperature in this range (1–21 d). For the second path, tests of β_{02}=0 and β_{12}=0 offered strong evidence that these parameters are different from zero (P<0.001 in each case). In particular, these results suggested for the age range 22–60 d, otolith growth rates decrease. The extent of the decrease is strongly associated with average temperature according to a quadratic relationship such that growth rates were more steeply decreasing with age for lower temperatures and then became shallower at higher temperatures. In summary, for temperatures at the lower and higher end of the observed temperature range, otolith growth rates for the age range 22–60 d were higher than they were in the middle of the observed temperature range.

Discussion

Growth in body length of juvenile spotted seatrout in Florida Bay was faster than growth of juveniles from Tampa Bay (Table 6, McMichael and Peters, 1989). Florida Bay is generally considered an oligotrophic system (Fourqurean and Robblee, 1999). Nevertheless, seagrass beds in western Florida Bay, where juvenile spotted seatrout are most common (Chester and Thayer, 1990), are significantly more dense than beds in northwestern Florida waters, slightly north of Tampa Bay (Iverson and Bittaker, 1986). Increased growth of juveniles in Florida Bay could be attributed to the dense seagrass beds that provide habitat for epifaunal crustaceans (Holmquist et al., 1989; Matheson et al., 1999), which are important in the diet of juve-

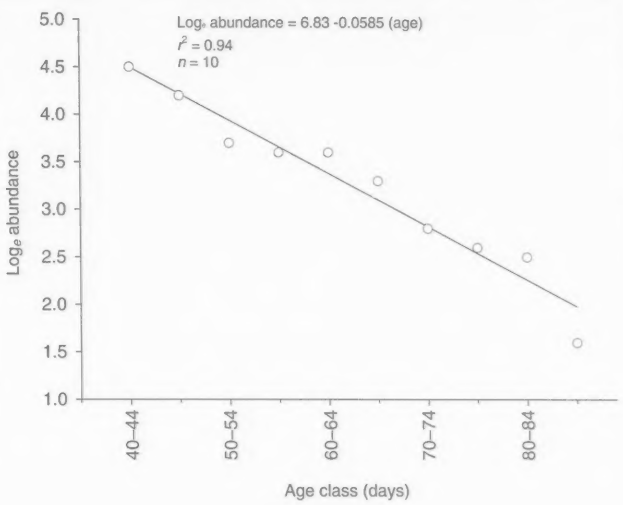

Figure 7

Catch curve of juvenile spotted seatrout (*Cynoscion nebulosus*) used to estimate daily instantaneous mortality (Z). Z = slope = –0.0585. Spotted seatrout were fully recruited to the gear at age 40–44 days.

Table 6

Comparison of spotted seatrout growth (size in mm SL at age) between Tampa Bay, Florida (McMichaels and Peters, 1989) and Florida Bay, Florida (this study).

	Age (days)								
Area	10	20	30	40	50	60	70	80	90
Tampa Bay	5.1	10.2	15.3	20.3	25.4	30.5	35.6	40.7	45.8
Florida Bay	4.4	10.3	16.9	23.3	31.4	39.2	47.2	55.6	64.1

nile spotted seatrout (Hettler, 1989; McMichael and Peters, 1989). Additionally, warmer water temperatures have been observed in Florida Bay (Boyer et al., 1999) compared to Tampa Bay (McMichael and Peters, 1989); these warmer temperatures could enhance growth if adequate food is available (Warren, 1971). However, our study and that of McMichael and Peters (1989) were quite a few years apart; hence differences that we observed could also be accounted for by interannual variability. In addition, differences in growth could also be attributed to differences in sampling gear between the two studies.

Florida Bay is a heterogenous ecosystem and consists of ecologically distinct regions (Phlips and Badylak, 1996; Fourqurean and Robblee, 1999); however, we did not detect any differences in growth of juvenile spotted seatrout among our three subdivisions. In general, juvenile collections from the central subdivision were from stations that were spatially dispersed; whereas, juvenile collections in the western and Gulf transition subdivisions were from relatively few stations (Table 1). Normally, the central subdivision is characterized by the highest salinities in the bay and the western and the Gulf transition are characterized by high salinities (Orlando et al., 1997). However, in our study, salinities in the three subdivisions were moderate and similar (Fig 4), and growth rates estimated for the three subdivisions could be useful as baseline rates, particularly in the central subdivision where salinities are commonly hyperhaline (Orlando et al., 1997).

The spawning habits of spotted seatrout throughout their entire range are generally similar. They have a protracted spawning season, are multiple spawners, and reach sexual maturity at an early age. Initiation of spawning might be temperature dependent, with water temperatures between 20° and 23°C necessary to initiate reproductive development (Brown-Peterson and Warren, 2001). Hatchdate distributions calculated for spotted seatrout in

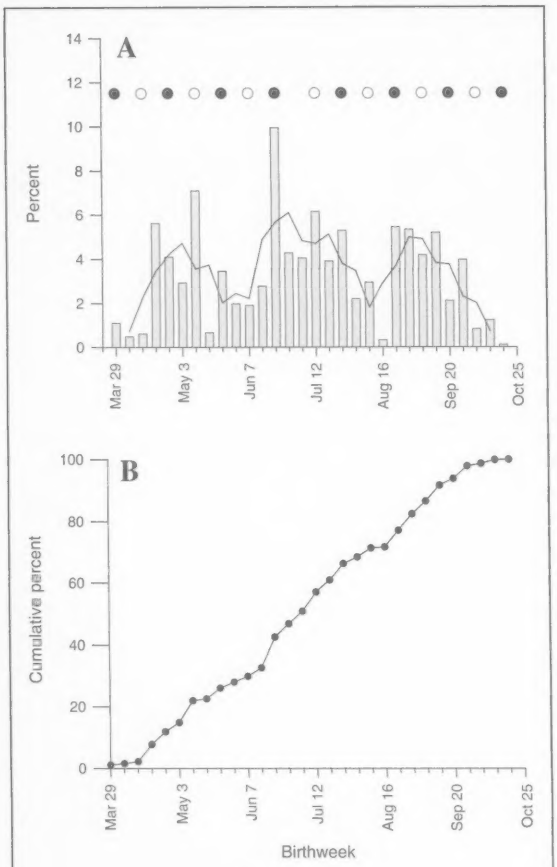

Figure 8

(**A**) Spotted seatrout (*Cynoscion nebulosus*) (n=417) weekly hatchdate distributions adjusted for mortality, including moon phases (●=new moon; ○=full moon), and 3-point moving average (solid line) of hatchdate distributions. (**B**) Cumulative frequency of spotted seatrout (n=417) hatchdate distributions.

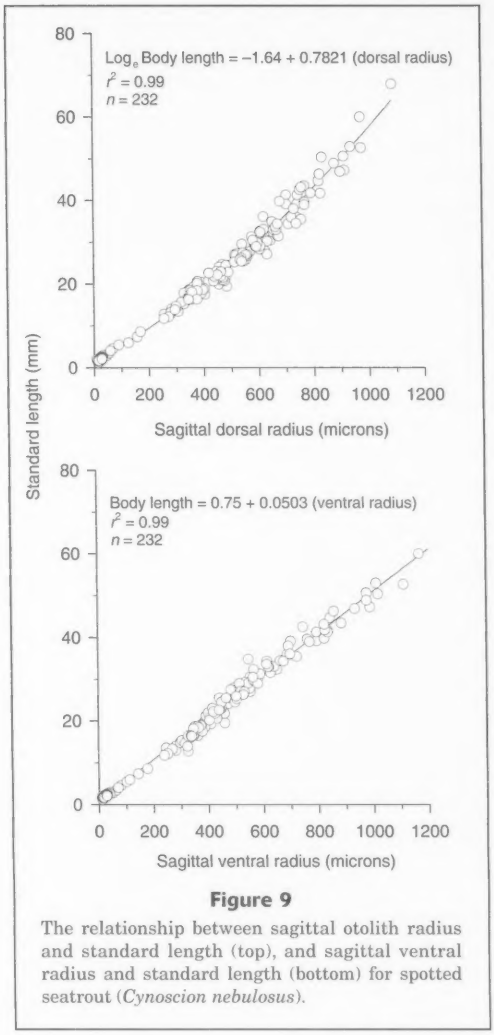
Log$_e$ Body length = −1.64 + 0.7821 (dorsal radius)
r^2 = 0.99
n = 232
Sagittal dorsal radius (microns)
Body length = 0.75 + 0.0503 (ventral radius)
r^2 = 0.99
n = 232
Sagittal ventral radius (microns)
Standard length (mm)

Figure 9

The relationship between sagittal otolith radius and standard length (top), and sagittal ventral radius and standard length (bottom) for spotted seatrout (*Cynoscion nebulosus*).

Florida Bay in this study along with early stage larval collections (Powell, 2003) indicate that spotted seatrout spawn between March and October (based on hatchdate distributions) and that the majority of spawning occurs between 27° and 35°C , with very little spawning between 20° and 26°C (based on early stage larval collections). Spawning peaks, based on larval collections in 1994–96, occurred in June, August, and September (Powell, 2003), and early May, late June, and late August through early September based on 1995 hatchdate distributions (this study). However, Stewart (1961) reported that spotted seatrout in Florida Bay spawned throughout the year and that spawning peaked in spring and fall. Another larval fish study in Florida Bay indicated that some spawning occurs as early as February and continues into December (Rutherford et al., 1989).

Peak spawning activity of spotted seatrout is highly variable (McMichael and Peters, 1989; Brown-Peterson and Warren, 2001). McMichael and Peters (1989) observed two spawning peaks: spring and summer. Older fish participate in two peak spawning periods (Tucker and Faulkner, 1987), and a portion of the larger spring-spawned fish (age-1+) enter the spawning population during their second summer, augmenting the number of summer spawning fish.

We found that spawning activity and moon phase were uncorrelated, which is not in concordance with observations of McMichael and Peters (1989). They found that distinct peaks in spawning (based on hatchdate distributions of larval spotted seatrout) occurred at monthly intervals, and this periodicity might coincide with moon phase. However, this monthly periodicity was not observed when their data for juvenile spotted seatrout were examined. Moreover, statistical tests were not performed on the data in their study.

Our inferences, from this study, in relation to spotted seatrout peak spawning are based on hatchdate distributions and should be viewed with caution because hatchdates are based on survivors. Differential survival for early life history stages can bias results. Hatchdate distributions are valuable when compared to egg or recently hatched larval densities and might suggest processes responsible for differential cohort survivorship. Because spotted seatrout undergo a protracted spawning period and because there is high variation associated with icthyoplankton samples (Cyr et al., 1992), intensive and extensive sampling of recently hatched larvae would be required over a long duration to answer these process-oriented mortality questions.

The daily instantaneous mortality rate of juvenile spotted seatrout was higher in Florida Bay than those reported from northwestern Florida systems (Nelson and Leffler, 2001). Mortality rates of juvenile spotted seatrout from Florida Bay were 5.7%/d; whereas, for the other systems, rates approximated 3%/d. In general, mortality rates might increase with increasing estuarine temperatures (Houde and Zastrow, 1993). Although we were unable to estimate instantaneous daily mortality rates for larval spotted seatrout, these data have been estimated for larvae (3.5–6.5 mm) in two southwestern Florida estuaries (Peebles and Tolly, 1988). Highly variable rates were reported between the two Florida estuaries (Naples Bay: 0.70 or 50%/d; and Fakahatchee area: 0.37 or 31%/d). Houde (1996) reported a generalized instantaneous daily mortality rate for marine fish larvae of 0.239 (21%/d). Estimating mortality rates for larval spotted seatrout in Florida Bay will be critical for calculating G:M ratios in order to evaluate stage-specific survival and to develop credible spatially explicit models.

Mortality rates of spotted seatrout cohorts could be calculated for only three of six cohorts (B, May; D, July; and F, September) because slopes were significantly different from zero for only these cohorts. Furthermore, mortality rates of two of the three cohorts (B and F) were associated with low r^2 values (Table 5); hence the G:M ratios along with the mortality rates for these three cohorts should be considered "rough" estimates. Attaining more accurate mortality estimates for spotted seatrout would be valuable in linking cohort variability with potential recruitment and stage-specific survival. For example, larval cohorts of bay anchovy (*Anchoa mitchilli*) from Chesapeake Bay, a temperate estuary, exhibit growth rates that are temporally variable and mortality rates that are spatially and temporally variable (Rilling and Houde, 1999). Temperature, zooplankton prey and gelatinous predators are believed to influence growth and mortality rates of the bay anchovy. For striped bass (*Morone saxatilis*) in a subestuary of Chesapeake Bay, cohorts exhibited highly variable seasonal G:M ratios that were strongly influenced by temperature (Houde, 1997). In a subtropical estuary, cohort-specific mortality rates for juvenile red drum varied temporally; early and late season cohorts exhibited the highest mortality rates, which coincided with highest growth rates and G:M ratios for midseason cohorts (Rooker et al., 1999). We agree with Houde (1997) that future research should focus on the variability and causes of variability in growth and mortality, both of which interact to determine stage-specific survival. The developmental stage or age where G:M variability is greatest, along with the relationship of this variability to recruitment, need to be determined for spotted seatrout in Florida Bay. No doubt a relationship exists between G:M ratios and recruitment. Future research should also determine if cohort G:M ratios and somatic growth rates are seasonally or spatially variable. If they are, then a limited spatial and temporal sampling program could be designed to annually evaluate G:M ratios at highly variable stages or ages as an index of year-class strength of spotted seatrout in Florida Bay. Such an index could be verified by examining year-class catch rates on an annual basis or by virtual population analysis.

In our study there was little temporal difference in growth of juvenile spotted seatrout cohorts. Larval growth and mortality, which was not treated adequately in our study, could be influenced by copepod prey—an important dietary component of larval spotted seatrout (McMichael and Peters, 1989). The copepod *Acartia tonsa* is dominant in Florida Bay, but egg production rates for this species are low in the bay compared to those in other systems (Kleppel et al., 1998). We suspect the "bottleneck" to recruitment of spotted seatrout could occur during the larval stage. Hence, future research should examine mortality and growth of larval and recently settled spotted seatrout; in particular the patterns of larval production potential (G:M ratios). Research in these areas should increase our understanding of the degree of variability in stage-specific survival and recruitment of spotted seatrout in Florida Bay (Houde, 1996).

For most species, especially those with protracted spawning habits, it is most informative to analyze cohort growth and mortality. For example, striped bass and bay anchovy cohorts in Chesapeake Bay exhibit highly variable growth rates, mortality rates, and stage durations (Rutherford and Houde, 1995; Rilling and Houde, 1999). This variability could cause differential survival for cohorts and result in frequency distributions of survivor hatchdates that do not resemble recently hatched larvae or egg-production frequency distributions (e.g. Crecco and Savoy, 1985; Rice et al., 1987).

We are unable to interpret the significance of the absolute value of the G:M ratio for juvenile spotted seatrout, because interannual comparisons were not made, but we presented the ratio for future comparisons. Generally, the G:M ratio is <1.0 during the early larval stage, indicating a decline in biomass. However, the G:M ratio of a cohort will eventually exceed 1.0 as a result of a relative decline in mortality as larvae grow (Houde and Zastrow, 1993). Clearly, stage specific analysis of the spotted seatrout from egg through juvenile stage would have been more informative in determining when the maximum G:M ratio occurs (when cohort biomass increases at a maximum rate) and in providing insight into stage-specific dynamics of spotted seatrout (Houde, 1997). A constraint of our study was our inability to estimate larval mortality rates; hence early life history stage dynamics could not be examined.

Size-selective mortality in the juvenile life history stages can have important consequences for recruitment. Sogard (1997) argued that "within-cohort size-selective mortality"

is more evident in the juvenile stage than during the egg and larval stages when random mortality independent of fish size is more likely to occur (e.g. dispersal of eggs and larvae away from suitable nursery areas). In addition, variation in size, which provides a "template" for size-selective processes, increases during the juvenile stage as larval size is constrained by egg size. Sogard (1997) cited a number of recent studies that suggest the early juvenile period plays a greater role in determining year-class strength than previously thought.

We were unable to determine if salinity influenced increment width (a surrogate for somatic growth) at early life stages. Understanding the relationship between salinity and growth is critical because Everglades restoration will most likely result in increased freshwater flows to Florida Bay, and during low rainfall periods, salinities in the north central portion of the bay can exceed 45 ppt (Orlando et al., 1997; Boyer et al., 1999). But, salinities were moderate and similar at most stations where juvenile trout were collected in the bay during 1995 (Fig. 4). Very few fish were collected at low salinities; in fact, juvenile spotted seatrout are not commonly collected at low-salinity stations (Table 1; Florida Department of Environmental Protection[1]), and hyperhaline conditions were not observed in 1995. Therefore, we were only able to determine if temperature could influence increment widths. The curvilinear relationship between otolith growth rate and temperature, although a statistically strong relationship, is difficult to explain biologically. Temperature could mask other factors, e.g. temporal variability in prey and predator availability, and optimal temperatures for growth (Rooker et al., 1999). We were able to demonstrate that one cohort grew faster than five other cohorts, possibly indicating differential prey availability in 1995. An individual-based bioenergetics model for spotted seatrout now in preparation (Wuenschel et al.[2]) should add to our understanding of the effects of salinity and temperature on larval and juvenile spotted seatrout

Acknowledgments

We are especially grateful to Al Crosby, Mike Greene, Mike LaCroix, and other Beaufort staff that participated in the field work. We thank James Waters of the NMFS Southeast Fisheries Science Center for computer programing assistance and Jon Hare of our laboratory for performing the circular statistics. We are grateful to Dean Ahrenholz, Jon Hare, Patti Marraro, Joseph Smith, and three anonymous reviewers for their valuable reviews of the manuscript. We also thank Steve Bobko at Old Dominion University for the image analysis macro used to obtain otolith increment widths.

[2] Wuenschel, M. J., R. G. Werner, D. E. Hoss, and A. B. Powell. 2001. Bioenergetics of larval spotted seatrout (*Cynoscion nebulosus*) in Florida Bay. Florida Bay Science Conference, April 23–26, 2001, p. 215–216. Westen Beach Resort, Key Largo, Florida. Abstract. Center for Coastal Fisheries and Habitat Research, Beaufort Laboratory, 101 Pivers Island Road, Beaufort, NC 28516.

Literature cited

Anderson, J. T.
1988. A review of size dependent survival during pre-recruit stages of fishes in relation to recruitment. J. Northw. Atl. Fish. Sci. 8:55–66.

Batschelet, E.
1981. Circular statistics in biology, 371 p. Academic Press, New York, NY.

Boyer, J. N., J. W. Fourqurean, and R. D. Jones.
1999. Seasonal and long-term trends in the water quality of Florida Bay (1989–1997). Estuaries 22:417–430.

Brown-Peterson, N. J., and J. W. Warren.
2001. The reproductive biology of spotted seatrout, *Cynoscion nebulosus*, along the Mississippi Gulf Coast. Gulf Mexico Sci. 2001:61–73.

Chester, A. J., and G. W. Thayer.
1990. Distribution of spotted seatrout (*Cynoscion nebulosus*) and gray snapper (*Lutjanus griseus*) juveniles in seagrass habitats of western Florida Bay. Bull. Mar. Sci. 46:345–357.

Crecco, V., and T. Savoy.
1985. Effects of biotic and abiotic factors on growth and relative survival of young American shad, *Alosa sapidissima*, in the Connecticut River. Can. J. Fish. Aquat. Sci. 42: 1640–1648.

Cyr, H., J. A. Downing, S. Lalonde, S. B. Baines, and M. L. Price.
1992. Sampling larval fish: choice of sample number and size. Trans. Am. Fish. Soc. 121:356–368.

Fourqurean, J. W., and M. B. Robblee.
1999. Florida Bay: a history of recent ecological changes. Estuaries 22:345–357.

Hare, J. A., and R. K. Cowen.
1997. Size, growth, development, and survival of the planktonic larvae of *Pomatomus saltatrix* (Pisces: Pomatomidae). Ecology 78:2415–2431.

Hettler, W. F., Jr.
1989. Food habits of juveniles of spotted seatrout and gray snapper in western Florida Bay. Bull. Mar. Sci. 44: 152–165.

Hettler, W. F., and A. J. Chester.
1990. Temporal distribution of ichthyoplankton near Beaufort Inlet, North Carolina. Mar. Ecol. Prog. Ser. 68: 157–168.

Holmquist, J. G., G. V. N. Powell, and S. M. Sogard.
1989. Decapod and stomatopod communities of seagrass-covered mud banks in Florida Bay: inter- and intrabank heterogeneity with special reference to isolated subenvironments. Bull. Mar. Sci. 44:251–262.

Houde, E. D.
1996. Evaluating stage-specific survival during the early life of fish. *In* Survival strategies in early life stages of marine resources (Y. Watanabe, Y. Yamashita, and Y. Oozeki, eds.), p. 51–66. Balkema, Brookfield, VT.
1997. Patterns and consequences of selective processes in teleost early life histories. *In* Early life history and recruitment of fish populations (R. C. Chambers and E. A. Trippel, eds.), p. 173–196. Chapman and Hall, London.

Houde, E. D., and C. E. Zastrow.
1993. Ecosystem-and taxon-specific dynamic and energetic properties of larval fish assemblages. Bull. Mar. Sci. 53: 290–335.

Iverson, R. L., and H. F. Bittaker.
1986. Seagrass distributions and abundances in eastern Gulf of Mexico coastal waters. Estuar. Coast. Shelf Sci. 1986:577–602.

Kleppel, G. S., C. A. Burkart, L. Houchin, and C. Tomas.
1998. Egg production of the copepod *Acartia tonsa* in Florida Bay during summer. 1. The roles of food environment and diet. Estuaries 21:328–339.
Matheson, R. E., Jr., S. M. Sogard, and K. A. Bjorgo.
1999. Changes in seagrass-associated fish and crustacean communities on Florida Bay mud banks: the effects of recent ecosystem changes? Estuaries 22:534–551.
McMichael, R. H., Jr., and K. M. Peters.
1989. Early life history of spotted seatrout, *Cynoscion nebulosus* (Pisces: Sciaenidae), in Tampa Bay, Florida. Estuaries 12:98–110.
Nelson, G. A., and D. Leffler.
2001. Abundance, spatial distribution, and mortality of young-of-the-year spotted seatrout (*Cynoscion nebulosus*) along the Gulf Coast of Florida. Gulf Mex. Sci. 19:30–42.
Neter, J., W. Wasserman, and M. H. Kutner.
1983. Applied linear regression models, 547 p. Richard D. Irwin, Inc., Homewood, IL.
Orlando, S. P., Jr., M. B. Robblee, and C. J. Klein.
1997. Salinity characteristics of Florida Bay: a review of the archived data set (1955–1995), 33 p. Office of Ocean Resources Conservation and Assessments, NOAA, Silver Spring, MD.
Peebles, E. B., and S. G. Tolley.
1988. Distribution, growth and mortality of larval spotted seatrout, *Cynoscion nebulosus*: a comparison between two adjacent estuarine areas of southwest Florida. Bull. Mar. Sci. 42:397–410.
Phlips, E. J., and S. Badylak.
1996. Spatial variability in phytoplankton standing crop and composition in a shallow inner-shelf lagoon, Florida Bay, Florida. Bull. Mar. Sci. 58:203–216.
Powell, A. B.
2003. Larval abundance and distribution, and spawning habits of spotted seatrout, *Cynoscion nebulosus*, in Florida Bay, Everglades national Park, Florida. Fish. Bull. 101: 704–711.
Powell, A. B., D. E. Hoss, W. F. Hettler, D. S. Peters, and S. Wagner.
1989. Abundance and distribution if ichthyoplankton in Florida Bay and adjacent waters. Bull. Mar. Sci. 44:35–48.
Powell, A. B., E. H. Laban, S. A. Holt, and G. J. Holt.
2000. Validation of age estimates from otoliths of larval and juvenile spotted seatrout, *Cynoscion nebulosus*. Fish. Bull. 98:650–654.
Rice, J. A., L. B. Crowder, and M. E. Holey.
1987. Exploration of mechanisms regulating larval survival in Lake Michigan bloater: a recruitment analysis based on characteristics of individual larvae. Trans. Am. Fish. Soc. 116:481–491.
Ricker, W. E.
1975. Computation and interpretation of biological statistics of fish populations. Bull. Fish. Res. Board. Can. 191, 382 p.
Rilling, G. C., and E. D. Houde.
1999. Regional and temporal variability in growth and mortality of bay anchovy, *Anchoa mitchilli*, larvae in Chesapeake Bay. Fish. Bull. 97:555–569.
Rooker, J. R., S. A. Holt, G. J. Holt, and L. A. Fuiman.
1999. Spatial and temporal variability in growth, mortality, and recruitment potential of postsettlement red drum, *Sciaenops ocellatus*, in a subtropical estuary. Fish. Bull. 97:581–590.
Rutherford, E. S., and E. D. Houde.
1995. The influence of temperature on cohort-specific growth, survival, and recruitment of striped bass, *Morone saxatilis*, larvae in Chesapeake Bay. Fish. Bull. 93:315–332.
Rutherford, E. S., E. B. Thue, and D. G. Buker.
1982. Population characteristics, food habits and spawning activity of spotted seatrout, *Cynoscion nebulosus*, in Everglades National Park, 48 p. United States Park Service, South Florida Research Center Report T-668, Homestead, Florida.
Rutherford, E. S., T. W. Schmidt, and J. T. Tilmant.
1989. Early life history of spotted seatrout (*Cynoscion nebulosus*) and gray snapper (*Lutjanus griseus*) in Florida Bay, Everglades National Park, Florida. Bull. Mar. Sci. 44:49–64.
Secor, D. H., J. M. Dean, and E. H. Laban.
1991. Manual for otolith removal and preparation for microstructural analysis, 85 p. Belle W. Baruch Institute for Marine Biology and Coastal Research Technical Publication 1990-01.
Sogard, S. M.
1997. Size-selective mortality in the juvenile stage of teleost fishes: a review. Bull. Mar. Sci. 60:1129–1157.
Stewart, K. W.
1961. Contributions to the biology of the spotted seatrout (*Cynoscion nebulosus*) in the Everglades National Park, Florida. M.S thesis, 103 p. Univ. Miami, Coral Gables, FL.
Thayer, G. W., A. B. Powell, and D. E. Hoss.
1999. Composition of larval, juvenile and small adult fishes relative to change in environmental conditions in Florida Bay. Estuaries 22:518–533.
Tucker, J. W., Jr., and B. E Faulkner.
1987. Voluntary spawning patterns of captive spotted seatrout. Northeast Gulf Sci. 9:59–63.
Turney, W. J., and B. F. Perkins.
1972. Molluscan distribution in Florida Bay. Sedimenta III, 37 p. Rosenstiel School of Atmospheric Science, Univ. of Miami, FL.
U. S. Naval Observatory Applications Department.
1997. Fraction of the moon illuminated. [Available at http//aa.usno.navy.mil/data/docs/Moon Fraction.html.] Last accessed 17 December 2001.
Ware, D. M.
1975. Relation between egg size, growth, and natural mortality of larval fish. J. Fish. Res. Board Can. 32:2503–2512.
Warren, C. E.
1971. Biology and water pollution control, 434 p. W. B. Saunders Company, Philadelphia, PA.

Abstract—Age and growth of the night shark (*Carcharhinus signatus*) from areas off northeastern Brazil were determined from 317 unstained vertebral sections of 182 males (113–215 cm total length [TL]), 132 females (111.5–234.9 cm) and three individuals of unknown sex (169–242 cm). Although marginal increment (MI) analysis suggests that band formation occurs in the third and fourth trimesters in juveniles, it was inconclusive for adults. Thus, it was assumed that one band is formed annually. Births that occur over a protracted period may be the most important source of bias in MI analysis. An estimated average percent error of 2.4% was found in readings for individuals between two and seventeen years. The von Bertalanffy growth function (VBGF) showed no significant differences between sexes, and the model derived from back-calculated mean length at age best represented growth for the species (L_∞=270 cm, K= 0.11/yr, t_0=–2.71 yr) when compared to the observed mean lengths at age and the Fabens' method. Length-frequency analysis on 1055 specimens (93–260 cm) was used to verify age determination. Back-calculated size at birth was 66.8 cm and maturity was reached at 180–190 cm (age 8) for males and 200–205 cm (age ten) for females. Age composition, estimated from an age-length key, indicated that juveniles predominate in commercial catches, representing 74.3% of the catch. A growth rate of 25.4 cm/yr was estimated from birth to the first band (i.e. juveniles grow 38% of their birth length during the first year), and a growth rate of 8.55 cm/yr was estimated for eight- to ten-year-old adults.

Manuscipt approved for publication 26 June 2003 by Scientific Editor.

Manuscript received 20 October 2003 at NMFS Scientific Publications Office.

Fish. Bull. 102:156–167 (2004).

Age determination and growth of the night shark (*Carcharhinus signatus*) off the northeastern Brazilian coast

Francisco M. Santana

Rosangela Lessa

Universidade Federal Rural de Pernambuco (UFRPE)
Departamento de Pesca, Laboratório de Dinâmica de Populações Marinhas - DIMAR
Dois Irmãos, Recife-PE, Brazil, CEP 52171-900

E-mail address (for R. Lessa, contact author): rplessa@ig.com.br

The night shark (*Carcharhinus signatus*) is a deepwater coastal or semi-oceanic carcharhinid that is found in the western Atlantic Ocean along the outer continental or insular tropical and warm temperate shelves, at depths exceeding 100 meters (Bigelow and Schroeder, 1948). The species has been recorded from Delaware to Florida, the Caribbean sea (Cuba), and northern South America (Guayana) (Compagno, 1984). It has also been recorded in southern Brazil, Uruguay, and Argentina (Krefft, 1968; Compagno, 1984; Marín et al., 1998), and on the seamounts off northeastern Brazil (02°16′ to 04°05′S and 033°43′ to 037°30′W, Menni et al., 1995) where it is called "toninha."

Since 1991, tuna longline vessels have targeted the night shark in northeastern Brazil (Hazin et al., 1998) because of its highly prized fins, the increasing value of shark meat in the local market, and their relatively large abundance and accessability on seamounts (Menni et al., 1995). This species is most important in the area, making up 90% of catches over shallow banks (CPUE, in number, is 2.94/100 hook), and only 15% of catches on the surrounding deep area, yielding 0.04/100 hook (Amorim et al., 1998).

Information on this species is restricted to taxonomic descriptions (Bigelow and Schroeder 1948; Cadenat and Blache, 1981; Compagno, 1984, 1988), and some biological aspects (Guitart Manday, 1975; Hazin et al., 2000). Night sharks reach >270–280 cm maximum total length (TL) (Compagno, 1984; Branstetter, 1990). Off northeastern Brazil, females mature at 200–205 cm TL, males at 185–190 cm. Litter sizes range from 10 to 15 pups and the gestation period may last one year (Hazin et al., 2000). The assumed size-at-birth off the United States is 60–65 cm TL (Compagno, 1984; Branstetter, 1990). Age and growth have not been estimated.

The aim of this study is to present the first growth curve for *Carcharhinus signatus* from vertebral and length-frequency analyses. This information will permit the use of age-based stock assessment methods for the management of the species in the Exclusive Economic Zone (EEZ) off Brazil.

Materials and methods

Sampling data and vertebrae were collected from November 1995 to November 1999 from commercial landings (Natal, Brazil) caught in deep (Aracati, Dois Irmãos, Fundo, Sirius) and shallow (Pequeno, Leste, and Sueste) seamounts with depths between 38 to 370 m at the summits (Fig. 1).

Commercial vessels were equipped with ~30 km Japanese-style multifilament longline gear (Suzuki et al., 1977). On average, each vessel used 970–980 hook per day; mainline sets began at ~02:00 h and ended at ~06:00 h. The retrieval of gear began at noon and finished by dusk. The Brazilian sardinella (*Sardinella brasiliensis)*, margined flyingfish (*Cypselurus cyanopterus*), and squid (*Loligo* sp.) were used as bait (Hazin et al., 1998).

A total of 1055 individuals, landed whole, eviscerated, or as carcasses (headless and finless), were sampled. The interdorsal space (posterior dorsal

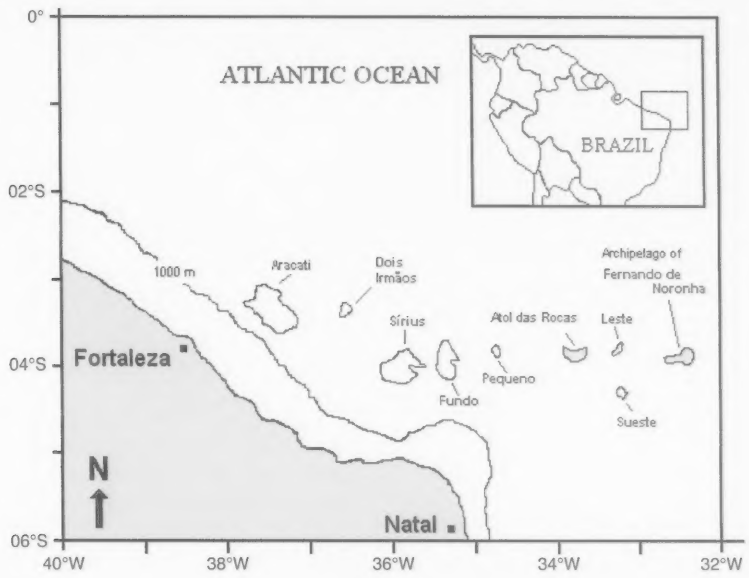

Figure 1

Location of the sampling area for the night shark (*C. signatus*) collected off northeastern Brazil.

fin base to origin of the second dorsal fin [IDS, cm]), total length (snout to a perpendicular line from the tip of the upper caudal fin [TL, cm]) and fork length (snout to fork of tail [FL, cm]) were measured. In carcasses, only IDS was measured, and IDS, FL, and TL were recorded for eviscerated or whole individuals. A set of five or six vertebrae were removed from below the first dorsal fin in 317 specimens. Total length was measured as the "natural length" (without depressing the tail) according to Garrick (1982).

To estimate TL for carcasses, relationships from subsamples of IDS versus TL and FL versus TL were established for males and females separately. Linear regressions derived for each sex were tested for homogeneity and analyzed for covariances (ANCOVA), resulting in TL=1.2049 FL + 1.7972 (r^2=0.944, n=668, P=0.41) and TL = 3.3467 IDS + 30.879 (r^2=0.824; n=764, P=0.161). Whenever length is mentioned hereafter, we always refer to TL.

Vertebrae were processed by removing excess tissue, fixed in 4% formaldehyde for 24 hours, and preserved in 70% alcohol. Each vertebra was embedded in polyester resin and the resulting block was cut to about a 1-mm thick section containing the nucleus by using a Buehler® low speed saw. Initially, alizarin-red-s stained sections (Gruber and Stout, 1983) were compared to unstained sections from the same individuals to define the best contrast for narrow and broad zones. In the first procedure, sections were immersed overnight in an aqueous solution of alizarin red s and 0.1% NaOH at a ratio of 1:9 and then rinsed in running tap water. In stained sections, narrow zones were visible as dark red and broad zones as light red, whereas in unstained sections translucent (narrow) and opaque (broad) zones were visible under transmitted light. Unstained sections produced comparable results to alizarin stained sections and were used for band observation in the study.

Bands counted in each section and distances from the focus to the margin of each narrow zone were recorded. Vertebral radius (VR) was measured by using a binocular dissecting microscope equipped with an ocular micrometer. Measurements were made at 10× magnification (1 micrometer unit=1 mm) with both reflected and transmitted light. The same reader read sections from the same specimen twice at different times without knowledge of the individual size or previous count. Whenever the counts differed between the two readings, a third reading was used for back-calculation of size-at-age.

The index of average percentage error (IAPE) (Beamish and Fournier, 1981) to compare reproducibility of age determination between readings was calculated.

$$IAPE = 1/N \sum \left(1/R \sum (|X_{ij} - X_j|/X_j\right) \times 100,$$

where N = the number of fish aged;
R = the number of readings;
X_{ij} = the mean age of j^{th} fish at the i^{th} reading; and
X_j = the mean age calculated for the j^{th} fish.

Marginal increment (MI) analysis to determine the time of band formation was used. The analysis was restricted to 1995–97, when samples were collected every month. The distance from the final band to the vertebral's edge (MI) was expressed as a percentage of the distance between the last two bands formed on vertebrae (Crabtree and Bullock, 1998). The distance between the last and the penultimate band was divided by the distance between the nucleus and the

last band for each vertebra that was measured, and we then calculated the mean of this number for the entire sample:

$$\sum\left((R_{n-1})-R_n\right)/n = 0.13(\mathrm{SE}=0.0009).$$

The expected distance between the last (R_n) and the penultimate (R_{n-1}) bands was estimated as a function of the distance between the vertebral nucleus and the last band (MI). The percent marginal increment (PMI) was calculated as

$$PMI = \left[MI/(0.13\times R_n)\right]\times 100.$$

Analysis of variance to test for differences in PMI by month was used. *Post-hoc* tests (Tukey honest significant differences ([HSD]) were performed to indicate which months were different.

Characterization of the vertebral edge was used to determine the time period of band formation (Carlson et al., 1999). Under reflected light, a narrow dark zone (MI 0), a narrow light zone (MI 0.1 to 0.5), and a broad light zone (MI 0.6 to 1) were observed. Absolute marginal increments (MI) were also analyzed by trimester for juveniles aged four and five years, and for adults (more than eight years) to confirm the time of translucent zone formation.

The relationship between VR and TL was calculated by sex, tested for normality, and compared by ANCOVA (Zar, 1996). The final regression in both sexes did not pass through the origin, thus suggesting that the Fraser-Lee method was the most appropriate for back-calculation (Ricker, 1969).

$$[TL]_n = (R_n/VR)([TL]-a)+a,$$

where $[TL]_n$ = the back-calculated length at age n;
R_n = vertebral radius at the time of the ring n;
VR = the vertebral radius at capture;
TL = the length at capture; and
a = the intercept on the length axis.

A von Bertalanffy growth function (VBGF) (von Bertalanffy, 1938) was fitted to back-calculated and observed length-at-age data with the following equation.

$$L_t = L_\infty\left[1-e^{-k(t-t_0)}\right],$$

where L_t = predicted length at age t;
L_∞ = mean asymptotic total length;
K = growth rate constant; and
t_0 = the age when length is theoretically zero.

To obtain parameters of VBGF, data were analyzed by using FISHPARM (Prager et al., 1987) for nonlinear least-squares parameter estimation. The Kappenman's method (1981), based on the sum of squares of the differences between observed and predicted lengths from a growth model, was used for comparing male and female growth curves. In addition, likelihood-ratio tests were used to compare parameter estimates of the von Bertalanffy equation between sexes (Cerrato, 1990).

Von Bertalanffy parameters (L_∞, K) were also estimated by the method of Fabens (1965) usually employed for recapture data and which takes into account the size at birth (L_0) instead of t_0. This method reconfigures VBGF and forces the regression through a known size at birth:

$$L_t = L_\infty(1-be^{-Kt}),$$

where $b = (L_\infty - L_0)/L_\infty$.

We used Fabens routine for growth increment data analysis of the FAO-ICLARM stock assessment tools (FISAT) program (Gayanilo et al., 1996), assuming that the time intervals ($=\Delta t$) for each size-at-age class were equal and had a periodicity identical to that obtained from the vertebral analysis.

The lengths of 1055 individuals were divided into 5-cm intervals and analyzed by the Shepherd method (1987) with the length-frequency data analysis program (LFDA). Initial values of L_∞ were based on results from maximal lengths in the sample and from literature (Compagno, 1984). K values ranging from 0.05 to 1.8 were used as input into the program, which was run repeatedly until the highest score function was obtained. The L_∞ and K values were then used to calculate t_0 (Sparre et al., 1989):

$$t_0 = t+(1/K)\left(\ln[L_\infty - lt]\right)/L_\infty).$$

Using an age-length key, based on 317 individuals for which vertebrae were read, we evaluated the age composition of the sample (Bartoo and Parker, 1983). Maximal ages in the sample were calculated by employing the inverted VBGF (Sparre et al., 1989). Further, the formula by Fabens (1965) [5(ln2)/K] for longevity estimation was used. All statistical inferences were made at a significance level of 0.05.

Results

The total sample size consisted of 1055 individuals: (551 males [93–248 cm], 499 females [110–252 cm], and 5 individuals of undetermined sex [169–260 cm]) (Fig. 2). Of these, vertebrae were removed from 317 specimens (182 males [113–215 cm], 132 females [111.5–234.9 cm], and 3 individuals of undetermined sex [169–242 cm]).

Differences in the relationship between VR and TL between sexes were not found to be significant (P=0.811). The regression for the overall sample showed a linear relationship: TL = 13.523VR + 41.824 (r^2=0.89; n=317), indicating that vertebrae are suitable structures for age determination, and methods based on direct proportion are appropriate for back-calculation.

The average percentage error, calculated between two readings, ranged from 0% to 4.5% in vertebrae with 2 to 17 bands and the average IAPE for the overall sample was 2.4%. Coefficient of variation (CV) between readings for total sample was 6.88%.

Monthly PMI analysis, for the entire sample, indicated that bands were formed from June to October, when high-

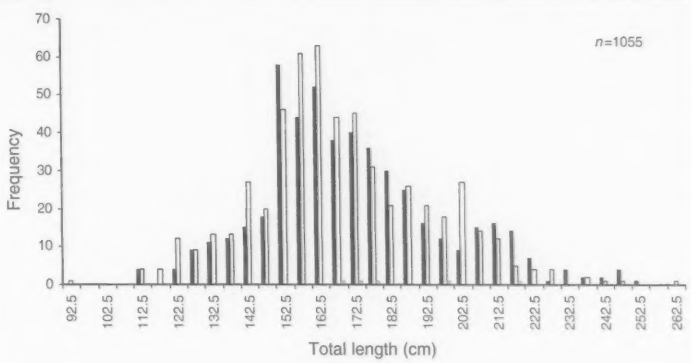

Figure 2

Length-frequency distribution for the night shark (*C. signatus*) caught off northeastern Brazil between 1995–99 (black bars=females; white bars = males; grey bars = undetermined sex).

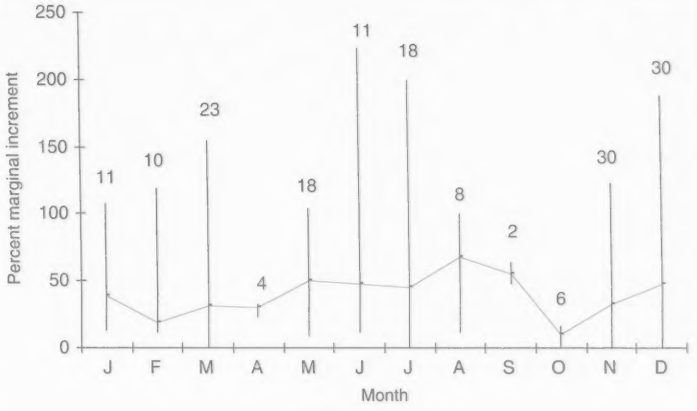

Figure 3

Percent marginal increments means (-) with the minimum and maximum values for the night shark (*C. signatus*) caught from 1995 to 1997 off northeastern Brazil (n=171). The number of individuals sampled per month is shown above the vertical bars.

est mean values are reached (Fig. 3). These values are followed by the lowest mean PMI in October, indicating that the new translucent zone forms from that point on. Monthly PMIs showed significant differences throughout the year (P=0.0463) and *post-hoc* comparisons detected differences in February, April, September, and October. Furthermore, monthly categorization of vertebral edges indicated that the highest frequency of broad light edges (MI 0.6–1) appears from July through December and narrow dark edges (MI 0) from March through December, with the exception for months of May and August (Fig. 4). Trimonthly frequency distribution of absolute marginal increments (MIs) was carried out for juveniles, revealing four and five bands, and for adults, revealing more than eight bands. For the former group, a higher number of broader increments and fully formed bands in the third and fourth trimesters were observed (Fig. 5). For adults, an unclear pattern was observerd perhaps because a smaller sample size was obtained.

Because there was no complete agreement on the time of band formation among different MI analysis for juveniles and adults, age was assigned by assuming an annual pattern of band deposition. The birth mark present in all analyzed vertebrae was not taken into account for age assignation. Under this assumption, band counts indicate relative age (years).

Mean observed lengths-at-age were higher than mean back-calculated lengths for males and females and were likely due to the strong variation in size for each age class (Table 1). The tendency of back-calculated lengths of older

Table 1

Mean back-calculated (BC) and observed length-at-age (OL) data for male and female night sharks (*C. signatus*) collected off northeastern Brazil (SD=standard deviation).

	Females		Males	
Age (yr)	BC (cm) ±SD	OL (cm) ±SD	BC (cm) ±SD	OL (cm) ±SD
0	66.8 ±1.78	—	67.3 ±1.41	—
1	91.9 ±1.31	—	92.3 ±1.37	—
2	113.4 ±2.13	122.5 ±16.93	113.3 ±1.48	120.1 ±4.21
3	128.8 ±2.21	132.9 ±9.77	128.6 ±1.54	135 ±8.91
4	142.7 ±2.41	149.8 ±7.75	142.4 ±1.94	151.5 ±9.72
5	154.7 ±2.92	160.7 ±7.21	154.5 ±2.7	157.5 ±7.86
6	165.9 ±3.46	166.8 ±10.32	166.3 ±3.25	167.5 ±8.1
7	176.8 ±3.4	179.8 ±9.56	177.4 ±2.64	177.6 ±9.34
8	185.9 ±3.71	184.9 ±9.12	187.4 ±2.22	189.8 ±6.53
9	194.8 ±3.82	197.1 ±6.49	195.8 ±2.25	199.9 ±5.26
10	202 ±4.75	208.2 ±3.89	202.4 ±2.78	204.3 ±3.13
11	206.9 ±5.56	202	209.8	212.5 ±3.54
12	215.7 ±2.4	218	—	—
13	222.2	—	—	—
14	226.9	—	—	—
15	231.7	234.4 ±0.63	—	—

fish in the early years to be systematically lower than younger ones at the same age (Lee's phenomenon) was not evident (Tables 1 and 2).

Using back-calculated lengths-at-age (Table 3), we plotted male and female growth curves separately and then tested the data; no indication of significant differences in growth was observed between sexes with both the Kapenman's (P>0.05) and likelihood ratio tests (Table 4). Data were then treated together, incorporating individuals of undetermined sex. VBGFs derived from observed length at age were not tested because of missing values in different age classes. The method of Fabens for combined sexes, fitted to back-calculated data, provided L_∞ and K, by using b = 0.781, L_0= 62.5 cm (Compagno, 1984) and, Δt = 1 year (Table 2).

Parameters from back-calculation were close to those derived from length-frequency analysis for 1055 specimens, whereas observed lengths and the Fabens method, provided the most varying parameters with lowest correlation and highest coefficients of variation (Table 2).

The smallest specimen in the vertebral sample showing two complete bands in sections was 111.5 cm, close to the estimated mean back-calculated length at age two of 113.7 cm (Table 3). Size at maturity, 185–190 cm for males and 200–205 cm for females, corresponded to 8- and 10-year-old individuals, respectively (Fig. 6). The largest and oldest specimen whose vertebrae were used, was 242 cm, which corresponded to 17-year-old individual.

A growth rate of 25.4 cm/yr was estimated from birth to the first band—a rate that corresponded to 38% of the birth length (the length at birth being 66.8 cm). Also, a mean rate of 8.55 cm/yr was calculated for 8- to 10-year-old individuals, when maturity is achieved (Table 3).

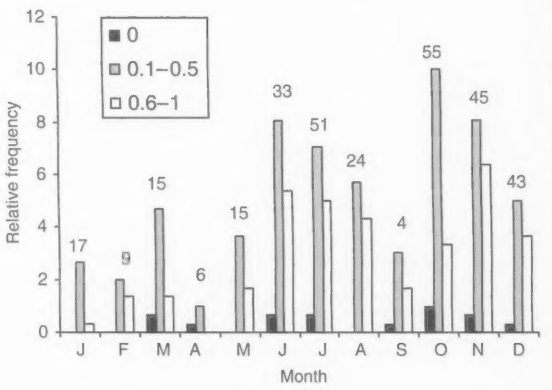

Figure 4

Categorization of edges by month for the night shark (*C. signatus*) off northeastern Brazil.

Considering mature individuals >185 cm, the age composition for the vertebral samples (n=317) indicated that 17.3% of specimens were adults (Table 5). Instead, for the total sample (n=1055), where the age ranged between 2 to ≥17 years, adults corresponded to 25.3% of the total sample

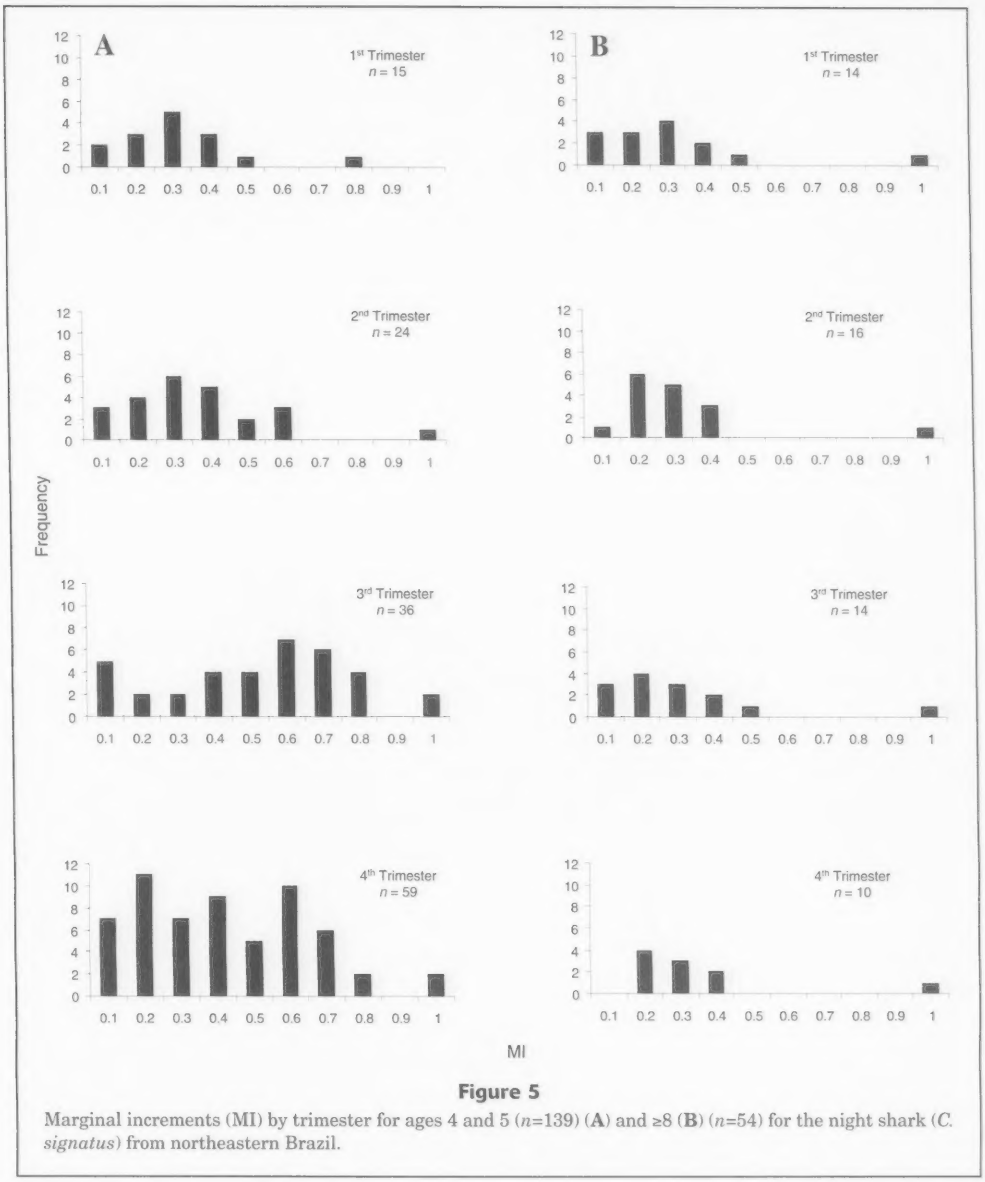

Figure 5

Marginal increments (MI) by trimester for ages 4 and 5 (n=139) (**A**) and ≥8 (**B**) (n=54) for the night shark (*C. signatus*) from northeastern Brazil.

(Fig. 7). According to the inverted back-calculated VBGF the oldest specimen in the sample was 31.7 years old (260 cm), whereas longevity was 31.5 years.

Discussion

Validating the time of band formation is considered critical when using hard parts for age estimates (Brothers, 1983), and validation is successful when growth zones are shown to form annually in all age groups of the population (Beamish and McFarlane 1983). Marginal increment analysis, carried out on younger and faster growing individuals, cannot always be used for validating older age groups, and therefore all ages must be ascertained (Brothers, 1983). In the present study, we obtained significant differences in marginal increments for the total sample. However, the significance level of the test (P=0.046) was close enough to 0.05 to cause us to suspect that the distributions could have been similar. The time of band formation varied when different age groups were analyzed separately, despite suggestions that bands are completed in the third and

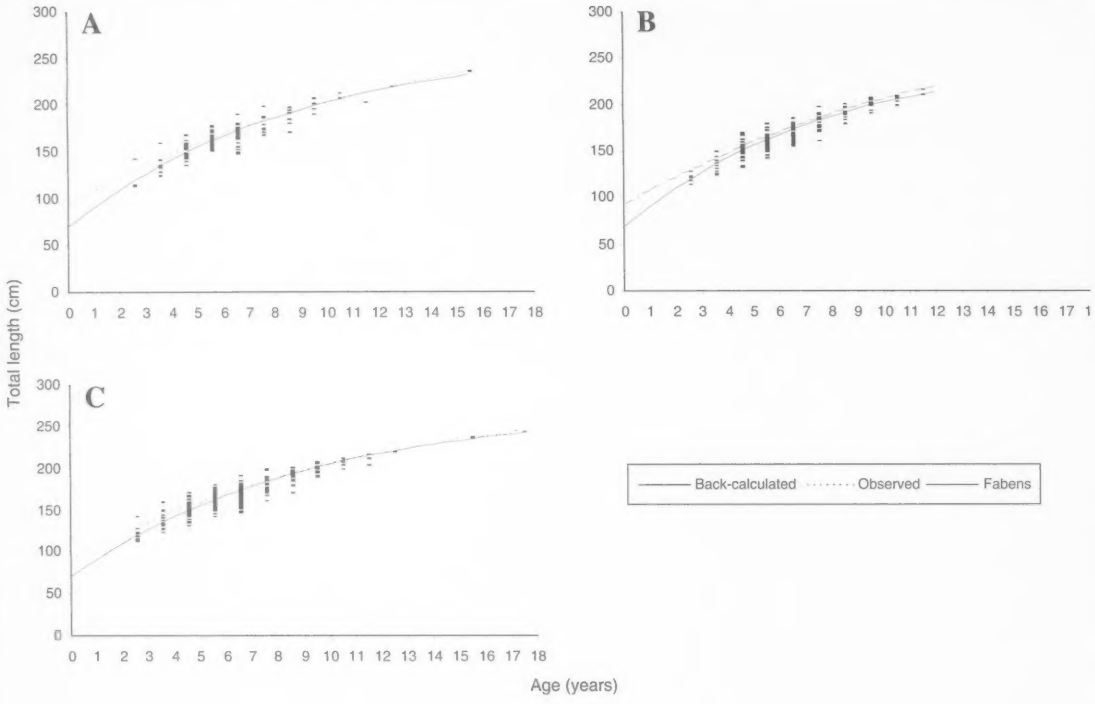

Figure 6

Growth curves generated from (**A**) females, (**B**) males, and (**C**) sexes combined for the night shark (*C. signatus*) off the northeastern Brazil.

Table 2

Von Bertalanffy parameters derived from back-calculated lengths (BC), observed lengths (OL), lengths from the Fabens method, and the length-frequency data analysis (LFDA) package for the pooled database (SE is standard error; CV is coefficient of variation).

Methods	Sex	L_∞ (cm)	SE	CV	K(/year)	SE	CV	t_0(year)	SE	CV	r^2
BC	Males	256.5	5.56	0.022	0.124	0.007	0.055	–2.538	0.119	0.047	0.999
	Females	265.4	4.15	0.016	0.114	0.005	0.045	–2.695	0.127	0.047	0.999
	Both	270	2.78	0.01	0.112	0.003	0.031	–2.705	0.099	0.037	0.999
OL	Males	306.1	37.71	0.117	0.076	0.02	0.267	–4.663	0.882	0.189	0.995
	Females	297.1	26.71	0.09	0.077	0.018	0.235	–4.853	0.977	0.201	0.99
	Both	289.9	7.6	0.026	0.085	0.006	0.077	–4.395	0.348	0.079	0.998
Fabens	Both	285.3	15.69	0.055	0.08	0.016	0.2	—	—	—	—
LFDA	Both	270.9	—	—	0.106	—	—	—	—	—	—

fourth trimesters (new bands begin to form in this period) in juveniles. Results were inconclusive for adults. For *C. obscurus* (Natanson et al., 1995), *C. plumbeus* (Sminkey and Musick 1995), *C. porosus* (Batista and Silva, 1995; Lessa and Santana, 1998), *C. acronotus* (Carlson et al., 1999), and *I. oxyrhynchus* (Lessa et al., 2000), inconclusive results for MI analysis were obtained. The inability to demonstrate the periodicity of band deposition in adult sharks

in the present study is similar to the outcome for *C. limbatus* older than four years (Wintner and Cliff, 1996). For the last mentioned species, the problem was circumvented by restricting MI analysis to juveniles (Killam and Parsons, 1989).

Age was assigned by assuming an annual pattern of deposition, as commonly occurs for most carcharhinids like *C. brevipinna* and *C. limbatus*, *Rhizoprionodon terraenovae* (Branstetter et al., 1987; Branstetter and Stiles, 1987), *Negaprion brevirostris* (Gruber and Stout, 1983), and *C. longimanus* (Seki et al., 1998; Lessa et al., 1999c). Three sources of bias generally occur with MI analysis: 1) sample sizes are small for any particular month or for any age class (Cailliet, 1990); 2) data are collected over a too long a period causing variability on account of annual marks that are not formed at the same time (Brothers, 1983) and 3) births occur over a long period (Brothers, 1983). All these may have biased MI analysis in the present study.

Research carried out in the study area by Hazin et al. (2000) indicated that copulation takes places throughout the austral summer. Embryos measuring 10 to 40 cm were collected in February, whereas 31.8 to 37.2 cm embryos were found in June. This remarkable variability in embryo size during the gestation period suggests that birth period lasts several months. Furthermore, with an estimated back-calculated birth length of 66.8 cm, individuals measuring ~40 cm in February will be born long before individuals that measured 37.2 cm in June. Such a protracted parturition period could lead to differences in MI of the same cohort. Thus, after an assumed ~12 months gestation period, individuals are born with birth dates varying by several months. Moreover, no significant differences in MI analysis was found for *C. porosus* and *I. oxyrhynchus*, which also have a protracted birth seasons (Lessa et al., 1999a, 1999b).

A comparison of growth model parameters by using known size information, such as size-at-birth and maximum observed size, can be

Table 3

Back-calculated and observed length-at-age data (cm) for combined sexes of the night shark (*C. signatus*) caught off northeastern Brazil. Numbers in parentheses are the number of individuals examined for each category of band count.

		Vertebral band count																
Age (yr)	*n*	0 (317)	1 (317)	2 (317)	3 (307)	4 (285)	5 (236)	6 (146)	7 (80)	8 (54)	9 (31)	10 (16)	11 (7)	12 (4)	13 (3)	14 (3)	15 (3)	16 (1)	17 (1)
Back calculated																			
2	10	65.1	90	112.1															
3	22	65.7	90.9	112.8	127.1														
4	49	57.8	93.5	115.4	130.9	144.2													
5	90	67.6	92.5	113.8	128.9	142.1	154												
6	66	67.6	91.6	112.1	126.7	139.7	151.6	162.3											
7	26	68.2	92.2	113.2	128.2	141.3	153.4	164.6	174.7										
8	23	68.5	92.6	113.4	128.2	141.9	153.9	165.3	175.9	185.1									
9	15	67.8	93.3	114.4	130.1	143.9	156	167.5	178.1	187.7	196.3								
10	9	67.1	93.2	112.9	127.9	141.5	153.6	165	175.7	185.6	194.3	201.6							
11	3	66.9	93	112.4	128.5	143.4	157.3	169	178.4	187	194.2	201.4	206.7						
12	1	64.3	90.8	110.7	129.2	143.8	155.7	167.7	178.3	187.5	195.5	202.1	208.7	214					
15	2	66.3	91.5	115.3	131	145.9	159.6	171.8	182.1	190.2	197.7	205.2	211.3	217.4	222.2	226.9	231.7		
17	1	65.5	93.3	119.7	133.6	146.1	157.2	168.3	179.4	189.2	198.9	207.2	214.2	219.8	225.3	229.5	233.7	237.8	240.6
Mean		66.8	92.2	113.7	129.2	143.1	155.2	166.8	177.8	187.5	196.1	203.5	210.2	217.1	223.8	228.2	232.7	237.8	240.6
SD		1.316	1.127	2.224	1.924	1.978	2.358	2.833	2.362	1.83	1.896	2.603	3.229	2.882	2.213	1.796	1.376	—	—
Observed																			
Mean		—	—	120.9	133.9	150.7	159	167.4	177.8	188.3	199	205.2	209	218	—	—	234.4	—	242
SD		—	—	8.765	9.185	8.803	7.688	9.003	9.354	7.556	5.641	3.509	6.557	0	—	—	0.629	—	0

Table 4

Likelihood ratio tests comparing estimates of von Bertalanffy parameters for males (noted as 1) and females (noted as 2) for *C. signatus* in the linear constraints.

Hypothesis	Linear constraints	Residual SS	χ^2_r	df	P
HΩ	none	60536.4			
Hω1	$L_{\infty 1} = L_{\infty 2}$	10511	0.049	1	0.996
Hω2	$K_1 = K_2$	10524.3	0.047	1	0.996
Hω3	$t_{01} = t_{02}$	10205.6	0.122	1	0.999
Hω4	Same L_∞, K, and t_0	24301.2	0.164	3	0.973

useful as a method of verification (Cailliet et al., 1983). Although no specimens younger than 2-years-old were caught (perhaps due to the gear selection bias), the presumed size at birth was about 60–65 cm (Compagno, 1984), which is similar to the estimated size in the present study (66.8 cm). Also, the estimated L_∞ value (270 cm), derived from the back-calculated or observed VBGF is close to the maximum size of 276 cm mentioned by Bigelow and Schroeder (1948), 280 cm off Cuba (Compagno, 1984), and 275 cm by Garrick (1985).

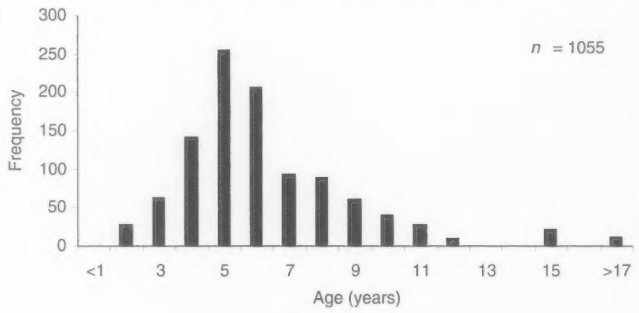

Figure 7

Age composition for the night shark (*C. signatus*) collected off northeastern Brazil.

Mean observed length-at-age is generally higher than back-calculated mean length-at-age (Bonfil et al., 1993; Lessa and Santana, 1998), leading to lower values of L_∞ and higher values of K. However, in the present study, although mean observed length-at-age is higher than mean back-calculated lengths, parameters derived from back-calculation provided a lower L_∞ and a higher K value. Inconsistency of the observed length-at-age set is attributed to the missing values in for ages 0, 1, 13, 14, and 16. This led to a VBGF which provided an unrealistic birth size of 90 cm and which present a flatter shape than the back-calculated curve.

Von Bertalanffy growth parameters generated from both back-calculation and by the Fabens method were all considered suitable and were of the same magnitude. However, taking into account 1) parameters close to those derived for length-frequency analysis, and 2) the best statistical fit, the back-calculated VBGF was chosen as best representing growth in the species.

Comparisions of biological features such as maturity size and maximum sizes have been used for inferences in growth and to explain differences between sexes (Natanson et al., 1995; Natanson and Kohler, 1996; Lessa et al., 2000). The studied species shows a disparity of ~15 cm in maturity sizes between sexes (Hazin, et al., 2000), corresponding to ~2 years. In addition, the largest specimen, for which sex was determined, was a 252-cm female and the largest male was 248 cm. These disparities, however, did not bring about differences in growth between sexes, as indicated by results of both tests used. Such a result can be explained by the number of juveniles used for age determination (~83%). Thus, the number of adults was not high enough to bring about any differences in the growth equation although differences frequently occur after maturity, caused by different growth rates between sexes (Natanson et al., 1995; Sminkey and Musick, 1995).

Assuming that the time elapsed between birth and the band corresponding to age 1 is one year, the species grows 38% of its birth length during the first year. This growth rate is close to that (50%) generally assumed (Branstetter 1990; Cortés, 2000). Furthermore, the estimated K value falls within the range suggested by the first author, and according to him, the night shark is a relatively fast growing species, presenting a life strategy similar to that of *C. falciformis*, and apparently depending on rapid growth for adequate neonate survival due to vulnerability to predation from large sharks.

In summary, considering the increasing fishing effort on the night shark as a targeted species and that catches are mainly composed by juveniles (representing 74.7% of specimens in landings), we believe that the K-selected characteristics of the species (including late maturity, long gestation period, and low fertility) should be taken into account in determining the management of this resource. Demographic analyses will be required for the examination of consequences of current levels of exploi-

Table 5

Age-length key (in percentages) for the night shark (*C. signatus*) caught off northeastern Brazil. Numbers in parentheses are the number of individuals examined in each age class.

		Age (years)															
TL (cm)	*n*	2 (10)	3 (22)	4 (49)	5 (90)	6 (66)	7 (26)	8 (23)	9 (15)	10 (9)	11 (3)	12 (1)	13 —	14 —	15 (2)	16 —	17 (1)
112.5	3	100	—	—	—	—	—	—	—	—	—	—	—	—	—	—	—
117.5	1	100	—	—	—	—	—	—	—	—	—	—	—	—	—	—	—
122.5	6	66.7	33.3	—	—	—	—	—	—	—	—	—	—	—	—	—	—
127.5	8	12.5	87.5	—	—	—	—	—	—	—	—	—	—	—	—	—	—
132.5	9	—	66.7	33.3	—	—	—	—	—	—	—	—	—	—	—	—	—
137.5	5	—	60	40	—	—	—	—	—	—	—	—	—	—	—	—	—
142.5	11	9.1	9.1	63.6	18.2	—	—	—	—	—	—	—	—	—	—	—	—
147.5	16	—	12.5	62.5	12.5	12.5	—	—	—	—	—	—	—	—	—	—	—
152.5	42	—	—	28.6	61.9	9.5	—	—	—	—	—	—	—	—	—	—	—
157.5	39	—	2.6	20.5	56.4	20.5	—	—	—	—	—	—	—	—	—	—	—
162.5	37	—	—	8.1	51.4	37.8	2.7	—	—	—	—	—	—	—	—	—	—
167.5	26	—	—	15.4	34.6	34.6	11.5	3.8	—	—	—	—	—	—	—	—	—
172.5	29	—	—	—	20.7	48.3	31	—	—	—	—	—	—	—	—	—	—
177.5	21	—	—	—	19	52.4	14.3	14.3	—	—	—	—	—	—	—	—	—
182.5	9	—	—	—	—	33.3	33.3	33.3	—	—	—	—	—	—	—	—	—
187.5	12	—	—	—	—	8.3	41.7	41.7	8.3	—	—	—	—	—	—	—	—
192.5	8	—	—	—	—	—	—	62.5	37.5	—	—	—	—	—	—	—	—
197.5	12	—	—	—	—	—	16.7	50	25	8.3	—	—	—	—	—	—	—
202.5	7	—	—	—	—	—	—	—	71.4	14.3	14.3	—	—	—	—	—	—
207.5	9	—	—	—	—	—	—	—	33.3	66.7	—	—	—	—	—	—	—
212.5	2	—	—	—	—	—	—	—	—	50	50	—	—	—	—	—	—
217.5	2	—	—	—	—	—	—	—	—	—	50	50	—	—	—	—	—
222.5	—	—	—	—	—	—	—	—	—	—	—	—	—	—	—	—	—
227.5	—	—	—	—	—	—	—	—	—	—	—	—	—	—	—	—	—
232.5	2	—	—	—	—	—	—	—	—	—	—	—	—	—	100	—	—
237.5	—	—	—	—	—	—	—	—	—	—	—	—	—	—	—	—	—
>242.5	1	—	—	—	—	—	—	—	—	—	—	—	—	—	—	—	100

tation to ensure the sustainability of the night shark in northeastern Brazil.

Acknowledgments

The present research was funded by Ministério do Meio Ambiente-MMA, Secretaria da Comissão Interministerial para os Recursos do Mar-SECIRM in the scope of Programa Nacional de Avaliação do Potencial Sustentável de Recursos Vivos–REVIZEE. We are grateful to Norte Pesca S. A. and to Conselho Nacional de Desenvolvimento Científico e Tecnológico-CNPq for scholarships and research grants (Procs: 301048/83, 38.0726/96-3 and 820652/87-3).

Literature cited

Amorim, A. F., C. A. Arfelli, and L. Fagundes.
1998. Pelagic elasmobranchs caught by longliners off Southern Brazil during 1974–97: an overview. Mar. Freshw. Res., 49:621–632.

Batista, V. S., and T. C. Silva.
1995. Age and growth of juveniles of junteiro shark *Carcharhinus porosus* in the coast of Maranhão, Brazil. Rev. Bras. de Biol. 55 (suppl. I):25–32.

Bartoo, N. V., and K. E. Parker.
1983. Reduction of bias generated by age-frequency estimation using the von Bertalanffy growth equation. *In* Proceedings of the international workshop on age determination of oceanic pelagic fishes: tunas, billfishes, and sharks (E. D. Prince and L. M. Pulos, eds.), p. 25–26. NOAA Technical Report NMFS 8.

Beamish, R. J., and D. A. Fournier.
1981. A method for comparing the precision of a set of age determinations. Can. J. Fish. Aquat. Sci., 38: 982–983.

Beamish, R. J., and G. A. McFarlane.
1983. Validation of age determination estimates: The forgotten requirement. *In* Proceedings of the international workshop on age determination of oceanic pelagic fishes: tunas, billfishes, and sharks (E. D. Prince and L. M. Pulos, eds.), p. 29–33. NOAA Technical Report NMFS circular 8.

Bigelow, H. B., and W. C. Schroeder.
1948. Fishes of the western North Atlantic, lancelets, cyclostomes, sharks, 576 p. Memoirs of Sears Foundation for Marine Research I.

Bonfil, R., R. Mena, and D. Anda.
1993. Biological Parameters of Commercially Exploited Silky Shark, *Carcharhinus falciformis*, from the Campeche Bank, Mexico. NOAA Technical Report NMFS 115:73–76.

Branstetter, S.
1990. Early life-history implications of selected carcharhinoid and lamnoid sharks of the northwest Atlantic. *In* Elasmobranchs as living resources: advances in the biology, ecology, systematics, and the status of the fisheries (H. Pratt, S. Gruber, and T. Taniuchi, eds.), 17–28. NOAA Technical Report NMFS 90.

Branstetter, S., J. A. Musick, and J. A. Colvocoresses.
1987. A comparison of the age and growth of the tiger shark, *Galeocerdo cuvieri*, from off Virginia and from the northwestern gulf of Mexico. Fish. Bull. 85:269–279.

Branstetter, S., and R. Stiles.
1987. Age and growth estimates of the bull shark, *Carcharhinus leucas*, from Northern Gulf of Mexico. Environ. Biol. Fish. 20(3):169–181.

Brothers, E. B.
1983. Summary of round table discussions on age validation. *In* Proceedings of the international workshop on age determination of oceanic pelagic fishes: tunas, billfishes, and sharks (E. D. Prince, L. M. Pulos, eds.), p. 35–44. NOAA Technical Report NMFS 8.

Cadenat J., and J. Blache.
1981. Requins de Méditerranée et d´Atlantique. Faune tropicale, 330 p. ORSTOM (Office de Recherche Scientifique et Technique d'Outre-Mer) 21.

Cailliet, G.
1990. Elasmobranch age determination and verification: an updated review. *In* Elasmobranchs as living resources: advances in biology, ecology, systematics and the status of the fisheries (H. L. Pratt Jr., S. H. Gruber, and T. Taniuchi, eds.), p. 157–165. NOAA Technical Report NMFS 90.

Caillet, G., K. L. Martin, D. Kusher, P. Wolf, and B. A. Welden.
1983. Techniques for enhancing vertebral bands in age estimation of California elasmobranchs. *In* Proceedings of the international workshop on age determination of oceanic pelagic fishes: tunas, billfishes, and sharks (E. D. Prince, L. M. Pulos, eds.), p. 157–165. NOAA Technical Report NMFS 8.

Carlson, J. K., E. Cortés, and A. G. Johnson.
1999. Age and growth of the blacknose shark *Carcharhinus acronotus* in the eastern Gulf of Mexico. Copeia 1999(3): 684–691.

Cerrato, R. M.
1990. Interpretable statistical tests for growth comparisons using parameters in the von Bertalanffy equation. Can. J. Fish. Aquat. Sci. 47(7):1416–1426.

Compagno, L. J. V.
1984. FAO species catalogue. Vol. 4: Sharks of the world, Part 2: Carcharhiniformes. FAO Fisheries Synopsis 125: 251–655. FAO, Rome.
1988. Sharks of the order Carcharhiniformes, 486 p. Princeton Univ. Press, Princeton, NJ.

Cortés, E.
2000. Life history and correlations in sharks. Rev. Fish. Sci. 8(4):299–344.

Crabtree, R. E., and L. H. Bullock.
1998. Age, growth, and reproduction of black grouper, *Mycteroperca bonaci*, in Florida waters. Fish. Bull. 96: 735–753.

Fabens, A. J.
1965. Properties and fitting of the von Bertalanffy growth curve. Growth 29:265–289.

Gayanilo, F. C. Jr., P. Sparre, and D. Pauly.
1996. FAO ICLARM stock assessment tools. User's manual. FAO computerized information series (Fisheries) 8, 126 p and 3 diskettes. FAO, Rome.

Garrick, J. A. F.
1982. Sharks of the genus *Carcharhinus*. NOAA Tech. Rep. NMFS circular, 194 p.
1985. Additions to a revision of the shark genus *Carcharhinus*: Synonymy of the *Aprionodon* and *Hypoprion* and descriptions of as new species of Carcharhinus (Carcharhinidae). NOAA Tech. Rep. NMFS 34, 26 p.

Gruber, S., and R. Stout.
1983. Biological materials for the study of age and growth in tropical marine elasmobranch, the lemon shark, *Negaprion brevirostris* (Poey). *In* Proceedings of the international workshop on age determination of oceanic pelagic fishes: tunas, billfishes, and sharks (E. D. Prince, and L. M. Pulos, eds.), 193–205. NOAA Technical Report NMFS 8.

Guitart Manday, D.
1975. Las pesquerias pelago-oceanicas de corto radio de acción en la région noroccidental de Cuba. ser. Oceanol. Acad. Cienc. Cuba 31, 26 p.

Hazin, F. H. V., J. R. Zagaglia, M. Broadhurst, P. Travassos, and T. R. Q. Bezerra.
1998. Review of a small-scale pelagic longline fishery off northeastern Brazil. Mar. Fish. Rev. 60(3):1–8.

Hazin, F. H., F. Lucena, T. S. L. Souza, C. Boeckman, M. Broadhurst, and R. Menni.
2000. Maturation of the night shark, *Carcharhinus signatus*, in the south-western equatorial Atlantic Ocean. Bull. Mar. Sci. 66(1):173–185.

Kappenman, R. F.
1981. A method for growth curve comparisons. Fish. Bull. 79:95–101.

Killam, K. A., and G. R. Parsons.
1989. Age and growth of the blacktip shark, *Carcharhinus limbatus*, near Tampa Bay, Florida. Fish. Bull. 87:845–857.

Krefft, G.
1968. Neue und erstmalig nachgewiesene Knorpelfische aus dem Archibenthal des Südwestatlantiks, einsliesslich einer Diskussion einiger *Etmopterus*-Arten Südlicher Meere. Arch. Fischereiwiss. 19(1):1–72.

Lessa, R., and F. M. Santana.
1998. Age determination and growth of the smalltail shark *Carcharhinus porosus* from northern Brazil. Mar. Freshw. Res. 49:705–711.

Lessa, R., V. Batista, and Z. Almeida.
1999a. Occurrence and biology of the daggernose shark *Isogomphodon oxyrhynchus* (Chondrichthyes: Carcharhinidae) off the Maranhão Coast (Brazil). Bull. Mar. Sci. 64(1):115–128.

Lessa, R., F. Santana, R. Menni, and Z. Almeida.
1999b. Population structure and reproductive biology of the smalltail shark (*Carcharhinus porosus*) off Maranhão. Mar. Freshw. Res. 50:383–388.

Lessa, R., F. M. Santana, and R. Paglerani.
1999c. Age, growth and stock structure of the oceanic whitetip shark, *Carcharhinus longimanus*, from the southwestern Equatorial Atlantic. Fish. Res. 42:21–30.

Lessa, R., F. M. Santana, V. Batista, and Z. Almeida.
2000. Age and growth of the daggernose shark, *Isogomphodon oxyrhynchus*, from northern Brazil. Mar. Freshw. Res. 51:339–347.

Marín, Y., F. Brum, L. F. Barea, and J. F. Chocca.
1998. Incidental catch associated with swordfish longline fisheries on the South-West Atlantic Ocean. Mar. Freshw. Res. 49:633–639.

Menni, R. C., F. H. V. Hazin, and R. P. Lessa.
1995. Occurrence of the night shark *Carcharhinus signatus*, and the pelagic stingray *Dasyatis violacea* off northeastern Brazil. Neotropica 41(105–106):105–110.

Natanson, L. J., J. G. Casey, and N. E. Kohler.
1995. Age and growth estimates for the dusky shark, *Carcharhinus obscurus*, in the western North Atlantic Ocean. Fish. Bull. 93:116–126.

Natanson, L. J., and N. E. Kohler.
1996. A preliminary estimate of age and growth of the dusky shark *Carcharhinus obscurus* from the South-West Indian Ocean, with comparisons to the Western North Atlantic population. S. Afr. J. Mar. Sci. 17: 217–224.

Prager, M. M., S. B. Saila, and C. M. Recksiek.
1987. FISHPARM: a microcomputer program for parameter estimationof nonlinear models in fishery science. Technical Report. 870:1–37. Dep. Oceanography, Old Dominion Univ., Norfolk, VA.

Ricker, W. E.
1969. Effects of size-selective mortality and sampling bias on estimates of groowth, mortality, production and yield. J. Fish. Res. Board Can. 26(3):479–541.

Seki, T., T. Taniuchi, H. Nakano, and M. Shimizu.
1998. Age, growth and reproduction of the oceanic whitetip shark, *Carcharhinus longimanus* from the Pacific Ocean. Fish. Sci. 64(1):14–20.

Shepherd, J. G.
1987. A weakly parametric method for estimating growth parameters from length composition data. *In* Length-based methods in fisheries research. ICLARM (International Center for Living Resources Management) conference proceedings 13 (D. Pauly and G. Morgan, eds.), p. 113–119. ICLARM, Manila, and the Kuwait Institute for Scientific Research, Safat, Kuwait.

Sminkey, T. R., and J. A. Musick.
1995. Age and growth of the sandbar shark, *Carcharhinus plumbeus*, before and after population depletion. Copeia 1995(4):871–883.

Sparre, P., E. Ursin, and S. C. Venema.
1989. Introduction to tropical fish stock. Part 1. Manual. FAO Fisheries Tech. Paper 306.1, 337 p. FAO, Rome.

Suzuki, Z., Y. Warashima, and M. Kishida.
1977. The comparison of catches by regular and deep tuna longline gear in the western and central equatorial Pacific. Bull. Far Seas Fish. Res. Lab. 15:51–89.

von Bertalanffy, L.
1938. A quantitative theory of organic growth. Hum. Biol. 10:181–213.

Wintner, S., and G. Cliff.
1996. Age and growth determination of the blacktip shark, *Carcharhinus limbatus*, from the east coast of South Africa. Fish. Bull. 94:135–144.

Zar, J. H.
1996. Biostatistical analysis, 3rd ed., 662 p. Prentice Hall, Upper Saddle River, NJ.

Abstract—The prowfish (*Zaprora silenus*) is an infrequent component of bottom trawl catches collected on stock assessment surveys. Based on presence or absence in over 40,000 trawl catches taken throughout Alaskan waters southward to southern California, prowfish are most frequently encountered in the Gulf of Alaska and the Aleutian Islands at the edge of the continental shelf. Based on data from two trawl surveys, relative abundance indicated by catch per swept area reaches a maximum between 100 m and 200 m depth and is much higher in the Aleutian Islands than in the Gulf of Alaska. Females weigh 3.7% more than males of the same length. Weight-length functions are W (g) = 0.0164 $L^{2.92}$ (males) and W = 0.0170 $L^{2.92}$ (females). Length at age does not differ between sexes and is described by $L = 89.3(1 - e^{-0.181(t+0.554)})$, where L is total length in cm and t is age in years. Females reached 50% maturity at a length of 57.0 cm and an age of 5.1 years. Prowfish diet is almost entirely composed of gelatinous zooplankton, primarily scyphozoa and salps.

Manuscript approved for publication 20 September 2003 by Scientific Editor.
Manuscript received 20 October 2003 at NMFS Scientific Publications Office.
Fish. Bull. 102:168–178 (2004).

Distribution and biology of prowfish (*Zaprora silenus*) in the northeast Pacific

Keith R. Smith
David A. Somerton
Mei-Sun Yang
Daniel G. Nichol
Alaska Fisheries Science Center
National Marine Fisheries Service
7600 Sand Point Way NE
Seattle, Washington 98115
E-mail address (for K. R. Smith, contact author): Keith.Smith@noaa.gov

Current taxonomy distinguishes the prowfish (*Zaprora silenus*, Fig. 1) as the only species and the only genus of the family Zaproridae. Other families in the encompassing suborder Zoarcoidei include Bathymasteridae (ronquils), Cryptacanthodidae (wrymouths), Pholidae (gunnels), and Stichaeidae (pricklebacks). Systematics of most families within Zoarcoidei, and of the suborder itself within the order perciforms, is uncertain (Nelson, 1994). Prowfish (adult) physical features include an elongate, laterally compressed body; a high convex brow and interorbital area ending with a short blunt snout; and a distinctive protruding area below a slightly upturned terminal mouth. Fins consist of: a long, moderately high dorsal fin; a moderately long anal fin; a discrete truncate caudal fin with a short, broad peduncle; and moderately large, rounded pectoral fins (pelvic fins are absent). Teeth are small, sharp, and close-set in a single row attached only to the jaws. Scales are ctenoid. Numerous distinctive large round pores occur on the sides and top of the head. Color is olive-gray to brown dorsally, shading lighter below, suffused on the sides and back with many small dark spots (Clemens and Wilby, 1961; Eschmeyer et al, 1983; Hart, 1973; Kessler, 1985). The maximum length reported is more than 1 m (Tokranov, 1999).

Since its original description (Jordan, 1897), the prowfish has been observed infrequently despite numerous and extensive bottom trawl surveys comprising thousands of net deployments off Alaska and the west coast of North America. It is not clear whether this lack of documentation indicates a species of low abundance or a preference by prowfish for a habitat, such as rough rock substrate or steep bottom gradients, that is poorly sampled by bottom trawl surveys. Nevertheless, the species is common enough to be considered representative of the ichthyofauna of certain benthic biotopes within its range (Allen and Smith, 1988; Tokranov, 1999). It has been encountered at locations along the outer continental shelf and upper slope ranging in a long arc from San Miguel Island, California, north through the Gulf of Alaska, west through the Bering Sea and Aleutian Islands to the Asiatic shelf, thence south to Hokkaido, at depths of 10–675 m (Allen and Smith, 1988; Hart, 1973). In addition to occurring in the catches on biological surveys, prowfish have been taken incidentally, and occasionally processed, in commercial fishing operations on the outer continental shelf (Smith, pers. obs.; Berger[1]).

Prowfish are known to be pelagic as pre-adults (Hart, 1973; Doyle et al, 2002). After larval transformation at 30 mm (Matarese et al., 1989), juveniles maintain close proximity to the medusae of pelagic cnidarians (Scheffer, 1940). Brodeur (1998) observed juveniles swimming near the bells of scyphomedusae *Cyanea capillata* and *Chrysaora melanaster* and retreating

[1] Berger, J. 2002. Personal commun. Alaska Fisheries Science Center, National Marine Fisheries Service, 7600 Sand Point Way NE, Bldg 4, Seattle, WA 98115-0070.

Figure 1
Aquarium prowfish specimen, National Marine Fisheries Service, Kodiak Laboratory, Kodiak, AK. Photograph by Jan Haaga.

behind the tentacles or within the bells of these jellyfish when approached by a remotely operated vehicle, apparently as a means of protection from predators. Prowfish are also believed to later become demersal and have a preference for rocky areas (Tokranov, 1999).

The association with scyphomedusae and other large gelatinous zooplankton exhibited by juveniles may continue throughout their lives, because such prey are reported to constitute a considerable portion of the prowfish diet (Carollo and Rankin, 1998). In the stomachs of 16 juveniles of 5–13.3 cm total length captured at midwater depths in Prince William Sound in 1995, Sturdevant[2] found prey biomass was composed principally of hyperiid amphipods but also found unquantifiable gelatinous matter which was thought to be the remains of jellyfish tentacles.

Little is known regarding possible predators of prowfish, the relative frequency of prowfish among prey items, or the sizes of prowfish consumed. Prowfish have been found in the diets of diving seabirds and have comprised 25% of food biomass delivered to tufted puffin (*Lunda cirrhata*) chicks (Sturdevant[2]). Yang (1993) found prowfish in only 0.3% of 467 stomachs of Pacific halibut (*Hippoglossus stenolepis*) taken by bottom trawl in the Gulf of Alaska in 1990, accounting for 0.03% (by weight) of total food present. Orlov (1998) found prowfish in 0.13% of stomachs of white-blotched skate (*Bathyraja maculata*) caught by bottom trawl off the Northern Kuril Islands and Southeastern Kamchatka in 1996. In comparisons of proximate composition among 17 taxa of forage-size fish from the northeastern Pacific (Van Pelt et al, 1997; Payne et al, 1999), juvenile prowfish averaged highest in moisture content (86–88% by weight) and relatively low in lipids (10.8±1.3%, dry weight analysis).

In this study we examined information on this little-known species, investigating spatial and depth distributions, size frequency, growth, reproduction, and diet in the waters off Alaska.

Materials and methods

Data and sample collection

Data used in this investigation were collected during bottom trawl surveys for groundfish and invertebrate stocks conducted by the Resource Assessment and Conservation Engineering (RACE) Division of the Alaska Fisheries Science Center (AFSC), National Marine Fisheries Service. Areas surveyed were the continental shelf and upper slope of the eastern Bering Sea, Aleutian Islands region (AI), Gulf of Alaska (GOA), and west coast of North America from Washington to California. Trawl catches were sorted to species, weighed, and individuals were counted, following procedures described in Wakabayashi et al. (1985).

[2] Sturdevant, M. V. 1999. Forage fish diet overlap, 1994–1996. *Exxon Valdez* oil spill restoration project final report (restoration project 97163C), 184 p. Alaska Fish. Sci. Cent., Auke Bay Laboratory, Natl. Mar. Fish. Serv., NOAA, Juneau, AK. [Available by order no. PB2000-100700 from Natl. Tech. Info. Serv, 5285 Port Royal Rd., Springfield, Virginia 22161.]

To characterize prowfish distribution we obtained catch data from 42,601 bottom trawl deployments (hauls) executed from 1953 through 2000 using a variety of net designs. We used these data to determine presence or absence of prowfish at each haul location. Previous observations have indicated that prowfish tend to be pelagic as larvae and become demersal as adults (Matarese et al., 1989; Hart, 1973). A full accounting of prowfish distribution by life stage is beyond the scope of this investigation, which focuses on adults. Therefore we confined our observations to haul catches taken on bottom, as opposed to in mid-water or at the surface.

On two of the bottom trawl surveys, one in the Gulf of Alaska from 22 May to 30 July 1996, and the other in the Aleutian Islands from 10 June to 11 August 1997, additional prowfish data were collected. Consistency between these surveys in sampling procedures and equipment (Martin, 1997, and Stark[3]) facilitated subsequent data comparisons.

Density of prowfish at each sampling location was estimated as the number caught divided by the km^2 of area swept by the trawl (catch per unit of effort, or CPUE). Research vessels on both surveys employed the standard RACE Division model poly-Nor'eastern high-opening bottom trawl net with roller gear, and hauls were made during daylight. Net configuration and bottom contact during trawling were monitored by Scanmar instrumentation. Data were obtained from 807 hauls in the Gulf of Alaska and 408 hauls in the Aleutian Islands. The average area swept per haul was 0.025 km^2 in the GOA and 0.024 km^2 in the AI.

All prowfish were sorted to sex by examination of the gonads and then length (total length; cm) was measured. Sample sizes were 84 males and 90 females for the Gulf of Alaska; 396 males and 431 females for the Aleutian Islands. Whole-body weights (g) of 83 male and 88 female prowfish from the Gulf of Alaska were measured and the sagittal otoliths were removed and stored in 50% ethanol. Whole ovaries from a representative subsample of 39 of the females were removed, frozen, and later stored in 10% buffered formalin solution.

Diet composition was examined from stomach contents of 76 individuals (18 from the Gulf of Alaska and 58 from the Aleutian Islands). Stomachs containing food and with no signs of regurgitation or net-feeding (e.g. the stomach was in an inverted or flaccid state or there was the presence of prey in the mouth or around the gills) were removed and preserved in 10% buffered formalin.

Laboratory procedures

Standard otolith-preparation techniques for age determination were modified to accommodate the relatively small size of prowfish otoliths (usually <5 mm long). An anterior portion of each otolith was removed by a transverse cut with scalpel perpendicular to the sagittal axis and anterior to the nucleus. The remainder, which contained the nucleus, was baked at 300–475°C for up to 17 min or heated over an alcohol flame to enhance visibility of annuli. The otoliths were then individually mounted on slides by completely embedding them in clear thermoplastic posterior end down. On hardening, each mount was wet-sanded on increasingly fine grades of sandpaper (400–2000 grit), parallel to the slide, until the surface intersected the otolith nucleus (transverse section). Preparing readable mounts was a delicate procedure; besides cutting and polishing the small otoliths precisely without fracturing them, precise heating temperature and time were especially critical to expose annuli without again causing fractures or burning the otolith. Our method had advantages over the standard "break and burn" method of simply coating the surface of a temporarily mounted specimen with oil to enhance visibility of annuli, in lieu of polishing. It allowed a more precise intersection of the nucleus by the viewed surface and eliminated the need to remove oil from specimens intended for further viewing in order to prevent blurring of annuli. After preparation, slides were placed in sufficient water to cover the surface scratches and were examined under a dissecting microscope with reflected light. Age in years was determined by counting the annuli or hyaline bands according to the criteria described in Chilton and Beamish (1982).

Prowfish ovaries were prepared for histological examination by removing a small portion from the middle of each ovary, which was then embedded in paraffin, sectioned at 6 μm, and stained with hematoxylin and eosin. The histological slides were examined under a compound microscope and donor females were classified as either sexually immature or mature based on the presence of yolk in the oocytes (i.e. vitellogenesis).

Prowfish stomachs were processed by first neutralizing the 10% formalin used for initial fixation and then by immediately transferring the stomachs into 70% ethanol. The food was removed, blotted with a paper towel, and examined with a dissecting microscope. Prey items were sorted to the lowest practical taxonomic level and then weighed to the nearest 0.1 gm. The percentage of total prey weight which each taxon comprised, as well as the percentage of stomachs containing each taxon, was calculated for each haul sample and then estimated for each of the two regions as the average of the per-haul percentages.

Analysis of data

The distribution of prowfish density over depth in the Gulf of Alaska and the Aleutian Islands was determined by calculating the mean CPUE for each 20-m depth interval from 20 m to 480 m. Both surveys utilized a stratified sampling design in which sampling density (hauls per unit area) varied by geographical subarea (Martin, 1997; Stark[3]). To compensate for this variation, the CPUE of each haul was weighted by the inverse of the sampling density in that geographic stratum. The mean bottom depth as weighted by prowfish density was calculated for each of the two regions as the weighted average of the midpoints of the depth intervals, where the weighting factors were the interval-mean CPUE values.

[3] Stark, J. 1998. Report to industry: fishing log for the 1997 bottom trawl survey of the Aleutian Islands. AFSC Proc. Rep. 98-06, 96 p. Alaska Fish. Sci. Cent., Natl. Mar. Fish. Serv., NOAA, 7600 Sand Point Way NE, Bldg. 4, Seattle, WA 98115-0070.

Frequency distributions of prowfish total length, separated by sex and region, were calculated as the weighted percent of measurements within 10-cm length intervals. The weighting factors were calculated for each fish measurement as the inverse of geographic-stratum sampling (i.e. haul) density, multiplied by the inverse of the individual haul area that was swept . Also, differences in mean length between sexes or regions were examined by using analysis of variance (ANOVA)[4] to test the significance of statistical differences based on the weighted lengths. Because potential grouping of prowfish by size could affect within-haul variance, source haul (i.e. that in which each measured fish was caught) was included in analyses as a possible random variable affecting length. Variances in length between regions and sexes were each tested for significance against variance among hauls. The significance of the haul variable was also checked by testing variance among hauls against that among measurements.

The relationship of body weight (g; W) to total length (cm; L) was assumed to be an exponential function:

$$W = e^{\alpha} L^{\beta},$$

for which the parameters α and β were estimated from the data by first log-transforming both variables and then calculating the intercept and slope of the least squares linear regression:

$$\ln(W) = \alpha + \beta \ln(L).$$

To determine whether the relationship differed by sex, analysis of covariance (ANCOVA; Statgraphics Plus, Manugistics, Inc., Rockville, MD) was used to compare the fit of a model with two regression lines, each with a sex-specific intercept and slope, to the fit of a two-line model with sex-specific intercepts and a common slope (null hypothesis). If no significant difference was observed, then a second test was performed by testing the latter model against the null hypothesis of a common regression line with single intercept and slope for both sexes combined. The relationships in the best-fit model were then transformed back to exponential form.

Prowfish growth was described by fitting the von Bertalanffy function to length (L) and age (year; t) data by using nonlinear least squares. The function is

$$L = L_{\infty}(1 - e^{-k(t - t_0)}),$$

where L_{∞} = asymptotic maximum length;
k = a constant (per year) affecting model early growth rate; and
t_0 = hypothetical age at 0 length.

To determine whether parameters differed between prowfish sexes, we fitted the function separately to the data from each sex as well as to the data for both sexes combined. A likelihood ratio test was then used to determine whether the separate-sex model fitted the data significantly better than the combined-sex model (Kimura, 1980). Significance of the likelihood ratio was based on the chi-squared statistic with degrees of freedom equal to the difference in number of parameters between the two models.

The proportion of prowfish females that were mature (P_{mat}) at a given length or age was described with logistic functions of the form $P_{mat} = 1/(1 + e^{\alpha + \beta X})$, where X is either length (L) or age in years (t), and α and β are function parameters. The models were fitted to the data by using maximum likelihood. After the relationships were estimated, the length and age at which 50% of females were mature were estimated by setting $P_{mat} = 0.5$ in each function and solving for X. The 95% confidence interval for each estimate was calculated by using the delta method (Seber, 1973).

Results

Geographic distribution

Prowfish distribution in the waters off Alaska, as indicated by their presence at 1528 out of a total of 35,159 historical bottom trawl locations, is shown in Figure 2. The total count of individuals in catches was 11,401. Distribution south of approximately 50°N latitude off Vancouver Island is not shown because here 6 of 7442 bottom trawl hauls caught a total of 8 prowfish. The southernmost occurrence was at 34°13.4′N latitude near San Miguel Island, southern California. Prowfish were taken at depths ranging from 24 m to 801 m but most frequently appeared in catches close to the break between the continental shelf and upper continental slope near 200 m depth.

Prowfish CPUE was greater than zero at 64 of 807 haul locations in the Gulf of Alaska in 1996 and at 48 of 408 locations in the Aleutian Islands in 1997. Over all areas at the depths fished the range of per-haul CPUE was 0–547.5 prowfish/km^2 (average=6.7 prowfish/km^2) in the GOA and 0–5220.1 prowfish/km^2 (average=65.1 prowfish/km^2) in the AI. The average CPUE within 20-m bottom depth intervals in each region indicated that fish tend to be most concentrated at intermediate depths (Fig. 3). Depth at trawl locations ranged from 20 to 479 m for the GOA and from 22 to 474 m for the AI, and prowfish were collected at 34–252 m (GOA) and 89–258 m (AI), respectively. The CPUE-weighted average bottom depth was 163.8 m for the GOA and 150.3 m for the AI.

The CPUE values within 20-m depth intervals (Fig. 3) indicated that the regional difference in mean density was largely due to differences at the same depth rather than differences between regions in the amount of area available at a given bottom depth.

Length distribution

Length-frequency histograms by region and sex for prowfish from the Gulf of Alaska (84 males, 90 females) and Aleutian Islands (396 males, 431 females) are shown in Figure 4. Analysis of variance tests for a difference in mean length

[4] Unless otherwise specified, ANOVA, log-likelihood, and nonlinear regression analyses were accomplished by using Systat 10 software (Systat 10 Statistics I, SPSS Inc.,Chicago, IL).

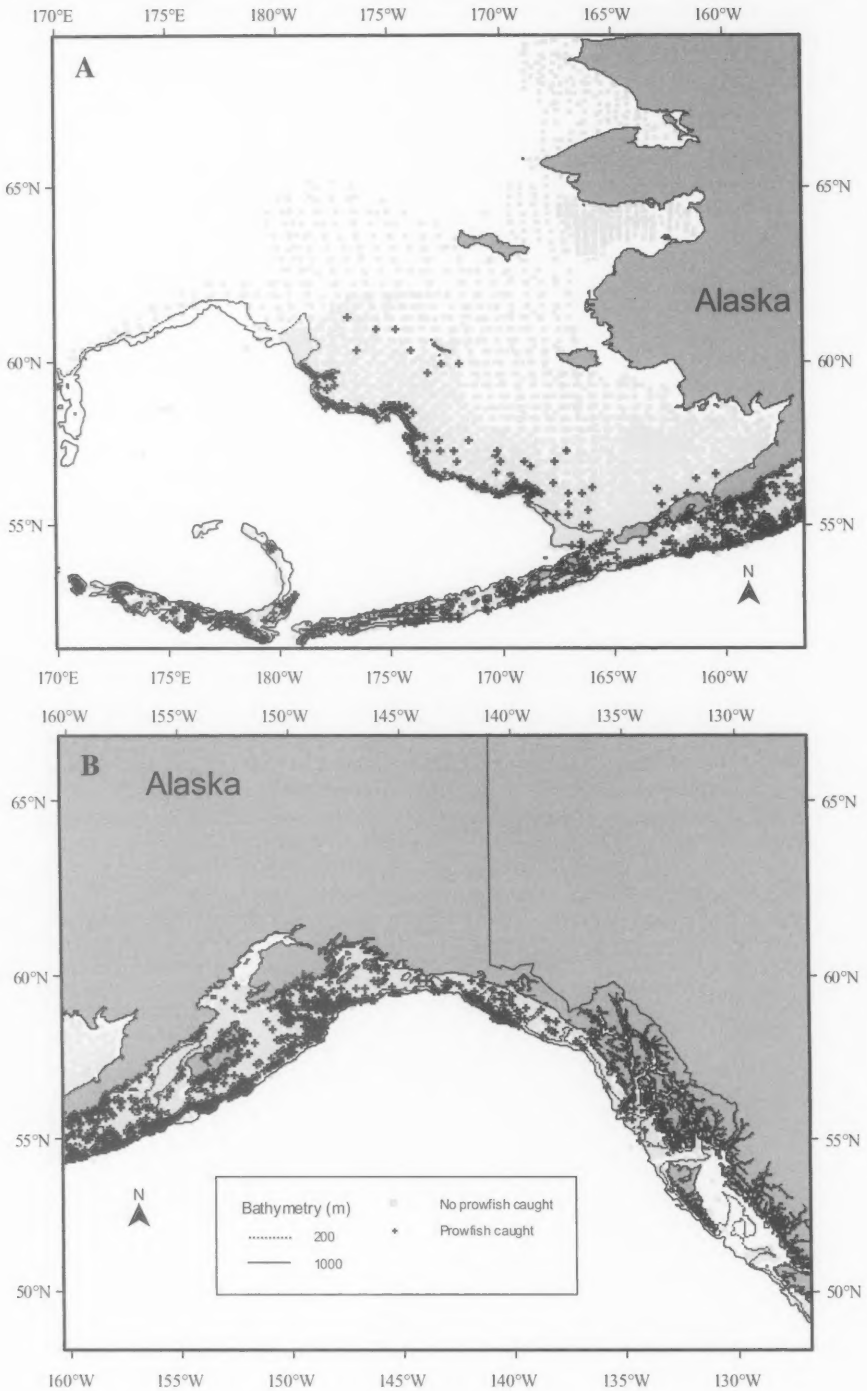

Figure 2

Locations of Alaska Fisheries Science Center groundfish survey bottom trawls (prior to year 2001) in (**A**) the eastern Bering Sea and the Aleutian Islands region and (**B**) the Gulf of Alaska, indicating trawls in which prowfish occurred.

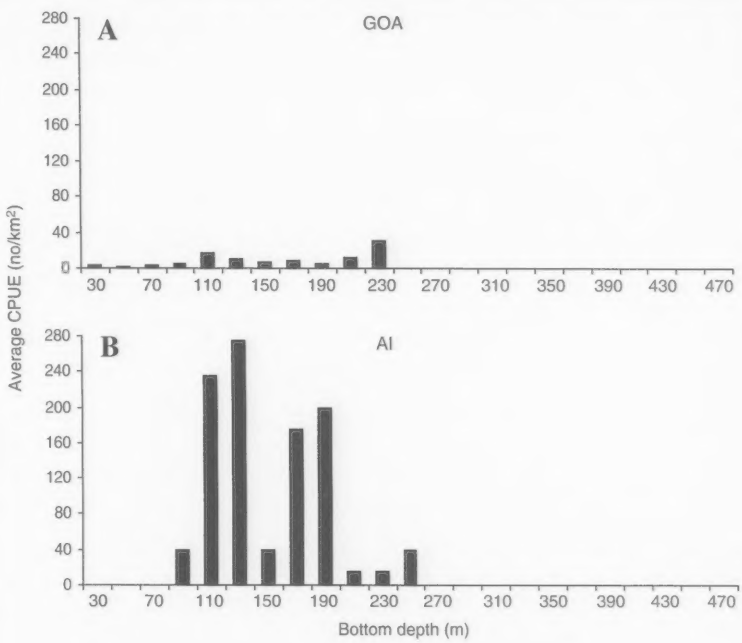

Figure 3

Average prowfish catch per unit of effort (CPUE; no/km^2) within 20-m intervals over the range of trawl depths of 20–479 m in the Gulf of Alaska (GOA) in 1996 (**A**) and 22–474 m in the Aleutian Islands (AI) in 1997 (**B**). The mean of interval midpoints, each weighted by interval average CPUE, was 163.8 m for the GOA and 150.3 m for the AI.

between sexes were not significant for either the GOA (P=0.83) or the AI (P=0.76). Although the weighted mean for both sexes combined was 61.0 cm (range: 11–90 cm) in the GOA and 51.9 cm (range: 25–87 cm) in the AI, the difference in length between regions was not significant (P=0.11). Grouping of prowfish of similar size within hauls was highly significant in both the GOA and the AI (P<<0.01).

Weight-length relationship

In the between-sex ANCOVA comparison of the linearized (i.e. log-transformed) weight-to-length relationships based on prowfish caught in the Gulf of Alaska, the slopes were not significantly different between sexes (P=0.38). However, the difference in intercepts was significant (P=0.044). Thus the best fitting model varied by sex with two regression lines of equal slope but with sex-specific intercepts. The equivalent functions in terms of the untransformed variables (Fig. 5) were

$$W_{males} = 0.0164 \times L^{2.922},$$

and

$$W_{females} = 0.017 \times L^{2.922}.$$

The model indicated that adult females are, on average, 3.7% heavier than males of the same length.

Age and growth

Readable otolith specimens were produced for 138 prowfish (71 males, 67 females) of the 172 from which samples were collected. Production of readable specimens did not appear related to fish size or age. The likelihood ratio test for a difference between males and females in the relationship of length to age was not significant (P=0.53), indicating that there was no difference in growth between sexes. The best-fit von Bertalanffy function (Fig. 6) had the following parameters (with 95% confidence intervals): L_∞ = 89.33 ±6.5 cm; k = 0.18 ±0.05/year; and t_0 = –0.55 ±0.12 year.

Female maturity

The proportions of females that were mature were highly significant logistic functions of length and age (P<0.005; Fig. 7). The fitted functions of length and age were

$$P_{mat} = 1/(1 + e^{371.14 - 6.51L});$$

and

$$P_{mat} = 1/(1 + e^{9.66 - 1.90t}).$$

The theoretical length and age at which 50% of females were mature, with respective 95% confidence limits, were 57.0 ±0.4 cm and 5.1 ±0.7 years.

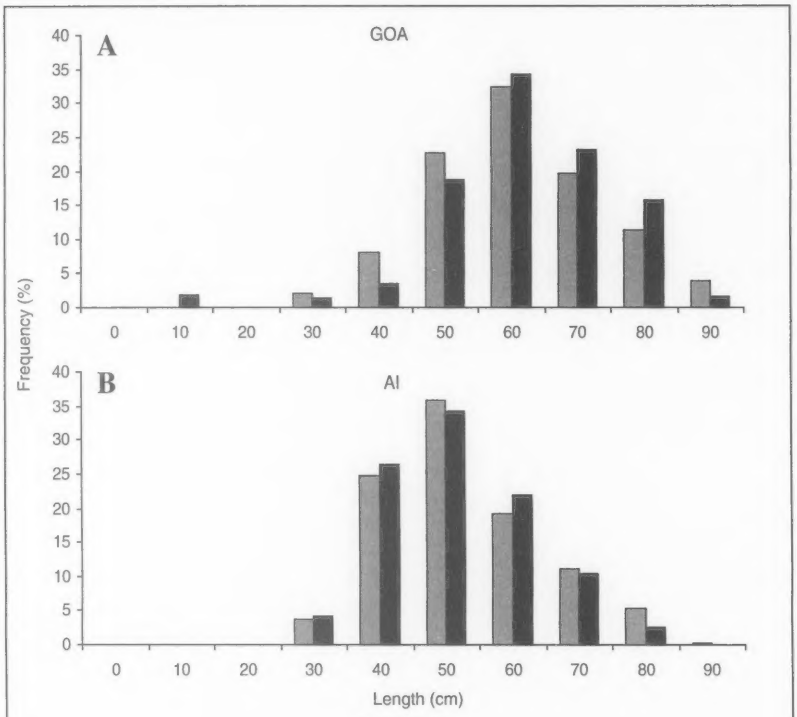

Figure 4

Frequency distribution of total lengths of (**A**) 84 male and 90 female prowfish from the Gulf of Alaska (GOA; 1996) and (**B**) 396 males and 431 females from the Aleutian Islands (AI; 1997). Gray bars show the percentage of male lengths and black bars the percentage of female lengths within continuous 10-cm intervals (e.g. 25–35 cm).

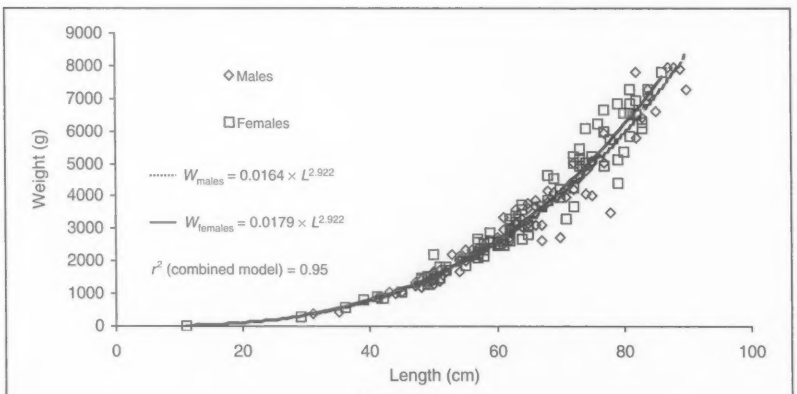

Figure 5

Prowfish body weight (W) fitted by an exponential function of fish total length (L) and sex. Data for males (n=83) are shown by diamonds and the fitted model by a dashed line. Data for females (n=88) are shown by squares and the fitted model by a solid line.

Food habits

Fish used for diet study averaged 63.8 cm in total length (range: 49–87 cm) in the Gulf of Alaska and 56.9 cm (range: 30–79 cm) in the Aleutian Islands. The contents of 18 prowfish stomachs from the Gulf of Alaska and 58 from the Aleutian Islands showed that jellyfish (99% and 31%

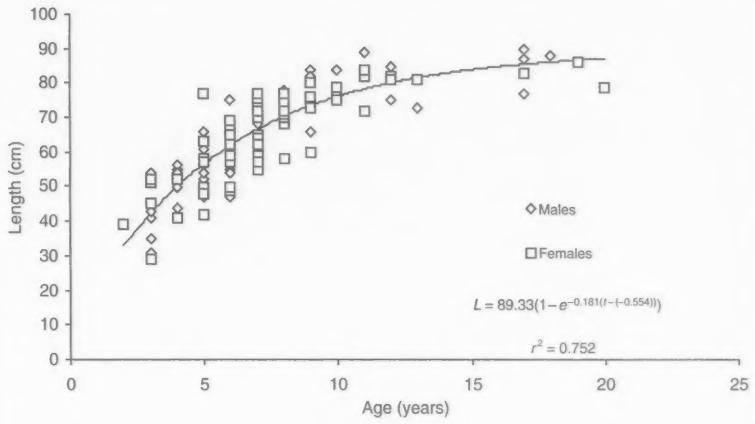

Figure 6

Prowfish total length (L) fitted by a von Bertalanffy function of age (t). Data for males (n=71) are shown by diamonds; data for females (n=67) are shown by squares. The fitted model is shown by a solid line.

Table 1

Mean percent weight (%W) and mean percent frequency of occurrence (%FO) of the prey items from 18 prowfish stomachs collected in the Gulf of Alaska (GOA; 1996; total prey weight=299 g) and 58 stomachs from the Aleutian Islands area (AI; 1997; total prey weight=1446.6 g). Sample prowfish had an average total length of 63.8 cm (range: 49–87 cm) from the GOA and and 56.9 cm (range: 30–79 cm) from the AI.

	GOA (n=18)		AI (n=58)	
Prey name	% W	% FO	% W	% FO
Scyphozoa (jellyfish)	98.84	100	30.45	29.88
Ctenophora (comb jelly)			0.09	1.23
Polychaeta (worm)			0.03	5.8
Calanoida (copepod)	0.26	28.13	0.04	29.14
Thysanoessa raschii (euphausiid)			0.05	6.67
Mysidacea Mysida (mysid)	0.01	3.13		
Hyperiidea (amphipod)			0.19	33.46
Gammaridea (amphipod)			0.12	30.49
Themisto sp. (amphipod)	0.32	28.57	0.14	36.91
Salpa sp. (pelagic salp)			34.06	46.79
Larvacea (pelagic tunicate)	0.13	12.5		
Sebastes sp. (rockfish) larvae, 5–8 mm long	0.43	42.86		
Microsomus pacificus (Dover sole) eggs	0.01	3.13		
Unidentified organic material			34.84	32.59

by weight of total food in the two regions, respectively) and gelatinous pelagic tunicates (*Salpa* spp.; 34% in the Aleutian Islands area only) were the most important food (Table 1). Although calanoid copepods and *Themisto* sp. (amphipod) were both often present in GOA specimens (28.13% and 28.57% of stomachs, respectively), they were not important food in terms of weight. The same was true in the AI for calanoid copepods, *Themisto* sp., gammaridean amphipods, and hyperiidean amphipods (29.14%, 36.91%, 30.49%, and 33.46% respectively). Mysids and larvaceans from GOA specimens as well as ctenophors, polychaetes, and euphasiids from AI specimens occurred in trace amounts. *Sebastes* larvae (5–8 mm standard length), the only fish species found, were found in 43% of Gulf of Alaska stomachs but made up only 0.43% of prey weight. Some Dover sole (*Microstomus pacificus*) eggs had also been consumed.

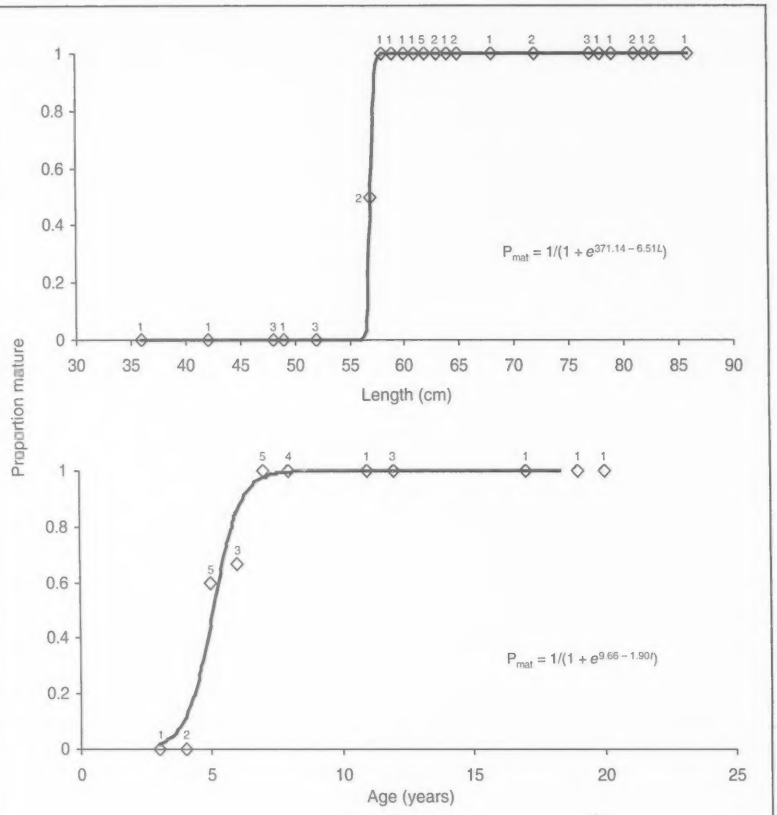

Figure 7

Proportion of female prowfish mature (P_{mat}) as logistic functions of length (L) and age (t). Data points based on 39 maturity-at-length and 27 maturity-at-age observations are shown by diamonds, and numbers of females of each cm-length and year-age class are shown next to the corresponding symbol. The fitted logistic models are shown by solid lines. The length and age at which $P_{mat} = 0.5$ with 95% confidence limits are 57.0 ±0.4 cm and 5.1 ±0.7 years.

Discussion

Geographic distribution

Historically occurring in the catch in AFSC bottom trawl surveys in areas of the eastern Bering Sea, Aleutian Islands, and Gulf of Alaska regions, prowfish were also observed more rarely farther south along the West Coast as far as the vicinity of San Miguel Island, California. This is the apparent southern limit of their range in the northeastern Pacific (Allen and Smith, 1988). They were most often encountered in the vicinity of the edge of the continental slope near 200 m depth (Fig. 2), although our data increase the maximum known depth of occurrence from 675 m (Allen and Smith, 1988) to 801 m. As indicated by survey CPUE, prowfish density was greatest between the depths of 100 m and 240 m (Fig. 3). Our distribution data show similarities with those of Tokranov (1999), who studied >300 bottom trawls executed in 1995–97 on the shelf and slope off the southern Kamchatka Peninsula and northern Kuril Islands, in which adult prowfish were taken at 100–480 m. Tokranov often found fish concentrated in areas of high-relief, rocky bottom—a common feature of the shelf edge in the Gulf of Alaska and Aleutian Islands regions. Such areas near the shelf break may be important prowfish habitat. Underwater videos taken in the northeast Gulf of Alaska by the Alaska Department of Fish and Game (Brylinsky[5]) show numerous adult fish resting on or just above this type of substrate.

Density was greater in the AI than in the GOA, over all bottom depths combined and in most cases by individual depth interval (Fig. 3). One reason may be that preferred habitat comprises a larger proportion of the Aleutian Is-

[5] Brylinsky, C. 2000. Pers. commun. Alaska Department of Fish and Game, 304 Lake Street, Sitka, AK 99835.

lands area. Because of the lack of a relatively broad shelf in the region, a larger proportion of trawls are in or near areas of steep seafloor gradient and therefore likely over rough bottom (Fig. 2).

Length distribution

In both the Gulf of Alaska and the Aleutian Islands, few prowfish <40 cm in length were captured (Fig. 4). This paucity of small prowfish is not due to size selection by the trawl net mesh because the codend is lined with small mesh (1.3 cm stretched measure) webbing that retains small individuals of other species. A different explanation, based on the observations of Brodeur (1998) and Scheffer (1940), is that pre-adult prowfish are pelagic, remaining in proximity with large coelenterates and thus avoiding bottom trawls. Thus, the minimum capture length may indicate the length at which prowfish recruit to a demersal habitat. Our data showed no statistically significant length difference between sexes, in contrast with the data of Tokranov (1999) who suggested a length dimorphism where females are generally longer than males.

Weight-length relationship

The best-fitting model of weight versus length predicts that for any length, female prowfish are, on average, 3.7% heavier than males (Fig. 5). It seems unlikely that this relationship exists over all developmental stages because our samples were almost all adults and such a (relative) difference might not remain constant during all ontogenetic sexual divergence. What is more certain is simply the existence of some small degree of length-weight dimorphism (females slightly heavier at a given length). Also, this dimorphism is not likely to stem primarily from a sexual difference in gonad weight because the maximum proportion of total female body weight composed of ovarian tissue was only 2.7%. Thus the difference is due to other morphological or behavioral differences.

Growth

There was no significant difference between sexes in length versus age. The predicted length of a prowfish of given age based on our samples was higher than that indicated by Tokranov (1999). In our study 5-year-old and 9-year-old fish averaged 56.6 cm and 73.5 cm in length, respectively. Tokranov (1999) considered that prowfish growth determined from otoliths of 102 specimens from the Northwest Pacific indicated a comparatively fast-growing species reaching an average length of 44.6 cm by 5 years of age and 67 cm after 9 years. These data suggest prowfish are indeed relatively fast growing and that growth rates for the Gulf of Alaska are faster than those for off southeastern Kamchatka and the northern Kuril Islands. Alternatively, size-dependent mortality from such elements as incidental capture by commercial fishing may affect the two populations differently.

Historically, two other prowfish have been aged from otoliths: a male 84 cm long taken near Eureka, CA (Fitch and Lavenberg, 1971), and a female 50.1 cm long (standard length) from off Monterey (Cailliet and Anderson, 1975). The ages estimated were 12 and 3 years, respectively. After converting the standard length record to an estimate of total length for the second specimen of 58 cm by using a ratio described by Baxter,[6] both lengths are slightly greater than our predictions for the same ages, albeit near the limits of our data range. This finding contrasts with the predictions of lesser length at a given age presented by Tokranov (1999).

Maturity

Little previous data exist with which to compare our observations of female prowfish rate of maturation. Cailliet and Anderson (1975) examined the ovaries of their 50.1-cm 3-year-old female specimen for vitellogenesis and predicted an age at first spawning of 4 years, slightly less than the lower 95% confidence limit of 4.4 years for our expected average age at 50% maturity.

Food habits

Our observation that gelatinous zooplankton was the largest constituent in the contents of prowfish stomachs (Table 1) is supported by Tokranov (1999), who found that the two most common prey taxa among the contents of 102 stomachs of adult specimens from the northwestern Pacific were Scyphozoa (59.6–62.0% of stomachs) and Ctenophora (6.0–15.4% of stomachs). Anecdotal observations have also been made of the feeding behavior of an aquarium specimen over an approximate 2-year period (Carollo and Rankin, 1998). When first obtained, the fish ate only various jellyfish species, rejecting other food, including a variety of live invertebrates. In our food samples, we observed other taxa, such as invertebrates and small fish, but these were a minor part, possibly first captured by jellyfish and then secondarily ingested by prowfish. Carollo and Rankin (1998) found that the aquarium specimen would ingest such items when eating the bells of *Chrysaora melanaster* in which such food had previously been placed, indicating the possibility of this occurring naturally. Possibly more reflective of the unnatural circumstances, the specimen later began accepting such items outside the bells of jellyfish.

Apparent adaptations of the prowfish to a diet of gelatinous zooplankton include the small, sharp, close-set teeth in a single row attached only to the jaws, which are capable of a 180-degree gape, and the large rough-scaled lips (Clemens and Wilby, 1961; Hart, 1973; Carollo and Rankin, 1998).

Acknowledgments

We are grateful for the expert advice given by Alaska Fisheries Science Center colleagues Delsa Anderl and Nancy

[6] Baxter, R. 1990. Unpubl. manuscript. Annotated key to the fishes of Alaska, 803 p. [Available from Sera Baxter, Box 182, Seldovia, AK 99663.]

Roberson regarding age-reading of prowfish otoliths, and by AFSC colleagues Kathy Mier and Susan Piquelle regarding statistical analyses of data.

Literature cited

Allen, James M., and Gary B. Smith.
1988. Atlas and zoogeography of common fishes in the Bering Sea and Northeastern Pacific. NOAA Tech. Rep. NMFS 66, 151 p.

Brodeur, R. D.
1998. In situ observations of the association between juvenile fishes and scyphomedusae in the Bering Sea. Mar. Ecol. Prog. Ser. 163:11–20.

Cailliet, G. M., and M. E. Anderson.
1975. Occurrence of prowfish *Zaprora silenus* Jordan, 1896 in Monterey Bay, California. Calif. Fish Game 61(1):60–62.

Carollo, M., and P. Rankin.
1998. The care and display of the prowfish, *Zaprora silenus*. Drum and Croaker 29:3–6.

Clemens, W. A., and G. V. Wilby.
1961. Fishes of the Pacific coast of Canada. Fish. Res. Board Can. Bull. 68, 2nd ed., 443 p.

Chilton, D. E., and R. J. Beamish.
1982. Age determination methods for fishes studied by the groundfish program at the Pacific Biological Station. Can. Spec. Pub. Fish. Aquat. Sci. 60, 102 p.

Doyle, M. J., K. L. Meir, M. S. Busby, and R. D. Brodeur.
2002. Regional variation in springtime ichthyoplankton assemblages in the northeast Pacific Ocean. Progress in Oceanography 53 (2–4):247–281

Eschmeyer, W. N., E. S. Herald, and H. Hammann.
1983. A field guide to Pacific Coast fishes of North America, 336 p. Peterson field guide ser. Houghton Mifflin, Boston, MA.

Fitch, J. E., and R. J. Lavenberg.
1971. Marine food and game fishes of California, 179 p. U.C. Press, Berkeley, CA.

Hart, J. L.
1973. Pacific fishes of Canada. Fish. Res. Board Can. Bull. 180, 740 p.

Jordan, D. S.
1897. Notes on fishes little known or new to science. Proc. Calif. Acad. Sci., 2nd ser., 6:203–205.

Kessler, D. W.
1985. Alaska's saltwater fishes and other sea life: a field guide, 358 p. Alaska Northwest, Anchorage, AK

Kimura, D. K.
1980. Likelihood methods for the von Bertalanffy growth curve. Fish. Bull. 77:765–776.

Martin, M. H.
1997. Data report: 1996 Gulf of Alaska bottom trawl survey. NOAA Tech. Memo. NMFS-AFSC-82, 235 p.

Matarese, A. C., A. W. Kendall, D. M. Blood, and B. M. Vinter.
1989. Laboratory guide to early life history stages of northeast pacific fishes. NOAA Tech. Rep. NMFS 80, 652 p.

Nelson, J. S.
1994. Fishes of the world, 3rd ed., 600 p. John Wiley, New York, NY..

Orlov, A. M.
1998. On feeding of mass species of deep-sea skates (*Bathyraja* spp., Rajidae) from the Pacific waters of the Northern Kurils and Southeastern Kamchatka. J. Icthyol. 38(8): 635–644.

Payne, S. A., B. A. Johnson, and R. S. Otto.
1999. Proximate composition of some north-eastern Pacific forage fish species. Fish. Oceanogr. 8(3): 159–177.

Scheffer, V. B.
1940. Two recent records of *Zaprora silenus* Jordan from the Aleutian Islands. Copeia 1940(3):203.

Seber, G. A. F.
1973. The estimation of animal abundance, 506 p. Hafner Press, New York, NY.

Tokranov, A. M.
1999. Some features of biology of the prowfish *Zaprora silenus* (Zaproridae) in the Pacific waters of the Northern Kuril Islands and Southeastern Kamchatka. J. Ichthyol. 39(6):475–478.

Van Pelt, T. I., J. F. Piatt, B. K. Lance, and D. D. Roby.
1997. Proximate composition and energy density of some North Pacific forage fishes. Comp. Biochem. Physiol. 118A(4):1393–1398.

Wakabayashi, K., R. G. Bakkala and M. S. Alton.
1985. Methods of the U.S.–Japan demersal trawl surveys. *In* Results of cooperative U.S.–Japan groundfish investigations in the Bering Sea during May–August 1979 (R. G. Bakkala and K. Wakabayashi, eds.), p. 7–26. Int. North Pac. Fish. Comm. Bull. 44.

Yang, Mei-Sun.
1993. Food habits of the commercially important groundfishes in the Gulf of Alaska in 1990. NOAA Tech. Memo. NMFS-AFSC-22, 150 p.

Fish lost at sea: the effect of soak time on pelagic longline catches

Peter Ward

Ransom A. Myers

Department of Biology
Dalhousie University
Halifax, B3H 4JI Canada
E-mail address (for P. Ward): ward@mathstat.dal.ca

Wade Blanchard

Department of Mathematics and Statistics
Dalhousie University
Halifax, B3H 44 Canada

Abstract—Our analyses of observer records reveal that abundance estimates are strongly influenced by the timing of longline operations in relation to dawn and dusk and soak time—the amount of time that baited hooks are available in the water. Catch data will underestimate the total mortality of several species because hooked animals are "lost at sea." They fall off, are removed, or escape from the hook before the longline is retrieved. For example, longline segments with soak times of 20 hours were retrieved with fewer skipjack tuna and seabirds than segments with soak times of 5 hours. The mortality of some seabird species is up to 45% higher than previously estimated.

The effects of soak time and timing vary considerably between species. Soak time and exposure to dusk periods have strong positive effects on the catch rates of many species. In particular, the catch rates of most shark and billfish species increase with soak time. At the end of longline retrieval, for example, expected catch rates for broadbill swordfish are four times those at the beginning of retrieval.

Survival of the animal while it is hooked on the longline appears to be an important factor determining whether it is eventually brought on board the vessel. Catch rates of species that survive being hooked (e.g. blue shark) increase with soak time. In contrast, skipjack tuna and seabirds are usually dead at the time of retrieval. Their catch rates decline with time, perhaps because scavengers can easily remove hooked animals that are dead.

The results of our study have important implications for fishery management and assessments that rely on longline catch data. A reduction in soak time since longlining commenced in the 1950s has introduced a systematic bias in estimates of mortality levels and abundance. The abundance of species like seabirds has been over-estimated in recent years. Simple modifications to procedures for data collection, such as recording the number of hooks retrieved without baits, would greatly improve mortality estimates.

Manuscript approved for publication 22 September 2003 by Scientific Editor.

Manuscript received 20 October 2003 at NMFS Scientific Publications Office.

Fish. Bull. 102:179–195 (2004).

Our knowledge of large pelagic fish in the open ocean comes primarily from tagging and tracking experiments and from data collected from longline fishing vessels since the 1950s. Abundance indices for pelagic stocks are often derived from analyses that model catch as a function of factors such as year, area, and season. However, the amount of time that baited hooks are available to fish is likely to be another important factor influencing catch rates (Deriso and Parma, 1987).

The activity of many pelagic animals and their prey vary with the time of day. Broadbill swordfish, for example, feed near the sea surface at night. They move to depths of 500 m or more during the day (Carey, 1990). Other species may be more active in surface waters during the day (e.g. striped marlin) or at dawn and dusk (e.g. oilfish). Longline fishing crews take a keen interest in the timing of their fishing operations and soak time (the total time that a baited hook is available in the water). However, assessments have not accounted for those factors in estimating the abundance or mortality levels of target species or nontarget species.

In many assessments that use pelagic longline catch rates, fishing effort is assumed to be proportional to the number of hooks deployed. The effects of soak time and timing may have been omitted because a clear demonstration of their effects on pelagic longline catch rates is not available. The few published accounts on soak time in pelagic longline fisheries have been based on limited data and a few target species. For example, in analyzing 95 longline operations or "sets" by research vessels Sivasubramaniam (1961) reported that the catch rates of bigeye tuna increased with soak time, whereas yellowfin tuna catch rates were highest in longline segments with intermediate soak times.

In contrast to the limited progress in empirical studies, theoretical approaches are well developed for modeling factors that may influence longline catch rates. Soon after large-scale longlining commenced, Murphy (1960) published "catch equations" for adjusting catch rates for soak time, bait loss, escape, hooking rates, and gear saturation. He suggested that escape rates could be estimated from counts of missing hooks and hooks retrieved without baits. Unfortunately, such data are rarely collected from pelagic longline operations.

More recently, hook-timers attached to longline branchlines have begun to provide information on the time when each animal is hooked and also whether animals are subsequently lost, e.g. Boggs (1992), Campbell et al.[1,2] Such data are particularly useful to under-

[1] Campbell, R., W. Whitelaw, and G. McPherson. 1997. Domestic longline fishing methods and the catch of tunas and non-target species off north-eastern Queensland (1st survey: October–December 1995). Report to the Eastern Tuna and Billfish Fishery MAC. 71 p. Australian Fisheries Management Authority, PO Box 7051, Canberra Business Centre, ACT 2610, Australia.

[2] *See next page.*

standing the processes affecting the probability of capture and escape.

The purpose of our study is to determine whether variations in the duration and timing of operations bias abundance and mortality estimates derived from longline catch rates. We present a theoretical model that is then related to empirical observations of the effects of soak time on catch rates. The strength in our approach is in applying a random effects model to large data sets for over 60 target and nontarget species in six distinct fisheries. We also investigate the survival of each species while hooked because preliminary analyses suggested that the effects of soak time on catch rates might be linked to mortality caused by hooking (referred to as "hooking mortality").

Factors affecting catch rates

To aid interpretation of our statistical analysis of soak time effects, we first developed a simple model to illustrate how the probability of catching an animal may vary with soak time.

The probability of an animal being on a hook when the branchline is retrieved is a product of two probability density functions: first the probability of being hooked and then the probability of being lost from the hook.[3] Influencing the probability of being hooked are the species' local abundance, vulnerability to the fishing gear, and the availability of the gear. Catches will deplete the abundance of animals within the gear's area of action, particularly for species that have low rates of movement. Movement will also result in variations in exposure of animals to the gear over time—for instance, as they move vertically through the water column in search of prey (Deriso and Parma, 1987).

Other processes that will reduce the probability of being hooked include bait loss and reduced sensitivity to the bait (Fernö and Huse, 1983). Longline baits may fall off hooks during deployment, deteriorate over time and fall off or they may lose their attractant qualities. They may be removed by target species, nontarget species, or other marine life, such as squids. Hooked animals may also escape by severing the branchline or breaking the hook. Sections of the longline may become saturated when animals are hooked, reducing the number of available baits (Murphy, 1960; Somerton and Kikkawa, 1995). After an animal has been hooked, it may escape, fall off the hook, be removed by scavengers, or it may remain hooked until the branchline is retrieved.

Some of the processes affecting the probability of an animal being on a hook when the the branchline is retrieved are species-specific, whereas other processes may affect all species. For example, bait loss during longline deployment will reduce the catch rates of all species. In contrast, the probability of a hooked animal escaping may be species-dependent; some species are able to free themselves from the hook whereas other species are rarely able to do this.

Our simple model of the probability of an animal being on a hook is based on a convolution of the two time-related processes described above: 1) the decay in the probability of capture with the decline in the number of baits that are available; and 2) gains due to the increased exposure of baits to animals and losses due to animals escaping, falling off, or being removed by scavengers.

The probability of an animal being on a hook when the branchline is retrieved is the integral of the probability density functions of capture and retention:

$$\pi(T) = \int_{t=0}^{T} P_c(t) P_r(T-t)\,dt, \tag{1}$$

where $\pi(T)$ = the "catch rate" or probability of an animal being on a hook when the branchline is retrieved at time T (T is the total soak time of the hook);
$P_c(t)$ = the probability density function of an animal being captured at time t; and
$P_r(t)$ = the probability density function of a captured animal being retained on the hook for a length of time t.

The probability density function of capture can be approximated with an exponential function:

$$P_c(t) = P_0 e^{-\alpha t}, \tag{2}$$

where P_0 = the probability of capture when the hook is deployed (t=0); and
α = a parameter determining the rate of change in capture probability over time.

After the animal is hooked, the probability density function of an animal being retained after capture can be approximated as

$$P_r(t) = e^{-\beta(t)}, \tag{3}$$

where β = the "loss rate," a parameter determining the rate of change in the probability of an animal being retained after it has been captured.

Substituting approximations 2 and 3 into Equation 1 gives

$$\begin{aligned}\pi(T) &= \int_{t=0}^{T} P_0 e^{-\alpha t} e^{-\beta(T-t)}\,dt \\ &= \frac{P_0}{\beta-\alpha}\left[e^{-\alpha T} - e^{-\beta T}\right].\end{aligned} \tag{4}$$

[2] Campbell, R., W. Whitelaw, and G. McPherson. 1997. Domestic longline fishing methods and the catch of tunas and nontarget species off north-eastern Queensland (2nd survey: May–August 1996). Report to the Eastern Tuna and Billfish Fishery MAC, 48 p. Australian Fisheries Management Authority, PO Box 7051, Canberra Business Centre, ACT 2610, Australia.

[3] In discussing continuous variables we use the terms "probability" and "probability density function" interchangeably.

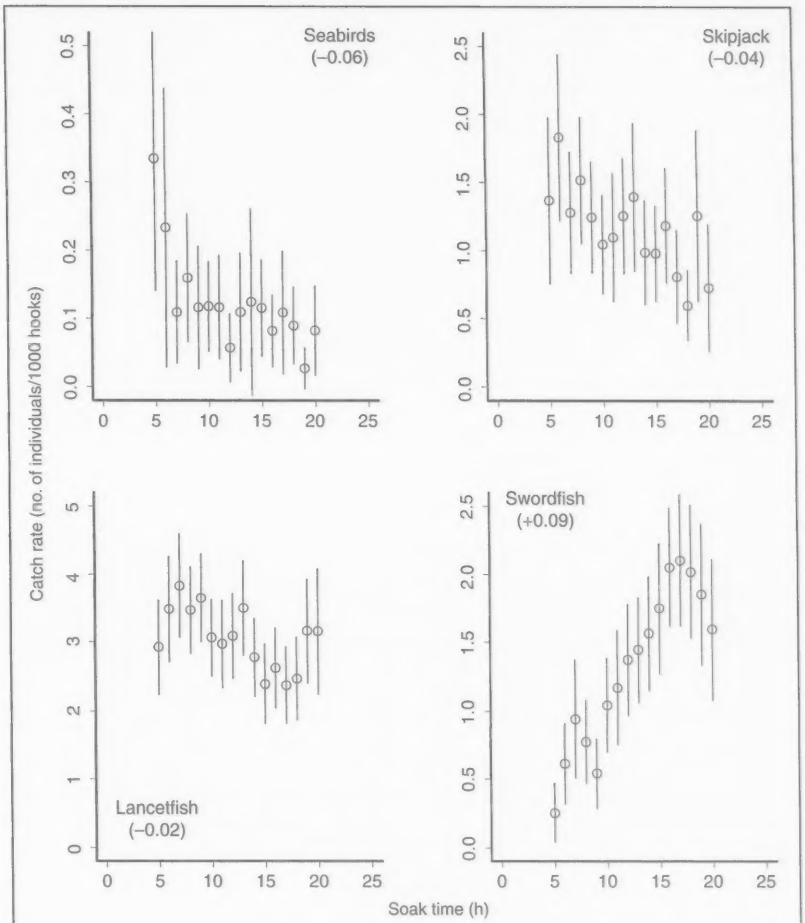

Figure 1

Mean catch rates plotted against soak time for skipjack tuna, long-nosed lancetfish, and swordfish in the South Pacific yellowfin tuna fishery and for "other seabirds" in the South Pacific bluefin tuna fishery. To reduce variability, the estimates were limited to longline segments with more than 25 hooks and soak times of 5–20 hours. Vertical bars are 95% confidence intervals for the mean hourly catch rate. In parentheses are the soak-time coefficients from random effects models (note that the soak-time coefficient is not the same as the slope coefficient of a regression of the data presented in this graph).

Our model is similar to the parabolic catch model examined by Zhou and Shirley (1997). It is simpler than catch equations developed by other authors because it does not include specific terms for the loss of baits, for fish competition, and gear saturation.

Preliminary plots of observer data indicated a variety of patterns in the relationship between catch rates and soak time (e.g. Fig. 1). By varying the values of P_0 (probability of capture), α (capture rate), and β (loss rate), our simple catch equation (Eq. 4) can mimic the observed patterns (Fig. 2). However, estimates of P_0, α , and β are not available. Instead, we used the empirical approach described in the following section to model the effect of soak time on catch rates. The relationship of soak time to catch rate represents the product of the probability of capture and the probability of being retained.

One approach to investigating the effects of soak time on catch rates is to fit linear regressions to aggregated data like those presented in Figure 1. Such an approach, however, would violate assumptions of independence (within each longline operation, catch rates in consecutive segments will be related), normality (these are binomial data), and homogeneity of variance (for binomial data, the variance is dependent on the mean).

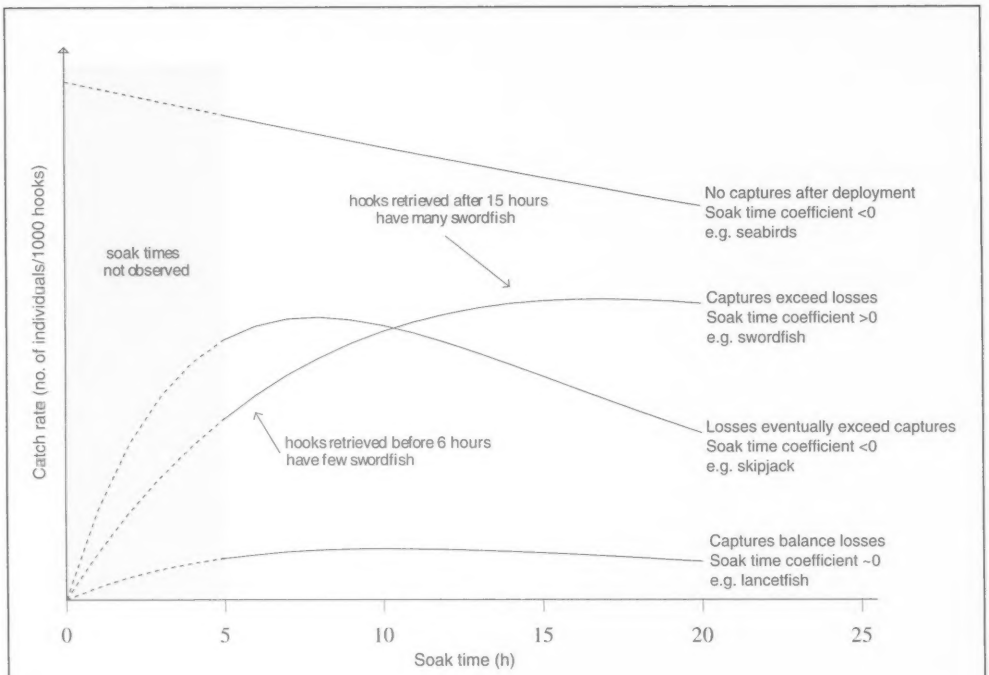

Figure 2

Illustration of different patterns in the theoretical relationship between longline catch rates and soak time. The probability of an animal being on a hook when a branchline is retrieved (the "catch rate") is estimated from Equation 4 by using soak times (T) ranging from 0 to 20 hours and three different combinations of values for P_0 (probability of capture), α (capture rate), and β (loss rate). For seabirds, the probabilities were estimated from Equation 6. The probabilities are not on the same scale for all species.

Another approach might be to fit separate logistic regressions to each operation and then to combine the parameter estimates. This would overcome the problems of normality and homogeneity of variance. However, the separate regressions would not incorporate information that is common to all operations.

Instead, we used a logistic regression with random effects. The key advantage in using random-effects models in this situation is that they carry information on the correlation between longline segments that is derived from the entire data set of operations.

Data and methods

Fisheries

We analyzed observer data from six different fisheries in the Pacific Ocean to determine the effects of soak time and timing on longline catch rates (Table 1, Fig. 3). These fisheries involve two different types of longline fishing operation: 1) distant-water longlining involves trips of three months or longer and the catch is frozen on board the vessel; and 2) fresh-chilled longlining, which involves small vessels (15–25 m) undertaking trips of less than four weeks duration, and the catch is kept in ice, ice slurries, or in spray brine systems. The fresh-chilled longliners deploy shorter longlines with fewer hooks (~1000 hooks) than the distant-water longliners (~3000 hooks per operation) (Ward, 1996; Ward and Elscot, 2000).

The six fisheries share many operational similarities, such as the types of bait used and soak time. However, they are quite different in terms of targeting, which is determined by fishing practices, e.g. the depth profile of the longline, timing of operations and the area and season of activity. South Pacific bluefin tuna longliners operate in cold waters (10–16°C) in winter to catch southern bluefin tuna. In the South Pacific yellowfin tuna longliners target tropical species, such as yellowfin and bigeye tuna, in warmer waters (19–22°C) (Ward, 1996). To target bigeye tuna, longlines in the Central Pacific bigeye fishery are deployed in the early morning with hook depths ranging down to about 450 m. The depths of the deepest hook are much shallower (~150 m) in the North Pacific swordfish fishery where the longlines are deployed late in the afternoon and retrieved early in the morning (Boggs, 1992).

Observer data

National authorities and regional organizations placed independent observers on many longliners operating in the six fisheries during the 1990s. The observer data consisted of records of the species and the time when each animal was brought on board. We restricted analyses to operations where the last hook that had been deployed was retrieved first ("counter-retrieved"), where there was no evidence of stoppages due to line breaks or mechanical failure, and where there was continuous monitoring by an observer. Combined with records of the number of hooks deployed and start and finish times of deployment and retrieval, the observer data allowed calculation of soak time and catch rates of longline segments. We aggregated catches and the number of hooks into hourly segments. The soak time was estimated for the midpoint of each hourly segment.

The Central Pacific bigeye tuna and North Pacific swordfish fisheries differed from the other four fisheries in the species that were recorded and the method of recording the time when each animal was brought on board. Observers reported catches according to a float identifier in the Central and North Pacific fisheries. Therefore we estimated soak times for each longline segment from the time when each float was retrieved. For those fisheries, observers reported the float identifier only for tuna, billfish, and shark (Table 2). Data are available for protected species, such as seals, turtles, and seabirds but were not sought for the present study.

We assumed a constant rate of longline retrieval throughout each operation. The number of hooks retrieved during each hourly segment was the total number of hooks divided by the duration of monitoring (decimal hours). For each species we analyzed only the operations where at least one individual of that species was caught.

Longline segments that involved a full hour of monitoring had several hundred hooks. Segments at either end of the longline involved less than an hour of monitoring and had fewer hooks. Catch rates may become inflated in segments with very small numbers of hooks. Therefore we arbitrarily excluded segments where the observer monitored less than 25 hooks.

For four of the fisheries, data were available on survival rates, allowing the investigation of the relationship between soak time and hooking mortality. For the Western Pacific and South Pacific fisheries, observers reported whether the animal was alive or dead when it was brought on board. We calculated survival rate (the number alive divided by the total number reported dead or alive) for species where data were available on the life status of more than ten individuals.

Generalized linear mixed model

Logit model We applied a generalized linear mixed model to the observer data. The model is based on a logistic regression, with the catch (y) on each hook assumed to have a binomial distribution with $y \sim b(n, \pi)$. π is the expected value of the distribution for a specified soak time. We refer to it as the probability of catching an animal or

Table 1

Summary of the six fisheries analyzed, showing the mean number of hooks per operation, mean duration of operations, mean catch rate of all species, the period of observer data, and the total number of longline operations. For the two Western Pacific fisheries, the catch rates are for the most common species only. NP = North Pacific; CP = Central Pacific; WP = Western Pacific; and SP = South Pacific.

Fishery name	Fleet	Area	Target species	Period	No. of operations	Hooks per operation	Duration (h)	Catch rate (no. of fish per 1000 hooks)
NP swordfish[1]	U.S. fresh-chilled	North Pacific	swordfish	1994–2002	1539	812	21	51
CP bigeye tuna[1]	U.S. fresh-chilled	Central Pacific	bigeye tuna, albacore	1994–2002	3243	1865	19	23
WP bigeye tuna	fresh-chilled (various flags)	Western Pacific	bigeye tuna, yellowfin tuna	1990–2001	1915	1620	21	28
WP distant	distant-water (various flags)	Western Pacific	bigeye tuna, yellowfin tuna	1990–2001	234	2347	22	30
SP yellowfin tuna	Japan distant-water	northeastern Australia	yellowfin tuna, bigeye tuna	1992–97	1419	3130	22	40
SP bluefin tuna	Japan distant-water	southeastern Australia	southern bluefin tuna	1992–97	666	3086	22	23

[1] We used the number of hooks between floats to distinguish the North Pacific swordfish fishery (<15 hooks between floats) from the Central Pacific bigeye tuna fishery (16 or more hooks between floats).

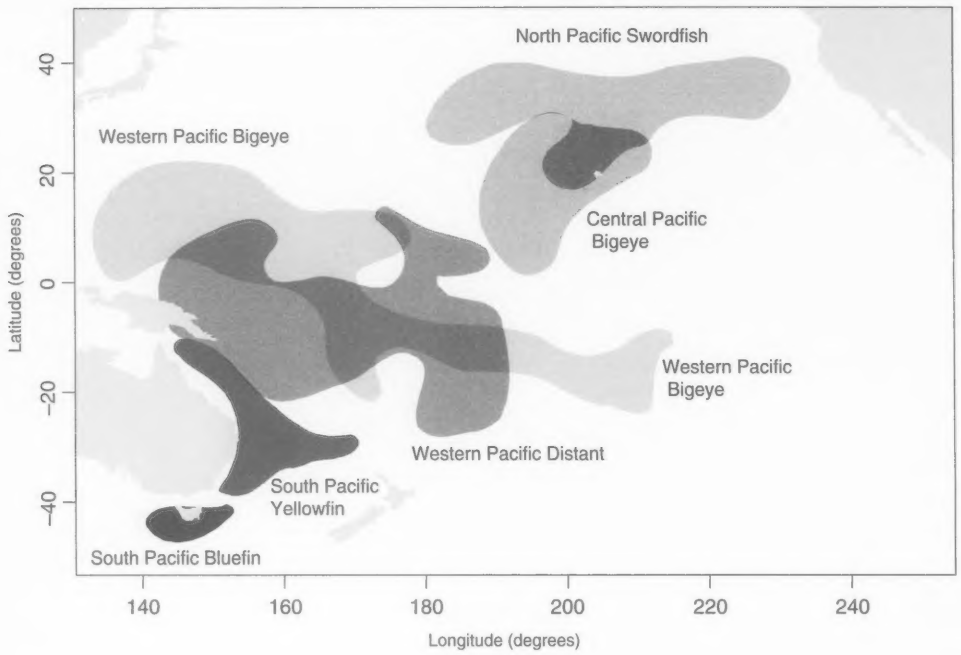

Figure 3
Geographical distribution of the observer data analyzed for each fishery.

the expected number of animals per hook. For each longline segment (j) within each operation (i), we link $\pi_{i,j}$ to a linear predictor ($\eta_{i,j}$) through the equation

$$\pi_{i,j} = \frac{e^{\eta_{i,j}}}{(1+e^{\eta_{i,j}})}.$$

$\eta_{i,}$ is then modeled as a function of soak time:

$$\eta_{i,j} = \beta_0 + \beta_1 T_{i,j}, \quad (5)$$

where $T_{i,j}$ = the hook's soak time (decimal hours) in longline segment j;
β_0 = the intercept; and
β_1 = the slope coefficient, which we term the "soak time coefficient."

Modeling the probability of a catch on each individual hook would result in large numbers of zero observations and thus test the limits of current computer performance. Therefore we aggregated hooks and catches into hourly segments for each longline operation.

We assumed that each longline segment had the same configuration and that the probability of capture was the same for each segment within a longline operation. The assumption may be violated where segments pass through different water masses or where they differ in depth profile or baits. Saturation of segments with animals will also alter the capture probability between segments. The effects of water masses, depth profiles, baits, and gear saturation were not analyzed in the present study.

Capture probability may also vary through the differential exposure of segments to the diurnal cycle of night and day. The addition of dawn and dusk as fixed effects allowed us to model diurnal influences on catch rates.

Fixed effects To explore factors that might affect the relationship between soak time and catch rate, we added four fixed effects to the logit model: year, season, and, as mentioned above, whether the segment was available at dawn or dusk. A full model without interaction terms would be

$$\eta_{i,j} = \beta_0 + \beta_1 T_{i,j} + \beta_2 A_{i,j} + \beta_2 P_{i,j} + \beta_3 S_{i,j} + \beta_4 Y_{i,j} + O_i,$$

where $T_{i,j}$ = the hook's soak time (decimal hours) in longline segment j;
$A_{i,j}$ = an indicator of whether the hook was exposed to a dawn period;
$P_{i,j}$ = an indicator of whether the hook was exposed to a dusk period;
$S_{i,j}$ = the season (winter or summer);
$Y_{i,j}$ = the year;
O_i = the random effect for operation that we modeled as an independent and normally distributed variable (see "Random effects" section); and
β_0–β_4 are parameters (fixed effects) to be estimated. We refer to β_1 as the "soak time coefficient."

Table 2

List of common and scientific names of the species analyzed. Also shown is the number of individuals of each species analyzed in each fishery. A dash indicates that the species was not analyzed in the present study; it does not necessarily mean that the species was not taken in the fishery. In particular, observer data on the time of capture were not available for "other bony fish" in the North Pacific swordfish and Central Pacific bigeye tuna fisheries. NP = North Pacific; CP = Central Pacific; WP = Western Pacific; SP = South Pacific; LN = long-nosed; and SN = short-nosed.

		Fishery					
Common name	Species	NP swordfish	CP bigeye tuna	WP bigeye tuna	WP distant	SP yellowfin tuna	SP Bluefin tuna
Tuna and tuna-like species							
Albacore	*Thunnus alalunga*	9707	23,128	14,194	11,976	21,550	1399
Bigeye tuna	*Thunnus obesus*	5409	45,476	9814	2581	1846	–
Butterfly mackerel	*Gasterochisma melampus*	—	—	—	—	—	533
Skipjack tuna	*Katsuwonus pelamis*	546	13,882	1456	445	691	—
Slender tuna	*Allothunnus fallai*	—	—	—	—	—	28
Southern bluefin	*Thunnus maccoyii*	—	—	—	—	1030	10,537
Yellowfin tuna	*Thunnus albacares*	2811	21,654	16,029	4689	12,454	—
Wahoo	*Acanthocybium solandri*	383	5508	1345	—	308	—
Billfish							
Black marlin	*Makaira indica*	25	41	353	226	160	—
Blue marlin	*Makaira nigricans*	981	2379	1467	529	179	—
Sailfish	*Istiophorus platypterus*	49	193	706	399	151	—
Shortbill spearfish	*Tetrapturus angustirostris*	543	5467	529	398	654	—
Striped marlin	*Tetrapturus audax*	1963	8332	681	182	724	—
Swordfish	*Xiphias gladius*	22,457	1680	1472	287	1173	92
Other bony fish							
Barracouta	*Thyrsites atun*	—	—	—	—	53	—
Barracudas	*Sphyraena* spp.	—	—	707	153	—	—
Escolar	*Lepidocybium flavobrunneum*	1208	3983	1343	878	1726	84
Great barracuda	*Sphyraena barracuda*	32	743	303	442	92	—
Lancetfish (LN)	*Alepisaurus ferox*	2788	30,136	325	419	2868	610
Lancetfish (SN)	*Alepisaurus brevirostris*	—	—	155	84	257	59
Lancetfishes	*Alepisaurus* spp.	—	—	1431	98	—	—
Long-finned bream	*Taractichthys longipinnis*	—	—	—	—	—	292
Mahi mahi	*Coryphaena hippurus*	17,463	19,090	1436	211	447	—
Oilfish	*Ruvettus pretiosus*	555	1091	420	456	653	900
Opah	*Lampris guttatus*	68	4724	527	129	80	213
Pomfrets	Family Bramidae	—	—	623	60	—	40
Ray's bream	*Brama brama*	—	—	—	—	1074	10,547
Ribbonfishes	Family Trachipteridae	—	—	—	—	—	22
Rudderfish	*Centrolophus niger*	—	—	—	—	—	90
Sickle pomfret	*Taractichthys steindachneri*	—	—	122	21	—	—
Slender barracuda	*Sphyraena jello*	—	—	—	—	121	—
Snake mackerel	*Gempylus serpens*	1971	9881	256	44	—	—
Snake mackerels	Family Gempylidae	—	—	456	10	—	—
Southern Ray's bream	*Brama* spp.	—	—	—	—	—	28
Sunfish	*Mola ramsayi*	—	—	—	—	249	99
Sharks and rays							
Bigeye thresher shark	*Alopias superciliosus*	149	1930	145	61	—	—
Blacktip shark	*Carcharhinus limbatus*	—	—	445	125	—	—
Blue shark	*Prionace glauca*	31,503	31,413	5601	1628	1689	12,797
Bronze whaler	*Carcharhinus brachyurus*	—	—	—	—	116	—
Crocodile shark	*Pseudocarcharias kamoharai*	—	—	153	73	—	—

continued

Table 2 (continued)

Common name	Species	Fishery					
		NP swordfish	CP bigeye tuna	WP bigeye tuna	WP distant	SP yellowfin tuna	SP Bluefin tuna
Sharks and rays (continued)							
Dog fishes	Family Squalidae	—	—	—	—	—	60
Dusky shark	*Carcharhinus obscurus*	—	112	—	—	20	—
Grey reef shark	*Carcharhinus amblyrhynchos*	—	—	282	64	—	—
Hammerhead shark	*Sphyrna* spp.	—	—	142	191	22	—
Long finned mako	*Isurus paucus*	—	83	108	15	—	—
Oceanic whitetip shark	*Carcharhinus longimanus*	568	2373	2376	384	142	—
Porbeagle	*Lamna nasus*	—	—	—	—	27	1011
Pelagic stingray	*Dasyatis violacea*	2374	2849	1212	248	534	109
Pelagic thresher shark	*Alopias pelagicus*	—	—	77	34	—	—
School shark	*Galeorhinus galeus*	—	—	—	—	—	143
Short finned mako	*Isurus oxyrinchus*	476	685	408	169	432	128
Silky shark	*Carcharhinus falciformis*	25	1433	5396	2406	8	—
Silvertip shark	*Carcharhinus albimarginatus*	—	—	168	74	—	—
Thintail thresher shark	*Alopias vulpinus*	—	74	—	—	—	31
Thresher shark	*Alopias superciliosus*	—	—	415	—	93	18
Tiger shark	*Galeocerdo cuvier*	—	—	56	18	38	—
Velvet dogfish	*Zameus squamulosus*	—	—	—	—	—	156
Whip stingray	*Dasyatis akajei*	—	—	78	15	—	—
Seabirds							
Albatrosses	Family Diomedeidae	—	—	—	—	—	88
Petrels	Family Procellariidae	—	—	—	—	—	29
Other seabirds	Family Procellariidae	—	—	—	—	38	200
All operations	104,054		238,340	73,212	30,222	51,699	40,343

To maintain a focus on the effects of soak time, the models were limited to simple combinations of fixed effects and interaction terms. Dawn and dusk were added to various models of each species in each fishery. To reduce complexity, year and season were limited to models of seven species (bigeye tuna, oilfish, swordfish, blue shark, albacore, southern bluefin tuna, long-nosed lancetfish) in the two South Pacific fisheries. The seven species represented four taxonomic groups and the full range of responses observed in preliminary analyses of the soak-time–catch-rate relationship.

Random effects We added random effects to all models to allow catch rates of segments within each longline operation to be related. The random effects model assumes that there is an underlying distribution from which the true values of the probability of catching the species, π, are drawn. The distribution is the among-operation variation or "random effects distribution." The operations are assumed to be drawn from a random sample of all operations, so that the random effects (O_i) in the relationship between catch rate and soak time for each operation (i) are independent and normally distributed with $O_i \sim N(0, \sigma^2)$. The random effects and various combinations of the fixed effects were added to the linear predictor presented in Equation 5.

For each species in the South Pacific yellowfin tuna data set we compared the performance of models under an equal correlation structure with that of models under an autoregressive correlation structure. Under an autoregressive structure, catch rates in the different hourly segments within the operations are not equally correlated. For example, the correlation between segments might be expected to decline with increased time between segments. However, we used an equal correlation structure for all models because the Akaike's information criterion (AIC) and Sawa's Bayesian information criterion (BIC) indicated that there was no clear advantage in using the autoregressive structure rather than an equal correlation structure.

Implementation We implemented the models in SAS (version 8.0) using GLIMMIX, a SAS macro that uses iteratively reweighted likelihoods to fit generalized linear

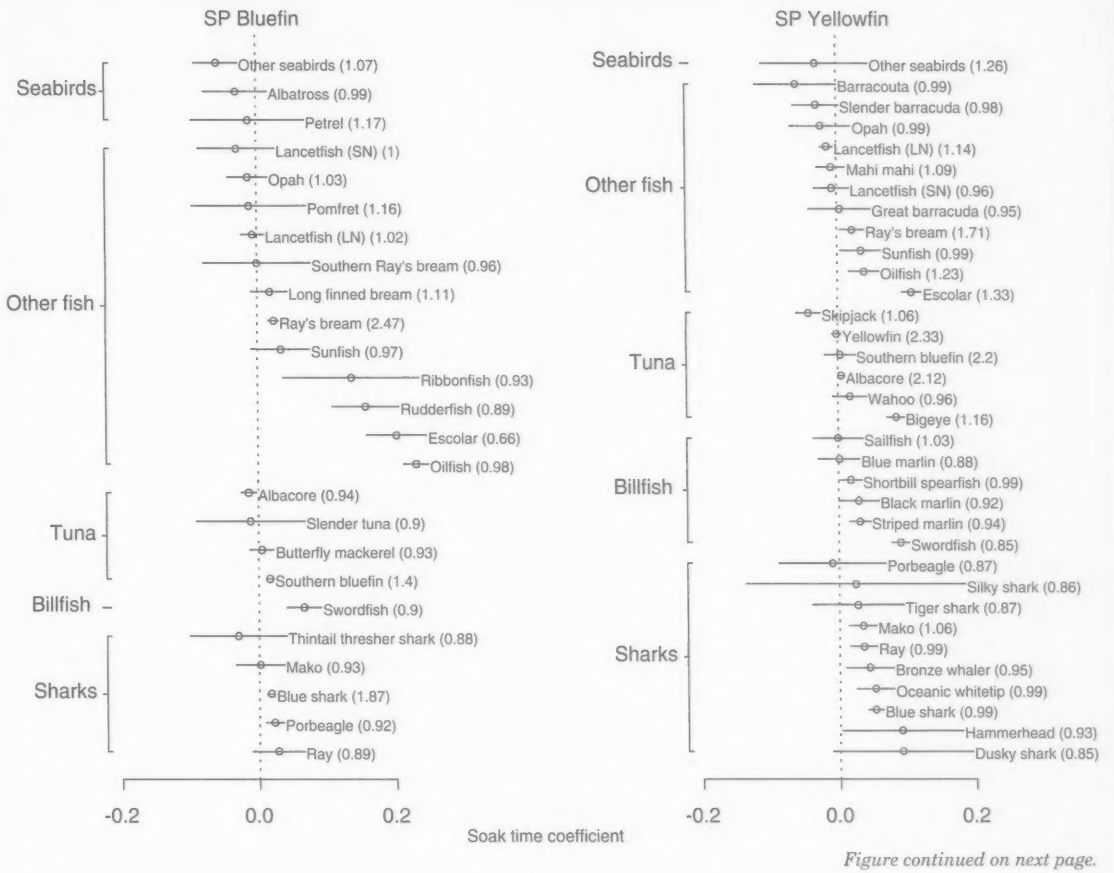

Figure continued on next page.

Figure 4

Coefficients for the effect of soak time on the catch rates of the most abundant species in each fishery. The coefficients are from random effects models where soak time is the only factor. Horizontal bars are 95% confidence intervals for the estimated coefficient. The dispersion parameter is shown in parentheses (it is 1.00 for species that are distributed as predicted by the model, but may be higher for species that have a more clumped distribution along the longline).

mixed models (Wolfinger and O'Connell, 1993). To judge the performance of the various model formulations, we checked statistics, such as deviance and dispersion, and examined scatter plots of chi-square residuals against the linear predictor (η) and QQ plots of chi-square residuals. We used the AIC and BIC to compare the performance of the various model formulations.

Variance in the binomial model depends on only one parameter, P. A dispersion parameter is therefore necessary to allow the variance in the data to be modeled. In effect, the dispersion parameter scales the estimate of binomial variance for the amount of variance in the data. The dispersion parameter will be near one when the variance in the data matches that of the binomial model. Values greater than one ("over-dispersion") imply that the species may have a clumped distribution along the longline.

Results

Soak time

For most species, soak time had a positive effect on catch rates (Fig. 4). In addition to being statistically significant, the effect of soak time made a large difference to catch rates at opposite ends of the longline. In the South Pacific yellowfin tuna fishery, for example, the expected catch rates of swordfish can vary from 0.6 (CI ±0.1) per 1000 hooks (5 hours) to 1.9 (CI ±0.3) per 1000 hooks (20 hours) (Table 3). A soak time of 5 hours and 3500 hooks (if that were possible) would result in a total catch of about two swordfish. In contrast, almost seven swordfish are expected from a longline operation of the same number of hooks with 20 hours of soak time.

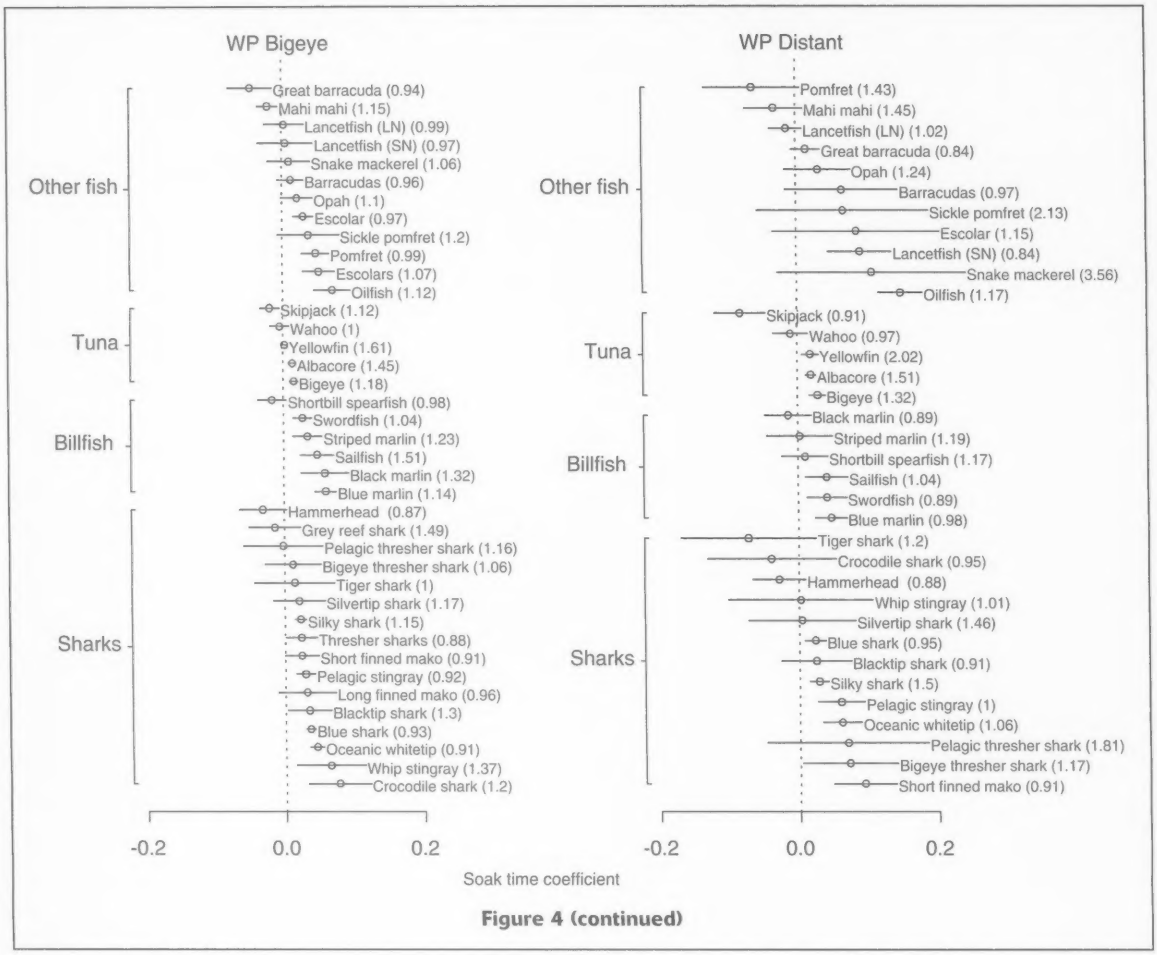

Figure 4 (continued)

For some species (e.g. seabirds, skipjack tuna, and mahi mahi), soak time had a negative effect on catch rates that was often statistically significant (Fig. 4). For skipjack tuna in the Western Pacific distant fishery, for example, catch rates decreased from 1.3 (CI ±0.2) per 1000 hooks for a soak time of 5 hours to 1.0 (CI ±0.1) per 1000 hooks (20 hours). Soak time had a small or statistically insignificant effect on catch rates for several species, such as yellowfin tuna and shortbill spearfish.

Fixed effects

Exposure to dusk had a positive effect on the catch rates for most species (Fig. 5). Dusk often had a negative effect on the catch rates of billfish, such as striped marlin and sailfish. For most species, however, the effect of dawn was weaker, and it influenced the catch rates of fewer species.

Like soak time, timing made a substantial difference to catch rates (Table 4). For a soak time of 12 hours in the South Pacific yellowfin fishery, for example, longline segments exposed to both dawn and dusk have a catch rate of 2.0 (CI ±0.5) escolar per 1000 hooks. The catch rate is 0.8 (CI ±0.1) per 1000 hooks for segments that were not exposed to dawn or dusk.

The effects of timing on catch rates were most pronounced in the South Pacific bluefin tuna fishery. The fishery also showed the greatest range in soak time coefficients, and the coefficients tended to be larger than those of other fisheries (Fig. 4).

Separately, the fixed effects often had statistically significant relationships with catch rates of the seven species that we investigated in detail. However, the interaction between soak time and each fixed effect was less frequently significant. Season was significant, for example, in none of the six models that included a soak-time–season interaction term. By comparison, season was significant in six of the 18 models that included season as a factor but not with a soak-time–season interaction term. The effect of soak time was not significant for southern bluefin tuna in any model for the South Pacific bluefin tuna fishery. It was significant

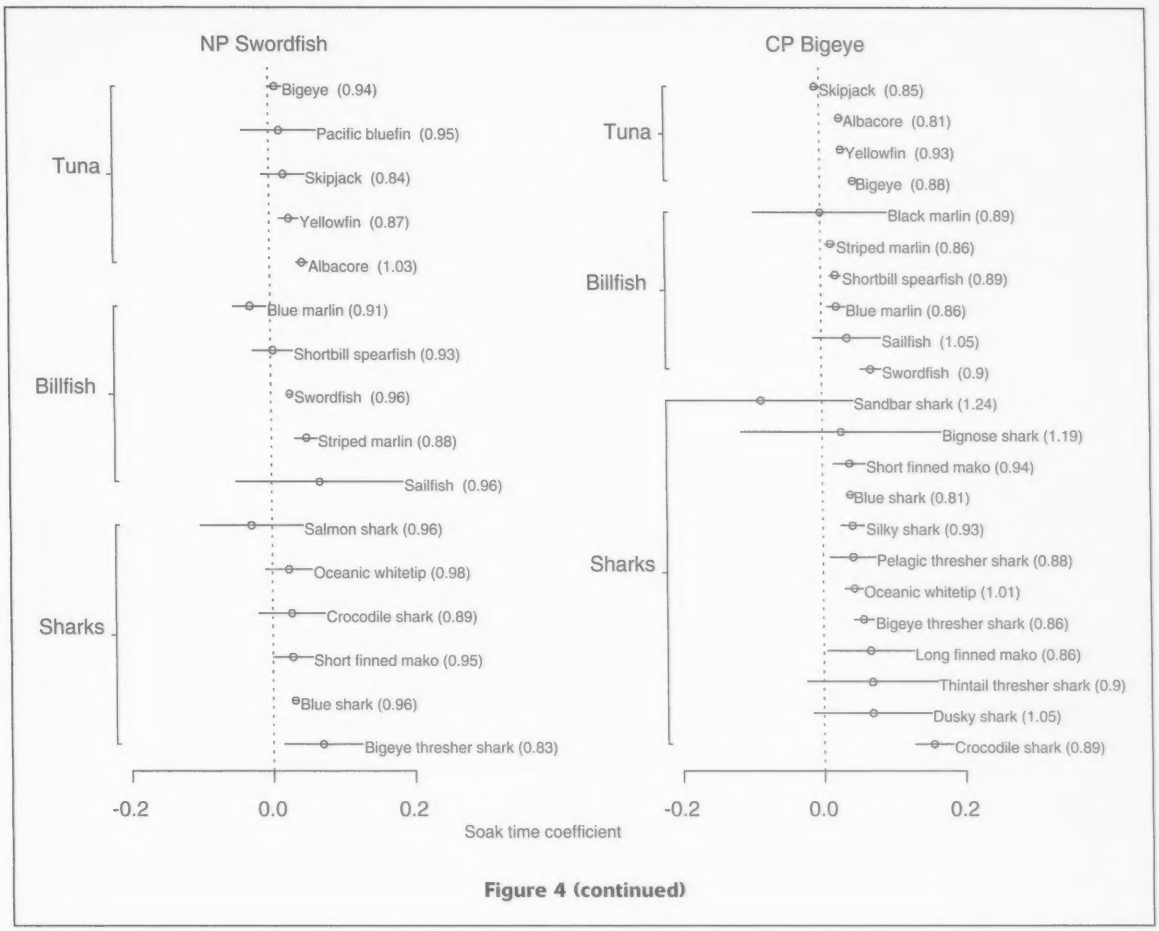

Figure 4 (continued)

in 36 of the 48 models for the other six species. We concluded that the fixed effects modified the intercept of the soak-time–catch-rate relationship, but they rarely altered the slope of the relationship.

Akaike's information criterion (AIC) and Sawa's Bayesian information criterion (BIC) both indicated that models with soak time as the only variable were the most or second most parsimonious model. This was the case for all models, except for several models of albacore and long-nosed lancetfish. Therefore the following discussion concentrates on the effects of soak time and timing on catch rates.

Discussion

In considering results of the random effects models, we examined patterns in the effects of soak time and timing among taxonomic groups, the mechanisms that may cause the patterns, and their implications. First, however, we investigated whether the effects were consistent for the same species between fisheries.

Comparison of fisheries

The effect of soak time was consistent for several species between the fisheries, despite significant differences in fishing practices and area and season of activity. For example, the soak time coefficients for species in the South Pacific yellowfin tuna fishery were very similar to those of the same species in the Central Pacific bigeye tuna fishery (r=0.79) (Fig. 6).

Several species had a narrow range of soak time coefficients over all the fisheries analyzed. Estimates of the coefficient of yellowfin tuna, for example, ranged from 0.00 (CI ±0.01) in the South Pacific yellowfin fishery to 0.04 (CI ±0.01) in the North Pacific swordfish fishery. A coefficient of 0.04 is equivalent to a difference of 1.3 yellowfin tuna per 1000 hooks between longline segments with soak times of 5 and 20 hours. The range in coefficients is also small for other abundant and widely distributed species, such as albacore (r=0.00–0.05) and blue shark (r=0.01–0.05).

For many species, however, the correlation between soak-time coefficients from different fisheries was poor (Fig. 6).

Table 3

Examples of the effect of soak time on expected catch rates of species in the South Pacific yellowfin tuna fishery. The expected catch rates (number per 1000 hooks) are predicted from the soak-time coefficient for each species for longline segments exposed to a dusk period with a soak time of 5 or 20 hours. Figure 4 shows the 95% confidence intervals for soak-time coefficients used to calculate the expected catch rates. LN = long-nosed; SN = short-nosed.

	Soak time (h)	
Species	5	20
Tuna and tuna-like species		
Albacore	15.5	13.4
Bigeye tuna	1.1	2.3
Skipjack tuna	1.3	1.0
Southern bluefin tuna	5.2	5.5
Yellowfin tuna	8.4	7.7
Billfish		
Black marlin	0.4	1.6
Blue marlin	1.2	0.4
Sailfish	0.8	1.0
Shortbill spearfish	1.0	1.6
Striped marlin	0.8	1.0
Swordfish	0.6	1.9
Other bony fish		
Barracouta	0.8	0.7
Escolar	0.8	3.1
Great barracuda	0.9	1.1
Lancetfish (LN)	2.7	2.4
Lancetfish (SN)	1.6	1.4
Mahi mahi	1.0	0.9
Oilfish	0.8	2.2
Opah	0.7	0.5
Ray's bream	1.8	2.0
Slender barracuda	1.7	1.6
Sunfish	0.6	1.3
Wahoo	1.0	1.1
Sharks and rays		
Blue shark	1.1	2.0
Bronze whaler	0.7	0.8
Dusky shark	0.4	0.8
Hammerhead	0.2	1.8
Mako	0.6	0.8
Oceanic whitetip	0.5	0.9
Porbeagle	1.2	1.1
Pelagic stingray	0.9	1.2
Thresher shark	0.6	1.0
Tiger shark	0.5	0.5

Table 4

Examples of the effect of timing on expected catch rates of species in the South Pacific yellowfin tuna fishery. The expected catch rates (number per 1000 hooks) are predicted from the soak-time coefficient for each species for a longline operation with a soak time of 12 hours. The different catch rates are for longline segments exposed to neither the dawn or dusk period, for dawn only, and for dawn and dusk periods. LN = long-nosed; SN = short-nosed.

	Period		
Species	Neither period	Dawn only	Dawn + dusk
Tuna and tuna-like species			
Albacore	12.3	14.0	16.5
Bigeye tuna	0.9	1.2	2.1
Skipjack tuna	1.4	1.2	1.0
Southern bluefin tuna	3.8	2.9	4.1
Yellowfin tuna	7.7	7.6	8.0
Billfish			
Black marlin	1.2	0.6	0.4
Blue marlin	0.4	1.0	1.4
Sailfish	0.8	0.7	0.7
Shortbill spearfish	1.3	0.9	0.9
Striped marlin	0.8	0.9	0.9
Swordfish	0.5	0.7	1.3
Other bony fish			
Barracouta	1.1	1.2	0.7
Escolar	0.8	1.0	2.0
Great barracuda	1.0	0.8	0.8
Lancetfish (LN)	2.8	2.7	2.5
Lancetfish (SN)	1.2	1.1	1.3
Mahi mahi	1.2	1.3	1.1
Oilfish	0.8	1.1	1.8
Opah	0.5	0.5	0.6
Ray's bream	0.8	0.7	1.6
Slender barracuda	2.0	1.5	1.2
Sunfish	0.8	0.6	0.7
Wahoo	1.2	1.3	1.1
Sharks and rays			
Blue shark	1.3	1.4	1.4
Bronze whaler	0.6	0.9	1.0
Dusky shark	0.1	0.1	0.6
Hammerhead	0.4	0.2	0.3
Mako	0.7	0.8	0.8
Oceanic whitetip	0.7	0.8	0.7
Porbeagle	1.0	0.6	0.6
Pelagic stingray	0.9	0.9	1.1
Thresher shark	0.6	0.6	0.7
Tiger shark	0.4	0.5	0.7

For a few species (e.g. tiger shark) the poor correlation may have been a function of small sample sizes and the wide confidence intervals of the estimates. For other species the estimates were well determined, yet poorly correlated, e.g. the coefficient for short-nosed lancetfish was 0.09 (CI ±0.05) in the Western Pacific distant fishery compared to 0.01 (CI ±0.04) in the Western Pacific bigeye tuna fishery. Therefore, we urge caution in applying our estimates to the same species in longline fisheries in other areas.

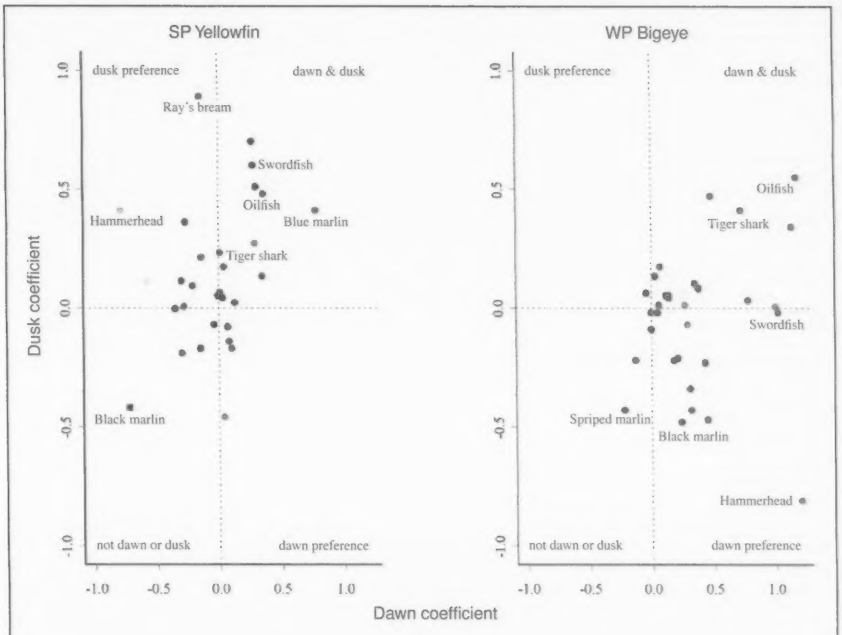

Figure 5

Pair-wise comparison of coefficients for the effects of dawn and dusk on catch rates for two fisheries. The shading of each symbol represents the sum of the standard errors of the dawn and dusk estimates (heavy shading for the lowest standard errors; light shading for large standard errors). Not all species names are shown.

Underlying mechanisms

The broad taxonomic groups taken by longline each represent a wide range of life history strategies and feeding behaviors. Nevertheless, the results show a tendency for soak time to have a positive effect on catch rates of most shark species (Fig. 4). It also had a positive effect on catch rates of many billfish species, including striped marlin, black marlin, and swordfish. There is no clear pattern in the effect of soak time on catch rates of tuna or other bony fish. It had a negative effect on the four seabird groups.

The results imply that the ability of a species to stay alive and to escape or avoid scavengers while hooked is important in determining the catch that is actually brought on board. The effect of soak time is significantly correlated with the ability of a species to survive while hooked on the longline in the four fisheries with data on survival (Fig. 7). Soak time has a strong, positive effect on catch rates of species like blue shark, which are almost always alive when branchlines are retrieved. Species like skipjack tuna and seabirds are usually dead. Soak time had a negative effect on their catch rates. The opposite trend would be expected if escape is a significant process that affects catch rates; if escape is important, soak time should have a *negative* affect on the catch rates of the most active species. Therefore removal by scavengers is likely to be more important than escape in determining catch rates for many species.

Longline branchlines are usually 20–30 m in length, allowing considerable room for a live, hooked animal to evade predators or scavengers. Or, scavengers may be attracted by immobile and dead animals. The scavenger avoidance hypothesis is attractive, but it is difficult to test with observer data. Data from hook-timer experiments may help to estimate the total number of animals that are lost or removed from the longline. Data presented by Boggs (1992) showed a large number of hook-timers that were triggered but which did not hold an animal when the branchline was retrieved, e.g. his data show that 2–4% of hook-timers on 10,236 branchlines that had "settled" were activated but did not have an animal. It is unclear whether the triggering of hook-timers was due to equipment malfunction or whether it represents high loss rates. Of particular significance to the question of loss rates is the fact that current hook-timer technology does not identify the species that were lost and whether they were alive or dead.

We noticed that soak-time coefficients tended to be poorly correlated between fisheries and that the effects of soak time on catch rates were most pronounced in the South Pacific bluefin tuna fishery. Our scavenging hypothesis might explain those observations as evidence that the activities of scavengers vary between fisheries. For example, blue shark might be an important scavenger. They are most abundant in temperate areas (Last and Stevens, 1994). Our analyses showed a predominance of negative soak-time coefficients

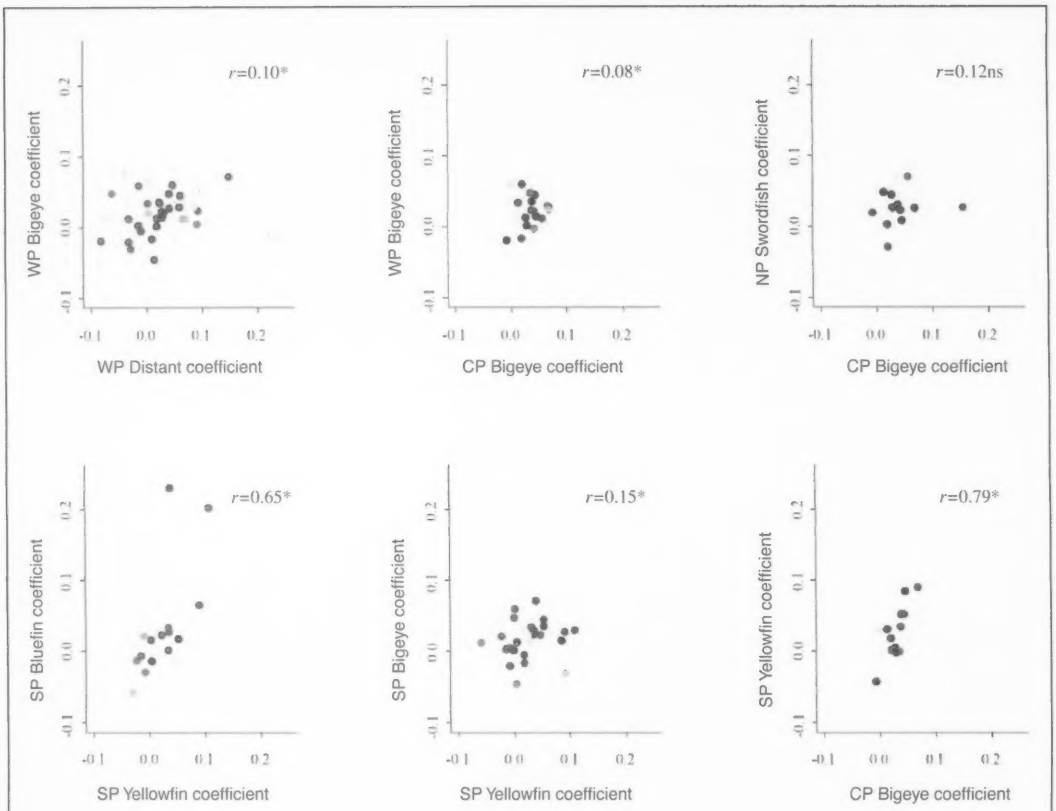

Figure 6

Pair-wise comparison of soak time coefficients for species that were common to fisheries. The coefficients are from random effects models where soak time is the only factor. The shading of each symbol represents the size of the standard error of the estimate. "*r*" is the correlation coefficient of a linear regression of coefficients (* indicates that the regression slope is significantly different from one at the 95% level, whereas "ns" indicates that the null hypothesis, that the regression slope equals one, cannot be rejected).

in the South Pacific bluefin tuna fishery—perhaps indicating that loss rates may be particularly high where blue shark are abundant.

Nevertheless, there are other plausible explanations for the differences in soak-time effects between fisheries. The movement of branchlines caused by wave action will cause animals to fall off hooks, especially when branchlines are near the sea surface. Rough seas are frequently experienced in the North Pacific swordfish and South Pacific bluefin tuna fisheries where the soak-time effects were most pronounced.

Another source of loss might be the breakage of longline branchlines. The animal's teeth or rostrum might abrade the branchline causing the branchline to fail and allowing the animal to escape. In this regard it is noteworthy that Central Pacific bigeye tuna longliners often use wire for the end of branchlines or "leader" whereas North Pacific wwordfish longliners use monofilament nylon leaders (Ito[4]).

Mortality estimates

The results of our study show that longline catch rates that are not adjusted for the effects of soak time will underestimate the level of mortality of several species because they are lost after being hooked. The soak time effect was negative for albatrosses and other seabirds. This finding agrees with field observations (e.g. Brothers, 1991) that most seabirds are taken during longline deployment in the brief period after the bait is cast from the vessel until the bait sinks beyond the depth that seabirds can dive to. Those observations indicate that counts of seabirds when they are brought on board do not cover the total number hooked because many fall off or are removed by scavengers or are lost during the operation.

[4] Ito, R. 2002. Personal commun. National Marine Fisheries Service (NOAA), 2570 Dole Street, Honolulu Hawaii 96822-2396.

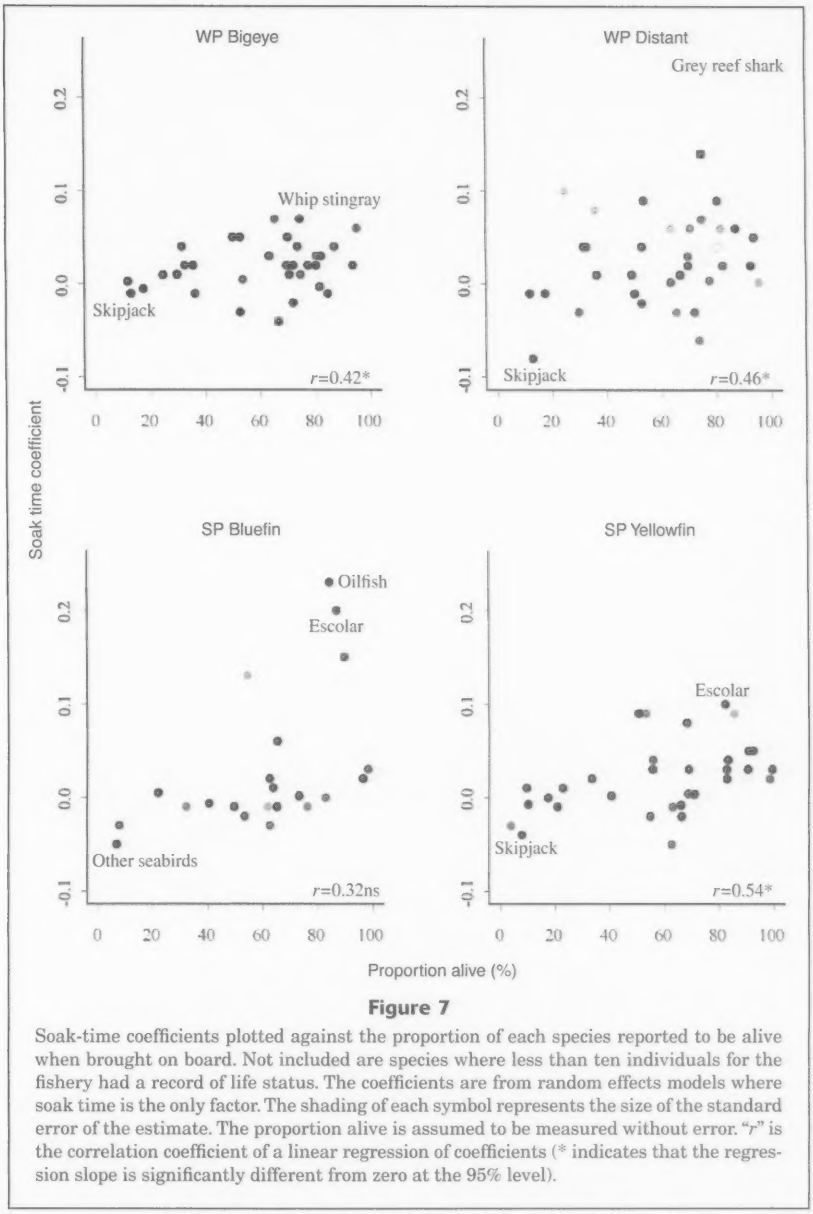

Figure 7

Soak-time coefficients plotted against the proportion of each species reported to be alive when brought on board. Not included are species where less than ten individuals for the fishery had a record of life status. The coefficients are from random effects models where soak time is the only factor. The shading of each symbol represents the size of the standard error of the estimate. The proportion alive is assumed to be measured without error. "r" is the correlation coefficient of a linear regression of coefficients (* indicates that the regression slope is significantly different from zero at the 95% level).

Seabirds provide a unique case for estimating loss rates because they are only caught when the longline is deployed (Brothers, 1991). Within minutes of the branchline being deployed, the capture rate (α in Eq. 4) falls to zero whereas the loss rate β might be constant or it might vary. Therefore, the probability of a seabird being on a hook when the branchline is retrieved is

$$\pi(T) = e^{-\beta T}. \quad (6)$$

We estimated a soak-time coefficient of –0.0302 (CI ±0.0462) for albatrosses in the South Pacific bluefin tuna fishery. Substituting 0.0302 for β in Equation 6 and 10.4 hours for T (the average soak time of hooks deployed by the longliners), we estimated that 27% of albatrosses are lost after being hooked but before the branchlines are retrieved. The loss rate is about 12% for petrels (β=0.0123) and 45% for other seabirds (β=0.0582). It is about 26% for other seabirds in the South Pacific yellowfin tuna fishery (β=0.0307, T=10.0 hours).

For fishes and sharks, we do not know how the probability of capture, or capture rate, or loss rate varies during a longline operation. However, hook–timer experiments

and observer programs may provide estimates of those parameters. Broad limits for the probability of capture may also be obtained if observers were to report the number of branchlines that are retrieved with missing baits or missing hooks.

For most species, capture rates must balance or outweigh loss rates. In this case, captures result from the increased exposure of animals to the longline as a result of movement and, perhaps, the dispersal of chemical attractants during the operation. However, we must stress that losses are also likely to be occurring for the species that have positive coefficients. The analyses indicate the relative levels of loss between longline segments of varying soak time. Other than those for seabirds, we cannot estimate the levels of catch that are lost.

Adding to the uncertainty over loss rates is the unknown fate of lost animals. For seabirds it is known that most drown soon after being hooked. The few seabirds that survive while hooked eventually drown during longline retrieval (Brothers, 1991). However, it is not known whether other lost animals are dead or alive.

Results of our analyses may also be useful for monitoring programs. Observers are increasingly being placed on longliners to collect data on bycatch and to independently verify data reported in logbooks. A sampling approach is necessary in some fisheries because observers are often unable to monitor the entire longline retrieval. Indications that catch rates of some species at the end of the retrieval are double those at the beginning necessitate care in designing observer monitoring protocols and in the interpretation of the data. Observers could also collect information on the number of hooks retrieved without baits. Such data would greatly improve the estimates of α and β required for the theoretical model. For the empirical model, catch rate data from research surveys where longline segments have very short (<4 hour) soak times would improve estimates of soak-time coefficients.

Historical changes

The interaction of year and soak time was rarely significant for the random effects models of the seven species examined in detail. This might suggest that soak-time–catch-rate relationships are stable over time. However, the range of years that we analyzed was limited to 1992–97. Over larger time scales there have been large variations in the abundance of individual species and the mix of species comprising the pelagic ecosystem. We cannot predict how soak-time–catch-rate relationships would change with those long-term variations.

Our original motivation for examining the effects of soak time was the hypothesis that the number of hooks per operation and soak time have increased since longlining commenced and that this may have resulted in an overestimation of billfish catch rates in early years. Ward[5] presented information on temporal trends in soak time and timing for several longline fleets. Although there is uncertainty over the early operations, the available information indicates significant historical changes in Japan's distant-water longline operations. Average soak time shows a decline from over 11.5 hours before 1980 to 10.0 hours in the 1990s. For species with a negative soak-time coefficient, this apparently modest reduction in soak time would inflate catch rate estimates for recent years. It would result in reduced catch-rate estimates for species with positive coefficients. For example, the expected catch rate for swordfish is 0.94 (CI ±0.06) per 1000 hooks for a soak time of 11.5 hours compared to 0.82 (CI ±0.06) per 1000 hooks for 10.0 hours.

More significant may be changes in the timing of operations. During 1960–80 most baits used with Japan's distant-water longliners were available to fish at dawn whereas about 50% were also available at dusk. Longlines were deployed and retrieved at later times in the 1990s so that about 30% of baits were available at dawn and about 70% available at dusk. In the case of swordfish, the changes in timing would moderate the effects of reduced soak time. The expected catch rate for swordfish is 0.89 per 1000 hooks in the early operations compared to 0.83 per 1000 hooks in the later operations.

Conclusions

The results have important implications for fishery management and assessments that rely on longline catch data. Modifications to data collection, such as recording the number of hooks with missing baits during longline retrieval, would greatly improve mortality estimates. The mortality of species like seabirds is significantly higher than previously estimated. Such underestimation may be particularly critical for the assessment and protection of threatened species of seabirds. Furthermore, the changes in timing and reduction in soak time have resulted in a systematic bias in estimates of mortality levels and abundance indices for many species. For species like swordfish, where soak time has a positive effect on catch rates, the stocks might be in better shape than predicted by current assessments (if assessments were solely based on catch and effort data). The opposite situation would occur for species with negative soak-time coefficients: assessments that use long time-series of longline catch data will over-estimate the species' abundance so that population declines are more severe than previously believed.

Acknowledgments

Grants from the Pew Charitable Trust, Pelagic Fisheries Research Program, and the Killam Foundation provided financial support for this work. Peter Williams (Secretariat of the Pacific Community), U.S. National Marine Fisheries Service staff (Kurt Kawamoto, Brent Miyamoto, Tom Swenarton, and Russell Ito) and Thim Skousen (Australian Fisheries Management Authority) provided observer data and operational information on the fisheries. We are espe-

[5] Ward, P. 2002. Historical changes and variations in pelagic longline fishing operations. http://fish.dal.ca/~myers/pdf papers.html. [Accessed 22 February 2003.]

cially grateful to the observers who collected the data used in this study and thank the masters, crew members, and owners of longliners for their cooperation with the observer programs. Pierre Kleiber, Ian Jonsen, Julia Baum, Boris Worm and an anonymous referee provided many useful comments on the manuscript.

Literature cited

Boggs, C. H.
1992. Depth, capture time, and hooked longevity of longline-caught pelagic fish: timing bites of fish with chips. Fish. Bull. 90:642–658.

Brothers, N.
1991. Albatross mortality and associated bait loss in the Japanese longline fishery in the Southern Ocean. Biol. Conserv. 55:255–268.

Carey, F. G.
1990. Further acoustic telemetry observations of swordfish. Mar. Recr. Fish. 13:103–22. Sportfishing Institute, Washington D.C.

Deriso, R. B., and A. M. Parma.
1987. On the odds of catching fish with angling gear. Trans. Am. Fish. Soc. 116:244–256.

Fernö, A., and I. Huse.
1983. The effect of experience on the behaviour of cod (*Gadus morhua* L.) towards a baited hook. Fish. Res. (Amst.) 2: 19–28.

Last, P. R., and J. D. Stevens.
1994. Sharks and rays of Australia. CSIRO Australia. 513 pages + color plates.

Murphy, G. I.
1960. Estimating abundance from longline catches. J. Fish. Res. Board Can. 17:33–40.

Sivasubramaniam, K.
1961. Relation between soaking time and catch of tunas in longline fisheries. Bull. Jpn. Soc. Sci. Fish. 27:835–845.

Somerton, D. A., and B. S. Kikkawa.
1995. A stock survey technique using the time to capture individual fish on longlines. Can. J. Fish. Aquat. Sci. 52: 260–267.

Ward, P. J.
1996. Japanese longlining in eastern Australian waters, 1962–90, 249 p. Bureau of Resource Sciences, Canberra.

Ward, P., and S. Elscot.
2000. Broadbill swordfish: status of world fisheries, 242 p. Bureau of Rural Sciences, Canberra.

Wolfinger, R. and M. O'Connell.
1993. Generalized linear mixed models: a pseudo-likelihood approach. J. Stat. Comput. Simul. 48:233–243.

Zhou, S., and T. C. Shirley.
1997. A model expressing the relationship between catch and soak time for trap fisheries. N. Am. J. Fish. Manag. 17: 482–487.

Abstract—Annual mean fork length (FL) of the Pacific stock of chub mackerel (*Scomber japonicus*) was examined for the period of 1970–97. Fork length at age 0 (6 months old) was negatively correlated with year-class strength which fluctuated between 0.2 and 14 billion in number for age-0 fish. Total stock biomass was correlated with FL at age but was not a significant factor. Sea surface temperature (SST) between 38–40°N and 141–143°E during April–June was also negatively correlated with FL at age 0. A modified von Bertalanffy growth model that incorporated the effects of population density and SST on growth was well fitted to the observed FL at ages. The relative FL at age 0 for any given year class was maintained throughout the life span. The variability in size at age in the Pacific stock of chub mackerel is largely attributable to growth during the first six months after hatching.

Effects of density-dependence and sea surface temperature on interannual variation in length-at-age of chub mackerel (*Scomber japonicus*) in the Kuroshio-Oyashio area during 1970–1997

Chikako Watanabe

Akihiko Yatsu

National Research Institute of Fisheries Science
Fisheries Research Agency
2-12-4 Fukuura, Kanazawa
Yokohama 236-8648, Japan
E-mail address (for C. Watanabe): falconer@affrc.go.jp

Manuscript approved for publication 22 September 2003 by Scientific Editor.
Manuscript received 20 October 2003 at NMFS Scientific Publications Office.
Fish. Bull. 102:196–206 (2004).

Variability in growth of marine fishes has been attributed to the effects of density-dependence or environmental factors such as water temperature, or to the effects of both factors (e.g. Moyle and Cech, 2002). Size-at-age data are crucial because they are necessary for stock assessment methods such as virtual population analysis, yield per recruit, and spawning-per-recruit analyses (Pauly, 1987; Mace and Sissenwine, 1993; Haddon, 2001) and are possibly useful for detecting regime shifts as well (Yatsu and Kidoroko, 2002). Around Japan, the effects of population density and sea water temperature on fish growth have been shown for the Pacific stock of chub mackerel (*Scomber japonicus*) (Iizuka, 1974), Japanese Spanish mackerel (*Scomberomorus niphonius*) (Kishida, 1990), the Pacific and Tsushima Current stocks of Japanese sardine (*Sardinops melanostictus*) (Hiyama et al., 1995; Wada et al., 1995), and Japanese common squid (*Todarodes pacificus*) (Kidokoro, 2001).

The Pacific stock of chub mackerel is one of the most important commercially exploited fish populations in Japan and has been managed by the total allowable catch (TAC) system in Japan since 1997. Chub mackerel seasonally migrate along the Pacific coast of Japan from Kyushu to Hokkaido. They spawn in the coastal waters around Izu Islands and off southwestern Japan between February and June (Fig. 1, Watanabe, 1970; Usami, 1973; Murayama et al., 1995; Watanabe et al., 1999). Adult fish (after spawning) and their offspring migrate eastward along the Pacific coast with the Kuroshio Current. Juvenile mackerel of about 6 months old usually recruit to the purse-seine and set-net fisheries off the coast of northeastern Japan at the end of summer (Fig. 1, Odate, 1961; Kawasaki, 1966; Watanabe, 1970; Iizuka, 1974). The total catch of the Pacific stock of chub mackerel increased during the 1960s and 1970s, peaked at 1.5 million metric tons in 1978, and then declined to 2.3 thousand tons in 1990 (Fig. 2). The estimated total biomass increased in the 1970s from 2.8 million tons in 1970 to 5.9 million tons in 1977, and the consecutive occurrences of large year classes exceeded 7 billion age-0 (6-month-old) fish in the early and mid 1970s. In 1990, the biomass was reduced to a minimum of 0.2 million tons in 1990 (Table 1, Fig. 2; Yatsu et al.[1]). Relatively large year classes occurred in 1992 (2.8 billion fish) and 1996 (4.5 billion fish), and the total biomass increased in the mid 1990s, but it remained at about 10% of the level attained in the mid 1970s (Yatsu et al.[1]).

On the basis of year-class strength and variations in fork length (FL) at ages 0–2 for the 11 year classes present from 1963 to 1973, Iizuka (1974) suggested an effect of density-dependent growth on young chub mackerels. In

[1] Yatsu, A., C. Watanabe, and H. Nishida. 2001. Stock assessment of the Pacific stock of chub mackerel in fiscal 2000 year. *In* Stock assessment report, p. 64–87. [In Japanese. Available from Fisheries Research Agency, 2-12-4 Fukuura, Kanazawa, Yokohama 236-8648, Japan.]

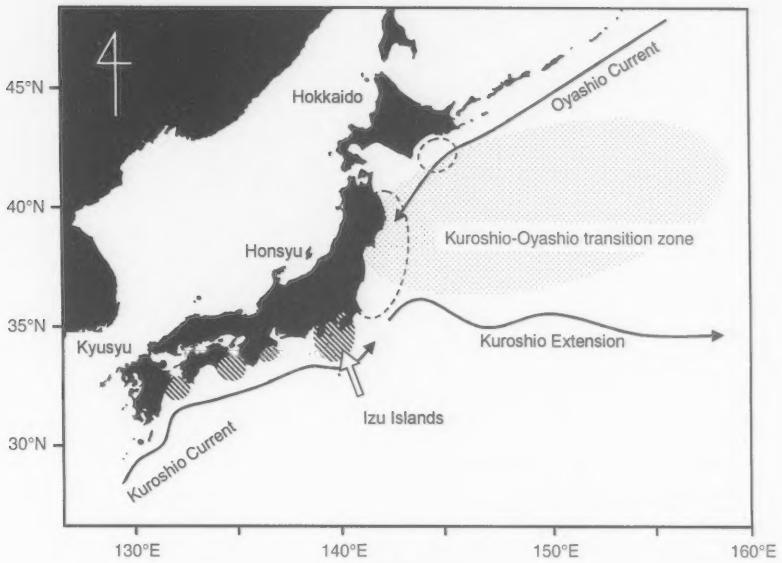

Figure 1

Distribution of the Pacific stock of chub mackerel (*Scomber japonicus*) and major oceanographic features around Japan. The hatched areas show spawning grounds. The dotted areas show feeding grounds. Major purse-seine fishing grounds are surrounded by dashed lines. The fishing grounds around the eastern coast of Hokkaido failed in 1977 with the decline in biomass (Hirai, 1991).

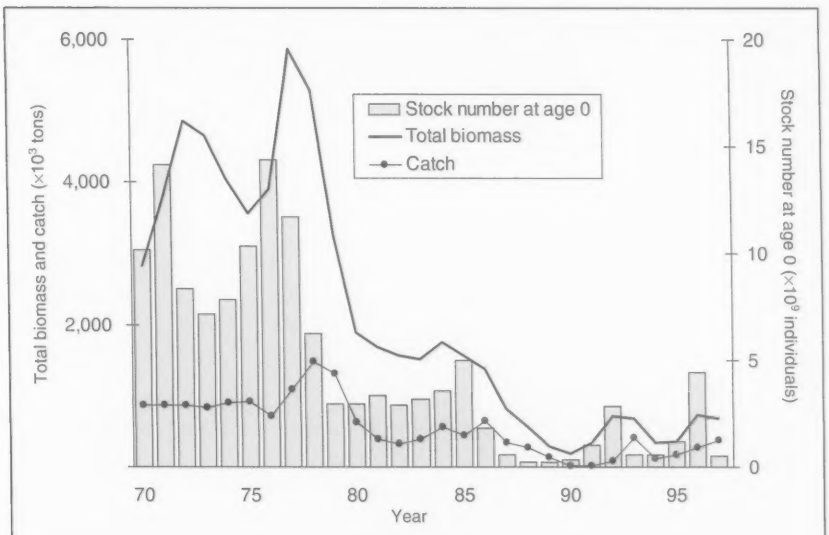

Figure 2

Total biomass, total catch, and year-class strength for the Pacific stock of chub mackerel (*Scomber japonicus*) (Yatsu, et al.[1]). Year-class strength was represented by the stock in number at age 0, estimated by virtual population analysis (Yatsu, et al.[1]).

this study we describe the variation in FL at age of the Pacific stock of chub mackerel in the Kuroshio–Oyashio area, using data from 1970 to 1997 when the stock biomass fluctuated between 0.2 and 5.9 million metric tons. We use these data to evaluate the effects of population density and sea surface temperature on FL at age.

Materials and methods

Biological data

Biological data have been compiled since 1964 for purse-seine, set-net, dip-net catches, and other catches by national fisheries research institutes and local government fisheries experimental stations in Japan. Fork length (FL) was measured for one thousand to 100 thousand fish per year and body weight (BW) and gonad weight were measured for 10–100% of these fish. The monthly FL compositions and the relationships of FL to BW were established for each year with this data set. Year-specific age-length keys from 1970 to 1994 were adopted from the reports of cooperative research on Pacific mackerel by local government agencies in Chiba, Kanagawa, Shizuoka, and Tokyo.[2] Between 1995 and 1997, age-length keys were developed by national fisheries research institutes and local government fisheries experimental stations.

For calculating the mean FL for ages 0, 1, 2, 3, 4, 5, and 6 years and older, we used data from the purse-seine fishery of northeastern Japan during September–December for 28 years, from 1970 to 1997. The catch of this fishery in these four months constituted 26–80% (the 28-year mean is about 63%) of the total annual catch of the Pacific stock of chub mackerel. Catch in number at FL class i (cm) of each month were calculated by

$$n_{a,i} = C_a \frac{d_{a,i}}{\sum_{k=1}^{50} d_{a,k} w_{a,k}}, \quad (1)$$

where $n_{a,i}$ = catch in number at FL class i (cm) {= 1, . . . , k, . . 50} of month a {= *Sep.*, *Oct.*, *Nov.*, *Dec.*};
$d_{a,i}$ = frequency at FL class i of month a;
$w_{a,i}$ = a mean weight of each FL class derived from the FL-BW relationship; and
C_a = a total catch of month a.

We then summed $n_{a,i}$ of 4 months to derive the annual catch in number at FL class i:

$$n_i = \sum_{a=Sep.}^{Dec.} n_{a,i}, \quad (2)$$

where n_i = the annual catch in number at FL class i.

Using the age-length key, we converted n_i to catch at FL class i at age j:

$$n_{i,j} = n_i \times r_{i,j}, \quad (3)$$

where $n_{i,j}$ = the annual catch in number at FL class i at age j; and
$r_{i,j}$ = the proportion of age j at FL class i ($r_{i,0} + r_{i,1} + \cdots + r_{i,k} = 1$).

From $n_{i,j}$, we calculated the mean and variance of FL at age j:

$$l_j = \frac{\sum_{i=1}^{k} n_{i,j} l_{i,j}}{\sum_{i=1}^{k} n_{i,j}} \quad (4)$$

and

$$Var(l_j) = \frac{\sum_{i=1}^{k} n_{i,j} (l_{i,j} - l_j)^2}{\left(\sum_{i=1}^{k} n_{i,j}\right) - 1}, \quad (5)$$

where l_j = mean FL at age j; and
$l_{i,j}$ = mean FL at FL class i at age j.

Sea surface temperature

Time-series data for sea surface temperature (SST, temperatures averaged over 10 days for 1° latitude × 1° longitude blocks over the northwestern North Pacific between 0–53°N and 110–180°E since 1950) were provided by the Oceanographical Division of the Japan Meteorological Agency. The SST data for each block was averaged for periods of three months (i.e. January–March, April–June, July–September, and October–December). The relationship between the SST of each block and FL at age 0 were examined from 1970 to 1997.

Autocorrelation

For correlation analysis, effective sample sizes (n^*) were calculated for all time series data to take autocorrelation into account. n^* was computed by the formula (Pyper and Peterman, 1998):

$$\frac{1}{n^*} = \frac{1}{n} + \frac{2}{n} \sum_{j=1}^{n/5} r_{XX}(j) r_{YY}(j), \quad (6)$$

where $r_{XX}(j)$ and $r_{YY}(j)$ are the autocorrelations of X and Y at lag j, defined here with the additional weighting factor proposed by Pyper and Peterman (1998):

$$r_{XX}(j) = \frac{n}{n-j} \frac{\sum_{t=1}^{n-j} (X_t - \overline{X})(X_{t+j} - \overline{X})}{\sum_{t=1}^{n} (X_t - \overline{X})^2}. \quad (7)$$

Growth model

We used the modified von Bertalanffy growth model to incorporate the effects of population density and sea sur-

[2] Age-length keys. *In* Kanto Kinkai no Masaba ni tuite, Appendix 1, vol. 30, 30 p. [In Japanese. Available from Kanagawa Prefectual Fisheries Research Institute, Jyogashima, Misaki, Miura, Kanagawa 238-0237, Japan.]

face temperature according to Millar and Myers,[3] who nvestigated three formulations of the modified von Bertalanffy equations: 1) a reversible effect on the growth constant k; 2) a reversible effect on the asymptotic length L_∞; and 3) an irreversible effect on L_∞ or k. We tested two of the models, 1 and 2, to investigate the effect of population density and SST. We did not test model 3 because we did not consider that the environmental effects on growth were permanent. Mean length at age i of year-class y was estimated with the following formulas:

Model 1: reversible environmental effect on k

$$\hat{L}_{i,y} = L_\infty(1-e^{-k_{0,y}t_0}) \quad (8)$$

$$\hat{L}_{i,y} = \hat{L}_{i-1,y} + (L_\infty - \hat{L}_{i-1,y})(1-e^{-k_{i,y}}) \quad (9)$$

$$k_{i,y} = k + \beta_1 T_{i+y} + \beta_2 D_{i,y}. \quad (10)$$

Model 2: reversible environmental effect on L_∞

$$\hat{L}_{0,y} = L_{\infty 0,y}(1-e^{-kt_0}) \quad (11)$$

$$\hat{L}_{i,y} = \hat{L}_{i-1,y} + (L_{\infty i,y} - \hat{L}_{i-1,y})(1-e^{-k}) \quad (12)$$

$$L_{\infty i,y} = L_\infty + \beta_1 T_{i+y} + \beta_2 D_{i,y}, \quad (13)$$

where t_0 = the age at length 0 (year);
L_∞ = the asymptotic length; and
k = the growth coefficient;
$L_{\infty i,y}$ = L_∞ at age i of year-class y;
$k_{i,y}$ = k at age i of year-class y;
T_{i+y} = the sea surface temperature in year i+y; and
$D_{i,y}$ = a population density presented by the number of stock at age i of year-class y.

These variables were z-score standardized. The model parameters α_1 and β_2 were estimated to represent the effects of T_{i+y} and $D_{i,y}$ on k or L_∞.

The parameters were estimated by maximizing the likelihood function which is represented by

$$L(i,y) = \hat{L}_{i,y} + \varepsilon_i, \quad (14)$$

$$\varepsilon_i \sim N(0,\sigma_i^2), \quad (15)$$

and

$$L(L_\infty, k, t_0, \beta_1, \beta_2, \sigma_i^2) = \prod_y \prod_i \left[2\pi\sigma_i^2\right]^{-\frac{1}{2}} \exp\left[-\frac{\left\{L(iy)-\hat{L}_{i,y}\right\}^2}{2\sigma_i^2}\right]. \quad (16)$$

[3] Millar, R. B., and R. A. Myers. 1990. Modeling environmentally induced change in growth for Atlantic Canada cod stock. ICES CM 1990/G:24.

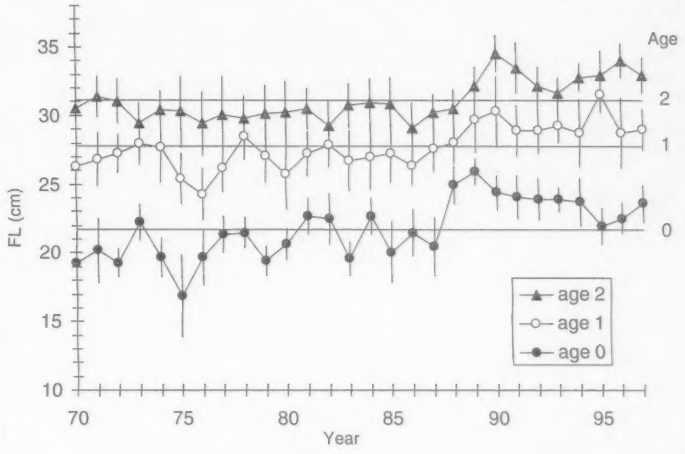

Figure 3

Interannual fluctuations in mean fork length (FL) at age 0, age 1, and age 2 for chub mackerel (*Scomber japonicus*) in 1970–97. Horizontal lines show the 28 year mean FL at age 0, 1, and 2, respectively. Vertical bars show standard deviations.

We ran the models with all possible combinations of explanatory variables (T, D, T, and D), and compared AIC with that obtained with the base parameters (L_∞, t_0, k).

Results

Fork length at age

Mean FL at age 0 varied substantially over the time series examined. For example, it ranged from 16.9 (Sd ±3.0) cm in 1975 to 25.9 (Sd ±1.0) cm in 1989. The mean FL for the 28 years period was 21.7 (±2.1) cm (coefficient of variation: CV=9.8%, Table 1, Fig. 3). The FL-at-age-0 values were smaller than the 28-year mean FL for the 1970s, varied around the mean in the early and mid 1980s, reached a maximum in 1989, and were at about 22–24 cm in the 1990s (Fig. 3).

Mean FL at age 1 was similarly variable; it ranged from 24.3 (±1.9) cm in 1976 to 31.6 (±1.4) cm in 1995. The 28-year mean FL was 27.7 (±1.6) cm (CV=5.6%, Table 1). The trend in interannual variability was similar to that in age 0, i.e. it was smaller in the 1970s and larger in the 1990s (Fig. 3). In age-2 fish the 28-year minimum FL of 29.1 (±1.8) cm was observed in 1986 and the maximum of 34.5 (±1.3) cm was observed in 1990 (the 28-year mean FL=31.1 (±1.5) cm, CV=4.7%, Table 1, Fig. 3).

In fish age 3 and older, mean FL varied year-to-year in a manner similar to that found in the younger ages (Table 1). Annual mean FLs for 3-, 4-, and 5-year-olds were 33.7 (±1.3) cm (3.8%), 36.2 (CI ±1.4) cm (CV=4.0%), and 38.5 (CI ±1.5) cm (CV=3.8%), respectively (Table 1). The mean FLs for ages 0–5 of each year were significantly different among different years (one-way ANOVA, $P<0.01$).

Table 1

Total biomass, year class strength (stock number at age 0; Yatsu, et al.[1]), SST, and mean fork length (FL) of *Scomber japonicus* from 1970 to 1997. Blanks show the lack of data.

Year	Total Biomass (10^3 t)	Stock number at age 0 (10^6 individuals)	SST (°C)[I]	Mean FL (SD) cm					
				0	1	2	3	4	5
1970	2833	10,199	11.5	19.2 (2.6)	26.3 (1.8)	30.5 (2.4)	34.2 (1.7)	37.7 (1.6)	40.5 (1.4)
1971	3781	14,138	10.9	20.2 (2.3)	26.8 (1.9)	31.4 (1.5)	34.3 (1.6)	37.7 (1.6)	40.4 (1.3)
1972	4860	8342	13.2	19.3 (1.0)	27.2 (1.4)	31.1 (1.6)	34.3 (1.5)	37.3 (1.7)	40.0 (1.5)
1973	4650	7154	11.1	22.2 (1.4)	27.9 (1.5)	29.4 (1.6)	31.2 (1.8)	33.1 (2.0)	36.1 (1.9)
1974	4048	7854	10.5	19.7 (1.4)	27.7 (2.5)	30.4 (1.4)	31.9 (1.7)	33.9 (1.8)	37.6 (1.7)
1975	3558	10,353	12.3	16.9 (3.0)	25.4 (1.8)	30.3 (2.6)	32.7 (1.6)	33.8 (1.6)	35.5 (1.7)
1976	3896	14,402	11.5	19.7 (2.0)	24.3 (1.9)	29.4 (2.4)	33.7 (1.9)	35.3 (1.8)	38.1 (1.8)
1977	5868	11,701	10.9	21.4 (1.3)	26.2 (1.8)	30.1 (2.8)	33.5 (2.2)	35.7 (1.7)	37.4 (1.4)
1978	5285	6249	10.0	21.5 (1.1)	28.5 (1.7)	29.8 (1.6)	32.1 (2.3)	34.5 (2.1)	36.1 (1.9)
1979	3250	2931	12.3	19.5 (1.1)	27.1 (2.0)	30.2 (2.0)	33.0 (1.7)	35.2 (1.6)	37.2 (1.3)
1980	1898	2952	11.3	20.7 (1.1)	25.8 (2.6)	30.3 (2.2)	32.4 (1.8)	33.9 (1.8)	35.6 (1.6)
1981	1683	3374	9.4	22.7 (1.3)	27.2 (1.7)	30.5 (1.5)	33.1 (2.1)	36.5 (1.8)	38.0 (1.5)
1982	1567	2883	10.8	22.5 (1.8)	27.9 (1.6)	29.3 (1.8)	33.6 (2.2)	36.6 (1.6)	38.3 (1.4)
1983	1516	3175	11.5	19.6 (1.2)	26.7 (2.2)	30.8 (1.6)	33.6 (1.5)	35.5 (2.0)	37.8 (1.2)
1984	1759	3605	9.3	22.7 (1.3)	27.0 (2.4)	31.0 (1.8)	34.8 (1.9)	36.6 (1.8)	38.2 (2.0)
1985	1565	4998	11.4	20.1 (2.2)	27.3 (2.1)	30.9 (1.9)	33.3 (1.9)	37.4 (1.7)	39.0 (1.8)
1986	1373	1833	9.7	21.5 (1.7)	26.4 (1.4)	29.1 (1.8)	32.5 (2.4)	35.9 (2.1)	38.9 (1.9)
1987	812	583	10.9	20.5 (2.1)	27.6 (1.7)	30.2 (1.3)	32.8 (1.6)	36.4 (2.3)	39.2 (0.8)
1988	555	236	11.4	24.9 (1.4)	28.1 (1.5)	30.5 (1.4)	32.8 (1.7)	36.8 (1.6)	40.1 (1.2)
1989	289	219	9.8	25.9 (1.0)	29.7 (2.3)	32.2 (1.4)	34.6 (1.5)	35.7 (1.5)	39.2 (1.5)
1990	185	356	11.7	24.4 (1.3)	30.3 (2.6)	34.5 (1.3)	35.8 (1.5)	38.2 (1.1)	39.7 (0.8)
1991	338	1017	12.2	24.1 (1.6)	28.9 (1.8)	33.5 (1.9)	35.5 (1.2)	36.7 (1.9)	39.0 (1.8)
1992	724	2839	9.7	24.0 (1.6)	29.0 (1.7)	32.1 (1.4)	34.1 (1.5)	37.5 (1.6)	40.5 (1.6)
1993	685	589	10.7	23.9 (0.9)	29.3 (1.3)	31.7 (1.1)	33.2 (0.5)		
1994	343	547	11.3	23.7 (1.7)	28.8 (2.5)	32.8 (1.0)	34.6 (0.8)	35.9 (0.7)	39.1 (1.0)
1995	351	1183	11.3	22.0 (1.3)	31.6 (1.4)	32.9 (1.8)	35.5 (1.8)	38.0 (1.3)	39.2 (0.8)
1996	726	4452	9.9	22.5 (1.1)	28.7 (2.5)	34.1 (1.2)	36.1 (1.1)	37.8 (0.9)	39.7 (0.7)
1997	682	529	9.9	23.6 (1.4)	29.0 (1.5)	33.0 (1.3)	35.4 (1.7)	37.6 (0.7)	38.6 (0.5)
28-year mean of FLs at ages				21.7 (2.1)	27.7 (1.6)	31.1 (1.5)	33.7 (1.3)	36.2 (1.4)	38.5 (1.5)

[I] SST during April–June in the waters bounded by 38–40°N and 141–143°E.

Mean growth increments I of each year class from age 0 (6 months old) to ages 1–5 (I_{0-i}) showed significantly negative correlations (Table 2). Correlations between the two variables tended to increase with age: –0.69 for I_{0-1}, –0.71 for I_{0-2}, –0.80 for I_{0-3}, and –0.77 for I_{0-4}.

The relative FL at age 0 for any given year class was maintained throughout the life span. A correlation between the mean FL at age 0 and age 1 within each year class (1970 to 1996 year class) was positive and statistically significant ($P<0.05$, Fig. 4). Similarly, the positive correlations between the mean FL at age 0 and age 3 (1970 to 1994 year class, $P<0.01$, Fig. 4), and age 0 and age 4 (1970 to 1993 year class, $P<0.05$, Fig. 4) were significant ($P<0.05$, Fig. 4).

Correlation between FL and population density

Population densities represented by stock in number at age 0 and total biomass were negatively correlated to FL at age. Negative correlations between the logarithm of abundance of age 0 ($\ln N_0$) and FL at ages were relatively high in age 0 to 3 (–0.69 to –0.83, Table 3) and low in age 4 and 5 (–0.63 and –0.64, Table 3). Correlations were statistically significant for ages 0, 2, and 3 (Table 3). Negative correlations between the logarithm of total biomass and FL at ages were relatively high at ages 0 to 2 (–0.73 to –0.75) and moderate for age 3 to 5 (–0.50 to –0.52, Table 4). However, the relationships were not statistically significant for all ages (Table 4).

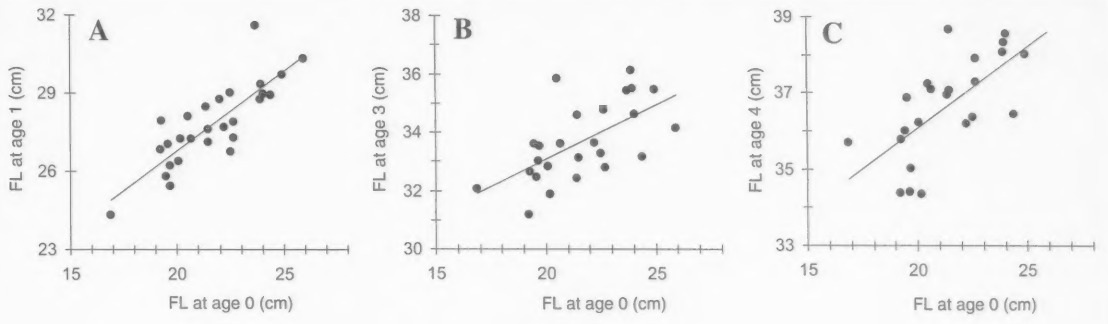

Figure 4

Scatter plots of FL at age 1 (**A**), age 3 (**B**) and age 4 (**C**) on FL at age 0 for chub mackerel (*Scomber japonicus*). Correlations between FL at age 1 with age 0 (r=0.83, n=28, actual sample size n^*=8, df=6), age 3 with age 0 (r=0.62, n=26, n^*=11, df =9) and age 4 with age 0 (r=0.67, n=24, n^*=10) were all significant at $P < 0.05$.

Table 2

Correlation of FL at age 0 and growth increment after age 0. n = actual sample size. n^* and degree of freedom (df) show the effective n and df when the data were corrected for autocorrelation (Pyper and Peterman, 1998). Significance level: **, P<0.01.

Growth increment	r	r^2	n	n^*	df
Ages 0–1	–0.69**	0.48	27	21	19
Ages 0–2	–0.71**	0.51	26	25	23
Ages 0–3	–0.80**	0.64	25	23	21
Ages 0–4	–0.77**	0.59	23	24	22
Ages 0–5	–0.78**	0.61	22	22	20

Table 3

Correlation between the natural logarithm of the abundance of age 0 and mean FL for each age. n = actual sample number. n^* and degree of freedom (df) show the significant n and df when autocorrelation was considered (Pyper and Peterman, 1998). Significance levels: *, $P < 0.05$.

Age	r	r^2	n	n^*	df
0	–0.75*	0.57	28	8	6
1	–0.69	0.48	27	7	5
2	–0.83*	0.69	26	6	4
3	–0.71*	0.51	25	9	7
4	–0.63	0.40	23	8	6
5	–0.64	0.40	22	6	4

Correlation between FL and SST

Growth in the first six months of life was correlated with SST. We detected significant negative correlation between FL-at-age 0 and SST between April and June in the waters bounded by 38–40°N and 141–143°E (r=–0.45, r^2=0.20, n=28, n^*=27, df=25, P<0.05, Fig. 5). The SST between July and September of this area was also negatively correlated with FL at age 0 although the correlation coefficient was not significant at 5% level.

Table 4

Correlation between natural logarithm of total biomass and mean FL for each age. n = actual sample size. n^* and dgree of freedom (df) show the effective n and df when the data were corrected for autocorrelation (Pyper and Peterman, 1998). No correlations were significant (P>0.05).

Age	r	r^2	n	n^*	df
0	–0.74	0.38	27	6	4
1	–0.73	0.32	27	6	4
2	–0.75	0.36	27	5	3
3	–0.52	0.26	27	11	9
4	–0.51	0.26	26	9	7
5	–0.50	0.22	26	7	5

Growth analysis

Model 1 that incorporated SST (T) and population density (D) gave a minimum Akaike's information criterion (AIC) of 457.68 (Table 5) and the model was expressed by

$$\hat{L}_{i,y} = 43.98\left\{1-\exp(-2.585)\exp\left(-\sum_{i=0}^{5} k_{i,y}\right)\right\} \quad (17)$$

$$k_{i,y} = 0.271 - 0.008T_{i+y} - 0.21D_{i,y}. \quad (18)$$

This model estimated the FL at ages 0–5 well (Fig. 6). The AIC of model 1 incorporating T and D was smaller than the AIC of model 2; therefore the environmental factors had an affect on k rather than L_∞.

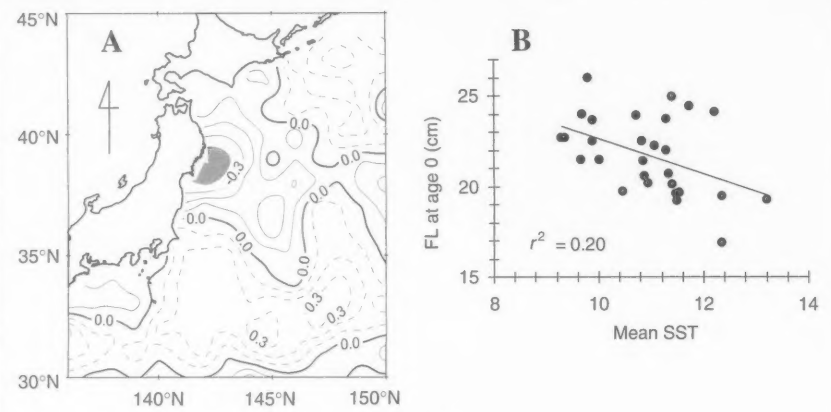

Figure 5

(**A**) Map to show correlation between sea surface temperatures (SST) and mean fork length (FL) at age 0 for chub mackerel (*Scomber japonicus*). The dotted area indicates the negative correlation coefficient r above 0.4. The contour interval is 0.1 of the correlation coefficient and positive contours are shown as dashes. (**B**) Relationship between mean SST for the area 38°–40°N and 141–143°E from April to June and mean FL at age 0. Correlation was significant at the 5% level (r=–0.45, n=28, n^*=27, df=25).

To investigate the effect of T and D, we calculated the total effect on k for year-class y according to Sinclair et al. (2002):

$$\frac{\sum_{i=0}^{5}\beta_1 T_{i+y}}{6} \text{ for } T, \text{ and } \frac{\sum_{i=0}^{5}\beta_2 D_{i,y}}{6} \text{ for } D.$$

Discussion

Estimated population abundance of age-0 fish and total biomass may explain density-dependent growth. FL at age 0, 2, and 3 of the Pacific stock of chub mackerel were negatively correlated with the number of age-0 recruits. Correlations between biomass and FL at ages 0–5 were low and not significant. Therefore, year-class strength is indicated to have a greater negative influence on the growth of the Pacific stock of chub mackerel than total biomass, as reported for the Atlantic mackerel (*Scomber scombrus*) (Agnalt, 1989; Overholtz, 1989; Neja, 1995) and Atlantic herring (*Clupea harengus*) (Toresen, 1990).

Density-dependent growth in fish populations seems to be a common phenomenon for pelagic fishes found in the temperate waters of Japan. The FL at age 0 of the 1963–69 year classes ranged from 16 to 20 cm, and were smaller than those of the 1970s, possibly indicating density-dependent growth (Iizuka, 1974). According to Honma et al. (1987), the stock abundance of the Pacific stock of chub mackerel from 1963 to 1969 was larger than it was in the 1970s. Wada et al. (1995) and Hiyama et al. (1995) found negative relationships between total biomass and body length in the Pacific and Tsushima Current stock of the Japanese sardine (*Sardinops melanostictus*). Kishida (1990) demonstrated a density-dependent relationship between the growth and total stock density (CPUE) of Japanese Spanish mackerel (*Scomberomorus niphonius*).

Our results do not agree with the positive effect of sea water temperature on somatic growth that has been shown for several species, including Japanese common squid (Kidokoro, 2001), Atlantic herring (Moores and Winters, 1981; Toresen, 1990), and Atlantic cod (*Gadus morhua*) (Brander, 1995; Dutil et al., 1999; Rätz et al. 1999; Otterson et al., 2002).

Table 5

Summary of statistics from the estimation of growth for chub mackerel (*Scomber japonicus*). AIC = Akaike's information criterion.

Model	Variables	No. of unknown parameters	Log likelihood	AIC
1	$L_\infty, k, t_0, \sigma_1 \ldots \sigma_5$	9	–280.20	578.40
	$L_\infty, k, t_0, \sigma_1 \ldots \sigma_5, \beta_1$	10	–270.10	560.20
	$L_\infty, k, t_0, \sigma_1 \ldots \sigma_5, \beta_2$	10	–222.38	464.77
	$L_\infty, k, t_0, \sigma_1 \ldots \sigma_5, \beta_1, \beta_2$	11	–217.84	457.68
2	$L_\infty, k, t_0, \sigma_1 \ldots \sigma_5$	9	–280.20	578.40
	$L_\infty, k, t_0, \sigma_1 \ldots \sigma_5, \beta_1$	10	–268.63	557.25
	$L_\infty, k, t_0, \sigma_1 \ldots \sigma_5, \beta_2$	10	–224.01	468.02
	$L_\infty, k, t_0, \sigma_1 \ldots \sigma_5, \beta_1, \beta_2$	11	–220.81	463.62

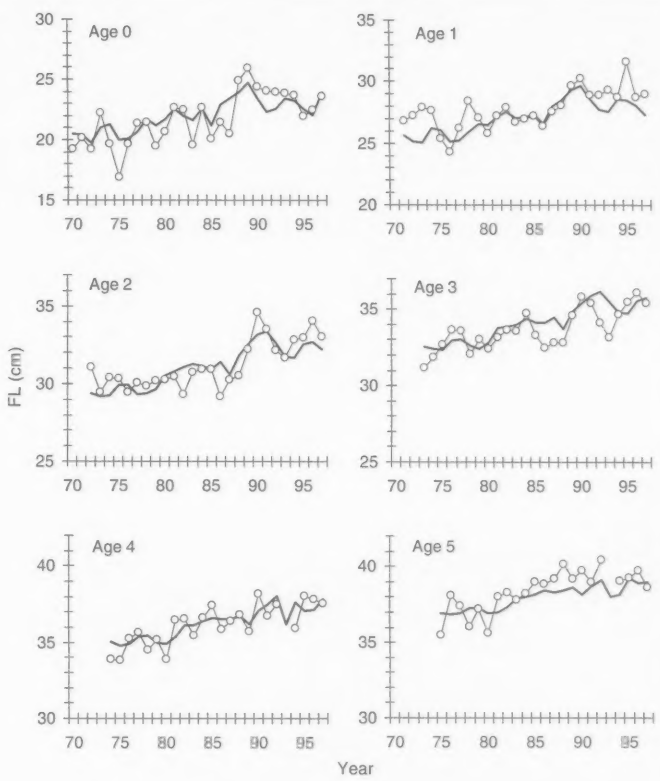

Figure 6

Time series of observed (open circles) and modeled (solid line) values of mean fork length (FL) at ages 0–5 during 1970–97 for chub mackerel (*Scomber japonicus*).

There was a positive correlation between FL at age 0 and 1°×1° block SST in the waters of 32–34°N and 144–149°E, located south of the Kuroshio Extension flowing eastward at the latitude of 35–37°N from April to June (Figs. 1 and 5A). But the correlation coefficient was not significant, and this area was not considered to be inhabited by juvenile mackerel (Watanabe, 1970). Thus, we considered that the SST in the waters of 32–34°N and 144–149°E was not a significant factor on the variation of FL at age 0.

The low SST in the waters bounded by 38–40°N and 141–143°E is indicative of a large inflow of Oyashio Current waters (Hirai and Yasuda, 1988), which is a cold water current and has high productivity (Odate, 1994), into the Kuroshio–Oyashio transition zone, where is one of the main feeding grounds of mackerels (Odate, 1961; Watanabe, 1970; Watanabe and Nishida, 2002; Fig. 1). Thus, we hypothesized that the large inflow of Oyashio current waters into the Kuroshio–Oyashio transition zone improved the feeding condition and accelerated the growth of juvenile mackerel. Jobling (1988) suggested a parabolic relationship between water temperature and fish growth. The range of SST in this area, which was negatively correlated with FL at age 0 of mackerel, was 9–13°C (Table 1). This temperature range is near the lowest nonstressful temperatures for mackerel (10–12°C, Schaefer, 1986). Thus, we do not consider that the negative relationship between growth and SST was the result of suppressed growth by the high ambient temperature.

In mackerel, maximum egg production appears to have shifted to later in spring during the 1990s, as compared to the late 1970s and 1980s, resulting in a shorter period of growth and thus smaller fish (Fig. 8, Mori et al.[4]; Kikuchi and Konishi[5]; Ishida and Kikuchi[6]; Zenitani et al.[7]; Kubota et al.[8]). In the early 1970s, the main spawning period was

[4] Mori, K., K. Kuroda, and Y. Konishi. 1988. Monthly egg production of the Japanese sardine, anchovy, and mackerels off the southern coast of Japan by egg censuses. Datum Collect. Tokai Reg. Fish. Res. Lab. 12:1–321. [In Japanese. Available from National Research Institute of Fisheries Science, 2-12-4 Fukuura, Kanazawa, Yokohama 236-8648, Japan.]

[5] *See next page.*

[6] *See next page.*

[7] *See next page.*

[8] *See next page.*

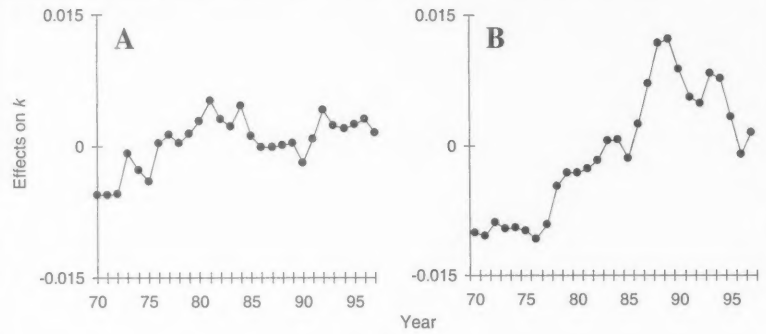

Figure 7

The total effect of (**A**) mean SST for the area of 38–40°N and 141–143°E from April to June, and (**B**) population density on k for each year class of chub mackerel (*Scomber japonicus*).

also in April (Kuroda[9]). Delayed spawning in the 1990s should have resulted in a reduction in the mean FL at ages during September–December in the 1990s compared to the 1970s and 1980s; however the present study showed the opposite result (Table 1). We hypothesize that the effect of the shift of spawning period on the FL at ages may have been overwhelmed by the effect of population density (Fig.7).

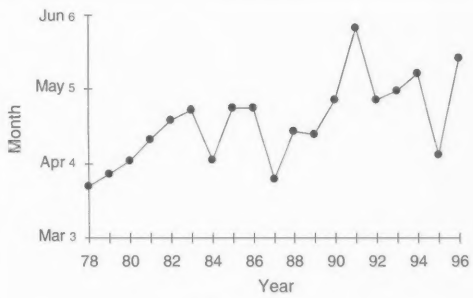

Figure 8

Interannual variation in the peak period (weighted monthly means) of egg production for the Pacific stock of chub mackerel (*Scomber japonicus*), which includes a small portion from the eggs of spotted mackerel (*Scomber australasicus*) (Mori et al.[4]; Kikuchi and Konishi[5]; Ishida and Kikuchi[6]; Zenitani et al.[7]; Kubota et al.[8]).

The estimated FL at age from our growth model, with the use of AIC, fitted well to the observed FL at age (Fig. 6). Mean growth increments I of each year class from age 0 (6 months old) to ages 1–5 (I_{0-i}) were significant and negatively correlated with FL at age 0 (Table 2), indicating that the growth rate of mackerel had changed from year to year for a given year class. This negative correlation indicated that the effects of population density and SST was temporal, and influenced k rather than L_∞. The negative correlation between FL at age 0 and growth increments also suggested that the FL at age of mackerel approximated the asymptotic length. Thus, mackerel growth was best fitted to the modified von Bertalanffy growth model with the temporal environmental effect on k (Table 5).

[5] Kikuchi, H., and Y. Konishi. 1990. Monthly egg production of the Japanese sardine, anchovy, and mackerels off the southern coast of Japan by egg censuses: January, 1987 through December, 1988, 72 p. National Research Institute of Fisheries Science, Tokyo. [In Japanese. Available from National Research Institute of Fisheries Science, 2-12-4 Fukuura, Kanazawa, Yokohama 236-8648, Japan.]

[6] Ishida, M. and H. Kikuchi. 1992. Monthly egg production of the Japanese sardine, anchovy, and mackerels off the southern coast of Japan by egg censuses: January, 1989 through December, 1990, 86 p. National Research Institute of Fisheries Science, Tokyo. [In Japanese. Available from National Research Institute of Fisheries Science, 2-12-4 Fukuura, Kanazawa, Yokohama 236-8648, Japan.].

[7] Zenitani, H., M. Ishida, Y. Konishi, T. Goto, Y. Watanabe, and R. Kimura. 1995. Distributions of eggs and larvae of Japanese sardine, Japanese anchovy, mackerels, round herring, jack mackerel and Japanese common squid in the waters around Japan, 1991 through 1993. Resources Management Research Report Series A-2, 368 p. National Research Institute, Japan Fisheries Agency, Tokyo. [In Japanese. Available from National Research Institute of Fisheries Science, 2-12-4 Fukuura, Kanazawa, Yokohama, 236-8648 Japan.]

[8] Kubota, H., Y. Oozeki, M. Ishida, Y. Konishi, T. Goto, H. Zenitani, and R. Kimura. 1999. Distributions of eggs and larvae of Japanese sardine, Japanese anchovy, mackerels, round herring, jack mackerel and Japanese common squid in the waters around Japan, 1994 through 1996, 352 p. Resources Management Research Report Series A-2., National Research Institute, Japan Fisheries Agency, Tokyo. [In Japanese. Available from National Research Institute of Fisheries Science, 2-12-4 Fukuura, Kanazawa, Yokohama 236-8648, Japan.]

[9] Kuroda, K. 2002. Personal commun. 1-1-3-406, Kasumi, Narashino, Chiba 275-0022, Japan.

The effect of population density on growth of mackerel was higher than the effect of SST (Fig. 7, Table 6). Our result agreed with the results for Japanese sardine (Wada et al., 1995) and Atlantic cod (Sinclair et al., 2002). Particularly, the effect of population density was significant in the late 1980s, which resulted in a remarkable increase in FL at age 0 (Figs. 3 and 7).

The relative size at age 0 was carried over to older ages (Fig. 4), indicating that the cohorts that were small at age 0 could not compensate for this early small size. Iizuka (1974) reported that the trend of growth established at age 0 for chub mackerel was maintained until age 2 for the 1963–73 year classes. Toresen (1990) demonstrated from length data that a trend in rate of growth for a given year class of Norwegian herring was determined at the immature stage and was consistent after maturation. Total length of Hokkaido-Sakhalin herrings (*Clupea pallasii*) at age 5 and older was positively correlated with the length at age 4 (Watanabe et al., 2002). Because fish first mature at age 4, this implied that the trend in total length of each year class was determined by the age at maturity. From these results we hypothesize that the variability in size at age in the Pacific stock of chub mackerel is largely attributable to growth before maturity, especially during the first 6 months after hatching.

Acknowledgments

We would like to thank K. Meguro of Chiba Prefecture Governmental Office and K. Kobayashi of Shizuoka Prefecture Governmental Office for providing insights into chub mackerel's growth and into age determination. We also thank T. Akamine, M. Suda, and N. Yamashita of the National Research Institute of Fisheries Science for advice on the statistical analysis. We also thank Y. Watanabe and C. B. Clarke of the Ocean Research Institute, University of Tokyo, for their constructive comments on this manuscript.

Literature cited

Agnalt, A. -L.
1989. Long-term changes in growth and age at maturity of mackerel, *Scomber scombrus* L., from the North Sea. J. Fish Biol. 35 (suppl. A):305–311.

Brander, K. M.
1995. The effect of temperature on growth of Atlantic cod (*Gadus morhua* L.). ICES J. Mar. Sci. 52:1–10.

Dutil, J. -D., M. Castonguay, D. Gilbert, and D. Gascon.
1999. Growth, condition, and environmental relationships in Atlantic cod (*Gadus morhua*) the northern Gulf of St. Lawrence and implications for management strategies in the Northwest Atlantic. Can. J. Fish. Aquat. Sci. 56: 1818–1831.

Haddon, M.
2001. Modelling and quantitative methods in fisheries, 406 p. Chapman&Hall/CRC, New York, NY.

Hirai, M.
1991. Fisheries oceanographic study on purse-seine fishing-grounds for chub mackerel in the Sanriku coastal waters. Bull. Tohoku Natl. Fish. Res. Inst. 53:59–147. [In Japanese.]

Hirai, M., and I. Yasuda.
1988. Interannual variability of the temperature field at 100 m depth near the east coast of Japan. Bull. Otsuchi Ocean Res. Center, Univ. Tokyo. 14:184–186.

Hiyama, Y , H. Nishida, and T. Goto.
1995. Interannual fluctuations in recruitment and growth of the sardine, *Sardinops melanostictus*, in the Sea of Japan and adjacent waters. Res. Popul. Ecol. 37(2):177–183.

Honma, M., Y. Sato, and S. Usami.
1987. Estimation of the population size of the Pacific mackerel by the cohort analysis. Bull. Tokai Reg. Fish. Res. Lab. 121:1–11. [In Japanese.]

Iizuka, K.
1974. The ecology of young mackerel in the north-eastern sea of Japan IV. Estimation of the population size of the 0-age group and the tendencies of growth patterns on 0, I, and II age groups. Bull. Tohoku Reg. Fish. Res. Lab. 34: 1–16. [In Japanese.]

Jobling, M.
1988. A review of the physiological and nutritional energetics of Cod, *Gadus morpha* L., with particular reference to growth under farmed conditions. Aquaculture, 70:1–19.

Kawasaki, T.
1966. Structure of the Pacific population of the mackerel. Bull. Tokai Reg. Fish. Res. Lab. 47:1–34. [In Japanese.]

Kidokoro, H.
2001. Fluctuations in body size and abundance of Japanese common squid (*Todarodes pacificus*) in the Sea of Japan. GLOBEC report 15:42.

Kishida, T.
1990. Relationship between growth and population density of Japanese Spanish mackerel in the central and western waters of the Seto Inland Sea. Bull. Nansei Natl. Fish. Res. Inst. 23:35–41. [In Japanese.]

Mace, P. M., and M. O. Sissenwine.
1993. How much spawning per recruit is enough? Can. Spec. Publ. Fish. Aquat. Sci. 120:101–118

Moores, J. A., and G. H. Winters.
1981. Growth patterns in a Newfoundland Atlantic herring (*Clupea harengus harengus*) stock. Can. J. Fish. Aquat. Sci. 39:454–461.

Moyle, P. B., and J. J. Cech Jr.
2002. Fishes: An introduction to ichthyology, 4th ed., 612 p. Prentice Hall, Englewood Cliffs, NJ.

Murayama,T., I. Mitani, and I. Aoki.
1995. Estimation of the spawning period of the Pacific mackerel *Scomber japonicus* based on the changes in gonad index and the ovarian histology. Bull. Jpn. Soc. Fish. Oceanogr. 59:11–17. [In Japanese.]

Neja, Z.
1995. The stock size and changes in the growth rate of the northwest Atlantic mackerel (*Scomber scombrus* L.) in 1971–1983. Acta Ichthyologica et Piscatoria 25:113–121.

Odate, K.
1994. Zooplankton biomass and its long-term variation in the western north Pacific ocean, Tohoku sea area, Japan. Bull. Tohoku Natl. Fish. Res. Inst. 56, 115–173. [In Japanese.]

Odate, S.
1961. Study on the larvae of the fishes in the north-eastern sea area along the Pacific coast of Japan. Part 1. Mackerel, *Pneumatophorus japonicus* (Houttuyn). Bull. Tohoku Reg. Fish. Res. Lab. 19:98–108. [In Japanese.]

Otterson, G., K. Helle, and B. Bogstad.
2002. Do abiotic mechanisms determine interannual vari-

ability in length-at-age of juvenile Arcto-Norwegian cod? Can. J. Fish. Aquat. Sci. 59:57–65.

Overholtz, W. J.
1989. Density-dependent growth in the northwest Atlantic stock of Atlantic mackerel (*Scomber scombrus*). J. Northw. Atl. Fish. Sci. 9:115–121.

Pauly, D.
1987. Application of information on age and growth of fish to fishery management. *In* Age and growth of fish (R. C. Summerfelt and G. E. Hall, eds.) p.495–506. Iowa State Univ Press, Ames, IA.

Pyper, B. J., and R. M. Peterman.
1998. Comparison of methods to account for autocorrelation in correlation analyses of fish data. Can. J. Fish. Aquat. Sci. 55:2127–2140.

Rätz, H. -J., M. Stein, and J. Lloret.
1999. Variation in growth and recruitment of Atlantic cod (*Gadus morhua*) off Greenland during the second half of the twentieth century. J. Northw. Atl. Fish. Sci. 25:161–170.

Schaefer, K. M.
1986. Lethal temperature and the effect of temperature change on volitional swimming speeds of chub mackerel, *Scomber japonicus*. Copeia 1986:37–44.

Sinclair, A. F., D. P. Swain, and J. M. Hanson.
2002. Disentangling the effects of size-selective mortality, density, and temperature on length-at-age. Can. J. Fish. Aquat. Sci. 59:372:382.

Toresen, R.
1990. Long-term changes in growth of Norwegian spring-spawning herring. J. Cons. Int. Explor. Mer 47:48–56.

Usami, S.
1973. Ecological studies of life pattern of the Japanese mackerel, *Scomber japonicus* Houttuyn: on the adult of the Pacific subpopulation. Bull. Tokai Reg. Fish. Res. Lab. 76: 71–178. [In Japanese.]

Wada, T., Y. Matsubara, Y. Matsumiya, and N. Koizumi.
1995. Influence of environment on stock fluctuations of Japanese sardine, *Sardinops melanostictus*. Can. Spec. Publ. Fish. Aquat. Sci. 121:387–394.

Watanabe, C., and H. Nishida.
2002. Development of assessment techniques for pelagic fish stocks: applications of daily egg production method and pelagic trawl in the northwestern Pacific ocean. Fisheries Science. 68:97–100.

Watanabe, C., T. Hanai, K. Meguro, R. Ogino, Y. Kubota, and R. Kimura.
1999. Spawning biomass estimates of chub mackerel *Scomber japonicus* of Pacific subpopulation off central Japan by a daily egg production method. Nippon Suisan Gakkaishi 65(4):695–702. [In Japanese.]

Watanabe, T.
1970. Morphology and ecology of early stages of life in Japanese common mackerel, *Scomber japonicus* Houttuyn, with special reference to fluctuation of population. Bull. Tokai Reg. Fish. Res. Lab. 62:1–283. [In Japanese.]

Watanabe, Y., Y. Hiyama, C. Watanabe, and S. Takayanagi.
2002. Inter-decadal fluctuations in length-at-age of Hokkaido-Sakhalin herring and Japanese sardine in the Sea of Japan. PICES Scientific Report 20:63–67.

Yatsu, A., and H. Kidokoro.
2002. Coherent low frequency variability in biomass and in body size of Japanese common squid, *Tadorodes padificus*, during 1964–2002, 89 p. Abstracts of PICES 11th annual meeting.

Latitudinal and seasonal egg-size variation of the anchoveta (*Engraulis ringens*) off the Chilean coast

Alejandra Llanos-Rivera

Leonardo R. Castro

Laboratorio de Oceanografía Pesquera y Ecología Larval
Departamento de Oceanografía
Universidad de Concepción
Casilla 160-C, Concepción, Chile

E-mail address (for L. R. Castro, contact author): lecastro@udec.cl

The anchoveta *Engraulis ringens* is widely distributed along the eastern South Pacific (from 4° to 42°S; Serra et al., 1979) and it has also supported one of the largest fisheries of the world over the last four decades. However, there are few interpopulation comparisons for either the adult or the younger stages. Reproductive traits, such as fecundity or spawning season length, are known to vary with latitude for some fish species (Blaxter and Hunter, 1982; Conover, 1990; Fleming and Gross, 1990; Castro and Cowen, 1991), and latitudinal trends for some early life history traits, such as egg size and larval growth rates, have been reported for others clupeiforms and other fishes (Blaxter and Hempel, 1963; Ciechomski, 1973; Imai and Tanaka, 1987, Conover 1990, Houde 1989). However, there is no published information on potential latitudinal trends during the adult or the early life history of the anchoveta, even though this type of information may help in understanding recruitment variability, especially during recurring large scale events (such as El Niño or La Niña) that affect the entire species range.

Egg volume has been found to vary widely among species and among populations of the same species. For fish that broadcast planktonic or benthic eggs, egg size often varies as the spawning season progresses (Bagenal, 1971), and the magnitude of this variation depends on the species. For instance, the egg volume of the pelagic spawners *Engraulis anchoita* and *Solea solea* decreases 23% and 38%, respectively, throughout the spawning season (Ciechomski, 1973; Rijnsdorp and Vingerhoed, 1994). Maternal and environmental factors may also affect egg volume (Bagenal, 1971; Thresher, 1984; Rijnsdorp and Vingerhoed, 1994; Chambers and Waiwood, 1996; Chambers, 1997). Variations in size of the spawning females and shifts in energy allocation from reproduction to growth as the spawning season progresses may influence the egg volume (Wootton, 1990). Alternatively, seasonal variations in photoperiod, seawater temperature, and food supply during the spawning season may affect the reproductive output (Wootton, 1990).

Scarce information exists on the variability of egg sizes for fishes in the Humboldt Current. In this extensive area, the heavily exploited anchoveta *Engraulis ringens* is the dominant small pelagic species. Throughout this range, three major stocks are recognized: the northern stock off northern Peru (the largest); the central stock off southern Peru and northern Chile (mid-size), and the southern stock off central Chile (the smallest of the three). For the entire distribution of anchoveta, the main spawning season is from July through September, but may extend to December or January (Cubillos et al., 1999). The wide latitudinal range and prolonged spawning period suggest the possibility of egg-size variation, as observed in other clupeifoms (Blaxter and Hempel, 1963; Ciechomski, 1973; Imai and Tanaka, 1987). Egg size correlates with larval characteristics such as larval length at hatching, the time to first feeding, and time before irreversible starvation (Shirota, 1970; Ware, 1975; Hunter, 1981; Marteinsdottir and Able, 1992). To explore whether differences in potential early-life-stage survival would exist among populations and (or seasons), the objective of our research was to determine whether variations in some early-life-stage characteristics occur among populations of *E. ringens* along its distribution. In this study, we 1) report changes in egg size throughout the anchoveta spawning season as well as for the peak months of the spawning season, 2) evaluate whether egg size varies with respect to latitude, and 3) evaluate whether differences in larval length and yolksac volume occur in hatching larvae from the two major spawning stocks along Chile (central and southern stocks).

Materials and methods

We collected anchovy eggs from four locations along the coastal zone (<20 nmi offshore) off northern and central Chile during the austral winter and spring spawning seasons 1995–97 (Fig. 1). Eggs were collected with a Calvet net (150 μm mesh) in Iquique and Antofagasta (northern Chile), with a standard conical net (330 μm) in Valparaíso and with either a Tucker trawl (250 μm mesh) or a standard bongo net (500 μm) in Talcahuano. The shorter axis of the anchovy eggs varied from 0.563 mm (SD=0.032) in Iquique to 0.657 mm (SD=0.027) in Talcahuano. Consequently, egg extrusion from the nets was ruled out as a potential source of variation in our collections. Egg size (length and width) was measured with an ocular micrometer on a dissecting microscope at 25× magnification. Upon collection, all eggs were preserved in 5% buffered formalin. Previous studies on anchoveta eggs have reported no egg size shrinkage or shape changes with formalin preservation (Fisher, 1958). Similarly, reports on this species and other anchovies show that egg-size variations throughout their development do not occur (*Engraulis ringens*, Fisher, 1958; *Engraulis japonica*, Imai and Tanaka, 1987). We tested this hypothesis using eggs that we collected in northern Chile and found no size differences among different egg stages (ANOVA, n=535, P=0.1176).

Manuscript approved for publication 12 August 2003 by Scientific Editor.

Manuscript received 20 October 2003 at NMFS Scientific Publications Office.

Fish. Bull. 102:207–212 (2004).

Egg volume was calculated considering the anchovy egg as an ellipsoid ($V=4\pi \times a \times b \times c/3$, where a, b and c are the ellipse radii).

Statistical analyses included one-way ANOVA tests for volume differences among eggs spawned in three subperiods during the spawning season (initial, middle, and final) in Valparaíso and Talcahuano (1996–97). We did not have samples from the start of the spawning season in 1996 for Valparaíso; thus, we used samples collected in late June 1995 for this subperiod (Table 1). Variations in the egg-size frequency distributions between contiguous subperiods were also tested with nonparametric tests (Kolmogorov-Smirnov test). Changes in egg volume with latitude were tested by using egg sizes measured at four localities (20°, 23°, 33°, and 36°S) during the peak spawning months (initial subperiod). The same statistical tests were used as in the previous objective (ANOVA, Kolmogorov-Smirnov test).

To evaluate the relationship between egg size and larval length at hatching, live eggs from ichthyoplankton samples from the field in August 2000 were transported to the laboratory and reared at the normal mixed-layer temperature off Antofagasta and Talcahuano (15°C and 12°C, respectively) (Escribano et al., 1995; Castro et al., 2000). A subsample of the incubated egg batch was preserved in 5% formalin and measured at the beginning of the experiments. The rest of the eggs were placed in 1-L flasks and incubated until hatching under 12h/12h photoperiod. This procedure was repeated twice (4 days apart) in each zone. From each rearing experiment, 30 just-hatched larvae (max. 30 min from hatch) were anesthetized and measured (notochord length) under a dissecting microscope with the aid of an ocular micrometer. Additionally, yolksac sizes of recently hatched larvae were measured and volume estimated as one half of an ellipsoid by using the algorithms given above.

Results

A total of 7196 anchovy eggs were measured. The egg size tended to decrease as the spawning season progressed (Fig. 2). From late June through January the mean volume decreased by about 20% in Valparaíso and by about 10% in Talcahuano (ANOVA, $P<0.05$)(Table 1). The size-frequency distribution between consecutive subperiods (initial, middle, and final) also differed in both areas (Kolmogorov-Smirnov test, $P<0.05$). The mean size of the eggs in Valparaíso was smaller than in Talcahuano during all subperiods (Table 1), and the largest difference between areas was at the end of the spawning season (15%).

During the spawning peak (spawning commencement), when the eggs were larger, the mean anchoveta egg size increased with latitude (ANOVA, $P<0.01$; Fig. 3). At Iquique (20°S), the mean egg volume was 21% smaller than at Antofagasta (23°S), 49% smaller than at Valparaíso (33°S), and 56% smaller than the eggs from Talcahuano (36°S), the southernmost location (Table 2). The egg-size frequency distribution differed between adjacent areas (Kolmogorov-Smirnov test, $P<0.05$). Interestingly, the smallest egg sizes measured in Iquique (<0.19 mm^3) did not occur in Talcahuano. Similarly, the largest sizes determined in Talcahuano (>0.30 mm^3) did not occur in Iquique, at the lowest latitude.

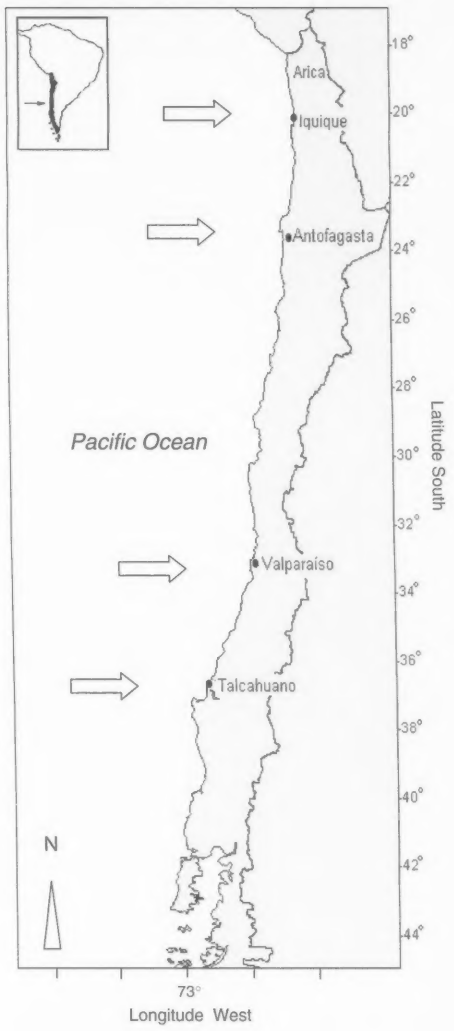

Figure 1

Areas where anchoveta eggs were collected to determine egg-size variations along the Chilean coast. Arrows show the locations depicted in Table 2.

Larval length at hatching determined in the rearing experiments at normal field temperatures was greater for the southernmost population (Talcahuano) (Table 3). The mean larval size for the southern location (2.70 mm notochord length) was 8.2% greater than the larvae hatched from eggs collected at the northern experimental location (Antofagasta, 2.50 mm). Furthermore, the yolksac volume in the recently hatched larvae in Talcahuano (0.130 mm^3)

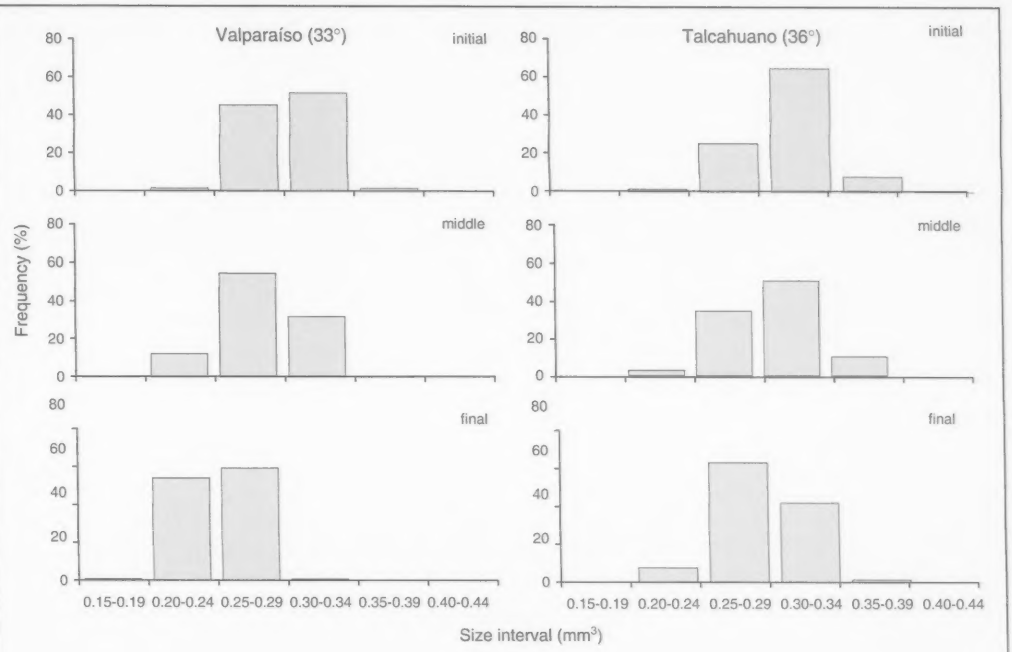

Figure 2

Seasonal variation in egg size of the anchoveta (*E. ringens*) off Valparaíso and Talcahuano. *Y*-axis is frequency over the total number of eggs measured at each locality. Initial, middle, and final are subperiods within the spawning season (see Table 2).

Table 1

Mean volume of *Engraulis ringens* eggs at the beginning, middle, and end of the spawning season off Valparaíso and Talcahuano, central Chile. SD = standard deviations. n = number of eggs measured.

	Valparaíso			Talcahuano		
	June 1995	October 1996	December 1996	August 1996	October 1996	January 1997
Volume (mm^3)	0.298	0.281	0.247	0.312	0.308	0.286
SD	0.026	0.029	0.022	0.030	0.034	0.029
n	62	759	630	1833	718	1099

was much larger (33% larger) than the yolk volume of the larvae hatched in Antofagasta (0.098 mm^3).

Discussion

The results of this study identified several trends that are related to egg-size variation. First, egg size tends to decrease with the progression of the spawning season. Second, egg size increases with latitude during the peak spawning period. Third, larval size at hatching is smaller in the northern latitude populations. Fourth, the yolk sac of recently hatched larvae is much larger than expected (based on the larval size at hatching) in the southern population.

A number of hypotheses have been proposed to explain egg-size variations in fish that spawn at multiple times as the reproductive season progresses. It has been proposed that in clupeiforms, the decrease in egg size may result from maternal reduction of energy reserves over the spawning season, a switch in the stored energy from reproduction to growth, seasonal changes in the age structure of the spawning population, or changes during ovogenesis that are correlated with temperature (Blaxter and Hunter, 1982; Chambers, 1997, for a recent review). In the anchoveta *E. ringens*, published data suggest that some

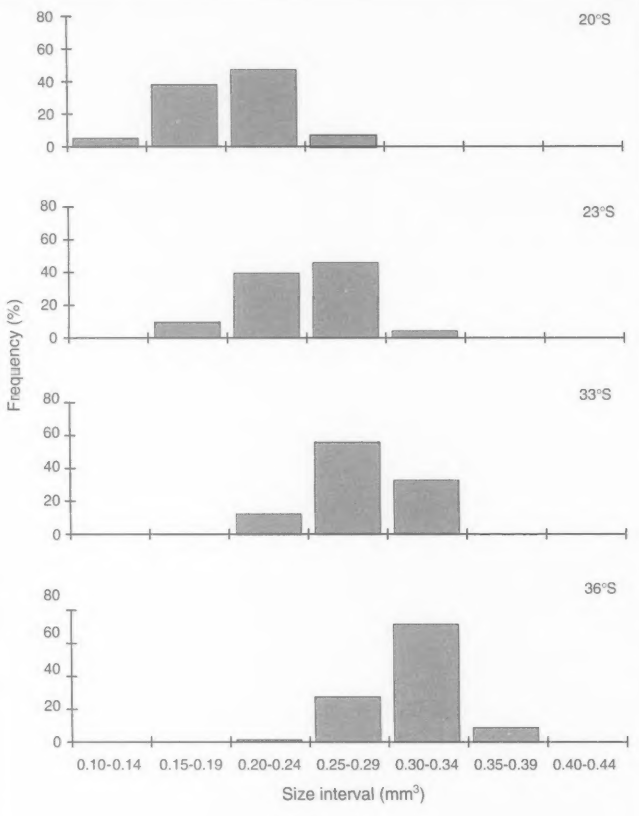

Figure 3

Latitudinal variation in egg size of the anchoveta (*E. ringens*) along northern and central Chile during the peak months of the spawning season. *Y*-axis is frequency over the total number of eggs measured at each locality.

of these factors co-occur. For instance, changes in growth rates for yearly cohorts during the spawning season (low at the beginning, fast at the end) have been documented for the southernmost population (Cubillos et al., 2001). Alternatively, variations in the population age structure during the spawning season have also been reported as the 1.5 year-old new recruits begin to spawn in early summer (late December–January, Cubillos et al., 1999, 2001). Changes in environmental factors affecting the spawning adults also correlate with the egg-size variations. The photoperiod and nearsurface temperatures increase as the spawning season progresses from mid-winter to late spring.

Larger egg size at the beginning of the spawning season in winter may be advantageous for these offspring because the chances of survival increase with the larger sizes of the hatching larvae. According to Cushing (1967), larger size larvae should be favored over smaller larvae in seasons with variable environmental conditions. In the Talcahuano area, strong fluctuations in the hydrographic regime occur during winter as strong north wind storms alternate with short periods of south winds, and also because of the increased river flow to the coastal zone (Castro et al., 2000). Larval food, although variable, seems to be sufficient to support most of the larval growth demands for larger exogenous feeding larvae during winter (Hernandez and Castro, 2000). For recently hatched larvae, however, the picture might be slightly different because, in addition to food supply variability, the strong turbulent environmental conditions may jeopardize first feeding success. In these highly variable areas, therefore, larger larval size at hatching and larger yolk reserves may be even more important than in other less hydrographically variable areas and seasons.

A remarkable increase in egg size at the peak spawning season occurred with respect to latitude. Egg from the northernmost (20°S) latitude were at a maximum 55% larger than eggs from the southernmost (36°S) latitude. Latitudinal variations in egg size have been previously reported for other anchovies (i.e. *Engraulis anchoita*; Ciechomski, 1973). However, egg-size variations for fishes

Table 2

Width, length, and volume of anchoveta eggs collected at different latitudes along the Chilean coast during the peak months of the spawning season. SD = standard deviations. n = number of eggs measured.

	Width (mm)		Length (mm)		Volume (mm^3)		
Latitude and area	mean	SD	mean	SD	mean	SD	n
20° Iquique	0.563	0.032	1.201	0.076	0.201	0.031	1670
23° Antofagasta	0.597	0.030	1.293	0.083	0.243	0.034	425
33° Valparaíso	0.643	0.023	1.373	0.064	0.298	0.026	62
36° Talcahuano	0.657	0.027	1.377	0.063	0.312	0.030	1833

Table 3

Morphological characteristics of recently hatched *Engraulis ringens* larvae from rearing experiments at normal field temperatures in Antofagasta (15°C) and Talcahuano (12°C). SD = standard deviations. N = number of eggs measured. Exp. = experiment.

		Egg volume (mm^3)		Larval length at hatching (mm)		Yolksac size at hatching (mm^3)	
		Exp. 1	Exp. 2	Exp. 1	Exp. 2	Exp. 1	Exp. 2
Antofagasta							
15°C	Mean	0.264	0.260	2.49	2.50	0.099	0.096
	SD	(0.023)	(0.023)	(0.170)	(0.104)	(0.012)	(0.012)
	n	358	325	30	30	30	30
Talcahuano							
12°C	Mean	0.302	0.292	2.71	2.69	0.126	0.134
	SD	(0.023)	(0.026)	(0.111)	(0.103)	(0.016)	(0.017)
	n	254	66	30	30	30	30

are not necessarily always associated with latitude (i.e. north Atlantic herring stocks) because local environmental conditions that trigger spawning (i.e. specific temperature or others) may have a stronger effect in some species (Chambers, 1997). Because of the extremely wide distribution range of the anchoveta (4–42°S) and its residence along an almost linear coast oriented exactly north–south, we proposed that any potential differences in egg size due to specific local conditions is probably over-driven by the larger scale changes in environmental conditions associated with latitude.

The strong latitudinal gradient in egg size of the anchoveta may be an adaptive measure if different egg sizes are favored at different latitudes or if there is a correlation between egg size and adult life history traits that maximize net reproductive output. Unfortunately, an analysis of the anchoveta in which fecundity, age of first reproduction, longevity, or other adult traits are compared in relation to latitude has not yet been carried out. The timing and length of the spawning season seem to be similar for the northern (Iquique, 20°S) and southern (Talcahuano, 36°S) stocks along Chile, despite the different temperatures at which anchoveta spawn (Castro et al., 2001). The decrease in egg size coincides with known temperature effects on physiological rates (Houde, 1989) and on ecological factors related to the need of anchoveta at early life stages to remain in nearshore environments (Bakun, 1996). At lower latitudes, the sea temperature is higher and the seaward surface Ekman transport is stronger and therefore eggs and larvae in such conditions would likely develop rapidly. Alternatively, anchovy egg and larvae at higher latitudes are retained nearshore in winter (because the Ekman transport is negative, Castro et al., 2000) but are exposed to lower temperatures and to strong turbulence that may not facilitate the first feeding of recently hatched larvae and subsequent rapid larval development. Larger eggs, larger larvae at hatching, and more energy reserves may be the favored early life history strategy in southern populations. How the latitudinal variations in environmental characteristics affect the rest of the life history traits of the different populations of *Engraulis ringens*, one of the most important fish species in the world in terms of catches, remains to be assessed.

Acknowledgments

We acknowledge help from R. Escribano (U. Antofagasta), G. Claramunt (U. Arturo Prat), and F. Balbontín (U. of Valparaíso) who facilitated ichthyoplankton collections.

H. Moyano (U. of Concepcion) allowed the use of his laboratory and optical material. This study was financed by the project FONDECYT 1990470 to L. R. Castro. E. Tarifeño, and R. Escribano. Alejandra Llanos-Rivera was also partially supported by the Graduate School of the Universidad de Concepcion.

Literature cited

Bagenal, T.B.
1971. The interrelation of the size of fish eggs, the date of spawning and the production cycle. J. Fish Biol. 3: 207–219

Bakun, A.
1996. Patterns in the ocean. Ocean processes and marine population dynamics, 233 p. California Sea Grant College Publ., NOAA in Cooperation with the Centro de Investigaciones Biologicas del Noreste, La Paz, BCS, Mexico.

Blaxter, J., and G. Hempel.
1963. The influence of egg size on herring larvae (*Clupea harengus* L.). J. Con. Perm. Int. Explor. Mer 28: 211–240.

Blaxter, J. H. S., and J. R. Hunter
1982. The biology of clupeoid fishes. Adv. Mar. Biol. 20: 3–194.

Castro, L. R., and R. K. Cowen
1991. Environmental factors affecting the early life history of bay anchovy (*Anchoa mitchilli*) in Great South Bay, New York. Mar. Ecol. Prog. Ser. 76:235–247.

Castro, L. R., G. R Salinas, and E. H. Hernández.
2000. Environmental influences on winter spawning of the anchoveta, *Engraulis ringens*, off Central Chile. Mar. Ecol. Prog. Ser. 197:247–258.

Castro, L. R., A. Llanos, J. L. Blanco, E. Tarifeño, R. Escribano, and M. Landaeta.
2001. Latitudinal variations in spawning habitat characteristics: influence on the early life history traits of the anchoveta, *Engraulis ringens*, off northern and central Chile. GLOBEC Report 16:42–45.

Chambers, R. C.
1997. Environmental influences on egg and propagule sizes in marine fishes. *In* Early life history and recruitment in fish populations (R. C. Chambers and E. A. Trippel, eds.), p. 63–102. Chapman & Hall, London.

Chambers, R. C., and K. Waiwood.
1996. Maternal and seasonal differences in egg sizes and spawning characteristics of captive Atlantic cod, *Gadus morhua*. Can. J. Fish. Aquat. Sci. 53:1986–2003.

Ciechomski, J. de
1973. The size of the eggs of the Argentine anchovy, *Engraulis anchoita* (Hubbs & Marini) in relation to the season of the year and the area of spawning. J. Fish Biol. 5:393–398.

Conover, D.
1990. The relation between capacity for growth and length of the growing season: evidence for and implications of countergradient variation. Trans. Am. Soc. 119:416–430.

Cubillos, L. A., D. Arcos, D. Bucarey, and M. Canales.
2001. Seasonal growth of small pelagic fish off Talcahuano, Chile (37°S, 73°W): a consequence of their reproductive strategy to seasonal upwelling? Aquat. Living Resour. 14:1–10.

Cubillos, L. A., M. Canales, D. Bucarey, A. Rojas, and R. Alarcón.
1999. Reproductive period and mean size at first maturity for *Strangomera bentincki* and *Engraulis ringens* from 1993 to 1997, off central-southern Chile. Invest. Mar. 27:73–85. [In Spanish.]

Cushing, D. H.
1967. The grouping of herring populations. J. Mar. Biol. Assoc. U.K. 47:193–208

Escribano, R., L. Rodriguez, and C. Irribarren
1995. Temporal variability of sea temperature in bay of Antofagasta, Northern Chile (1991–1995). Estud. Oceanol. 14:39–47. [In Spanish.]

Fisher, W.
1958. Huevos, crías y primeras prelarvas de la anchoveta *Engraulis ringens* Jenyns. Rev. Biol. Mar. 8 (1-2-3):111–124.

Fleming, I. A., and M. Gross.
1990. Latitudinal clines: a trade-off between egg number and size in pacific salmon. Ecology 71(1):1–11.

Hernández, E. H., and L. R. Castro.
2000. Larval growth of the anchoveta, *Engraulis ringens*, during the winter spawning season off central Chile. Fish. Bull. 98:704–710.

Houde, E. D.
1989. Comparative growth, mortality and energetics of marine fish larvae: temperature and implied latitudinal effects. Fish. Bull. 87:471–495.

Hunter, J. R.
1981. Feeding ecology and predation of marine fish larvae. *In* Marine fish larvae (R. Lasker, ed.), p. 34–77. Univ. Washington Press, Seattle, WA.

Imai, Ch., and S. Tanaka.
1987. Effect of sea water temperature on egg size of Japanese anchovy. Nippon Suisan Gakkaishi 53(12): 2169–2178.

Marteinsdottir, G., and K. Able.
1992. Influence of egg size on embryos and larvae of *Fundulus heteroclitus* (L.). J. Fish Biol. 41:883–896.

Rijnsdorp, A., and B. Vingerhoed.
1994. The ecological significance of geographical and seasonal differences in egg size in sole *Solea solea* (L.). Neth. J. Sea Res. 32(3/4):255–270.

Serra J., O. Rojas, M. Aguayo, F. Inostroza, and J. Cañon.
1979. Anchoveta (*Engraulis ringens*). *In* Estado actual de las principales pesquerías nacionales. Bases para un desarrollo pesquero, 36 p. Corporación de fomento de la producción. Instituto de Fomento Pesquero. Santiago, Chile.

Shirota, A.
1970. Studies on the mouth size of fish in the larval and fry stages. Bull. Jap. Soc. Sci. Fish. 36:353–368.

Thresher, R. E.
1984. Reproduction in reef fishes, 399 p. T.F.H. Publications, Inc. Ltd.,The British Crown Colony of Hong Kong.

Ware, D. M.
1975. Relation between egg size, growth, and natural mortality of larval fish. J. Fish. Res. Board Can. 32: 2503–2512.

Wootton, R.
1990. Ecology of teleost fishes, 404 p. Chapman & Hall. London.

Molecular methods for the genetic identification of salmonid prey from Pacific harbor seal (*Phoca vitulina richardsi*) scat

Maureen Purcell

Greg Mackey

Eric LaHood

Conservation Biology Molecular Genetics Laboratory
Northwest Fisheries Science Center
National Marine Fisheries Service, NOAA
2725 Montlake Blvd. E.
Seattle, Washington 98112-2097

Harriet Huber

National Marine Mammal Laboratory
Alaska Fisheries Science Center
National Marine Fisheries Service, NOAA
7600 Sand Point Way NE
Seattle, Washington 98115

Linda Park

Conservation Biology Molecular Genetics Laboratory
Northwest Fisheries Science Center
National Marine Fisheries Service, NOAA
2725 Montlake Blvd. E.
Seattle, Washington 98112-2097

E-mail address (for L. Park, contact author): linda.park@noaa.gov

Twenty-six stocks of Pacific salmon and trout (*Oncorhynchus* spp.), representing evolutionary significant units (ESU), are listed as threatened or endangered under the Endangered Species Act (ESA) and six more stocks are currently being evaluated for listing.[1] The ecological and economic consequences of these listings are large; therefore considerable effort has been made to understand and respond to these declining populations. Until recently, Pacific harbor seals (*Phoca vitulina richardsi*) on the west coast increased an average of 5% to 7% per year as a result of the Marine Mammal Protection Act of 1972 (Brown and Kohlman[2]). Pacific salmon are seasonally important prey for harbor seals (Roffe and Mate, 1984; Olesiuk, 1993); therefore quantifying and understanding the interaction between these two protected species is important for biologically sound management strategies. Because some Pacific salmonid species in a given area may be threatened or endangered, while others are relatively abundant, it is important to distinguish the species of salmonid upon which the harbor seals are preying. This study takes the first step in understanding these interactions by using molecular genetic tools for species-level identification of salmonid skeletal remains recovered from Pacific harbor seal scats.

Most studies of harbor seal food habits rely on morphological identification of indigestible parts (e.g. otoliths and bones) from scat. Otoliths can be used to identify fish species (Ochoa-Acuna and Francis, 1995) but are not always present in scats, which can result in an underestimate of the number of species and the number of fish consumed (Harvey, 1989). Skeletal remains in scat are much more common and generally bones can be identified to the species level (Cottrell et al., 1996). Morphological identification is possible to the family level only with Pacific salmonid bones; however, genetic markers have the ability to discriminate between species, and the feasibility of extracting DNA from bones has been clearly demonstrated (Hochmeister et al., 1991).

Mitochondrial DNA (mtDNA) has been widely employed in systematic studies (reviewed by Avise, 1994) making it ideal for animal species identification. In this study, we explored three regions of the mitochondrial genome that have been previously characterized in Pacific salmonids (Shedlock et al., 1992; Domanico and Phillips, 1995; Parker and Kornfield, 1996). DNA sequencing of these regions provided an unambiguous way to determine species identity. Because high throughput sequencing can be prohibitively expensive for laboratories with limited facilities, restriction fragment length polymorphism (RFLP) analysis was also explored as an alternative for species identification. A previous study had established a species-specific polymerase chain reaction (PCR) test for Pacific Northwest salmon and coastal trout species (McKay et al., 1997). The PCR test is based on the initial amplification of an approximately 1000-bp fragment of the nuclear growth hormone 2 gene. The degraded state of the DNA isolated from bones recovered from scat has generally limited successful PCR to amplicons of 300 bp or less (data not shown). Furthermore, the amount of DNA isolated from bone fragments can be quite small; mtDNA is present in higher copy number per cell than is nuclear DNA. Thus, we considered mtDNA it to be a more

[1] http://www.nwr.noaa.gov/1salmon/salmesa/specprof.htm. [Accessed June 17, 2003.]

[2] Brown, R. F., and S. G. Kohlman. 1998. Trends in abundance and current status of the Pacific harbor seal (*Phoca vitulina richardsi*) in Oregon: 1977–1998. ODFW (Oregon Department of Fish and Wildlife) Wildlife Diversity Program Technical Report, 98-6-01, 16 p. [Available from ODFW, 7118 NE Vandenberg Ave. Corvallis, OR 97333.]

Manuscript approved for publication 9 October 2003 by Scientific Editor.

Manuscript received 20 October 2003 at NMFS Scientific Publications Office.

Fish. Bull. 102:213–220 (2004).

appropriate target for our assay. We chose to explore smaller regions of the mitochondrial genome, including the d-loop (Shedlock et al., 1992), a portion of the 16s ribosomal gene (Parker and Kornfield, 1996), and a region spanning the cytochrome oxidase III, t-RNA glycine, and ND3 genes (hereafter, referred to as COIII/ND3) (Domanico and Phillips, 1995). Significant interspecific variation but not intraspecific variation was observed in the COIII/ND3 region among salmonid species in previous studies, making it a particularly good candidate region for the development of diagnostic markers (Domanico and Phillips, 1995).

In the first phase of the study, we developed and validated the genetic tools for species identification by using frozen or ethanol-preserved tissues collected from known species and populations. In the second phase, we applied these tools to the identification of bone remains from harbor seal scats collected at the Umpqua River (Oregon). A number of Pacific salmonid species are present in the Umpqua River but of particular concern were the sea-run cutthroat (*Oncorhynchus clarki*) that were listed as endangered under the ESA during 1996 (Johnson et al., 1999). Here we report the method associated with these two phases of the project. The salmonid bones that were identified genetically were incorporated into a larger study of the harbor seal diet and are reported in a companion paper (Orr et al., 2004).

Materials and methods

Salmonid tissue samples of known species have been collected over the past decade by geneticists from the Conservation Biology Molecular Genetics Laboratory (NOAA/NMFS/NWFSC) or generously donated by others (see "Acknowledgments" section) and maintained either frozen at –80°C or preserved in 95% ethanol. Reference populations were chosen to represent the geographic range of chinook salmon (*O. tshawytscha*), coho salmon (*O. kisutch*), sockeye salmon (*O. nerka*), pink salmon (*O. gorbuscha*), chum salmon (*O. keta*), steelhead (*O. mykiss*), coastal cutthroat trout (*O. clarki clarki*), and Yellowstone cutthroat trout (*O. clarki bouvieri*) (collection information is listed in Table 1). Tissues were extracted with either a standard phenol and chloroform extraction (Sambrook et al., 1989) or by using the DNAeasy 96-well tissue kit (Qiagen, Valencia, CA), following the manufacturer's instruction for tissue preparations. PCR primers were either taken directly from the published studies or designed from the reported sequences (Table 2). All primers were cycled with 2.5 mM $MgCl_2$, 0.8 mM dNTPs, 0.04 μM primers, 0.25 units of *Taq* DNA polymerase (Promega, Madison, WI), 20–40 ng of DNA, and cresol red loading buffer (final concentration 2% sucrose and 0.005% cresol red) for 35–45 cycles of 94°C for 45 seconds, 55°C for 45 seconds, and 72°C for 1 minute.

A single individual of each salmonid species listed in Table 1 was sequenced for both the 16s rRNA and COIII/ND3 regions. For DNA sequencing, the PCR products were purified with an Ultrafree MC column (Millipore, Beverly, MA) and resuspended in 20 μL of sterile water. The purified product (1–10 μL depending on band intensity) was manually sequenced by using the USB ThermoSequenase cycle sequencing kit (Cleveland, OH), following the manufacturer's instructions. MACDNASIS (Miraibio Inc., Alameda, CA) and SEQUENCHER (Gene Codes Corp., Ann Arbor, MI) were used for sequence alignment and identification of diagnostic restriction enzyme cut sites.

RFLP analysis of the unpurified COIII/ND3 PCR product was performed in the presence of a cresol red loading buffer. Restriction digests were incubated for 6 to 12 hours at 37°C for *Dpn* II, *Sau* 96I, *Fok* I, *Ase* I, at 50° for *Apo* I, and at 60°C for *Bst* NI with the supplied buffers (NEB, Beverly, MA) and 1–5 units of enzyme. Restricted products were electrophoresed in a 4% 3:1 high-resolution and medium-resolution agarose gel (Continental Laboratory Products, San Diego, CA). DNA bands on the agarose gels were visualized with SYBR Gold, following the manufacturer's instructions (Molecular Probes, Eugene, OR).

Personnel from the National Marine Mammal Laboratory (NMML) collected and processed harbor seal scat samples from the Umpqua River (Orr et al., 2004). NMML researchers identified bone remains to either family or species level by using morphological characteristics of skeletal remains (Orr et al., 2004). From 39 harbor seal scats, 116 bones were identified morphologically to the genus *Oncorhynchus* and subjected to DNA analysis for species identification. For a positive DNA extraction control, we simulated digestion by treating coastal cutthroat bones (collected from Cowlitz Trout Hatchery, Winlock, WA) in a mixture of laboratory-grade trypsin (a digestive enzyme), baking soda, and water for 1 to 2 days. These trypsin-treated bones from a coastal cutthroat trout were used as positive DNA extraction and amplification control.

To prepare samples for DNA extraction, bones were soaked in 10% sodium hypochlorite for 10 minutes to destroy any contaminating DNA that may have adhered to the outside of the bone and were rinsed twice in sterile water. Bones ranged in weight from 0.1 to 105.6 mg and included teeth, vertebrae, gillrakers, radials, and bone fragments (hereafter, all bony parts and teeth will be referred to as "bone"). The bones were decalcified overnight in 0.5M EDTA solution (Hochmeister et al., 1991); fragile or small fragments were not decalcified. The EDTA was removed and the decalcified samples were extracted with the QIAamp tissue extraction kit (Qiagen, Valencia, CA) according to the manufacturer's instructions with the following modifications: 1) samples were proteinase K digested overnight or until completely digested; 2) 10 mg/μL yeast t-RNA carrier was added to the extractant before placement on the QIAQuick column; and 3) DNA was eluted in a reduced volume (50–100 μL) of buffer AE. Negative controls containing no tissue were simultaneously processed to verify that the extraction was free of contaminating DNA. The trypsin-treated coastal cutthroat bones were used as positive extraction and PCR controls.

Five to ten microliters of the extracted DNA were used in each amplification reaction. Amplification success was determined by electrophoresis through a 2% agarose gel followed by staining with ethidium bromide or the more sensitive SYBR Gold (Molecular Probes). Species identifi-

Table 1

Species, locations, and sample sizes (n) examined for RFLP analysis.

Species	Population	Location	n
Chinook	Walker Creek	Upper Frasier River, British Columbia	10
	Grovers Creek Hatchery	Puget Sound, Washington	12
	Lookingglass Hatchery	Snake River, Oregon	12
	Carson Hatchery	Columbia River, Washington	12
	Abernathy Hatchery.	Columbia River, Washington	11
	Upper Sacramento Mainstem	Sacramento River, California	10
Coho	Edison Creek	Oregon Coast	13
	Sandy River	Columbia River, Oregon	15
	North Fork Moclips River	Washington Coast	15
	Minter Creek Hatchery	Puget Sound, Washington	15
	Yakoun River	Queen Charlotte Island, British Columbia	7
Sockeye	Nehalem Ponds	Oregon Coast	4
	Redfish Lake	Snake River, Idaho	4
	Alturas Lake	Snake River, Idaho	2
	Ozette Lake	Washington Coast	14
	Lake Wenatchee	North Cascades,Washington	10
	Babine Lake	Central British Columbia	2
	Kamchatka River	Kamchatka Peninsula, Russia	9
Chum	Hamma Hamma River	Hood Canal, Washington	11
	Frosty Creek	Alaskan Peninsula	12
	Utka River	Chucotka Peninsula, Russia	9
	Miomote River	West Honshu, Japan	11
Pink	Nisqually River	South Puget Sound, Washington	6
	Snohomish River Even Year	North Puget Sound, Washington	12
	Skagit River	North Puget Sound, Washington	7
	Hood Canal Hatchery	Hood Canal, Washington	9
Steelhead	Gaviota Creek	South California Coast	4
	Coquille River	Oregon Coast	8
	Upper Tucannon River	Snake River, Washington	12
	Finney Creek	Puget Sound, Washington	12
	Quinault Hatchery	Washington Coast	12
	Tigil River	Kamchatka Peninsula, Russia	12
Cutthroat[1]	Alsea River	Oregon Coast	2
	Alsea Hatchery	Oregon Coast	3
	Duwamish River	Puget Sound Washington	12
	Yellowstone River	Yellowstone River, Montana	5

[1] Cutthroat trout from the Yellowstone River are a different subspecies (*O. clarki bouvieri*) from the Washington and Oregon coastal cutthroat trout (*O. clarki clarki*).

cation was accomplished by sequencing of either the d-loop or the COIII/ND3 region. RFLP analysis was performed as described above with the following modifications: *Bst* NI was excluded because it is redundant with *Dpn* II, the enzyme amount was reduced to 0.4–1.0 units per reaction, and incubation time did not exceed 2 hours. The COIII/ND3 primers are specific to the family Salmonidae. To test the possibility that the failure to obtain amplification with the COIII/ND3 primers was due to morphological misidentification of an *Oncorhynchus* species we used the 16s primers that are conserved across a broad set of taxa from Platyhelminthes through Chordata (Parker and Kornfield, 1996).

Results

The COIII/ND3 and 16s sequences were confirmed for all seven salmonid naturally present in the Pacific Northwest (Figs. 1 and 2) and deposited in Genbank (COIII/ND3: AF294827-AF294833; 16S: AF296341-AF296347). Two chinook salmon were sequenced representing two *Dpn* II

Table 2

Primer sequences, size of amplified product in base pairs, and references for mitochondrial loci used in this study.

Locus	Primer sequences (5′ to 3′)	Product size	Reference
d-loop	P2: tgt taa acc cct aaa cca g P4: gcc gaa tgt aaa gca tct ggt	230	Shedlock et al., 1992
COIII/ ND3	F: tta caa tcg ctg acg gcg R: gaa aga gat agt ggc tag tac tg	368	Domanico and Phillips, 1995
16sV	F: tac ata aca cga gaa gac c R: gtg att gcg ctg tta tcc	260	Parker and Kornfield, 1997

Table 3

Restriction fragment length polymorphisms of the cytochrome oxidase III and ND3 region digested with six restriction enzymes. The "A" haplotype does not cut with the enzyme, "B" cuts with the enzyme, and "C" cuts with the enzyme but at a different site than "B."

Species	*Dpn* II	*Sau* 96I	*Fok* I	*Ase* I	*Apo* I	*Bst* NI
Chinook	A/B[1]	B	B	A	A	A
Coho	A	A	B	A	A	A
Sockeye	A	A	A	A	C	B
Chum	A	A	A	B	C	A
Pink	C	A	A	B	C	C
Steelhead	A	A	A	B	B	A
Cutthroat	A	A	A	A	A	A

[1] Spring-running chinook from the Columbia and Snake Rivers were polymorphic for the *Dpn* II cut site. Spring chinook from Carson Hatchery (derived from the upper Columbia River spring-running ESU [evolutionary significant unit]) had the "A" haplotype at a frequency of 0.91 (n=12) and spring chinook from Lookingglass Hatchery (Snake River spring-summer-running ESU) had the "A" haplotype at a frequency of 0.83 (n=12). All other chinook samples from Table 1 were invariant for the "B" haplotype.

haplotypes (A and B) and their sequences are presented in Figure 1; the chinook salmon individuals were from the Upper Columbia River summer and fall ESU (Methow River, WA). A second intraspecific polymorphism in chinook salmon was observed at position 341 between our ND3 sequence and the published sequence (Domanico and Phillips, 1995) (Fig.1). Sufficient nucleotide variation exists in the d-loop (Shedlock et al., 1992) and in the COIII/ND3 region (Fig. 1) to distinguish among the salmon species by sequencing; both regions were used for bone identification.

Six restriction enzymes were selected from the COIII/ ND3 sequence that appeared to distinguish among all the species (*Dpn* II, *Sau* 96I, *Fok* I, *Ase* I, *Apo* I, and *Bst* NI) (Fig. 1). The *Dpn* II and *Bst* NI cut patterns are redundant in that only one of these enzymes is required for species identification when used in conjunction with the other four enzymes (however, only *Dpn* II exhibits the intraspecific chinook polymorphism, see below). Haplotype patterns for all species are listed in Table 3. The haplotypes were scored with a simple alphabetic system: "A" was uncut (368 base-pair (bp) band) and "B" was cut (the size differed depending on enzyme). A few of the enzymes had an alternative cut site, and the resulting haplotype we labeled "C." The "B" haplotype produced by *Apo* I occurs in steelhead and the bands migrate at 300 and 68 bp, whereas the bands of the "C" haplotype in sockeye, chum, and pink salmon migrate at 250 and 118 bp. The enzyme *Bst* NI also has two cut patterns: the sockeye salmon "B" haplotype bands migrate at 282 and 87 bp and the "C" haplotype bands in pink salmon migrate at 271 and 98 bp. The *Dpn* II "B" haplotype in chinook salmon creates two fragments, 290 and 80 bp; the "C" haplotype in pink salmon creates three fragments, 292, 53, and 24 bp.

To confirm that the restriction enzyme polymorphisms were diagnostic within each species, we surveyed all seven Pacific salmon species representing multiple populations spanning a large geographic range (Table 1). No intraspecific polymorphisms were detected among populations with the exception of chinook salmon (Tables 1 and 3). A single intraspecific polymorphism was found with the *Dpn* II enzyme in chinook salmon lineages in the Columbia and Snake River basins (Tables 1 and 3). Chinook salmon from the Snake River spring-summer run (Lookingglass

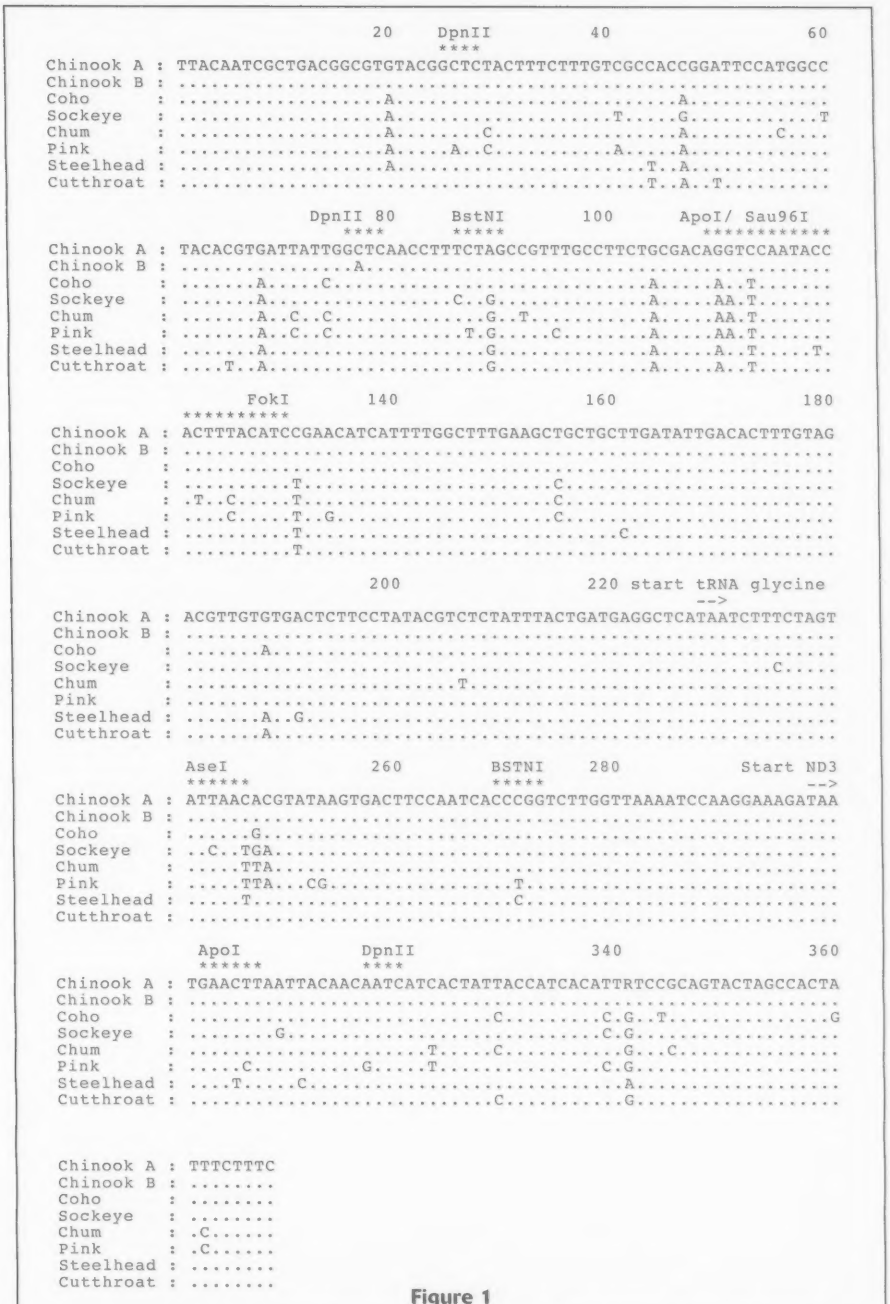

Figure 1

Aligned sequences of the 3′ region of the cytochrome oxidase III gene (COIII), the tRNA glycine gene, and the 5′ region of the ND3 gene for seven species of the genus *Oncorhynchus*. The cutthroat trout sequence is represented by the coastal cutthroat subspecies (*O. clarki clarki*). Chinook "A" refers to the "A" *Dpn* II haplotype; chinook "B" refers to the "B" *Dpn* II haplotype. Sequence identity relative to the chinook salmon "A" sequence is denoted by dots; nucleotide substitutions are indicated. The arrow at basepair (bp) 230 is the start of the tRNA glycine gene and the arrow at bp 300 is the start of the ND3 gene. Stars above the sequence correspond to restriction enzyme cut sites used in this study. At position 341 in chinook, the R represents an A or G.

```
                                20                  40                  60
Chinook    : GGAGCTTTAGACACCAGGCAGATCACGTCAAACAACCTTGAATTAACAAGTAAAAACGCAGT
Coho       : ..........................................G.....................
Sockeye    : ....................................................................
Chum       : ..........................................C.....................
Pink       : ..............C...........A...A..........................C.......
Steelhead  : ..............................G.....................................
Cutthroat  : ..............................G.....................................

                           80                  100                 120
Chinook    : GACCCCTAGCCCATATGTCTTTGGTTGGGGCGACCGCGGGGGAAAATTAAGCCCCCATGTGG
Coho       : ....................................................................
Sockeye    : ............G.......................................................
Chum       : ..............................................A.....................
Pink       : ..............................................A.....................
Steelhead  : ....................................................................
Cutthroat  : ..................................T..............C.....................

                         140                 160                 180
Chinook    : ATGGGGGCATGCCCCCACAGCCAAGAGCCACAGCTCTAAGCACCAGAATATCTGACCAAAAA
Coho       : ..............T.............T...A.............................C.....
Sockeye    : ....................................................................
Chum       : ......................G.....T.....................T.....C.....C.....
Pink       : ............T.........G.....T..............C.....C.....C.....C.....
Steelhead  : ......................G.....T.....C.....C.....C.....C.....C.....T.
Cutthroat  : ......................G.....T..G..C.....C.....C.....C.....C.....C.....

                       200                 220
Chinook    : TGATCCGGCAAACGCCGATCAACGGACCGAGTTACCCTAG....
Coho       : .............................................
Sockeye    : .............................................
Chum       : .............................................
Pink       : ..........G..................................
Steelhead  : .........G.....C.....C.....C.....C.....C.....
Cutthroat  : .............................................
```

Figure 2

Aligned sequences of a variable portion of the 16s gene for seven species of the genus *Oncorhynchus*. Sequence identity in relation to the chinook salmon "A" sequence is denoted by dots; nucleotide substitutions are indicated.

Hatchery) and hatchery stocks descended from the Upper Columbia River spring run (Carson Hatchery) had the "A" (uncut) haplotype at a frequency of 83% and 91%, respectively, whereas those from the Lower Columbia River ESU were invariant for the "B" (cut) haplotype. The "B" haplotype was also invariant in the other lineages examined (Sacramento River, CA; Puget Sound, WA; and the Fraser River, BC). Despite this *Dpn* II polymorphism, the haplotype patterns were still chinook-specific.

Extractions from the trypsin-treated cutthroat trout bones, used as positive controls, were amplified consistently, but of the 116 salmonid bones from harbor seal scats, only 78 (67%) were amplified. Failed samples were repeated several times with all possible primer sets. Because each scat contained multiple bones, we were able to amplify bones representing 35 of the 39 scats (90%). The smallest bone we successfully amplified was a 0.2-mg tooth and the largest was a 21.8-mg vertebra. There did not appear to be a relationship between bone size and DNA extraction success; no significant difference in mean bone size was detected between 32 bones that either amplified or failed (P=0.280; unpaired t-test; SYSTAT 8.0 [Chicago, IL]). The bone samples that failed to amplify repeatedly were also tested by using the evolutionarily conserved 16s primers. Some samples were still refractory to PCR, indicating that the overall DNA quality or quantity was insufficient for this assay; however, those samples that did amplify were identified by sequencing as salmon. In an unrelated study using river otter bones (data not presented), one bone sample morphologically identified as salmonid yielded a sequence with 100% identity to the published 16s sequence available for Northern squawfish (*Ptychocheilus oregonensis*) (Simons and Mayden, 1998).

After verifying the specificity of the RFLP analysis for differentiating the Pacific salmon species, the assay was applied to the bone samples. Restriction enzyme digestion required some modification when applied to bone. On occasion, the restriction enzyme protocol developed for the fresh tissue resulted in degradation of the amplified bone PCR product. Enzyme amount and digestion times were scaled back for the analysis of the bone samples. The *Fok* I enzyme proved the most difficult for the bone samples, which was likely due to nonspecific restriction that occurs when the enzyme is present at a high concentration in relation to its target or if the reaction is allowed to digest for more than two hours. In some cases, only very weak amplification was achieved with the bone samples and it was difficult to get digestion without degradation. Although sequencing was the main technique used for bone identification, 23 bones in this study were identified by using the RFLP technique. Fourteen of these 23 bones were additionally confirmed by sequencing and the two techniques gave matching results.

Discussion

This study focused on the development of tools for the genetic identification of Pacific salmon skeletal remains recovered from harbor seal scats. These tools help to determine the diet of marine mammals and can also be used to address direct management questions regarding interspecific interactions in rivers such as the Umpqua River where salmonid species of concern (cutthroat trout) occur with protected marine mammal species. The harbor seal diet in the Umpqua River consisted of nonsalmonid fish and chinook, coho, and steelhead; no cutthroat trout were observed in the scat samples (Orr et al., 2004). The majority of salmonid species identifications were possible only by using genetic methods because very few otoliths were recovered in the Umpqua River scats. A number of other sites exist were this technology may also be applicable. In Hood Canal (WA) the summer chum salmon run is listed as threatened under the ESA. A report of seal diets in Hood Canal determined that 27% of the fish consumed by harbor seals were salmonids (Jeffries et al.[3]). The study used both bones and otoliths, but only 25% of the samples contained otoliths that allowed species-level identification. In the Alsea River (OR), coho salmon are listed as threatened. A report by Riemer et al.[4] indicated that 6% of fish consumed by pinnipeds in the Alsea River are salmonids; none of the salmonid remains were morphologically identifiable to species.

Extraction of DNA from bones can be done with a commercially available kit with minor modifications. In our study, only 67% of the bone DNA extracts could be amplified by PCR. PCR failure could be due to DNA degradation during the digestive process or to environmental exposure after defecation. However, multiple bones are often present in scats and we were able to amplify DNA from at least one bone representative from 35 out of the 39 scats examined. Sequencing or RFLP analyses of the COIII/ND3 locus are both viable methods of identifying the seven common *Oncorhynchus* species. This study used manual sequencing with radioactivity and we did have better results using this method compared to the RFLP method. A recently published study also identified restriction enzymes in the cytochrome B gene that distinguish among the salmonid species (Russell et al., 2000). The study reported diagnostic RFLP differences among these species but did not confirm the lack of intraspecific variation in a wide geographic survey of each species. The goal of the cytochrome B RFLP assay designed by Russell et al. (2000) was to identify salmon species found in processed food products but the primers may also prove useful in species identification of bone remains. The 16s primer set is also valuable for bones that are morphologically unidentifiable. However for salmonid species identification, the 16s region contains fewer diagnostic nucleotide substitutions in relation to the d-loop and the COIII/ND3 region. Overall, the techniques established here would be useful for further study of marine mammal diets and may have the potential for forensic application.

[3] Jeffries, S. J., J. M. London, and M. M. Lance. 2000. Observations of harbor seal predation on Hood Canal summer chum salmon run 1998–1999. Annual progress report to Pacific States Marine Fisheries Commission, 39 p. [Available from WDFW, Marine Mammals Investigations, 7801 Phillips Rd. SW, Tacoma, WA 98498.]

[4] Riemer, S. D., R. F. Brown, B. E. Wright and M. I. Dhruv. 1999. Monitoring pinniped predation on salmonids at Alsea River and Rogue River, Oregon: 1997–1999. Oregon Department of Fish and Wildlife, Marine Mammal Research Program, Corvallis, OR, 36 p. [Available from ODFW, 7118 NE Vandenberg Ave., Corvallis, OR 97333.]

Acknowledgments

The authors acknowledge Robert Delong for suggesting this study. Jon Baker at the Northwest Fisheries Science Center and Paul Spruell at the University of Montana kindly provided cutthroat DNA. James Shaklee at the Washington Department of Fish and Wildlife kindly provided pink salmon samples. Sam Wasser and Virginia Butler provided advice on the recovery of DNA from scat and bone samples. Gail Bastrup assisted in technical aspects of this study.

Literature cited

Avise, J. C.
1994. Molecular markers, natural history, and evolution, p. 44–91. Chapman and Hall, New York, NY.

Cottrell, P. E., A. W. Trites, and E. H. Miller.
1996. Assessing the use of hard parts in faeces to identify harbour seal prey: results of captive-feeding trials. Can. J. Zool. 74:875–880.

Domanico, M. J., and R. B. Phillips.
1995. Phylogenetic analysis of Pacific salmon (genus *Oncorhynchus*) based on mitochondrial DNA sequence data. Mol. Phylogenet. Evol. 4:366–371.

Harvey, J. T.
1989. Assessment of errors associated with harbour seal (*Phoca vitulina*) faecal sampling. J. Zool. 219:101–111.

Hochmeister, M. N., B. Budowle, U. V. Borer, U. Eggmann, C. T. Comey, and R. Dirnhofer.
1991. Typing of deoxyribonucleic acid (DNA) extracted from compact bone from human remains. J. Forensic Sci. 36: 1649–1661.

Johnson, O., M. Ruckelshaus, W. Grant, F. Waknitz, A. Garrett, G. Bryant, K. Neely, and J. Hard.
1999. Status review of coastal cutthroat trout from Washington, Oregon, and California. NOAA Tech. Memo. NMFS-NWFSC-37, p 138–139.

McKay, S. J., M. J. Smith, and R. H. Devlin.
1997. Polymerase chain reaction-based species identification of salmon and coastal trout in British Columbia. Mol. Mar. Biol. Biotechnol. 6:131–140.

Ochoa-Acuna, H., and J. M. Francis.
1995. Spring and summer prey of the Juan Fernandez fur seal, *Arctocephalus philippii*. Can. J. Zool. 73:1444–1452.

Olesiuk, P. F.
1993. Annual prey consumption by harbor seals (*Phoca vitulina*) in the Strait of Georgia, British Columbia. Fish. Bull. 91:491–515.

Orr, A., A. Banks, S. Mellman, and H. Huber.
2004. Examination of Pacific harbor seal (*Phoca vitulina richardsi*) foraging habits to describe their use of the

Umpqua River, Oregon, and their predation on salmonids. Fish. Bull.102:108–117.

Parker, A., and I. Kornfield.
1996. An improved amplification and sequencing strategy for phylogenetic studies using the mitochondrial large subunit rRNA gene. Genome 39:793–797.

Roffe, T., and B. Mate.
1984. Abundance and feeding habits of pinnipeds in the Rogue River, OR. J. Wildl. Manag. 48:1262–1274.

Russell, V. J., G. L. Hold, S. E. Pryde, H. Rehbein, J. Quinteiro, M. Rey-Mendez, C. G. Sotelo, R. Perez-Martin, A. T. Santos, and C. Rosa.
2000. Use of restriction fragment length polymorphism to distinguish between salmon species. J. Agricult. Food Chem. 48:2184–2188.

Sambrook, J., E. F. Fritsch, and T. Maniatis.
1989. Molecular cloning: a laboratory manual, p. 9.17–9.19. Cold Spring Harbor Laboratory, Cold Spring Harbor, NY.

Shedlock, A. M., J. D. Parker, D.A. Crispin, T. W. Pietsch, and G. C. Burmer.
1992. Evolution of the salmonid mitochondrial control region Mol. Phylogenet. Evol. 1:179–192.

Simons, A. M., and R. L. Mayden.
1998. Phylogenetic relationships of the western North American phoxinins (Actinopterygii: Cyprinidae) as inferred from mitochondrial 12S and 16S ribosomal RNA sequences. Mol. Phylogenet. Evol. 9:308–329.

Diel vertical migration of the bigeye thresher shark (*Alopias superciliosus*), a species possessing orbital retia mirabilia

Kevin C. Weng
Barbara A. Block
Tuna Research and Conservation Center
Hopkins Marine Station of Stanford University
120 Oceanview Boulevard
Pacific Grove, California 93950
E-mail address (for K. C. Weng): kevin.cm.weng@stanford.edu

The bigeye thresher shark (*Alopias superciliosus*, Lowe 1841) is one of three sharks in the family Alopiidae, which occupy pelagic, neritic, and shallow coastal waters throughout the tropics and subtropics (Gruber and Compagno, 1981; Castro, 1983). All thresher sharks possess an elongated upper caudal lobe, and the bigeye thresher shark is distinguished from the other alopiid sharks by its large upward-looking eyes and grooves on the top of the head (Bigelow and Schroeder, 1948). Our present understanding of the bigeye thresher shark is primarily based upon data derived from specimens captured in fisheries, including knowledge of its morphological features (Fitch and Craig, 1964; Stillwell and Casey, 1976; Thorpe, 1997), geographic range as far as it overlaps with fisheries (Springer, 1943; Fitch and Craig, 1964; Stillwell and Casey, 1976; Gruber and Compagno, 1981; Thorpe, 1997), age, growth and maturity (Chen et al., 1997; Liu et al., 1998), and aspects of its reproductive biology (Gilmore, 1983; Moreno and Moron, 1992; Chen et al., 1997).

Limited information on the movement patterns of bigeye thresher sharks has been obtained from mark-recapture studies by using conventional tags. The longest straight-line movement of a conventionally tagged bigeye thresher shark to date is 2767 km from waters off New York to the eastern Gulf of Mexico (Kohler and Turner, 2001). The bigeye thresher shark has been captured on longlines set near the surface at night (0 m to 65 m, Fitch and Craig, 1964; Stillwell and Casey, 1976; Thorpe, 1997; Buencuerpo et al., 1998) and at 400 m to 600 m during the day (Nakamura[1]). There is no published information available regarding its habitat and behavior, although Francis Carey tracked a bigeye thresher with an acoustic tag for six hours (Carey[2]).

Endothermy is a rare trait in fishes and has been demonstrated only in tunas (Thunnini), billfishes (Xiphiidae, Istiophoridae), and lamnid sharks (Lamnidae) (Carey and Teal, 1969; Carey, 1971, 1982a; Block, 1991). In all endothermic fishes, the blood supply to aerobic tissues such as slow-twitch swimming muscle, visceral organs, extraocular muscles, retina, and brain occurs by counter-current heat exchangers known as retia mirabilia. The vascular supply reduces heat loss to the environment and enables heat conservation in metabolically active tissues (Carey, 1971). Lamnid sharks have retia mirabilia in the circulatory anatomy supplying the slow-oxidative swimming muscles, viscera, brain, and eyes (Burne, 1924; Block and Carey, 1985; Tubbesing and Block, 2000). In many lamnid species, tissue temperatures significantly above ambient have been recorded from freshly captured specimens and through telemetry studies of swimming animals (Carey, 1971; Carey et al., 1981, 1982, 1985; McCosker, 1987; Goldman, 1997; Tubbesing and Block, 2000).

The anatomy of alopiid sharks suggests that endothermy may occur in this family. The bigeye thresher and the common thresher (*Alopias vulpinus*) have centrally located slow-oxidative muscle and primitive retia mirabilia supplying blood to them (Carey, 1982b; Bone and Chubb, 1983). Burne (1924) noted a coiling of the pseudobranchial artery supplying the orbit and cranial regions in the common thresher. No internal tissue temperature measurements have been taken for free-swimming thresher sharks to ascertain whether heat is conserved in oxidative tissues. A freshly caught bigeye thresher shark was found to have a body-core thermal excess of 4°C (Carey, 1971); thus the species may have the ability to conserve metabolic heat.

In this study we present electronic tagging data on the movements, diving behavior, and habitat preferences of the bigeye thresher shark based on two individuals studied with pop-up satellite archival tags. In addition, we provide a brief description of the orbital rete mirabile of the species. The presence of this highly developed rete mirabile within the orbital sinus suggests a physiological mechanism to buffer the eyes and brain from the large temperature changes associated with diel vertical migration, potentially conferring enhanced physiological performance.

Materials and methods

The movements of two bigeye thresher sharks were monitored with pop-up satellite archival tags (PAT tag version 2.00, Wildlife Computers, Redmond, WA; Gunn and Block, 2001; Marcinek et al., 2001). The first shark was captured on a longline set in the Gulf of Mexico at 26.5°N, 91.3°W on 12 April

[1] Nakamura, I. 2002. Personal commun. Institut National des Sciences et Technologies de la Mer, 28 rue 2 Mars 1934, 2025 Salammbo, Tunisia.

[2] Carey, F. G. (deceased). 1990. Personal commun. Woods Hole Oceanographic Institution, Woods Hole, MA 02543.

Manuscript approved for publication 15 August 2003 by Scientific Editor.
Manuscript received 20 October 2003 at NMFS Scientific Publications Office.
Fish. Bull. 102:221–229 (2004).

2000 in waters with a surface temperature of 21.9°C. The longline set contained 184 hooks set at depths between 70 m and 90 m and was made at 06:00 h and retrieved at 09:00 h. Circle hooks (L2045 20/0 circle hook, Eagle Claw, Denver, CO) were used to avoid hooking of the gut, and the shark in this study was hooked in the corner of the jaw. Hooks were baited with squid, and chemical light sticks were attached to every other line. The mass of the shark was visually estimated at 170 kg by an experienced commercial longline fisherman, which corresponds to a fork length of 229 cm, and a total length of 377 cm, based on the weight-length relationship of Kohler et al. (1995). According to this size estimation and the published size-at-maturity data (Chen et al., 1997; Liu et al., 1998), the shark was mature. The sex of the shark was not determined. The second shark was captured by hook-and-line gear near Hawaii at 19.5°N, 156.0°W on 13 May 2003 in waters with a surface temperature of 25.5°C. A baited circle hook set at a depth of 40 m was taken by the shark at 02:00 h. The mass of the shark was estimated at 200 kg by an experienced sportfishing captain, which corresponds to a fork length of 242 cm, and a total length of 400 cm (after Kohler et al., 1995). Given this size, the shark was mature (Chen et al., 1997; Liu et al., 1998), but its sex was not determined.

Each pop-up satellite archival tag was attached to a titanium dart (59 mm × 13 mm) with a 17 cm segment of 136-kg monofilament line (300-lb test extra-hard Hi-Catch, Momoi Fishing Net Mfg. Co. Ltd., Ako City, Hyogo prefecture, Japan). The dart was inserted into the dorsal musculature of the shark at the base of the first dorsal fin, such that the tag trailed behind the fin. Following attachment of each tag, the fishing line was cut near the hook and both sharks swam away vigorously. Tagging locations were recorded by using the vessel's global positioning system. After the Gulf of Mexico shark was tagged, a depth-temperature recorder (ABT-1, Alec Electronics, Kobe, Japan) was used to determine the temperature-depth profile of the upper 200 m of the ocean at the release site, at a resolution of 1 m.

The pop-up satellite archival tag deployed in the Gulf of Mexico was programmed to collect pressure and temperature data at two-minute intervals, which the on-board software (PAT software version 1.06, Wildlife Computers, Redmond, WA) summarized into six-hour bins. This version of PAT software did not permit light-based geolocation. The summary data for each time interval comprised percentage distributions of time-at-depth and time-at-temperature, and profiles of temperature-at-depth. Temperature-depth profiles for this generation of software were recorded at intervals by measuring a single temperature at depths of 0, 25, 50, 75, 100, 125, 150, 200, 250, 300, 350, and 400 meters for the deepest dive. A mean temperature-depth profile was obtained by calculating the mean temperature at each specified depth for all profiles taken during the track. The endpoint position of the shark's track was obtained from the tag's radio transmissions to the Argos satellites. The six-hour bins were later combined into 12-hour bins representing day (06:00 to 17:59 h local time) and night (18:00 to 05:59 h local time). At the time and place of tag deployment, sunrise occurred at 05:45 h and sunset at 18:28 h; whereas at the popup time and position, sunrise occurred at 05:02 h and sunset at 18:55 h (U.S. Naval Observatory), such that the day and night bin cutoffs were always within one hour of true sunrise and sunset.

The pop-up satellite archival tag deployed off Hawaii collected data at 30-second intervals and summarized them into four-hour bins (PAT software version 2.08e, Wildlife Computers, Redmond, WA). The data were later combined into day and night bins as for the first tag, and the actual sunrise and sunset times were within one hour of 06:00 h and 18:00 h, respectively (U.S. Naval Observatory). The tag measured the minimum and maximum temperature at the surface, maximum depth, and six intermediate depths, for the deepest dive in each time interval. Temperature-depth profiles for each time interval were later constructed by using the maximum temperature at each depth for all profiles taken during the track, and a curve was fitted by using a LOWESS (locally weighted regression smoothing) function (Cleveland, 1992). Version 2.08e PAT software collected light data for geolocation; however the diel dive pattern of the shark prevented the calculation of accurate positions.

The vascular circulation to the brain and eyes was examined in two bigeye thresher sharks: one common thresher shark and one pelagic thresher shark (*Alopias pelagicus*). A female bigeye thresher (1.5 m fork length) was captured off Cape Hatteras, North Carolina, and a male (1.4 m fork length) was captured in the Gulf of Mexico. The circulatory systems of the bigeye threshers were injected with latex to aid in identifying the blood vessels. A male common thresher (1.3 m fork length) was captured off Cape Hatteras, North Carolina, and was examined without being frozen or preserved. An immature female pelagic thresher shark (1.37 m fork length) was captured in the Indian Ocean. The orbital retia mirabilia were prepared from casts of the vascular circulation that were removed from the orbit.

Results

One bigeye thresher shark was tracked in the Gulf of Mexico for 60 days, and another in the Hawaiian Archipelago for 27 days, by using pop-up satellite archival tags. Both tags released from the sharks as programmed and transmitted summary information to Argos satellites. The tag deployed in the Gulf of Mexico popped up on 10 June 2000 at 27.95°N, 89.54°W (Fig. 1A). The shark moved a straight-line distance of 320 km during the track, starting from the central Gulf in depths exceeding 3000 m and moving to waters 150 km south of the Mississippi Delta where depths were approximately 1000 m. The second shark was tagged off the Kona coast of Hawaii and the tag released on 9 June 2003 at 24.2°N, 165.6°W, northeast of French Frigate Shoals, a straight-line distance of 1125 km from the deployment position (Fig. 1B).

The depth and temperature distributions of the bigeye thresher sharks showed a strong diel movement pattern (Fig. 2). The Gulf of Mexico shark spent the majority of the daytime (84% [±2.3%], mean [±1 SE]) below the thermocline between 300 m and 500 m and the majority of nighttime (80% [±4.7%], mean [±1 SE]) in the mixed layer

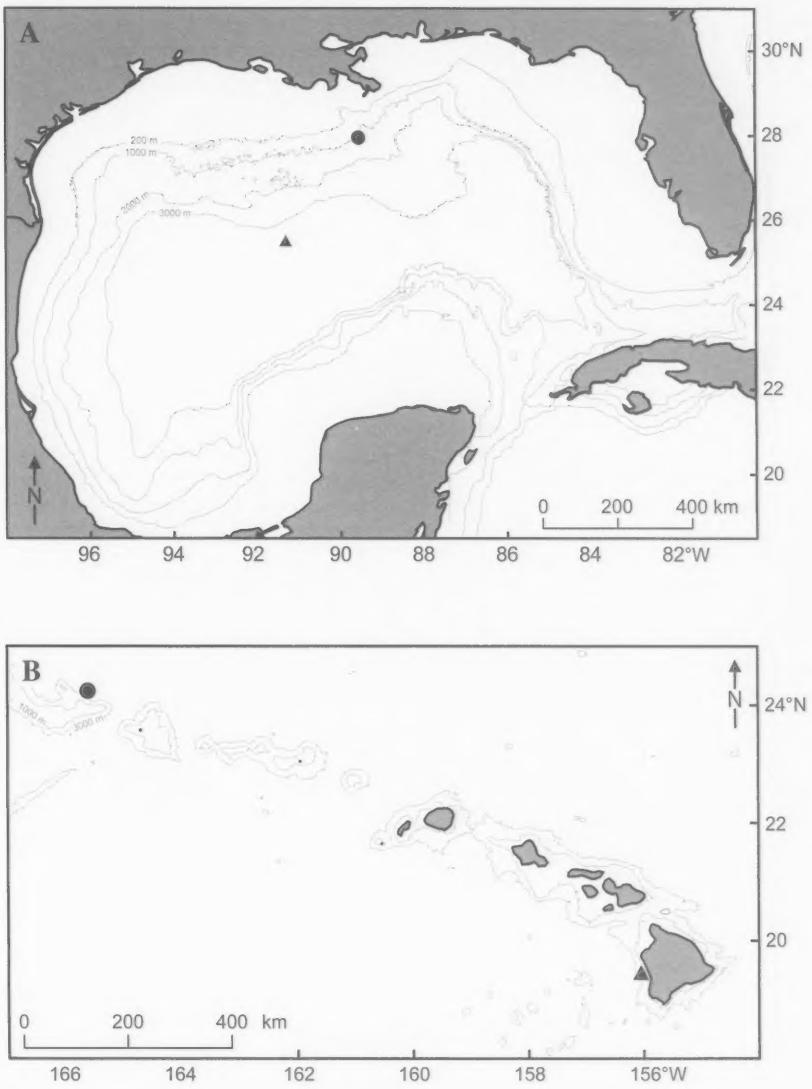

Figure 1

Deployment (▲) and end-point (●) positions for the two pop-up satellite archival tags attached to bigeye thresher sharks. Both tags surfaced on the programmed dates and transmitted data to Argos satellites. Pressure sensors in the tags confirmed that the tags remained attached to the sharks for the duration of the tracks. (**A**) In the Gulf of Mexico a shark was tagged and released on 12 April 2000 and the tag surfaced on 10 June 2000. The shark moved a straight-line distance of 320 km during the 60-day track. (**B**) In the Hawaiian Archipelago a shark was tagged on 13 May 2003 off Kona, Hawaii, and the tag surfaced on 9 June 2003 northeast of French Frigate Shoals. The shark moved a straight-line distance of 1125 km during the 27-day track.

and upper thermocline between 10 m and 100 m (Fig. 2A). The shark spent most of the daytime in deeper waters of 6°C to 12°C (70% [±4.4%], mean [±1 SE]), and most of the nighttime in shallower waters from 20°C to 26°C (70% [±2.7%], mean [±1 SE]) (Fig. 2B). A temperature-depth profile taken by the tag during the first day of the shark's track closely matched a profile taken from the vessel with a bathythermograph (Fig. 3A). The mean temperature-depth profile for the 60-day track (Fig. 3B), when compared with the shark's depth preferences (Fig. 2A), indicated that

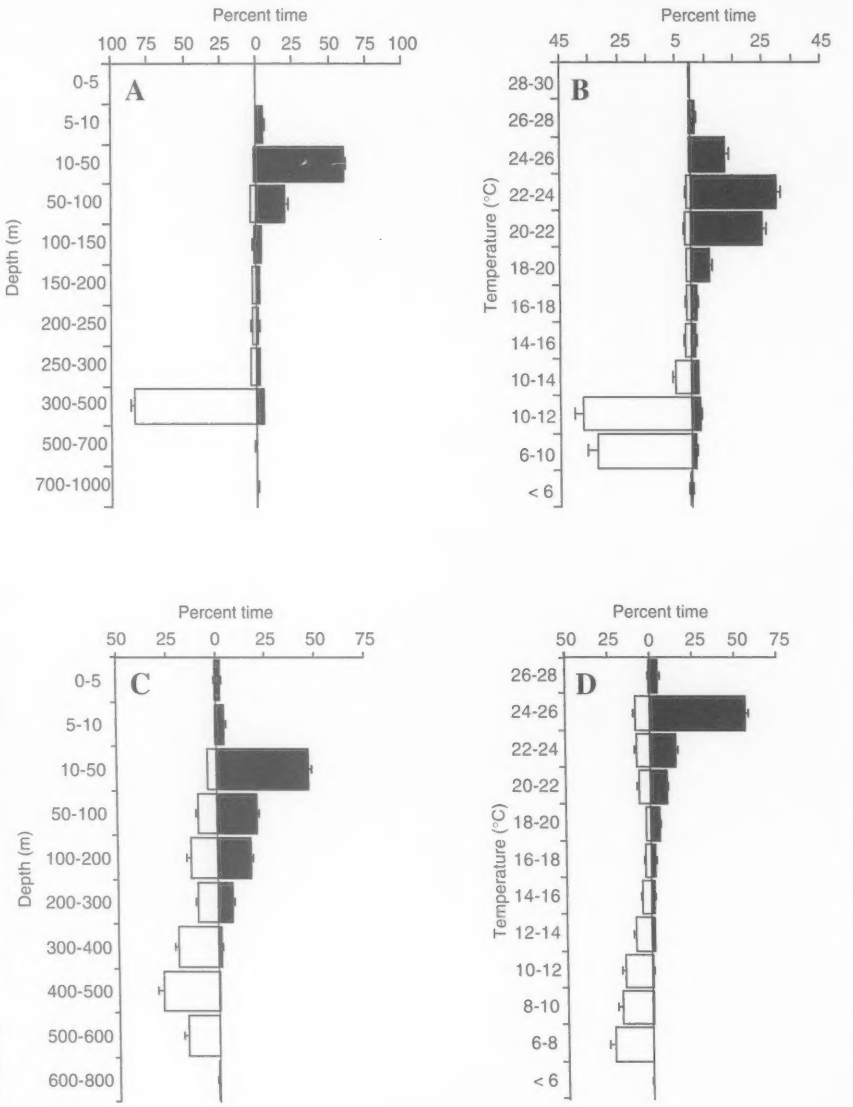

Figure 2

Depth and temperature distributions of two bigeye thresher sharks showing diel vertical migration. The tags recorded depth and temperature at two-minute (**A, B**) or 30-second (**C, D**) intervals; data are summarized into a series of bins for the full duration of each track. (A) Depth distribution for the Gulf of Mexico shark is shown as the percentage of day (□) and night (■) spent within depth bins ranging from the surface to 1000 m. Error bars are 1 SE. (B) Temperature distribution for the Gulf of Mexico shark is shown as the percentage of day (□) and night (■) spent within temperature bins ranging from 6°C to 30°C. The shark occupied cool waters during the day and warm waters during the night, a consequence of its deep daytime and shallow nighttime habitats. Error bars are 1 SE. (**C**) Depth distribution for the Hawaii shark showing diel vertical migration. The shark spent most of the daytime at the base of the thermocline and most of the nighttime in the mixed layer and upper thermocline. (**D**) Temperature distribution for the Hawaii shark showing cool daytime and warm nighttime water temperatures.

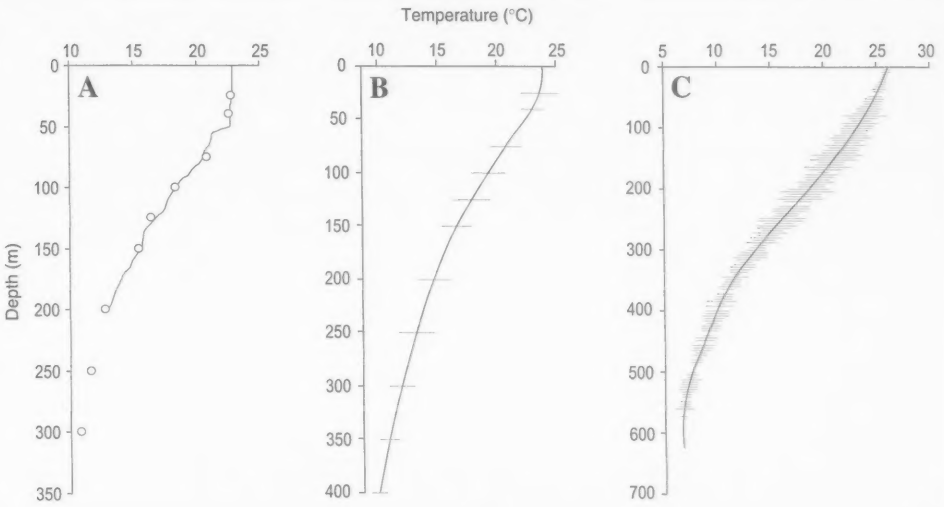

Figure 3

Temperature-depth profiles characterizing the thermal habitat of two bigeye thresher sharks. (**A**) Profiles of the Gulf of Mexico taken with a bathythermograph (——) sampling at 1-m intervals deployed from the fishing vessel after the tagging event, and by the pop-up satellite archival tag (○) during the first day it was attached to the bigeye thresher shark. The two profiles are similar, indicating that the pop-up satellite archival tag is capable of characterizing thermal habitat. (**B**) Average temperature-depth profile for the 60-day track of the bigeye thresher shark in the Gulf of Mexico, showing a mixed layer shallower than 50 m and a thermocline extending beyond 400 m where waters were 10°C. The curve was fitted by using a LOWESS function and error bars are 1 SD, because 1 SE bars are invisible at this scale. (**C**) Average temperature-depth profile for the 27-day track of the bigeye thresher shark in the Hawaiian Archipelago, showing a shallow mixed layer a thermocline extending to approximately 600 m where waters were 6°C. Curve was fitted by using a LOWESS function and error bars are 1 SD, because 1 SE bars are invisible at this scale.

the shark spent most of the daytime below the maximum gradient of the thermocline where temperatures were approximately 10°C. On 25 April and 25 May 2000 the shark spent two hours of the day in waters between 4°C and 6°C. The Hawaii shark showed a similar diel vertical migration, with a lesser contrast between day and night (Fig. 2, C and D). The shark's modal nighttime depth was between 10 m and 50 m, whereas its modal daytime depth was between 400 m and 500 m (Fig. 2C). The temperature-depth profile for the Hawaii shark (Fig. 3C) indicated that it spent nighttime above the thermocline and daytime below it.

The bigeye thresher shark possesses a large arterial plexus between the posterior part of the eye and the wall of the orbital sinus, which appears to be a rete mirabile (Fig. 4). The orbital rete is bathed in venous blood from the orbital sinus and its anterior surface is contoured to the posterior surface of the eye. The sources of venous input to the orbital sinus remain unknown but are most likely within the surrounding extraocular muscles, which are large and comprise numerous aerobic muscle fiber types, and the retina. The rete shown in Figure 4 measures 72 mm by 49 mm by 19 mm. A reduced structure of similar form is also found in the pelagic thresher shark, but is not present in the common thresher. The orbital rete of the bigeye and pelagic threshers is larger in absolute size and occupies a greater cross sectional proportion of the orbital sinus than the lamnid orbital rete noted by Burne (1924). The arterial vessels form a finer and more orderly meshwork than those in the lamnid sharks (Block and Carey, 1985; Tubbesing and Block, 2000) and appear similar in physical structure to the mammalian carotid rete used for brain cooling (Baker, 1982).

Discussion

Observations of the biological features of the bigeye thresher shark are rare and our knowledge of the species is based primarily on incidental catches in fisheries. Using pop-up satellite archival tags we were able to record behavior for a total of 87 days, and for individual periods up to 60 days without recapturing or following the study animals. We observed a pronounced diel alternation between warm shallow waters and cool deep waters and a rete mirabile that may confer physiological benefits during deep dives by stabilizing brain and eye temperatures.

The depth data obtained for the bigeye thresher shark shows a striking pattern of diel vertical migration. The bigeye thresher shark's vertical movement pattern is distinct from those of most other sharks for which observations

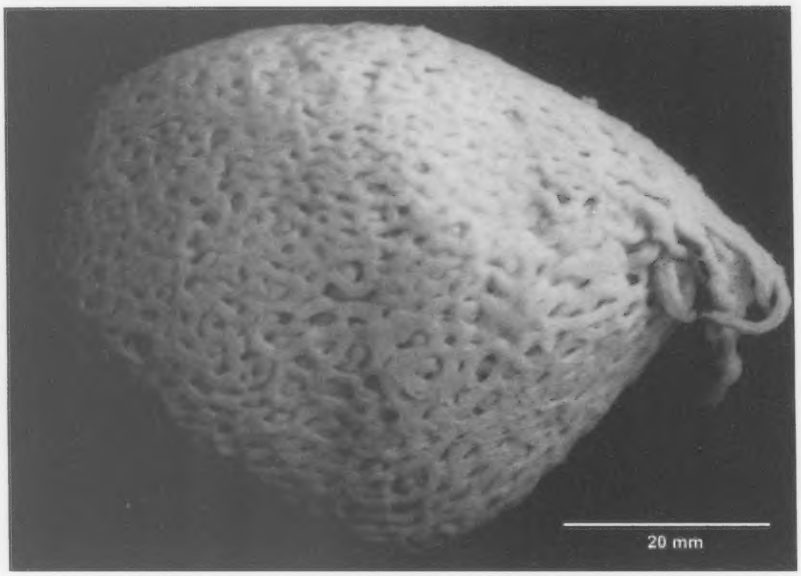

Figure 4

Orbital rete of a bigeye thresher shark, showing the highly developed arterial network. The rete was injected with latex so that the arterial structure (72 mm by 49 mm by 19 mm) could be photographed. The structure of the rete and its position in the orbital sinus suggest that it may be a heat exchanging vascular plexus. Retention of metabolic heat in the eyes and brain would buffer these sensitive organs from the large ambient temperature swings that occur as a result of the bigeye thresher shark's diel vertical migrations. A smaller but similar structure is found in *A. pelagicus* but not in *A. vulpinus*.

exist. In satellite or acoustic tracks, diel vertical migration was not observed for white sharks (*Carcharodon carcharias*; Carey et al., 1982; Goldman and Anderson, 1999; Boustany et al., 2002), salmon sharks (*Lamna ditropis*; Block et al.[3]), shortfin mako (*Isurus oxyrhynchus*; Carey, 1982b; Holts and Bedford, 1993), blue (*Prionace glauca*, Carey, 1982b; Carey and Scharold, 1990), sixgill (*Hexanchus griseus*; Carey and Clark, 1995), tiger (*Galeocerdo cuvier*; Tricas et al., 1981; Holland et al., 1999), Pacific angel (*Squatina californica*; Standora and Nelson, 1977), whale (*Rhincodon typus*; Gunn et al., 1999), or scalloped hammerhead sharks (*Sphyrna lewini*; Klimley, 1993).

Diel vertical migration has been observed in the swordfish (*Xiphias gladius*; Carey and Robison, 1981; Carey[4]), the megamouth shark (*Megachasma pelagios*; Nelson et al., 1997), and the school shark (*Galeorhinus galeus*; West and Stevens, 2001). Carey and Robison (1981) and Carey[4] studied swordfish in both the Pacific and Atlantic Oceans, acoustically tracking fish that moved from the surface at night to over 600 m during day. A megamouth shark showed a strong diel vertical migration when tracked acoustically off southern California (Nelson et al., 1997) with shallow nighttime and deep daytime distribution in a vertical range of 20 m to 160 m. West and Stevens (2001) studied school sharks in southern Australia using archival tags and noted that they ascended in the water column at night.

The ambient temperature at the modal day- and nighttime depths of the two bigeye thresher sharks differed by 15° to 16°C, requiring them to be eurythermal. The sharks spent most of the nighttime in shallow waters warmer than 20°C and commonly spent 8 or more hours during the daytime in deep waters cooler than 10°C. The coolest waters occupied had temperatures between 4°C and 6°C. The bigeye thresher sharks tracked in our study spent a higher proportion of their time in waters below 10°C than did white sharks (Carey et al., 1982; Boustany et al., 2002) and mako sharks (Carey and Scharold, 1990; Klimley et al., 2002).

The presence of a rete mirabile in the cranial region may indicate a mechanism for heat conservation. Heat conservation in the brain and eyes would enable the big-

[3] Block, B. A., K. G. Goldman, and J. A. Musick. 1999. Unpubl. data. Hopkins Marine Station of Stanford University, 120 Oceanview Boulevard, Pacific Grove, CA 93950.

[4] Carey, F. G. 1990. Further acoustic telemetry observations of swordfish. *In* Planning the future of billfishes; proceedings of the second international billfish symposium, 1–5 August 1988, Kailua-Kona, Hawaii (R. H. Stroud, ed.), p. 103–122. National Coalition for Marine Conservation, 3 North King St., Leesburg, VA 20176.

eye thresher shark to prolong its foraging time beneath the thermocline, as we observed for both of the sharks tagged in our study. The retina and brain are extremely temperature sensitive in most vertebrates and the large changes in depth and temperature recorded would impose significant effects on the biochemical processes occurring in these tissues (Block and Carey, 1985; Block, 1994). Delayed responses to retinal stimulation can be caused by cooling, whereas increased noise and random firing of neurons can be caused by warming—both responses having adverse affects on sensory function (Konishi and Hickman, 1964; Friedlander et al., 1976; Prosser and Nelson, 1981).

Anatomical and physiological adaptations to warm the brain and eyes have evolved independently in divergent pelagic fish lineages, including the lamnid sharks (Block and Carey, 1985), billfishes of the Xiphiidae and Istiophoridae (Carey, 1982a; Block, 1983) and some scombrid fishes (Linthicum and Carey, 1972). A cranial rete mirabile also has been identified in mobulids (Schweitzer and Notarbartolo di Sciara, 1986) and is thought to be a heat exchanger (Alexander, 1995, 1996). Although it is premature to suggest that the orbital rete of the bigeye thresher shark is a heat exchanger without direct evidence of elevated tissue temperatures in the brain and eyes, the structure is larger than the rete mirabile of lamnid sharks, for which elevated brain and eye temperatures have been demonstrated (Block and Carey, 1985). The anatomical arrangement of an arterial plexus in an orbital sinus is correlated with heat conservation strategies in other vertebrates (Baker, 1982). The phylogenetic relationships of the alopiid and lamnid sharks (Compagno, 1990; Naylor et al., 1997) suggest that endothermic traits evolved independently in the two families.

This note presents new information on the depth and ambient temperature preferences of the bigeye thresher shark based on observations of two individuals, as well as the anatomy of the orbital rete mirabile, which appears to function as a vascular heat exchanger. Behavior of many organisms varies with ontogeny, season and location; therefore the present study should be considered as only the beginning of an understanding of the bigeye thresher shark's physical habitat preferences and adaptations to temperature change. Further studies on individuals of different sizes and in different regions will enhance our understanding of the behavior, and morphological and physiological adaptations, of the bigeye thresher shark to variations in temperature.

Acknowledgments

This research was supported by grants from the National Marine Fisheries Service, the National Fish and Wildlife Federation and the Packard Foundation. The authors wish to thank Captain David Price and crew of the FV *Allison*, and Captain John Bagwell and crew of the FV *Silky*. Shana Beemer provided scientific assistance on the cruise and Captain McGrew Rice assisted in tagging and releasing the Gulf of Mexico shark. This research was conducted under Scientific Research Permit TUNA-SRP-2000-002, issued by the Office of Sustainable Fisheries, National Marine Fisheries Service, Silver Spring, MD 20910.

Literature cited

Alexander, R. L.
1995. Evidence of counter-current heat exchanger in the ray, *Mobula tarapacana* (Chondrichthyes: Elasmobranchii: Batoidea: Myliobatiformes). J. Zool. (Lond) 237:377–384.
1996. Evidence of brain-warming in the mobulid rays, *Mobula tarapacana* and *Manta birostris* (Chondrichthyes: Elasmobranchii: Batoidea: Myliobatiformes). Zool. J. Linn. Soc. 118:151–164.

Baker, M. A.
1982. Brain cooling in endotherms in heat and exercise. Annu. Rev. Physiol. 44:85–96.

Bigelow, H. B., and W. C. Schroeder.
1948. Sharks. *In* Fishes of the western North Atlantic, part one (A. Parr and Y. Olsen, eds), p. 59–546. Sears Found. Mar. Res., Yale Univ., Mem. 1.

Block, B. A.
1983. Brain heaters in the billfish. Am. Zool. 23:936.
1991. Endothermy in fish: thermogenesis ecology and evolution. *In* Biochemistry and molecular biology of fishes. Volume 1: Phylogenetic and biochemical perspectives (P. Hochachka and T. Mommsen, eds.), p. 269–311. Elsevier, Amsterdam.
1994. Thermogenesis in muscle. Annu. Rev. Physiol. 56: 535–577

Block, B. A., and F. G. Carey.
1985. Warm brain and eye temperatures in sharks. J. Comp. Physiol. B. Biochem. Syst. Environ. Physiol. 156: 229–236.

Bone, Q., and A. D. Chubb.
1983. The retial system of the locomotor muscles in the thresher shark (*Alopias vulpinus*). J. Mar. Biol. Assoc. U.K. 63:239–242.

Boustany, A. M., S. F. Davis, P. Pyle, S. D. Anderson, B. J. Le Boeuf, and B. A. Block.
2002. Satellite tagging: expanded niche for white sharks. Nature 415:35–36.

Buencuerpo, V., S. Rios, and J. Moron.
1998. Pelagic sharks associated with the swordfish, *Xiphias gladius*, fishery in the eastern North Atlantic Ocean and the strait of Gibraltar. Fish. Bull. 96:667–685.

Burne, R. H.
1924. Some peculiarities of the blood vascular system of the porbeagle shark (*Lamna cornubica*). Philos. Trans. R. Soc. Lond. B. Biol. Sci. 212B:209–257.

Carey, F. G.
1971. Warm bodied fish. Am. Zool. 11:135–143.
1982a. A brain heater in the swordfish (*Xiphias gladius*). Science 216:1327–1329.
1982b. Warm fish. *In* A companion to animal physiology; 5th international conference on comparative physiology; Sandbjerg, Denmark, July 22–26, 1980 (C. R. Taylor, K. Johansen and L. Bolis, eds.), p. 216–234. Cambridge Univ. Press, Cambridge, England; New York, NY.

Carey, F. G., J. G. Casey, H. L. Pratt, D. Urquhart, J. E. McCosker, J. A. Seigel, and C. C. Swift.
1985. Temperature, heat production and heat exchange in lamnid sharks. *In* Biology of the white shark (J. A. Seigel and C. C. Swift, eds.), p. 92–108. Mem. South. Calif. Acad. Sci., vol. 9, Fullerton, CA.

Carey, F. G., and E. Clark.
1995. Depth telemetry from the sixgill shark, *Hexanchus griseus*, at Bermuda. Environ. Biol. Fishes 42:7–14.

Carey, F. G., J. W. Kanwisher, O. Brazier, G. Gabrielson, J. G. Casey, and H. L. J. Pratt.
1982. Temperature and activities of a white shark, *Carcharodon carcharias*. Copeia 1982:254–260.

Carey, F. G., and B. H. Robison.
1981. Daily patterns in the activities of wwordfish, *Xiphias gladius*, observed by acoustic telemetry. Fish. Bull. 79: 277–292.

Carey, F. G., and J. V. Scharold.
1990. Movements of blue sharks (*Prionace glauca*) in depth and course. Mar. Biol. 106:329–342.

Carey, F. G., and J. M. Teal.
1969. Mako and porbeagle: warm-bodied sharks. Comp. Biochem. Physiol. 28:199–204.

Carey, F. G., J. M. Teal, and J. W. Kanwisher.
1981. The visceral temperatures of mackerel sharks (Lamnidae). Physiol. Zool. 54:334–344.

Castro, J. I.
1983. The sharks of North American waters, 180 p. Texas A&M Univ. Press, College Station, TX.

Chen, C.-T., K.-M. Liu, and Y.-C. Chang.
1997. Reproductive biology of the bigeye thresher shark, *Alopias superciliosus* (Lowe, 1839)(Chondrichthyes: Alopiidae), in the northwestern Pacific. Ichthyol. Res. 44: 227–235.

Cleveland, W. S., E. Grosse, and W. M. Shyu.
1992. Local regression models. Chapter 8 *in* Statistical models in S (J. M. Chambers and T. J. Hastie eds.), 608 p. Wadsworth & Brooks/Cole, Pacific Grove, CA.

Compagno, L. J. V.
1990. Relationships of the megamouth shark, *Megachasma pelagios* (Lamniformes: Megachasmidae), with comments on its feeding behavior. *In* Elasmobranchs as living resources: advances in the biology, ecology, systematics, and the status of the fisheries (H. L. J. Pratt, S. H. Gruber, and T. Taniuchi, eds.), p. 357–379. NOAA Technical Report 90.

Fitch, J. E., and W. L. Craig.
1964. First records for the bigeye thresher (*Alopias superciliosus*) and slender tuna (*Allothunnus fallai*) from California, with notes on eastern Pacific scombrid otoliths. Calif. Fish Game 50:195–206.

Friedlander, M. J., N. Kotchabhakdi, and C. L. Prosser.
1976. Effects of cold and heat on behavior and cerebellar function in goldfish. J. Comp. Physiol. A Sens. Neural. Behav. Physiol. 112:19–45.

Gilmore, R. G.
1983. Observations on the embryos of the longfin mako, *Isurus paucus* and the bigeye thresher, *Alopias superciliosus*. Copeia 1983:375–382.

Goldman, K. J.
1997. Regulation of body temperature in the white shark, *Carcharodon carcharias*. J. Comp. Physiol. B. Biochem. Syst. Environ. Physiol. 167:423–429.

Goldman, K. G., and S. D. Anderson.
1999. Space utilization and swimming depth of white sharks, *Carcharodon carcharias*, at the South Farallon Islands, central California. Environ. Biol. Fishes 56:351–364.

Gruber, S. H., and L. J. V. Compagno.
1981. Taxonomic status and biology of the bigeye thresher, *Alopias superciliosus*. Fish. Bull. 79:617–640.

Gunn, J. S., J. D. Stevens, T. L. O. Davis, and B. M. Norman.
1999. Observations on the short-term movements and behaviour of whale sharks (*Rhincodon typus*) at Ningaloo Reef, Western Australia. Mar. Biol. 135:553–559.

Gunn, J. S., and B. A. Block.
2001. Advances in acoustic, archival and satellite tagging of tunas. *In* Tunas: physiology, ecology and evolution (B. A. Block and E. D. Stevens, eds.), p. 167–224. Academic Press, San Diego, CA.

Holland, K. N., B. M. Wetherbee, C. G. Lowe, and C. G. Meyer.
1999. Movements of tiger sharks (*Galeocerdo cuvier*) in coastal Hawaiian waters. Mar. Biol. 134:665–673.

Holts, D. B., and D. W. Bedford.
1993. Horizontal and vertical movements of the shortfin mako shark, *Isurus oxyrinchus*, in the southern California bight. Aust. J. Mar. Freshw. Res. 44:901–909.

Klimley, A. P.
1993. Highly directional swimming by scalloped hammerhead sharks, *Sphyrna lewini*, and subsurface irradiance, temperature, bathymetry, and geomagnetic field. Mar. Biol. 117:1–22.

Klimley, A. P., S. C. Beavers, T. H. Curtis, and S. J. Jorgensen.
2002. Movements and swimming behavior of three species of sharks in La Jolla Canyon, California. Environ. Biol. Fishes 63:117–135.

Kohler, N. E., J. G. Casey, and P. A. Turner.
1995. Length-weight relationships for 13 species of sharks from the western North Atlantic. Fish. Bull. 93:412–418.

Kohler, N. E., and P. A. Turner.
2001. Shark tagging: A review of conventional methods and studies. Environ. Biol. Fishes 60:191–223.

Konishi, J., and C. P. Hickman.
1964. Temperature acclimation in the central nervous system of rainbow trout (*Salmo gairdnerii*). Comp. Biochem. Physiol. 13:433–442.

Linthicum, D. S., and F. G. Carey.
1972. Regulation of brain and eye temperatures by the bluefin tuna. Comp. Biochem. Physiol. A Comp. Physiol. 43:425–433.

Liu, K.-M., P.-J. Chiang, and C.-T. Chen.
1998. Age and growth estimates of the bigeye thresher shark, *Alopias superciliosus*, in northeastern Taiwan waters. Fish. Bull. 96:482–491.

Marcinek, D. J., S. B. Blackwell, H. Dewar, E. V. Freund, C. Farwell, D. Dau, A. C. Seitz, and B. A. Block.
2001. Depth and muscle temperature of Pacific bluefin tuna examined with acoustic and pop-up satellite archival tags. Mar. Biol. 138:869–885.

McCosker, J. E.
1987. The white shark, *Carcharodon carcharias*, has a warm stomach. Copeia 1987:195–197.

Moreno, J. A., and J. Moron.
1992. Reproductive biology of the bigeye thresher shark *Alopias superciliosus* Lowe 1839. Aust. J. Mar. Freshat. Res. 43:77–86.

Naylor, G. J. P., A. P. Martin, E. G. Mattison, and W. M. Brown.
1997. Interrelationships of lamniform sharks: Testing phylogenetic hypotheses with sequence data. *In* Molecular systematics of fishes (T. D. Kocher and C. A. Stepien, eds.), p. 199–218. Academic Press, San Diego, CA.

Nelson, D. R., J. N. McKibben, W. R. Strong Jr., C. G. Lowe, J. A. Sisneros, D. M. Schroeder, and R. J. Lavenberg.
1997. An acoustic tracking of a megamouth shark, *Megachasma pelagios*: A crepuscular vertical migrator. Environ. Biol. Fishes 49:389–399.

Prosser, C. L., and D. O. Nelson.
1981. Role of nervous systems in temperature adaptation of poikilotherms. Annu. Rev. Physiol. 43:281–300.
Schweitzer, J., and G. Notarbartolo di Sciara.
1986. The *rete mirabile cranica* in the genus *Mobula*: a comparative study. J. Morphol. 188:167–178.
Springer, S.
1943. A second species of thresher shark from Florida. Copeia 1943:54–55.
Standora, E. A., and D. R. Nelson.
1977. A telemetric study of the behavior of free swimming Pacific angel sharks *Squatina californica*. Bull. South. Calif. Acad. Sci. 76:193–201.
Stillwell, C. E., and J. G. Casey.
1976. Observations on the bigeye thresher shark, *Alopias superciliosus*, in the western North Atlantic. Fish. Bull. 74:221–225.
Thorpe, T.
1997. First occurrence and new length record for the bigeye thresher shark in the northeast Atlantic. J. Fish Biol. 50: 222–224.
Tricas, T. C., L. R. Taylor, and G. Naftel.
1981. Diel behavior of the tiger shark *Galeocerdo cuvier* at French Frigate Shoals Hawaiian Islands USA. Copeia 1981:904–908.
Tubbesing, V. A., and B. A. Block.
2000. Orbital rete and red muscle vein anatomy indicate a high degree of endothermy in the brain and eye of the salmon shark. Acta Zool. (Stockh.) 81:49–56.
West, G. J., and J. D. Stevens.
2001. Archival tagging of school shark, *Galeorhinus galeus*, in Australia: Initial results. Environ. Biol. Fishes 60: 283–298.

Superintendent of Documents **Publications** Order Form

*5178

☐ YES, please send me the following publications:

____ Subscriptions to *Fishery Bulletin*
for $55.00 per year ($68.75 foreign)

The total cost of my order is $ _____ . Prices include regular domestic postage and handling and are subject to change.

_____
(Company or Personal Name) (Please type or print)

_____
(Additional address/attention line)

_____
(Street address)

_____
(City, State, ZIP Code)

_____
(Daytime phone including area code)

_____
(Purchase Order No.)

Charge your order. IT'S EASY!

VISA

MasterCard

Please Choose Method of Payment:

☐ Check Payable to the Superintendent of Documents
☐ GPO Deposit Account ☐☐☐☐☐☐☐–☐
☐ VISA or MasterCard Account
☐☐☐☐☐☐☐☐☐☐☐☐☐☐☐☐
☐☐☐☐ (Credit card expiration date)

To fax your orders (202) 512-2250

_____
(Authorizing Signature)

Mail To: Superintendent of Documents
P.O. Box 371954, Pittsburgh, PA 15250-7954

Thank you for your order!

Fishery Bulletin

Guidelines for contributors

Content of papers

Articles

Articles are reports of 10 to 30 pages (double spaced) that describe original research in one or a combination of the following fields of marine science: taxonomy, biology, genetics, mathematics (including modeling), statistics, engineering, economics, and ecology.

Notes

Notes are reports of 5 to 10 pages without an abstract that describe methods and results not supported by a large body of data. Although all contributions are subject to peer review, responsibility for the contents of articles and notes rests upon the authors and not upon the editor or the publisher. It is therefore important that authors consider the contents of their manuscripts carefully. Submission of an article is un-derstood to imply that the article is original and is not being considered for publication elsewhere. Manuscripts must be written in English. Authors whose native language is not English are strongly advised to have their manuscripts checked for fluency by English-speaking colleagues prior to submission.

Preparation of papers

Text

Title page should include authors' full names and mailing addresses (street address required) and the senior author's telephone, fax number, e-mail address, as well as a list of key words to describe the contents of the manuscript. **Abstract** must be less than one typed page (double spaced) and must not contain any citations. It should state the main scope of the research but emphasize the author's conclusions and relevant findings. Because abstracts are circulated by abstracting agencies, it is important that they represent the research clearly and concisely. **General text** must be typed in double-spaced format. A brief introduction should state the broad significance of the paper; the remainder of the paper should be divided into the following sections: Materials and methods, Results, Discussion (or Conclusions), and Acknowledgments. Headings within each section must be short, reflect a logical sequence, and follow the rules of multiple subdivision (i.e. there can be no subdivision without at least two subheadings). The entire text should be intelligible to interdisciplinary readers; therefore, all acronyms and abbreviations should be written out and all lesser-known technical terms should be defined the first time they are mentioned. The scientific names of species must be written out the first time they are mentioned; subsequent mention of scientific names may be abbreviated. Follow *Scientific style and format: CBE manual for authors, editors, and publishers* (6th ed.) for editorial style and the most current issue of the *American Fisheries Society's common and scientific names of fishes from the United States and Canada* for fish nomenclature. Dates should be written as follows: 11 November 1991. Measurements should be expressed in metric units, e.g. metric tons (t). The numeral one (1) should be typed as a one, not as a lower-case el (l).

Footnotes

Use footnotes to add editorial comments regarding claims made in the text and to document unpublished works or works with local circulation. Footnotes should be numbered with Arabic numerals and inserted in 10-point font at the bottom of the first page on which they are cited. Footnotes should be formatted in the same manner as citations. If a manuscript is unpublished, in the process of review, or if the information provided in the footnote has been conveyed verbally, please state this information as "unpubl. data," "manuscript in review," and "personal commun.," respectively. Authors are advised wherever possible to avoid references to nonstandard literature (unpublished literature that is difficult to obtain, such as internal reports, processed reports, administrative reports, ICES council minutes, IWC minutes or working papers, any "research" or "working" documents, laboratory reports, contract reports, and manuscripts in review). If these references are used, please indicate whether they are available from NTIS (National Technical Information Service) or from some other public depository. Footnote format: author (last name, followed by first-name initials); year; title of report or manuscript; type of report and its administrative or serial number; name and address of agency or institution where the report is filed.

Literature cited

The literature cited section comprises works that have been published and those accepted for publication (works in press) in peer-reviewed journals and books. Follow the name and year system for citation format. In the text, write "Smith and Jones (1977) reported" but if the citation takes the form of parenthetical matter, write "(Smith and Jones, 1977)." In the literature cited section, list citations alphabetically by last name of senior author: For example, Alston, 1952; Mannly, 1988; Smith, 1932; Smith, 1947; Stalinsky and Jones, 1985. Abbreviations of journals should conform to the abbreviations given in the *Serial sources for the BIOSIS previews database*. Authors are responsible for the accuracy and completeness of all citations. Literature citation format: author (last name, followed by first-name initials); year; title of report or article; abbreviated title of the journal in which the article was published, volume number, page numbers. For books, please provide publisher, city, and state.

Tables

Tables should not be excessive in size and must be cited in numerical order in the text. Headings in tables should be short but ample enough to allow the table to be intelligible on its own. All unusual symbols must be explained in the table legend. Other incidental comments may be footnoted (use italic arabic numerals for footnote markers). Use asterisks only to indicate probability in statistical data. Place table legends on the same page as the table data. We accept tables saved in most spreadsheet software programs (e.g. Microsoft Excel). Please note the following:

- Use a comma in numbers of five digits or more (e.g. 13,000 but 3000).
- Use zeros before all decimal points for values less than one (e.g. 0.31).

Figures

Figures include line illustrations, computer-generated line graphs, and photographs (or slides). They must be cited in numerical order in the text. Line illustrations are best submitted as original drawings. Computer-generated line graphs should be printed on laser-quality paper. Photographs should be submitted on glossy paper with good contrast. All figures are to be labeled with senior author's name and the number of the figure (e.g. Smith, Fig. 4). Use Helvetica or Arial font to label anatomical parts (line drawings) or variables (graphs) within figures; use Times Roman bold font to label the different sections of a figure (e.g. **A**, **B**, **C**). Figure legends should explain all symbols and abbreviations seen within the figure and should be typed in double-spaced format on a separate page at the end of the manuscript. We advise authors to peruse a recent issue of *Fishery Bulletin* for standard formats. Please note the following:

- Capitalize the first letter of the first word of axis labels.
- Do not use overly large font sizes to label axes or parts within figures.
- Do not use boldface fonts within figures.
- Do not create outline rules around graphs.
- Do not use horizontal lines through graphs.
- Do not use large font sizes to label degrees of longitude and latitude on maps.
- Indicate direction of degrees longitude and latitude on maps (e.g. 170°E).
- Avoid placing labels on a vertical plane (except on *y* axis).
- Avoid odd (nonstandard) patterns to mark sections of bar graphs and pie charts.

Copyright law

Fishery Bulletin, a U.S. government publication, is not subject to copyright law. If an author wishes to reproduce any part of *Fishery Bulletin* in his or her work, he or she is obliged, however, to acknowledge the source of the extracted literature.

Submission of papers

Send four printed copies (one original plus three copies)—clipped, *not stapled*—to the Scientific Editor, at the address shown below. Send photocopies of figures with initial submission of manuscript. Original figures will be requested later when the manuscript has been accepted for publication. Do not send your manuscript on diskette until requested to do so.

Dr. Norman Bartoo
National Marine Fisheries Service, NOAA
8604 La Jolla Shores Drive
La Jolla, CA 92037

Once the manuscript has been accepted for publication, you will be asked to submit a software copy of your manuscript. The software copy should be submitted in WordPerfect or Word format (in Word, save as Rich Text Format). Please note that we do not accept ASCII text files.

Reprints
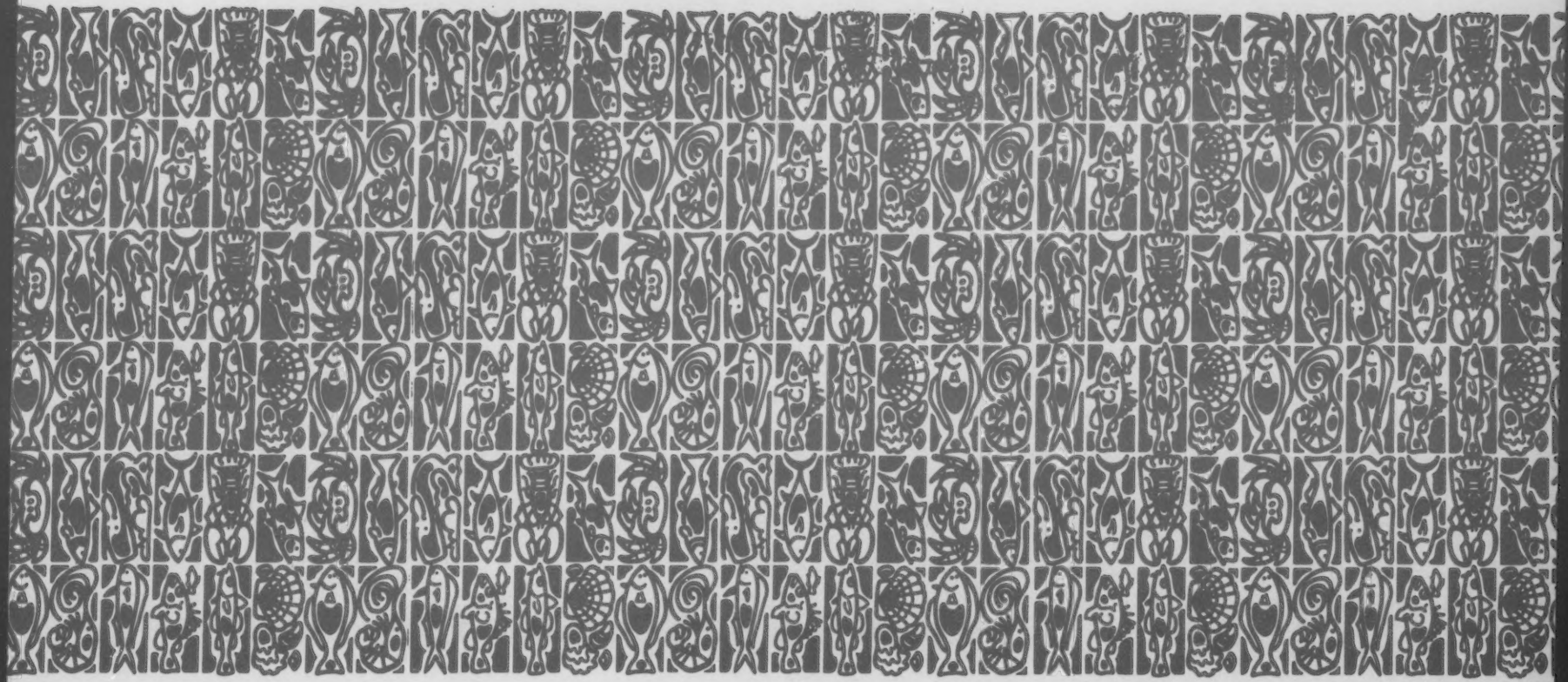
Copies of published articles and notes are available free of charge to the senior author (50 copies) and to his or her laboratory (50 copies). Additional copies may be purchased in lots of 100 when the author receives page proofs.